EFFECT OF BAMBARA GROUNDNUT FLOUR ON THE STABILITY AND RHEOLOGICAL PROPERTIES OF OIL-IN-WATER EMULSION

by

OLADAYO ADEYI
B.Tech. (Hons.) (Ogbomoso), M.Sc. (Ibadan),

Thesis submitted in fulfillment of the requirements for the degree

Doctor of Technology: Chemical Engineering

in the Faculty of Engineering

at the Cape Peninsula University of Technology

Supervisor: Prof Ikhu-Omoregbe Daniel
Co-supervisor: Prof Victoria Jideani

Cape Town

May 2014

DECLARATION

I, Oladayo Adeyi, declare that the contents of this dissertation/thesis represent my own unaided work, and that the dissertation/thesis has not previously been submitted for academic examination towards any qualification. Furthermore, it represents my own opinions and not necessarily those of the Cape Peninsula University of Technology.

Signed **Date**

ABSTRACT

The effect of bambara groundnut flour (BGNF) on the stability and rheological properties of sunflower oil-in-water (o/w) emulsions was studied. BGNF dispersions were gelatinized and used to stabilize sunflower o/w emulsions. The sunflower oil-in-water emulsions were prepared by homogenizing gelatinized BGNF and sunflower oil using the Ultra Turrax T-25 homogenizer. D-optimal response surface methodology (RSM) was used to investigate the effect of BGNF and sunflower oil (SFO) on emulsion stability. Emulsion stability was studied using Turbiscan MA 2000 by observing changes in the average Δ-backscattering flux (%) at 20°C. Quantification of droplet size and droplet size distribution of emulsions was done by image analysis. Emulsion stability parameters such as microstructure, droplet size ($d_{3,2}$ and $d_{4,3}$), initial backscattering (BS_{AVO}) and equilibrium backscattering (BS_{eq}) values were quantified and modeled using RSM. The time-dependent, steady shear and visco-elastic properties were studied using Rheolab MC 1 and Discovery HR-1 rheometers. The rheological behaviours were modeled using rheological equations and predictive equations were developed using RSM. Both BGNF and SFO concentration affected the emulsion stability and rheological properties of emulsions. Increase in oil phase fraction and BGNF concentration improved emulsion stability. The linear and interaction effects of BGNF and SFO were found significant ($p < 0.05$) on droplet size and BS_{AVO}. BGNF-stabilized emulsions showed multiple destabilization mechanism with flocculation/coalescence more prevalent. Kinetics of destabilization showed that increase in SFO and BGNF concentration has profound effect on emulsion destabilization. Increased BGNF in the emulsion decreased particle size. A quadratic polynomial relationship was found between the emulsion main components and droplet sizes ($d_{3,2}$ and $d_{4,3}$) and BS_{AVO}. However, a linear relationship was established between BGNF and SFO for BS_{eq}. Emulsion formulated with 7% (w/w) BGNF and 40% (w/w) SFO possessed highest stability with equilibrium backscattering and desirability values of -0.084% and 89.3% respectively. Regarding the rheological properties, all emulsions were thixotropic, pseudoplastic and viscoelastic fluids. The time-dependent behaviour of the emulsions was well modeled by Weltman, Figoni and Shoemaker and Hahn's models. Both the shear rate and emulsion main components (BGNF and SFO) greatly influenced the time-dependent model parameters. First order stress decay with a zero equilibrium stress value was found not suitable to predict the time-dependent rheological properties of BGNF stabilized emulsions. The time-independent characteristics of the BGNF-stabilized emulsions were well predicted by the Power law, Herschel-Bulkley, Bingham and Casson model (high R^2 and low RMSE and SE). All emulsions possessed viscous (G') and elastic (G") properties. The G', G" and recoverable strain (Q (t)%) of the emulsion were found to

depend on BGNF and SFO concentrations. The linear and quadratic equations were appropriate to describe the relationship between rheological parameters and emulsion components as the case may be. However the emulsion formulated with 7% (w/w) BGNF and 40% (w/w) SFO which possessed maximum storage stability also recorded the highest thixotropic area, pseudo-plasticity, G', G" and Q (t)%. The result strongly indicated a close relationship between emulsion stability and rheological properties for BGNF-stabilized emulsions. Varietal differences of BGNF was insignificant ($p < 0.05$) on the stability parameters such as microstructure, oil-droplet size, BS and BS_{eq} and on rheological properties such apparent viscosities, thixotropic area, power law parameters (K and n), Weltman parameters, G', G" and Q(t)%. Food additives (NaCl, vinegar and citric acid) significantly affected emulsion stability and rheological properties of BGNF stabilized emulsions. Storage stability results indicated that all emulsions were most stable at low temperature of $5^{o}C$ and least stable at high temperature of $45^{o}C$. Destabilization due to oil droplet aggregation was prevalent in all the emulsions. The rheological behaviour during storage was a peculiarity of each of the studied emulsion systems. However, most of the emulsions showed significant ($p < 0.05$) initial increase in rheological parameters (such as apparent viscosity and consistency coefficient of power law equation) in the first three days of study. There was however no general descriptive trend as a function of storage days at all investigated temperatures. All experimental results demonstrated that BGNF may find applications in food emulsion deliveries if appropriately engineered. All the developed empirical models may find uses during formulation of BGNF stabilized emulsions of predetermined stability and rheological properties. Additives may as well be used to control the rheology and physical stability of such emulsions and the presence of BGNF may present the structures (in terms of the matrix) necessary for rigidity during long term storage stability, particularly if BGNF is used as a stabilizer.

ACKNOWLEDGEMENTS

I wish to thank:

- Almighty God, for the gift of life, His love, provision, care and protection. I thank him for His all-time guidance and privilege to complete this study.
- My supervisor, Prof Ikhu-Omoregbe Daniel for the opportunity given to me to undertake this study and his assistance towards the completion of this project. Thank you very much sir.
- My co-supervisor, Prof Victoria Jideani for her sacrifice of time, energy and laboratory assistance towards the completion of this project**.** I will forever be indebted to you ma.
- Prof Tunde Ojumu for his all-time assistance and words of encouragement. I will forever be grateful to you sir.
- Dr. Seun Oyekola for his assistance and love
- Faculty of Engineering and Built Environment for the position of research assistant in 2012 and bursary award of 2014 to enable me complete my study.
- Department of Chemical Engineering for the opportunity to teach in 2012 and 2013 academic sessions, without which I may not be able to pay my fees.
- Cape Peninsula University of Technology, for the award of University Research Fund to study Doctor of Tech., Chemical Engineering in the institution and for sponsoring my trip to Kansas city, USA to attend a conference.
- My colleagues: Patrick, Claudine, Zolelwa and Yvonne for the moral and technical support given to me.
- My good friends
    - Dr. Ayeleso, without who I would not have been able to undertake this programme. May the Almighty God reward you abundantly. Thank you for you have not forgotten the struggles of the past. I will forever be grateful to you.
    - Dr Ayanda, I will forever remember you. Thank you for the accommodation you gave to me when I first arrived in South Africa, your words of encouragement and your assistance.
    - Dr. Ajuwon, for his brotherly love, advice and concern during my hard times in South Africa.
    - Dr. Olatunji, for his brotherly advice, moral support and all time financial assistance. May all mighty God reward you abundantly sir.

  - Engr. Ogidan, Mr Imisi, Mr Ogbomoiko James and Mr Akinsoji for their love, brotherly care and concern.
  - Mrs Fasinu Ebunoluwa, I owe her many thanks for her advice, concern, words of encouragement and for believing in me.
  - Late Fowe Soji, I will always remember you.
- Prof. Fakunle. Thank you daddy for believing in me and your all time advice.
- Pastor Dele Olutona, for being there at all times. Thank you sir.
- My parents, Mr and Mrs Adeyi for their words of advice and encouragement and financial support. Their prayers contributed immensely to the success of this research work.
- My brother, Engr. Adeyi Abiola, I will forever be grateful to you. Thank you for all you have done for me. I pray that God Almighty will continue to bless you. May you achieve all your goals in life.
- My beautiful wife, Mrs. Adeyi Bolanle Yemisi for her patience, love, prayers, care and for standing by me. I am sorry to have abandoned you for more than three years now. Nothing will ever separate us in Jesus name. Amen.
- The Redeemed Christian Church of God (RCCG), The House Hold of God Parish, Bellville, South Africa
- My sisters and brothers: Mr. Oyewola Ayobami, Adeyi Oluwaseun, Mrs Amoo Motolani, Engr. Adeyi Abiola, Mrs Odunayo Ojediran, Adeyi Oluwabusayo, Joshua, Samson and Sayo. We shall all live long to achieve our purpose in life in Jesus name. Amen.

DEDICATION

This thesis is dedicated to Almighty God who started with me and assisted me throughout this research

TABLE OF CONTENTS

LIST OF FIGURES

LIST OF TABLES

LIST OF APPENDICES

GLOSSARY

Symbol	Meaning & Units
BGN	Bambara groundnut
BGNF	Bambara groundnut flour
GBGNFD	Gelatinized bambara groundnut flour dispersion
O/W	Oil-in-water
W/O	Water-in-oil
SFO	Sunflower oil
rpm	revolution per minute
ν_o	Rate of creaming/sedimentation for dilute emulsion
r	Radius of oil droplet
$\Delta\rho$	Density difference
η_o	Viscosity of the continuous phase
Φ	Dispersed phase fraction
ν	Rate of creaming/sedimentation for concentrated emulsion
V_m	Molar volume of dispersed phase in Kelvin equation
S(r)	Solubility of particle with radius r in Kelvin equation
S (∞)	Solubility of particle with infinite radius in Kelvin equation
R_g	Gass constant
T	Absolute temperature
CI	Extent of creaming
H_s	Height of serum
H_E	Height of emulsion
λ_e	Structural parameter at equilibrium state for structural kinetic model
K	Rate constant (s^{-1})
n	Order of structural kinetic model

$d_{3,2}$	Volume surface mean diameter (μm)
$d_{4,3}$	Equivalent volume mea diameter (μm)
n_i	Number of droplet
d_i	Droplet diameter (μm)
T	Transmitted fluxes (%)
T_o	Transmittance of the continuous phase (%)
r_i	Measurement cell internal radius (μm)
l^*	Photon mean free path
d	Particle mean diameter
BS	Backscattering flux (%)
Q_s	Optical parameter of Mie theory
g	Acceleration due to gravity
gr	Optical parameter of Mie theory
BS_{eq}	Equilibrium backscattering flux (%)
K	Consistency coefficient for upward measurement of Power law model
K'	Consistency coefficient for downward measurement of Power law model
n	Flow behavior index for upward measurement of Power law model
n'	Flow behavior index for downward measurement of Power law model
τ	Shear stress (Pa)
γ	Shear rate (s^{-1})
τ_o^B	Yield stress of Bingham rheological model (Pa)
$\tau_{oc}^{0.5}$	Casson yield stress (Pa)
$K_{oc,}$	Casson constant
A	Parameter of Weltman model representing the initial shear stress value
B	Parameter of Weltman model representing the extent of structural breakdown

τ_e	Equilibrium stress value (Pa)
P	Parameter of Hahn model representing the initial shear stress value
α	Parameter of Hahn model representing the rate of structural breakdown
t	Time of shearing (s)
τ_0	Parameter representing the initial shear stress (Pa)
k	Kinetic constant of structural breakdown (s^{-1})
G’	Storage/elastic modulus (Pa)
G’’	Loss/viscous modulus (Pa)
Q (t)	Recoverable strain (%)
J	Compliance (Pa^{-1})

CHAPTER ONE

INTRODUCTION

1.1 Background

Emulsions are a class of dispersed systems that consist of two immiscible liquids, with one of the liquid dispersed as small droplets in the other called continuous phase (McClements, 1999). Emulsion forms the basis of most food and delivery systems and their properties define their eventual applications. Among important emulsion properties are emulsion stability and rheological behavior. Emulsion stability is the ability of the emulsion to resist changes over time. Depending on the application, most commercial food emulsions are expected to have shelf life of more than a year or two. Some of the factors having profound effects on the properties of food emulsions are the aqueous phase compositions such as additives, external stresses such as temperature and ageing. Generally, emulsions are thermodynamically unstable and have tendencies to break down over time due to the difference in specific gravity between the oil droplets and medium usually water (Samavati *et al.,* 2011). Apart from creaming, food emulsions can also destabilize via other phenomena, such as droplet flocculation, coalescence and Ostwald ripening or combination of two or more phenomena.

Food emulsions can therefore be made kinetically stable by adding an emulsifier which keeps the dispersed phase suspended in a continuous phase. This is made possible because of the intrinsic properties of the emulsifier. The effectiveness and functionalities of synthetic surfactants such as acyl lactylates, dioctyl sodium sulfosuccinate, propylene glycol monoesters, sucrose esters and sorbitan esters have made them found applications as food emulsifier and modifiers in food applications (Akoh, 1994). There have been reports of polyglycerol fatty acid ester (PGFE), polyoxyethelene sorbitan monolaurate (Tween 20), and sucrose fatty acid ester (Kobayashi and Nakajima, 2002), sucrose palmitate (Partal *et al.,* 1994), dioctyl sodium sulfosuccinate (Higuchi *et al.,* 1962) and polyglycerol esters of fatty acids (Tan and Nakajima, 2005) as food emulsifiers. However, the unending demand for more natural products by the consumers and increasing legislations for safe and healthy food by governments has made synthetic emulsifiers in food systems increasingly unpopular. Finding natural emulsifier and stabilizers that have comparable and required functionalities in food systems has therefore remained a significant interest (Yang *et al.,* 2013) and challenge in food industries. Researches have therefore been directed towards finding natural emulsifiers and stabilizers of comparable and better functionalities to replace the existing synthetic emulsifiers and stabilizers.

The potential of both animal and plant proteins have been investigated and documented (Young, 1976; Pearce and Kinsella, 1978). The use of phosphatides (Ishii *et al.,* 1990), egg yolk (Mine, 1998), hydrocolloids (Mirhosseini *et al.,* 2008) and starches from various agricultural origins as emulsifiers and stabilizers have been reported (Aktaş and Genccelep, 2006). However, due to abundant availability, emulsifier and stabilizers from plant and agricultural origin seems to be relatively promising. Plant proteins from chick pea (Zhang *et al.,* 2009), sweet potato (Gharsallaoui *et al.,* 2012), and lentil (Can Karaca *et al.,* 2011) have been isolated and starches such as yam (Ibrahim and Achunda, 2011) and maize (Bortnowska *et al.,* 2014) have been extracted and their respective ability to emulsify/stabilize oil-in-water food emulsion have been documented. Whole legumes have also shown high tendencies as auxiliary stabilizers and can improve food emulsion properties. Lentil pulses have been recently reported to increase emulsion stability and recoverable strain of pulse supplemented mayonnaise-like food emulsion relative to the control formulation (Ma and Boye, 2013). However no work is yet available on the use of whole legume as the main stabilizing or emulsifying composition in food systems.

Bambara groundnut (BGN) is a leguminous plant which belongs to the family fabaceae. It is cultivated throughout Africa, from Senegal across to Kenya and from Sahara to South Africa (Brough *et al.,* 1993). BGN contained carbohydrate contents of 49 - 63.5%, protein content of about 15 – 25%, fat contents of about 4.5 - 7.4%, fiber content of 5.2 - 6.4, ash of 3.2 - 4.4% and 2% mineral (Murevanhema and Jideani, 2013). It has also been reported to have great health significance. The high percentage of protein and carbohydrate contents as well as the probable protein-carbohydrate interactions during gelatinization and emulsion preparation made BGN to have high potential as main emulsifier/stabilizer in food emulsions. Therefore understanding the behaviour of food emulsions stabilized with whole bambara groundnut, may be necessary for the future adoption of BGN as food stabilizer.

1.2 Statement of Research Problem

A fast growing area in food emulsion technology research is finding new alternatives for improving the stability and physical properties of emulsions. This is because consumers are demanding more natural products. One of such promising alternatives is in the area of plant - derived emulsifiers and stabilizers. Like other legumes (e.g. flaxseed and soybean) BGN has recently been shown to possess stabilizing and emulsifying properties (Adebowale and Lawal, 2002). The nutritional composition of BGN indicates its potential as food emulsifier/stabilizer.

The seed is regarded as a balanced food because it is rich in iron and the protein contains high lysine and methionine (Okpuzoor *et al*., 2010). Despite all these numerous advantages, BGN still remains one of the neglected and under-utilized crops in Africa. Oil-gelatinized BGN flour emulsion is a novel emulsion system that may have potential applications in food industries but whose stability and rheological data have never been reported in the literature. Stability of food emulsions determines the shelf life and their rheological properties are necessary to evaluate their behaviour during processing, storage and in overall plant design. The ability to control the rheological properties of emulsions depends on the quantitative understanding of the relationship between the rheology, composition and microstructure. There is therefore need to investigate the (1) contributions of each of the main components/ingredients of the emulsion and their interactions to the stability and rheological characteristics of the BGN stabilized oil-in-water emulsions (2) influence of food additives on the stability and rheological properties and (3) changes in their intrinsic properties during storage with a view to establish the suitability of bambara groundnut flour (BGNF) as natural stabilizing agent.

1.3 Broad Objectives

The aim of this research work was to evaluate the potential effect of BGNF and sunflower oil on some emulsion stability parameters (droplet-size, microstructure, droplet-size distribution and creaming or aggregation) and on the rheological parameters (viscosity, visco-elasticity and time dependent flow behavior) of oil-in-water emulsions.

Specific objectives are to:

1. Investigate the effects of bambara groundnut flour (BGNF) and sunflower oil (SFO) concentrations, on the stability of oil-in-water emulsion stabilized with gelatinized BGNF and optimize and model the emulsion stability parameters as function of main emulsion components (BGNF and SFO) using response surface methodology (RSM).

2 Characterize and describe the time dependent rheological behaviour observed in the sunflower oil-in-water emulsions stabilized with gelatinized BGNF using the hysteresis loop area and constant shear stress decay methods and develop empirical equations for the time dependent properties as a function of BGNF and SFO.

3 Characterize and describe the time independent rheological properties of the oil-in-water emulsion stabilized with gelatinized BGNF using steady shear rheological equations and to model the intrinsic rheological properties as a function of emulsion components.

4 Characterize the viscoelastic rheological behaviour of the oil-in-water stabilized with gelatinized BGNF and model the intrinsic properties as a function of BGNF and SFO.

5 Investigate the effect of some food additives on the emulsion stability and rheological properties (time dependent, time dependent and visco-elastic properties) of optimum formulation in (1)

6 Investigate the effect of storage temperatures and time on the stability and rheological properties of the optimum oil-in-water emulsion and emulsions containing additives.

7 Investigate the relationship between emulsion stability and rheological parameters.

1.4 Research Hypotheses

1. Bambara groundnut flour (BGNF), sunflower oil and additives, all affect significantly the stability and rheological properties of sunflower oil-in-water emulsion (SOWE) stabilized by gelatinized BGNF dispersion.

2. The time dependent, time independent and viscoelastic behaviours of sunflower oil-gelatinized bambara groundnut dispersion can be fitted and predicted by the existing rheological models and the viscous and viscoelastic properties greatly depend on the composition of the emulsion.

3. Optimum amount of BGNF and oil concentration will yield the most stable (best) emulsions.

4. Storage temperatures and time will significantly improve the stability and rheological properties of the most stable formulation of SOWE and emulsions containing food additives.

5. Long term emulsion stability can be explained in terms of short term rheological measurements.

1.5 Significance of the Research

The result of the research will give a better insight into exploiting other functional use of bambara groundnuts. It will also provide a cheap source of emulsifying/stabilizing agents for food, industries and others like pharmaceutical, cosmetics and chemical. The result of the research work is hoped to give a new formulation of oil-in-water emulsion using BGNF as emulsifying agents. The outcome of BGNF influences on the oil-in-water emulsion systems provide us with information on the nature, characteristics use and functions to which such emulsions can be subjected. Information about the emulsion stability will enable understanding of instability of the system and hence the shelf-life of the emulsions, while the rheological properties will give insight into the nature and viscoelasticity of the emulsion and its applications.

1.6 Expected Outcomes

Findings of this research work will be presented in international conferences and published in accredited journals, in addition, the following are expected to be unveiled:

(a) The influence of BGNF on the stability of oil-in-water emulsion which ultimately determines the shelf-life of the emulsions.
(b) The inherent rheological properties of oil-in-water emulsions stabilized with BGNF which determines its processability and functional uses.
(c) The link between long term emulsion stability and short term rheological responses.
(d) The influence of food additives such as NaCl and acidulants on the stability and rheological behaviour of oil-in-water emulsion which determines its applications.
(e) The ageing of BGNF stabilized emulsions which elucidates their behaviour during storage.

1.7 Delineation of the Study

Laboratory studies mainly were conducted to determine, evaluate and generalize the effect of various factors on the parameters of oil-in-water emulsion stabilized with gelatinized BGNF. No proximate composition of the BGNF was conducted prior to laboratory studies. Extensive work was only done on brown BGN variety, although comparative studies were conducted on the other four varieties available in South Africa. Sun flower oil was used as the only hydrophobic phase and commercially available brand was used without further purification. Emulsion stability and rheological properties were the only two properties investigated. Image analysis

method of quantifying droplet size and distribution was used because of the nature of the BGNF stabilized emulsion. Droplet size measurements using light diffraction method (Malvern mastersizer) could not differentiate between the flour particles and the oil-droplets. The observed rheological characteristics were described using the existing rheological models, although models predicting the observed intrinsic characteristics as function of emulsion components were developed using response surface methodology (RSM). No sensory studies were conducted on the emulsions.

1.8 Chapter Overview

This thesis describes the effect of bambara groundnut flour on the stability and rheological properties of oil-in-water emulsion with particular interest in food systems. The influences of food additives and ageing on the properties of the oil-in-water emulsions were also described. The background of the study, problem of the research statement, aim and objectives of the research and significance of research was described in Chapter 1. Chapter 2 considered the review of relevant literatures regarding the research work. Chapter 3 described the experiments performed to study the:

(a) Optimization of processing parameters necessary to investigate the behaviour of oil-in-water emulsion stabilized with BGNF.
(b) Optimization of main emulsion components and effect on the stability and rheological properties of oil-in-water emulsions stabilized with BGNF.
(c) Effects of some food additives on the properties of most stable oil-in-water emulsion stabilized with BGNF.
(d) Ageing of most stable emulsions with and without additives at different storage temperatures.

The results of the experimental studies were described in Chapter 4 while Chapter 5 gave the summary of the research work, future recommendations and conclusions.

CHAPTER TWO

LITERATURE REVIEW

2.1 Overview of Food Emulsion

2.1.1 Emulsion types and emulsification process

An emulsion is a biphasic, metastable coarse dispersion of two immiscible materials, usually liquids (typically oil and water), that produces a semisolid (Sarker, 2013). Emulsions can be classified as oil-in-water (O/W), water-in-oil (W/O) and oil-in-oil (O/O). The preference for the oil-in-water (O/W) or water-in-oil (W/O) type is dictated primarily by the wettability of the dispersed particle, with preferentially oil wetted particle favouring water-in-oil (W/O) emulsion. Emulsion-phase characterization can be done by Copenhagen Radiometer CDM3 Instrument with a model CDC314 glass probe (Saleh *et al.,* 2005). In order to disperse two immiscible liquids a third component is required, namely the emulsifier. Emulsion may be classified according to the nature of the emulsifier or the structure of the system. Such classification is given in the Table 2.1.

Table 2.1 Classification of emulsion types

Nature of emulsifier	Structure of the system
Simple molecule and ions	Nature of internal and external phase
Nonionic surfactants	O/W, W/O
Surfactant mixture	Micellar emulsions (micro emulsions)
Ionic surfactants	Macroemulsions
Nonionic polymers	Macroemulsions
Polyelectrolytes	Double and multiple emulsions
Mixed polymers and surfactants	Mixed emulsions
Liquid crystalline phases	Glassy emulsion
Solid particles	Pickering emulsions

Source: Tadros, 2009

Several industrial systems consist of emulsions of which the following are worthy of mention (Tadros, 2009):

(a) Food emulsions, such as mayonnaise, salad creams and beverages.

(b) Personal care and cosmetics such as lotion and hand cream.

(c) Pharmaceuticals, such as anesthetics of O/W emulsion, lipid emulsions, double and multiple emulsions.
(d) Paints, such as emulsions of alkyd resins and latex emulsions.
(e) Dry-cleaning formulations
(f) Emulsions in oil industry
(g) Oil slick dispersants-oil spilled from tankers must be emulsified and then separated.

The manufacture of an oil-in-water emulsion requires intense energy in order to disperse the organic phase (oil) in continuous phase (water). The extent of the disorderliness (entropy) of the system determines the degree of size reduction of the organic phase and hence the increase in droplet number. The mechanism of colloidal emulsification is based on particle (emulsifiers) adsorption at the oil/water interface. Emulsification process include two steps, deformation and disruption of droplets, and the stabilization of the newly formed interface by surfactant or emulsifier (Tantayotai and Pongsawatmanit, 2005). Different machines are available for the emulsification process such as rotor-stator systems and high-pressure homogenizer.

2.2 Food Emulsion Stability

Among important emulsion properties are emulsion stability, interfacial properties and interactions, texture and flavour. Emulsion stability determines the shelf-life of food emulsion-products. Stability of an emulsion can be defined as the maintenance of an initial state that was attained after homogenization of the two (or more) phases. Emulsions are thermodynamically unstable and have tendency to breakdown overtime (Friberg and Larsson, 1997). Several processes relating to breakdown of emulsions may occur on storage. Such processes depended on:

(a) The distribution of the oil droplets and the difference in density between the droplets and the medium.
(b) The magnitude of the attractive versus repulsive forces, which determines flocculation
(c) The solubility of the dispersed droplets and the particle size distribution, which in turn determines Ostwald ripening
(d) The stability of the liquid film between the droplets, which determines coalescence
(e) Phase inversion (Friberg and Larsson, 1997).

The destabilization may however be simultaneous rather than consecutive and may involve more than one emulsion destabilization phenomena. Food emulsion stability are affected by factors such as, emulsifier and oil phase concentration (Sun and Gunasekaran, 2009; Dluzewska *et al.,* 2006; Ibrahim and Najwa, 2012), pH (Surh *et al.,* 2006; Demetriades *et al.,* 1997), homogenizer type and processing variables (Huck-Iriart *et al.,* 2011; Tantayotai and Pongsawatmanit, 2005; Thiebaud *et al.,* 2003) and additives such as sodium chloride salt (Tantayotai and Pongsawatmanit, 2005; Demetriades, *et al.,* 1997).

2.2.1 Mechanisms of emulsion instabilities

The summary of emulsion breakdown processes encountered on storage is given in Figure 2.1

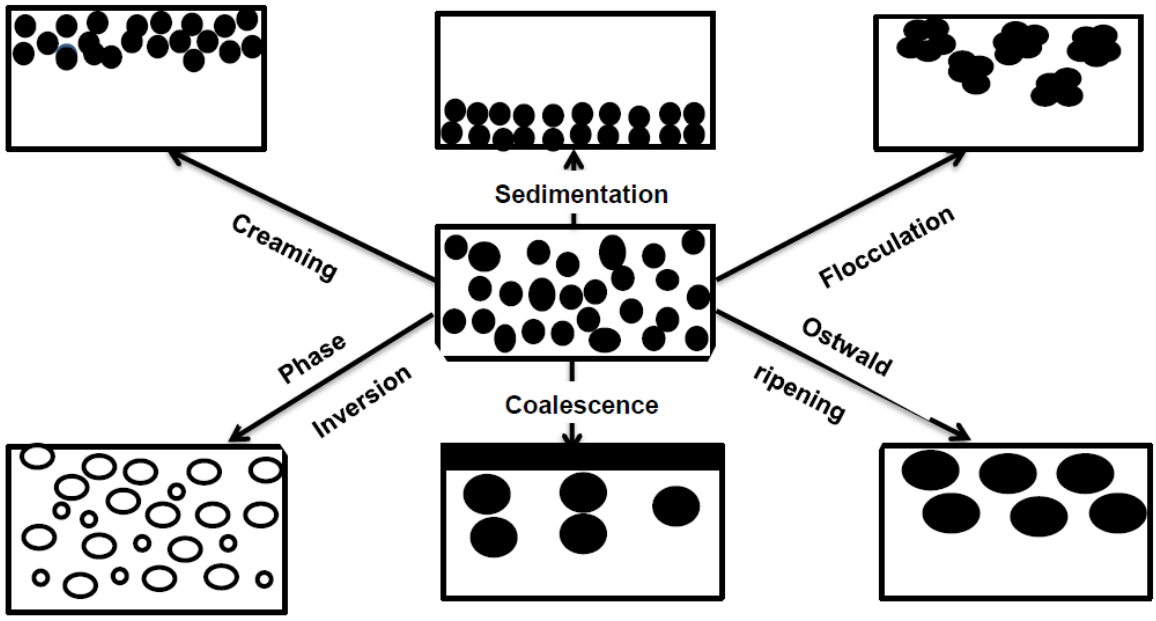

Figure 2.1 Representation of breakdown processes in emulsion (Adapted from Tadros, 2004)

Generally, the three main types of interaction energies between emulsion droplets are:

(a) The van der Waals attractions of which London dispersion interactions are the most important.

(b) Electrostatic repulsion

(c) Steric repulsion

The van der Waals forces of attraction are majorly responsible for the breakdown of an emulsion system (Tadros, 2009). Frequently encountered food emulsion destabilization mechanisms are discussed below.

2.2.1.1 Flocculation

This occurs when oil droplets in an emulsion aggregate without the rupture of the stabilizing layer at the interface (Silset, 2008). Aggregation through droplet flocculation may result when van der Waals energy exceeds the repulsive energy (Verwey *et al.,* 1999). When there is no repulsion among the oil droplets in the emulsion system, there is higher tendency for the emulsions to flocculate very rapidly thereby producing large clusters leading to an increase in the emulsion viscosity (McClements, 2005). Flocculation may be reversible or irreversible. Irreversible flocculation is called coagulation. The driving forces for flocculation can be body forces such as gravity and centrifugation, Brownian forces or thermo-capillary migration (Abdel-Raouf, 2011). Assessment of the emulsion flocculation can be done by direct droplet counting. The phenomenon can however be eliminated or minimized by reducing the van der Waals force of attraction either electrostatically or sterically.

2.2.1.2 Coalescence

This mechanism of destabilization involves fusing or joining of two or more droplets together to form a single larger droplet by the rupturing of the interface stabilizing films with the eventual separation of the oil. The thinning and disruption of liquid films between the approaching droplets in cream layer, in a floc or during Brownian diffusion provides the driving force for the rate of coalescence. Coalescence is an irreversible phenomenon (Abdel-Raouf, 2011) and may be reduced by using a mixed surfactant film and formation of 'lamellar' liquid crystalline phases at the O/W interface (Tadros, 2009).

2.2.1.3 Creaming or sedimentation

The processes of flocculation and coalescence are followed by phase separation. Emulsion creaming/sedimentation is a result of density difference between the continuous phase and the dispersed phase. The rate of creaming or sedimentation (v_o) of very dilute emulsion followed the Stokes law (equation 2.1) (Tadros, 2004).

$$v_o = \frac{2}{9}\frac{r^2 \Delta\rho g}{\eta_o} \qquad (2.1)$$

Where r is the particle radius, $\Delta\rho$ is the density difference, g is the acceleration due to gravity and η_o is the viscosity of the continuous phase.

However for a concentrated emulsion (high dispersed volume fraction (ϕ)) the rate of creaming/sedimentation (v) is reduced below Stokes law (equation 2.2) (Tadros, 2004).

$$v = v_o\ (1 - 6.55\ \phi) \quad (2.2)$$

Creaming/sedimentation phenomenon can be reduced sterically by adding a thickener to the continuous phase of the emulsion (Tadros, 2004). Thickeners are high molecular weight, pseudoplastic polymers that give very high viscosity and yield value at low shear rates.

2.2.1.4 Ostwald ripening

Ostwald ripening is a phenomenon that occurs as a result of the difference in solubility between small and large particles (Tadros, 2004). Ostwald ripening is often found in oil-in-water emulsions that contain more water-soluble lipids or when the aqueous phase contains alcohol (Agboola and Dalgleish, 1996). Ostwald ripening causes small particles to decrease in size while large particles grow even larger. This is because oil molecules diffuse through the aqueous continuous phase and join larger oil droplets which lead to phase separation over time. Kelvin equation, which relates the solubility of a particle with radius *r*, *S*(*r*) to that of a particle with infinite radius *S* (∞) is presented in equation 2.3 (McClement, 2005).

$$S(r) = S\ (\infty)\ \exp\left(\frac{2\gamma V_m}{R_g T r}\right) \quad (2.3)$$

Where V_m is the molar volume of the dispersed phase, γ is the interfacial tension and R_g is the gas constant and *T* is the absolute temperature. However, for two droplets, the Ostwald equation is given by equation 2.4 (Tadros, 2004).

$$\left(\frac{R_g T}{V_m}\right) \ln\left(\frac{S_1}{S_1}\right) = 2\ \gamma\ \left(\frac{1}{r_1} - \frac{1}{r_2}\right) \quad (2.4)$$

Where S_1 and S_2 are the solubilities of oil droplets with radius r_1 and r_2 respectively
Among the methods employed to reduce Ostwald ripening are reduction of interfacial tension, and enhancement of the Gibbs elasticity.

2.2.1.5 Phase inversion

Phase inversion is the process whereby a system changes from oil-in-water emulsion to a water-in-oil emulsion or vice versa (Moreira de Morais *et al.,* 2006). Phase inversion is usually caused by some changes in the composition or environmental conditions of an emulsion such

as disperse phase volume fraction, emulsifier type, emulsifier concentration, solvent conditions, temperature or mechanical agitation (McClement, 2005). The most common procedure to assess phase inversion is to measure the conductivity or the viscosity of the emulsion as a function of dispersed phase, increase of temperature and/or addition of electrolyte (Tadros, 2004).

2.2.2 Methods and equipment for studying emulsion instability

2.2.2.1 Zeta- potential

Zeta-potential measurement is one of the most widely used methods of emulsion stability characterization. Zeta-potential is defined as the value of the electrical potential at the shear plane of the particle and it provides an estimate of net charge on the particle (Surh *et al.,* 2006). Zeta-potential is dependent on the actual charge of the particle, the adsorbed layer at the interface and the nature and composition of the surrounding medium. Its value range provides information regarding electrostatic charge repulsion and attraction between particles and thus plays a role in aggregative stability. Emulsions with high zeta potential (negative or positive) tend to have high degree of electrostatic stability while a lower zeta potential leads to high particle aggregation (Wang *et al.,* 2010b) mainly by Van der Waals inter particle attractions. Therefore, detailed analysis of zeta potential of particles in a medium gives understanding of the origin of dispersion aggregation and flocculation and its knowledge could be applied to improve dispersion formulation. Some available instruments for measuring zeta potential of a surface are electrophoretic mass transport analyzer, streaming current detector and electrokinetic sonic amplitude device. However, zeta potential is nowadays determined by measuring the electrophoretic mobility of the dispersed particles in a charged field (Roland *et al.,* 2003).

2.2.2.2 Particle/droplet size measurements

Particle size determination of emulsion is probably the most important way of emulsion characterization (Dapčević Hadnađev, 2013). This is because particle size influences other properties of emulsions such as texture, creaming velocity and rheology (Chanamai and McClements, 2000), tastes, appearance, etc. Particle size of emulsions are normally reported in various forms, such as the volume mean diameter (Agboola *et al.,* 1998; Ibrahim and Achundan, 2011; Zúñiga *et al.,* 2012; Sun and Gunasekaran, 2009), number mean diameter (Dapčević Hadnađev, 2003) and the equivalent volume mean diameter (Gharibzahedi *et al.*, 2012; Jafari *et al.*, 2012; Palazolo *et. al.*, 2005). Among the widely reported methods of particle size analysis is the laser diffraction method (Agboola *et al.,* 1998; Lorenzo *et al.,* 2008; Camino

and Pilosof, 2011; Blijdenstein *et al.,* 2003; Wang *et al.,* 2010a; Ibrahim and Najwa, 2012; Koocheki and Kadkhodaee, 2011). Other popular methods are electrical sensing method, photon correlation spectroscopy or ultrasonic spectroscopy (Roland *et al.,* 2003). In principle, the beam passes through the dispersed sample and the angular variation in the intensity of the light scattered is measured, and analyzed by using Mie theory for information regarding the size of particle responsible for creating the scattering pattern.

Although particle sizes of emulsions have been widely reported by workers in the field of emulsion science by using laser diffraction method it however has its disadvantages. Like some other mentioned methods such as electrical zone sensing method and photon correlation spectroscopy laser diffraction method requires dilution of samples prior to measurements. Dilution in water may induce physicochemical changes in the environment of the droplet leading to completely unreliable data (Roland *et al*., 2003). Agboola *et al.* (1998) investigated the destabilization of oil-in-water emulsions formed using highly hydrolyzed whey protein. Particle size was measured by using laser diffraction method as one of the properties of emulsion. They concluded that small angle laser light scattering was inadequate to accurately size these emulsions because the size distribution data did not represent particle size ranges observed through microscopy. The probable reason provided by the authors were that the large particles of the emulsion are outside the range of the focal length used in the Mastersizer and or that the large oil droplets were broken down in the turbulent shear field of the Mastersizer before reaching the measuring equipment.

Droplet size quantification and distribution of emulsions by the use of image analysis is also widely reported (Zúñiga *et al.,* 2012; Payet, & Terentjev, 2008; Perrechil and Cunha, 2010; Perrechil *et al.,* 2010; Santana *et al.,* 2011; Freire *et al.,* 2005; de Castro Santana *et al.,* 2012; Trindade *et al.,* 2008). Generally, emulsion samples are poured onto microscope slides, which will then be covered with the glass cover slip and subsequently observed at various magnifications. Depending on the clarities of the microscopic images, most micrographs are normally processed before being subjected to analyses. Santana *et al.* (2011) investigated the emulsifying properties of collagen fibers and the effect of homogenization pressure on the particle size. Particle sizes of the emulsions were determined by image analysis method. Images of emulsions that were prepared by rotor-stator device were analyzed by transforming them into 8-bit grey scale binary images with 640-480 pixels and then segmented by thresholding. Droplets that were at image border were suppressed. The micrographs of emulsions homogenized by high pressure showed that the droplets were less than 5 µm and therefore these images were analyzed by measuring at least 500 droplets one at a time using

the public domain software image J v1.36b. The use of image analyzes algorithm available in Matlab has also been reported (Freire *et al.,* 2005). Most images processing in Matlab requires a three step sequence of image binarization, droplet quantification and evaluation of statistical parameters.

Creaming stability of emulsion is largely dependent on the particle size. The larger the oil droplet the higher the creaming rate. The particle size effect on creaming velocity can be explained using Stokes law in equation 2.3 (Chanamai and McClements, 2000). However a study conducted by Lorenzo *et al.* (2011) on the stability of gel-like emulsions stabilized with bovine gelatin showed that emulsion stability could largely depended on the emulsifier molecular weight rather than the dispersed droplet size of the emulsion. They reported that emulsions with higher droplet size but stabilized with high molecular weight protein was more stable than emulsion with lower droplet size stabilized with low molecular weight protein. In another study by Tse and Reineccius (1995) to investigate methods for predicting the physical stability of flavor-cloud emulsion, methods such as particle size determination, centrifugation and storage at elevated temperatures were studied. The workers concluded that particle size determination method was not accurate due to its inability to consider emulsion instability caused by flocculation and coalescence.

2.2.2.3 Emulsion stability measurement

One of many and popularly measured indicators of emulsion instability is creaming index. Creaming index provides indirect information about the extent of droplet aggregation in an emulsion, that is, the higher the creaming index, the faster the droplets move and therefore the more droplets aggregation has occurred (Onsaard *et al.,* 2005). Creaming tests are used to gain insights into the causes of emulsion instability. Laboratory analysis of creaming mechanism could be done by visual observation, optical imaging and accelerated optical imaging methods. Creaming tests provide information on how various parameters affect the emulsion stability.

There are various documentations of the procedures for visual studying and quantification of emulsion stability. For instance Wang *et al.* (2010b) studied emulsion stability of soybean oil-in-water emulsions stabilized by concentrated flaxseed protein by placing the emulsions in tightly sealed glass test tubes for seven days. The total height of the emulsion (H_E) and the height of the serum (H_s) were measured and extent of creaming (CI) was determined using the equation 2.5.

$$CI = {}^{H_s}/_{H_E}\ X\ 100 \qquad (2.5)$$

A similar method was also reported by Keowmaneechai and McClements (2002), Sun and Gunasekaran (2009), Surh *et al.* (2006) and Lorenzo *et al.* (2008). CI can provide indirect information about the extent of droplet aggregation in an emulsion (Sun and Gunasekaran, 2009). Slightly different approach was however reported by Nikovska (2010). In his report, creaming stability of walnut oil-in-water emulsion was studied by centrifuging at 3000 rpm for 15 minutes in order to accelerate creaming. Three layers were identified and measured to quantify emulsion stability or instability namely, the serum, emulsion and creamed layers. Emulsion stability under centrifugation was also reported by Ibrahim and Najwa (2012).

Optical characterization of emulsion by vertical scan analyzer is also widely reported (Camino and Pilosof, 2011; Huck-Iriart *et al.,* 2011; Lemarchand *et al.,* 2003; Roland *et al.,* 2003; Daoud-Mahammed *et al.,* 2007; Palazolo *et al.,* 2005). Optical characterization has been used to identify and quantify destabilization mechanisms prevalent in an emulsion system. One of the mostly used and reported vertical scanners is Turbiscan M.A 2000 (Blijdenstein *et al.,* 2003; Blijdenstein *et al.,* 2004; Lemarchand *et al.,* 2003; Álvarez Cerimedo *et al.,* 2010). Emulsion sample was put in the tube and the tube was in turn inserted in the analyzer and scanned from bottom to the top in order to monitor the optical properties, this allows physical evolutions of the process without disturbing the original system and with good accuracy and reproducibility (Alvarez Cerimedo *et al.*, 2010). The vertical scanner is made up of a light source which is an electro luminescent diode in the near infra-red (λ = 850nm) and two synchronous optical sensors namely transmission detector and backscattering detector. In principle, during optical scanning, the light passes through the dispersion and both the transmission and backscattering detectors receive light transmitted through the sample at an angle of 180^o and light backscattered by the sample at an angle of 45^o from the incident light, respectively (Figure 2.2)

Emulsion destabilization mechanisms such as creaming, sedimentation, coalescence and flocculation could be identified by scanning the emulsion sample repeatedly at a different time interval to get superimposition of the product fingerprint (Figure 2.3). Instability due to creaming was characterized by variation of the particle concentration between the top and the bottom of the cell. This was observed as a decrease and increase in the backscattering flux at the bottom and top of the sample, respectively when the backscattering profile was put in the reference mode (Figure 2.4). Coalescence and flocculation destabilization phenomena are although physico-chemically very different both behave the same way when Turbiscan MA 2000

is used. The particle variation induced by these phenomena can easily be observed as a decrease of the backscattering over the whole height of the sample which indicated a

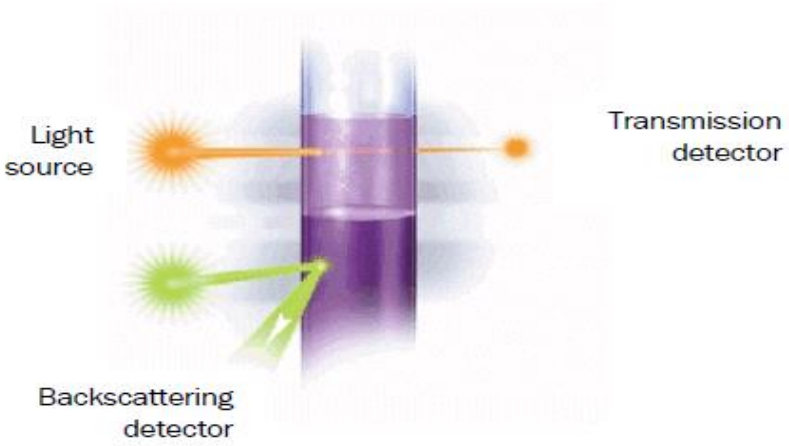

Figure 2.2 **Principle of measurement of the Turbiscan® (Source: Turbiscan® Manual, Turbiscan® MA 2000, Formulaction Toulouse, France)**

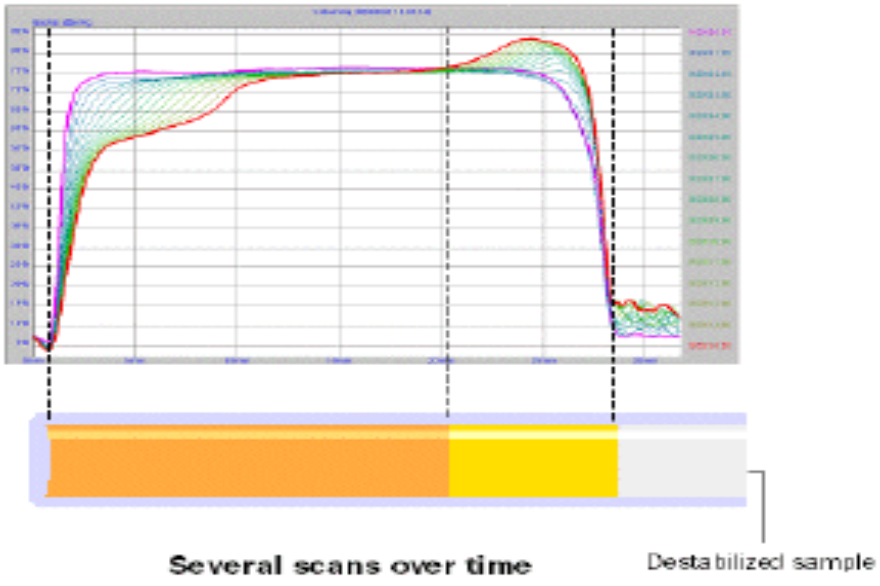

Figure 2.3 **Turbiscan® backscattering multiple scanned profile (Source: Turbiscan® Manual, Turbiscan® MA 2000, Formulaction Toulouse, France).**

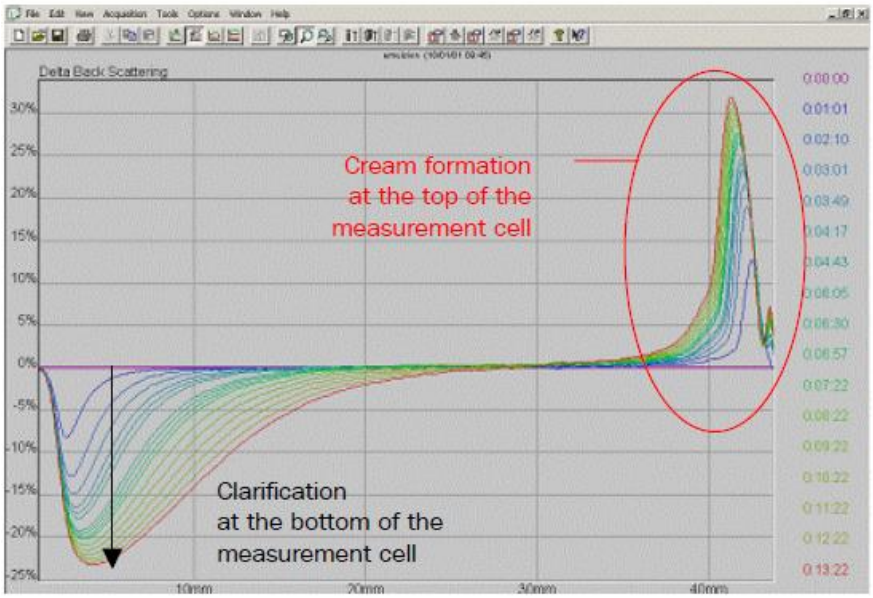

Figure 2.4 **Data in reference of creaming emulsion (Source: Turbiscan® Manual, Turbiscan® MA 2000, Formulaction Toulouse, France)**

progressive increase in particle size (Figure 2.5). However, some emulsions can show multiple destabilization mechanisms where creaming, flocculation and coalescence are happening simultaneously (Figure 2.6).

Huck-Iriart *et al.* (2011) investigated the effect of processing conditions and composition on sodium caseinate emulsions stability using Turbican M.A 2000. Creaming and flocculation phenomena were noticed in the emulsions. Creaming destabilization phenomenon showed as a peak at height between 0 - 20 mm of the tube and creaming kinetics was evaluated by measuring the peak thickness at 50% of the height at different times. The slope of the peak thickness vs time was obtained as an indication of migration rate. The observed flocculation phenomenon was followed by measuring the average backscattering flux as a function of storage time in the middle of the tube. Emulsion stability using a spectrophotometric method was also reported by Zuniga *et al.* (2012). In their study, light transmittance of hydroxypropyl methylcellulose based oil-in-water emulsions was measured at 850 nm using a spectrophotometer. Transmittance measurements were obtained by a double beam arrangement such that the transmittance of the emulsion was measured relative to the reference sample.

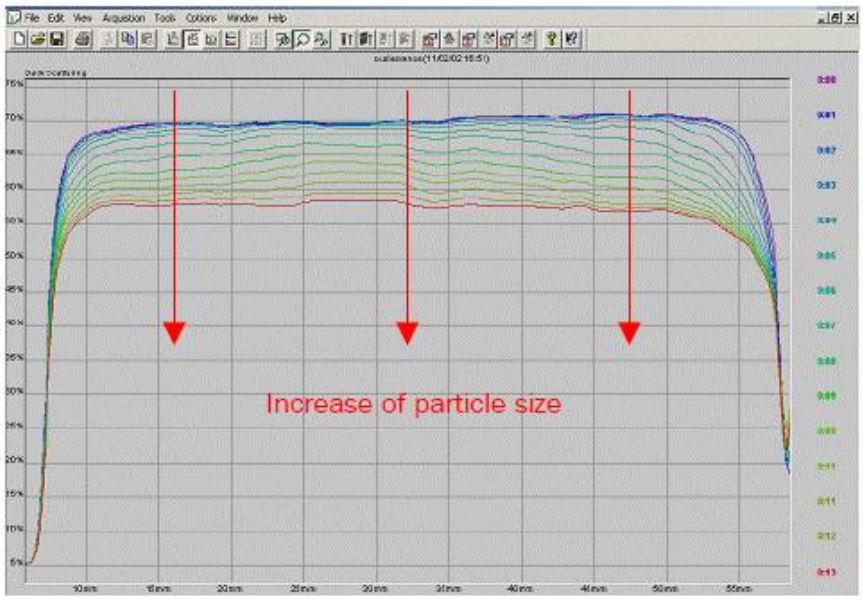

Figure 2.5 **Data in reference of coalescing emulsion (Source: Turbiscan® Manual, Turbiscan® MA 2000, Formulaction Toulouse, France)**

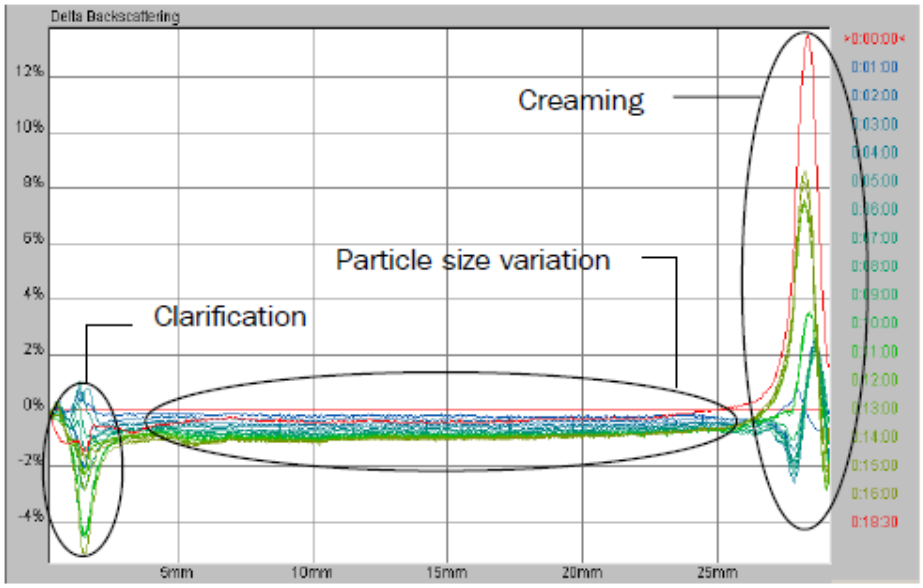

Figure 2.6 **Data in the reference of an emulsion that creamed and coalesced (Source: Turbiscan® Manual, Turbiscan® MA 2000, Formulaction Toulouse, France)**

2.3 Rheological Behaviour of Food Dispersions

Rheology is defined as the science that is concerned with the deformation and flow of matter (Macosko, 1994). The knowledge of the rheological properties of food dispersions cannot be over emphasized for numerous reasons. Rheological data of food products are needed in shelf life testing, process engineering calculations, determination of ingredient functionality, quality control and in sensory evaluations (Steffe, 1996). Rheological data are also useful during food product development stage (Fischer and Windhab, 2011) and could address the industrial production of food (stirring, pumping, dosing, dispersing and spraying), home based cooking as well as consumption of food (oral perception, digestion and well-being) (Gao *et al.,* 2011). From a technological point of view, the rheology of food dispersions is fundamental mainly due to its relationships with emulsion stability (Gallegos *et al.,* 2004). Food emulsions are compositionally and structurally complex materials that can exhibit a wide range of different rheological behaviours, ranging from low viscosity fluids, to viscoelastic gels, to fairly hard solids (McClements, 2005). The rheological behaviour of particular food dispersion depends on the type and concentration of ingredients that it contains, as well as the processing and storage conditions (McClement and Jochen, 2005) and as such, the precise equations used to describe rheological properties depend on the characteristics of the system. The flow and viscoelastic characterization of food dispersions provide the necessary rheological information on both the viscous and viscoelastic properties. In order to relate the long term physical stability with short term rheological measurements in the first few weeks of storage, three rheological methods that may be applied are (a) Steady state shear stress-shear rate measurements (using a controlled shear rate instrument). (b) Constant stress (creep) measurements (carried out using a constant stress instrument). (c) Dynamic (oscillatory) measurements (preferably carried out using a constant strain instrument) (Tadros, 2004).

2.3.1 Steady flow characterization of food dispersions

Most rheological tests involve applying a specific force to a material and measuring the corresponding flow or deformation of the material. The composition of dispersed systems has a profound effect on its rheological properties. In general, food emulsion rheology depends on droplet size distribution, rheology of the continuous phase, inter-particle interactions and processing conditions such as energy input during emulsification, residence time, application of thermal treatments and so on. (Gallegos *et al.,* 2004). The flow characterization tests give information regarding the viscous characteristics of a material and can either be performed by stepped shear stress / shear rate or ramped shear stress/ shear rate (Mezger, 2006). Viscous

behaviour of food dispersions are always described using rheograms, which shows the relationship between the applied load/force and the resulting flow of the material.

Fluid materials can exhibit shear thinning, shear thickening, plastic or complex flow behaviour when sheared over a broad range. Figure 2.7 shows the flow diagram of frequently encountered fluid behaviours. Most food dispersions are non-Newtonian and tend to have a shear thinning behaviour when sheared (Gallegos *et al.,* 2004). The distortion of the equilibrium structure of the dispersion changes the inter-particle spacing and Brownian contribution to the viscosity change and particles are observed to line up into a string parallel to the direction of flow. This is perhaps the most widely encountered type of time-independent behaviour in food systems. It is characterized by an apparent viscosity which gradually decreases with increasing shear rate (Mezger, 2006). For example, food emulsions stabilized by flaxseed protein concentrate containing–mucilage (FPCCM), whey protein isolate (WPI) and xanthan gum and green banana pulp, all showed shear thinning behaviours as suggested by rheological curves (Wang *et al.,* 2010b; Nayebzadey *et al.,* 2007; Izidoro *et al.,* 2008). Also a study of the steady flow properties of low-in fat oil in water emulsion stabilized by xanthan /guar mixture conducted by Lorenzo *et al.* (2008) showed a shear thinning characteristics with three well defined regions at low, medium, and high shear stresses.

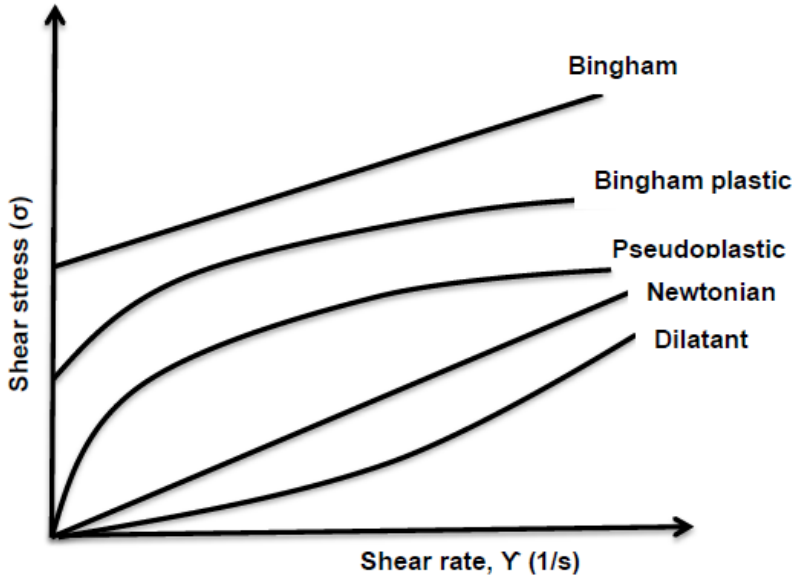

Figure 2.7 Characteristic flow diagrams of fluids

Steady flow behaviours of food dispersions have been described by flow models. A flow model may be considered to be a mathematical equation that can describe rheological data, such as shear rate versus shear stress, in a basic shear diagram and that provides a convenient and concise manner of describing the data (Rao, 2014). Fundamental flow models describe the simple flow behaviour of fluids. They are well suited to studying materials over a small shear range or where only a simple relationship is required. Flow characterization of most shear thinning food dispersions over a small shear range have been modeled by using power law (Izidaro *et al.,* 2008), and Herschel Bulkley model (Ibrahim *et al*., 2011; Ikhu-Omoregbe and Bushi, 2008). However, most materials including food dispersions start to deviate from these relationships over a sufficiently large shear range and therefore exhibit more complex flow behaviours. Dispersions with complex behaviours fitted well to Ellis model (Arora *et al.,* 2003); Lorenzo *et al.,* 2008), Cross model (Roberts *et al.,* 2001) and Sisko model (Lupi *et al.,* 2011).

2.3.2 Time-dependent behavior of food dispersions

Time-dependent characteristic of materials is related to internal structural destruction during flow and as such it is as a result of structural changes due to shearing. Time-dependent flow properties reflect the nature of a system's structure and can be as a result of viscoelasticity, structural changes, or both (Cheng and Evans, 1965). Time-dependent rheological behavior manifests as a progressive decrease in viscosity (break down of structure) when a material is sheared at a constant shear rate over a period of time and such structure may be recoverable when the system is left unperturbed (Tunan and Tiu, 1991). Such material is said to be thixotropic in nature. Time-dependent rheological behavior is therefore very important for understanding the products changes that occur during processing (Augusto *et. al.,* 2012). Reliable and accurate characterizations of time-dependent properties of foodstuffs are necessary for the quality control, product optimization, texture, shelf-life and for the design of processing equipment (Steffe,1996). Characterization of time-dependent rheological properties of food systems is also important in order to establish relationships between structure and flow and to correlate physical parameters with sensory attributes (Figoni and Shoemaker, 1983). Generally, two approaches always adopted to represent the thixotropy of a complex solution are the transient rheological approach and the hysteresis loop approach (Kooceki and Razavi, 2009). In hysteresis loop method, the shear rate is systematically increased and decreased between zero and a maximum value. A thixotropic material will describe a hysteresis loop when the transient data are plotted as shear stress (σ) versus shear rate (Υ) (Barnes, 1997) (Figure 2.8).

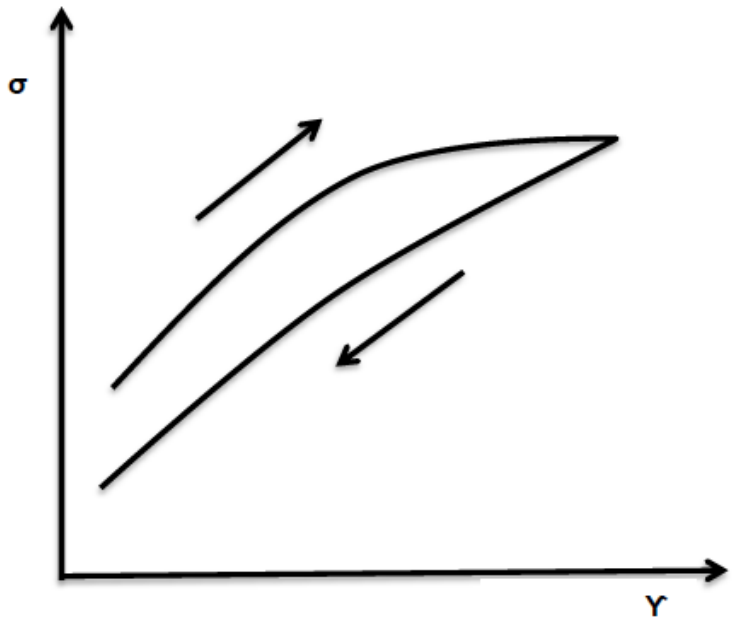

Figure 2.8 Shear stress versus shear rate data of a thixotropic material

Time-dependent rheological characteristics of semi-solid food materials have been described in the literature using the Figoni-Shoe maker model (Augusto *et al.,* 2012), Wetman model (1943), and Hahn-Ree-Eyring model (1959). Bellalta *et al.* (2012) also employed Structural kinetic (SK) model for studying time-dependent rheological behaviour of whey protein isolate-stabilized emulsions. SK model assumes that the changes in the time-dependent rheological behaviour are associated with shear induced breakdown of internal structure of non-food and food products. SK model as given by Bellalta *et al.* (2012) is expressed as in equation 2.6.

$$\frac{d\lambda}{dt} = -K(\lambda - \lambda_e)^n \qquad (2.6)$$

In the equation 2.4, K is the rate constant (s^{-1}) and a function of shear rate, λ_e is the structural parameter at the equilibrium state. The model is an n^{th} order kinetic equation that described the structural breakdown of material under shearing by means of a time dependent structural parameter.

2.3.3 Viscoelastic characterization of food dispersions

Viscoelasticity is a term used to mean the existence of the viscous and elastic properties and it provides information on the intermolecular and interparticle forces in materials. Linear viscoelasticity is the simplest viscoelastic behaviour in which the ratio of the stress to strain is a function of time alone and not of the strain or stress magnitude (Barbosa-Canovas *et al.,* 1996). Linear viscoelastic behaviour of a material can be obtained when the applied strain is sufficiently small enough not to affect the molecular structure of the material. Various types of tests exist which may be used to study viscoelastic material to determine the relationships between stress, strain, and time for a given type of deformation and a given type of loading pattern. Most popular among the tests include creep compliance and recovery test, stress relaxation test and oscillatory test. Some of the models for studying the viscoelastic behaviour of materials are the Maxwell and Kelvin-Voigt models, however due to the complex composition of food materials these models and their combination is valid only when the experimental data are obtained within the linear viscoelastic region (Barbosa-Canovas *et al.,* 1996).

2.4 Appraisal of the Use of Natural Polymers of Plant-Derivatives in Food Emulsions and Their Contribution to the Stability and Rheological Properties

For the sake of discussions, polymers of plant derivatives and of agricultural origins and their applications in food emulsions are grouped basically into three, viz, applications of protein isolates and hydrolase, native and modified starches, and hydrocolloids and whole legume flours. Their probable interactions with co emulsifiers or stabilizers were also discussed. The use of natural polymers of plant derivatives and agricultural origins are endless in the literature, however the following are considered relevant to this study.

2.4.1 Use of proteins and hydrolases and contribution to emulsion properties

Studies have explored the use of natural proteins and hydrolases of plant derivative as emulsifiers and findings on their ability to form emulsions and contribution to emulsion properties is largely dependent on the nature of the protein, aqueous and hydrophilic phase composition among others. For example, Wang *et al.* (2010b) investigated the effect of concentrated flaxseed protein (FPCCM) on the stability and rheological properties of soybean oil-in-water emulsion. Information regarding droplet size, zeta potential, creaming index and viscosity of the emulsions were determined. They reported that FPCCM and oil-phase volume concentration significantly affected zeta potential, creaming rate and emulsion viscosity. Increase in FPCCM resulted in a more negative droplet charge and a lower creaming rate while

increase of oil phase volume fraction increased both oil droplet size and emulsion viscosity while creaming index and creaming rate decreased. Papalamprou *et al.* (2006) investigated the stability of model salad dressing emulsion as affected by the type of the lupin seed protein isolate. Model salad dressing emulsions of an oil volume fraction of 0.50 were prepared using two types of lupin seed protein isolate (LSPI). The proteins differed in the method applied for their isolation and their protein composition. The result indicated that model salad dressing emulsions containing the isolate that were mainly composed of lupin globulins exhibited higher stability and more pronounced rheological characteristics compared to those prepared with the isolate enriched in albumins or with the mixture of the two isolates. Guo and Mu (2011) investigated and reported the effect of sweet potato protein (SPP) concentration on the properties of oil-in-water emulsion. Parameters such as emulsifying stability index (ESI), droplet size, rheological properties, and interfacial properties were reported. Result showed that increasing of protein concentration greatly decreased droplet size, emulsifying activity index (EAI) and apparent viscosity of SPP emulsions. The rheological curve suggested that SPP emulsions were shear-thinning non-Newtonian fluids.

2.4.2 Use of native and modified starches and contribution to emulsion properties

Influence of starches on the properties of food emulsion was found to depend predominantly on the nature of the starch and on the type of modifications used. Generally the performance of modified starches on the emulsion properties (particularly physical stability and rheological characteristics) was found to be better than natural starches. For instance, Moghaddam *et al.* (2013) investigated the effect of native and modified (hydroxypropylated di starch phosphate and acetylated di starch adipate) on physical and rheological properties of French dressing during storage. They identified that one of the problems with products such as salad dressing is related to reduction in viscosity during storage. Emulsion samples were formulated by adding 1.6 - 2.2% of each type of starch instead of xanthan and guar which were used as the usual thickeners in control. Emulsion stability and viscosity of the samples were the measured parameters of interest. Their results showed that emulsion stability and viscosity of samples, formulated with modified starch, were improved compared to native one and between two types of modified starches, acetylated di-starch adipate produced more stable and viscous product.

Ibrahim and Achunda (2011) investigated the physical properties and stability of emulsions as affected by the native and modified yam starches. Both the native and modified starches were used to supplement mayonnaise-like emulsion. Two modification procedures were used to modify native yam starches, viz, pre-gelatinization and cross linking

phosphorylation. Emulsions stabilized with pre-gelatinized starch recorded the highest viscosity and good stability. Emulsions with cross linked phosphorylation also had a significant low droplet size. The performance of the modified starch samples in mayonnaise-like emulsions was reported to be better when compared with native yam starch. Bortnowska *et al.* (2014) investigated the effects of pre-gelatinized waxy maize starch (WMS) concentration (0.0 - 5.0 wt%) on the physicochemical properties and stability of model low-fat (20.0 wt% rapeseed oil) oil-in-water emulsions, made with dried egg yolk or sodium caseinate (2.0 wt%). Herschel-Bulkley's model fitted well the behaviour of the emulsion and were reported to exhibit shear-thinning flow behaviour, yield stress, consistency coefficient (K), and flow behavior index (n) were highly affected ($p < 0.001$) by WMS addition. WMS concentration was reported to have a significant ($p < 0.001$) impact on the emulsions stability with respect to creaming and fat holding capacity. Izidoro *et al.* (2008) investigated the rheological properties of emulsions stabilized by green banana and was fitted by power law model. Response surface methodology was employed in their investigation and three emulsion components were tested namely banana pulp, soy oil and water. All the emulsions showed pseudoplatic characteristics and were perfectly described by power law rheological model. The rheological properties were reported to be influenced by the difference in green banana pulp proportions and also by the temperatures. The quadratic polynomial model of response surface was found appropriate to describe the intrinsic rheological properties as a function of main emulsion component. The consistency coefficient increasing with the interaction between the emulsion components and the flow behaviour index was a function of added water.

2.4.3 Use of hydrocolloids and legume flour and contribution to emulsion properties

Aqueous phase composition plays a more dominant role in determining the performance of hydrocolloids in food emulsion systems. Hydrocolloids in emulsion systems have been reported to thicken the aqueous phase. The type and nature of the primary emulsifier and hydrocolloids in an emulsion system determine the compatibilities between them and this can greatly affect the properties of food emulsion. Wang *et al.* (2011) investigated the effects of gum arabic (GA) (0 – 4%, w/w) on stability of oil-in-water emulsion stabilized by flaxseed protein concentrate (FPC) and soybean protein concentrate (SPC). They reported that emulsions stabilized by both proteins in the presence of the 2% gum Arabic (w/w) have better stability than its absence. This was achieved by increasing the emulsion viscosity of the FPC stabilized emulsion and causing competitive adsorption between the GA and SPC layer to give a steric repulsion for the SPC stabilized emulsion. Erçelebi and Ibanoflu (2009a) studied the effect of guar gum and pectin on

the rheological properties of whey protein isolate stabilized emulsion at pH of 7.0. Emulsions were prepared in the presence of 0.1 or 0.5% (w/v) pectin/guar gum. Their results showed that viscosity and also consistency index of emulsions increased with hydrocolloid concentration and the flow behaviour index of all emulsions containing 0.5% (w/v) guar gum was in the range of 0.9 – 1.0, which corresponds to near-Newtonian behaviour while emulsions containing 0.5% (w/w) guar gum were shear thinning in nature. Emulsions behaved like a liquid with viscous modulus (*G*") greater than elastic modulus (*G*') at lower frequencies; and like an elastic solid with *G*'' > *G*' at higher frequencies. Effect of guar gum was reported to be more pronounced on dynamic properties of studied emulsions. Vega *et al*. (2005) investigated the effect of k-carrageenan on dairy emulsions containing sodium caseinate and locust bean gum (LBG). It was found that sodium caseinate and LBG were incompatible and there were phase separations in the emulsions. K-carrageenan was not so effective at inhibiting the formation of the cream layer in sodium caseinate emulsions and this was attributable to k-carrageenan's self-association, rather than interaction with casein proteins.

Erçelebi and Ibanoğlu (2009b), investigated phase separation behavior of egg white-pectin/guar gum mixtures. Different polysaccharides concentrations (0% to 0.5% [w/v]) were studied and measured parameter of interest were emulsifying activity index (EAI), emulsifying stability index (ESI), creaming stability, microstructure, and rheological properties. They reported that the emulsion systems led to phase separation which arose by either depletion flocculation or thermodynamic incompatibility of the emulsifiers/stabilizers. However the addition of polysaccharides improved emulsion stability against creaming, increase in pectin and guar gum concentration from 0.01% to 0.5% significantly improved EAI by 51% and 25%, respectively. All emulsions with polysaccharides were pseudoplastic in nature. Polysaccharides, especially at high concentrations, affected the viscoelastic behavior of the emulsions. The storage (*G*') and loss modulus (*G*'') was reported to cross-over at lower frequency values as compared to that of emulsions containing no polysaccharide. Heyman *et al.* (2010) investigated the effects of non-starch hydrocolloids (NSH) on the physicochemical properties and stability of a béchamel sauce. The two non-starch hydrocolloids of interest were the guar-gum and carboxymethyl cellulose. The hydrocolloids were investigated at two concentrations of 0.10 wt% and 0.25 wt%. Sauce batches were stored at refrigerated temperatures for four weeks and were rheologically characterized at day 2, 16 and 30 after preparation. The addition of all hydrocolloids caused a marked increase of the consistency index compared to the model system whereas this parameter decreased for all sauces during refrigerated preservation.

Nor Hayati *et al.* (2009) investigated the droplet characteristics, flow properties and stability of egg yolk-stabilized oil-in-water (O/W) emulsions as affected by the presence of selected polysaccharides. Among the investigated hydrocolloids were, carboxymethyl cellulose (CMC), guar gum (GG), locust bean gum (LBG) and gum Arabic (AG). The same concentrations of each of the polysaccharides were investigated. The presence of CMC, GG and LBG significantly decreased the droplet mean diameters of the emulsion. LBG, GG and CMC emulsions exhibited a shear-thinning behavior but AG emulsion exhibited a Bingham plastic behavior while the emulsion without gum (control) almost exhibited a Newtonian behavior. Both emulsions containing AG and control exhibited a severe phase separation after 30 days of storage at 5^{o}C. Increases in droplet mean diameters and decreases in flow properties were found in stored GG and LBG emulsions and these were attributed to droplet coalescence. The results supported the ability of CMC, GG and LBG in reducing partial coalescence either by providing a sufficiently thick continuous phase or by acting as a protective coating for oil droplets. Lorenzo *et al.* (2008) investigated and modeled the effect of composition on the rheological properties and stability of low-in-fat o/w emulsions formulated using xanthan/guar gum mixture in an acidic aqueous solution containing 2% NaCl. Emulsions were shear thinning and viscoelastic in nature, however the viscoelastic behaviour was mainly governed by the hydrocolloid content and that all emulsions were stable after eight months.

The use of legume flour as supplements was reported by Ma and Boye (2013). In their study, the microstructure, physical stability and rheological properties of salad dressing emulsions supplemented with various pulse flour namely red lentil, green lentil, desi chickpea, kabuli and yellow pea were investigated. They reported that supplementation with pulse flour significantly increased the consistency coefficient and flow behaviour index of the control dressing during steady state flow test. The pulsed supplemented dressings were also reported to show increase in the recoverable strain when compared with the control samples. The physical stability of the emulsions with pulse flours was also greatly improved. In a related study, raw lentil flour and lentil flour and seeds subjected to different thermal processing treatments (i.e., ground roasted seeds; roasted flours; pre-cooked, ground and freeze-dried seeds; pre-cooked, ground and spray-dried seeds) were used to supplement salad dressing emulsions (Ma *et al.,* 2013). The effect of lentil on physical stability and rheological properties were evaluated among others. Addition of pulse flours had a thickening effect and had improved viscoelastic properties of the salad dressing emulsions. Dressings supplemented with pre-cooked, freeze and spray-dried lentil flours were reported to have the highest rheological

properties. There are however no work on the use of bambara groundnut flour as main emulsifying composition in food systems.

2.5 Chemical Composition and Functional Properties of Flour and Starch from Bambara Groundnut

Bambara groundnut (*Vigna subterranea*) (Figure 2.9) is an indegenous Africa legume grown by subsistence farmers primarily for its seeds (Ayamdoo, 2013; Brough *et al.,* 1993). The main producing areas of bambara groundnut (BGN) in South Africa are Limpopo, Mpumalanga and Kwazulu-Natal (Swanevelder, 1998). It is the third most important legume after groundnut (*Arachis hypogea*) and cowpea (*Vigna unguiculata*) (Vurayai *et al.,* 2011). It is a herbeceous, intermediate, annual plant with creeping stem at ground level. The pods usually develop underground and may reach up to 3.7 cm depending on the number of seeds they contain. Mature pods are indehiscent, often wrinkled, ranging from a yellowish to reddish dark brown colour. Seed colour also varies from white to cream, yellow, brown, purple, red or black. In most traditional farming systems, the crop is grown by women as an intercrop in association with one or more species. It is traditionally grown on poor soil and in hot climates, generally in regions where the cultivation of other legumes such as groundnut is too risky because of the threat of drought (Brough *et al.,* 1993).

Figure 2.9 Bambara groundnut

The immature seeds are normally eaten fresh, grilled or boiled while dried seeds are also sometimes roasted and ground into flour (Swanevelder, 1998). Seven varieties of bambara groundnut are black, cream/black eye, cream/brown eye, cream/no eye, red, specked/flecked and brown (Swanevelder, 1998).

On average, the seeds were found to contain 63% carbohydrate, 19% protein and 6.5% oil (Bamshaiye *et al.,* 2010). Sirivongpaisal (2007), prepared flour and isolated starch from BGN, and reported that the flour contained 11.51% moisture content, 7.90% fat, 15.48% protein, 4.19% ash, 2.54% fiber and 58.38% carbohydrate while the extracted starch contained 8.9% moisture, 0.44% fat, 0.61% protein, 0.47% ash, 0.60% fiber and 88.98% carbohydrate. Table 2.2 summarized the proximate composition of different varieties of bambara groundnut seeds, flour and seed coat as reported by Ojimelukwe and Ayernor (1992).

Table 2.2 Proximate compositions of different varieties of bambara groundnut seeds, flour and seed coat

Cultivars	Crude protein	Fat %	Moisture content	CHO soluble	CHO content	Ash content
Red	19.5	6.5	8.0	7.6	54.4	3.0
Black	21.7	8.5	9.0	4.0	52.8	3.5
Cream	19.5	6.0	9.7	6.5	56.0	2.5
Brown	19.0	6.5	10.3	12.0	54.4	3.0
	FLOUR					
Red	20.9	3.0	9.3	2.2	48.0	2.0
Black	22.6	4.0	9.0	1.4	32.0	2.0
Cream	22.3	3.0	9.0	1.6	49.6	1.5
Brown	19.4	3.5	10.0	2.9	48.0	2.0
	SEED COAT					
Red	5.7	0.5	3.0	2.6	8.4	1.0
Black	6.1	2.0	3.5	3.0	6.0	1.5
Cream	6.8	1.0	3.0	1.8	9.2	1.0
Brown	6.3	2.0	3.0	0.5	9.1	1.0

Source: Ojimelukwe and Ayernor, 1992.

Although there may not be conspicuous disparities in the proximate compositions of all the varieties as pointed out by Bamshaiye *et al.* (2011), the table however shows slight differences in composition. In another study conducted by Yusuf *et al.* (2007) to determine the functional properties of raw and roasted Nigerian beninseed and BGN, it was unveiled that oil absorbtion capacity (OAC) of BGN flour was high which could be due to high content of hydrophobic proteins. The foaming capacity (FC) of BGN flour was reported as 72% which was below the value obtained for benninseed flour. Bambara groundnut flour and beninseed however showed a high emulsion capacity of 83.0 and 78.5 g/oil protein respectively.

The difference in total protein composition (soluble and insoluble) as well as components other than protein (possibly carbohydrate and fat), may have substantial contribution to the emulsifying properties of protein-containing products like legumes flour. Furthermore, the factors affecting emulsification are related to the physicochemical characteristics of protein-surface hydrophobicity and charge, steric effects, elasticity-rigidity, viscosity in solution and the ability of the macromolecules to rearrange after adsorbing at the interface and form a continous film of high mechanical strength (Sikorski, 2002). The potential of BGN has been investigated for the vegetable milk production (Brough *et al.,* 1993).

CHAPTER THREE

RESEARCH DESIGN AND METHODOLOGY

3.1 Materials and Equipment

Dried Bambara groundnut (BGN) seeds of brown, brown eye, black eye and red varieties were purchased from Triotrade Gauteng CC, South Africa. The seeds were washed, and dried at 50^{o}C for 48 hrs by using cabinet drier (Model: 1069616). The dried seeds were milled into flour using a hammer mill and screened through 90 µm sieve to give bambara groundnut flour (BGNF). A commercial brand (Ritebrand) of 100% sunflower oil (SFO) purchased from a local supermarket was used without purification as the hydrophobic dispersed phase in this work. Milli-Q water was used in the preparation of all the emulsions. Food grade additives namely, sodium chloride (NaCl), vinegar and citric acid were purchased from a local store in Bellville, South Africa. Major equipment used in this study were Turbiscan MA 2000 (Formulaction, Toulouse), Rheolab MC 1 (Physica Inc., Stuttgard Germany), Discovery HR-1 rheometer (TA Instruments), Ultra Turrax homogenizer (IKA, Germany), and Ken-A-Vision microscope (TU-19542C Inc.USA). Figure 3.1 gives the summary of the work accomplished in this chapter.

3.2 Effect of Processing Variables on Emulsion Properties.

Oil-in-water emulsions containing sunflower oil at a concentration of 20% (w/w) were prepared. BGNF dispersion of brown variety at a fixed concentration of 8% (w/w) was gelatinized at a temperature of 84^{o}C for 10 minutes and used to stabilize the oil-droplets. Emulsification was performed using an Ultra Turrax T-25 homogenizer (IKA, Germany) at different homogenization speed (4000 – 12000 rpm) and homogenization time (3 - 12 min). The effect of the homogenization time was performed at a fixed homogenization speed of 10000 rpm in order to determine the optimum homogenization time. The effect of homogenization speed was thereafter carried out at the optimum homogenization time. Droplet size distribution was carried out using image analysis according to section 3.3.2. Apparent viscosity measurement was conducted using a shear rate controlled rheometer (Rheolab MC 1, Physica Inc., Stuttgard Germany). Emulsion viscosity was measured over a shear rate range of 40 – 750 s^{-1} without prior shearing at temperature of 20^{o}C. The test geometry was coaxial cylinder geometry conforming to Z3 DIN (bob radius: 12.5 mm: length 37 mm: cup radius: 13.5 mm). Processing variables (homogenization time and speed) that gave most desirable emulsion properties were selected and used for futher emulsification. All measurements were performed in duplicates.

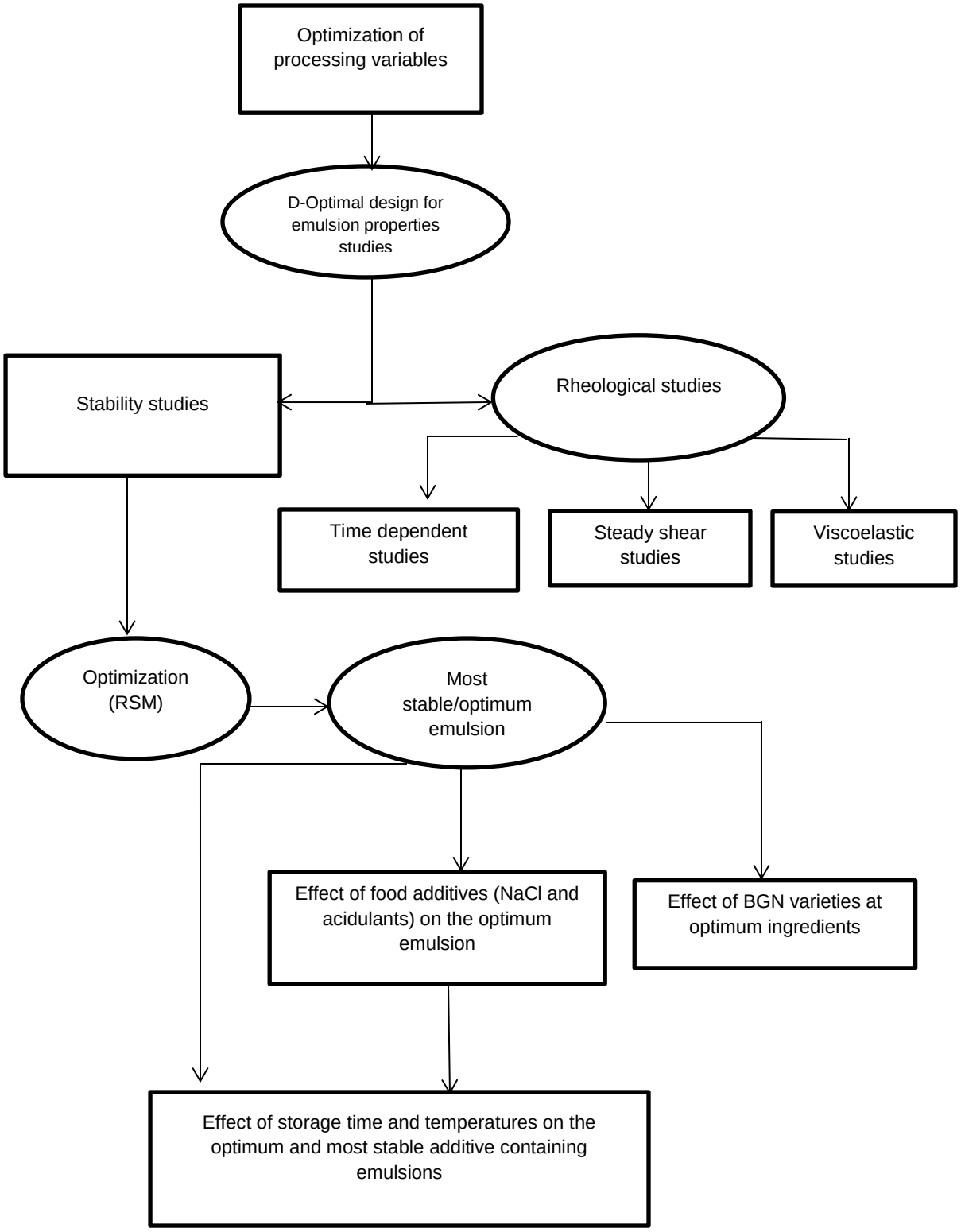

Figure 3.1 Chapter Overview

3.3 Optimization of Emulsion Components and Effects on Emulsion Physical Stability

Response surface methodology (RSM) D-optimal was used for this study. The independent variables (BGNF and SFO) and experimental design in the coded and uncoded forms are as shown in Table 3.1. Nine formulations of emulsions were made in duplicate. All emulsions were prepared according to section 3.3.1 without additives added to either the hydrophobic or the hydrophilic phase.

The emulsions were characterized by determining:

(i) Droplet size and distribution using image analysis by image J software according to section 3.3.2

(ii) Optical characterization of emulsion according to section 3.3.3

Empirical models were developed for droplet size and backscattering as a function of emulsion components (SFO and BGNF) according to section 3.6. Numerical optimization algorithm (Design-Expert 9) was used to estimate the optimal SFO and BGNF for a stable emulsion.

Table 3.1 Response surface D-optimal design for BGNF stabilized emulsion[1]

Independent variables				
	Coded levels		Uncoded levels	
Run	BGNF	Oil-phase	BGNF %(w/w)	Oil-phase %(w/w)
1	+1	+1	5	30
2	+1	0	5	35
3	+1	-1	5	40
4	0	+1	6	30
5	0	0	6	35
6	0	-1	6	40
7	-1	+1	7	30
8	-1	0	7	35
9	-1	-1	7	40

+1 refers to the minimum level; 0 is the center point; -1 is the maximum level; BGNF refers to bambara groundnut flour; SFO is the sunflower oil.

3.3.1 Emulsion preparation

Emulsions were prepared from a dispersed phase and a continuous phase. The dispersed phase consisted of SFO and continuous phase was gelatinized bambara groundnut flour (BGNF) dispersion. BGNF dispersions of specific concentrations were prepared according to Table 3.1 by dispersing measured amount of BGNF in known quantity of Milli-Q water. The resulting dispersions were gelatinized at a temperature of 84^{o}C for 10 minutes with constant stirring. The resulting gelatinized BGNF dispersions (GBGNFD) were weighted in order to ascertain the amount of water loss during gelatinization. Water loss during gelatinization was compensated for by adding Milli-Q water to the GBGNFD, stirred and allowed to cool down to 20^{o}C. Measured quantities of SFO according to Table 3.1 were added into the gelatinized BGNF to achieve different oil concentrations. Emulsions (100 g) were made by homogenizing SFO and gelatinized BGNF at 20^{o}C using an Ultra Turrax T-25 homogenizer (IKA, Germany) (Cerimedo et al., 2010) for 10 minutes at the speed of 11000 rpm (as determined from section 3.2). The Ultra Turrax T-25 homogenizer (IKA, Germany) is shown in Figure 3.2.

Figure 3.2 Ultra Turrax T-25 homogenizer (IKA, Germany)

3.3.2 Quantification of droplet sizes and distributions of emulsion by image analysis

Microstructure of the emulsions immediately after emulsion preparation was analyzed in terms of droplet size and droplet size distribution. Each emulsion was diluted with Milli Q-water at a ratio of 1:5 (w/w) in order to avoid overlapping and agglomeration of oil droplets which can affect further image analysis and processing. Droplet sizes were determined from the images of the oil-in-water emulsion obtained with a light microscope (Ken-A-vision). The Ken-A-vision microscope is connected to an output display unit as shown in Figure 3.3. Emulsion samples were poured onto microscope slides and covered with glass cover slips and visualized using X40 objective lens. The microscope focus and the light intensity were carefully controlled and optimized in order to obtain the sharpest possible boundaries between the oil-droplets and the surrounding GBGNFD. The images were captured with a digital camera mounted on the microscope. Image processing and further analysis was carried out using public domain software image J v1.36b (Caubet *et al.,* 2011; Perrechil and Cunha, 2010). The diameters of the oil droplets were measured one by one by an operator according to the method of Tcholakova (2004). A substantial number of droplets (N = 1000) were counted in order to obtain statistical estimate of the oil-droplet diameters and oil droplet size distribution in each sample. Droplet size distributions were generated by grouping the droplets into classes belonging to a common interval.

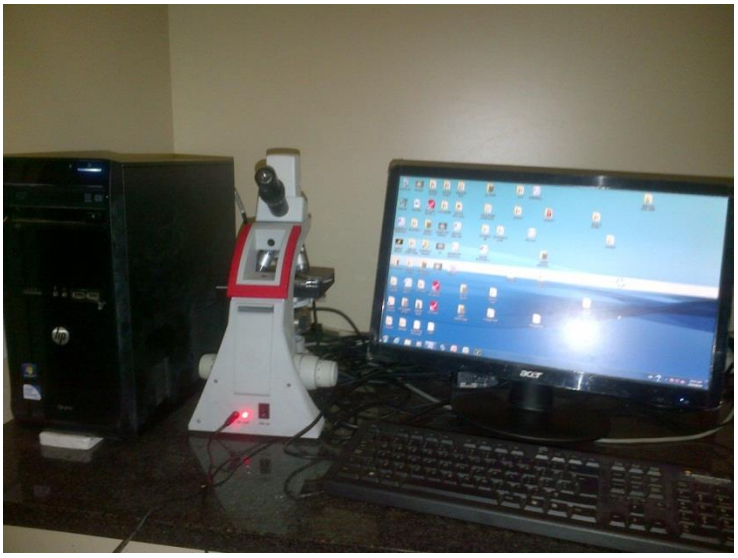

Figure 3.3 Ken-A-Vision microscope unit (TU-19542C Inc.USA)

Droplet size frequency distributions were computed using MS-Excel (Microsoft™ Excel 2007) (Bellalta *et al*., 2012). Oil-droplet sizes were obtained in terms of volume-surface mean diameter ($d_{3,2}$) and equivalent volume-mean diameter ($d_{4,3}$). The volume–surface mean diameter ($d_{3,2}$) and equivalent volume-mean diameter, $d_{4,3}$ were calculated using equation 3.1 and 3.2, respectively.

$$D_{3,2} = \frac{\sum n_i d_i^3}{\sum n_i d_i^2} \quad (3.1)$$

$$D_{4,3} = \frac{\sum n_i d_i^4}{\sum n_i d_i^3} \quad (3.2)$$

Where n_i is the number of droplets with diameter d_i (µm).

3.3.3 Optical characterization of emulsion stability

The stability of oil-in-water emulsions stabilized with (BGNF) was monitored using Turbiscan MA 2000 (Formulaction, France). The Turbiscan MA 2000 was connected to an output display unit as shown in Figure 3.4. BGNF stabilized emulsion (6 mL) were introduced in a cylindrical glass cell and inserted into Turbiscan MA 2000. The optical reading head of the machine scanned the whole length of the sample and acquired both the transmission and backscattered data every 40 µm and 30 minutes for 6 hr. The transmission and backscattering curves generated provided transmission and backscattered light flux in percentage (%) relative to the internal standard of the machine as a function of sample height. Both the transmission and backscattering fluxes were dependent on the particle mean diameter, d, and volume fraction ɸ of the particles according to the equations 3.3 and 3.4 & 3.5 and 3.6, respectively (Camino *et al,* 2011).

$$T = T_o e^{\frac{-2ri}{l^*}} \quad (3.3)$$

$$l = \frac{2d}{3\phi Q_s} \quad (3.4)$$

$$BS = \frac{1}{\sqrt{l^*}} \quad (3.5)$$

$$l = \frac{2d}{3\phi(1-gr)Q_s} \quad (3.6)$$

Where T, T_o, r_i, l^*, d, ϕ, BS are transmitted fluxes, transmittance of the continuous phase, measurement cell internal radius, photon mean free path, particle mean diameter, particle

volume fraction, backscattered flux respectively Q_s and gr are optical parameters given by Mie theory.

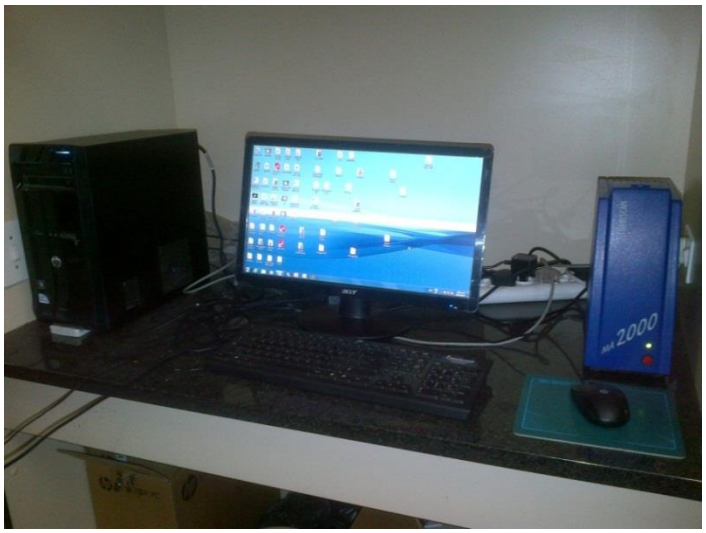

Figure 3.4 Turbiscan MA 2000 unit

The analysis of the emulsion stability was carried out as a variation of backscattering profiles over time because of the opaque nature of the emulsion nil transmission flux. The stability or instability of the dispersion was observed and evaluated by conducting repeated multiple scans overtime, each one providing a curve and all curves were overlaid on one graph to show stability or otherwise of the dispersion over time.

3.4 Optimum Emulsion and Preparation

The emulsion containing 7% BGNF and 40% SFO was selected to possess highest stability by maximizing the equilibrium backscattering value (BS_{eq} (%)). The continuous phase of optimum emulsion was hence prepared by dispersing 7 g of BGNF in 53 g of Milli-Q water. The dispersion was gelatinized at a temperature of 84^{o}C for 10 minutes with constant stirring. The gelatinized dispersion was allowed to cool down to 20^{o}C and the water loss during gelatinization was compensated for by adding Milli-Q water to the gelatinized dispersion. 40 g of SFO was added to the gelatinized dispersion and emulsion was made by homogenizing SFO and gelatinized dispersion using an Ultra Turrax T-25 homogenizer (IKA, Germany) (Cerimedo et al., 2010).

3.5 Rheological Measurement and Modeling of Emulsions

3.5.1 Time-dependent rheological measurement

Time-dependent rheological experiments of the emulsions prepared according to section 3.3.1, Table 3.1 were conducted. Rheological measurements were conducted using a shear rate controlled rheometer (Rheolab MC 1, Physica Inc., Stuttgard Germany). Rheolab MC 1 was connected to external display unit as shown in Figure 3.5. All the experiments were performed at 20^{o}C without previous shearing. Samples were carefully transferred into the rheometer cup and allowed to rest for about 10 minutes. Viscosity was measured as a function of increasing shear rate from 40 to 750 s^{-1} followed by a decreasing rate from 750 to 40 s^{-1}. In order to describe the time dependent flow behavior, experimental data (shear stress-shear rate) of forward and backward curves were fitted to Power law model (Eq. 3.12). The hysteresis loop area was calculated as the area between the upstream data and downstream data using equation 3.7 (Koocheki and Razavi, 2009 and Tarrega *et al.,* 2004).

$$\text{Hysteresis loop area} = \int_{\gamma_1}^{\gamma_2} \mathrm{K}\gamma^{\mathrm{n}} - \int_{\gamma_1}^{\gamma_2} \mathrm{K}'\gamma^{\mathrm{n}'} \qquad (3.7)$$

Where, K, K' are the consistency coefficient and n, n' are the flow behavior indices for upward and downward measurements, respectively. Each experiment was performed in duplicate.

Figure 3.5 Rheolab MC 1 measuring unit

In the second part of this work, the time-dependent rheological properties were investigated by shearing oil-in-water emulsion stabilized with BGNF samples at 20 minutes at constant shear rates of 50, 100 and 150 s^{-1}. Then the emulsion viscosity was measured as a function of shearing time. All measurements were done at a constant temperature of 20^{o}C. The data were modeled in order to describe the time-dependent flow properties of the BGNF-stabilized emulsions using standard rheological models such as (1) Weltman model (2) Hahn model (3) Figoni and Shoemaker model (4) First-order stress decay, with a zero equilibrium stress value. (Razavi and Karazhiyan, 2009)

1. Weltman Model

Weltman model is generally expressed as below

$$\tau = A + B\,In(t) \qquad (3.8)$$

Where, τ is the shear stress, t is the shearing time, and A and B are constants that characterize a material's time dependent behavior. Parameter A represents the initial shear stress and parameter B; the time coefficient of thixotropic breakdown is the product of rate in breakdown of thixotropic structure and time of agitation at constant rate of shear (Koocheki and Razavi, 2009).

2. Hahn model

Hahn model according to Singla *et al.* (2013) is expressed in equation 3.9.

$$\text{Log}\,(\tau - \tau_e) = P - \alpha t \qquad (3.9)$$

Where τ_e is the equilibrium stress value, *P* is the initial shear stress and α is the rate of structural breakdown for the sample

3. First-order stress decay with a non-zero equilibrium stress value (Figoni and Shoemaker model)

Figoni and Shoemaker model is generally expressed as in equation 3.10 (Singla *et al.,* 2013).

$$\tau = \tau_e + (\tau_0 - \tau_e)e^{-kt} \qquad (3.10)$$

Where, τ_e is the equilibrium shear stress value, τ_o is the initial shear stress and *k* is the kinetic constant of structural breakdown.

4. First-order stress decay, with a zero equilibrium stress value

First order stress decay with a zero-equilibrium stress value is expressed as in equation 3.11.

$$\tau = \tau_0 e^{-kt} \quad (3.11)$$

Where, τ_0 is the initial shear stress value, and k is the breakdown rate constant.

Parameters of Weltman model, Hahn model, Figoni and Shoemaker model and first order stress decay with zero equilibrium were obtained by using least square method described in section 3.7. In order to select the most appropriate model for the prediction of time-dependent flow behavior in oil-in-water emulsion stabilized with BGNF, coefficient of determination R^2 (equation 3.19); root mean square error (RMSE, equation 3.20) and standard error (SE, equation 3.21) were used. Model equations were developed for parameters of magnitude of hysteresis loop area as function of emulsion components according to section 3.6.

3.5.2 Steady shear rheological measurement

Steady state shear experiments of the emulsions were conducted according to Table 3.1. Steady shear rheological tests were made in a shear rate controlled rheometer (Rheolab MC 1, Physica Inc., Stuttgard Germany) (Figure 3.5). Samples (17 mL) were carefully transferred into rheometer cup and allowed to equilibrate for 10 minutes before shearing test proceeded. Emulsions were first sheared at constant shear rate of 100 s^{-1} for 1200 seconds in order to eliminate the structure responsible for time dependence. After the elimination of flow time dependence, emulsion viscosity was measured over a shear rate range of 40 – 750 s^{-1}. The test temperature was maintained at 20^{o}C and the test geometry was coaxial cylinder geometry conforming to Z3 DIN (bob radius: 12.5 mm: length 37 mm: cup radius: 13.5 mm). All measurements were performed in triplicates.

Experimental flow data were evaluated and fitted according to the rheological models of Power Law (equation 3.12), Herschel-Bulkley (equation 3.13), Bingham model (equation 3.14) and Casson model (equation 3.15).

$$\tau = K\gamma^n \quad (3.12)$$

$$\tau = \tau_o + K\gamma^n \quad (3.13)$$

$$\tau = \tau_o^B + K^B\gamma' \quad (3.14)$$

$$\tau^{0.5} = \tau_{oc}^{0.5} + K_{oc}\gamma^{0.5} \quad (3.15)$$

Where, τ is the shear stress, τ_o is the yield stress, γ is the shear rate, K is the consistency coefficients, K^B is the Bingham plastic viscosity, n is the flow behavior index, $\tau_{oc}^{0.5}$ is the Casson yield, $K_{oc,}$ is the Casson constant, τ_o^B is the Bingham yield stress and k' is the Bingham viscosity (Holdsworth, 1993; Keshani *et al.,* 2012). All rheological parameters were obtained using least square method and suitability of the models to describe the emulsions were judged using R^2 (equation 3.19), RMSE (equation 3.20) and SE (equation 3.21) as described in section 3.7. Empirical equations were developed for rheological parameters of Power law, Herschel-Bulkley, Bingham and Casson rheological models as function of emulsion components according to section 3.6.

3.5.3 Oscillatory experiment

Oscillatory experiment was conducted on emulsions prepared as described in section 3.3.1 and Table 3.1. Oscillatory experiment was conducted using Discovery HR-1 rheometer (TA Instruments) equipped with temperature control. The Discovery HR-1 rheometer unit is shown in Figure 3.6. During the experiments, the temperature was maintained constant at 20^{o}C. Serrated parallel plates of 1 mm gap were used for all the experiments. Emulsions were carefully loaded into the rheometer and allowed to rest for 10 minutes before rheological test proceeded. Amplitude experiment were conducted at constant frequency of 6.28 rad/s and the storage and loss moduli were recorded as a function of stress (0.01 – 100 Pa). In order to determine the linear viscoelastic region, the storage modulus was plotted against shear stress.

Figure 3.6 Discovery HR-1 rheometer

A shear stress of 0.1 Pa was afterwards selected for further frequency sweep experiment. Frequency sweep experiment was conducted at over a frequency range of 0.628 – 62.8 rad/s at a constant stress of 0.1 Pa which has been previously determined during amplitude test. The fingerprint of each emulsion sample in terms of storage and loss moduli was then plotted as a function of frequency. All experiments were duplicated.

Model equations were developed for visco-elastic parameters (G' and G") as a function of emulsion components according to section 3.6.

3.5.4 Creep and recovery experiment

Compliance and recovery properties of the emulsions prepared as described in section 3.3.1 and Table 3.1 were conducted. Creep and recovery studies were conducted in a controlled stress Discovery HR-1 rheometer (Figure 3.6). Initial pre-shear of 300 s^{-1} was used on the emulsions for 240 s and equilibration time of 120 s was allowed before a creep and recovery experiment. During the creep-compliance experiment, fresh emulsion samples were suddenly subjected to a constant shear stress of 0.5 Pa which has been previously determined to be in the linear visco-elastic region (LVR). The deformation of the sample was recorded as a function of time during a period of 500 s. The stress was suddenly removed and the recoverable stress was further monitored for another 500 s (Ma and Boye, 2013). The linear visco-elastic region of the emulsions was determined by an amplitude sweep experiment in the range of 0.01 to 100 Pa at a frequency of 1 Hz and constant temperature of 20^{o}C prior to creep and recovery experiment. All experiments were duplicated.

Model equations were developed for recoverable strain (Q (t)) as a function of emulsion components according to section 3.6.

3.6 Empirical Modeling and Response Surface Analysis

Stability and rheological data obtained from the D-Optimal experimental design in Table 3.1 were treated using the Response Surface Methodology (RSM) in order to establish the relationship between the measured parameters and main emulsion component (BGNF and SFO). All experiments as designed were performed in duplicates for this study. The variance for each parameter assessed was divided into linear, quadratic, and interactive components and was represented using a second-order polynomial model (equation 3.16):

$$Y = b + \sum b_i X_i + \sum b_{ii} X_i^2 + \sum b_{ij} X_i X_j \qquad (3.16)$$

Where Y is the estimated parameters response; equation coefficients were represented by b (constant term), b_i (linear effect), b_{ii} (quadratic effect) and b_{ij} (interaction effect). X_i and X_j are the emulsion components (BGNF and SFO). The statistical significance of each parameter was determined by analysis of variance (ANOVA) at 5% (Izidoro *et al.,* 2008). The surface graphical presentations of the response surface models were performed using Design Expert 9 software.

The quality of the fit of the polynomial model was judged by coefficient of determination R^2, R^2_{adj} as expressed below in equations 3.17 and 3.18 respectively.

$$R^2 = 1 - \frac{SS_{residual}}{SS_{model}+SS_{residual}} \quad (3.17)$$

$$R^2_{adj} = 1 - \frac{SS_{residual}/DF_{residual}}{SS_{model}+SS_{residual}/DF_{model} + DF_{residual}} \quad (3.18)$$

SS is the sum of squares and *DF* is the degrees of freedom

3.7 Data Analysis

Mean and standard deviation were calculated using IBM SPSS version 21 software. Curve fittings for steady shear and time dependent rheological models was performed using the solver function in Microsoft Excel adopting the generalized reduced gradient (GRG2) nonlinear optimization code to determine the rheological parameters. The best fit line with minimum sum of square errors (SSE) was used as the sole criterion during curve fitting. The goodness of fit, R^2 was calculated as

$$R^2 = 1 - \frac{SSE}{SST} \quad (3.19)$$

where SST is the total corrected sum of square (Walpole *et al.,* 2002; Chin *et al.,* 2009).

The best fit model was selected on the basis of high coefficient of determination R^2, low root mean square error (RMSE, equation 3.20) and standard error (SE, equation 3.21).

$$RMSE = \left[\frac{\sum(Y_m - Y_c)^2}{n}\right]^{1/2} \quad (3.20)$$

$$SE = \left[\frac{\sum(Y_m - Y_c)^2}{n-1}\right]^{1/2} \quad (3.21)$$

Where Y_m is the measured value, Y_c is the calculated value for each data point, and n is the number of observations (Nindo *et. al.* 2007; Keshani *et. al.* 2012).

3.8 Effect of Bambara Groundnut Varieties on Optimal Emulsion Stability and Rheological Properties

A comparative study was conducted to evaluate the effect of different varieties of BGN on emulsion stability and rheological properties. Optimum emulsion formulation in section 3.4 were prepared using four different flours from BGN namely brown, brown eyed, black eyed and red varieties. The following tests were conducted on each emulsion:

(a) Quantification of droplet size and distribution using image analysis as described in section 3.3.2
(b) Optical characterization of emulsion as detailed in section 3.3.3
(c) Rheological measurements as detailed in section 3.5. Time dependent rheological properties were described by hysteresis loop area method and Weltman model (equation 3.8). Power law (equation 3.12) was used for steady shear properties.

3.9 Effect of Food Additives on Optimal Emulsion Stability and Rheological Properties

The following food additives and concentrations were added to the Milli-Q water used for continuous phase preparations of the optimum emulsion described in section 3.4:

(a) Sodium chloride (25 – 300 mM)
(b) Vinegar (0.5 – 8% (w/w))
(c) Citric acid (0.5 - 6% (w/w))

Continuous phase was then made by dispersing 7 g BGNF in 53 g of additive containing Milli-Q water. The dispersions were gelatinized and the additive containing emulsions were prepared as described in section 3.4.

The following tests were done on the additive containing emulsions:

(a) Quantification of droplet size and distribution using image analysis as detailed in section 3.3.2
(b) Optical characterization of emulsion as detailed section 3.3.3
(c) Rheological measurements as described in section 3.5. Time dependent rheological properties were described by Weltman model. (Equation 3.8) and hysteresis loop area method (equation 3.7). Power law (equation 3.12) was used for steady shear rheological properties.

3.9.1 Composition and Preparation of Most Stable Additive Containing Emulsions

(A) Most stable sodium chloride (NaCl) containing emulsion

Optimal emulsion containing 25 mM NaCl was identified as the most stable NaCl containing emulsion. 1.46 g of NaCl was dissolved in 1L of Milli-Q water to make 25 mM NaCl solution. Continuous phase was prepared by dispersing 7 g BGNF in 53 g of 25 mM NaCl solution. The dispersion was gelatinized at a temperature of 84^{o}C for 10 minutes with constant stirring. The gelatinized dispersion was allowed to cool down to 20^{o}C and the water loss during gelatinization was compensated for by adding Milli-Q water to the gelatinized dispersion. 40 g of SFO was added to the gelatinized dispersion and emulsion was made by homogenizing SFO and gelatinized dispersion using an Ultra Turrax T-25 homogenizer (Figure 3.1). Emulsion was stored in a plastic bottle prior to analysis.

(B) Most stable vinegar containing emulsion

Optimal emulsion containing 8% (w/w) vinegar was identified as the most stable vinegar containing emulsion. 8 g of vinegar was weighed using a balance and added to 92 g of Milli-Q water in a 500 mL beaker to make 8% (w/w) vinegar solution. Continuous phase was prepared by dispersing 7 g BGNF in 53 g of 8% (w/w) vinegar solution. The dispersion was gelatinized at a temperature of 84^{o}C for 10 minutes with constant stirring. The gelatinized dispersion was allowed to cool down to 20^{o}C and the water loss during gelatinization was compensated for by adding Milli-Q water to the gelatinized dispersion. 40 g of SFO was added to the gelatinized dispersion and emulsion was made by homogenizing SFO and gelatinized dispersion using an Ultra Turrax T-25 homogenizer (Figure 3.1). Emulsion was stored in a plastic bottle prior to analysis.

(C) Most stable citric acid containing emulsion

Optimal emulsion containing 0.5% (w/w) citric acid was identified as the most stable citric acid containing emulsion. 0.5 g of citric acid was weighed using a balance and added to 99.5 g of Milli-Q water in a 500 mL beaker to make 0.5% (w/w) citric acid solution. Continuous phase was prepared by dispersing 7 g BGNF in 53 g of 0.5% (w/w) citric acid solution. The dispersion was gelatinized at a temperature of 84^{o}C for 10 minutes with constant stirring. The gelatinized dispersion was allowed to cool down to 20^{o}C and the water loss during gelatinization was compensated for by adding Milli-Q water to the gelatinized dispersion. 40 g of SFO was added to the gelatinized dispersion and emulsion was made by homogenizing SFO and gelatinized

dispersion using an Ultra Turrax T-25 homogenizer (Figure 3.2). Emulsion was stored in a plastic bottle prior to analysis.

3.10 Effect of Storage Time and Temperature on Emulsion Stability and Rheological Properties of Optimum and Most Stable Additive Containing Emulsions

Behaviors of the under listed emulsions were studied under storage at low, room and high temperatures of 5, 20 and 45^{o}C respectively for twenty days.

(a) Optimum emulsion in section 3.4.
(b) Most stable sodium chloride containing emulsion in section 3.9.1 (A).
(c) Most stable vinegar containing emulsion in section 3.9.1 (B).
(d) Most stable citric acid containing emulsion in section 3.9.1 (C).

All measurements were done at 20^{o}C. Emulsions were put in covered plastic containers and stored at 5, 20 and 45^{o}C. All emulsions stored at 5 and 45^{o}C were removed from refrigerator and incubator respectively 2 hr before measurements to attain the room temperature of 20^{o}C according to the method of Goncalves and Maia Campos (2009). The following tests were conducted on each emulsion on the first, 3rd, 9th, 15th and 20th day of storage

(i) Optical characterization of emulsion as described in section 3.3.3

(ii) Rheological measurement as described in section 3.5. Time dependent and steady shear properties were assessed by using hysteresis loop method (equation 3.7) and Power law rheological model (equation 3.12).

CHAPTER FOUR

RESULTS AND DISCUSSION

4.1 Effect of Processing Variables on Droplet Size and Apparent Viscosity

Optimum conditions necessary for the processing of emulsions stabilized with BGNF was investigated. BGNF of brown variety was used for this investigation. Parameters such as droplet size and apparent viscosities were used to assess some important processing conditions such as homogenization time and speed. This section therefore reported the results of the effect of homogenization time and speed on droplet size and apparent viscosity of BGNF-stabilized emulsion.

4.1.1 Effect of homogenization time on droplet size distribution of BGNF stabilized emulsion

Effect of homogenization time on droplet size was investigated at an arbitrary speed of 10000 rpm. Figure 4.1 shows the effect of homogenization time (4 - 12 minutes) on the droplet size distribution of emulsion formulated with 8% (w/w) bambara groundnut flour (BGNF) and 20% (w/w) sunflower oil (SFO). Homogenization time affected the droplet size distribution of the emulsion.

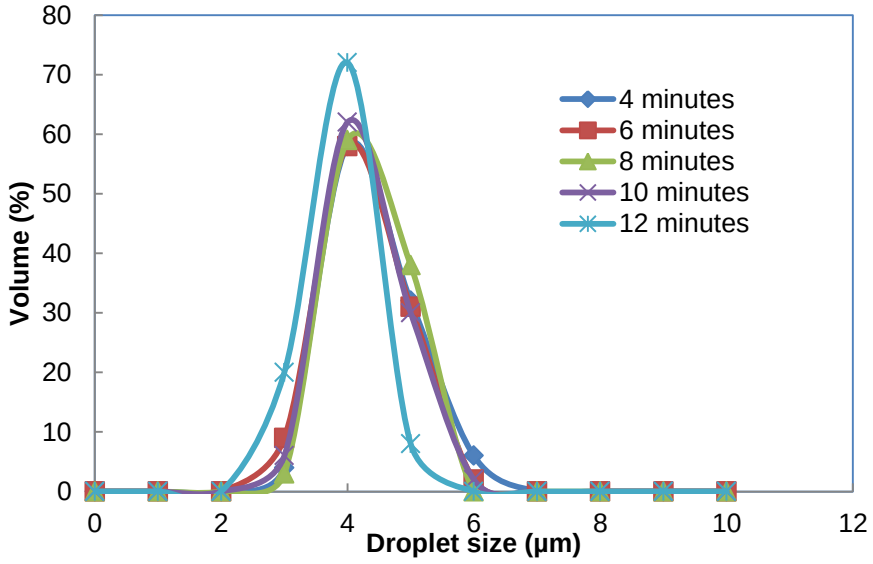

Figure 4.1 **Effect of homogenization time on particle size distribution of emulsion formulated with 8% (w/w) BGNF and 20% (w/w) SFO**

Emulsion homogenized for 4, 6, 8 and 10 minutes at 10000 rpm showed a slight difference regarding the width and height of the distribution which signifies high similarities in the droplet distribution. The droplet size distribution of emulsion homogenized for 12 minutes however showed a clear difference from the rest of homogenization time. The distribution was narrower and was shifted to the left side when compared with the other selected homogenization time. The effect of homogenization time on the oil droplet size is detailed in Table 4.1. Oil droplet size of the emulsions are expressed in terms of volume surface mean diameter $d_{3,2}$ and equivalent volume-mean diameter, $d_{4,3}$. The $d_{3,2}$ and $d_{4,3}$ ranged from 3.55 - 4.01 and 3.62 - 4.09 µm respectively. The droplet sizes of the emulsions at 12 minutes homogenization were significantly ($p < 0.05$) lower compared to those at 4, 6, 8, 10 minutes.

Table 4.1 Effect of homogenization time on droplet size[1,2]

Homogenization time (minutes)	$d_{3,2}$ (µm)	$d_{4,3}$ (µm)
4	4.01 ± 0.17^{b}	4.09 ± 0.10^{c}
6	3.92 ± 0.03^{b}	4.02 ± 0.04^{bc}
8	3.96 ± 0.01^{b}	4.01 ± 0.04^{b}
10	3.86 ± 0.07^{b}	3.92 ± 0.09^{b}
12	3.55 ± 0.10^{a}	3.62 ± 0.06^{a}

[1]Values are means ± standard deviations; Mean with different letters within the same column are significantly different from each other ($p < 0.05$).
[2] $d_{3,2}$ refers to the volume surface mean diameter of the emulsions; $d_{4,3}$ is the equivalent volume-mean diameter of the emulsions.

This could be as a result of high interaction time which enhanced breaking up of big oil droplet there by resulting into finer droplets.

4.1.2 Effect of homogenization time on the apparent viscosity of BGNF stabilized emulsion

Figure 4.2A and B show the effect of homogenization time on the apparent viscosity of the emulsion. There was notable decrease in apparent viscosity with increase in shear rate at all the homogenization time. Although homogenization time did not affect the overall behaviour of the emulsion, there was observable influence on the relative position of the apparent viscosity curves. The apparent viscosity curves tended to move higher as the homogenization time increases for a given shear rate. As the homogenization time increased the particles were

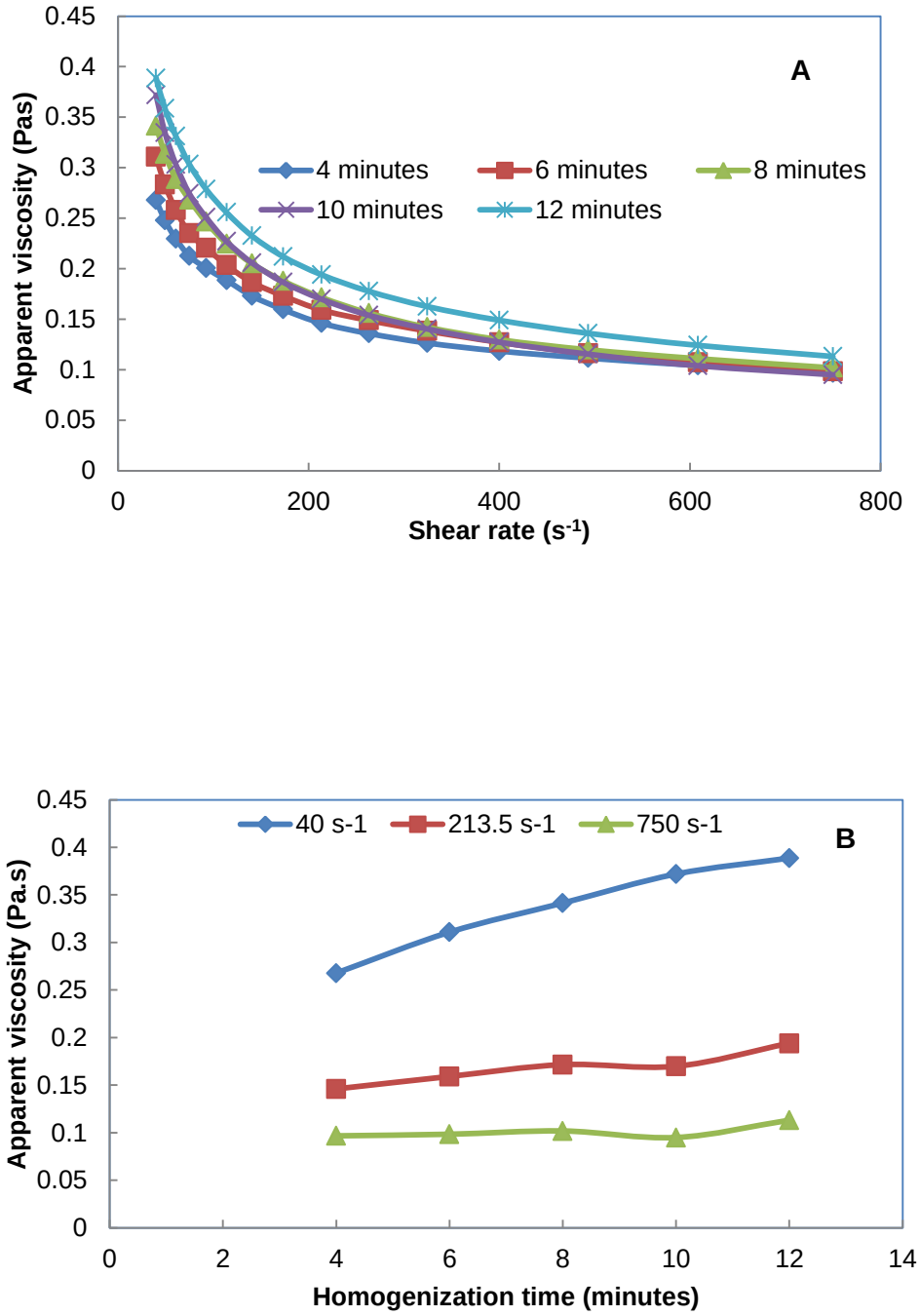

Figure 4.2 **Effect of homogenization time on the apparent viscosity (A) shear rate of 40 – 750 s^{-1} (B) selected shear rates**

reduced in size and increased in number. The interaction between the high numbers of oil droplets must have resulted into a much more flocculated emulsion system and this has increased the apparent viscosity of the emulsion. The apparent viscosities of the emulsions at selected shear rates are presented in Table 4.2. The apparent viscosity at 40, 213.5 and 750 s^{-1} ranged from 0.27 - 0.39, 0.15 - 0.19 and 0.1 - 0.11 Pas respectively. Homogenization time had effect on the apparent viscosities of the emulsions at lower shear rates. Apparent viscosity of the emulsion tended to increase significantly ($p < 0.05$) at the shear rate of 40 and 213.5 s^{-1} while there was no significant difference in the apparent viscosity of emulsions homogenized for 4, 6, 8 and 10 minutes at shear rate of 750 s^{-1} ($p > 0.05$).

Table 4.2 Effect of homogenization time on apparent viscosity at selected shear rates[1]

Homogenization time	Apparent viscosity (Pas)		
(min)	40 s^{-1} (Pas)	213.5 s^{-1}	750 s^{-1}
4	0.27 ± 0.01^{a}	0.15 ± 0.00^{a}	0.10 ± 0.01^{a}
6	0.31 ± 0.01^{b}	0.16 ± 0.00^{b}	0.10 ± 0.01^{a}
8	0.34 ± 0.00^{c}	0.17 ± 0.00^{c}	0.10 ± 0.01^{a}
10	0.37 ± 0.00^{d}	0.17 ± 0.00^{c}	0.10 ± 0.01^{a}
12	0.39 ± 0.00^{e}	0.19 ± 0.00^{d}	0.11 ± 0.01^{a}

[1]Values are means ± standard deviations; mean with different letters within the same column are significantly different from each other ($p < 0.05$).

The increase in the apparent viscosity with homogrnization time was as a result of increased number of the oil-droplets and their interactions. The highest apparent viscosity ($p < 0.05$) at the three selected shear rates belonged to emulsion homogrnized for 12 minutes. Although 12 minutes of homogrnization gave a narrower oil-droplet distribution, minimum droplet sizes, highest apparent viscosity at all the selected shear rates when compared with other homogenization time, it however generated a lot of heat energy. Homogenization time of 10 minutes did however generate moderate heat energy but produced comparable viscosity at higher shear rate with homogenization time of 12 minutes. Homogenization time of 10 minutes was therefore selected instead for further emusification and investigation.

4.1.3 Effect of homogenization speed on droplet size distribution of BGNF stabilized emulsion

The effect of homogenization speed on emulsion parameters were conducted at 10 minutes homogenization. Figure 4.3 shows the influence of homogenization speed on the oil-droplet

distribution curves. Similar to what was observed earlier on the influence of homogenization time, homogenization speed had dissimilar effects on particle size distribution. While emulsions processed at 4000, 6000, 8000 and 10000 rpm showed broad widths, droplet distribution of emulsion processed at 12000 appeared narrower.

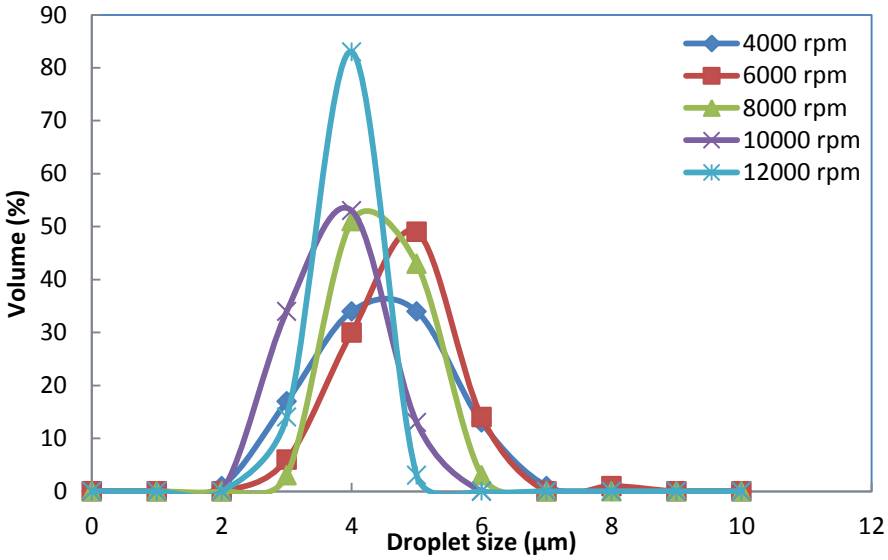

Figure 4.3 **Effect of homogenization speed on particle size distribution of emulsion formulated with 8% (w/w) BGNF and 20% (w/w) SFO**

Table 4.3 details the observed particle sizes in terms of $d_{3,2}$ and $d_{4,3}$. The $d_{3,2}$ was in the range of 3.41 - 4.47 µm and $d_{4,3}$ was between and 3.44 and 4.58 µm. Droplet particle sizes were observed to decrease significantly ($p < 0.05$) with increased homogenization speed. The lowest value of $d_{3,2}$ and $d_{4,3}$ belonged to emulsion homogenized at 12000 rpm. This could be as a result of increased energy input (homogenization intensity) into the system and this promoted the breaking up of big oil droplet to produce finer droplets. The droplet breakup in the homogenizing device has been explained as a result of equilibrium between the destructive forces and viscous forces and that the effect of the homogenizing pressure is dependent on the operating conditions and physical properties of the material (Floury *et al.,* 2000).

Table 4.3 Effect of homogenization speed on the particle size[1,2]

Homogenization (rpm)	$d_{3,2}$ (μm)	$d_{4,3}$ (μm)
4000	4.47 ± 0.06[c]	4.58 ± 0.01[c]
6000	4.35 ± 0.08[c]	4.55 ± 0.04[c]
8000	4.07 ± 0.11[b]	4.15 ± 0.18[b]
10000	3.45 ± 0.04[a]	3.54 ± 0.04[a]
12000	3.41 ± 0.01[a]	3.44 ± 0.01[a]

[1]Values are means ± standard deviations; mean with different letters within the same column are significantly different from each other ($p < 0.05$).
[2]$d_{3,2}$ refers to the volume surface mean diameter of the emulsions; $d_{4,3}$ is the equivalent volume-mean diameter of the emulsions.

4.1.4 Effect of homogenization speed on the apparent viscosity

Figure 4.4A and B show the effect of homogenization speed on the apparent viscosity of emulsion formulated with 8% (w/w) BGNF and 20% (w/w) SFO. Similar to the effect of homogenization time, homogenization speed did not change the behaviour of the emulsion and the emulsion remained shear thinning. There was an observed decrease in emulsion viscosity with increased shear rate for all homogenization speeds. The influence of homogenization speed on apparent viscosity of emulsions was observable on the flow curves. The flow curves tended to move higher as the homogenization speed increased (Figure 4.4B). Emulsion processed at 12000 rpm recorded highest viscosities at all shear rates investigated. Figure 4.4 B showed an increase in emulsion viscosities at three selected shear rates. The influence of homogenization speed on the viscosity of emulsions at three shear rate was summarized in Table 4.4. The apparent viscosity at 40, 213.5 and 750 s^{-1} ranged between 0.25 - 0.47, 0.15 - 0.19 and 0.09 - 0.12 Pas, respectively. The apparent viscosity at the three selected shear rate was observed to increase significantly ($p < 0.05$) as the homogenization speed increased. This can be explained in terms of increased number of oil droplet as homogenization speed is increased. The increased number had resulted in increased interactions among oil-droplets and between oil droplets and BGNF matrix (Franco *et al.,* 1998) which resulted to increased apparent viscosity. Emulsion treated at 12000 rpm had the highest apparent viscosity at all the selected shear rates. Homogenization speed of 12000 rpm was however rejected because foams were being generated at this homogenization speed. Hence, subsequent work used homogenization speed of 11000 rpm.

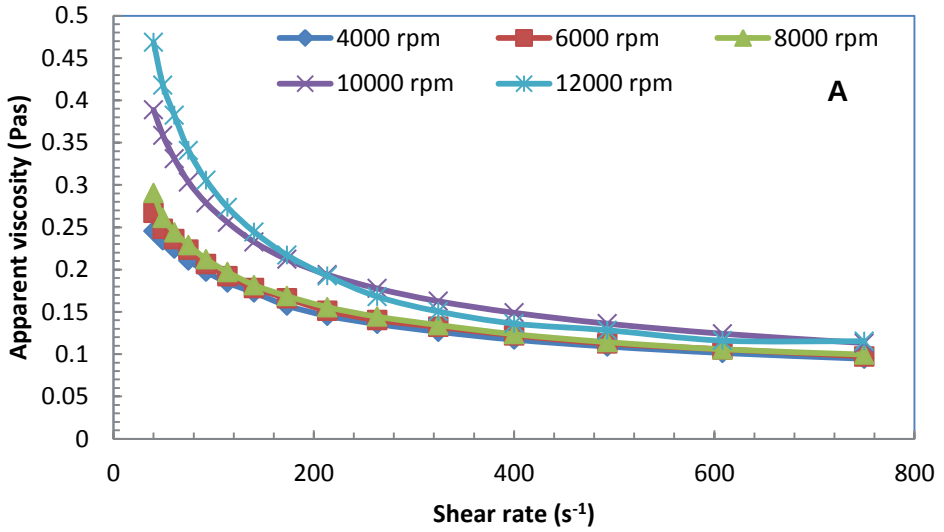

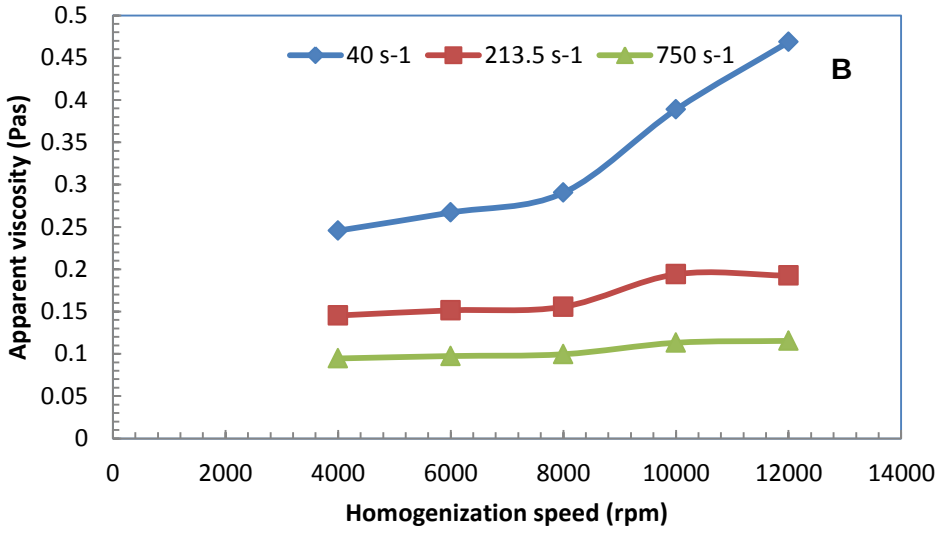

Figure 4.4 **Effect of homogenization speed on the apparent viscosity (A) shear rate of 40 – 750 s^{-1} (B) selected shear rates**

Table 4.4 Effect of Homogenization speed on apparent viscosity at selected shear rates[1]

Homogenization speed (rpm)	Apparent viscosity at 40 s^{-1} (Pas)	Apparent viscosity at 213.5 s^{-1} (Pas)	Apparent viscosity at 750 s-1 (Pas)
4000	0.25 ± 0.02^{a}	0.15 ± 0.00^{a}	0.09 ± 0.00^{a}
6000	0.27 ± 0.00^{ab}	0.15 ± 0.00^{a}	0.10 ± 0.00^{b}
8000	0.29 ± 0.02^{c}	0.16 ± 0.00^{a}	0.10 ± 0.00^{b}
10000	0.39 ± 0.01^{d}	0.19 ± 0.01^{b}	0.11 ± 0.00^{c}
12000	0.47 ± 0.02^{e}	0.19 ± 0.01^{b}	0.12 ± 0.00^{d}

[1]Values are means ± standard deviations; mean with different letters within the same column are significantly different from each other ($p < 0.05$).

4.1.5 Summary on the effect of processing conditions on emulsion properties

Processing variables were found to have profound effect on the oil droplet distribution, droplet size and the apparent viscosities of BGNF stabilized emulsions. Increased speed and time of homogenization were found to decrease or increase the droplet size and apparent viscosity (particularly at low shear rate) of the emulsions respectively. Similar observation was reported by Franco *et al.* (1998) for lupin protein-stabilized emulsions and Floury *et al.* (2000) for whey protein stabilized emulsions. Although the homogenization time of 12 minutes and speed of 12000 rpm gave the minimum droplet size and highest emulsion viscosity, high temperature and foaming characterized the operation at these conditions, emulsification time and speed of 10 minutes and 11000 rpm respectively were therefore selected because of the moderate heat energy and minimal foaming at these conditions for further work.

4.2 Emulsion Stability and Component Optimization of Oil-in-water Emulsion

The results of the effect of BGNF and SFO concentrations on emulsion stability parameters such as droplet size, microstructure and storage stability were reported. The parameters were afterwards described as function of emulsion components using linear and quadratic models. The prevalent mechanism of emulsion destabilization was as well identified. Optimization of emulsion components (BGNF and SFO) that resulted into highest emulsion stability was also reported.

4.2.1 Effect of BGNF and SFO on droplet size distribution

Figure 4.5 shows the oil droplet size distribution of all the studied emulsions. Figure 4.5A, B and C are the oil droplet size distribution of freshly prepared emulsions containing 30, 35 and

40% SFO, stabilized with 5, 6 and 7% (w/w) gelatinized bambara groundnut flour (BGNF) dispersions respectively. None of the distribution showed a perfect Gaussian shape and all tended to have a shoulder which is an indication of second population and therefore are poly dispersed in nature. The mean droplet size of the emulsion is as detailed in Table 4.5. The $d_{3,2}$ is the volume-surface mean diameter or the Sauter-diameter of the emulsions and it provides information regarding the mean diameter where most of the particles fall (Gu *et al.,* 2005; Camino and Pilosof, 2011). The $d_{3,2}$ is as well important when the study of a catalyst or the amount of surfactants are of interest (Ibrahim and Achundan, 2011). The $d_{4,3}$ on the other hand is the equivalent volume-mean diameter or De Broucker diameter. It is important when total amount of oil in the dispersed phase is significant. The $d_{4,3}$ is related to changes in particle size involving destabilization process and hence is more sensitive to existence of large particles and fat droplet aggregation (Camino and Pilosof, 2011). Thus $d_{4,3}$ is more sensitive to the phenomenon of droplet flocculation (Ibrahim and Achundan, 2011). The oil-droplet size distribution shows that both the BGNF and SFO concentrations clearly affected the oil-droplet size. The volume-surface mean diameter, $d_{3,2}$ of BGNF emulsions was in the range of 2.80 - 5.35 µm while the $d_{4,3}$ in the range of 2.89 - 5.92 µm. The emulsions stabilized with 5% (w/w) BGNF recorded the highest oil-droplet size diameters ($d_{3,2}$ and $d_{4,3}$) while emulsions stabilized with 7% (w/w) recorded the least.

The emperical model developed for $d_{3,2}$ and $d_{4,3}$ as a function of BGNF and SFO, as well as the analysis of variance (ANOVA) and coefficients of regression are as presented in Table 4.6. The response surface graphs are also presented in Figure 4.6. The quadratic polynomial was significant ($p < 0.0001$) and with high values of R^2, making it suitable for predicting the droplet size as a function of of emulsion components. The linear terms of SFO and BGNF and quadratic term of BGNF were the only significant model terms ($p < 0.005$) for the $d_{3,2.}$ The interaction between BGNF and SFO and the quadratic effect of SFO did not have significant effect on $d_{3,2}$. The linear terms of BGNF and SFO were negative while the quadratic effect of BGNF was positive on droplet size ($d_{3,2}$). Regarding $d_{4,3}$, all model terms were significant ($p < 0.05$) except the interaction term of SFO and BGNF. The effect of the linear terms of BGNF and SFO and their quadratic terms were negative and positive, respectively. The interaction between BGNF and SFO did not have a significant effect on both $d_{3,2}$ and $d_{4,3}$. (Figure 4.6). As expected, there was an increase in oil droplet size with an increase in dispersed phase (SFO) concentration for all BGNF concentration studied (Figure 4.6). Similar trend were reported by Wang *et. al.* (2010a) for soybean oil-in water emulsions. However, the increase in $d_{3,2}$ was moderate, for example $d_{3,2}$ for emulsions containing 30% (w/w), 35% (w/w) and 40% (w/w)

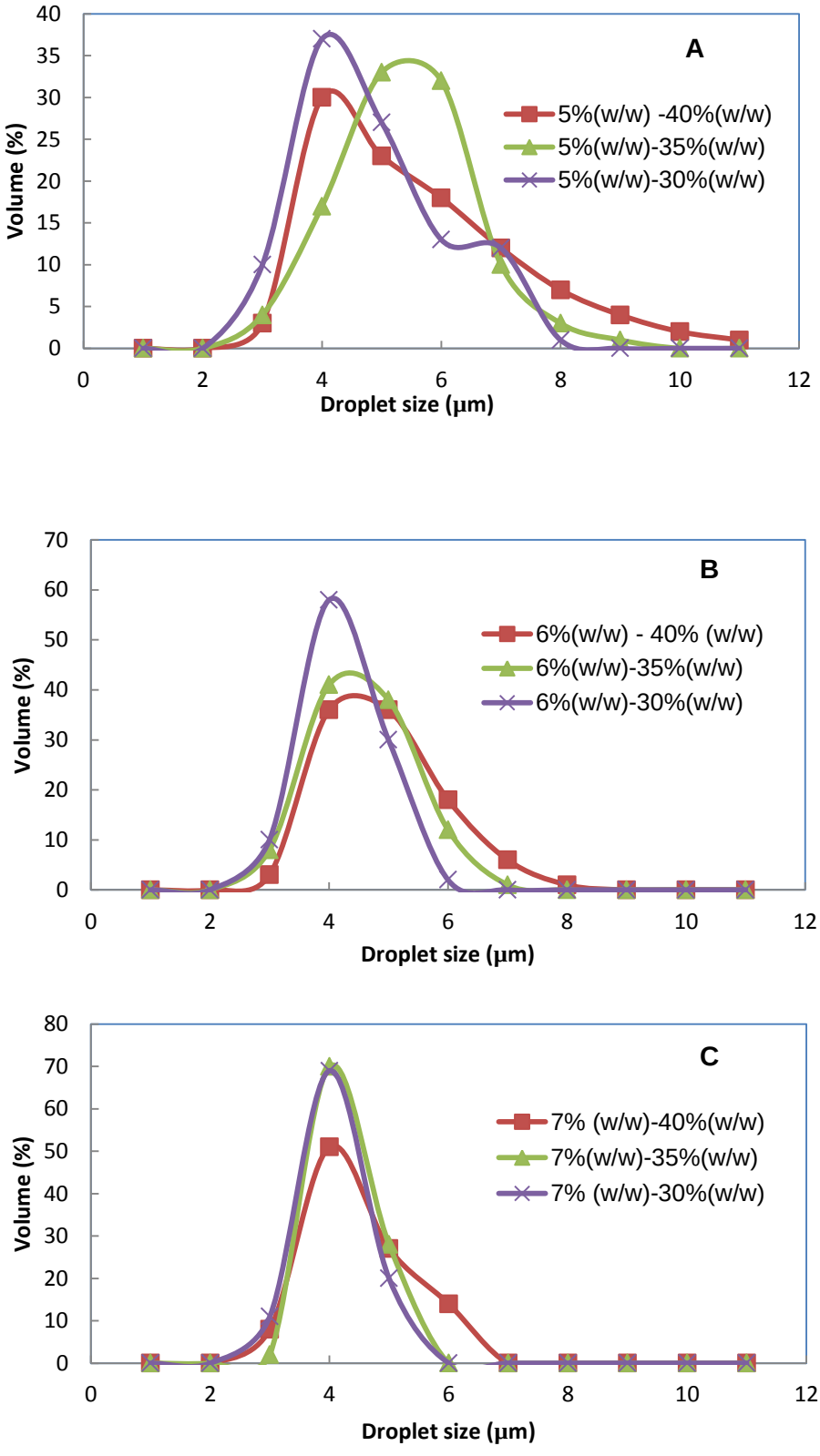

Figure 4.5 **Droplet size distribution of dispersed phase particles in emulsion stabilized with BGNF (A) 5% (w/w) (B) 6% (w/w) (C) 7% (w/w)**

Table 4.5 Average diameters (µm) De-Sauter ($d_{3,2}$) and De Brouker ($d_{4,3}$) of the BGNF stabilized emulsion[1]

Emulsion BGNF (%w/w)	SFO (%w/w)	$d_{3,2}$ (µm)	$d_{4,3}$ (µm)
5	30	4.05	4.36
	35	4.53	4.77
	40	5.35	5.92
6	30	3.07	3.19
	35	3.45	3.61
	40	3.90	4.16
7	30	2.80	2.89
	35	2.91	3.00
	40	3.45	3.66

[1]BGNF equals bambara groundnut flour; SFO is the sunflower oil

stabilized with 5% (w/w) BGNF were 4.05 µm, 4.53 µm and 5.35 µm respectively. The effect of BGNF concentration on oil-droplet size was also significant ($p < 0.05$). With an increase in the BGNF concentration, the $d_{3,2}$ decreased. For example, the $d_{3,2}$ of the emulsions containing 40% (w/w) SFO, stabilized with 5% (w/w), 6% (w/w) and 7% (w/w) are 5.35 µm, 3.90 µm and 3.45 µm, respectively.

The decrease in the particle size with the addition of polymer has been explained to be due to an increase in viscosity of the continuous phase of the emulsion. For a given speed of the homogenizer, the shear stresses are higher when the viscosity of the continuous phase of the emulsion is high and hence finer droplets are produced in the mixer (Pal, 1996; Payet and Terentjev, 2008). The De Broucker diameter, $d_{4,3}$ which is related to destabilization processes was found to increase with an increase in sunflower oil concentration and decreased with an

increase in BGNF concentration. The behavior of colloidal systems in terms of creaming and coalescence has been explained to be dependent on the population of higher droplet sizes in the system. The higher the droplet sizes in an emulsion system, the greater the tendency to coalesce is high because the impact forces and their magnitudes are higher during collision (McClements, 1999; Camino and Pilosof, 2011).

Table 4.6 Analysis of variance (ANOVA) for the quadratic model of oil-droplet size[1]

		$d_{3,2}$ (μm)				$d_{4,3}$ (μm)		
Source	DF	Coefficient	Sum of square	F-ratio p-value	DF	Coefficient	Sum of square	F-ratio p-value
Model	5	+18.55	11.04	<0.0001	5	+24.527	15.05	<0.0001
Linear								
b_1	1	-0.1137	2.58	<0.0001	1	-0.3157	3.63	<0.0001
b_2	1	-4.1392	7.62	<0.0001	1	-4.8942	10.08	<0.0001
Quadratic								
b_{11}	1	+5.73E3	0.082	0.0634	1	+9.46E3	0.22	0.0146
b_{22}	1	+0.3733	0.56	0.0002	1	+0.4467	0.80	0.0002
Interaction								
b_{12}	1	-0.0325	0.21	0.0066	1	-0.0395	0.31	0.0056
Residual	12		0.24		12		0.33	
Pure error	9		0.20		9		0.24	
Lack of fit	3		0.040	0.6287	3		0.0090	0.3888
Total	17		11.28		17		15.38	
R^2		0.9791				0.9785		
Adj-R^2		0.9704				0.9695		
CV		0.9496				4.20		
Adequate precision		31.143				30.605		

[1]b_1 and b_2 equal the coefficient of the linear term of bambara groundnut flour and sunflower oil; b_{11} and b_{22} are the coefficients of the quadratic terms of the bambara groundnut flour and sunflower oil; b_{12} equals the coefficients of interaction between the bambara groundnut flour and sunflower oil; DF equals degree of freedom; R^2 is the coefficient of determination; Adj R^2 equals the adjusted coefficient of determination; CV is the coefficient of variation.

The variation of oil-droplet size as a function of BGNF and SFO is therefore in line with earlier hypothesis that emulsion components will have significant effect on the properties of BGNF stabilized oil-in-water emulsion. The significance dependence of oil-droplet sizes on the emulsion components (BGNF and SFO) may therefore have notable differences on their respective microstructure and eventual emulsion stability.

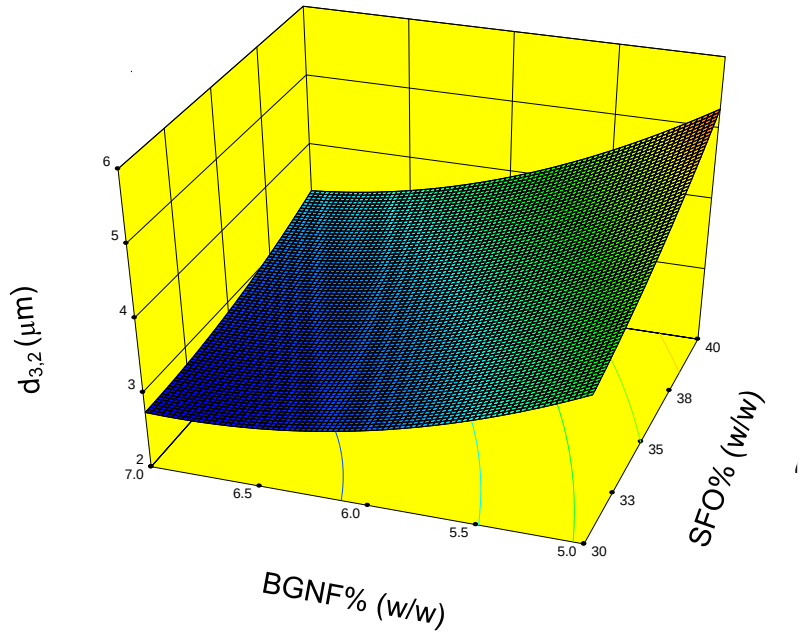

A

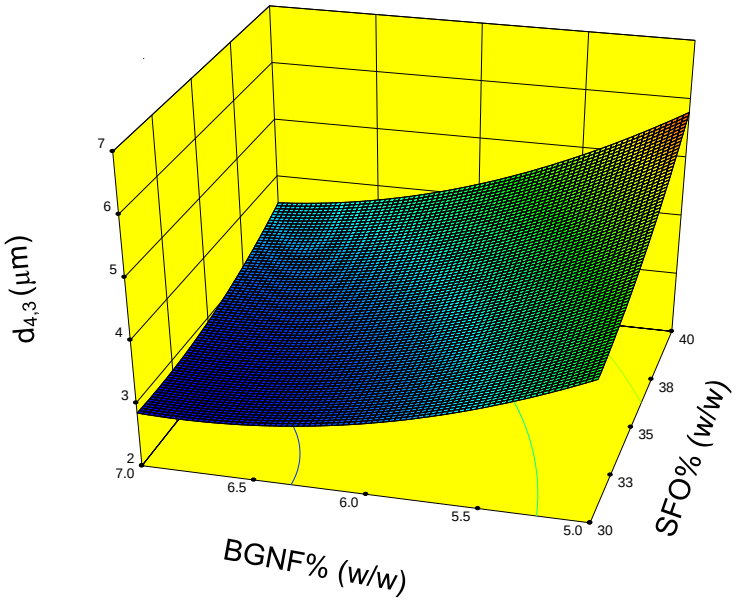

B

Figure 4.6 **Response surface for the effect of bambara groundnut flour (BGNF) and sunflower oil (SFO) concentrations on (A) De-Sauter ($d_{3,2}$) (B) De Brouker ($d_{4,3}$)**

4.2.2 Effect of BGNF and SFO on emulsion microstructure

Figures 4.7, 4.8 and 4.9 show the microscopic images of the emulsions. The images are the microstructure of freshly prepared emulsions.

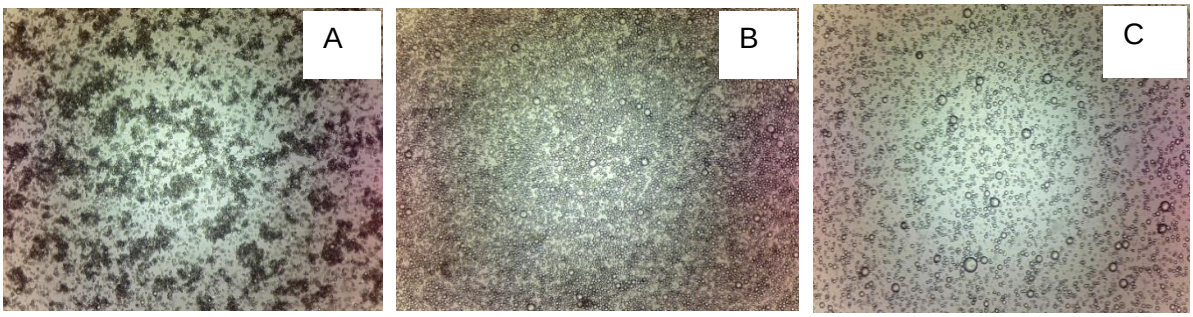

Figure 4.7 **Photo micrographs of emulsion stabilized with 5% (w/w) BGNF (A) 30% (w/w) SFO (B) 35% (w/w) SFO (C) 40% (w/w) SFO**

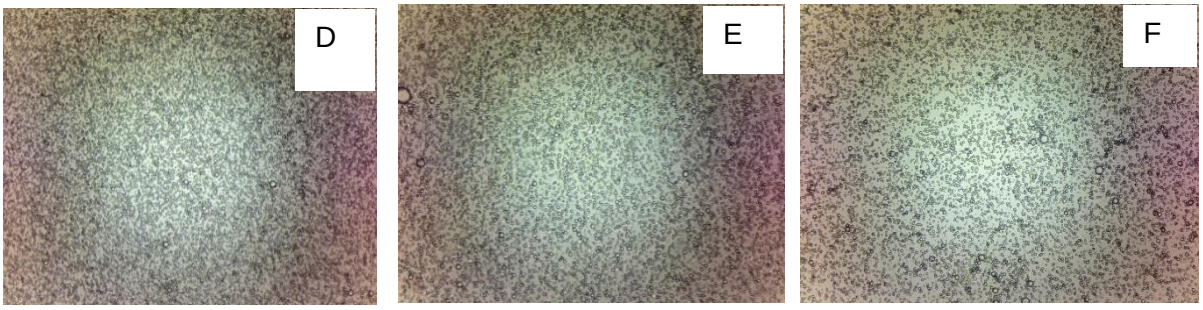

Figure 4.8 **Photo micrographs of emulsion stabilized with 6%(w/w) BGNF (D) 30% (w/w) SFO (E) 35% (w/w) SFO (F) 40% (w/w) SFO**

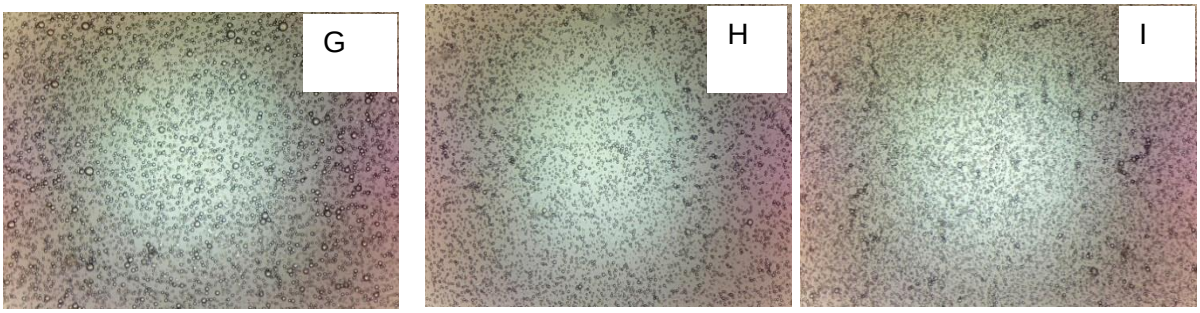

Figure 4.9 **Photo micrographs of emulsion stabilized with 7% w/w) BGNF (G) 30% (w/w) SFO (H) 35% (w/w) SFO (I) 40% (w/w) SFO**

The small drops correspond to the oil and the empty space represents the continuous phase (Izidoro *et al.,* 2008). In this work, the drops were the sunflower oil while the watery phase is gelatinized bambara groundnut flour dispersion (GBGNFD). The images revealed a steady poly dispersed systems. The optical micrographs revealed bigger drops as the sunflower concentration in the emulsion increased. However the drops became reduced as the BGNF concentration increased. Droplet aggregation was also noticed in all the emulsion systems and tended to increase as the dispersed phase fraction (sunflower oil) increased. All emulsions containing 40% (w/w) SFO were most affected by droplet aggregation irrespective of the BGNF concentrations. Emulsions containing 30% (w/w) SFO presented aggregation as observed from the micrographs. The difference in the intensity of the droplet aggregation in the emulsions may be unconnected with the earlier observed changes in oil-droplet size as affected by the emulsion components in the section 4.2.1.

4.2.3 Effect of BGNF and SFO on emulsion storage stability

Figures 4.10, 4.11 and 4.12 show the emulsion stability (multiple backscattering profiles) for emulsions (stored at 20^{o}C) in Figure 4.5, analyzed at 30 minutes interval for 360 minutes. Two sets of graphs were displayed, the Turbiscan graphs at its normal mode to the left and their corresponding reference modes, placed to the right of their respective normal modes. The Turbiscan normal modes depicted the variation of the actual backscattering flux (%) over a period and from which other information such as initial backscattering flux (%) was obtained. The reference mode was constructed by making the first scans of the normal mode as a reference relative to other scans and was assigned a backscattering flux value of zero. The reference modes allow better visualization and analysis of the stability or instability of emulsion systems with respect to the relative positions of the subsequent scans to the reference scan.

Emulsion stability refers to its ability to resist changes in its properties with time (Camino and Pilosof, 2011). The initial mean backscattering values along the entire tube (BS_{Avo}) from backscattering (*BS*) profile for emulsion stabilized with 5% (w/w), 6% (w/w) and 7% (w/w) were detailed in Table 4.7. The initial backscattering profiles give information on the microstructure of the freshly prepared emulsions (Palazolo *et al.,* 2005) and a relation between BS_{Avo} and $d_{3,2}$ has been found in soy stabilized emulsion (Marquez *et al.,* 2005). *BS* is a parameter that is directly dependent on the droplet mean diameter and oil volumetric fraction (Cerimedo *et. al.,* 2010). The initial backscattering (BS_{Avo}) profile corresponds to freshly prepared emulsions where the droplets are uniformly distributed.

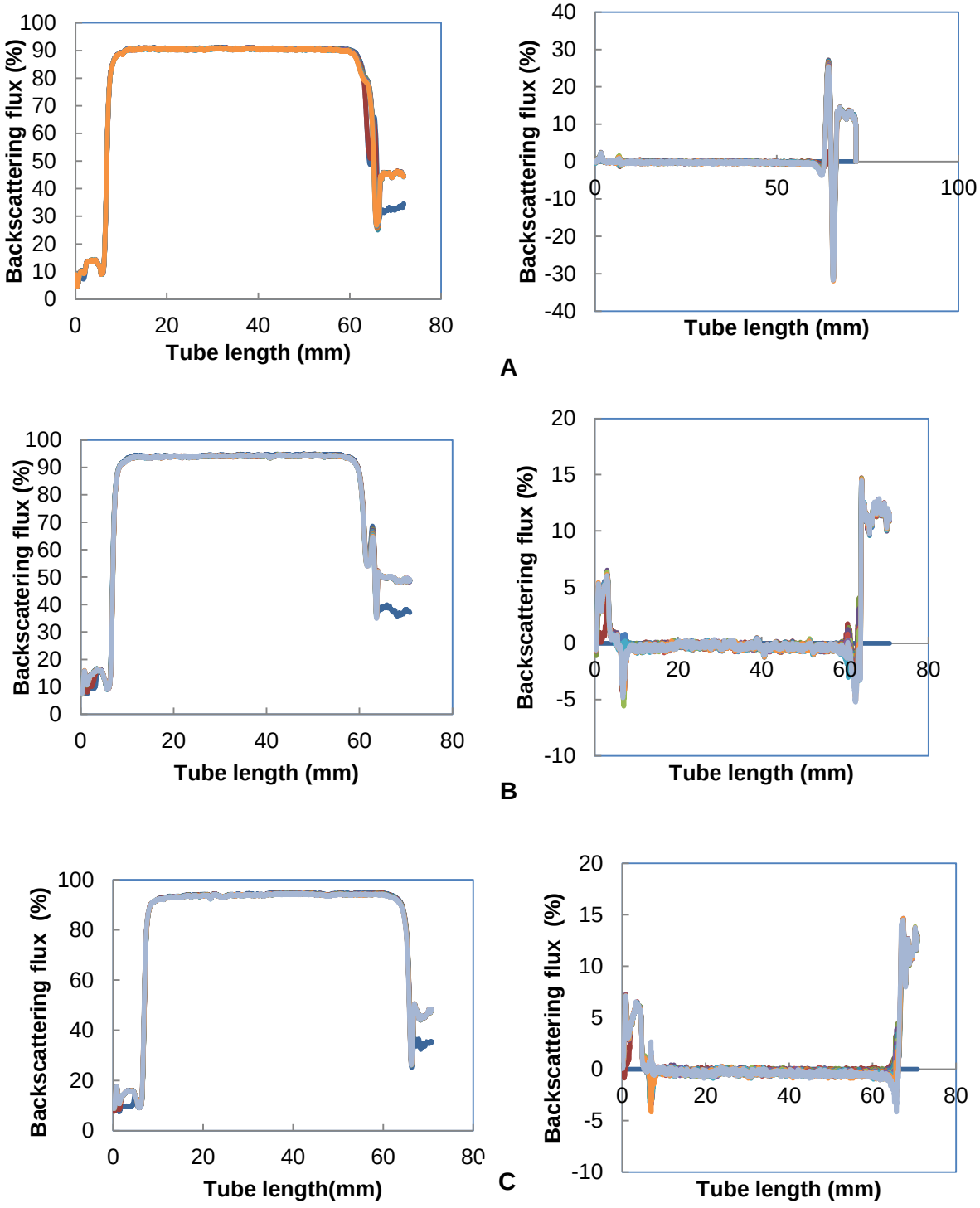

Figure 4.10 **Changes in backscattering profile (BS%) as a function of sample height with storage time of 5% (w/w) BGNF stabilized emulsion containing (A) 30% SFO (B) 35% SFO (C) 40% SFO**

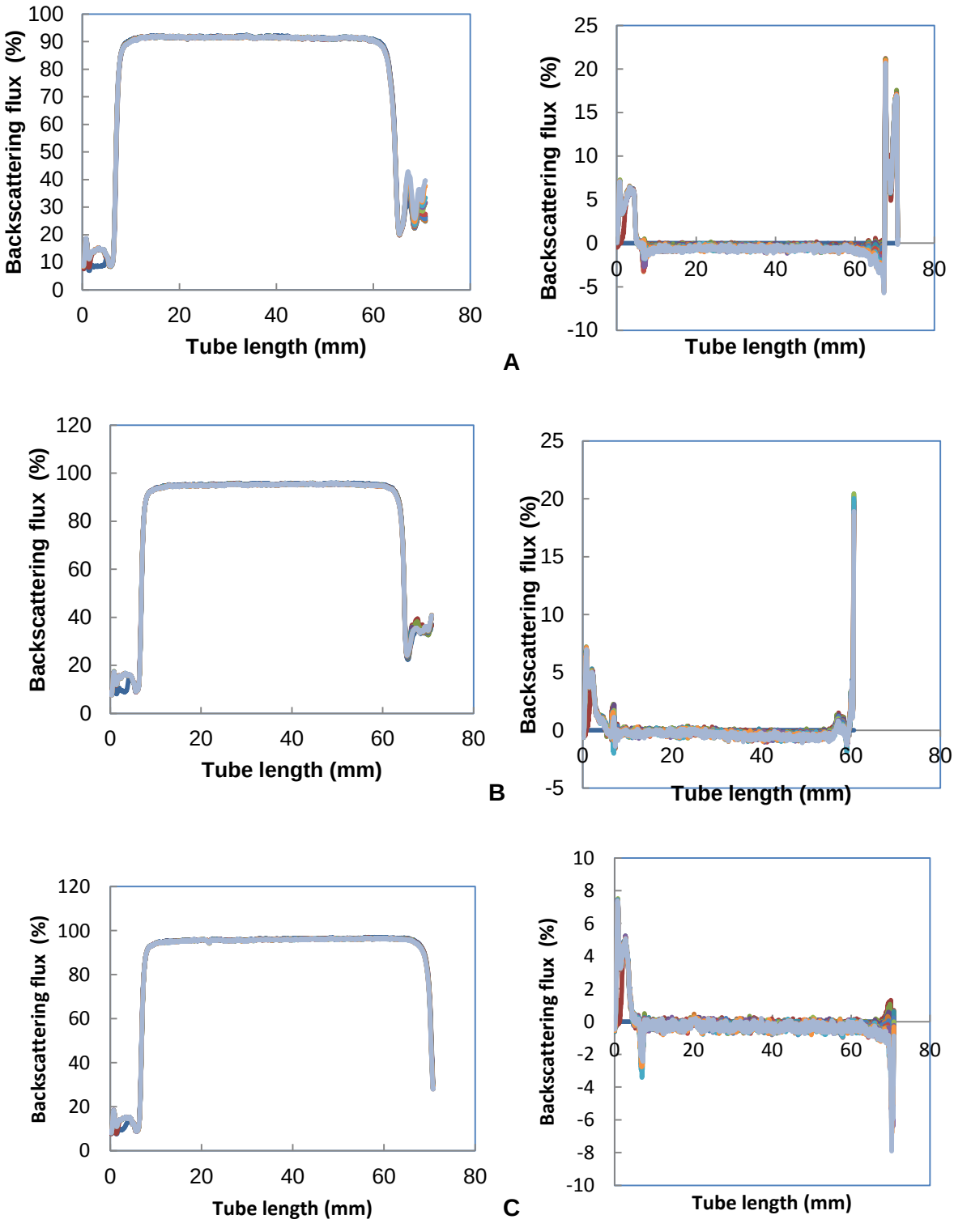

Figure 4.11 **Changes in backscattering profile (BS%) as a function of sample height with storage time of 6% (w/w) BGNF stabilized emulsion containing (A) 30% SFO (B) 35% SFO (C) 40% SFO**

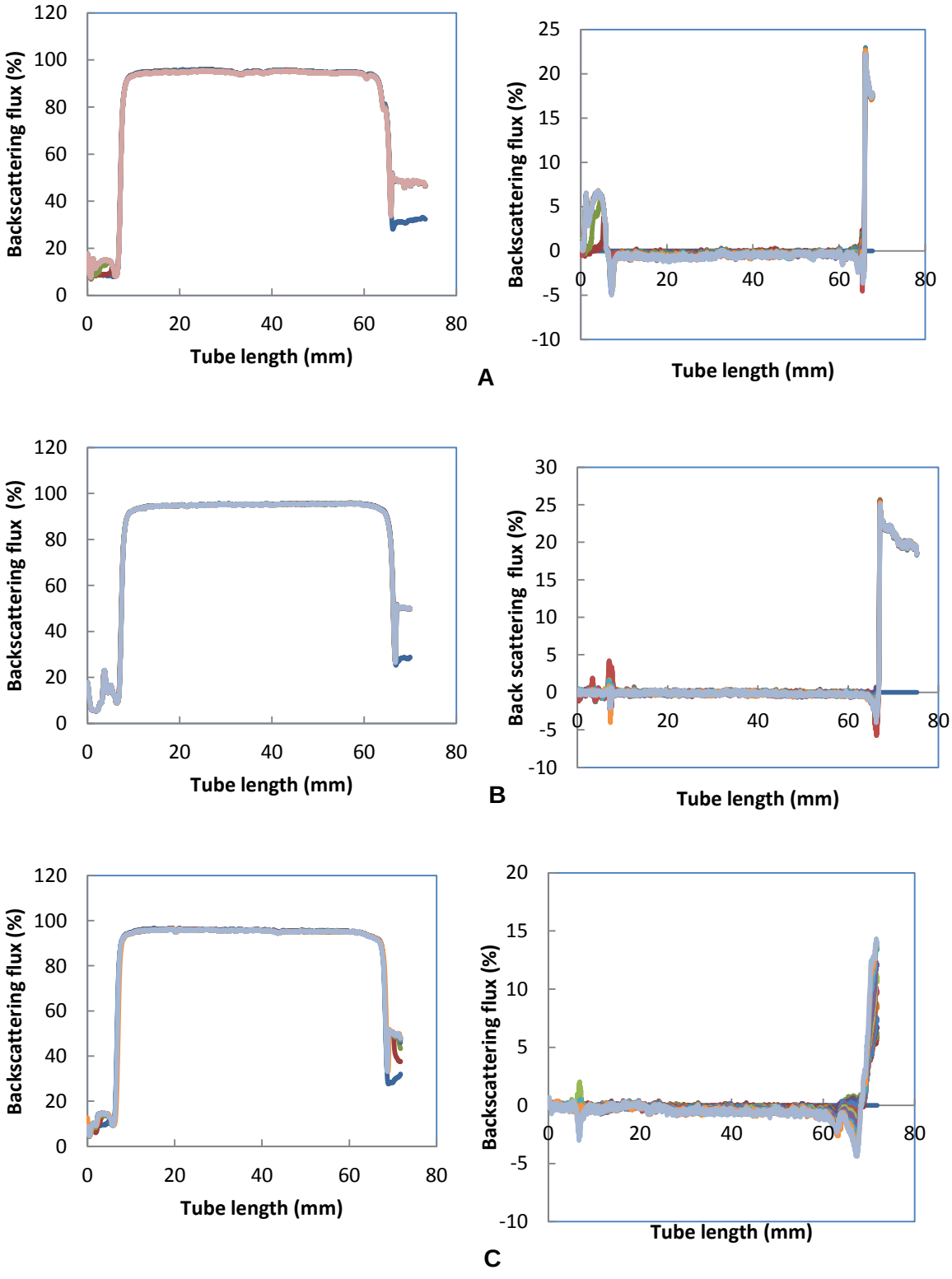

Figure 4.12 **Changes in the backscattering profile (BS%) as a function of sample height with storage time of BGNF 7% (w/w) stabilized emulsion containing (A) 30% SFO (B) 35% SFO (C) 40% SFO**

Table 4.7 Average backscattering of emulsions stabilized with BGNF[1,2]

Emulsion BGNF (%w/w)	SFO (%w/w)	Initial backscattering value [BS_{AVo}] (%)
5	30	91.27 ± 0.13
	35	94.24 ± 0.54
	40	95.01 ± 0.53
6	30	92.71 ± 0.01
	35	95.47 ± 0.14
	40	96.06 ± 0.40
7	30	95.29 ± 0.01
	35	95.77± 0.54
	40	96.15± 0.01

[1]Values are means ± standard deviations.
[2]BGNF equals Bambara groundnut flour; SFO is the sunflower oil

With a constant volumetric fraction, the backscattering is only dependent on the droplet diameter and therefore *BS* is expected to respond (move up or down) to changes in the droplet size. The emulsion containing lower droplet size disperses a higher quantity of light which means higher percentage of backscattering. This is in accordance with what was obtained in Figure 4.5. The emperical model developed for BS_{Avo} as a function of BGNF and SFO, as well as the ANOVA and coefficients of regression are presented in Table 4.8. The response surface graphs is also presented in Figure 4.13. The quadratic polynomial model was significant ($p < 0.0001$) and with high values of R^2 of 0.93, making the models suitable for predicting the BS_{AVO} as a function of of emulsion components. The linear terms of SFO and BGNF, quadratic term of SFO and the interaction between SFO and BGNF were the only significant ($p < 0.005$) model terms for BS_{AVO}.

Table 4.8 Analysis of variance (ANOVA) for the quadratic model of backscattering flux (%)[1]

	BS_{AVO} (%)			
Source	DF	Coefficient	Sum of Square	p-value
Model	5	+7.605	42.44	<0.0001
Linear				
b_1	1	+3.229	21.04	<0.0001
b_2	1	+7.717	14.94	<0.0001
Quadratic				
b_{11}	1	-0.1437	2.26	0.0122
b_{22}	1	-0.0300	0.068	0.6170
Interaction				
b_{12}	1	-0.1437	4.13	0.0422
Residual	11		3.12	
Pure error	8		1.40	
Total	17		45.56	
Lack of fit	3		1.72	0.0554
R^2	0.9316			
Adj-R2	0.9031			
CV	0.54			
Adequate precision	17.08			

[1] b_1 and b_2 equal the coefficient of the linear term of bambara groundnut flour and sunflower oil; b_{11} and b_{22} are the coefficients of the quadratic terms of the bambara groundnut flour and sunflower oil; b_{12} equals the coefficients of interaction between the bambara groundnut flour and sunflower oil; DF equals degree of freedom; R^2 is the coefficient of determination; Adj R^2 equals the adjusted coefficient of determination; CV is the coefficient of variation.

The linear terms of BGNF and SFO were positive while the quadratic term of SFO and the interaction of BGNF and SFO were negative on the BS_{AVO} (Figure 4.13). For all the emulsions, BS_{AVO} is highly dependent on both the BGNF and SFO concentrations. BS_{AVO} tended to increase with an increase in BGNF and SFO concentration. The interaction effect between BGNF and SFO decreased significantly BS_{AVO} ($p < 0.005$). For example, emulsion samples containing 30% (w/w) sunflower oil stabilized with 5, 6 and 7% (w/w) BGNF have average BS_{AVO} of 91.27%, 92.71% and 95.29%, respectively. The same trend of increase was observed in emulsions containing 35% and 40% SFO stabilized with 5, 6 and 7% (w/w) BGNF. This suggested that the droplet population and interaction increased with increased BGNF and SFO in the emulsion.

In order to study the global stability of the BGNF stabilized emulsion, *BS* profiles were analyzed at room temperature (20^oC) and at different storage times to gain insights into the destabilization kinetics. These profiles constitute the macroscopic fingerprint of emulsion samples at a given time (Mengual *et al.,* 1999; Cerimedo *et al.,* 2010).

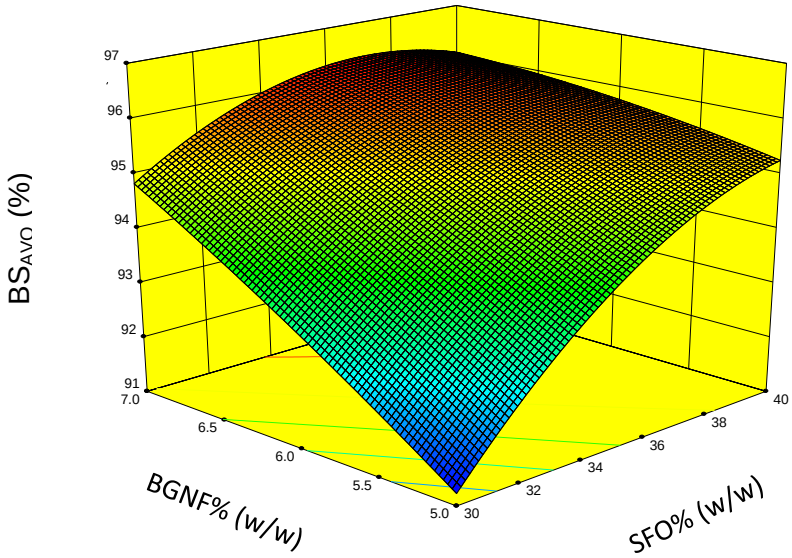

Figure 4.13 Response surface for the effect of bambara groundnut flour (BGNF) and sunflower oil (SFO) concentrations on backscattering (%)

All the emulsions showed similar multiple destabilization mechanism as evident from the reference mode of *BS*-profile (Figures 4.10, 4.11 & 4.12). The backscattering profiles for all the formulations showed a peak at the bottom of the tube between 0 - 20 mm zone (in reference mode) which could be attributed to creaming. There was also a noticeable decrease in the average backscattering along the whole length of the tube, indicative of flocculation and or coalescence. Emulsion destabilization by creaming is a characteristic of low volumetric relation between the dispersed phase and continuous phase and flocculation present a high influence in the creaming process and could favour gravitational separation depending on the droplet size and the flocs structure (McClements, 1999; Palazolo *et al.*, 2005; Camino and Pilosof, 2011). In a more concentrated dispersed phase, the droplets lose their mobility and could stay intact during a long period of time which induces coalescence (Palazolo *et al.,* 2005; Camino and Pilosof, 2011). When there are no external forces, coalescence is a slow process in comparison with creaming and flocculation. The nature of colloidal interaction between the droplets and interfacial film resistance will determine the degree of emulsion destabilization (McClements, 1999; Camino and Pilosof, 2011). The creaming quantification was made by

using the migration software available in the Turbiscan vertical scanner. However, the result showed that all the emulsions were resistant to creaming as the migration rates of all the emulsions were zero. This is in accordance to what was observed visually.

In order to quantify phenomenon that occurred repeatedly through particle size variation such as flocculation and coalescence in the emulsions, the variation in backscattering in the 20 - 40 mm zone with storage time was determined and it is as shown in Figure 4.14A, B and C. It gives information on the spatial distribution of the oil droplets with time, and hence the farther the graphs from the origin, the more unstable the emulsion becomes with time. A well - structured emulsion (better stability) has the kinetic graph (in terms of backscattering %) either on the zero base line or closer at any point in time. All the destabilization kinetics followed the same trend. Both BGNF and SFO were found to affect the mechanism of destabilization. Increase in BGNF and SFO concentrations simultaneously in the emulsions improved stability. However, the consecution of an extensive flocculated state could be related to an improvement in creaming stability by immobilization of droplets in the network (Franco *et al.,* 2000). The differences observed in the BGNF stabilized emulsions is not unrelated to the oil-droplet sizes and microstructure of their respective emulsion observed in sections 4.2.1 and 4.2.2, respectively. All emulsions with higher concentration of SFO showed better stability. The present observation could be attributed to the formation of a droplet network and the resulting greater number of interdroplet interaction within the network (Nikovska, 2010). The droplet network could also be responsible for the reduced frequency of oil droplet collision which has resulted into better stabilization. The results show a clear picture of the gel strength of the individual BGNF concentrations used to achieve emulsions stabilization and the nature and strength of the interdroplet interactions. The backscattering (%) at equilibrium time of 360^{th} minute (BS_{eq}%) was modeled as a function of emulsion component (BGNF and SFO) in order to gain insight into the stability of the emulsions at the final time of storage stability.

Table 4.9 gave the analysis of variance (ANOVA) and coefficients of the of developed empirical linear model. The model was significant ($p < 0.001$) and the significant lack of fit shows that the model can be used to prdict the instrinsic variation of BS_{eq} as a function of emulsion components. The linear model terms were significant ($p < 0.001$) and positive on the $BS_{eq..}$ Figures 4.15 A, B and C show the influence of BGNF and SFO on the BS_{eq}. Increase in concentration of BGNF and SFO independently led to an increase in $BS_{eq.}$ The increase is unc onnected with the increased droplet network formed as the BGNF and SFO increased in the emulsion.

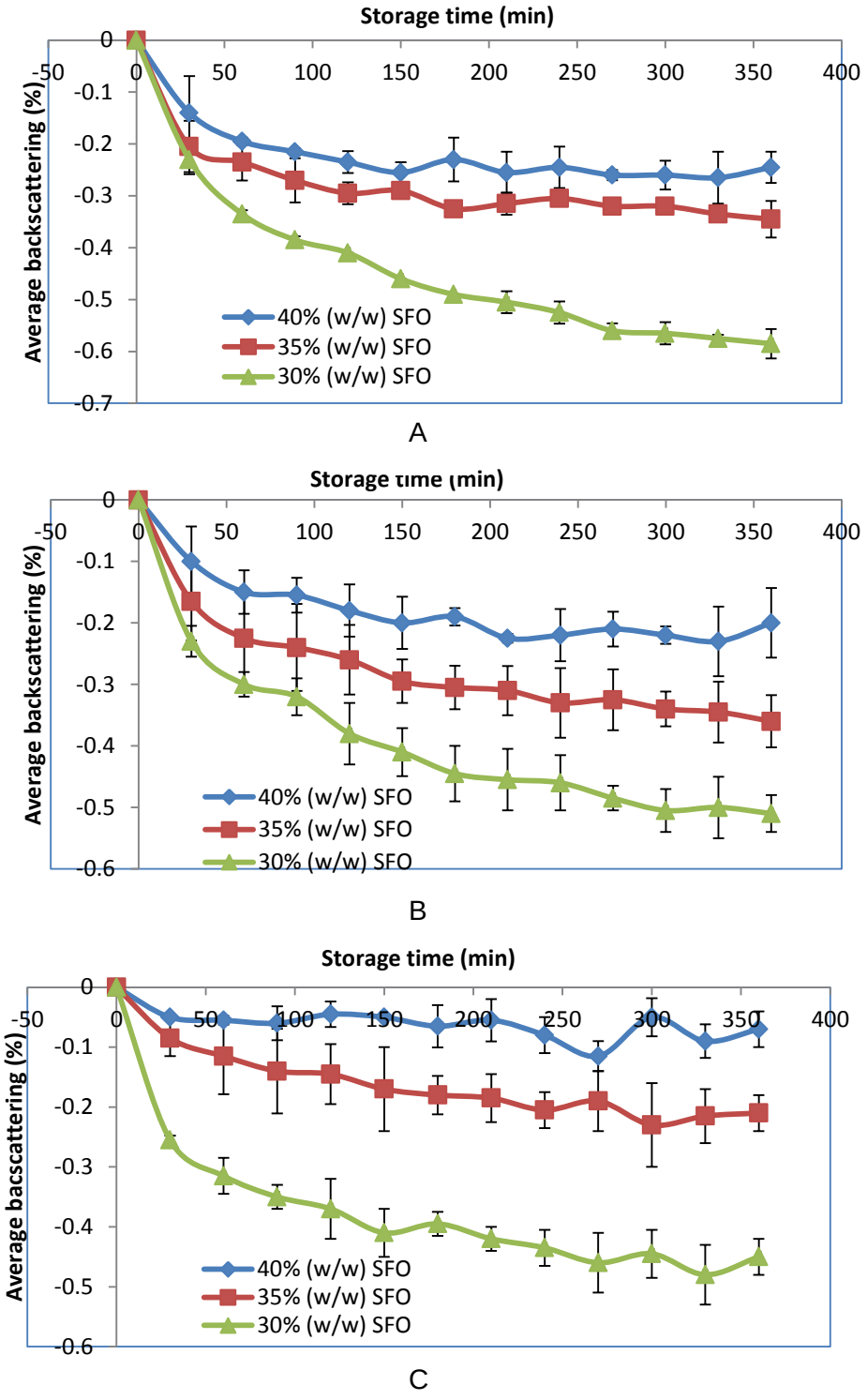

Figure 4.14 **Variation in backscattering in the 20 – 40 mm zone monitored over 360 minutes for sampled stored in quiescent condition at 20°C. Emulsion stabilized with (A) 5% (w/w) (B) 6% (w/w) (C) 7% (w/w) Bambara groundnut flour (BGNF) containing 30%, 35% and 40% (w/w) sunflower oil (SFO)**

Table 4.9 **Analysis of variance (ANOVA) for the linear model of equilibrium backscattering (BS_{eq}%) responses[1]**

Source		BS_{eq} (%)		
	DF	Coefficient	Sum of square	p-value
Model	2	-0.33	0.63	<0.001
Linear				
b1	1	+0.17	0.53	<0.0001
b2	1	+0.075	0.10	<0.0001
Lack of fit	6			0.2884
Total	26			
R2		0.8457		
Adj-R2		0.8671		
CV		18.33		
Adequate precision		24.391		

[1]b_1 and b_2 equal the coefficient of the linear term of bambara groundnut flour and sunflower oil; DF equals degree of freedom; R^2 is the coefficient of determination; Adj R^2 equals the adjusted coefficient of determination; CV is the coefficient of variation.

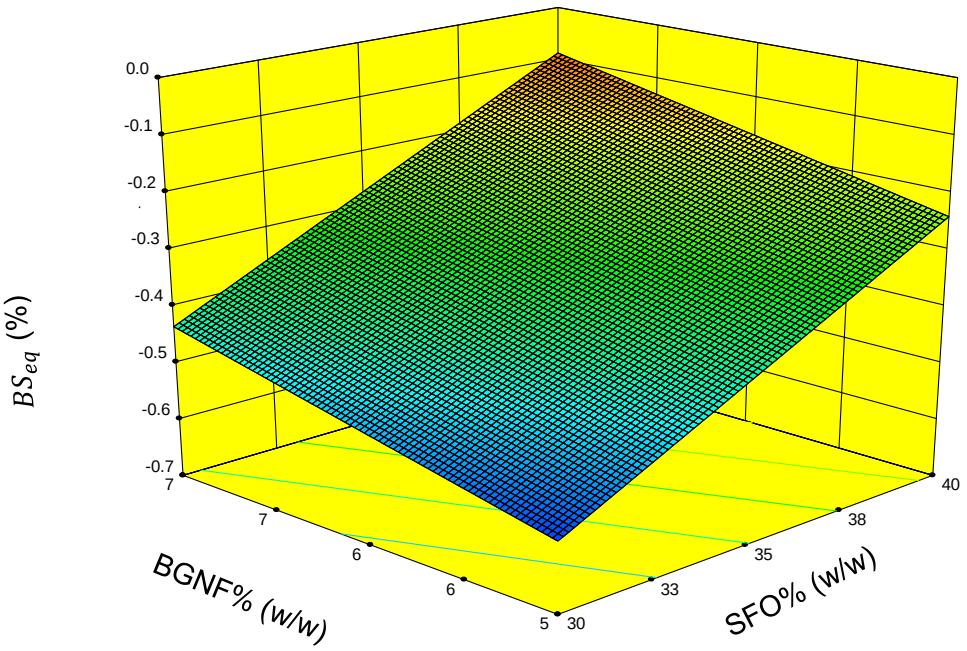

Figure 4.15 **Response surface for the effect of bambara groundnut flour (BGNF) and sunflower oil (SFO) concentrations on equilibrium backscattering obtained at the 360th minute of stability study.**

4.2.4 Optimization of the main components (BGNF and SFO concentrations) of the emulsion

Numerical optimizer available in the Design Expert software was used to obtain the components (BGNF and SFO) of the most stable emulsion with highest emulsion stability. For this purpose, the equilibrium backscattering (BS_{eq}%), which gave the information regarding emulsion stability at the 360th minutes of study and whose value is a function of other emulsion stability parameters such as the particle size, was used. The backscattering of the most stable emulsion formulation is expected to be very close to the zero line (Figures 4.14A, B and C), which implies minimum spatial shift in oil droplets (maximum droplet interaction) and therefore maximizing the BS_{eq}% (Table 4.10), within the range of BGNF and SFO gave the desirable optimization goal. The results of the numerical optimization are shown in Table 4.11

Table 4.10 Optimization constraints and goal[1]

Constraint Name	Goal	Lower limit (%)	Upper limit (%)
A:SFO	Is in range	30	40
B:BGNF	Is in range	5	7
BS_{eq}	Maximize	-0.62	-0.02

[1]BGNF equals Bambara groundnut flour; SFO is the sunflower oil; BS_{eq} is the equilibrium backscattering flux

Table 4.11 Numerical optimization solution

Solution Number	SFO (w/w)	BGNF (w/w)	BS_{eq} (%)	Desirability	
1	40.000	7.000	-0.084	0.893	Selected
2	40.000	6.989	-0.085	0.891	
3	40.000	6.964	-0.087	0.888	
4	39.621	7.000	-0.097	0.871	
5	39.519	7.000	-0.101	0.865	

[1]BGNF equals Bambara groundnut flour; SFO is the sunflower oil; BS_{eq} is the equilibrium backscattering flux

Emulsion formulated with 7% (w/w) BGNF and 40% (w/w) SFO with BS_{eq}% value of -0.084% and desirability of 0.893 was selected as the most stable formulation. This indicated that

emulsion formulated with 7% (w/w) BGNF and 40% SFO was the emulsion with the minimum oil-droplets spatial shift and maximum oil-droplets interaction.

4.2.5 Summary on emulsion stability and component optimization of oil-in-water emulsion

Sunflower oil-in-water emulsion was stabilized using gelatinized bambara groundnut flour dispersions. Both the BGNF and SFO concentrations have noticeable influence on the oil-droplet size and particle size distribution. Increase in SFO increased oil-droplet size while increase in BGNF decreased oil-droplet size. Emulsion microstructure showed that all studied emulsion were flocculated systems however, degree of flocculation depended greatly on the relative concentrations of both BGNF and SFO. BGNF and SFO concentrations affected emulsion stability and BGNF stabilized emulsions showed multiple destabilization mechanism. However, increasing BGNF and SFO greatly improved destabilization. Response surface methodology was found to be very useful in predicting and describing some useful emulsion stability parameters which can be very useful in formulation design of predetermined emulsion properties. Emulsion formulated with 7% (w/w) BGNF and 40% (w/w) SFO was the most stable.

4.3 Time-Dependent Rheology of BGNF Stabilized Emulsion

Time-dependent rheological properties of BGNF-stabilized emulsions were quantified by using the hysteresis loop area and constant shear decay methods. The individual and interactive contributions of BGNF and SFO to the time-dependent properties were further modeled using the response surface methodology. The observed time-dependent parameters were explained and related to emulsion stability. This section therefore reported the results of the effects of the BGNF and SFO on the time-dependent rheological characteristics of the BGNF-stabilized emulsion.

4.3.1 Effect of BGNF and SFO on hysteresis loop area

The shear rate sweep of BGNF stabilized emulsions at different BGNF and SFO concentrations are as presented in Figures 4.16A, B and C. Hysteresis loop areas were observed when the BGNF emulsions were subjected to increasing and decreasing shear rate. The hysteresis area has been explained to represent an index of energy per unit of time and per unit of volume needed to eliminate the influence of time in the flow behavior (Koocheki and Razavi, 2009). The existence of the hysteresis area between the increasing and decreasing shear rate curves indicated that all the BGNF stabilized emulsions were time dependent and thixotropic in nature

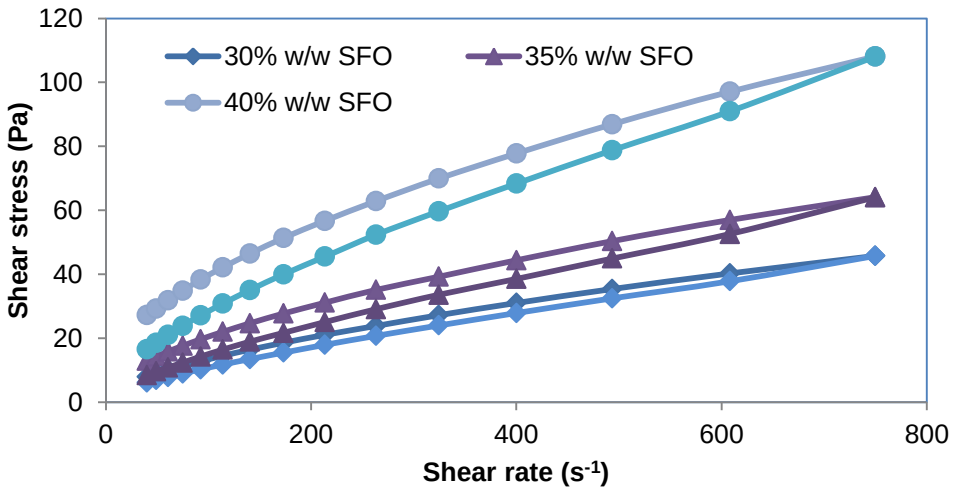

A

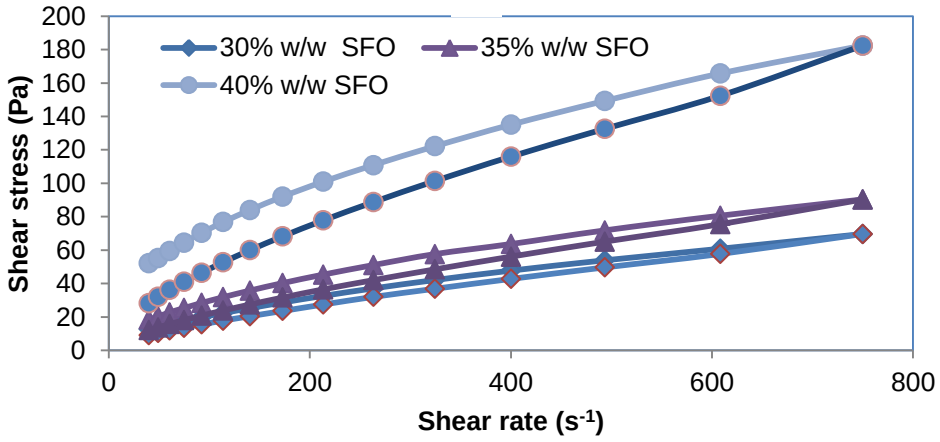

B

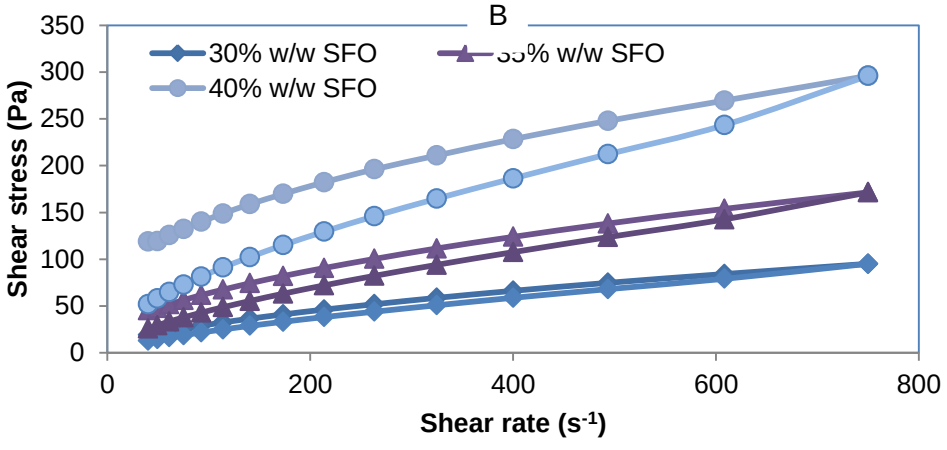

C

Figure 4.16 **Hysteresis loop obtained for emulsions containing 30% (w/w), 35% (w/w) and 40% (w/w) sunflower oil (SFO), stabilized with (A) 5% (w/w) (B) 6% (w/w) (C) 7% (w/w) bambara groundnut flour (BGNF)**

(Emadzadeh and Razavi, 2012). The thixotropy of a material has been interpreted as the continuous breakdown or rearrangement of the network links and this could be quantified by the evaluation of the magnitudes of the areas of hysteresis loops between the upward and downward curves (Tarrega *et al.,* 2004; Koksoy and Kilic, 2003). It has been reported that the larger the magnitude of the area, between the flow curves, the higher the thixotropic effect (Mathias *et al.,* 2011). Table 4.12 showed the magnitudes of the hysteresis loop areas for the emulsions at different BGNF and SFO concentrations. The mean values of hysteresis loop areas ranged from 36.2 to 694 Pas^{-1}. Time dependency was also found in vegetable-based infant purees (Dolores and Canet, 2013); ayran (Koksoy and Kilic 2003), and semi-solid dairy desserts (Tarrega *et al.,* 2004).

Table 4.12 Hysteresis loop area obtained for BGNF stabilized[1]

Emulsion				
BGNF (%w/w)	SFO (%w/w)	Integrating area for upward curve	Integrating area for downward curve	Hysteresis loop area (Pas^{-1})
5	30	322 ± 5.61	285 ± 1.88	36.2 ± 3.73
	35	472 ± 5.93	398 ± 1.58	74.2 ± 4.35
	40	855 ± 9.33	704 ± 15.3	151 ± 5.98
6	30	495 ± 7.94	434 ± 5.06	61.1 ± 2.88
	35	678 ± 8.99	572 ± 5.44	105 ± 3.56
	40	1453 ± 95.4	1175 ± 51.4	269 ± 44.0
7	30	697 ± 10.3	597 ± 9.07	100 ± 1.23
	35	1349 ± 38.2	1110 ± 21.0	239 ± 17.2
	40	2683 ± 85.4	1989 ± 20.7	694 ± 64.6

[1] BGNF is banbara groundnut flour; SFO is sunflower oil.

The ANOVA for the quadratic models developed for the hysteresis loop area is presented in Table 4.13. The model for the hysteresis loop area as a function of emulsion components was significant ($p < 0.0001$) with high R^2, coefficient of variation, adequate precision values and no significant lack of fit. All model terms were significant ($p < 0.05$) for the hysteresis loop areas. The effect of the linear term of SFO and BGNF were both negative. The quadratic effect of BGNF and SFO and interaction effect of BGNF and SFO were positive on the hysteresis loop area. The response surface for the individual and simultaneous increase of SFO and BGNF on the hysteresis loop area is shown in Figure 4.17. Hysteresis loop area was

dependent on both the BGNF and SFO contents in the emulsions. Increase in the BGNF and SFO independently increased the hysteresis loop area of the emulsions. This observation can also be visualized in Figure 4.16 where hysteresis loop area was smaller at lower BGNF and SFO concentrations and increased as the concentration of BGNF and SFO increased.

Table 4.13 Quadratic model prameters for the Hysteresis loop area

Hysteresis loop area (Pas^{-1})				
Source	DF	Coefficient	Sum of Square	p-value
Model	5	+4053.93	103700	<0.0001
Linear				
b_1	1	-155.53	82070.26	<0.0001
b_2	1	-621.78	48976.85	<0.0001
Quadratic				
b_{11}	1	+1.55	4726.52	0.0057
b_{22}	1	+25.56	2033.00	0.0443
Interaction				
b_{12}	1	+11.49	11548.40	0.0003
Residual	10		83437.39	
Pure error	8		2318.45	
Total	15		107500	
Lack of fit	2		1527.43	0.3913
R^2	0.9642			
Adj-R2	0.9463			
CV	15.01			
Adequate precision	19.107			

[1]b_1 and b_2 equal the coefficient of the linear term of bambara groundnut flour and sunflower oil; b_{11} and b_{22} are the coefficients of the quadratic terms of the bambara groundnut flour and sunflower oil; b_{12} equals the coefficients of interaction between the bambara groundnut flour and sunflower oil; DF equals degree of freedom; R^2 is the coefficient of determination; Adj R^2 equals the adjusted coefficient of determination; CV is the coefficient of variation.

Simultaneous increase of SFO and BGNF however caused a significant increase in the hysteresis loop area. This indicated that the thixotropic behavior of the entire emulsion samples were built up with an increase in the concentration of BGNF and SFO and this might be due to the increase in the viscosity as the concentration of BGNF and SFO increased. Emulsion formulated with 7% (w/w) BGNF and 40% (w/w) SFO showed the highest hysteresis loop area, while emulsion formulated with 5% (w/w) BGNF and 30% (w/w) SFO had the least. Therefore, if it is assumed that hysteresis loop area is an index of the energy needed to destroy the structure responsible for flow time dependence, the emulsion with 7% (w/w) BGNF and 40% (w/w) SFO was the sample that needed the highest energy to breakdown such structure. This could be as a result of the observed high viscosity of the emulsion. The high stability possessed

by emulsion formulated with 7% (w/w) BGNF and 40% SFO was therefore connected to high structural formation (high droplet-droplet interaction) which subsequently led to high viscosity. This has led to the high time-dependence (rigidity) and correspondingly high index of energy necessary to destroy the droplet-droplet structures. However, as reported by Tarrega *et al.* (2004) and Koocheki and Razavi (2009), a high viscous thixotropic fluid may show a larger hysteresis area than one with a lower viscosity even if the latter undergoes a stronger structural destruction.

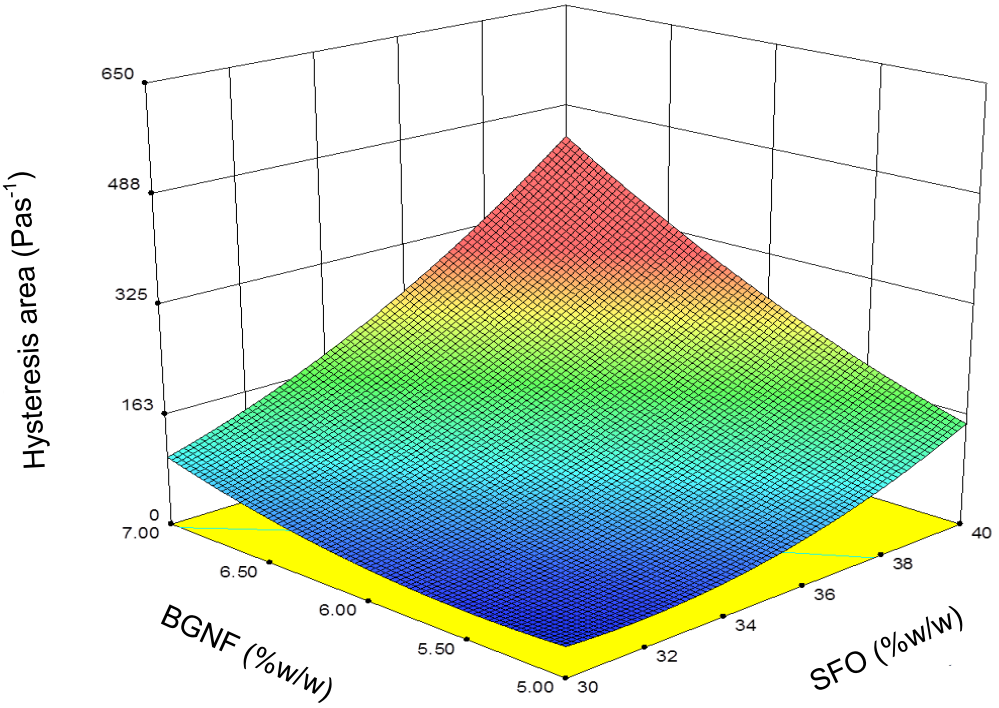

Figure 4.17 Response surface for the effect of BGNF and SFO concentrations on Hysteresis loop area

Therefore comparison of straight loop areas between viscous systems may not render valid conclusions on the extension of time dependent structural breakdown and therefore different time-dependent rheological models may be necessary for the evaluation of this phenomenon in emulsions stabilized by BGNF (Koocheki and Razavi, 2009).

4.3.2 Time-dependent rheological modeling: Effect of constant shear decay on apparent viscosity

Figures 4.18, 4.19 and 4.20 show the effect of shearing time on the apparent viscosity of concentrated oil-in-water emulsion containing 30, 35 and 40% (w/w) SFO, stabilized with 5, 6 and 7% (w/w) BGNF concentrations. The thixograms of the BGNF stabilized emulsions were different and dependent on the BGNF and SFO concentration as well as the rate of shearing. All the emulsion presented a time-dependent behavior when constant shear rates were applied. The apparent viscosity of the emulsion decreased with shearing time, which is a characteristic behaviour for thixotropic fluids. There was a greater dependency of apparent viscosity on time at the initial stage of the shearing process. The dependency of viscosity decreased as a function of shearing time, and it reached a steady state at about 800 seconds. Similar observation was reported for egg and eggless mayonnaise (Singla *et al.,* 2013), coffee flavored yogurt (Mathias *et al.,* 2011) and semi dairy desserts (Tarraga *et al.,* 2004). In addition, the viscosity tended to decay at a faster rate at higher shear rates towards a steady state viscosity and was lower than the steady state viscosity at low shear rates. This observation implied that the breakdown rate of samples under a shear field accelerates at high shear rates (Razavi and Karazhiyan, 2009). It is clear from Figures 4.18, 4.19 and 4.20 that BGNF concentration, SFO concentration and rate of shearing all affected the changes in the apparent viscosity from the initial value to final value. The higher changes were found between the initial and final values of apparent viscosity when the BGNF and SFO concentrations in the sample emulsions were increased. Emulsions that exhibit thixotropic properties do often contain oil droplets that are aggregated by weak forces and shearing causes the aggregated droplets to be progressively deformed and disrupted, thereby decreasing the resistance to flow and therefore causing a reduction in viscosity over time (Bellalta *et al.,* 2012). Furthermore, it is expected that the degree of oil droplet coalescence increase with increased oil content which led to an increment in the rate of structural breakdown. This result is in agreement with the report of Bellalta *et al.* (2012) that changes in apparent viscosity when a constant shear rate is applied are higher when oil content in the emulsion increases. Emulsion containing 40% (w/w) SFO, stabilized with 7% (w/w) BGNF showed the highest changes in apparent viscosity when sheared over a period of 1200 seconds.

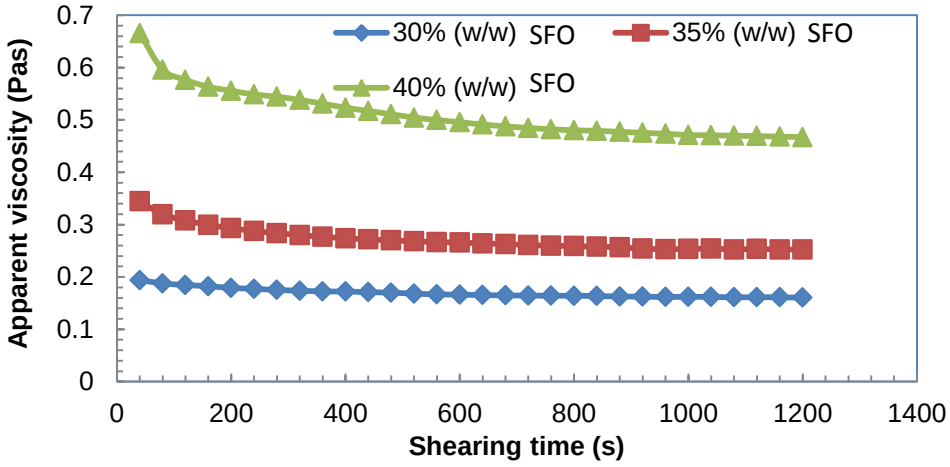

A

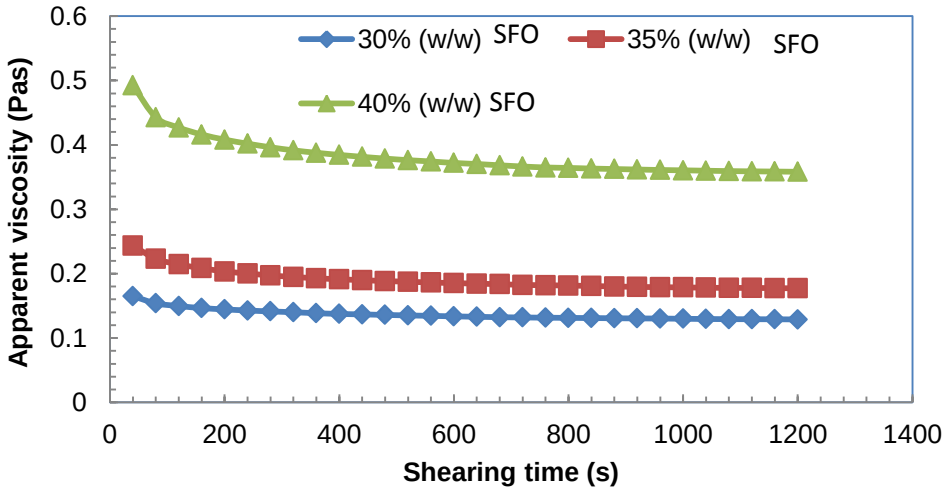

B

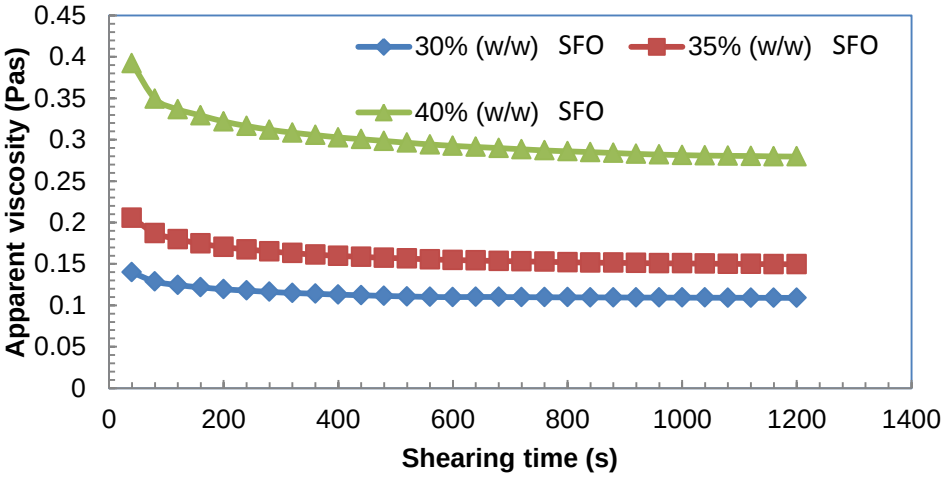

C

Figure 4.18 **Relationship between apparent viscosity and shearing time of emulsions stabilized with 5% (w/w) Bambara groundnut flour (BGNF) at (A) 50 s^{-1} (B) 100 s^{-1} (c) 150 s^{-1}**

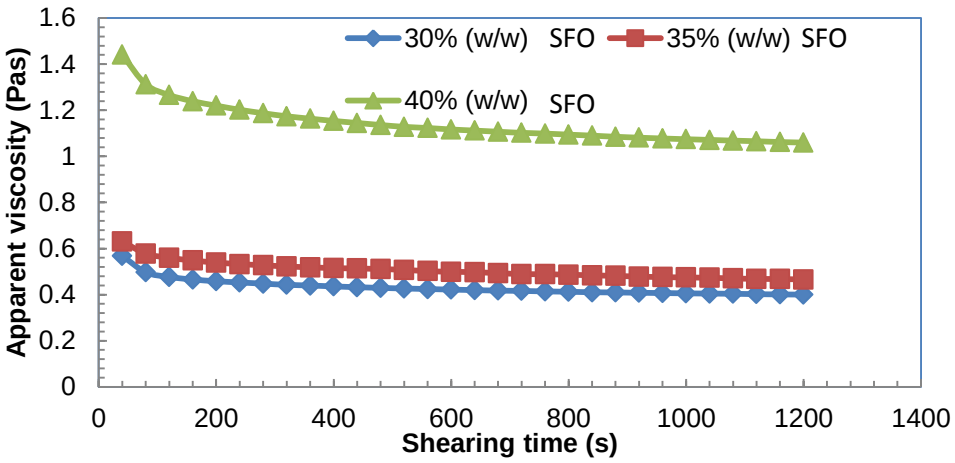

A

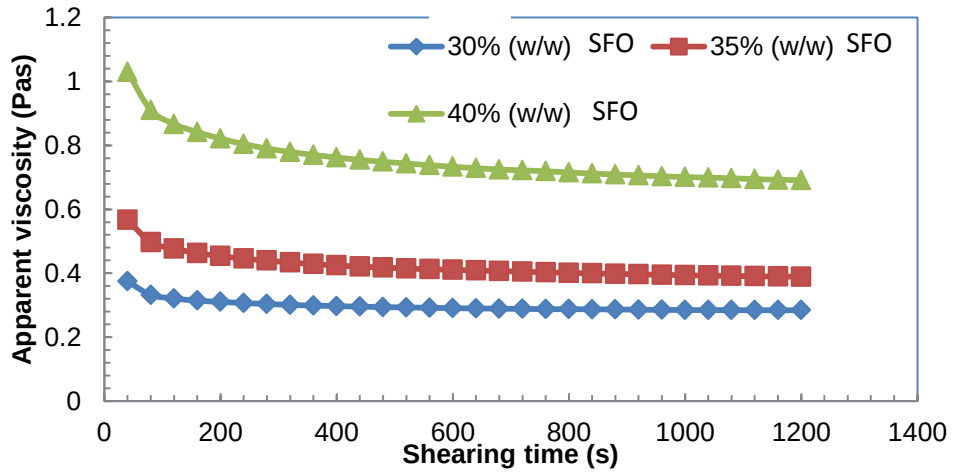

B

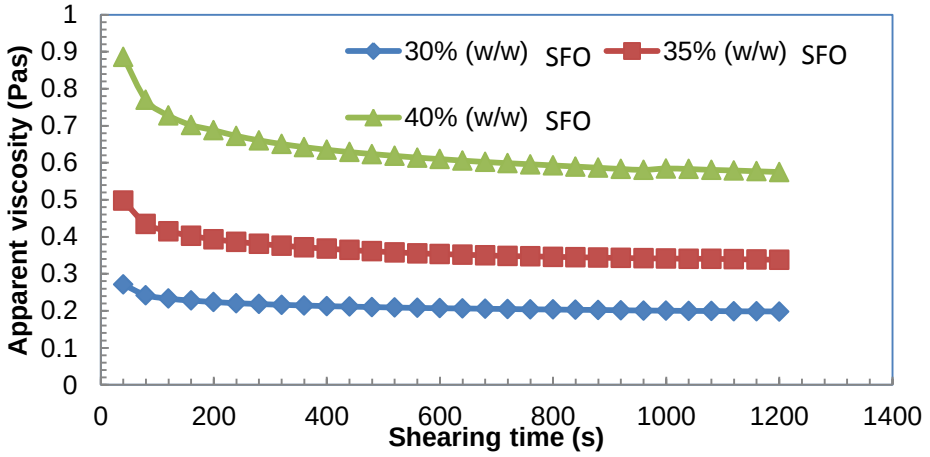

C

Figure 4.19 **Relationship between apparent viscosity and shearing time of emulsions stabilized with 6% (w/w) Bambara groundnut flour (BGNF) at (A) 50 s^{-1} (B) 100 s^{-1} (c) 150 s^{-1}**

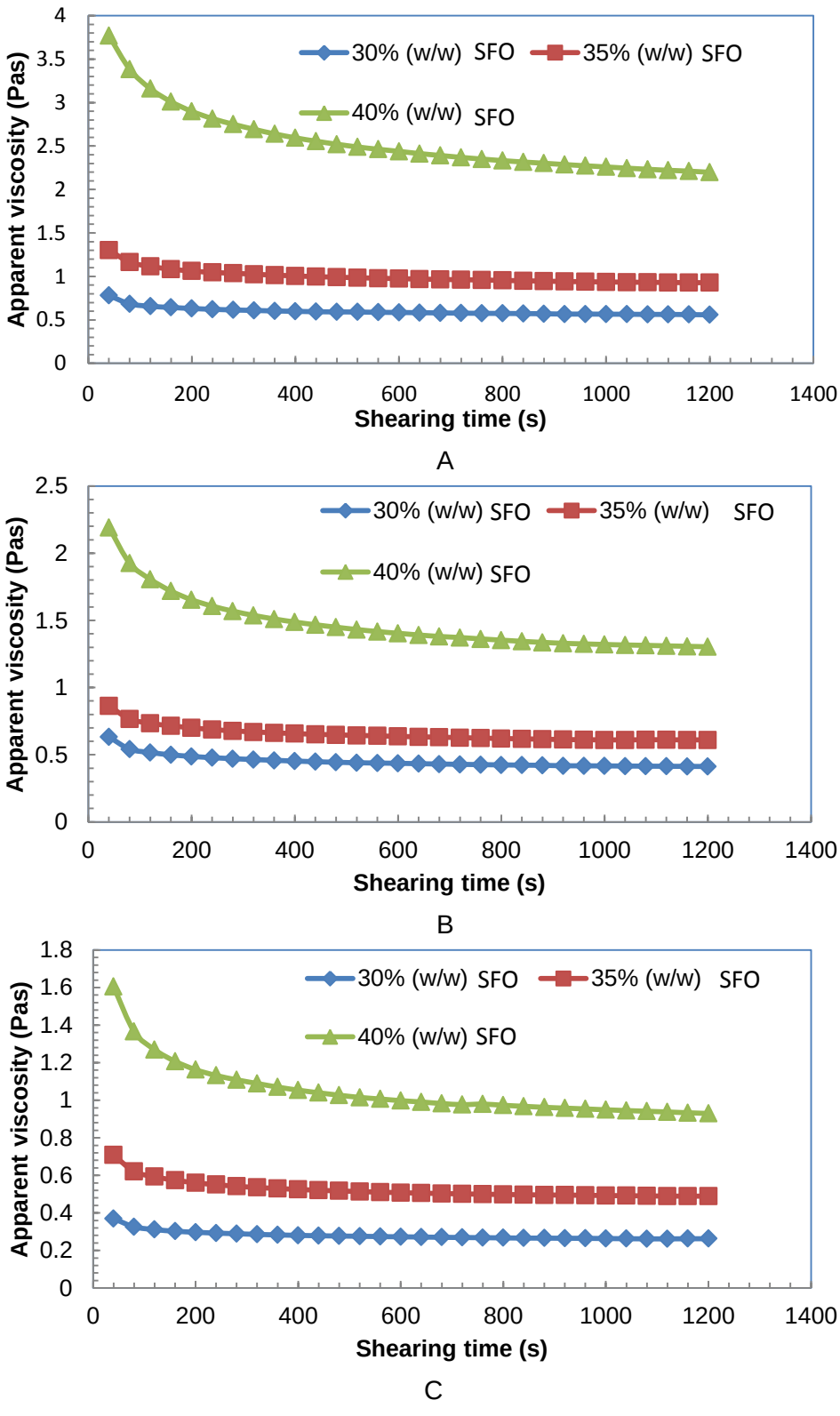

Figure 4.20 **Relationship between apparent viscosity and shearing time of emulsions stabilized with 7% (w/w) bambara groundnut flour (BGNF) at (A) 50 s^{-1} (B) 100 s^{-1} (C) 150 s^{-1}**

4.3.3 Thixotropic modeling of BGNF stabilized emulsion

4.3.3.1 Thixotropic modeling of BGNF stabilized emulsion using Weltman model

The observed time dependent behaviors of the samples were modeled using Weltman equation (Equation 3.8). Table 4.14 shows the Weltman model parameters at shear rates of 50, 100 and 150 s^{-1} as a function of BGNF and SFO concentration. Parameter *A* in the Weltman model is the quantification of initial stress of the emulsions while the parameter *B* value is an indication of the extent of thixotropy. A negative value of *B* measures how fast the shear stress drops from the initial value to final equilibrium value (Koocheki and Razavi, 2009). The mean of initial stress of the emulsions ranged from 11.7 to 315 Pa, while the extent of thixotropy ranged from 0.52 to 25.54 Pa. The high coefficient of determination (> 0.92) showed the appropriateness of Weltman model to describe the time dependent properties of the emulsions. Weltman model has been reported suitable to characterize the time dependent behaviour of food products like semi-solid dairy desserts (Tarrega *et al.,* 2004) and salad dressing (Paredes *et al.,* 1988). The coefficients of Weltman model obtained for BGNF stabilized emulsions were comparable to other food products reported in the literature. For example, Razavi *et al.* (2010) characterized and modeled the time dependent properties of pistachio butter with varying amount of lecithin and monoglyceride contents at 25 and 40^{o}C. They reported initial stress value (*A)* and extent of thixotropy (*B*) at 150 s^{-1} to be in the range of 376.43 - 2213.49 Pa and 21.62 - 235.19 Pa, respectively. In a related study conducted to characterize the time-dependent rheological properties of sesame paste/date syrup blend at 25^{o}C (Razavi and Habibi-Najafi, 2006), Weltman parameter *A* and *B* were reported in the range of 189.2 - 730.6 Pa and 0.278 - 1.571 Pa, respectively. Singla *et al.* (2013) also found parameter *A* and *B* for mayonnaise at 20^{o}C and 10 s^{-1} in the range of 5.051 - 5.106 Pa and 0.0005 - 0.0007 Pa, respectively.

The fittings of the experimental data of the emulsion samples to Weltman model are shown in Figures 4.21, 4.22 and 4.23 for emulsions stabilized with 5, 6 and 7% (w/w), respectively. The Weltman model (solid line), fits well the relationship between shear stress and shearing time of concentrated oil-in-water emulsions stabilized with BGNF for all BGNF and SFO concentrations and shear rates tested. Results showed that shear stress decreased with increasing time of shearing for all the emulsions, indicating that all BGNF stabilized emulsions exhibited thixotropic behavior. Decreases in shear stress were more pronounced in emulsion with higher concentration of BGNF and SFO at higher shear rates.

Table 4.14 Weltman model parameter for emulsion stabilized with BGNF[1]

BGNF (%w/w)	SFO (% w/w)	$\gamma\ (s^{-1})$	$A\ (Pa)$	$-B\ (Pa)$	R^2	$RMSE$	SE
5	30	50	11.7 ± 1.37	0.52 ± 0.18	0.99	0.03	0.04
		100	19.8 ± 5.92	0.99 ± 0.44	0.99	0.10	0.10
		150	24.4 ± 6.52	1.20 ± 0.34	0.99	0.06	0.07
	35	50	21.7 ± 2.70	1.30 ± 0.28	0.99	0.12	0.12
		100	30.1 ± 1.95	1.79 ± 0.18	0.98	0.24	0.24
		150	37.7 ± 1.32	2.23 ± 0.11	0.96	0.39	0.39
	40	50	42.3 ± 1.62	2.72 ± 0.08	0.98	0.28	0.36
		100	59.8 ± 0.88	3.49 ± 0.29	0.97	0.52	0.53
		150	72.0 ± 1.47	4.36 ± 0.15	0.97	0.69	0.70
6	30	50	34.1 ± 1.73	2.02 ± 0.25	0.95	0.41	0.41
		100	42.7 ± 2.67	2.10 ± 0.34	0.95	0.43	0.43
		150	48.4 ± 2.20	2.69 ± 0.27	0.95	0.81	0.52
	35	50	39.0 ± 0.23	2.39 ± 0.22	0.99	0.16	0.16
		100	69.7 ± 4.23	4.45 ± 0.42	0.96	0.80	0.81
		150	92.0 ± 3.45	6.01 ± 0.62	0.95	1.18	1.20
	40	50	85.3 ± 8.43	4.99 ± 0.80	0.98	0.58	0.59
		100	129 ± 15.08	8.72 ± 1.40	0.97	1.35	1.36
		150	167 ± 6.40	11.8 ± 1.15	0.95	2.17	2.20
7	30	50	46.0 ± 2.03	2.61 ± 0.19	0.93	0.62	0.63
		100	57.4 ± 2.97	3.45 ± 0.34	0.94	0.70	0.72
		150	66.5 ± 6.25	3.97 ± 0.52	0.94	0.87	0.88
	35	50	79.2 ± 6.64	4.74 ± 0.35	0.96	0.80	0.82
		100	104 ± 8.89	6.50 ± 0.64	0.96	1.16	1.18
		150	129 ± 10.7	8.15 ± 0.90	0.93	1.82	1.85
	40	50	263 ± 27.1	22.0 ± 2.66	0.99	1.87	1.90
		100	296 ± 11.9	24.1 ± 0.60	0.97	3.39	3.42
		150	315 ± 4.29	25.5 ± 0.09	0.95	5.04	5.13

[1]γ is the shear rate (s^{-1}); A is the initial shear stress (Pa); B is the extent of thixotropy (Pa); R^2 is the coefficient of determination between the experimental data and predicted Weltman model data;RMSE refers to the root mean square error between the experimental and predicted model data; SE refers to the standard error value between the experimental and predicted model data.

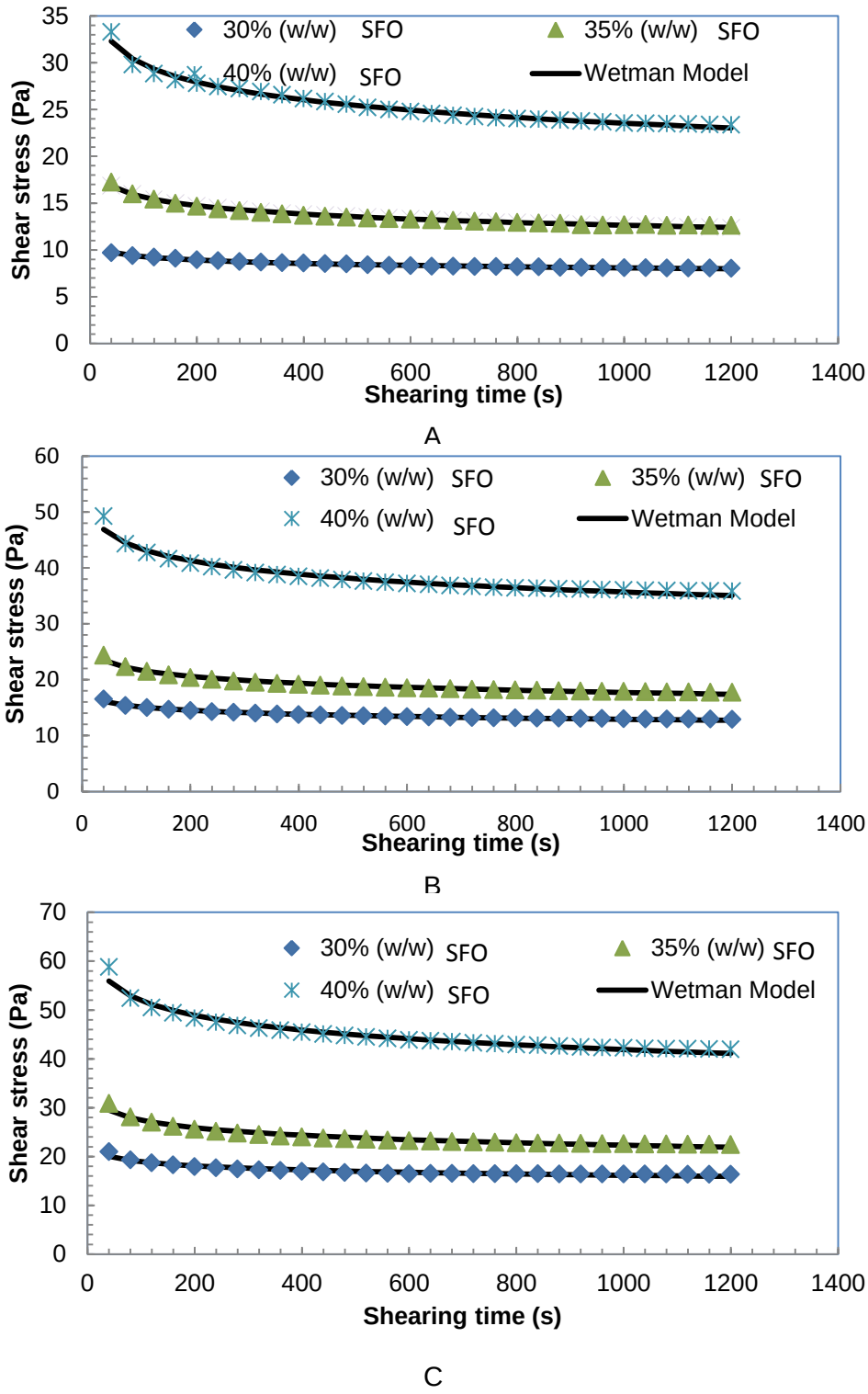

Figure 4.21 **Shear stress Vs shearing time of emulsions stabilized with 5% (w/w) BGNF (A) 50 s^{-1} (B) 100 s^{-1} (C) 150 s^{-1} modeling with Weltman equation**

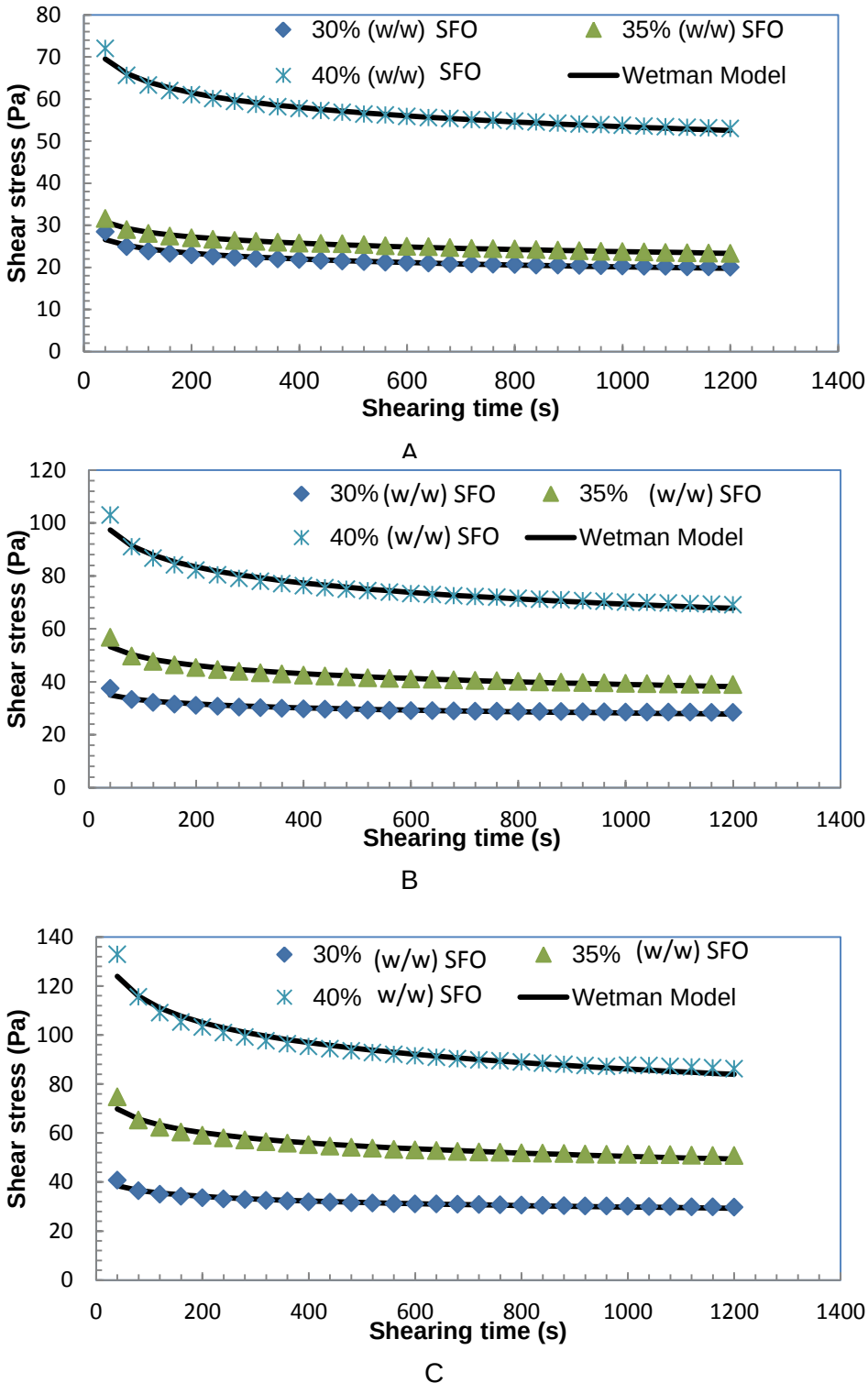

Figure 4.22 **Shear stress Vs shearing time of emulsions stabilized with 6% (w/w) BGNF (A) 50 s^{-1} (B) 100 s^{-1} (c) 150 s^{-1} modeling with Weltman equation**

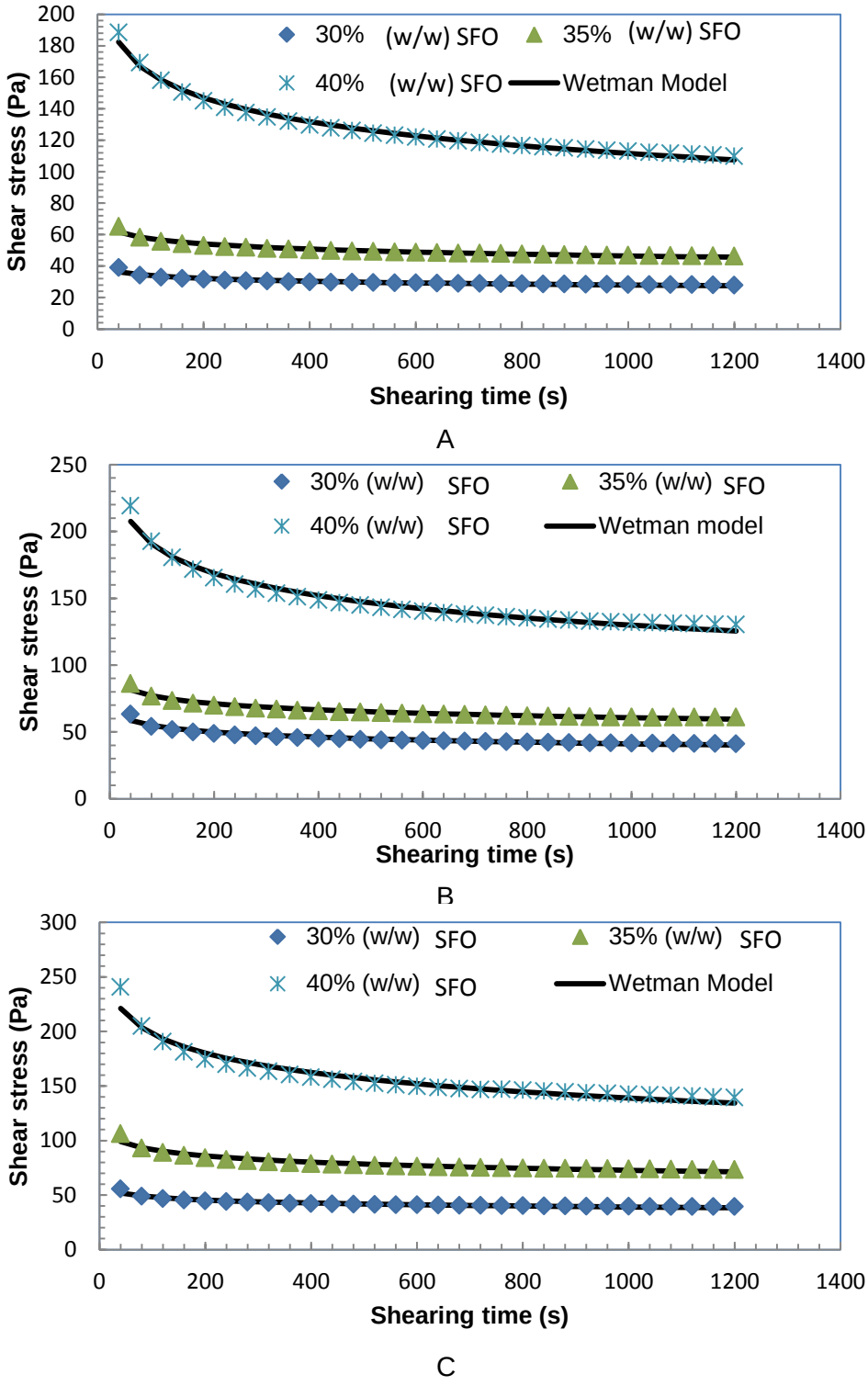

Figure 4.23 **Shear stress Vs shearing time of emulsions stabilized with 7% (w/w) BGNF (A) 50 s^{-1} (B) 100 s^{-1} (c) 150 s^{-1} modeling with Weltman equation.**

The same results were obtained for *Alyssum homolocarpmum* seed solution (Koocheki and Razavi, 2009) and low-fat sesame pastes (Razavi *et al.,* 2008).

The three-way analysis of variance showed that the coefficients of Weltman model were also significantly affected by concentration of BGNF, SFO and shear rate. In addition, other interaction effects including the interaction of BGNF, SFO and shear rate had significant effect on Weltman model parameters (Table 4.15). In all the emulsions, parameters *A* and *B* increased significantly as the shear rate increased. The increase in *B* with increase in shear rate is in agreement with that of Razavi *et al.* (2008) and Razavi and Karazhian (2009) for low fat sesame paste/date syrup blend and Salep respectively. It is however in contrast with the report of Nguyen *et al.* (1998) that *B* decreased with increased shear rate for maize and waxy starch pastes. Also parameters *A* and *B* increased significantly with increase in SFO and BGNF concentrations. For example, at a constant shear rate of 50 s^{-1} and SFO concentration of 30% (w/w), *A* and *B* values, increased from 11.68 ± 1.37 to 46.04 ± 2.03 Pa and 0.52 ± 0.18 to 2.61 ± 0.19 Pa for 5 to 7% (w/w) BGNF, respectively.

Table 4.15 Adjusted mean square for coefficient of Weltman model at different concentration of BGNF and SFO and shear rate[1]

Source of variation	df	*A (Pa)*	p	*B (Pa)*	p
BGNF	2	91866.50	<0.0001	590.88	<0.0001
SFO	2	106590.63	<0.0001	723.31	<0.0001
SRT	2	9139.41	<0.0001	42.71	<0.0001
BGNF*SFO	4	26843.58	<0.0001	243.39	<0.0001
SRT*BGNF	4	546.37	<0.0001	3.94	<0.0001
SRT*SFO	4	866.48	<0.0001	5.42	<0.0001
SRT*BGNF*SFO	8	155.25	0.0212	1.51	0.0114
Error	54	61.79	<0.0001	0.54	<0.0001

[1]A is the initial shear stress of the Weltman model; B is the extent of thixotropy.; BGNF equals bambara groundnut flour; SFO is sunflower oil; BGNF*SFO is the interaction between the bambara groundnut flour and sunflower oil; SRT*BGNF refers to the interaction between the shear rate of shearing and bambara groundnut flour; SRT*SFO refers to the interaction between shear rate and sunflower oil; SRT*BGNF*SFO is the interaction between the shear rate, bambara groundnut and sunflower oil.

Similar increase was observed at constant shear rates of 100 and 150 s^{-1} and at all the three levels of BGNF. The same trend was also observed when SFO concentration was increased from 30 to 40% (w/w) at constant BGNF concentration for all shear rates studied. In other word, increased BGNF and SFO concentration in the emulsion led to increased initial stress value which can be interpreted as an increased viscosity (Razavi and Habibi-Najafi, 2006, Razavi *et al.,* 2010). The larger the *B* value the greater the departure from thixotropy behavior (Razavi and Habibi-Najafi, 2006). Increased degree of thixotropy as a function of both emulsion components indicated increased structural breakdown. Emulsions formulated with lower concentrations of SFO and BGNF were less thixotropic at all shear rates. Emulsion formulated with 5% (w/w) BGNF and 30% (w/w) SFO possessed the lowest values of parameters *A* and *B*, while the highest values of parameters *A* and *B* belonged to sample formulated with 7% (w/w) and 40% (w/w) SFO. It is interesting to know that emulsions formulated with 7% (w/w) BGNF and 40% (w/w) SFO also possessed the highest initial backscattering (BS_{AVo} (%)) and equilibrium backscattering (BS_{eq}) and hence highest stability. The high stability possessed by the emulsion probably originated from its high viscosity (parameter *A*) which could be as a result of high structural network formed by the BGNF-SFO interactions. Razavi and Habibi-Najafi (2006) also linked emulsion stability to increased Weltman parameter *A* and *B*.

4.3.2.2 Thixotropic modeling of BGNF stabilized emulsion using Hahn model

The observed time dependent flow properties of BGNF stabilized emulsions were modeled by Hahn model (Equation 3.9). The *P* parameter in Hahn model represents initial shear stress (Pa), α indicates rate of structural breakdown for the sample (s^{-1}) and τ_e is the equilibrium shear stress value. Figures 4.24, 4.25 and 4.26 showed the effect of shearing time on the shear stress of concentrated oil-in-water emulsions containing 30, 35 and 40% (w/w) SFO, stabilized with 5, 6 and 7% (w/w) BGNF concentrations. As shown in the Figures, the Hahn model (solid line), fitted well the relationship between shear stress and shearing time of concentrated oil-in-water emulsions stabilized with BGNF for all BGNF and SFO concentrations and at all shear rates. Singla *et al.* (2013) and Razavi *et al.* (2010) also found Hahn model suitable to characterize the time dependent flow behavior of mayonnaise and pistachio butter, respectively. The coefficients of Hahn model were significantly affected by concentration of BGNF, SFO and shear rate (SRT) (Table 4.16). In addition, except for the interaction of SRT, BGNF and SFO all other linear and interaction effects were significant on τ_e. The linear effect of BGNF, SFO and SRT and interaction effect of BGNF and SFO, and SRT, BGNF and SFO were significant on parameters α and *P*.

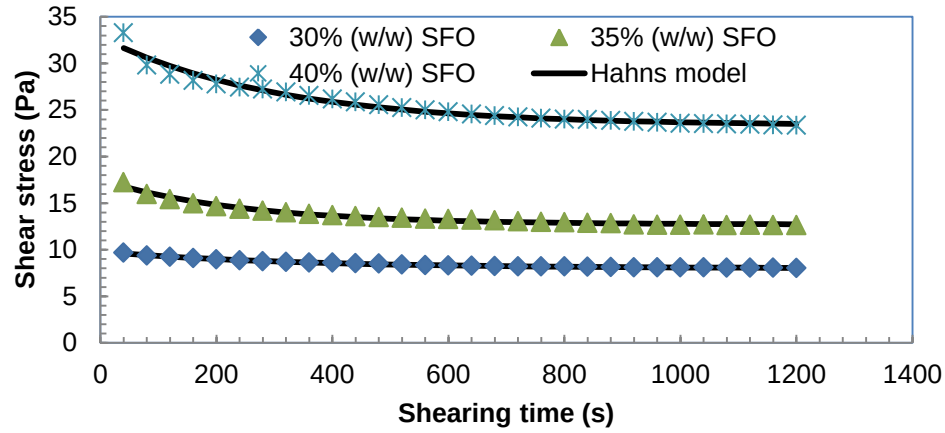

A

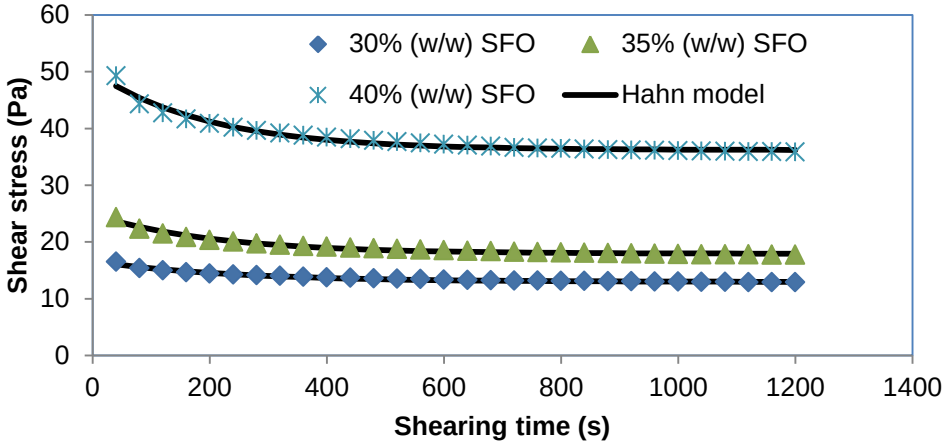

B

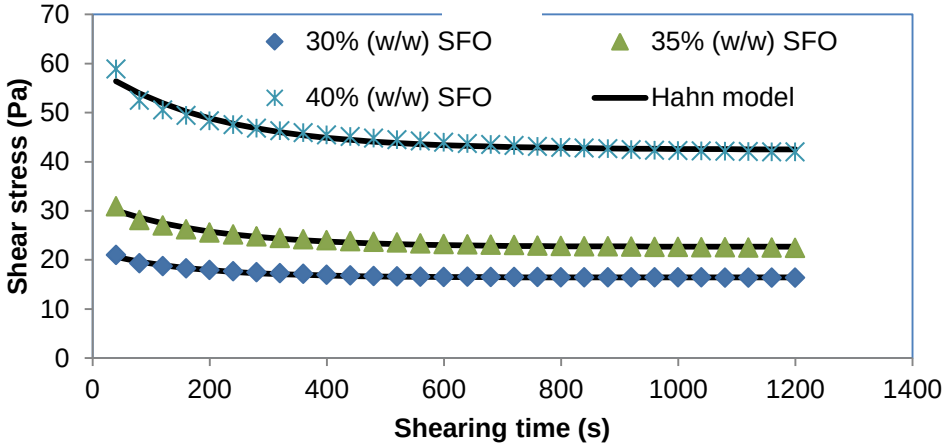

C

Figure 4.24 **Shear stress Vs shearing time of emulsions stabilized with 5% (w/w) BGNF (A) 50 s^{-1} (B) 100 s^{-1} (c) 150 s^{-1} modeling with Hahn- Re equation**

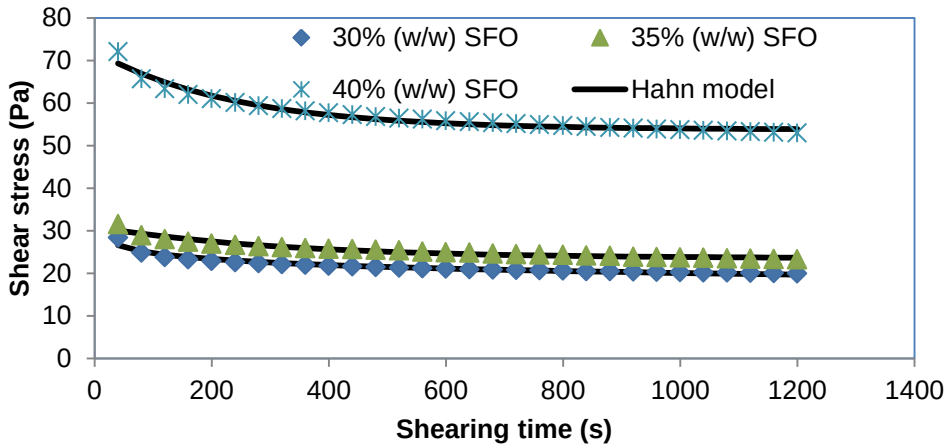

A

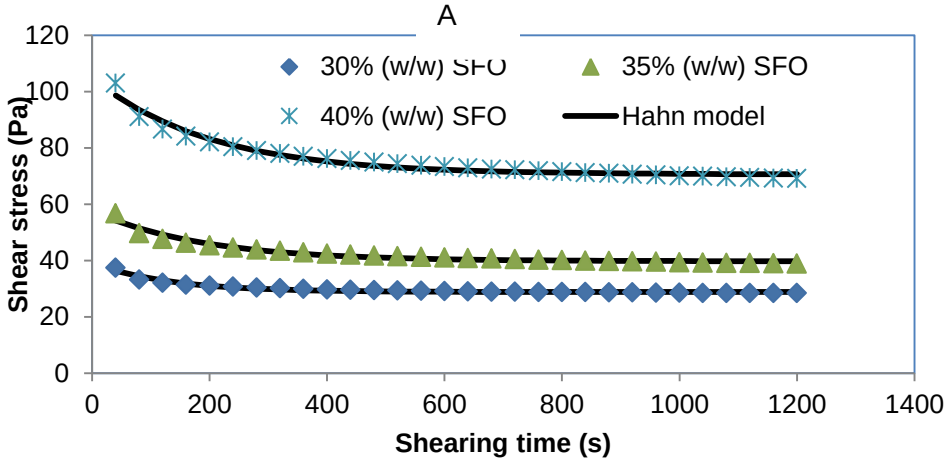

B

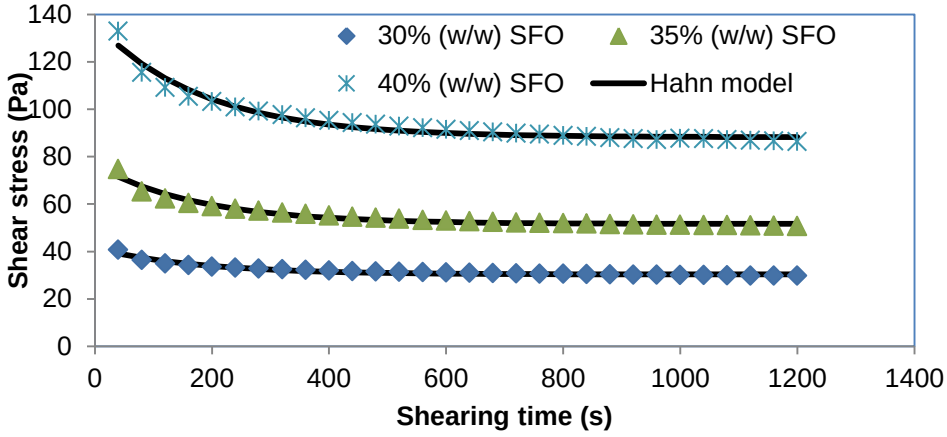

C

Figure 4.25 **Shear stress Vs shearing time of emulsions stabilized with 6% (w/w) BGNF (A) 50 s^{-1} (B) 100 s^{-1} (c) 150 s^{-1} modeling with Hahn - Re equation.**

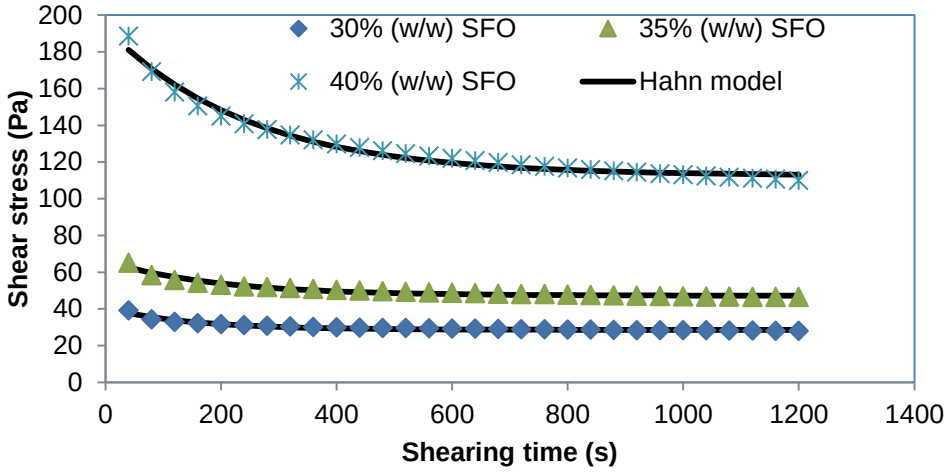

A

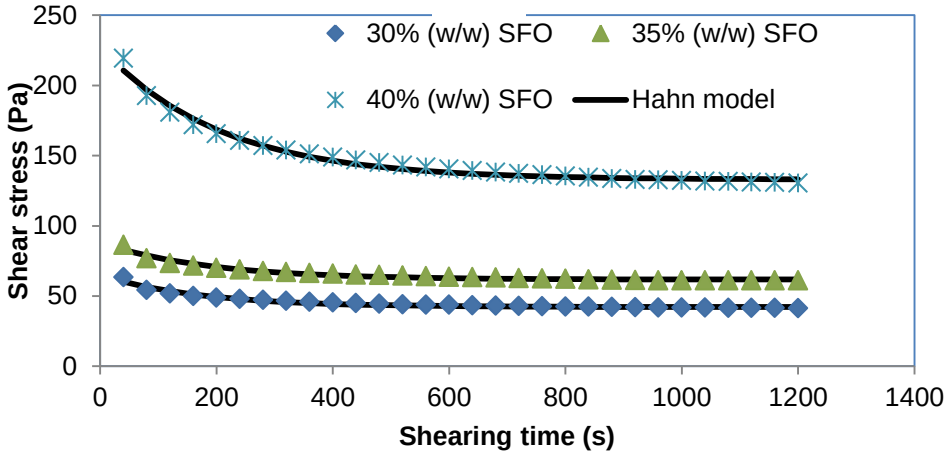

B

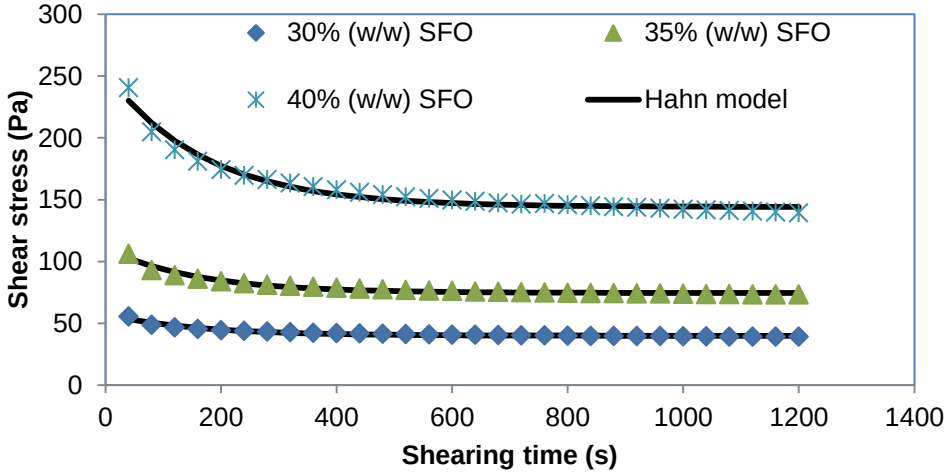

C

Figure 4.26 **Shear stress Vs shearing time of emulsions stabilized with 7% (w/w) BGNF (A) 50 s^{-1} (B) 100 s^{-1} (c) 150 s^{-1} modeling with Hahn- Re equation**

Table 4.16 Adjusted mean square for coefficient of Hahn model at different concentrations of BGNF and SFO and shear rate[1].

Source of variation	df	Υ_e	p	*P*	p	α x10^{-7}	p
BGNF	2	19564.76	<0.0001	17.72	<0.0001	83.9	<0.0001
SFO	2	20910.75	<0.0001	15.17	<0.0001	50.8	0.0004
SRT	2	27.68.99	<0.0001	3.11	<0.0001	139.9	<0.0001
BGNF*SFO	4	3411.75	<0.0001	0.41	<0.0001	24.1	0.0043
SRT*BGNF	4	99.39	<0.0001	0.10	0.013	23.8	0.0046
SRT*SFO	4	201.54	<0.0001	0.033	0.367	4.0	0.5841
SRT*BGNF*SFO	8	23.79	0.0698	0.097	0.004	21.1	0.0015
Error	54	12.14	<0.0001	0.029	<0.0001	5.6	<0.0001

[1]P is the initial shear stress of the Hahn model; ά is the structural breakdown from Hahn model; Υ_e refers to the equilibrium shear stress obtained from Hahn model; BGNF equals Bambara groundnut flour; SFO equals sunflower oil; BGNF*SFO is the interaction between the bambara groundnut flour and sunflower oil; SRT*BGNF refers to the interaction between the shear rate of shearing and bambara groundnut flour; SRT*SFO refers to the interaction between shear rate and sunflower oil; SRT*BGNF*SFO is the interaction between the shear rate, bambara groundnut and sunflower oil.

However, the interaction effects of SRT and SFO are not significant on both parameters. Table 4.17 shows the Hahn model parameters at shear rates of 50, 100 and 150 s^{-1} as a function of BGNF and SFO concentrations for the emulsions. The mean values of the initial shear stress of the emulsion ranged from 0.57 to 4.69 Pa, α value ranged from 3.10 to 5.93 s^{-1} while Υ_e is from 7.98 to 144 Pa. The high coefficient of determination, R^2 (0.93 - 0.99) and low RMSE (0.03 - 3.77) and SE (0.03 - 3.84) made Hahn model also suitable for the predictions of time-dependent characteristics of BGNF stabilized emulsions There was an increase in parameters *P,* α and Υ_e with increase in shear rate. Also parameters *P* and ά increased with increase in SFO and BGNF concentrations. This implied that, increased BGNF and SFO concentrations led to increased emulsion viscosity. The rate of structural breakdown α did not seem to have a definite trend.

Table 4.17 Hahn model parameter for emulsion stabilized with BGNF[1]

BGNF (%w/w)	SFO (%w/w)	$\gamma\ (s^{-1})$	Υ_e (Pa)	*P* (Pa)	α X10^{-3}(s^{-1})	R^2	$RMSE$	SE
5	30	50	7.98 ± 0.28	0.57 ± 0.31	3.10 ± 1.02	0.99	0.03	0.03
		100	13.0 ± 3.06	1.23 ± 0.45	4.00 ± 1.52	0.98	0.13	0.13
		150	16.3 ± 4.32	1.65 ± 0.45	6.17 ± 2.38	0.99	0.12	0.12
	35	50	12.7 ± 0.79	1.55 ± 0.24	4.03 ± 0.45	0.98	0.15	0.15
		100	17.9 ± 0.75	1.93 ± 0.12	4.73 ± 0.15	0.98	0.22	0.23
		150	22.7 ± 0.57	2.21 ± 0.07	5.33 ± 0.49	0.98	0.26	0.27
	40	50	23.3 ± 1.27	2.25 ± 0.05	3.33 ± 0.39	0.96	0.43	0.44
		100	36.2 ± 2.39	2.63 ± 0.09	5.10 ± 0.43	0.97	0.52	0.53
		150	42.5 ± 0.83	2.83 ± 0.09	4.93 ± 0.76	0.96	0.72	0.74
6	30	50	20.5 ± 0.08	2.09 ± 0.09	5.47 ± 0.40	0.93	0.45	0.45
		100	28.8 ± 0.40	2.32 ± 0.14	7.63 ± 0.66	0.95	0.43	0.43
		150	30.3 ± 0.45	2.40 ± 0.10	5.57 ± 0.05	0.95	0.51	0.52
	35	50	22.1 ± 1.47	2.10 ± 0.09	3.00 ± 0.20	0.96	0.37	0.38
		100	39.7 ± 1.39	2.89 ± 0.08	5.33 ± 0.35	0.96	0.80	0.82
		150	51.6 ± 1.91	3.22 ± 0.08	5.70 ± 0.61	0.96	1.01	1.02
	40	50	53.8 ± 1.74	2.90 ± 0.15	4.20 ± 0.29	0.96	0.80	0.82
		100	70.6 ± 5.62	3.53 ± 0.17	5.00 ± 0.36	0.97	1.37	1.38
		150	88.1 ± 2.52	3.87 ± 0.06	5.53 ± 0.85	0.96	1.97	2.00
7	30	50	28.6 ± 0.69	2.46 ± 0.06	6.63 ± 0.10	0.94	0.55	0.56
		100	34.5 ± 0.86	2.67 ± 0.09	5.80 ± 0.52	0.95	0.65	0.66
		150	40.0 ± 2.76	2.85 ± 0.09	6.23 ± 0.40	0.95	0.73	0.74
	35	50	47.2 ± 4.31	2.94 ± 0.07	5.17 ± 0.31	0.96	0.85	0.86
		100	61.7 ± 4.55	3.26 ± 0.11	5.33 ± 0.21	0.96	1.09	1.11
		150	74.5 ± 4.68	3.58 ± 0.17	6.33 ± 0.14	0.96	1.32	1.34
	40	50	112 ± 9.67	4.39 ± 0.14	4.13 ± 0.55	0.98	2.43	2.47
		100	132 ± 7.89	4.55 ± 0.03	4.90 ± 0.36	0.98	2.81	2.86
		150	144 ± 3.93	4.69 ± 0.04	5.93 ± 0.32	0.97	3.77	3.84

[1]BGNF equals Bambara groundnut flour; SFO equals sunflower oil; γ is the shear rate (s^{-1}); P is the initial shear stress (Pa); α is the extent of structural destruction (s^{-1}); Υ_e equals to the equilibrium shear stress estimated from Hahn model; R^2 is the coefficient of determination between the experimental data and predicted Hahn model data; RMSE refers to the root mean square error between the experimental and predicted model data; SE refers to the standard error value between the experimental and predicted model data

4.3.2.3 Thixotropic modeling of BGNF stabilized emulsion using Figoni and Shoemaker model

The thixotropic model of Figoni and Shoemaker as given in Equation 3.10 was used to fit the shear stress-time data of the emulsions for the purpose of finding its suitability to describe the time dependent behaviour and inspecting the non-zero equilibrium stress of BGNF stabilized emulsions. The decay constant (k) in the expression is a measure of the rate at which the BGNF stabilized emulsion under the influence of shear reaches the equilibrium stress values. τ_e is called the equilibrium stress and it quantifies the shear stress of the samples after a time of shearing, long enough to break the internal structure of the sample. τ_0 is the initial shear stress and represents the shear stress at the beginning of shearing process. The parameter ($\tau_o - \tau_e$) in Figoni and Shoemaker model is comparable to parameter *P* of Hahns model and *A* of Weltman model and it represents the shear stress needed to initiate the structural breakdown during shearing of the samples (Singla *et al.,* 2013).

Figures 4.27, 4.28 and 4.29 are the fittings of the experimental data of shear stress versus shearing time of emulsions containing 30, 35 and 40% (w/w) SFO stabilized with 5, 6 and 7% (w/w) BGNF respectively for Figoni and Shoemaker model. The experimental data were well fitted to Figoni and Shoemaker model (solid lines). The prediction of Figoni and Shoemaker model was similar to the prediction of Weltman and Hahn model. Table 4.18 shows that the coefficients of Figoni and shoemaker model were significantly affected by individual levels and interactions of BGNF, SFO and shear rate. Apart from the interaction of shear rate, BGNF and SFO on the equilibrium stress value, τ_e and interaction of SFO and SRT on k parameter, all other interaction effects were significant ($p < 0.05$) on the model parameters. Parameters of Figoni and Shoemaker model at shear rate of 50, 100 and 150 s^{-1} as a function of BGNF and SFO concentrations for the BGNF stabilized emulsion samples are shown in Table 4.19. The mean values of initial stress, τ_0, ranged from 9.82 to 253 Pa., equilibrium shear stress, τ_e, was from 7.98 to 144 Pa while the decay constant (k) was from 3.10 E-3 to 7.63 E-3 s^{-1}. The high R^2 (0.93 - 0.99) and low RMSE (0.03 – 3.77) and SE (0.03 – 3.84) made Figoni and Shoemaker model suitable for the prediction of thixotropic characteristics of the BGNF stabilized emulsion. Figoni and Shoemaker model was also found suitable for the description of thixotropic properties of several food stuffs (such as tomato juice (Augusto *et al.,* 2012); mayonnaise (Figoni and Shoemaker 1981), Gilaboru Juice (*Viburnum opulus* L) (Altan *et al.,* 2005)) and hydrocolloids such as *Alyssum homolocarpum* seed gum solution (Koocheki and

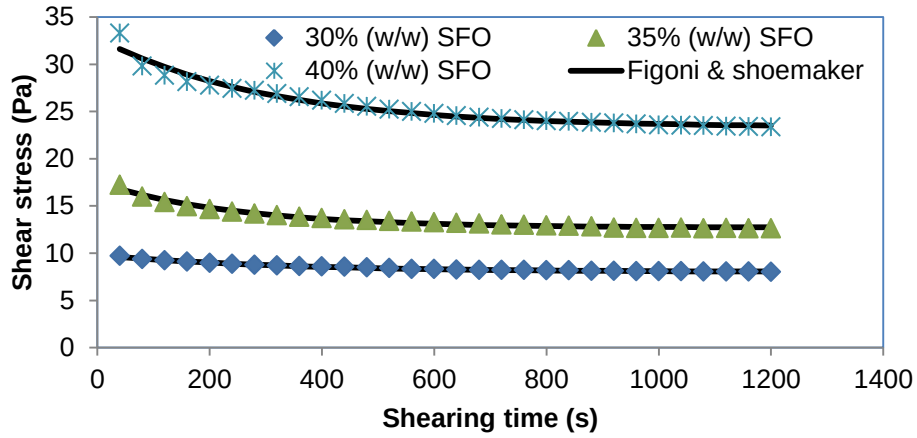

A

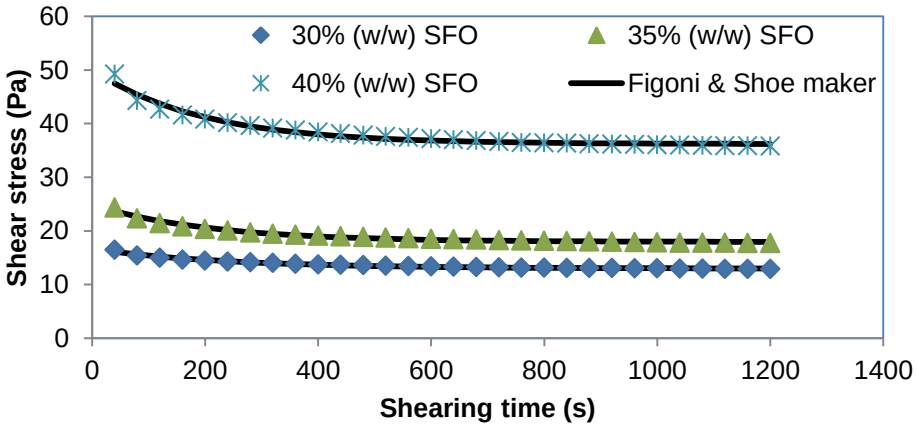

B

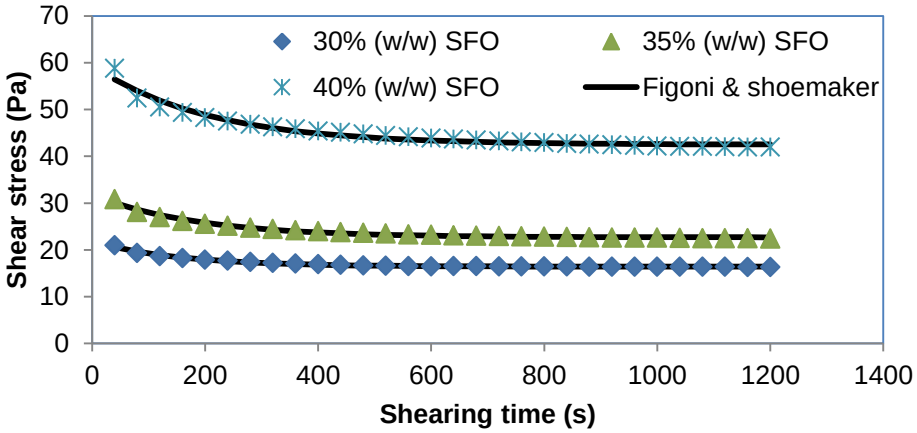

C

Figure 4.27 Shear stress Vs shearing time of emulsions stabilized with 5% (w/w) BGNF (A) 50 s^{1} (B) 100 s^{-1} (C) 150 s^{-1}modeling with Figoni & Shoemaker equation

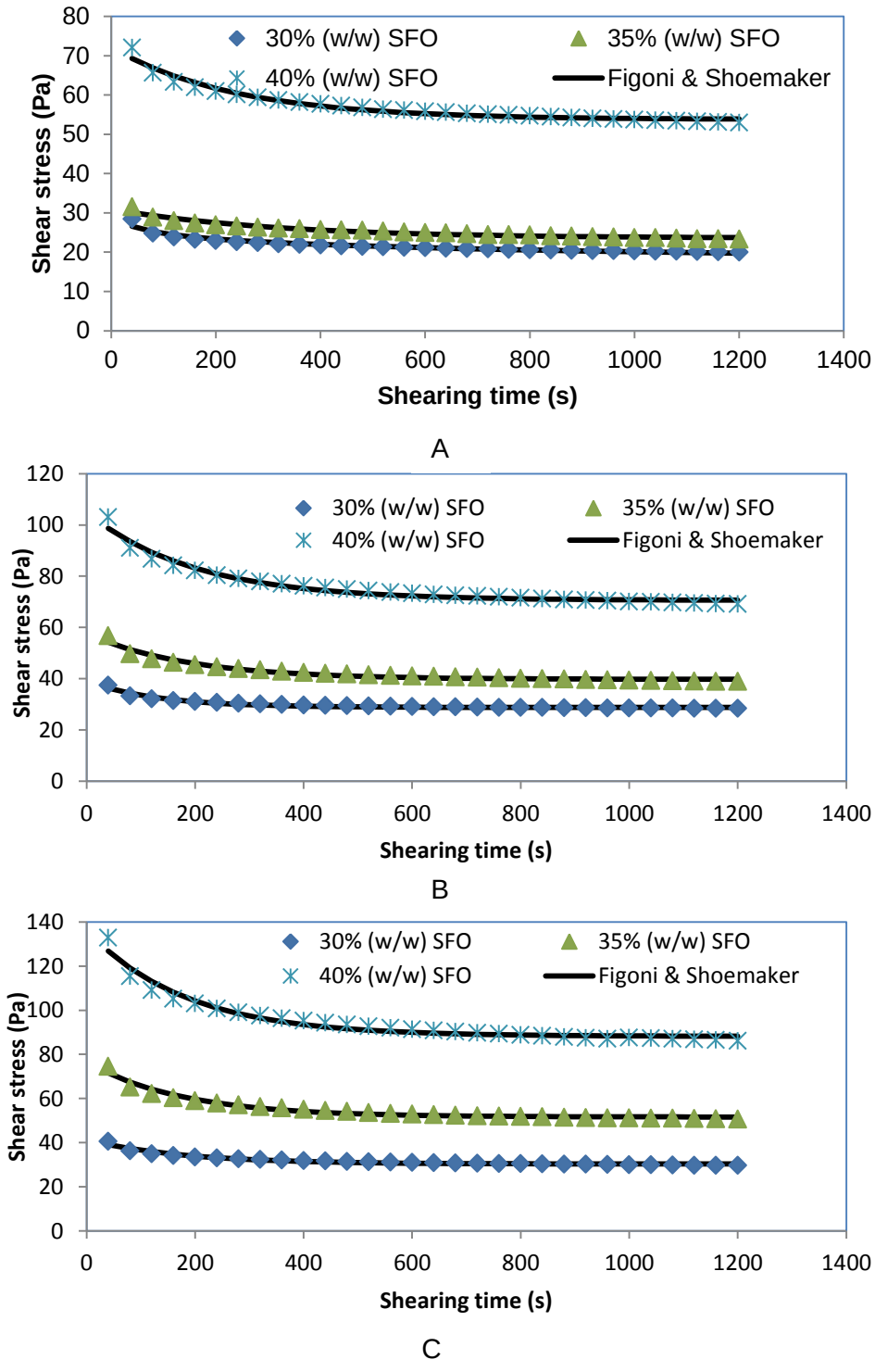

Figure 4.28 **Shear stress Vs shearing time of emulsions stabilized with 6% (w/w) BGNF (A) 50 s^{-1} (B) 100 s^{-1} (C) 150 s^{-1}modeling with Figoni & Shoemaker equation**

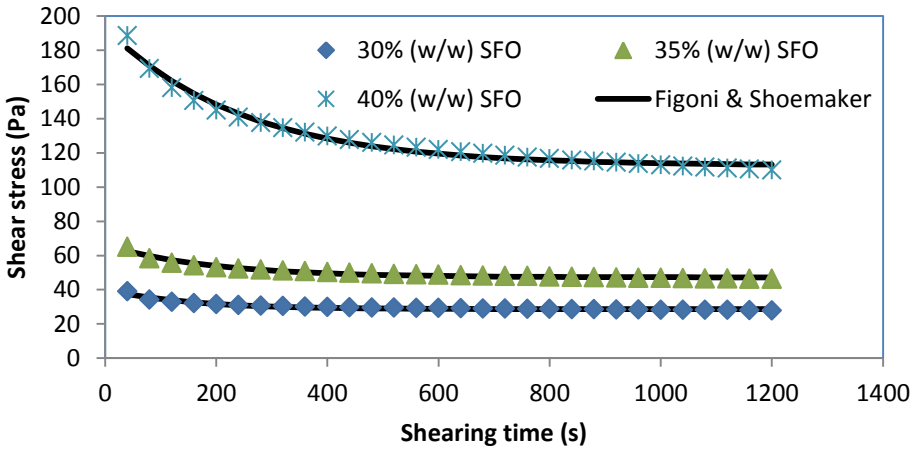

A

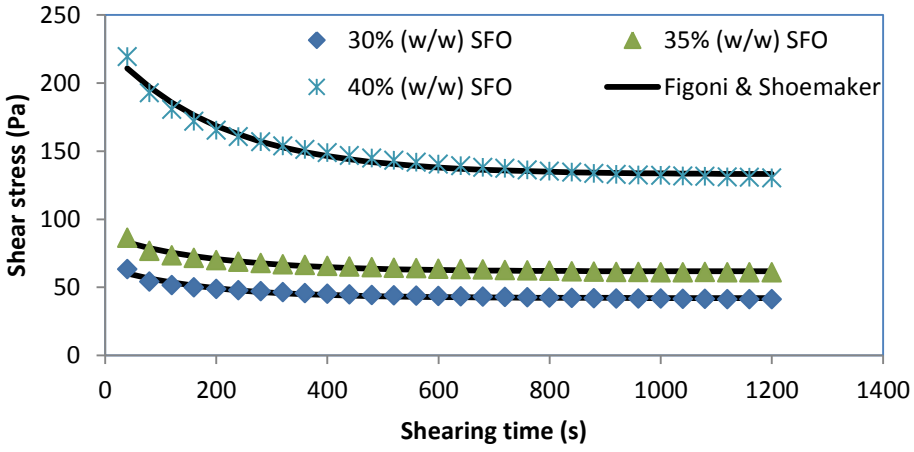

B

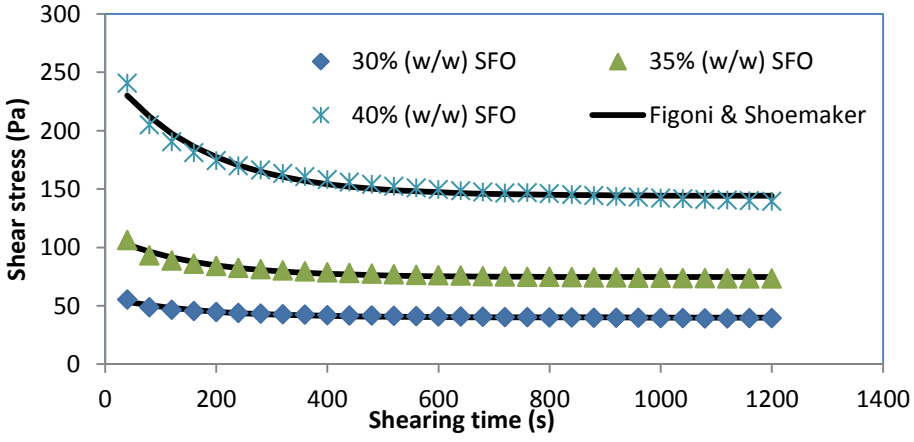

C

Figure 4.29 **Shear stress Vs shearing time of emulsions stabilized with 7% (w/w) BGNF (A) 50 s^{-1} (B) 100 s^{-1} (C) 150 s^{-1}modeling with Figoni & Shoemaker equation**

Razavi, 2009). The Figoni and Shoemaker model parameters were found to depend on BGNF, SFO and SRT at all levels.

Table 4.18 Adjusted mean square for coefficient of Figoni and shoemaker model at different concentration of BGNF and SFO and shear rate[1]

Source of variation	df	Υ_0	p	Υ_e	p	k x10^{-7}	p
BGNF	2	56944.27	<0.0001	19567.35	<0.0001	84.2	<0.0001
SFO	2	61976.32	<0.0001	20910.19	<0.0001	50.6	0.0004
SRT	2	7394.46	<0.0001	2768.03	<0.0001	139.8	<0.0001
BGNF*SFO	4	14142.50	<0.0001	3411.98	<0.0001	24.3	0.0041
SRT*BGNF	4	397.01	<0.0001	99.58	<0.0001	23.9	0.0045
SRT*SFO	4	745.70	<0.0001	201.17	<0.0001	4.0	0.5837
SRT*BGNF*SFO	8	88.04	0.0285	23.97	0.0680	21.1	0.0014
ERROR	54	37.05	<0.0001	12.16	<0.0001	35.7	<0.0001

Υ_0 is the initial shear stress and k is the structural breakdown obtained from Figoni and shoemaker model; Υ_e refers to the equilibrium shear stress obtained from Figoni and shoemaker model; BGNF equals Bambara groundnut flour; SFO equals sunflower oil; SRT is the shear rate; BGNF*SFO is the interaction between the bambara groundnut flour and sunflower oil; SRT*BGNF refers to the interaction between the shear rate of shearing and bambara groundnut flour; SRT*SFO refers to the interaction between shear rate and sunflower oil; SRT*BGNF*SFO is the interaction between the shear rate, bambara groundnut and sunflower oil.

All parameters of Figoni and Shoemaker model for BGNF stabilized emulsion increased as the SRT level increased. Similar reports were documented for egg and eggless mayonnaise (Singla *et al.,* 2013), Salep (Razavi and Karazhiya, 2009), gilabaoru juice (Altan *et al.,* 2005), tomato juice (Augosto *et al.,* 2012) and sesame paste (Abu-Jdayil, 2002). Both Υ_e and Υ_o showed dependence on the BGNF and SFO concentrations. Increased BGNF and SFO concentrations led to increased initial stress, Υ_o and equilibrium stress, Υ_e. However no clear relationship was found between the decay constant k, BGNF and SFO concentrations. Koocheki *et al.* (2009) also reported a no-trend relationship between decay constant, k and gum concentration for *Alyssum homolocarpum* seed gum. Emulsions containing least SFO (30% (w/w) at all levels of BGNF and SRT recorded the lowest Υ_e and Υ_o. This implied that all the emulsions formulated with 30% (w/w) SFO irrespective of BGNF concentrations had lowest initial and final apparent viscosity. The highest value of Υ_e however belonged to emulsion formulated with 7% (w/w) BGNF and 40% (w/w) SFO.

Table 4.19 Figoni and Shoe maker model parameter for emulsion stabilized with BGNF[1]

BGNF (% w/w)	SFO (% w/w)	γ (s^{-1})	Υ_e (Pa)	Υ_0 (Pa)	k X10^{-3}(s^{-1})	R^2	$RMSE$	SE
5	30	50	7.98 ± 0.28	9.82 ± 0.67	3.10 ± 0.89	0.99	0.03	0.03
		100	13.0 ± 3.06	16.7 ± 4.88	4.00 ± 0.99	0.98	0.13	0.13
		150	16.4 ± 4.38	22.0 ± 6.99	6.17 ± 2.38	0.99	0.12	0.12
	35	50	12.7 ± 0.79	17.5 ± 1.90	4.03 ± 0.45	0.98	0.15	0.15
		100	17.9 ± 0.75	24.9 ± 0.12	4.73 ± 0.15	0.98	0.22	0.23
		150	22.7 ± 0.57	31.8 ± 0.07	5.33 ± 0.49	0.98	0.26	0.27
	40	50	23.3 ± 1.27	32.8 ± 0.04	3.33 ± 0.38	0.96	0.43	0.44
		100	36.2 ± 2.39	50.1 ± 0.09	5.10 ± 0.43	0.97	0.52	0.53
		150	42.5 ± 0.83	59.4 ± 0.09	4.93 ± 0.76	0.96	0.72	0.74
6	30	50	20.5 ± 0.08	28.6 ± 0.09	5.47 ± 0.40	0.93	0.45	0.45
		100	28.8 ± 0.40	39.0 ± 1.82	7.63 ± 0.66	0.95	0.43	0.43
		150	30.3 ± 0.45	41.3 ± 1.48	5.57 ± 0.05	0.95	0.51	0.52
	35	50	22.1 ± 1.47	30.3 ± 0.73	3.00 ± 0.20	0.96	0.37	0.38
		100	39.7 ± 1.39	57.7 ± 2.81	5.33 ± 0.35	0.96	0.80	0.82
		150	51.6 ± 1.91	76.6 ± 0.08	5.70 ± 0.61	0.96	1.01	1.02
	40	50	53.8 ± 1.74	72.2 ± 4.39	4.20 ± 0.29	0.96	0.80	0.82
		100	70.6 ± 5.62	104 ± 10.8	5.00 ± 0.36	0.97	1.37	1.38
		150	88.1 ± 2.52	136 ± 3.87	5.53 ± 0.85	0.96	1.97	2.00
7	30	50	28.6 ± 0.69	40.3 ± 1.06	6.63 ± 0.10	0.94	0.55	0.56
		100	34.5 ± 0.86	49.0 ± 1.89	5.80 ± 0.52	0.95	0.65	0.66
		150	40.0 ± 2.76	57.2 ± 4.32	6.23 ± 0.40	0.95	0.73	0.74
	35	50	47.2 ± 4.31	66.1 ± 5.57	5.17 ± 0.31	0.96	0.85	0.86
		100	61.7 ± 4.55	88.0 ± 7.36	5.33 ± 0.21	0.96	1.09	1.11
		150	74.5 ± 4.68	110 ± 9.57	6.33 ± 0.14	0.96	1.32	1.34
	40	50	112 ± 9.67	193 ± 20.4	4.13 ± 0.55	0.98	2.43	2.47
		100	133 ± 7.89	227 ± 8.28	4.90 ± 0.36	0.98	2.81	2.86
		150	144 ± 3.93	253 ± 7.11	5.93 ± 0.32	0.97	3.77	3.84

[1]BGNF equals Bambara groundnut flour; SFO equals sunflower oil; γ is the shear rate (s^{-1}); Υ_0 is the initial shear stress (Pa); k is the extent of structural destruction obtained from Figoni and shoemaker model (Pa); Υ_e refers to the equilibrium shear stress (Pa); R^2 is the coefficient of determination between the experimental data and predicted Figoni and shoemaker model data; RMSE refers to the root mean square error between the experimental and predicted model data; SE refers to the standard error value between the experimental and predicted model data.

This implied that emulsion formulated with 7% (w/w) BGNF and 40% (w/w) SFO was the most viscous (most structured) even after shearing for 1200 seconds compared to other formulations.

4.3.2.4 Thixotropic modeling of BGNF stabilized emulsion using first order stress decay with a zero equilibrium stress value model

The shear stress decay time data were fitted to first order stress decay with a zero equilibrium stress value model (Eq. 3.11). The parameters τ_o and k of first order stress decay with a zero equilibrium model are comparable to the parameters of Figoni and Shoemaker model. τ_o is a measure of the initial stress value and k is the rate of breakdown of the BGNF stabilized emulsions. Table 4.20 shows the parameters of first order stress decay with a zero equilibrium model obtained using a least square technique. The low R^2 (0.61 - 0.86) and high RMSE (0.17 – 12.0) and SE (0.17 – 12.2) is an indication that this model was not suitable for describing the time-dependent behaviour of BGNF stabilized emulsions. Razavi and Karazhiyan (2009) also reported non-suitability of first-order stress decay model for describing the time dependent properties of selected hydrocolloids. This model was however found appropriate for milled sesame (tehineh) (Abu-Jdayil *et al.,* 2002). The mean values of parameters of first order stress decay model with a zero equilibrium stress values were found in the range of 9.22 - 193 Pa and 1.39 - 3.90 s^{-1} for τ_o and k, respectively. τ_o and k for hydrocolloid obtained from Balangu seed were also reported to be in the range of 134.18 - 144.62 Pa and 0.0096 – 0.0023 s^{-1}, respectively when sheared between the shear rate of 50 s^{-1} and 150 s^{-1} (Razavi and Karazhiyan, 2009).

Figure 4.30, 4.31 and 4.32 show the fittings of the model to the experimental data. The experimental data were not perfectly described by this model. However, the first order stress decay with a zero equilibrium model indicated that all BGNF stabilized emulsions were time dependent and exhibited thixotropic behavior. The analysis of variance (ANOVA) table showing the significance of the linear and interaction effects of BGNF, SFO and shear rate levels on the first order stress decay with a zero equilibrium model parameters is in Table 4.21. The coefficients of the model were significantly affected by individual components and interactions of BGNF, SFO and shear rate. Except for the interaction of shear rate, BGNF and SFO, all other linear and interaction effects were significant ($p < 0.05$) on the initial stress value, τ_o. The linear effect of SRT and the interaction effects of SRT and BGNF, SRT and SFO were not significant on k however, the linear effect of SFO and BGNF and their interaction and interaction of BGNF, SFO and SRT were significant on k parameter. Similar to other examined models, the coefficients of first-order stress decay with a zero equilibrium model were dependent on the BGNF, SFO and shear rate at all

Table 4.20 Parameters of first-order stress-decay with a zero equilibrium stress value model for emulsion stabilized with BGNF[1]

BGNF (% w/w)	SFO (% w/w)	$\gamma\ (s^{-1})$	$\tau_0\ (Pa)$	kX10^{-4}	R^2	$RMSE$	SE
5	30	50	9.22 ± 0.57	1.39 ± 0.48	0.86	0.17	0.17
		100	15.0 ± 3.83	1.56 ± 0.47	0.78	0.39	0.40
		150	18.6 ± 4.75	1.42 ± 0.14	0.62	0.64	0.65
	35	50	15.5 ± 1.35	2.09 ± 0.31	0.79	0.50	0.51
		100	21.5 ± 1.09	2.01 ± 1.17	0.75	0.76	0.77
		150	27.0 ± 0.79	1.96 ± 0.53	0.70	1.04	1.05
	40	50	29.5 ± 1.21	2.39 ± 0.06	0.82	0.96	0.78
		100	43.0 ± 1.73	1.94 ± 0.26	0.72	1.57	1.60
		150	51.1 ± 0.76	2.07 ± 0.05	0.73	1.91	1.93
6	30	50	24.6 ± 0.85	1.92 ± 0.20	0.71	0.93	0.95
		100	32.5 ± 1.03	1.43 ± 0.02	0.61	1.16	1.18
		150	35.4 ± 0.95	1.96 ± 0.17	0.71	1.24	1.27
	35	50	27.7 ± 0.76	2.25 ± 0.04	0.86	0.75	0.76
		100	48.4 ± 2.28	2.23 ± 0.01	0.72	2.02	2.05
		150	63.1 ± 1.29	2.32 ± 0.03	0.69	2.85	2.90
	40	50	64.1 ± 3.64	1.90 ± 0.02	0.78	1.98	2.02
		100	87.9 ± 8.59	2.47 ± 0.02	0.74	3.79	3.86
		150	111 ± 1.65	2.65 ± 0.03	0.71	5.40	5.49
7	30	50	33.4 ± 1.18	1.80 ± 0.10	0.66	1.31	1.34
		100	41.1 ± 0.98	2.03 ± 0.02	0.69	1.65	1.67
		150	47.3 ± 3.85	1.97 ± 0.05	0.67	1.96	1.99
	35	50	56.5 ± 4.99	2.03 ± 0.05	0.73	2.11	2.15
		100	74.3 ± 5.55	2.10 ± 0.10	0.71	2.98	3.02
		150	89.7 ± 6.51	2.13 ± 0.02	0.66	4.09	4.16
	40	50	160.7 ± 15.1	3.90 ± 0.17	0.81	8.04	8.18
		100	182.7 ± 9.54	3.60 ± 0.10	0.76	10.1	10.3
		150	194 ± 3.64	3.50 ± 0.10	0.70	12.0	12.2

[1] BGNF equals bambara groundnut flour; SFO equals sunflower oil; γ is the shear rate (s^{-1}); τ_0 is the initial shear stress (Pa); k is the extent of structural destruction obtained from First-order stress-decay with a zero equilibrium stress value model (Pa); τ_e refers to the equilibrium shear stress (Pa); R^2 is the coefficient of determination between the experimental data and predicted First-order stress-decay with a zero equilibrium stress value model data; RMSE refers to the root mean square error between the experimental and predicted model data; SE refers to the standard error value between the experimental and predicted model data;

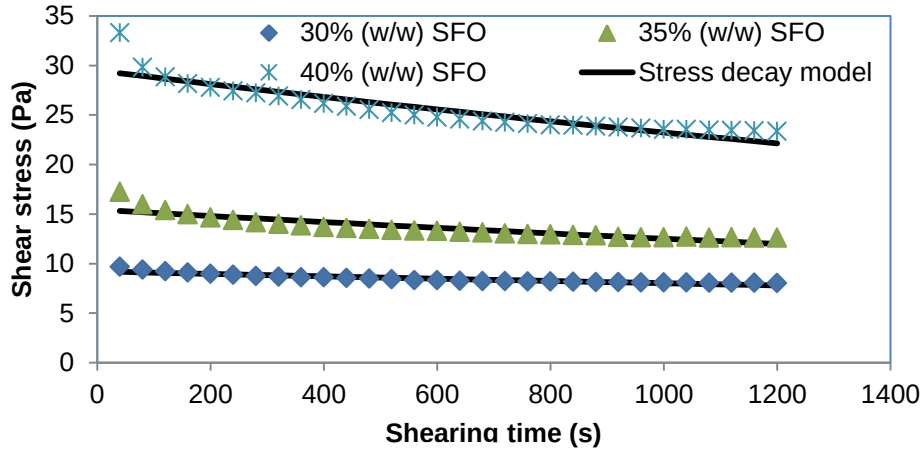

A

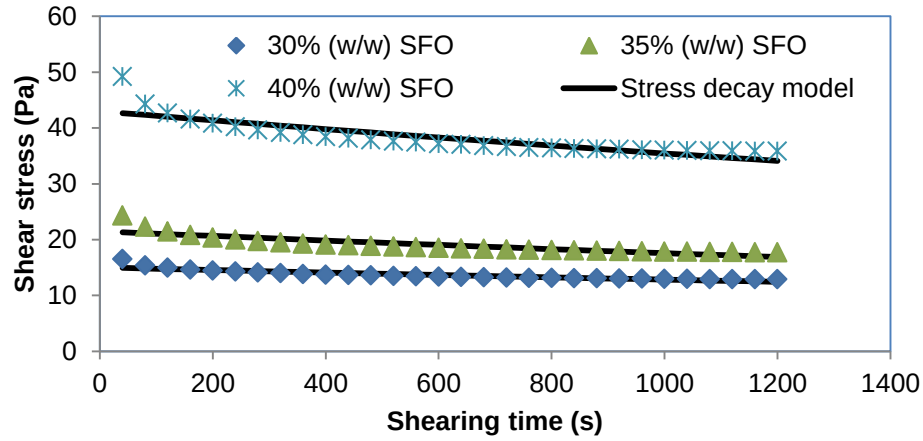

B

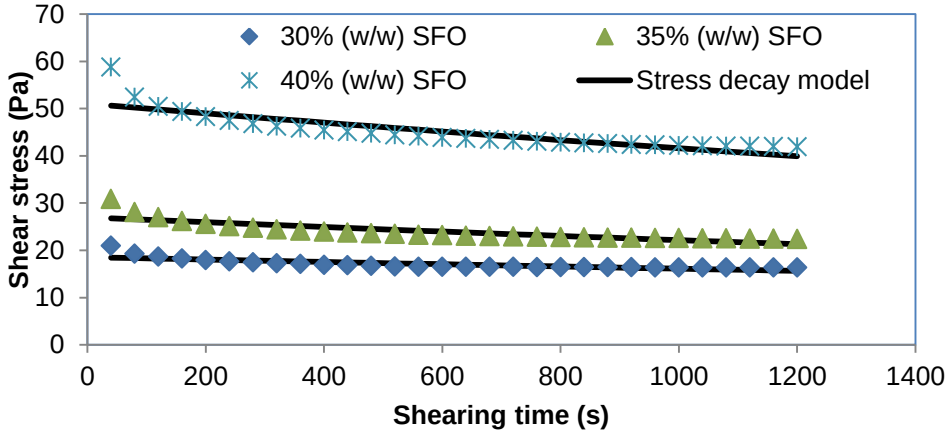

C

Figure 4.30 **Shear stress Vs shearing time of emulsions stabilized with 5% (w/w) BGNF (A) 50 s^{-1} (B) 100 s^{-1} (C) 150 s^{-1} modeling with first order stress decay with zero equilibrium equation**

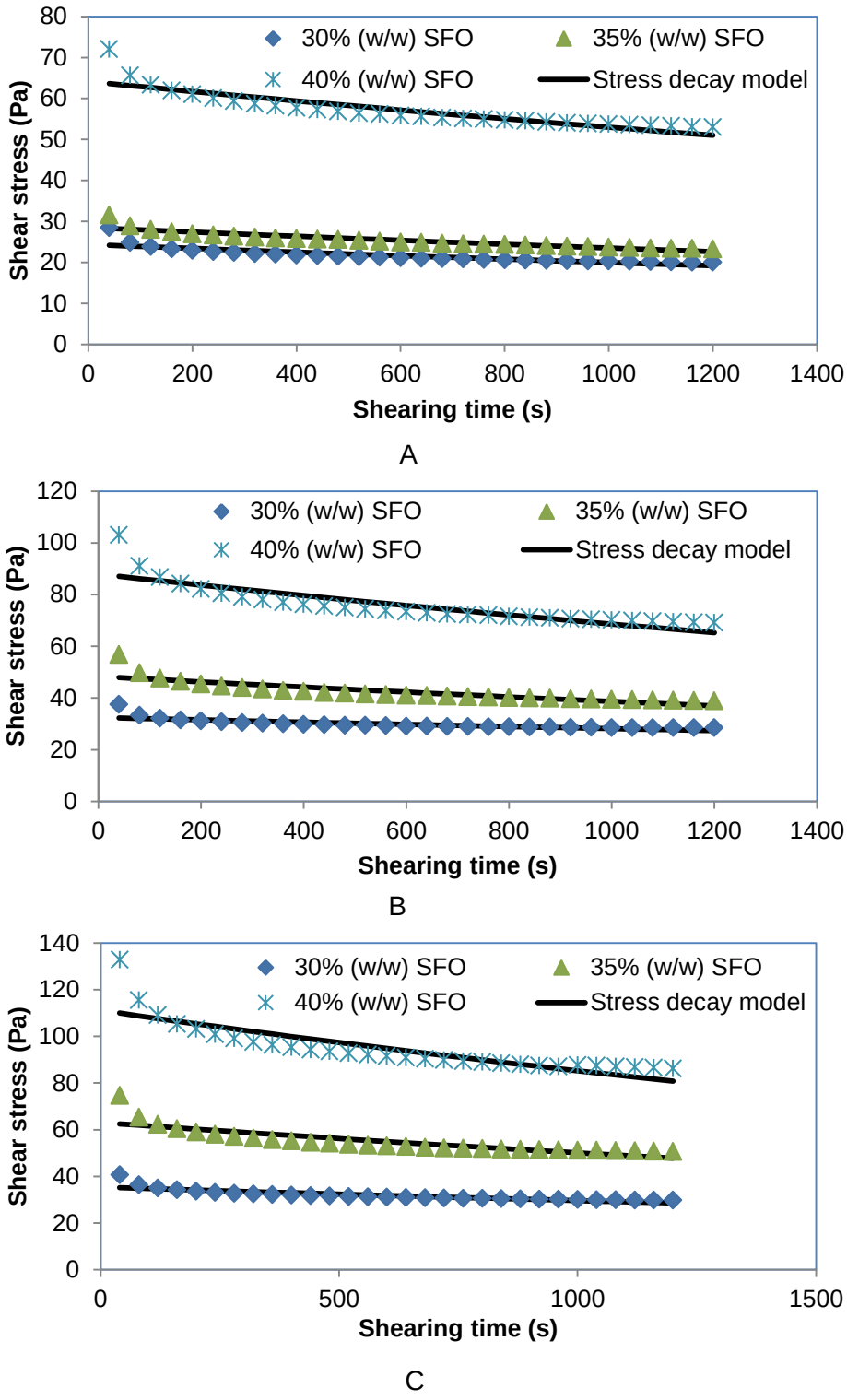

Figure 4.31 **Shear stress Vs shearing time of emulsions stabilized with 6% (w/w) BGNF (A) 50 s^{-1} (B) 100 s^{-1} (C) 150 s^{-1} modeling with first order stress decay with zero equilibrium equation**

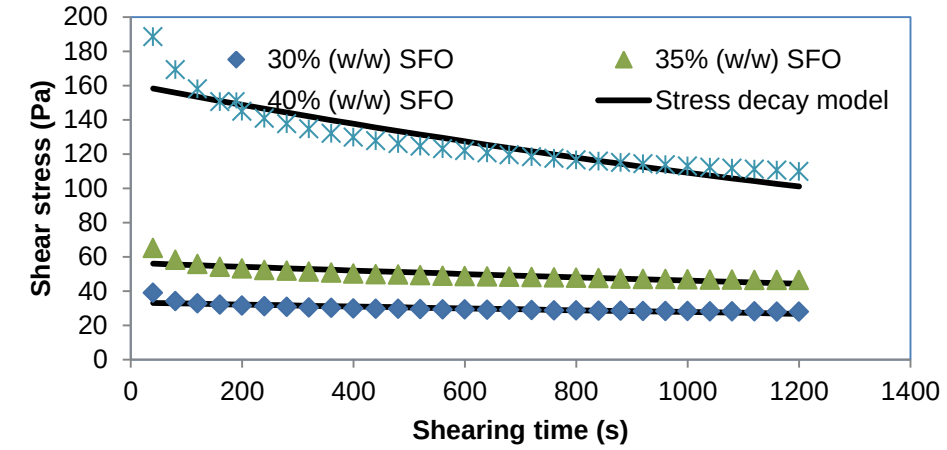

A

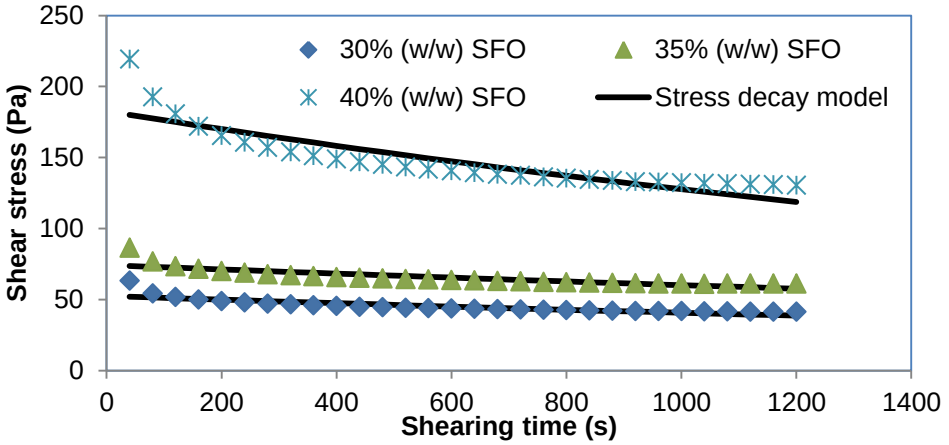

B

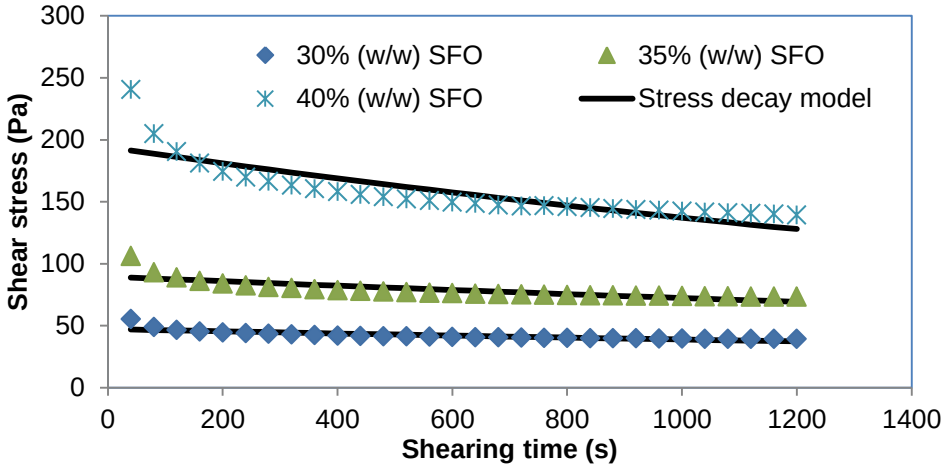

C

Figure 4.32 **Shear stress Vs shearing time of emulsions stabilized with 7% (w/w) BGNF (A) 50 s^{-1} (B) 100 s^{-1} (C) 150 s^{-1} modeling with first order stress decay with zero equilibrium equation**

component levels. The initial stress τ_0, increased with an increase in shear rate, BGNF and SFO concentrations. The obtained result of increased τ_0 with an increase in shear rate and concentration was in accordance with the report of Razavi and Habibi-Najafi (2006) for low fat sesame paste/date syrup blends (Halwa-Ardeh).

Table 4.21 Adjusted mean square for coefficient of first order stress decay with a zero equilibrium model of three replicates at different concentration of BGNF and SFO and shear rate[1]

Source of variation	df	τ_0	p	kx 10-^{10}	p
BGNF	2	21.97	<0.0001	334.22	<0.0001
SFO	2	35527.24	<0.0001	697.01	<0.0001
SRT	2	40189.69	<0.0001	1.52	0.7224
BGNF*SFO	4	3925.90	<0.0001	177.29	<0.0001
SRT*BGNF	4	8250.21	<0.0001	8.91	0.1221
SRT*SFO	4	174.89	<0.0001	0.17	0.9971
SRT*BGNF*SFO	8	300.82	0.0591	20.94	0.0003
ERROR	54	44.75	<0.0001	4.66	<0.0001

[1]τ_0 is the initial shear stress and k is the structural breakdown obtained from First order stress decay with a zero equilibrium model; BGNF*SFO is the interaction between the bambara groundnut flour and sunflower oil; SRT*BGNF refers to the interaction between the shear rate of shearing and bambara groundnut flour; SRT*SFO refers to the interaction between shear rate and sunflower oil; SRT*BGNF*SFO is the interaction between the shear rate, bambara groundnut and sunflower oil.

Similar observation of increased τ_0 with increased shear rate was also reported for milled sesame (tehineh) (Abu-Jdayil, 2002) and Balangu seed gum (Razavi and Karazhiyan, 2009). No trend was however observed for the k parameter on shear rate, BGNF and SFO concentrations. The present observation was in contrary to the results of Razavi *et al.* (2008) for low fat sesame paste and Razavi and Karazhiyan (2009) for hydrocolloids from salep and Balangu that k value increased and decreased with increased shear rate, respectively. The deviation in this study may probably be as a result of the inability of the model to represent the experimental data (low R^2 and high RMSE and SE observed).

4.3.2.5 Comparison of the time-dependent rheological models for predicting BGNF stabilized emulsion

The coefficient of determination for the Weltman, Hahn and Figoni-Shoemaker time dependent rheolological models was close to unity. Their RMSE and SE values were also very low. This is an indication that they can all perfectly predict the time dependent flow

behavior of the BGNF-stabilized emulsion at the shear rate and time investigated. However, the root mean square error and standard error (SE) for the first order stress decay with a zero equilibrium model were relatively higher than the corresponding prediction of the Weltman, Hahn and Figoni-Shoemaker models. Moreover, the observed R^2, was lower for all predictions of first order stress decay with a zero equilibrium model compared to all other tested models making the first order stress decay model not suitable for the prediction of the time-dependent properties of BGNF stabilized emulsion.

4.3.2.6 Summary on time-dependent rheological characterization of BGNF-stabilized emulsions

Among the principal reasons for time-dependent rheological characterization of food systems (including emulsions) are to establish connections between structure and flow, to relate physical parameters with sensory evaluation and for the purpose of optimization of processing stages such as mixing, handling, storage, and final quality (Razavi *et al.,* 2010)

Both the magnitude of hysteresis loop area quantification and steady shear decay method indicated that BGNF stabilized emulsions were time dependent and thixotropic in nature. The time dependent property was a function of both SFO and BGNF concentrations and their interactions. Constant shearing of the BGNF stabilized emulsions at all the tested shear rates for 1200 s was enough to destroy the structures responsible for flow time dependency (rigidity) in all of the emulsions. The time-dependency of the BGNF stabilized emulsions was due to the increased interactions between the BGNF and SFO as their concentrations increased. Increased interactions between SFO and BGNF subsequently led to increased emulsion viscosity. It therefore seemed that the time dependent thixotropic characteristic of BGNF-stabilized emulsions is highly dependent on structural formation. It is not surprising therefore that the most viscous formulation (7% (w/w) BGNF and 40% (w/w) SFO) was identified as the most thixotropic emulsion system. Emulsion containing 7% (w/w) BGNF and 40% (w/w) SFO had aggregated droplets network suspended in continuous BGNF phase (matrix). The very high droplet population (highest in this study) as evident from initial backscattering result made it the most structured emulsion system. The high structure of the emulsion is as a result of the contribution of the SFO and BGNF concentrations and this manifested as very high viscosity and stability. Therefore, it is not unlikely that the high thixotropy of the emulsion is unrelated to high structural formation and emulsion stability.

4.4 Time-independent (Steady Shear) Rheology of BGNF Stabilized Emulsion

Both steady shear behavior of gelatinized BGNF dispersions and BGNF stabilized emulsions were evaluated. The intrinsic rheological properties of BGNF-stabilized emulsions were identified and modeled by using some popular steady shear rheological models. The relationship between the emulsion components (BGNF and SFO) and rheological parameters were described using RSM. The observed steady shear parameters were explained and related to emulsion stability. This section reported the effect of the BGNF and SFO on the time-independent rheological properties of BGNF-stabilized emulsions.

4.4.1 Rheology of gelatinized bambara groundnut flour dispersion

Figure 4.33 shows the plots of apparent viscosity (η) vs shear rate for three different gelatinized BGNF dispersions (BGNFD) that formed the continuous phases of the BGNF stabilized emulsions. All the BGNFD (5%, 6% and 7%) were non-Newtonian fluids. The viscosity of all the BGNF dispersions tended to decrease as the shear rate increases suggesting a shear thinning (indicative of structural destruction) material for these solid content range and a shear rate range of 40 - 750 s^{-1}. Rao *et al.* (1997) observed that the time and temperature of gelatinization affect granule swelling of starches which invariably affect their rheological behaviors and thus the workers showed that gelatinized corn starch dispersion exhibited shear thickening and shear thinning at various stages of granule swelling. In a related study, Bagley and Chritianson (1982) also observed that shear rate range has significant influence on the rheological behaviors of biopolymers. At any given shear rate however, it was observed that the viscosity of gelatinized BGNF dispersions increased with an increase in concentration of BGNF indicated by upward shift of the curve (Figure 4.33). This could be connected with an increase in the cross-links (gel formation) in the structure of the dispersions as the concentration increases, therefore requiring much more force to disrupt the structure. Legume flours contain high protein and starch contents and the gelation capacity of flours is influenced by a physical competition for water between protein gelation and starch gelatinization (Singh, 2001; Kaur and Singh 2005). Gelation takes place more readily at higher protein concentration because of the greater intermolecular contacts during heating (Prinyawiwatkul *et al.,* 1997). Schmidt (1981) has also explained gelation in legume flours to involve the formation of a protein–polysaccharide complex. A number of studies conducted on the rheological behavior of biopolymer dispersions (predominantly gelatinized starches) have revealed that most parts exhibit pseudoplastic flow behaviors and that starch granule mass fraction which was referred to as 'notional volume fraction' plays an important role (Rao *et al.,* 1997). Therefore the non-Newtonian behaviour of the gelatinized BGNF dispersions in this chosen solid range could have a significant effect on the overall properties of the emulsions which they stabilize.

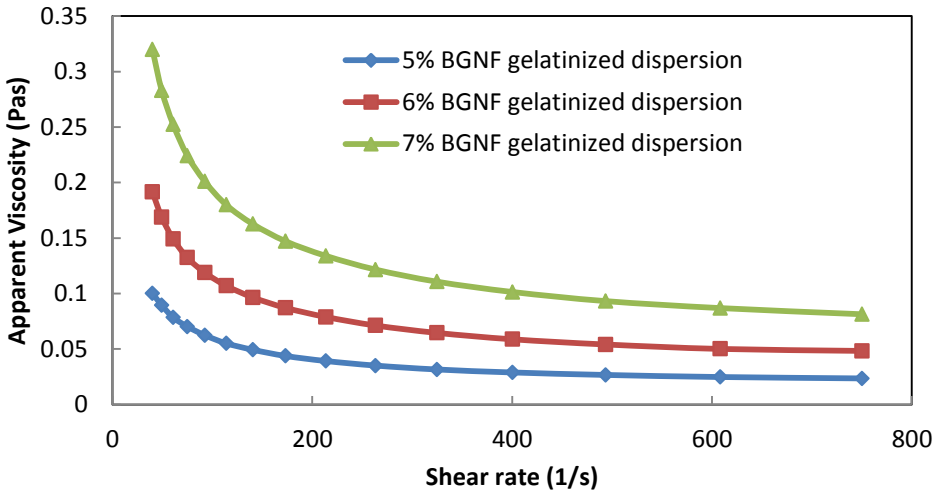

Figure 4.33 Apparent viscosity as a function of shear rate for dispersions of bambara groundnut flour (BGNF)

The possibilities for the emulsions to exhibit and manifest the inherent characteristics of each of the gelatinized BGNF dispersions used to achieve emulsion stabilization can not be ruled out.

4.4.2 Effect of BGNF and SFO on the steady shear rheology of o/w emulsion

Steady shear rheology of BGNF emulsions were investigated after the initial structures responsible for time dependency had been destroyed in order to attain the steady state condition. This was achieved by preshearing the emulsions for 1200 s observed in section 4.3.1 at shear rate of 100 s^{-1} before shearing test proceeded.

Flow curves of the studied emulsions as a function of SFO concentration [30-40% (w/w)] and BGNF concentration [5-7% (w/w)] are as presented in Figure 4.34A, B and C. All the emulsions depicted non-Newtonian behavior since the viscosities of all the emulsions were not constant for all shear rate range. The emulsions flow curves were similar in shape to that of the BGNF dispersions (Figure 4.33). Apparent viscosity of the emulsions decreased with increased shear rate, indicating a shear thinning-behavior due to progressive disruption of the flocs as the shear stress was increased (Mothe *et al.,* 2001; Samavati *et al.,* 2011). Shear-thinning behaviour was also found in food emulsions such as walnut oil-in-water emulsion (Nikovska, 2010), soybean oil-in-water emulsion stabilized with concentrated faxseed protein (Wang *et al.,* 2010b), low-in-fat emulsion stabilized with xanthan/guar mixture (Lorenzo *et al.,* 2008) and sodium-caseinate stabilized oil-in-water emulsion (Surh *et al.,* 2006).

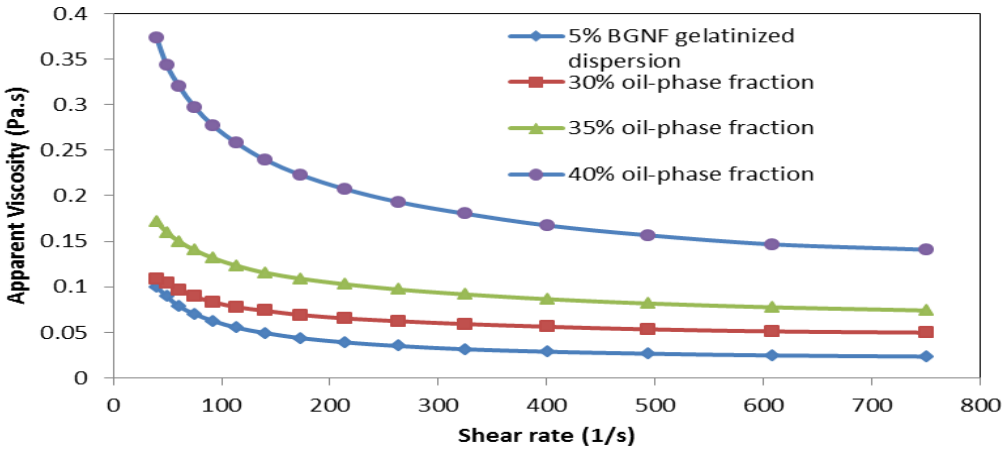

A

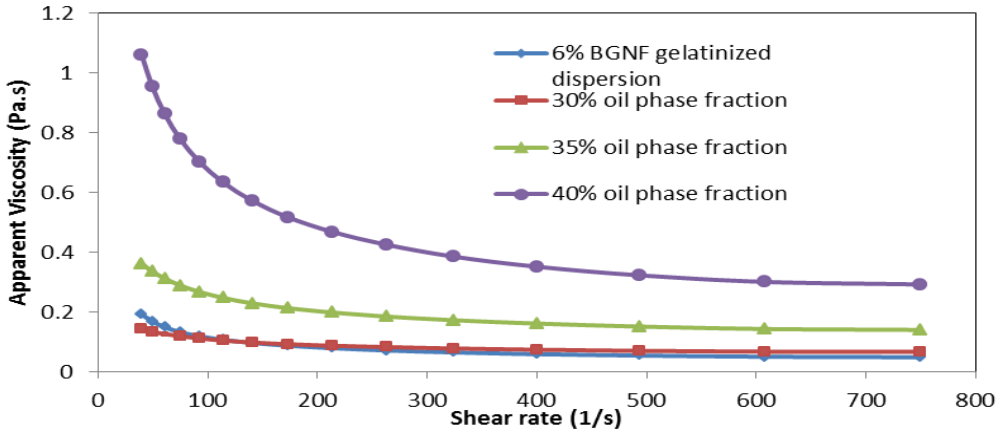

B

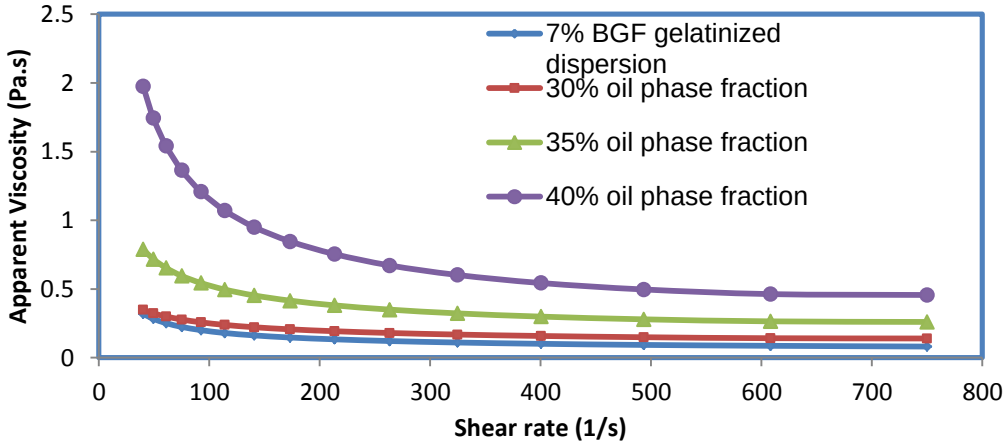

C

Figure 4.34 **Influence of oil-phase concentration on the apparent viscosity of the emulsions stabilized by gelatinized BGNF (A) 5% BGNF, (B) 6% BGNF and (C) 7% BGNF**

This behavior could be explained by the molecular structural breakdown generated and the increased constituent alignment of molecules with increased shear rate (Alparsan and Hayta, 2002). Small hydrodynamic flocs at low shear rate are not able to disrupt flocs and as an effect of increasing the shear rate, the hydrodynamic forces dominate and disrupt the flocs causing a reduction in viscosity (McClements, 1999; Sherman, 1993; Taherian *et al.,* 2006).

The apparent viscosities of emulsions increased slowly initially as there was no conspicous difference between the flow curves of all the emulsions with 30% (w/w) oil concentration and flow curves of their corresponding gelatinized BGNF dispersions of 5% (w/w), 6% (w/w) and 7% (w/w) (Figure 4.34A, B and C). As the oil-phase fraction (concentration) increased, the oil droplets came into close proximity then dispersions became more flocculated and viscosity increased. Consequently, flow curves shifted upwards to higher viscosities due to the increase in packing fraction of oil droplets. Increase in dispersion's viscosity has been related to droplet flocculation because the effective volume fraction of the particles (oil-droplets) in the system is increased due to the presence of the continuous phase trapped between the droplets in the flocs (McClements, 1999; Klinkesorn *et al.,* 2004; Taherian *et al.,* 2006; Samavati *et al.,* 2011). The present observation is in agreement with the report of Sun and Gunasekaran (2009) and Moros *et al.* (2002) that apparent viscosities of emulsions increased with oil concentration. Emulsions of flocculated droplets tend to exhibit a pronounced shear thinning behavior since the hydrodynamic forces generated at low shear stresses may possibly not be large enough to disrupt the flocs and as such the agglomerates could behave like drops of a fixed size and shape resulting in a constant viscosity (Samavati *et al.,* 2011). Furthermore the flow curves of all the emulsions showed a relatively constant viscosity at high shear rates. This could be because all of the flocs are completely disrupted or the number of flocculated droplets remains constant since the rate of flocs formation is equal to the rate of flocs disruption at equilibrium (Campanella *et al.,* 1995; Samavati *et al.,* 2011).

There was an appreciable increase in apparent viscosities with an increased BGNF concentration (Figure 4.34). This may be probably linked to the flow behaviors of their respective continuous phases having different BGNF concentrations (Figure 4.33). The increased concentration of the BGNF in the formulations made the emulsion with higher BGNF to be less susceptible to breakdown by shear stress because more cross-links were formed as the concentration of BGNF increased. Similar results were reported by Samavati *et al.* (2011) and Taherian *et al.* (2006) in their work to investigate the effect of polysaccharide on emulsion rheology. Therefore, shear thinning behavior of the emulsions was as a result of both oil droplet defloculation as the shear rate increased and non-Newtonian characteristics of the continuous phase.

4.4.3 Modeling of steady-shear flow behavior of oil-in-water emulsions stabilized by BGNF

4.4.3.1 Modeling of BGNF-stabilized emulsions using Power law model

Power law model (Equation 3.12) was used to describe the flow curves of the dispersions. Power law model contains only two parameters (K and n) that can describe shear stress-shear rate relationship, thus it is used extensively to characterize fluid foods (Keshani *et al.,* 2012). Power law is popular because the logarithm of shearing rheological behavior of a fluid is represented simply by a straight line (Steffe, 1996; Keshani *et al.,* 2012). The slope of the straight line is the flow behaviour index (n), which indicates the tendency of a fluid to shear thinning and the intercept equals log K, from which the consistency coefficient can be evaluated. The consistency coefficient serves as the viscosity index of the system (Friberg and Lasson, 1997). Table 4.22 compares the flow properties of emulsions at different oil and BGNF concentration. The results showed reasonably good fitting to power law model. The coefficient of determination was more than 0.98 for all measurements which indicated a high level of relation between the data points. The mean consistency coefficient (K) ranged from 0.25 - 10.37 Pas^n and the mean value of flow behavior index (n), varied between 0.52 - 0.76 indicating a shear thinning behavior since the values were less than unity.

The rheological properties of BGNF stabilized emulsion (in terms of power law parameters) were modeled as a function of main emulsion components (BGNF and SFO) in order to understand the individual and combined effects of these ingredients on emulsion properties. Such models can be useful in the design and formulation of BGNF emulsions of predetermined rheological properties. The coefficient of determination, linear, quadratic, interaction effects and p-values for power law model parameters are presented in Table 4.23. The relationship between BGNF and SFO concentrations on the power law model parameters was non-linear. The response models obtained for the consistency coefficient, (K) and flow behavior index, (n) were significant ($p < 0.0001$) with high R^2 of 0.996 and 0.997, respectively. Adequate precision of 95.2 and 68.5 were obtained for the models of K and n, respectively. High value of R^2 and adequate precison is an indication that the obtained response surface models can be accurately employed for predicting the intrinsic rheological emulsion properties as a function of BGNF and SFO. For K, the linear, quadratic and interaction terms of both BGNF and SFO were significant ($p < 0.001$). However, for n, the linear terms, quadratic effect of SFO and the interaction effect of both SFO and BGNF were the only significant model terms ($p < 0.05$). The quadratic effect of the BGNF was non-significant ($p > 0.05$). The effects of SFO and BGNF on K were both negative and positive for the linear and quadratic terms ($p < 0.0001$). The effects of both components

(BGNF and SFO) were however positive and negative on n for linear and quadratic terms, respectively. The interaction effect of BGNF and SFO was positive and negative on K and n,

Table 4.22 Power law model parameters for the emulsion stabilized with BGNF[1,2]

Emulsion BGNF (%w/w)	SFO (%w/w)	K (Pa·s^n)	n	R^2	RMSE	SE
5	30	0.25 ± 0.05	0.76 ± 0.03	0.99	0.32	0.33
	35	0.48 ± 0.05	0.71 ± 0.02	0.99	0.22	0.23
	40	1.19 ± 0.04	0.68 ± 0.01	0.99	0.69	0.71
6	30	0.32 ± 0.01	0.76 ± 0.01	0.99	0.54	0.56
	35	1.05 ± 0.05	0.69 ± 0.01	0.99	1.22	1.26
	40	4.71 ± 0.16	0.68 ± 0.01	0.99	3.96	4.10
7	30	0.93 ± 0.05	0.71 ± 0.01	0.99	1.39	1.45
	35	2.59 ± 0.04	0.65 ± 0.00	0.99	3.55	3.68
	40	10.4 ± 0.64	0.52 ± 0.00	0.98	9.50	9.83

[1]Mean values ± standard deviations of three samples
[2]K equals the consistency coefficient; n equals the flow behavior index; R^2 is the coefficient of determination; RMSE equals root mean square error; SE is the standard error.

respectively. The relationships between K and n was illustrated using three dimensional response surface. The individual and cummulative effects of BGNF and SFO on K and n values are as represented in Figures 4.35A and B, respectively. Increasing the level of BGNF and SFO independently led to an increase in the K which manifested as an increase in emulsion viscosity. Increased K with increasing SFO indicated that oil phase volume fraction enhanced droplet interactions and the emulsions were more structured (Sun and Gunasekaran, 2009). Similarly, the observed increase in K when BGNF was increased from 5% (w/w) to 7% (w/w) could be due to the non-Newtonian behavior of the continuous phase as shown in Figure 4.33. The interaction effect of BGNF and SFO drastically increased value of K. The increased value of K can be interpreted as increased emulsion viscosity and stability for the BGNF-stabilized emulsions. For the flow behavior index (Figure 4.35B), an increase in both the BGNF and SFO independently produced a moderate decrease in n value of power law model. This could be linked to the BGNF stabilized emulsions being

more flocculated as SFO and BGNF increased. The interaction of the BGNF and SFO led to a drastic increase in pseudo-plasticity of the emulsions.

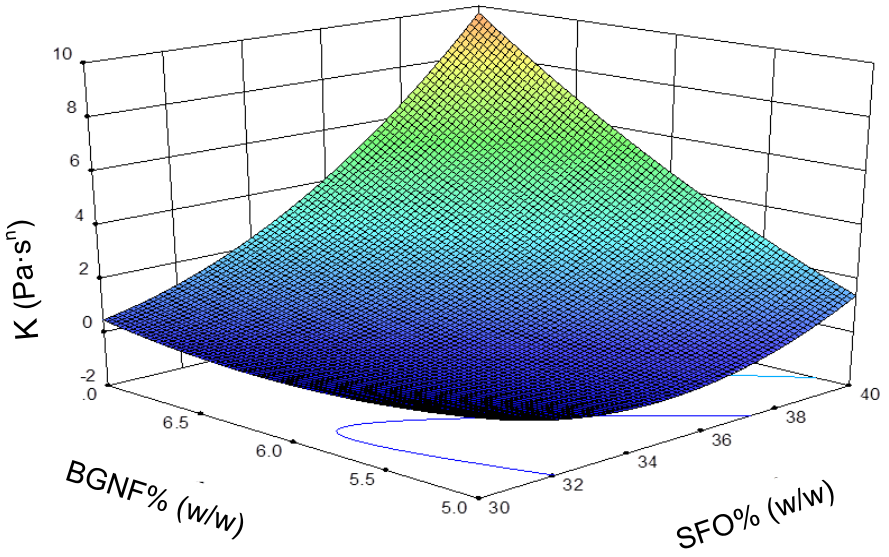

A

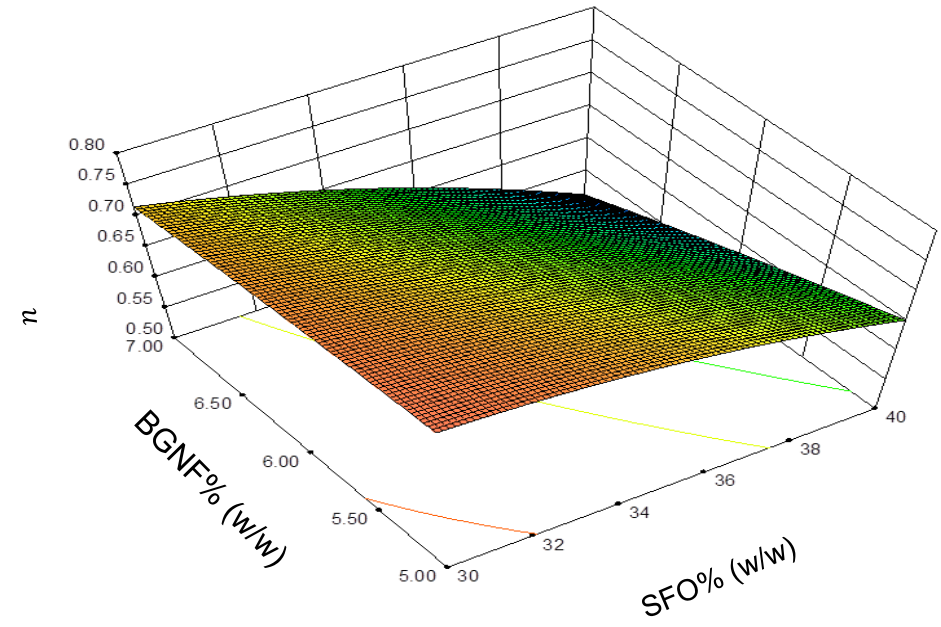

B

Figure 4.35 Response surface for the effect of bambara groundnut (BGNF) and sumflower oil (SFO) concentrations on (A) K value and (B) n-value of Power law model

Table 4.23 Analysis of variance (ANOVA) for the quadratic model of power law rheological responses[1]

		K(Pa·s^n)				n		
Source	DF	Coefficient	Sum of square	F-ratio p-value	DF	Coefficient	Sum of square	F-ratio p-value
Model	5	65.532	9.76	<0.0001	5	-0.557	0.15	<0.0001
Linear								
b_1	1	-0.2.164	4.23	<0.0001	1	0.074	0.0065	<0.0001
b_2	1	-11.306	6.68	<0.0001	1	0.123	0.0087	<0.0001
Quadratic								
b_{11}	1	0.018	0.21	<0.0001	1	-0.0027	0.0027	<0.0001
b_{22}	1	0.484	0.47	<0.0001	1	-0.0055	0.00005	0.1820
Interaction								
b_{12}	1	0.187	0.66	<0.0001	1	-0.0027	0.00053	0.0044
Residual	21		9.51		13		0.00004	0.4330
Pure error	12				11		0.00005	
Total	9.78				18		0.15	
R^2		0.997				0.996		
Adj-R^2		0.9970				0.9946		
CV		3.77				1.02		
Adequate precision		95.2				68.5		

[1]K is the consistency coefficient; n is the flow behavior index; b_1 and b_2 equal the coefficient of the linear term of bambara groundnut flour and sunflower oil; b_{11} and b_{22} are the coefficients of the quadratic terms of the bambara groundnut flour and sunflower oil; b_{12} equals the coefficients of interaction between the bambara groundnut flour and sunflower oil; DF equals degree of freedom; R^2 is the coefficient of determination; Adj R^2 equals the adjusted coefficient of determination; CV is the coefficient of variation.

4.4.3.2 Modeling of BGNF-stabilized emulsions using Herschel-Bulkley model

Herschel-Bulkley (H-B) model (Equation 3.13) parameters are as presented in Table 4.24. The coefficients of determination (R^2) were high indicating a high level of correlation between the experimental and predicted rheological data. Quantification by H-B model showed that the entire emulsions studied possessed yield stresses (τ_o) from 0.89 to 2.18 Pa. The mean consistency coefficient (K) of all the emulsion ranged from 0.23 - 9.83 Pas^n while the flow behavior index (n) was between 0.52 - 0.77. The empirical models were developed as the inverse of the parameters (transposition). The empirical model as a function of BGNF and SFO, as well as the ANOVA results are as presented in Table 4.25. The response surface is also presented in Figures 4.36A and B and 4.37. All the developed models were significant ($p < 0.0001$) and with high nalues of R^2, making the models suitable for predicting the properties of the parameters as a function of emulsion components. Both

the linear terms of SFO and BGNF and their interraction were significant ($p < 0.05$) for all of the empirical models.

Table 4.24 Herschel-Bulkley model parameters for the emulsion stabilized by BGNF[1,2]

Emulsion BGNF (%w/w)	SFO (%w/w)	τ_o (Pa)	K(Pa·s^n)	n	R^2	RMSE	SE
5	30	0.92 ± 0.18	0.23 ± 0.13	0.77 ± 0.08	0.99	0.13	0.13
	35	0.96 ± 0.09	0.39 ± 0.10	0.75 ± 0.04	0.99	0.08	0.09
	40	1.03 ± 0.00	1.07 ± 0.03	0.69 ± 0.01	0.99	0.59	0.61
5	30	0.89 ± 0.01	0.31 ± 0.08	0.76 ± 0.04	0.99	0.34	0.35
	35	1.01 ± 0.00	0.94 ± 0.04	0.71 ± 0.01	0.99	1.10	1.14
	40	1.29 ± 0.01	4.47 ± 0.16	0.58 ± 0.00	0.99	3.85	3.98
7	30	1.00 ± 0.00	0.82 ± 0.05	0.73 ± 0.01	0.99	1.27	1.32
	35	1.12 ± 0.00	2.44 ± 0.04	0.65 ± 0.00	0.99	3.43	3.55
	40	2.18 ± 0.32	9.83 ± 0.56	0.52 ± 0.00	0.98	9.33	9.66

[1] Values are mean ± standard deviation of three samples

[2] τ equals the yield stress; K is the consistency coefficient; n equals the flow behavior index; R^2 is the coefficient of determination; RMSE is the root mean square error; SE is the standard error.

The linear terms of BGNF and SFO were positive while the interaction between BGNF and SFO (b_{12}) were negative on the $1/\tau_o$. Independent increase in BGNF and SFO produced an increase in $1/\tau_o$ while the interaction of BGNF and SFO decreased $1/\tau_o$. Apparent yield stress has been interpreted as the applied stress that must be exceeded in order to make a structured fluid to flow (Steffe, 1996) and it is a significant factor in many industrial processes such as pumping, spreading and coating. Yield stress could however be desirable in some product design where the purpose is to keep the particles suspended in the medium. Regarding $1/K$, an increase in BGNF and SFO independently decreased $1/K$ while the interaction of BGNF and SFO led to an increase in $1/K$.

Table 4.25 Analysis of variance (ANOVA) for the linear model of the transposed Herschel-Bulkley law rheological responses

	$1/\tau_o$ (Pa^{-1})				$1/K$ (Pas^n)$^{-1}$				$1/n$			
Source	DF	Coefficient	Sum of square	F-ratio p-value	DF	Coefficient	Sum of square	F-ratio p-value	DF	Coefficient	Sum of square	F-ratio p-value
Model	3	-1.29	0.93	<0.0001	3	+51.37	68.5	<0.0001	3	+0.307	0.17	<0.0001
Linear												
b_1	1	+0.086	0.51	<0.0001	1	-1.218	36.4	<0.0001	1	+0.019	0.11	<0.0001
b_2	1	+0.567	0.30		1	-6.621	24.8		1	+0.154	0.048	<0.0001
Interaction												
b_{12}	1	-0.0198	0.12	0.0007	1	+0.156	7.27	0.0018	1	-5.88E-3	0.010	0.0069
Residual	23		0.18		23		13.5		23			
Pure error	18		0.11		18				18			
Total	26		1.11		26		82.0		26			
R^2		0.839				0.836				0.861		
Adj-R^2		0.818				0.814				0.843		
CV		9.47				45.3				5.01		
Adequate Precision		17.6				17.6				19.6		

[1] $1/\tau_o$ is the inverse of yield stress; $1/K$ is the inverse of consistency coefficient; $1/n$ is the flow behavior index; b_1 and b_2 equal the coefficient of the linear term of bambara groundnut flour and sunflower oil; b_{12} equals the coefficients of interaction between the bambara groundnut flour and sunflower oil; DF equals degree of freedom; R^2 is the coefficient of determination; Adj R^2 equals the adjusted coefficient of determination; CV is the coefficient of variation.

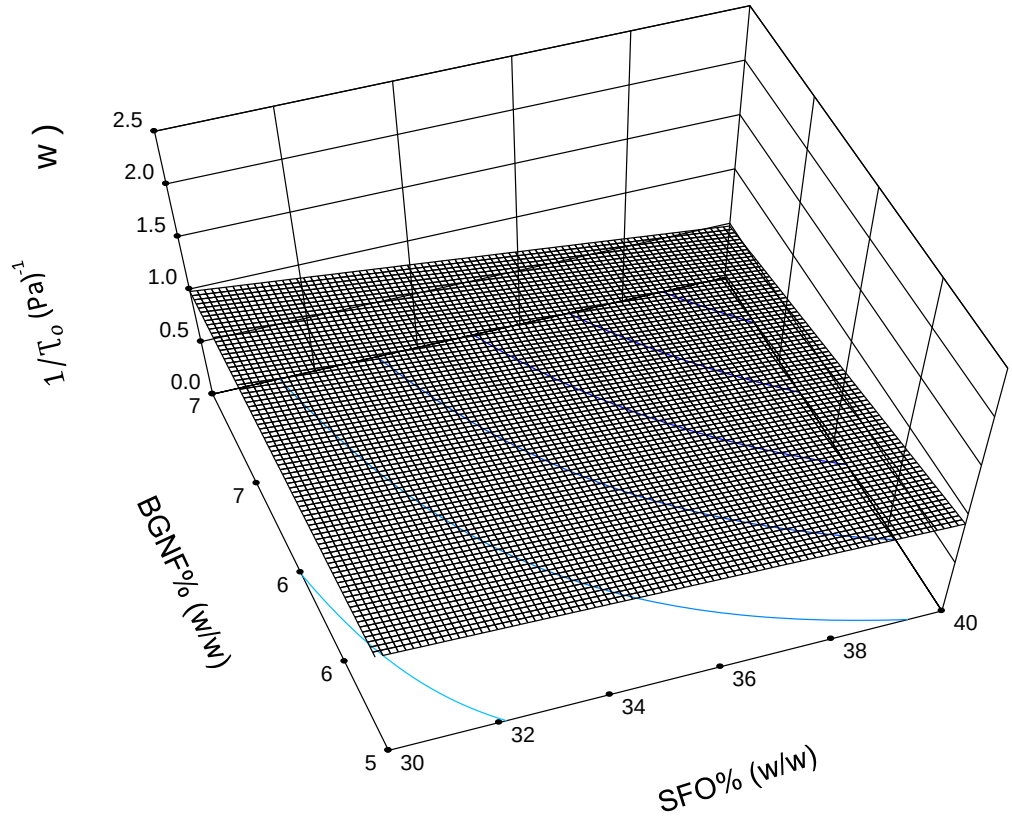

A

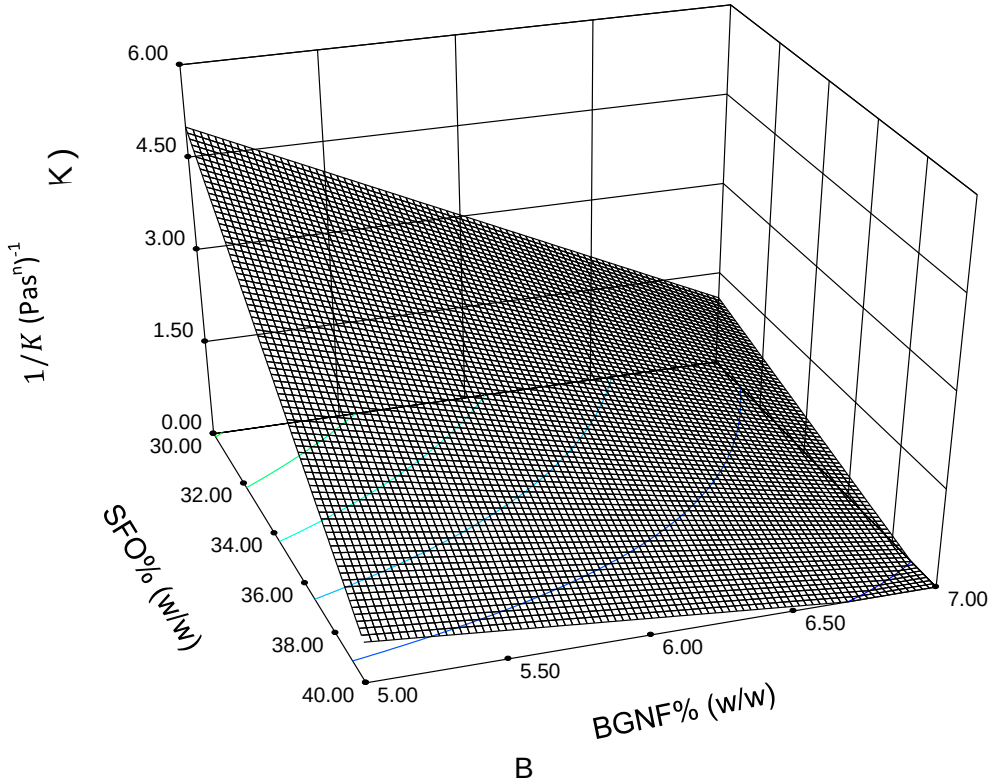

B

Figure 4.36 **Response surface for the effect of BGNF and SFO concentrations on (A) inverse of yield stress ($1/\tau_o$) (B) inverse of consistency coefficient ($1/K$) of Herschel-Bulkley model**

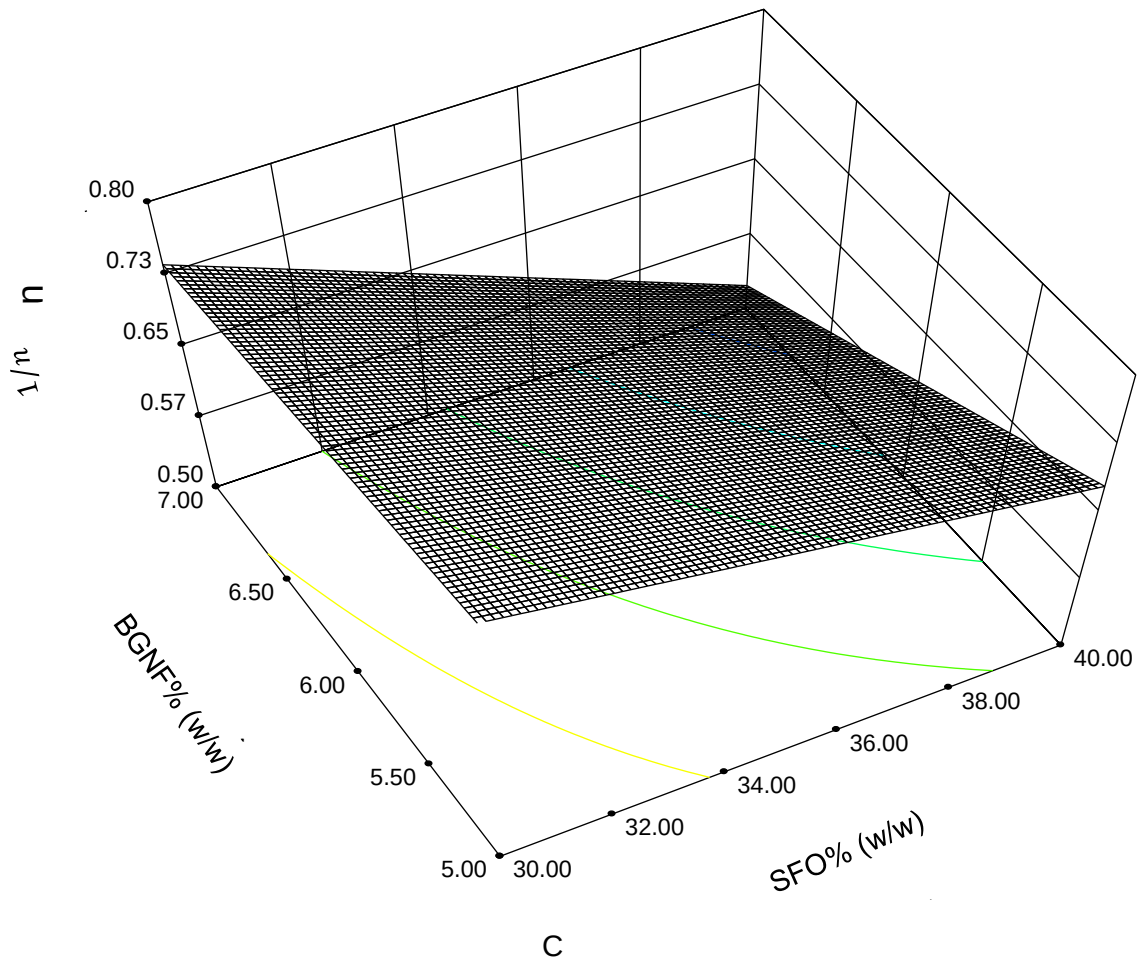

Figure 4.37 Response surface for the effect of bambara groundnut flour (BGNF) and sunflower oil (SFO) concentrations on the inverse of flow behaviour index ($1/n$) value of Herschel-Bulkley model

This could as well be attributed to stronger interaction between SFO droplets as the oil concentration increases and the non-Newtonian effect of the continuous gelatinized BGNF dispersion. On the other hand, $1/n$ increased when SFO and BGNF were increased independently. The interaction effect of BGNF and SFO decreased $1/n$ significantly.

4.4.3.3 Modeling of BGNF-stabilized emulsions using Bingham plastic model

Emulsions were modeled using Binghan plastic model (Equation 3.14). Fluids obeying this model are called Bingham plastic fluids. This category of fluids often has a critical stress below which they do not flow. Fluids obeying this model tend to exhibit a linear shear stress - shear rate behavior after an initial shear stress threshold has been attained. This model requires two parameters, that is, K^B which is the Bingham plastic viscosity and τ_o^B, the yield stress and both parameters can be acquired from the linear graph (Keshani *et al.,* 2012).

The results showed a reasonable good fitting of these data to Bingham model with high coefficient of determination (R^2 > 0.99). The parameters estimated were summarized in Table 4.26.

Table 4.26 Bingham model parameters for the emulsion stabilized with BGNF[1,2]

Emulsion BGNF (%w/w)	SFO (%w/w)	τ_o^B (Pa)	K^B(Pa·s)	R^2	RMSE	SE
5	30	3.51 ± 0.54	0.05 ± 0.00	0.99	0.56	0.57
	35	5.97 ± 0.23	0.07 ± 0.00	0.99	1.17	1.21
	40	14.2 ± 0.15	0.13 ± 0.00	0.99	2.59	2.68
6	30	4.64 ± 0.31	0.06 ± 0.00	0.99	0.75	0.78
	35	13.2 ± 0.12	0.12 ± 0.00	0.99	2.01	2.08
	40	42.3 ± 2.09	0.24 ± 0.02	0.99	4.99	5.16
7	30	12.2 ± 0.26	0.12 ± 0.01	0.99	1.74	1.79
	35	29.2 ± 0.55	0.22 ± 0.00	0.99	3.43	3.55
	40	77.6 ± 4.81	0.35 ± 0.02	0.99	6.64	6.88

[1]Values are mean ± standard deviation of three samples
[2]BGNF is bambara groundnut flour; SFO is sunflower oil; τ_o^B equals Bingham yield stress; K^B equals Bingham plastic viscosity; R^2 is the coefficient of determination; RMSE equals root mean square error; SE is the standard error.

The yield stress and Bingham plastic viscosities were in the range 3.51 - 77.63 (Pa) and 0.05 - 0.35 (Pa·s) respectively. The coefficients of equations representing the parameters of Bingham model (τ_o^B and K^B) as functions of BGNF and SFO are presented in Table 4.27. The quadratic polynomial models obtained for the Bingham model parameters that is, Bingham yield stress, τ_0^B, and viscosity, K^B were significant ($p < 0.0001$) with high R^2 (0.99 and 0.98 for τ_0^B, and K^B , respectively) and adequate precision (186 and 61.2 for τ_0^B and K^B, respectively).

Table 4.27 Analysis of variance (ANOVA) for the quadratic model of Bingham law rheological responses

		τ_0^B (Pa)				K^B (Pa·s^n)		
Source	DF	Coefficient	Sum of square	F-ratio p-value	DF	Coefficient	Sum of square	F-ratio p-value
Model	5	544.88	857.54	<0.0001	5	+2.103	0.24	<0.0001
Linear								
b_1	1	-18.255	412.53	<0.0001	1	-0.0081	0.12	<0.0001
b_2	1	-96.706	628.94	<0.0001	1	-0.3556	0.10	<0.0001
Quadratic								
b_{11}	1	0.156	14.67	<0.0001	1	0.0008	0.0022	0.0003
b_{12}	1	4.250	33.35	<0.0001	1	0.014	0.0013	0.003
Interaction								
b_{22}	1	1.633	44.44	<0.0001	1	0.007	0.016	<0.0001
Residual					21		0.0024	
Pure error	11		0.53		18		0.00167	
Total	16		858.07		26		0.24	
R^2		0.99				0.98		
Adj-R^2		0.99				0.99		
CV		1.79				7.17		
Adequate Precision		186				61.2		

[1]τ_o^B is the Bingham yield stress; K^B is the Bingham plastic viscosity; b_1 and b_2 equal the coefficient of the linear term of bambara groundnut flour and sunflower oil; b_{11} and b_{22} are the coefficients of the quadratic terms of the bambara groundnut flour and sunflower oil; b_{12} equals the coefficients of interaction between the bambara groundnut flour and sunflower oil; DF equals degree of freedom; R^2 is the coefficient of determination; Adj R^2 equals the adjusted coefficient of determination; CV is the coefficient of variation

Hence, the models were employed for predicting the intrinsic rheological emulsion properties as a function of main emulsion components. For the τ_0^B and K^B, ($p < 0.05$), the linear, quadratic and interaction terms were significant.

The effect of SFO and BGNF were negative and positive for the linear and quadratic terms, respectively ($p < 0.0001$). Similarly, the effects of both components (BGNF and SFO) were negative and positive on K^B for linear and quadratic terms, respectively. The interaction effect of BGNF and SFO were both positive on the Bingham yield stress and K^B respectively. The relationships between BGNF and SFO on Bingham yield stress, τ_0^B, and viscosity, K^B were illustrated using three dimensional response surface (Figure 4.38A and B). Increasing the concentration of BGNF and SFO independently (Figure 4.38A) led to an overall increase in the τ_0^B. At the initial stage, an increase in the BGNF and SFO presented a decrease in the τ_0^B and progressively increased as BGNF and SFO concentration increased. The simultaneous effect (interaction) of increase in BGNF and SFO drastically

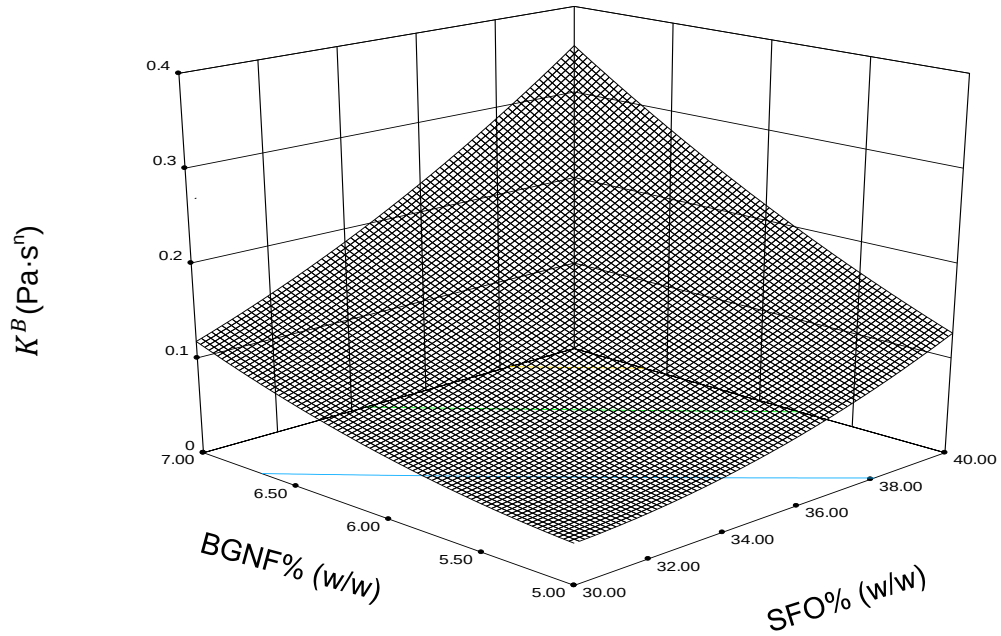

A

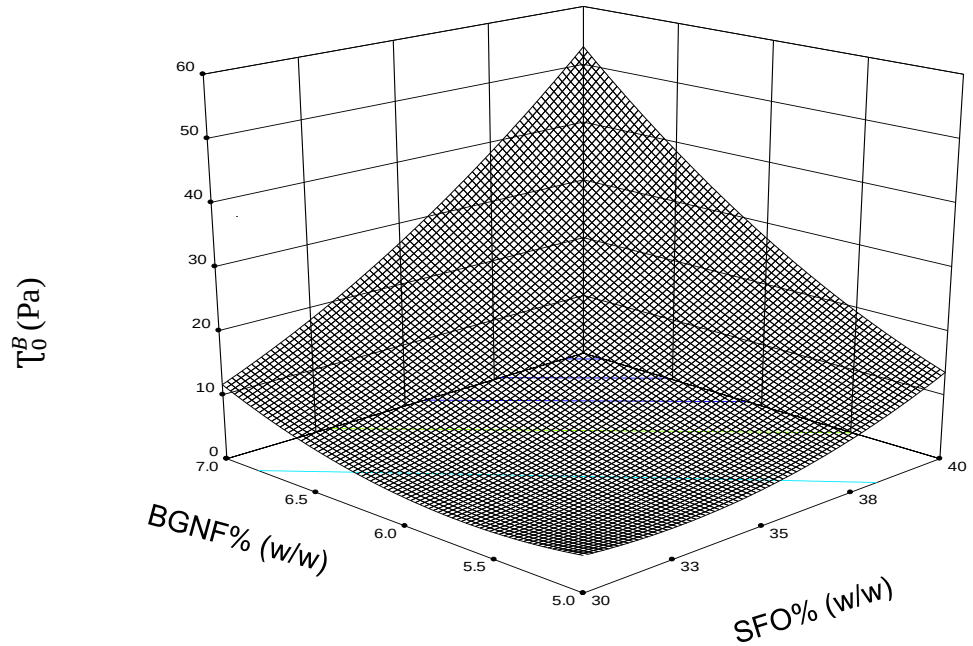

B

Figure 4.38 **Response surface for the effect of bambara groundnut flour (BGNF) and sunflower oil (SFO) concentrations on (A) Bingham plastic viscosity (K^B) and (B)Bingam yield stress (τ_0^B)**

increased τ_0^B. The implication is that BGNF stabilized emulsions have tendency to remain rigid when the magnitude of shear stress is smaller than yield stress. Regarding, K^B, (Figure 4.38B), an increase in both the BGNF and SFO independently produced a moderate increase in K^B value of Bingham model. However, simultaneous increase in the concentration of the BGNF and SFO led to a drastic increase in K^B of the emulsions.

4.4.3.4 Modeling of BGNF-stabilized emulsions using Casson model

The Casson model (Equation 3.15) had been reported to apply widely for a range of food products (Holdsworth, 1993). Casson model is closely related with the effect of particle size distribution on the flow behavior of pigment-oil suspensions (Chuah *et al.,* 2007; Keshani *et al.,* 2012). There are two parameters determined from Casson model, namely Casson yield $\tau_{oc}^{0.5}$, and the Casson Plastic viscosity K_{oc} and are tabulated in Table 4.28. The coefficient of determination R^2 obtained for all the emulsions was relatively high ($R^2 > 0.99$). All the emulsion samples exhibited definite yield stress due to significant particle-particle interactions throughout the range of BGNF and SFO. Casson yield stress and Casson plastic viscosity ranged respectively from 0.95 - 6.32 ($Pa^{0.5}$) and 0.19 - 0.43 ($Pas^{0.5}$).

Table 4.29 is the ANOVA of quadratic models of Casson rheological model parameters as a function of BGNF and SFO concentrations. The coefficient of determination, regression, linear, quadratic, interaction effects and p-values are also presented. The quadratic polynomial models obtained for the model parameters that is, Casson yield stress, $\tau_{oc}^{0.5}$, and viscosity, K_{oc} were significant ($p < 0.0001$) with R^2 of 0.994 and 0.990 and adequate precisions of 62.4 and 53.6 for $\tau_{oc}^{0.5}$ and K_{oc}, respectively. For the, $\tau_{oc}^{0.5}$, p-values of all the model terms were less than 0.05 ($p < 0.05$) indicating that the linear, quadratic and interaction terms were significant. However, for K_{oc}, the linear terms of BGNF and SFO, quadratic effect of SFO and the interaction effect of BGNF and SFO were significant ($p < 0.05$). The quadratic effect of the BGNF was not significant ($p > 0.05$). Figures 4.39A and B are the three dimensional response surface graph of the relationship between the Casson model parameters ($\tau_{oc}^{0.5}$, and K_{oc}) and the main emulsion components (BGNF and SFO). The response surface analysis showed the dependence of the model parameters on the BGNF and SFO. Analysis of the model terms revealed that the effect of SFO and BGNF were negative and positive on Casson yield stress for the linear and quadratic terms respectively ($p < 0.0001$) while the effects of both components (BGNF and SFO) were positive and negative on Casson viscosity for linear and quadratic terms respectively. The statistical analysis further showed that the interaction effect of BGNF and SFO were positive and negative on the $\tau_{oc}^{0.5}$ and K_{oc} respectively. The prediction of Casson model however was the same with Bingham rheological model. Increasing the concentration of BGNF and SFO independently led to an overall increase in $\tau_{oc}^{0.5}$.

Table 4.28 Casson model parameters for the emulsion stabilized with BGNF

Emulsion BGNF (%w/w)	SFO (%w/w)	$\Upsilon_{oc}^{0.5}$ $(Pa)^{0.5}$	$K_{oc}(Pa{\cdot}s)^{0.5}$	R^2	RMSE	SE
5	30	0.95 ± 0.15	0.19 ± 0.01	0.99	0.02	0.03
	35	1.27 ± 0.04	0.23 ± 0.00	0.99	0.06	0.06
	40	2.13 ± 0.01	0.30 ± 0.00	0.99	0.09	0.10
6	30	1.09 ± 0.06	0.21 ± 0.01	0.99	0.04	0.04
	35	2.06 ± 0.03	0.29 ± 0.01	0.99	0.07	0.07
	40	4.34 ± 0.10	0.38 ± 0.01	1.00	0.12	0.12
7	30	1.94 ± 0.04	0.30 ± 0.01	0.99	0.06	0.06
	35	3.33 ± 0.05	0.38 ± 0.00	0.99	0.08	0.09
	40	6.32 ± 0.26	0.43 ± 0.01	0.99	0.16	0.16

[1] Values are mean ± standard deviation of three samples

[2]BGNF is Bambara groundnut flour; SFO is the sunflower oil; $\Upsilon_{oc}^{0.5}$ equals Casson yield stress; K_{oc} equals Casson plastic viscosity; R^2 is the coefficient of determination; RMSE equals root mean square error; SE is the standard error.

Initially, an increase in the BGNF and SFO presented a decrease in the $\Upsilon_{oc}^{0.5}$. A further increase progressively led to an increase in $\Upsilon_{oc}^{0.5}$ as BGNF (> 6.5% w/w) and SFO (> 36% w/w) concentrations were increased. The simultaneous effect (interaction) of increase in BGNF and SFO drastically increased $\Upsilon_{oc}^{0.5}$. Regarding K_{oc}, (Figure 4.39A), an increase in both the BGNF and SFO independently produced an increase in K_{oc}. However, simultaneous increase in the concentration of the BGNF and SFO led to a moderate increase in K_{oc} of the emulsions. This indicated an increase in emulsion viscosity and subsequent stability as BGNF and SFO increased in the emulsion.

Table 4.29 Analysis of variance (ANOVA) for the quadratic model of Casson model rheological responses

			$\Upsilon_{oc}^{0.5}$ (Pa)$^{0.5}$				K_{oc} (Pa·s)$^{0.5}$	
Source	DF	Coefficient	Sum of square	F-ratio p-value	DF	Coefficient	Sum of square	F-ratio p-value
Model	5	33.07233	12.14	<0.0001	5	-1.6106	0.11	<0.0001
Linear								
b_1	1	-1.09961	3.95	<0.0001	1	0.054	0.059	<0.0001
b_2	1	-6.29391	6.40	<0.0001	1	0.155	0.058	<0.0001
Quadratic								
b_{11}	1	0.00976	0.14	<0.0001	1	-0.00039	0.00041	0.0225
b_{22}	1	0.29779	0.35	<0.0001	1	-0.0011	0.000005	0.7762
Interaction								
b_{12}	1	0.10723	0.86	<0.0001	1	-0.0018	0.00038	0.0275
Residual	0.079				0.0011			
Pure error	0.067				0.0008			
Total	12.22				0.11			
R^2		0.994				0.990		
Adj-R^2		0.991				0.990		
CV		3.98				2.60		
Adequate Precision		62.4				53.6		

[1]$\Upsilon_{oc}^{0.5}$ is the Casson yield stress; K_{oc} is the Casson plastic viscosity; b_1 and b_2 equal the coefficient of the linear term of bambara groundnut flour and sunflower oil; b_{11} and b_{22} are the coefficients of the quadratic terms of the bambara groundnut flour and sunflower oil; b_{12} equals the coefficients of interaction between the bambara groundnut flour and sunflower oil; DF equals degree of freedom; R^2 is the coefficient of determination; Adj R^2 equals the adjusted coefficient of determination; CV is the coefficient of variation

4.4.3.5 Comparison of selected time-independent rheological models

The coefficient of determination for all rheological flow models was close to unity. This was an indication that they can all perfectly predict the flow behavior of the SFO-gelatinized BGNF emulsion within the range of shear rate studied. However, the root mean square error and standard error (SE) values for Casson model were lower than the corresponding prediction of the power law, Herschel-Bulkley and Bingham models. In addition the observed R^2, was highest for all predictions of Casson model compared to all other tested models. Hence, Casson model is the best predictor within the studied range of BGNF and oil-phase concentrations. The consistency coefficients were slightly higher for power law model than for Herschel-Bulkley model (Table 4.22 and Table 4.24). However, the flow behavior index was slightly lower for the power law than the Herschel Bulkley model. This probably may be due to the yield stress being an integral part of H-B model while power law

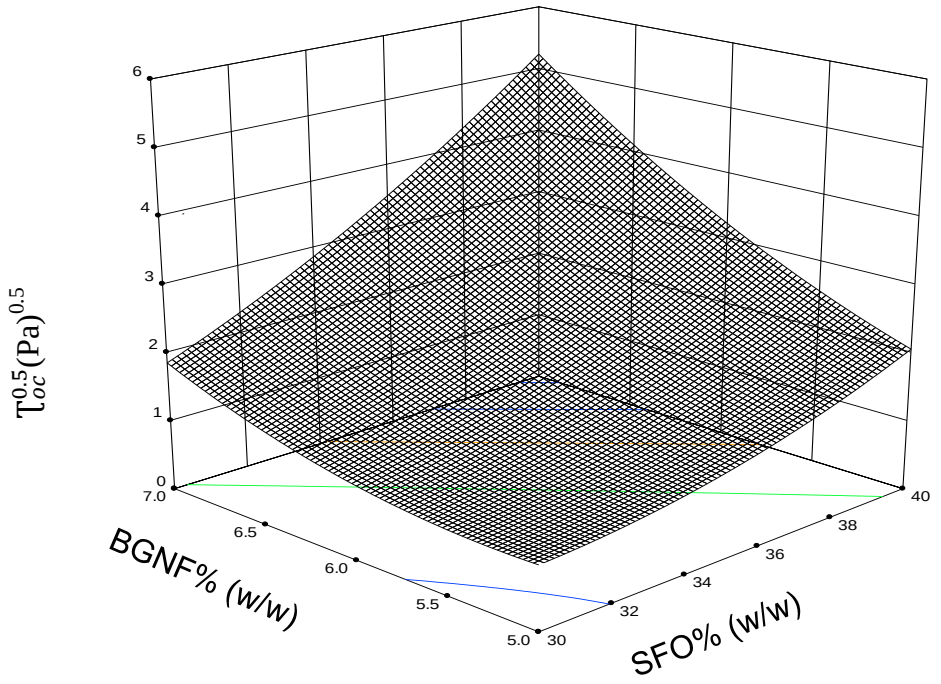

A

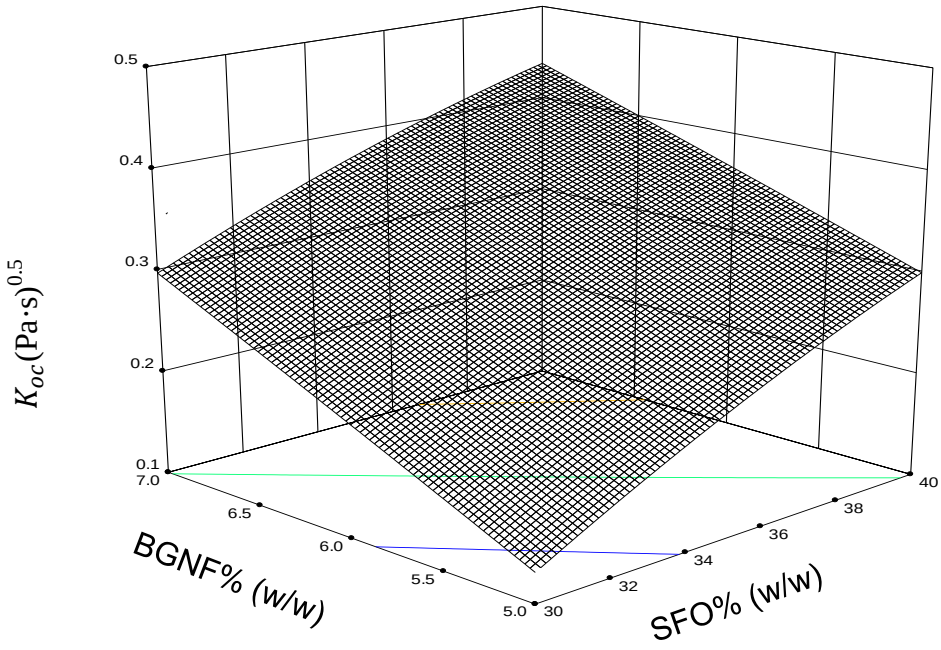

B

Figure 4.39 **Response surface for the effect of bambara groundnut flour (BGNF) and sunflower oil (SFO) concentrations on (A) Casson yield stress ($\tau_{oc}^{0.5}$) and (B) Casson viscosity (K_{oc})**

model disregards the yield stress. Keshani *et al.* (2012) reported a similar observation while studying the rheological properties of pomelo juice concentrates.

4.4.3.6 Summary on time-independent characterization of BGNF-stabilized emulsions

Steady state flow curves of both continuous phase (gelatinized BGNF dispersions) and emulsion showed shear thinning characteristics. Increase in SFO and BGNF concentrations increased system flocculation which manifested as an increase in apparent viscosity of the emulsions. The pseudoplastic nature of the emulsions was as a result of both oil-droplet deflocculation as the shear rate increased and the non-Newtonian nature of the gelatinized bambara groundnut flour. All tested models can reasonably predict steady shear behavior of emulsions stabilized with BGNF. Both power law and Herschel-Bulkley models predicted an increase in consistency coefficient and decrease in flow behavior index with an increase in oil-phase and BGNF concentrations. Fitting of rheological data to Bingham, Herschel-Bulkley and Casson model revealed that all BGNF emulsion samples possessed yield stress which increased as the BGNF and oil phase concentration increased. However, Casson model was the best predictor because of its relatively highest coefficient of determination (R^2), lowest root mean square error (RMSE) and standard error (SE). Response surface methodlogy was found suitable for determining the relationship between the level of emulsion components (BGNF and SFO) and rheological parameters of the fitted models. Bambara groundnut flour therefore, conferred high consistency, viscosity and yield on emulsion systems. This could be as a result of the psedoplastic nature of bambara groundnut flour dispersions.

4.5 Viscoelastic Properties of BGNF Stabilized Emulsions

Oscillatory and creep and recovery tests were employed to investigate the viscoelastic properties of BGNF-stabilized emulsions. The relationships between the emulsion components and some important viscoelastic parameters such as loss and storage moduli and recoverable strain were also established by using RSM. Viscoelastic parameters that translated to high emulsion stability were identified, modeled and explained.

4.5.1 Effect of BGNF and SFO on storage and loss moduli

The effect of BGNF and SFO on the viscoelastic properties of oil-in-water emulsions was also assessed. Material functions in the linear viscoelastic range of the emulsions were used to assess the emulsions stability. To achieve this, shear stress amplitude experiment was conducted at constant frequency of 6.28 rad/s and storage and loss moduli were recorded as a function of stress (0.01-100 Pa). Figures 4.40, 4.41 and 4.42 show the shear stress amplitude sweep of emulsions formulated with 30, 35 and 40% (w/w) SFO and

stabilized with 5, 6 and 7% (w/w) BGNF respectively. The results were displayed on the logarithmic scale where the material functions (properties) were placed on the Y-axis and shear stress amplitude was on the X-axis. All the emulsions possessed linear viscoelastic region (LVR). The LVR of the BGNF stabilized emulsions is the range at which both the elastic/storage modulus (G') and viscous/loss modulus (G") tended to show a constant plateau within the portion of the tested shear stress amplitude (Figures 4.40, 4.41 and 4.42). The existence of LVR was due to the resistance of emulsion structures to increased shear stress. The extended or increased plateau (LVR) is therefore related to the stability of the emulsion as increased shear stress will be required to overcome the high structural resistance of the emulsions. The more extended the LVR the higher the structural strength and hence the more stable the emulsion. The structure of the emulsion within the LVR is preserved. However, the structural breakdown is usually observed outside the LVR.

The spectra of the emulsions showed that at low amplitude G' is always above G'' within the observed LVR. This behaviour is associated with the gel character of the BGNF stabilized emulsion within the range of BGNF and SFO concentrations tested. Materials that showed G' above G'' within the LVR tended to exhibit some rigidity and therefore have greater tendencies to be very stable (Mezger, 2006). On the contrary, if G" is observed to be higher than G' within the LVR, such material tended to exhibit a liquid character and therefore are usually not stable. Increased G' is therefore related to increased elasticity and rigidity which translate to high emulsion stability. In other words, all the studied BGNF stabilized emulsions were gel like stable emulsions.

In order to assess the effect of BGNF and SFO on the emulsions LVR (relative stability), the G' was plotted against shear amplitude for all the emulsion formulations. G' allows the comparison of the elasticity of the emulsions as a function of BGNF and SFO concentration. Figure 4.43 shows the graphs of the G' as a function of amplitude for all the emulsions. The effect of BGNF and SFO concentrations was profound on the G' and LVR of the emulsions. There were observed extended increase in the LVR with an increase in BGNF and SFO concentration. Emulsions formulated with 40% (w/w) and 30% (w/w) SFO irrespective of the BGNF concentration had the highest and lowest G' values and LVR respectively. Figure 4.44 shows the effect of BGNF concentration on emulsions containing 40% (w/w) SFO. Emulsion stabilized with 7% (w/w) and 5% (w/w) BGNF had the highest and lowest G' values and LVR respectively. This observation is directly related to their respective structural stability. In other words, emulsion containing 40% (w/w) SFO and stabilized with 7% (w/w) BGNF had the strongest and most elastic structure. This is related to both individual contributions of BGNF and SFO and high structural interactions between the BGNF and SFO to structural formation of the emulsion.

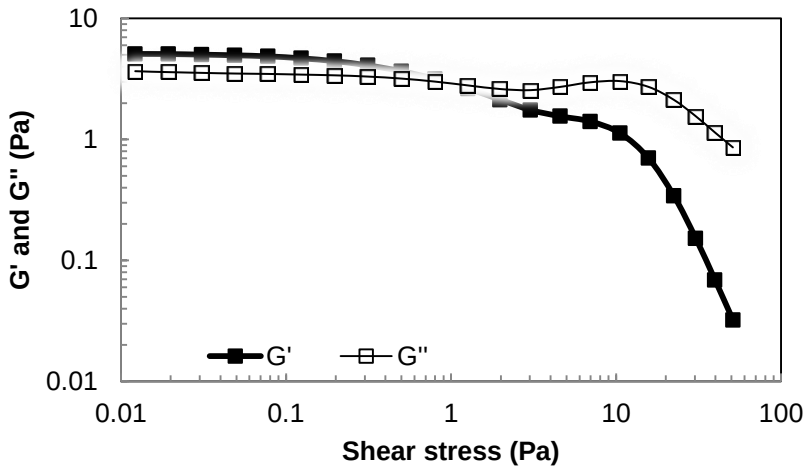

A

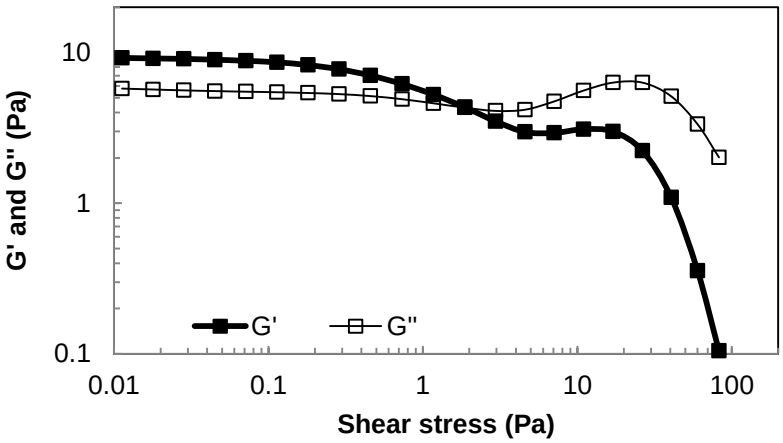

B

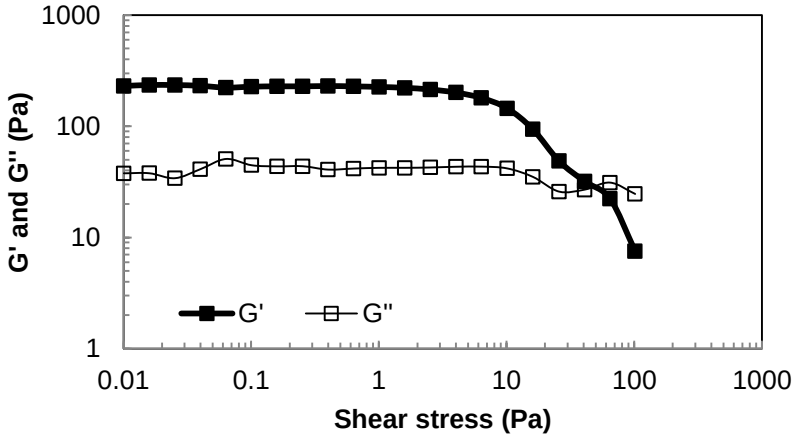

C

Figure 4.40 **Shear stress amplitude sweep of emulsions stabilized with 5% (w/w) bambara groundnut flour (BGNF) (A) 30% (w/w) SFO (B) 35% (w/w) SFO (C) 40% (w/w) sunflower oil (SFO)**

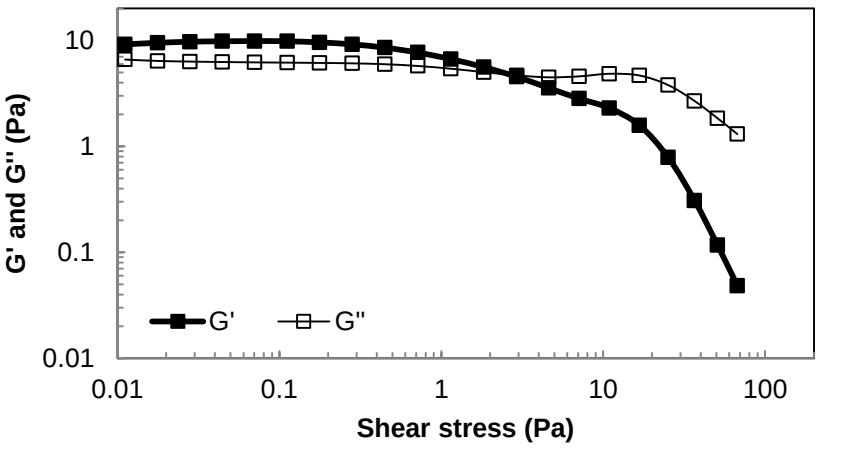

A

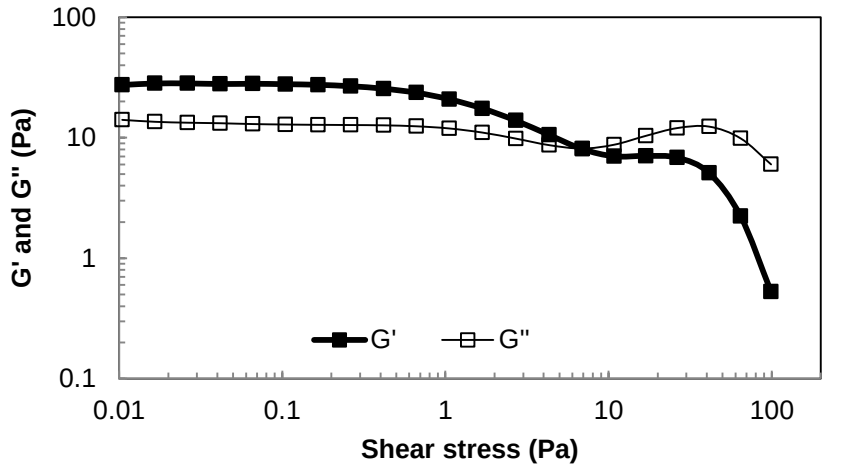

B

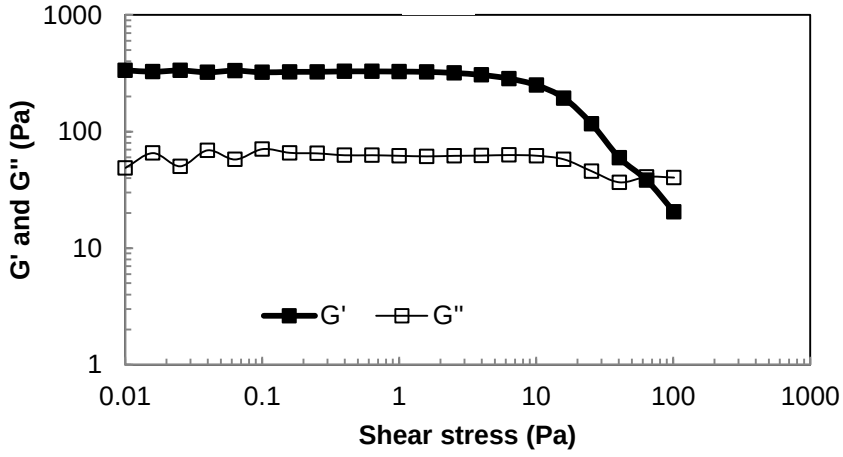

C

Figure 4.41 **Shear stress amplitude sweep of emulsions stabilized with 6% (w/w) Bambara groundnut (BGNF) (A) 30% (w/w) SFO (B) 35% (w/w) SFO (C) 40% (w/w) sunflower oil (SFO)**

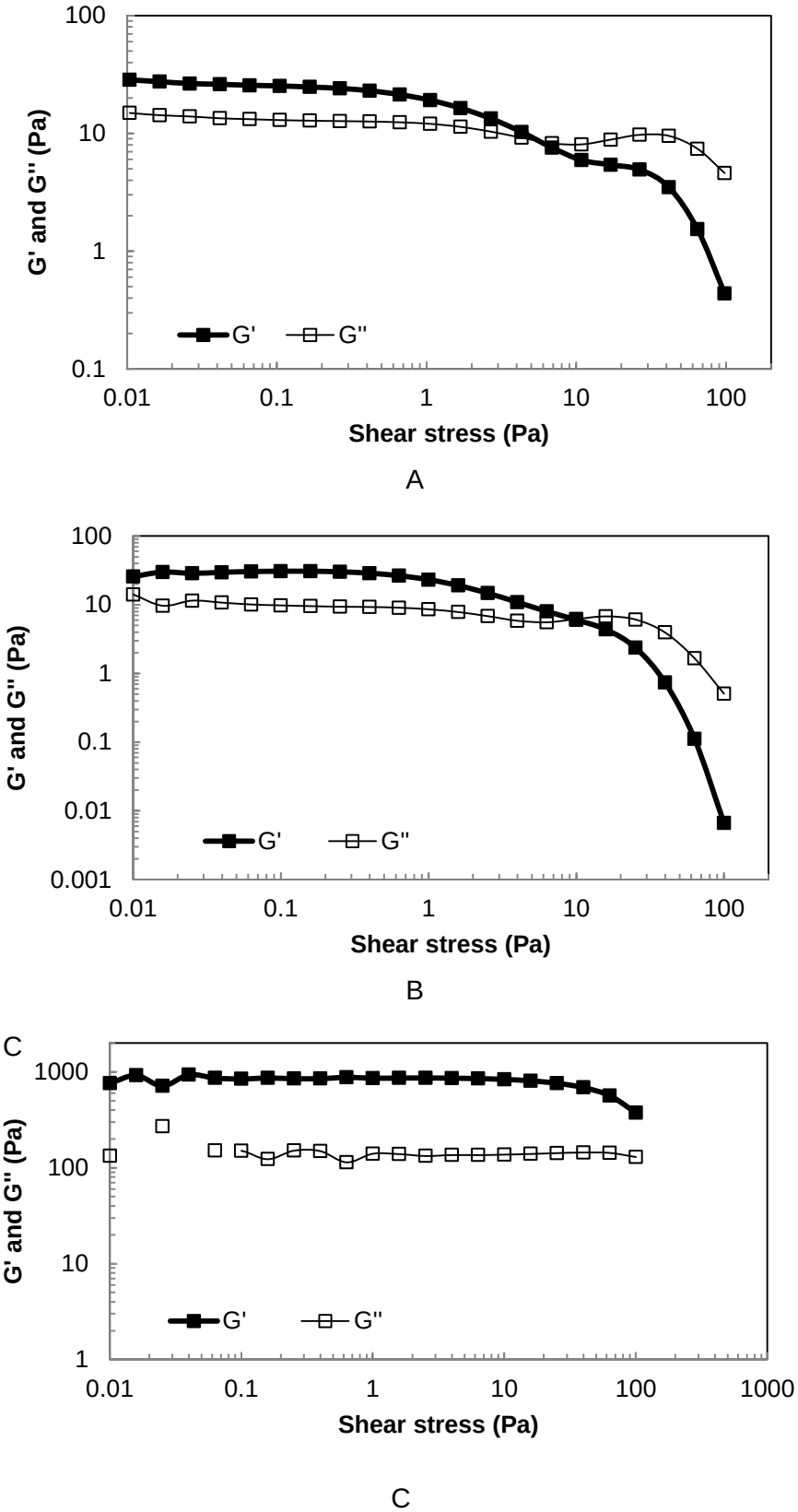

Figure 4.42 **Shear stress amplitude sweep of emulsions stabilized with 7% (w/w) BGNF (A) 30% (w/w) SFO (B) 35% (w/w) SFO (C) 40% (w/w) SFO**

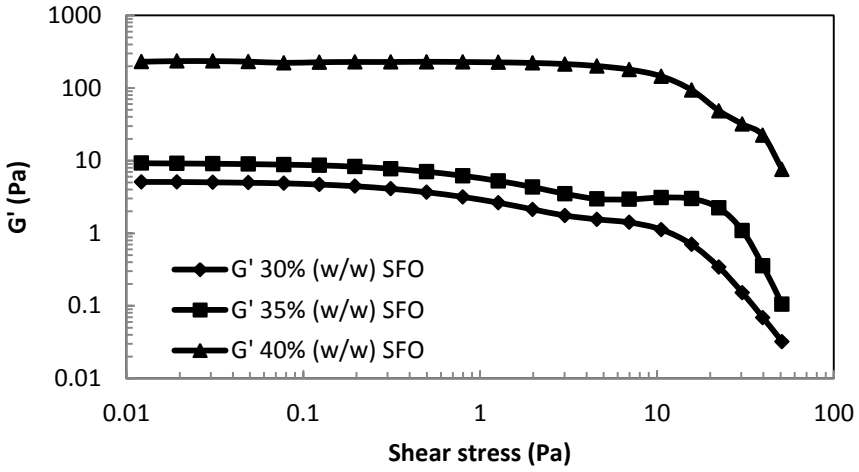

A

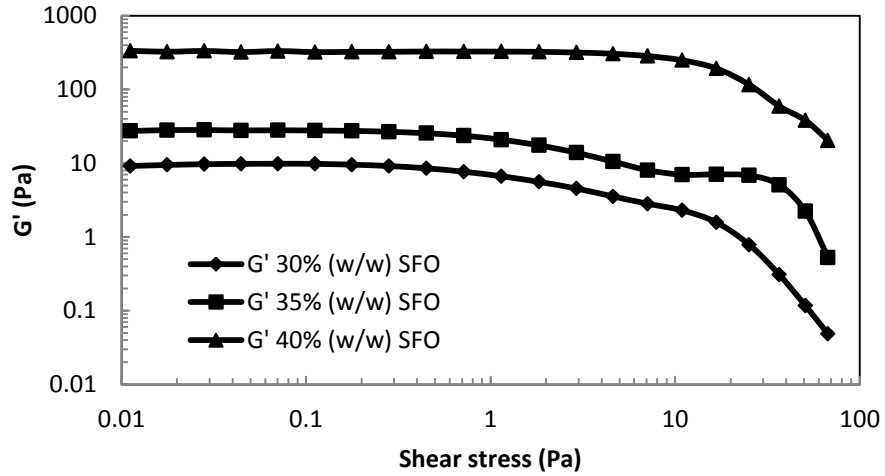

B

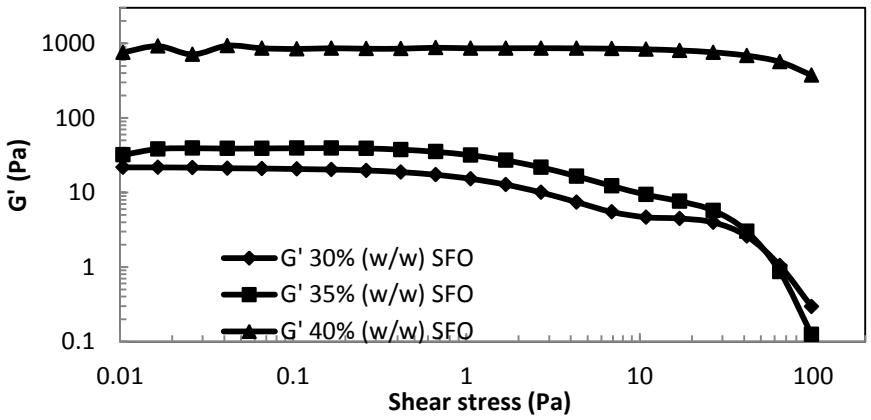

C

Figure 4.43 Effect of SFO concentrations on the LVR of emulsions stabilized by (A) 5% (w/w) BGNF (B) 6% (w/w) BGNF (C) 7% (w/w) BGNF

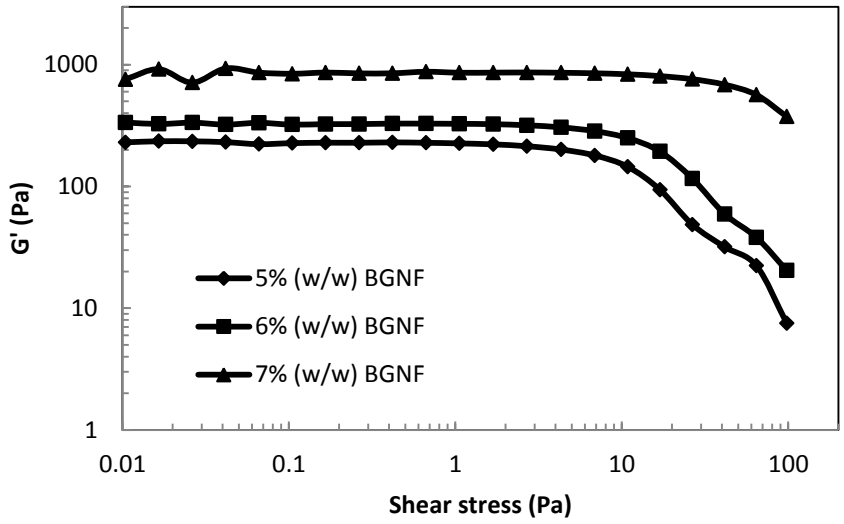

Figure 4.44 Effect of bambara groundnut (BGNF) concentrations on the LVR of emulsions formulated with 40% (w/w) sunflower oil (SFO)

Frequency sweep experiment was conducted within the LVR in order to obtain the finger print of the emulsions as a function of time. The purpose of the test is to monitor the micro and macro structural rearrangements (stability) with time. In other words, the time-dependent shear behaviour of the emulsions within the LVR was determined. To this effect, shear stress amplitude of 0.1 Pa which was within the LVR (previously determined) was imposed on all the emulsions. Figures 4.45, 4.46 and 4.47 show the results of the frequency sweep experiments obtained for emulsions formulated with 30, 35 and 40% (w/w) SFO and stabilized with 5, 6 and 7% (w/w) BGNF, respectively. The logarithms of G', G" and complex viscosity (η^*) were plotted on the Y-axis as a function of logarithm of the frequency on the X-axis. All the BGNF stabilized emulsion exhibited both the $G^{'}$ and $G^{"}$. G' was higher than G'' curve at the low frequencies and tended to show a constant limiting value for all the emulsions. The η^* was also increasingly rising towards an infinitely high value at low frequencies. These observations are characteristics of gels. The high values of G' at low frequency is an indication of high structural strength of the emulsions. The emulsions therefore exhibit the tendencies to be rigid, possess high flow resistance and therefore form stability at rest (during storage). Both the storage and loss modulus showed significant dependence on the frequency and were increased with increase in frequency for emulsions containing 30 and 35% (w/w) SFO and stabilized with 5 and 6 and 7% (w/w) BGNF. This rheological characteristic typifies emulsions with weak gels (Heyman, 2010). Emulsions containing 30 and 35% (w/w) SFO stabilized with 5% (w/w) BGNF showed a solid-like behaviour at low frequencies where G' dominated and was larger than the G''

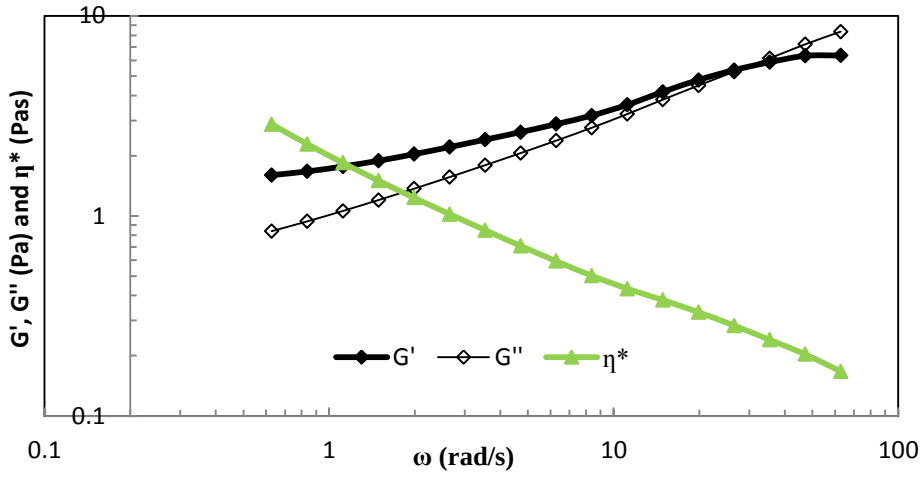

A

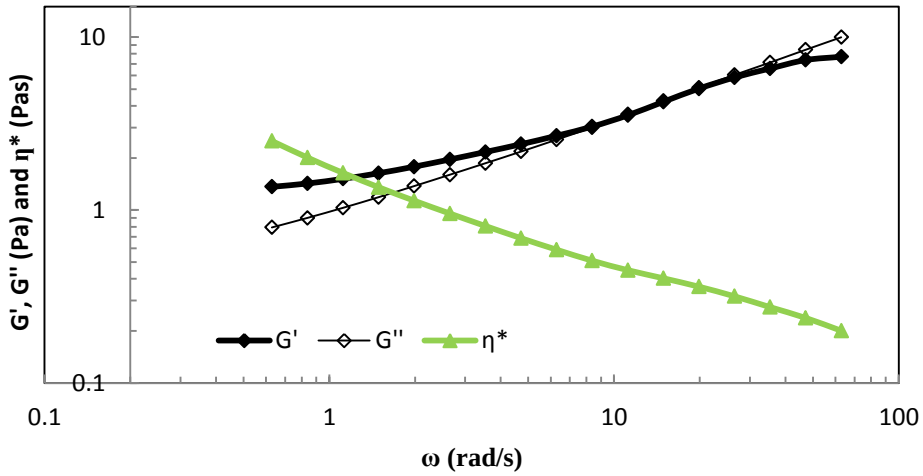

B

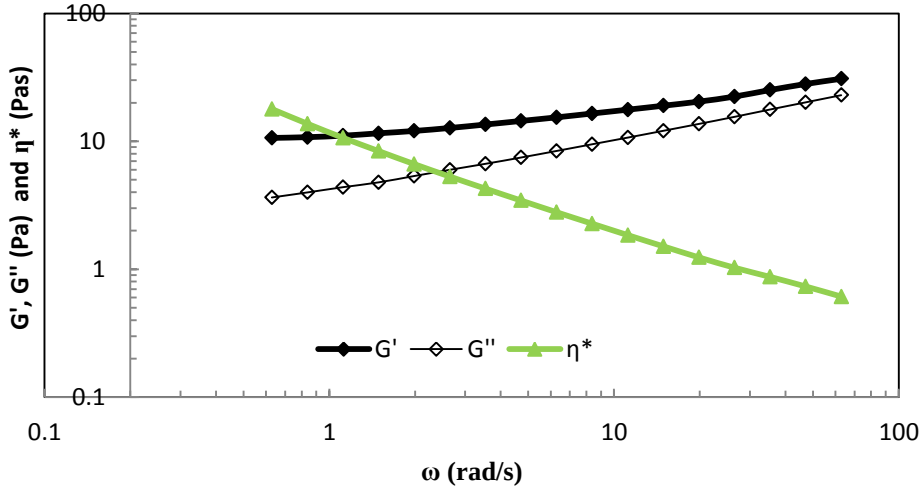

C

Figure 4.45 **Frequency sweep of emulsions stabilized 5% (w/w) BGNF formulated with (A) 30% (w/w) SFO (B) 35% (w/w) SFO (C) 40% (w/w) SFO**

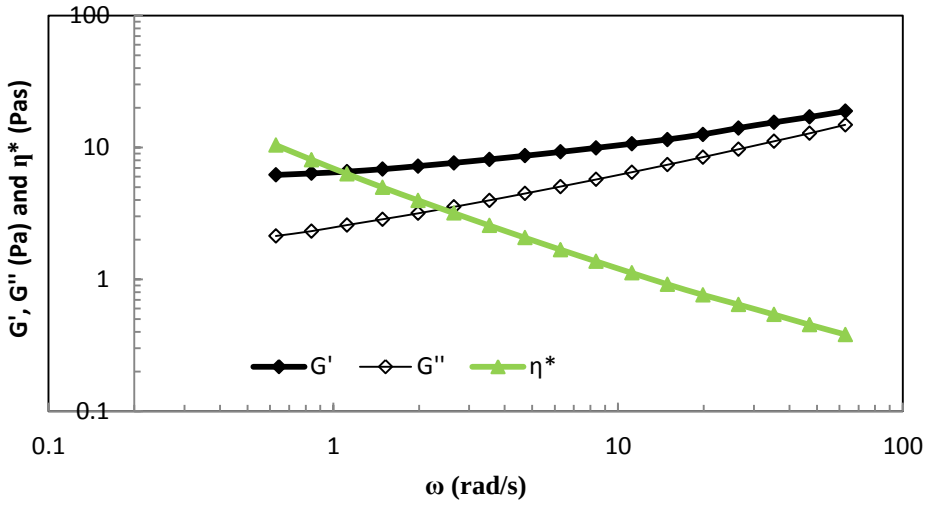

A

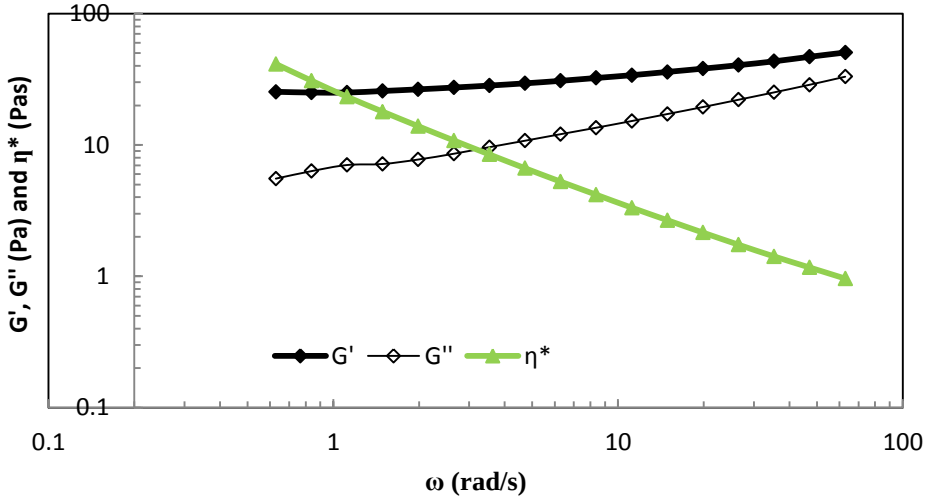

B

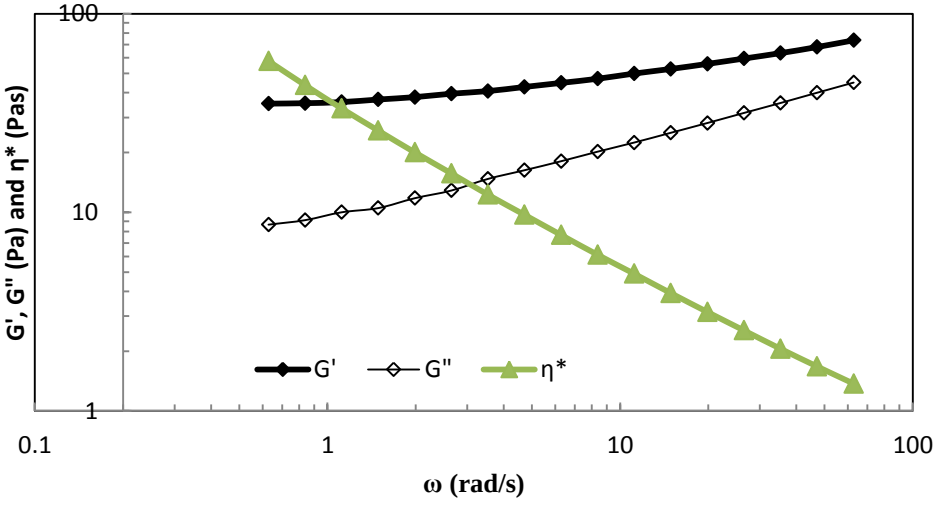

C

Figure 4.46 **Frequency sweep of emulsions stabilized 6% (w/w) BGNF formulated with (A) 30% (w/w) SFO (B) 35% (w/w) SFO (C) 40% (w/w) SFO**

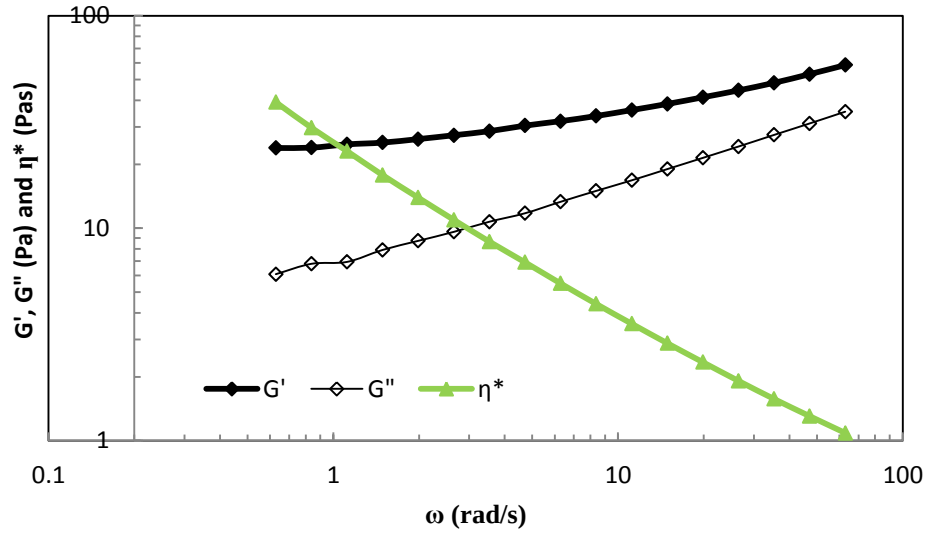

A

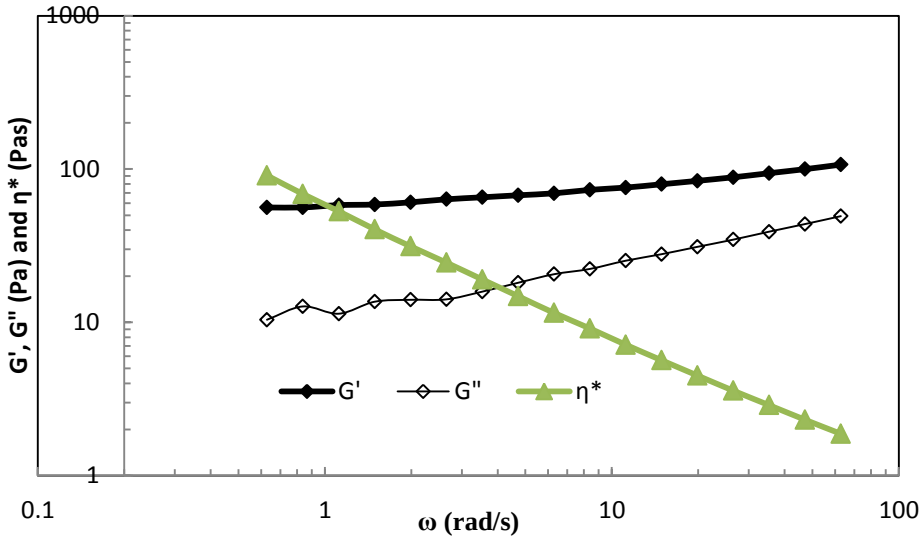

B

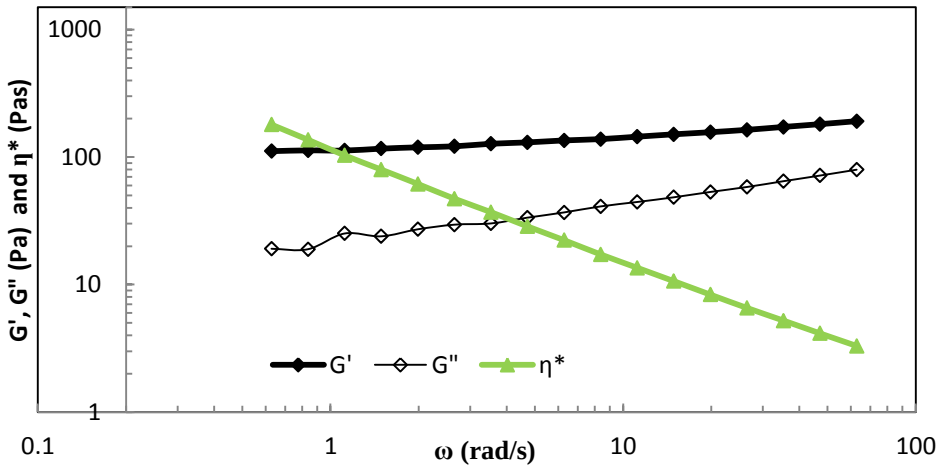

C

Figure 4.47 **Frequency sweep of emulsions stabilized 7% (w/w) BGNF formulated with 30% (w/w) SFO (B) 35% (w/w) SFO (C) 40% (w/w) SFO**

(Lorenzo *et al.,* 2011). There was observed cross over at higher frequency of about 35.33 rad/s and with G'' was observed to be higher than G' there by showing a liquid-like behaviour at higher frequency for both formulations. This behaviour is typical of polymeric solutions and was found in low-in-fat oil in water emulsion stabilized with xanthan/guar mixture (Lorenzo *et al.,* 2008). This behaviour may be unconnected with the behaviour of BGNF used to achieve emulsion stabilization.

Emulsions containing 40% (w/w) SFO, stabilized with, 5, 6 and 7% (w/w) BGNF showed less dependence on the frequency and significant increase in G' than the G''. This implied predominance in elastic characteristic over viscous behaviour at the frequency range considered suggesting that the emulsions were weak gels. Weak gel characteristics were also found for salad dressing emulsions supplemented with various pulse flours (Ma and Boye, 2013), emulsions stabilized with bovine gelatin (Lorenzo *et al.,* 2011), polymer-thickened oil-in-water emulsions (Pal, 1996) and low-in-fat emulsion stabilized with xanthan/guar mixture (Lorenzo *et al.,* 2008). Both the G' and G'' tended to form a plateau at higher frequency. The plateau region is an intermediate zone of mechanical spectra between the terminal and the transition zone (Lorenzo *et al*. 2011). Figures 4.48A and B and 4.49 show the effect of SFO and BGNF on the G' and G'' of the emulsions. The effect of BGNF and SFO concentrations were noticeable on the material functions. Both G' and G'' were observed to increase with an increase in both BGNF and SFO concentrations. Higher G' was due to increased flocculation in the emulsions as the concentrations of the components increased resulting in more interactions and consequent emulsion stability (Lorenzo *et. al.* 2011). Table 4.30 shows the G' and G'' values obtained for the BGNF stabilized emulsions at low frequency of 0.628 rad/s. The mean values of G' and G'' ranged from 1.50 to 99.0 Pa and 0.76 to 17.1 Pa, respectively. Emulsions containing 30% (w/w) SFO stabilized with 5% (w/w) BGNF and 40% (w/w) SFO stabilized with 7% (w/w) BGNF recorded the lowest and highest G' and G'', respectively. The coefficients of equations representing the material functions (G' and G") as a function of BGNF and SFO are presented in Table 4.31. The quadratic polynomial models obtained for G' and G" were significant ($p < 0.0001$) with high R^2 of > 0.96 (for G' and G") and adequate precision (23.2 and 31.8 for G' and G", respectively) making the models to be accurately employed for predicting the intrinsic rheological emulsion properties as a function of main emulsion components. For the G', p-values of the SFO quadratic model term were greater than 0.05 ($p > 0.05$) indicating that the linear, quadratic term of BGNF and interaction term of BGNF and SFO were significant model terms. Likewise the linear effects of BGNF and SFO and their interaction terms were significant ($p < 0.0001$).

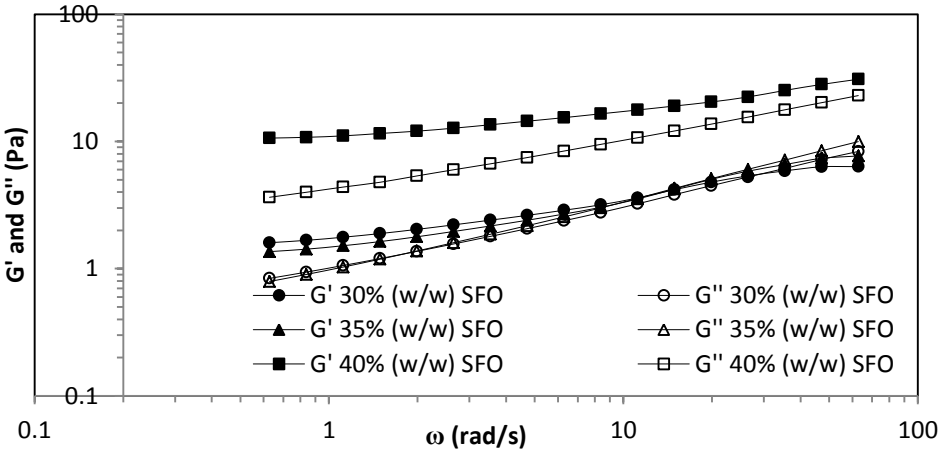

A

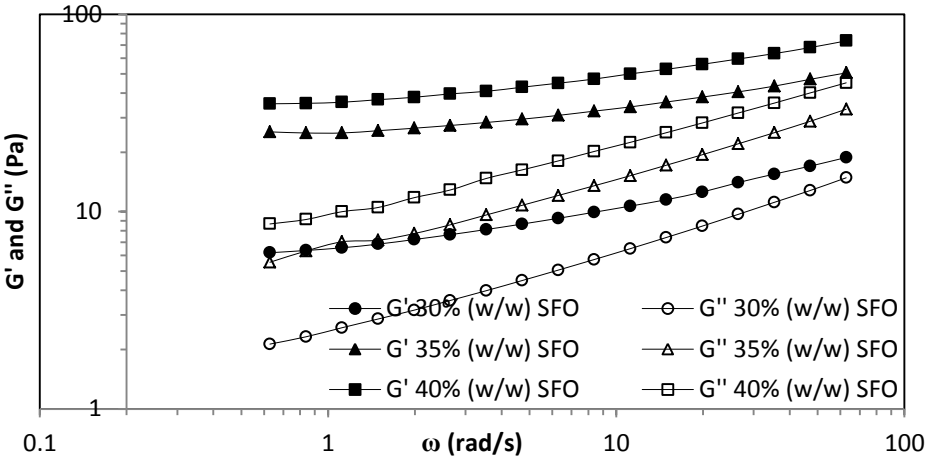

B

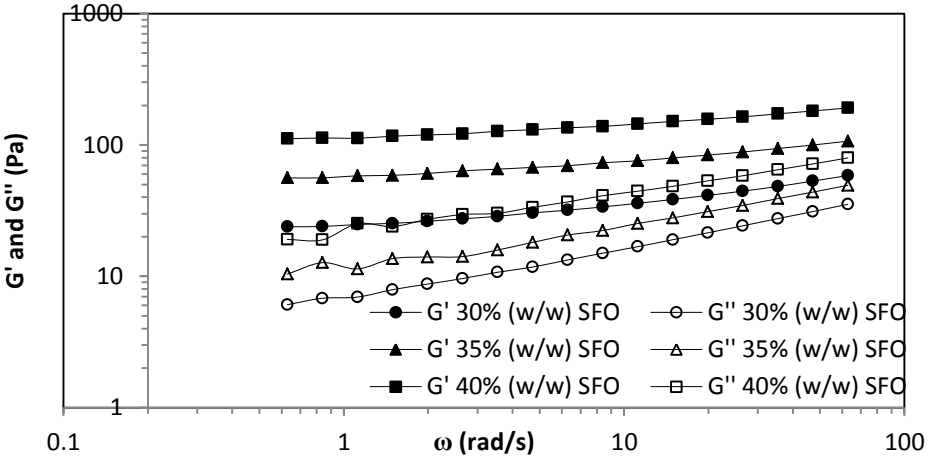

C

Figure 4.48 **Storage (G') and loss (G") moduli as a function of angular frequency during dynamic oscillatory tests of sunflower oil-in-water emulsion stabilized with (a) 5% (w/w) BGNF (B) 6% (w/w) BGNF (C) 7% (w/w) BGNF**

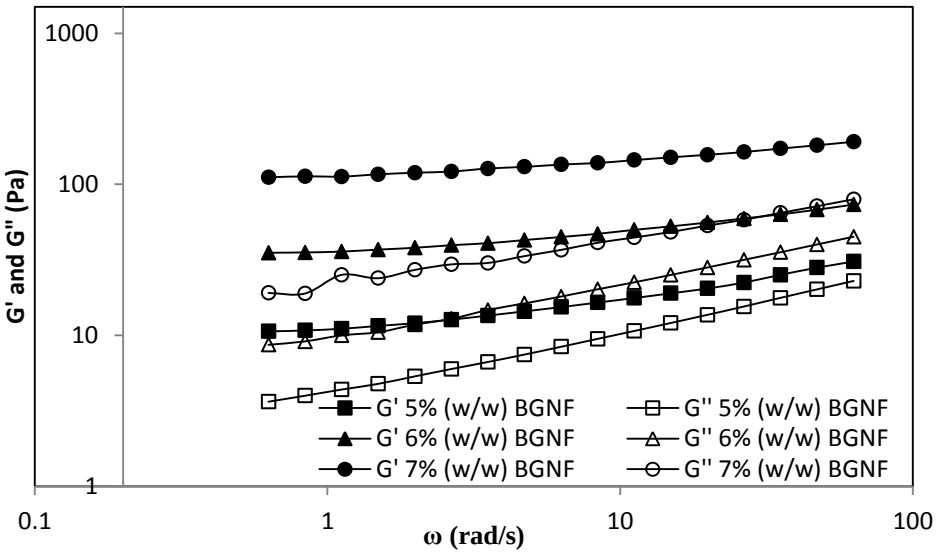

Figure 4.49 Storage (G') and loss (G") moduli as a function of angular frequency of emulsions containing 40% (w/w) SFO stabilized with 5, 6 and 7% (w/w) BGNF

Table 4.30 Storage and loss moduli of BGNF stabilized emulsions at 0.628 rad/s[1]

Emulsion BGNF (%w/w)	SFO (%w/w)	Storage modulus (G') Pa	Loss modulus (G'') Pa
5	30	1.50 ± 0.14	0.76 ± 0.11
	35	1.70 ± 0.48	0.77 ± 0.04
	40	9.75 ± 1.24	3.36 ± 0.39
6	30	6.85 ± 0.93	2.10 ± 0.04
	35	26.2 ± 1.07	5.82 ± 0.39
	40	33.5 ± 2.53	6.03 ± 0.07
7	30	24.2 ± 0.49	6.03 ± 0.07
	35	61.4 ± 7.41	10.3 ± 0.13
	40	99.0 ± 17.5	17.1 ± 2.82

[1]BGNF refers to bambara groundnut flour; SFO is sunflower oil; G' is storage modulus; G'' is the loss modulus

Table 4.31 Analysis of variance (ANOVA) for the response model of storage and loss moduli at 0.628 rad/s[1]

	G' (Pa)				G" (Pa)			
Source	DF	Coefficient	Sum of square	F-ratio p-value	DF	Coefficient	Sum of square	F-ratio p-value
Model	5	+779.16	16506.4	<0.0001	3	+42.96	442.14	<0.0001
Linear								
b_1	1	-14.582	4008.69	<0.0001	1	-1.8690	134.89	<0.0001
b_2	1	-217.07	9818.30	<0.0001	1	-10.058	271.41	<0.0001
Quadratic								
b_{11}	1	-0.0246	1.52	0.8629	-	-	-	-
b_{22}	1	+10.768	463.81	0.0095	-	-	-	-
Interaction								
b_{12}	1	+3.327	2214.10	<0.0001	1	+0.423	35.38	<0.0001
Residual	11		586.34		14		58.93	
Pure error	8		371.00		9		25.43	
Total	15		17092.7		17		3103.8	
Lack of fit	3		215.33	0.2280	5		33.10	0.2230
R^2		0.9657				0.9643		
Adj-R^2		0.9514				0.9567		
CV		23.83				17.77		
Adequate Precision		23.233				31.816		

[1]G' is the storage modulus; G'' is the loss modulus; b_1 and b_2 equal the coefficient of the linear term of bambara groundnut flour and sunflower oil; b_{11} and b_{22} are the coefficients of the quadratic terms of the bambara groundnut flour and sunflower oil; b_{12} equals the coefficients of interaction between the bambara groundnut flour and sunflower oil; DF equals degree of freedom; R^2 is the coefficient of determination; Adj R^2 equals the adjusted coefficient of determination; CV is the coefficient of variation.

The effect of SFO and BGNF were negative for the linear and quadratic term of BGNF ($p < 0.0001$). Similarly the effects of both components (BGNF and SFO) were negative on G" for linear term. The interaction effect of BGNF and SFO were both positive on the storage (G') and loss moduli (G"), respectively. The relationships between BGNF and SFO on G' and G" were illustrated using three dimensional response surface (Figures 4.50A and B). Increasing the concentration of BGNF and SFO independently (Figure 4.50A) led to an increase and decrease in the G' respectively. The simultaneous effect (interaction) of increase in BGNF and SFO drastically increased G'. Regarding G", (Figure 4.50B), an increase in both the BGNF and SFO independently produced a moderate increase in G" value. However, simultaneous increase in the concentrations of the BGNF and SFO led to a drastic increase in G" of the studied emulsions. This implied that the interactive effect of simultaneous increase

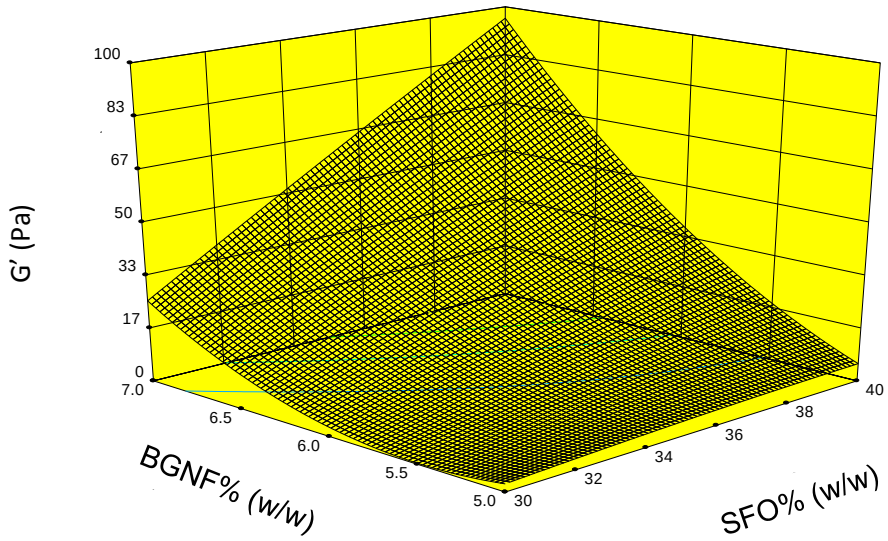

A

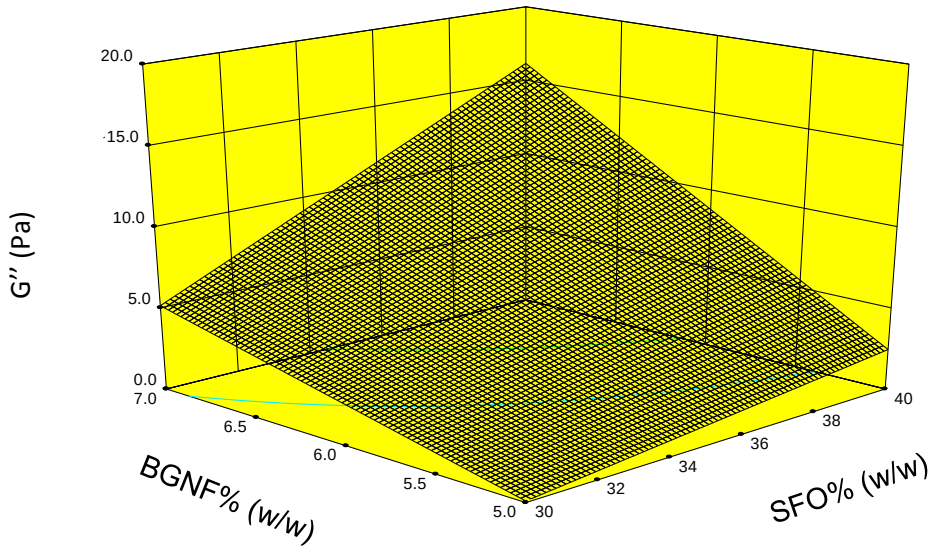

B

Figure 4.50 Response surface for the effect of BGNF and SFO concentrations on (A) storage (G') and (B) loss moduli (G'')

of BGNF and SFO in the emulsion produced a drastic increase in elaticity, viscosity and subsequent stability.

4.5.2 Effect of BGNF and SFO on compliance and recoverable strain

Creep and recovery test was performed to gain insight into deformation and recovery behaviour as a function of time. This shows the rigidity (stability) of the emulsion formulations under a low shear stress over a long period of time such as conditions encountered during storage. BGNF-stabilized emulsions were subjected to a constant shear stress of 0.5 Pa (previously determined to be within linear viscoelastic region) and the stress was suddenly removed. Both the deformation and the recoverable strain were recorded as a function of time during a period of 500 s. Figures 4.51A, B and C show the plot of compliance (J), defined as the ratio of strain to applied stress (Pal, 1996) against time (s). The figures showed two part of the creep and recovery experiment. The first part is when a stress was imposed on the structure of the emulsion (creep stage) for the first 500 s and the second part was when the stress was suddenly removed (recovery stage) for the next 500 s. All the emulsions showed typical viscoelastic characteristics during creep and recovery phases. The creep and recovery curves were also similar for all the samples. For instance, J steadily increased when a stress of 0.5 Pa was imposed on all the emulsions (creep stage) and the elastic component of the deformation recovered instantaneously when the load was removed (Figure 4.51A, B and C). This is shown as a sharp decrease at the beginning of the recovery stage. The present observation is similar to the behaviour of salad dressing type emulsion supplemented with pulse (Ma and Boye, 2013). The emulsion containing lowest amount of BGNF and SFO recorded the highest J value while the emulsion containing the highest BGNF and SFO recorded the lowest creep J value. The high J showed a negligible instantaneous elastic compliance and indicated that the network of the emulsion structure is weak and less rigid. Lower J however is a pointer to stronger structural interactions (high rigidity) in emulsion indicating a relatively small deformation when the stress was imposed on them. Both the BGNF and SFO had profound influence on the J values. Increase in BGNF and SFO (Figure 4.51 and 4.52) decreased J. This is as a result of increased structural formation which increased emulsion rigidity. Table 4.32 shows the recoverable strain Q (t)% obtained for the studied emulsion. The greater the extent of recoverable strain, the greater is the elasticity of the sample (Ma and Boye, 2013) and stability. The mean of Q (t)% ranged between 7.57 to 59.4% for all the emulsions. The emulsion containing 30% (w/w) SFO, stabilized with 5% (w/w) had the lowest value of Q (t)% indicating that this emulsion had the lowest elasticity and stability among the emulsions formulated. Emulsion with 40% (w/w) SFO, stabilized with 7% (w/w) recorded the highest elasticity.

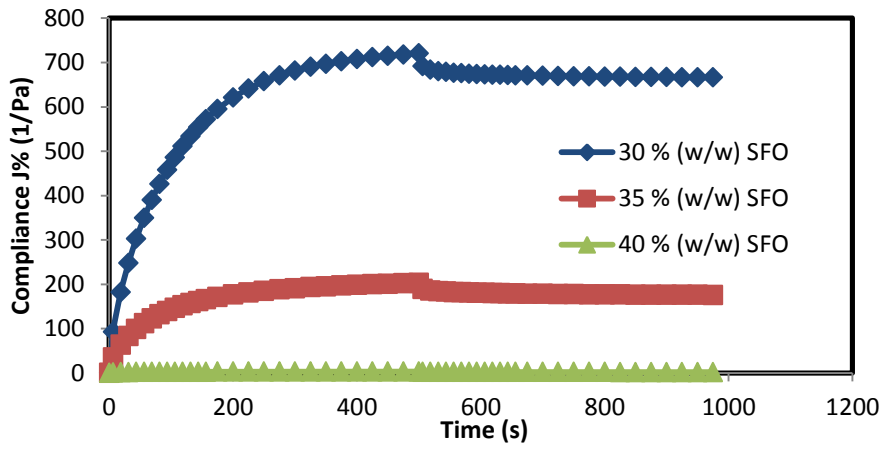

A

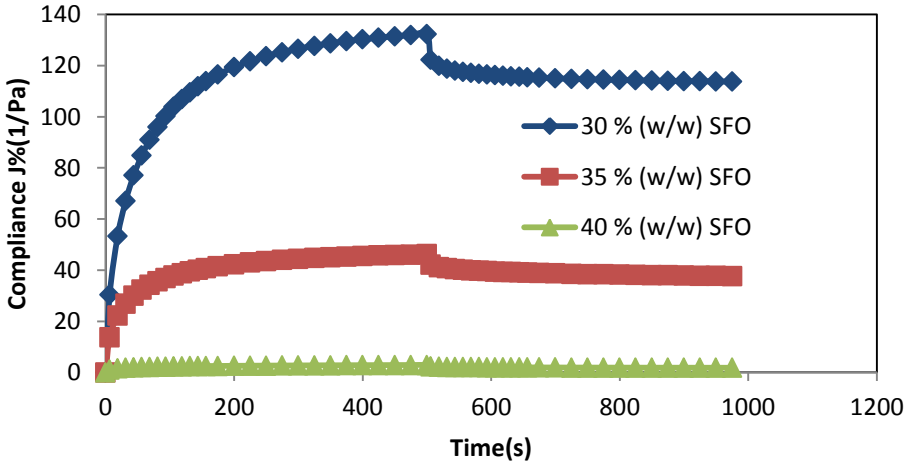

B

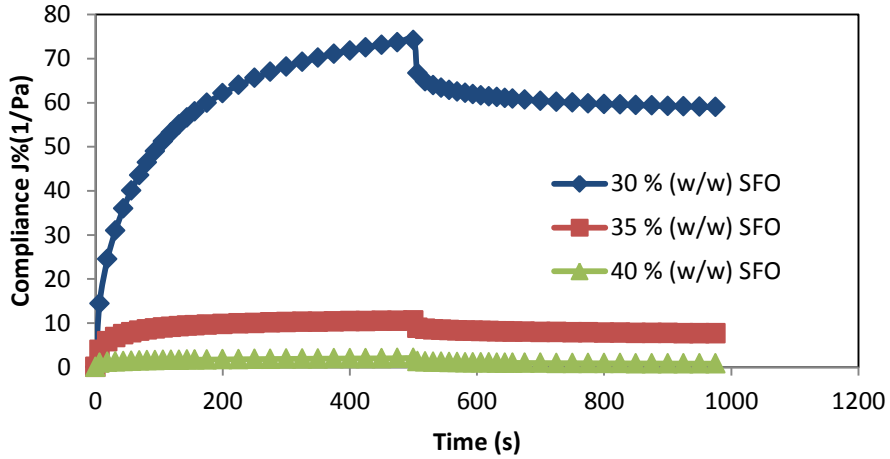

C

Figure 4.51 **Creep and recovery curves of oil-in-water emulsion containing sunflower oil (SFO) stabilized with (A) 5% (w/w) (B) 6% (w/w) (C) 7% (w/w) bambara groundnut flour (BGNF).**

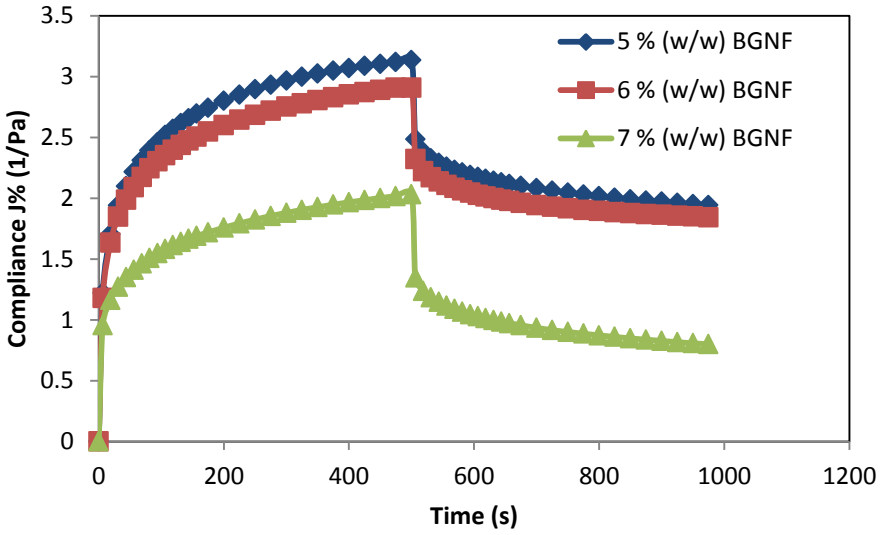

Figure 4.52 **Creep and recovery curves of emulsions containing 40% (w/w) sunflower oil (SFO) stabilized with 5, 6 and 7% (w/w) bambara groundnut flour (BGNF)**

Table 4.32 **Recoverable strain of BGNF stabilized emulsion[1]**

Emulsion BGNF (%w/w)	SFO (%w/w)	Recoverable strain (Q (%))
5	30	7.57 ± 0.93
	35	12.1 ± 1.94
	40	35.5 ± 0.71
6	30	14.2 ± 1.25
	35	18.4 ± 2.29
	40	40.1 ± 1.95
7	30	20.1 ± 3.09
	35	27.5 ± 0.17
	40	59.4 ± 1.68

[1]BGNF refers Bambara groundnut flour; SFO refers to sunflower oil; Q is the recoverable strain

The ANOVA for the quadratic models developed for the recoverable strain is presented in Table 4.33. The quadratic polynomial for the recoverable strain as a function of emulsion components was significant ($p < 0.0001$) with high R^2, coefficient of variation, adequate precision and significant lack of fit. The linear term of BGNF and SFO, the

quadratic term of BGNF and the interaction term of BGNF and SFO are the significant model terms ($p < 0.05$) for the recoverable strain (Q (t)%). The effect of the linear term of SFO and BGNF were both negative. The quadratic effect of BGNF and interaction effect of BGNF and SFO were positive on the recoverable strain. The response surface for the individual and simultaneous increase of SFO and BGNF on the recoverable strain is shown in Figure 4.53.

Table 4.33 ANOVA for the quadratic model of recoverable strain (Q (t)%)

	Recoverable strain (Q (t)%)			
Source	DF	Coefficient	Sum of Square	p-value
Model	5	+517.89	3045	<0.0001
Linear				
b_1	1	-26.919	2364.95	<0.0001
b_2	1	-35.485	723.56	<0.0001
Quadratic				
b_{11}	1	+0.413	366.95	<0.0001
b_{22}	1	+0.392	22.79	0.0636
Interaction				
b_{12}	1	+0.414	28.27	0.0422
Residual	11		58.93	
Pure error	8		25.43	
Total	15		3103.85	
Lack of fit	3		33.10	0.0690
R^2	0.9810			
Adj-R2	0.9724			
CV	9.60			
Adequate precision	33.854			

[1]Q (t) refers to recoverable strain; b_1 and b_2 equal the coefficient of the linear term of bambara groundnut flour and sunflower oil; b_{11} and b_{22} are the coefficients of the quadratic terms of the bambara groundnut flour and sunflower oil; b_{12} equals the coefficients of interaction between the bambara groundnut flour and sunflower oil; DF equals degree of freedom; R^2 is the coefficient of determination; Adj R^2 equals the adjusted coefficient of determination; CV is the coefficient of variation.

The recoverable strain was dependent on both the concentration BGNF and SFO. Increase in the BGNF and SFO independently, increased the recoverable strain of the studied emulsion. Simultaneous increase of SFO and BGNF however caused a significant increase in the recoverable strain. This indicated that the elastic behavior of the entire emulsions was strongly dependent on BGNF and SFO concentrations and their interactions.

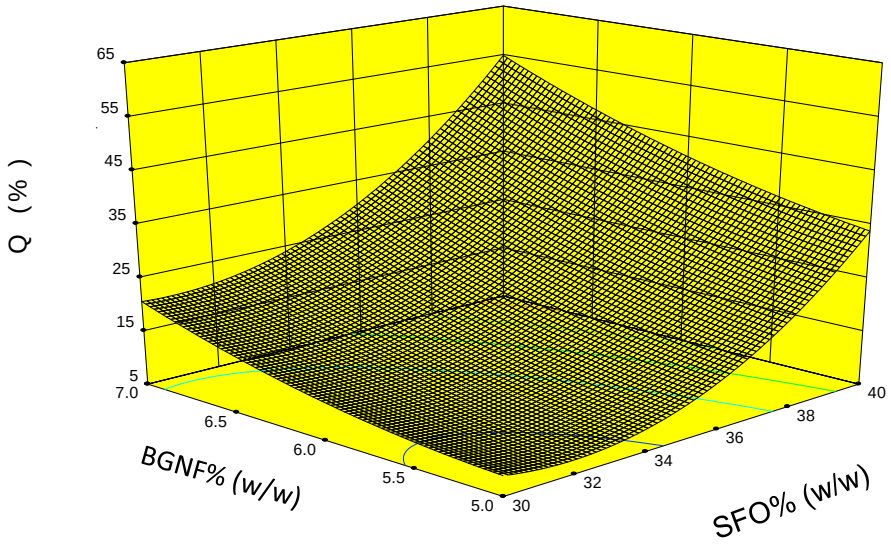

Figure 4.53 Response surface for the effect of BGNF and SFO concentrations on recoverable strain

4.5.3 Summary on viscoelastic properties of BGNF stabilized emulsions

This section studied the effect of BGNF and SFO on the viscoelastic properties of oil-in-water emulsions stabilized with BGNF. All the studied BGNF stabilized emulsions were viscoelastic materials. There was dominance of elastic property (G') over viscous properties (G") at low frequency and the complex viscosity tended to rise indefinitely irrespective of BGNF and SFO concentrations. Emulsions formulated with 5% (w/w) BGNF and 30 or 35% (w/w) SFO showed cross over to more viscous character at high frequency which implied a high tendency to structural breakdown (destabilize) when shaken perhaps during transportation. All of the emulsions formulated with 40% (w/w) (high dispersed phase) showed less dependency on frequency and indicated high structural strength. Increased in BGNF and SFO concentrations contributed greatly to the structural strength of the emulsions by increasing the elastic modulus and therefore emulsions have the potential of remaining highly rigid and stable over time. There were also decrease in compliance and increased recoverable strain with increased emulsion components. This is as a result of high structural interactions which increased the elasticity and rigidity of the emulsions by forming increased droplet network within BGNF matrix. Response surface methodology was found useful for modeling the viscoelastic parameters as function of BGNF and SFO.

4.6 Effect of Different Varieties of Bambara Groundnut Flour (BGNF) on O/W Emulsion Stability and Rheology

The proximate composition of different varieties of BGNF has been reported by Ojimelukwe and Ayernor (1992). There is slight difference in the composition of the varieties of BGNF investigated in terms of crude protein, fat, moisture, soluble and total carbonhydrate and ash contents (Table 2.2). This section reported the results of the varietal difference on the stability and rheological properties of optimal BGNF-stabilized emulsion. All the intrinsic stability and rheological properties peculiar to each BGNF varieties were evaluated and explained. The respective ability of all the varieties of BGNF to stabilize oil-in-water emulsion was also evaluated and compared.

4.6.1 Effect of BGNF varieties on emulsion stability with regard to droplet size distribution

Four different BGNF varieties were used to stabilize sunflower oil-in-water emulsions at optimum ingredient (BGNF and SFO) concentrations as predicted by RSM in section 4.2.4. Emulsions (100 g) containing 7% (w/w) BGNF of each four varieties and 40% (w/w) sunflower oil were prepared separately and their properties studied. Figure 4.54 is the droplet size distribution of oil-in-water emulsions stabilized with black eye (BE), brown eye (BRE), red (RED) and brown (BV) varieties of BGN. This is an indication that all the studied bambara groundnut varieties can form oil - water emulsions.

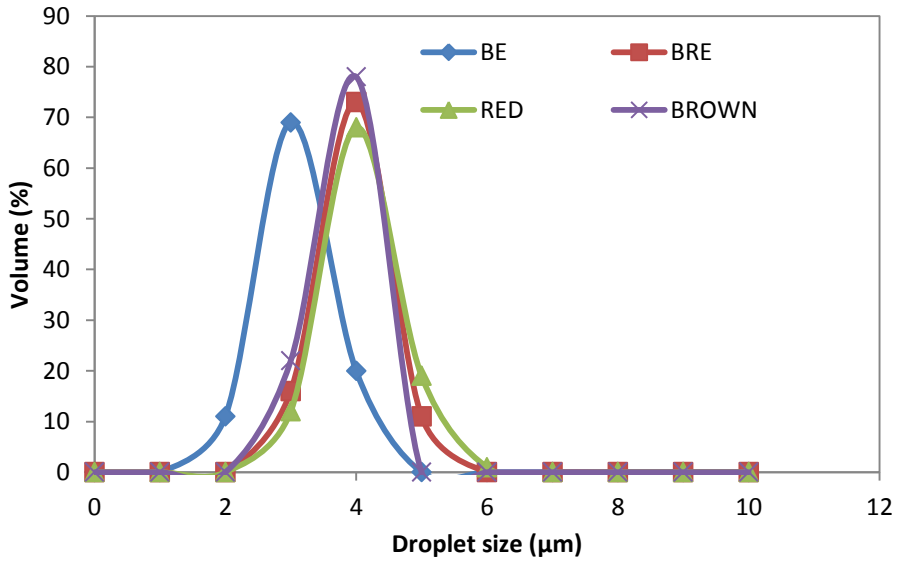

Figure 4.54 **Droplet size distribution of dispersed phase particles in emulsion stabilized with four varieties of BGN**

The oil-droplet distribution of the emulsions showed close similarities. Close similarities in the distribution curve is an indication that all the four varieties have comparable matrix and strength to achieve emulsion formation. Table 4.34 presents the oil-droplet sizes of the emulsions stabilized with four varieties of BGNF. The mean of $d_{3,2}$ was between 3.34 and 3.77 µm while $d_{4,3}$ was between 3.38 and 3.87 µm. The $d_{4,3}$ was relatively higher than the corresponding $d_{3,2}$ as expected. The $d_{4,3}$ is a measure of changes in oil-droplet size involving emulsion destabilization process while $d_{3,2}$ gives information regarding size of the emulsion where most oil-droplet fall.

Table 4.34 Effect of BGNF variety on particle size[1,2]

BGNF variety	$d_{3,2}$ (µm)	$d_{4,3}$ (µm)
Black- eye	3.34 ± 0.05^{a}	3.38 ± 0.12^{a}
Brown-eye	3.52 ± 0.04^{a}	3.58 ± 0.10^{ab}
Red	3.77 ± 0.12^{b}	3.87 ± 0.08^{c}
Brown	3.45 ± 0.10^{a}	3.66 ± 0.11^{ab}

[1]Values are mean ± standard deviations; Mean with different letters within the same column are significantly different from each other ($p < 0.05$).
[2]$d_{3,2}$ refers to the volume surface mean diameter of the emulsions; $d_{4,3}$ is the equivalent volume-mean diameter of the emulsions; BGNF is bambara groundnut flour

Except for red variety, the $d_{3,2}$ and $d_{4,3}$ of emulsions stabilized with black eye, brown eye and brown bambara groundnut varieties did not have any significant difference. This implies that the effect of brown, black eye and brown eye varieties was similar regarding their ability to form emulsions. Emulsion stabilized with red variety showed higher $d_{3,2}$ and $d_{4,3}$ relative to others. The relative difference in BGNF varieties could be related to the differences in their proximate compositions.

4.6.2 Effect of BGNF varieties on emulsion stability with regard to microstructure

The effect of varieties of BGNF on microstructure of the emulsion is presented in Figures 4.55A, B, C and D. The photographs were taken immediately after preparation and thus the images are the representation of the abilities of various BGNF to stabilize oil-in-water emulsion. All the varieties of BGNF formed oil-in-water emulsion of similar microstructure. All the micrographs showed various oil-droplets sizes in the BNGF matrix. In addition, the microstructures of the emulsions revealed highly flocculated systems. The differences in BGNF varieties was however not noticeable on the microstructure of the emulsions. It appeared that all of the BGNF varieties have comparable strength necessary for emulsion formation.

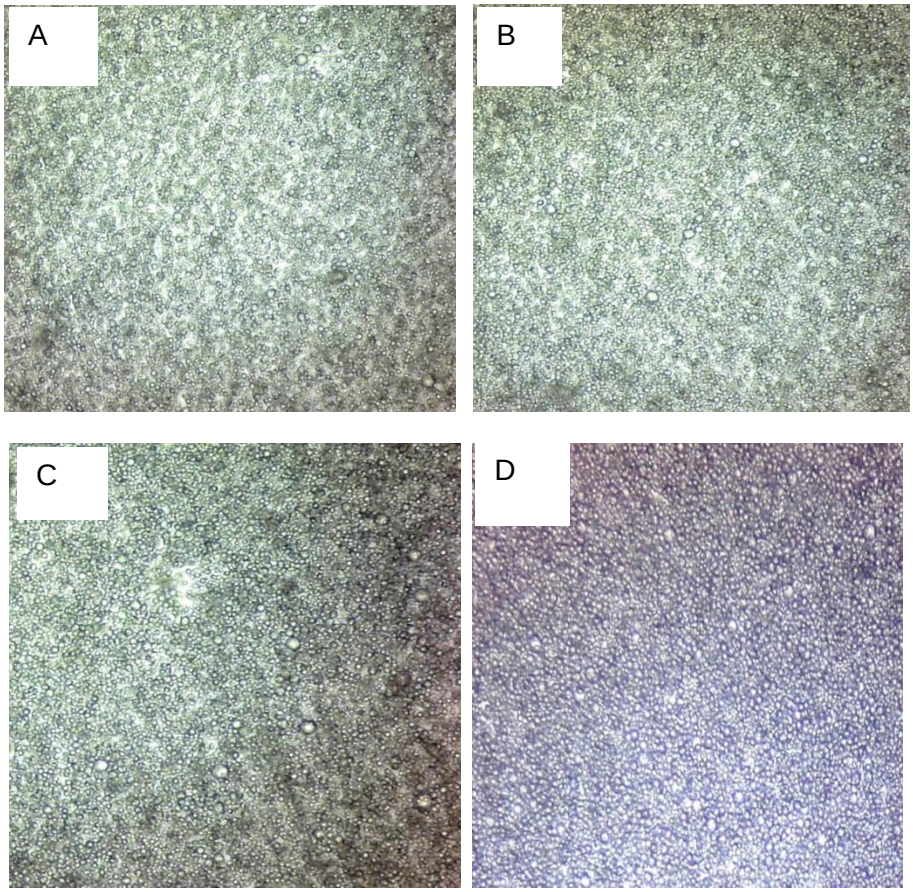

Figure 4.55 Micrographs (X 40 magnifications) of emulsions stabilized with (A) Black-eye (B) Brown-eye (C) Red (D) Brown bambara groundnut flour (BGNF)

4.6.3 Effect of BGNF varieties on emulsion storage stability

Figures 4.56 and 4.57 are the Turbiscan profiles of the emulsions stabilized with different varieties of BGNF measured at 30 minutes interval for a period of 360 minutes at 20^{o}C. The left hand side graphs were the presentation in the normal turbiscan mode while those at the right hand sides were the corresponding reference mode. The reference mode of the Turbiscan profile is an alternative way of visualizing the stability graph and allows better analysis of the curves. When the profiles were presented in the reference mode, other scans were measured relative to the first scan whose backscattering flux was assigned a value of 0%. In the Turbiscan normal mode, the first scan in each of the emulsion stability curves gave the intrinsic information regarding the emulsions and its backscattering (%) represented the microstructure of the recently prepared emulsions. The higher the initial backscattering flux (%), the more the population of the oil in the BGNF matrix. Hence, the initial backscattering was used as a standard to quantitatively measure the relative strength of the matrix of each BGNF variety to form emulsion. Table 4.35 show the effect on BGN

varieties on the initial backscattering flux (%) [BS_{AVo} (%)]. The mean of BS_{AVo} (%) values were between 96.1 and 96.4% for all the emulsions stabilized with the four BGN varieties.

Table 4.35 Effect of BGNF varieties on the initial backscattering flux (%)[1,2]

BGNF variety	Initial backscattering flux (%)
Black-eye	96.2 ± 0.17[a]
Brown-eye	96.4 ± 0.16[a]
Red	96.1 ± 0.06[a]
Brown	96.2 ± 0.06[a]

[1] Values are means ± standard deviations; Means with different letters within the same column are significantly different from each other ($p < 0.05$).
[2] BGNF is bambara groundnut flour

Emulsions stabilized with all the four varieties presented similar BS_{AVo} (%) which implied no significant difference existed in their abilities to form oil-in-water emulsions.

The result of the reference mode Turbiscan profile (Figures 4.56 and 4.57) showed relative changes with respect to time in all of the emulsions. Although the peak between 0 - 10 mm in all the emulsion samples could be attributed to creaming phenomenon, however the oil-droplet migration rates were all zero when assessed using migration software available in the Turbiscan machine. This implies that all the emulsions were stable to creaming within the time frame of the experiment. It was also observed that there was a decrease in backscattering flux (%) along the entire tube length in all the emulsions. Decreased backscattering flux (%) was as a result of oil droplet aggregation which could have resulted from oil-droplet flocculation or coalescence. The observed decrease in the backscattering flux overtime was as a result of increased oil-droplet size which caused the mean path of photon (l*) to increase because of an increased average distance between the oil-droplets. Emulsion stabilized with the four varieties presented similar destabilization mechanisms with oil-droplet aggregation being the most dominant destabilization phenomenon. Therefore, the kinetics of the most dominant destabilization phenomenon were assessed and compared among the emulsions stabilized with the four varieties of BGNF. To this effect, the mean value kinetics for coalescence/flocculation in the middle of the tube (20 - 40 mm) was analyzed. Figure 4.58 showed the effect of BGN varieties on the backscattering flux (%) mean value kinetics of the emulsions. BGNF varieties had closely identical effects on emulsion stability over time. The results were marked with high standard deviation making the graph to be highly unresolved. It is therefore very difficult to make tangible conclusions regarding the BGN variety that gave the best emulsion stability.

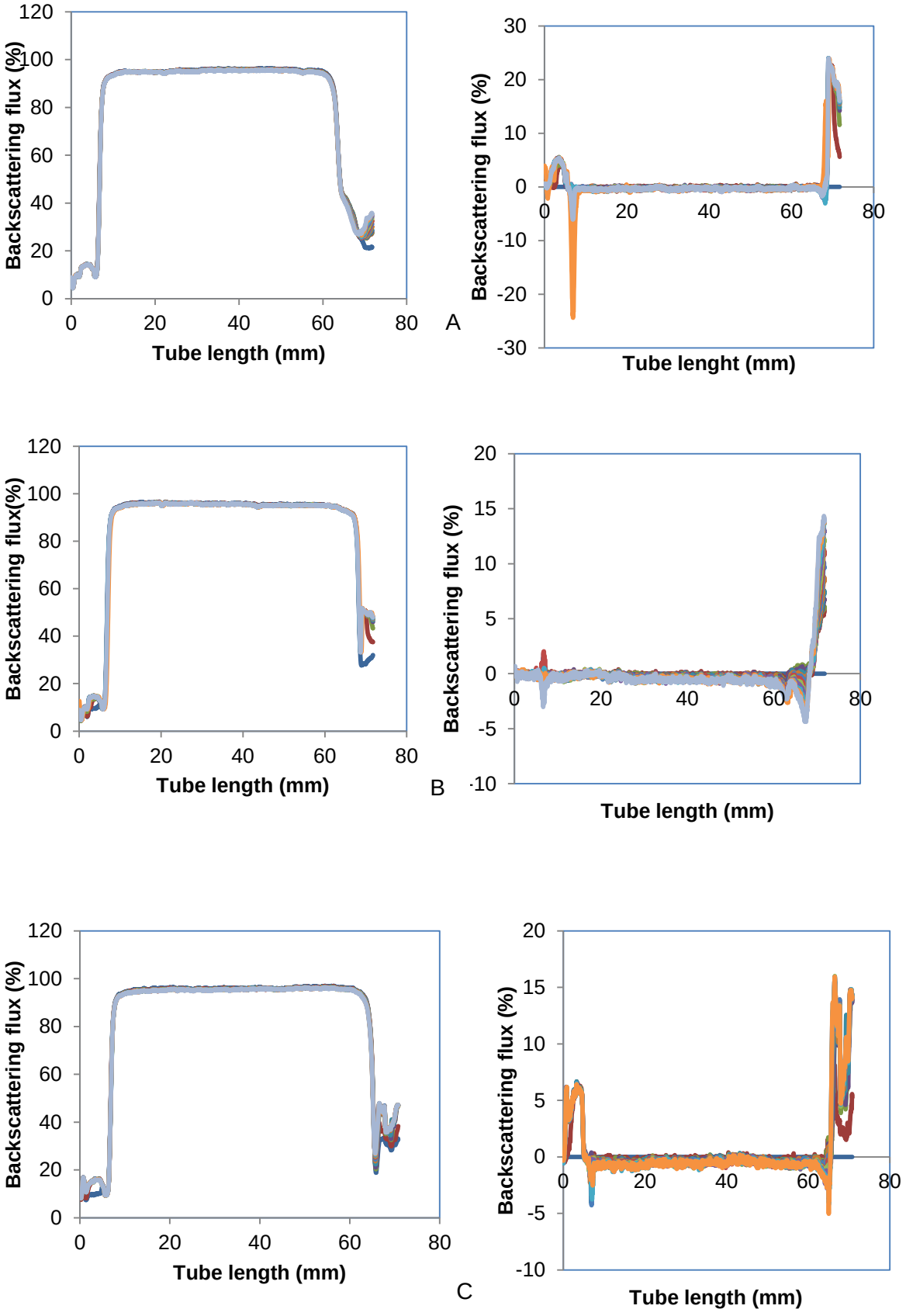

Figure 4.56 **Changes in the backscattering profile (BS%) as a function of sample height during storage of emulsions stabilized by different varieties of BGNF (A) Black-eye (B) Brown-eye (C) Red**

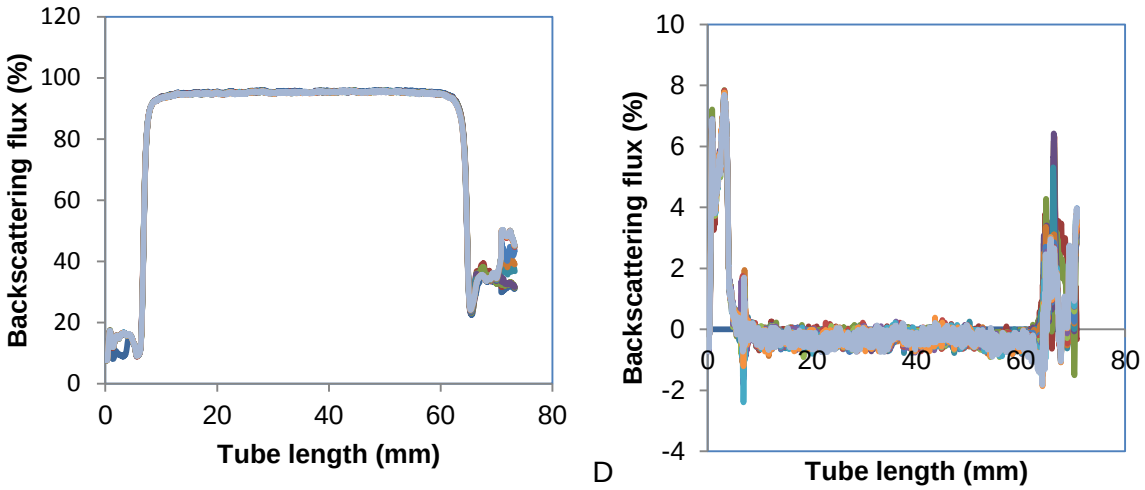

Figure 4.57 **Changes in the backscattering profile (BS%) as a function of sample height during storage of emulsions stabilized by different varieties of BGNF (D) Brown**

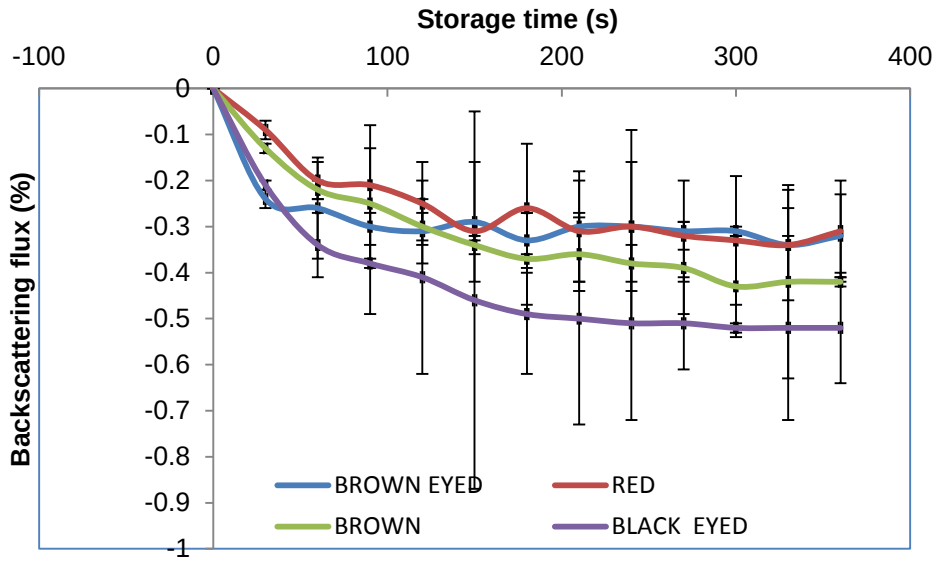

Figure 4.58 **Variation in backscattering in the 20 – 40 mm zone monitored over 360 minutes for samples stored in quiescent condition at 20°C (emulsion stabilized with different varieties of bambara groundnut flour).**

Stability of the emulsions was measured at equilibrium time in order to assess and compare the performance of different studied varieties of BGN. The backscattering flux (%) at equilibrium time was plotted for each variety as shown in Figure 4.59. The equilibrium backscattering flux (%) is the final backscattering flux (%) attained at the equilibrium time. All the emulsions had attained their respective equilibrium state at 360 minutes where there

were minimum changes in the backscattering flux (%) with time (Figure 4.58). Therefore the backscattering flux (%) at the end of the studied time (360 minutes) was assessed and plotted for each varieties studied. Although Figure 4.59 showed that BGN varieties have effects on the average equilibrium backscattering flux (%), the effect were very minimal (backscattering of < 0.2% between the maximum and minimum) and the results were marked with high standard deviations.

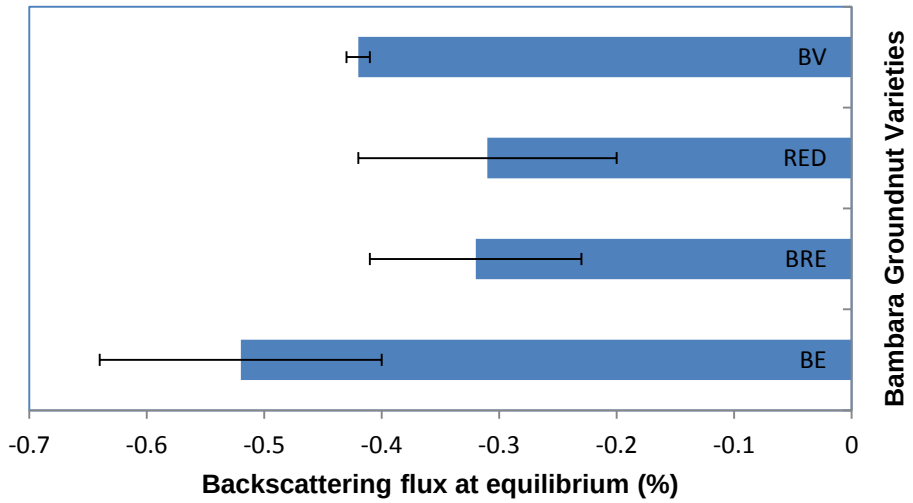

Figure 4.59 Effect of varieties of BGNF on emulsion stability (Average backscattering flux at equilibrium state)

4.6.4 Effect of BGNF varieties on rheological properties with regard to flow curves and hysteresis loop area of emulsions

The shear stress sweep experiment was conducted to assess and compare the rheological behaviours of emulsions stabilized with different varieties of BGNF. The effect of BGNF varieties on the flow curves of oil-in-water emulsions were presented in Figure 4.60. The upper curve is referred to the ascending curve and was developed first while the one below was developed as a result of backward shear stress sweep. The relative position of the two curves showed that all the studied emulsions were time dependent thixotropic fluid and that the structures of the emulsions have been destroyed during the forward sweep. This has resulted into hysteresis loop created between the forward and backward curves. The rheograms of all the emulsions started above the origin implying a positive yield stress which is desirable for the stability of semi-solid fluids (Goncalves and Maia Campos, 2009). All of the emulsions stabilized with different varieties showed similar rheological behaviour of comparable loop areas.

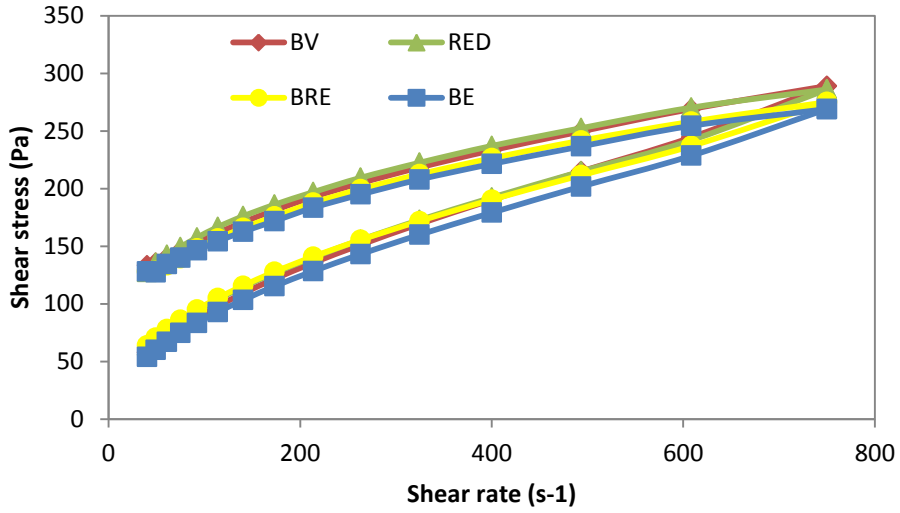

Figure 4.60 **Effect of bambara groundnut flour variety on the rheological behavior of optimized emulsion**

The similarities in the flow curves and comparable hysteresis loop areas were indications of closely related BGNF matrix strength and structural formation. Although the proximate compositions of these varieties are slightly different (Table 2.2) there seems not to be observable differences in the flow properties of their respective emulsions. Table 4.36 shows the mean apparent viscosities of the studied emulsions at three shear rates. There were no appreciable differences between the emulsions stabilized by different varieties of BGNF. All of the emulsion showed similar characteristics and this could be related to the similar stabilizing properties of all the BGNF studied.

The flow curve of Figure 4.60 was further analyzed by power law rheological model. Power law rheological model was selected for the analysis because of its high suitability to describe the time-independent properties of BGNF emulsions as demonstrated in section 4.4.

Table 4.36 **Apparent viscosities of emulsions stabilized with different varieties of BGN at different shear rates**

Shear rate (s^{-1})	Black-eye	Brown-eye	Red	Brown
40	3.20	3.19	3.18	3.32
263.3	0.740	0.758	0.795	0.778
750	0.365	0.369	0.386	0.388

The parameters of power law model as well as the magnitude of the hysteresis loop area obtained for the emulsions are presented in Table 4.37. The high coefficients of determination (0.99) implied that power law rheological model described the rheological behaviours of the emulsions. The K and n parameters in the power law rheological model represented the consistency coefficient which was a measure of the viscosity of the material and flow behaviour index which measured the fluid resistance to flow. The mean of consistency coefficient for the forward and backward curves ranged from 44.9 to 45.7 and 7.60 to 10.8 Pas^n, respectively. The mean value of n-parameter ranged from 0.27 to 0.28 for the forward curve and 0.48 to 0.56 for the backward curve. The flow behaviour indexes for the forward and backward curves were less than unity indicating that all the emulsions were pseudoplastic in nature. As expected the K and n parameter values for the forward curve were higher and lower than the backward curves, respectively. This was an evidence that the structure of the emulsions have been destroyed in the forward sweep experiment. There was no observable significant difference in the power law parameters of the emulsions stabilized with different varieties of BGNF.

The magnitude of hysteresis loop area quantifies the extent of thixotropy in a material. Table 4.37 presented the observed magnitude of hysteresis loop area of the emulsions. The mean of magnitude of hysteresis loop area of the emulsions ranged between 764 and 794 Pas^{-1}. The magnitudes of hysteresis loop area of all the emulsion were closely related. Since the magnitude of the hysteresis loop area depends mainly on the strength of the matrix and the oil-droplet interactions in the BGNF stabilized emulsion, it can be said that the four varieties of BGNF had comparable matrix strength and capability of forming emulsion structures.

4.6.5 Effect of BGNF varieties on rheological properties with regard to steady shear decay

Steady state shear decay experiment was further conducted to elucidate more on the time dependent thixotropic properties observed in the emulsions stabilized with different BGNF varieties. All of the emulsions were sheared and the decay behaviors were compared at a shear rate of 50 s^{-1}. Figures 4.61 and 4.62 show the thixograms of the oil-in-water emulsions containing fixed amount of SFO (40% w/w) but stabilized with 7% w/w BGNF from different varieties of BGN. All emulsions showed identical behavior with decreased viscosity over time. The much observed changes in the viscosity of the emulsions were at the initial shearing time where much of the structures were rapidly destroyed. The initial viscosity (at t = 0) of all the formulations were closely related showing a comparable emulsion structures. Weltman model was used to quantify and compare the structural breakdown observed in the

Table 4.37 Effect of BGNF varieties on Power law parameters and hysteresis loop area [1,2]

BGNF (% w/w)	K (Pas^n)	n	R^2	K' (Pas^n)	n'	R^2	Hysteresis loop area (Pas^{-1})
Black-eye	44.9 ± 0.91[a]	0.27 ± 0.00[a]	0.99	7.75 ± 0.33[a]	0.53 ± 0.00[a]	0.99	783 ± 13.9[a]
Brown-eye	44.7 ± 0.71[a]	0.27 ± 0.01[a]	0.99	10.8 ± 0.11[a]	0.48 ± 0.00[a]	0.99	774 ± 40.9[a]
Red	44.9 ± 0.81[a]	0.28 ± 0.00[a]	0.99	8.88 ± 2.02[a]	0.54 ± 0.06[a]	0.99	763 ± 33.5[a]
Brown	44.9 ± 0.87[a]	0.28 ± 0.06[a]	0.99	7.60 ± 0.53[a]	0.56 ± 0.03[a]	0.99	771 ± 44.2[a]

[1]Values are mean ± standard deviation; Means with different letters within the same column are significantly different from each other ($p < 0.05$).

[2]BGNF is bambara groundnut flour; K refers to the consistency coefficient of the forward sweep; K' is the consistency coefficient of the backward sweep; n is the flow behaviour index of the forward sweep; n' is the flow behaviour index of the backward sweep; R^2 is the coefficient of determination between the experimental data and power law model prediction

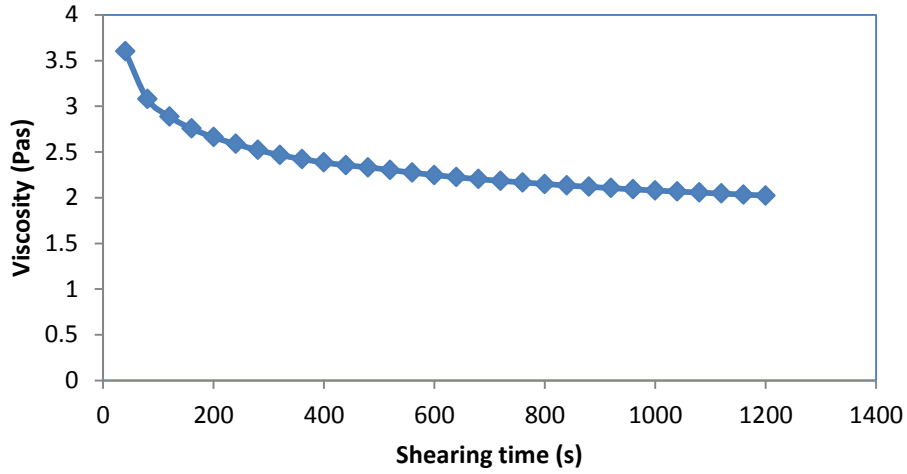

A

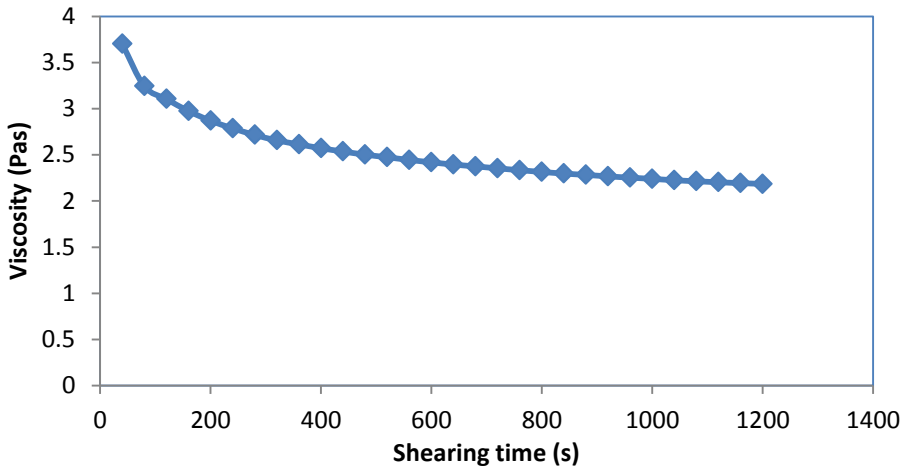

B

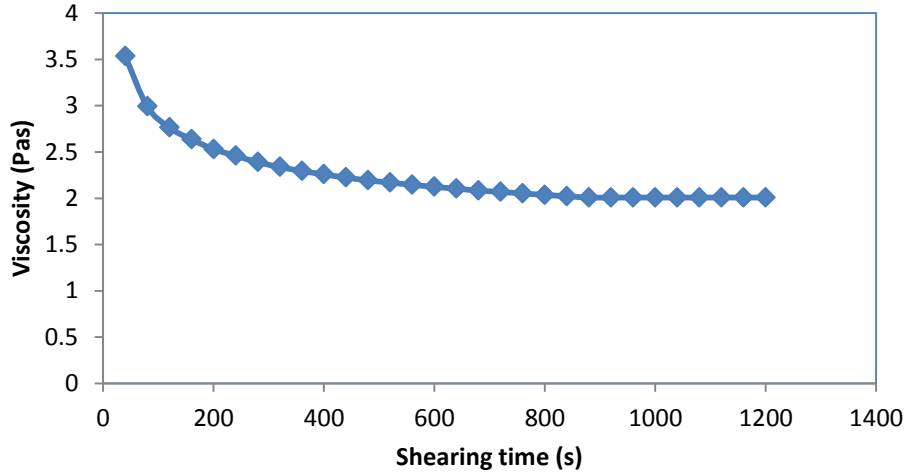

C

Figure 4.61 **Effect of BGNF varieties on thixotropic characteristics of emulsion at 50 s^{-1} (A) Black-eye (B) Brown-eye (C) Red**

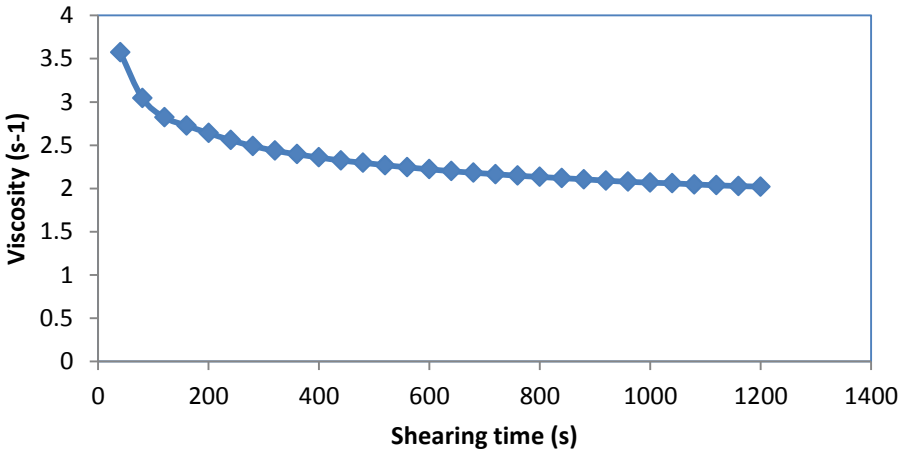

Figure 4.62 Effect of Brown BGNF varieties on thixotropic characteristics of emulsion at 50 s^{-1}

Weltman model was used to quantify and compare the structural breakdown observed in the emulsions because of it high suitability to describe the time-dependent rheological properties of BGNF emulsions (Section 4.3). This was used as a means to assess and quantify the matrix strength of different BGNF varieties and structural strength of their respective emulsions. Table 4.38 is the presentation of the model parameters obtained for the emulsions along with the coefficient of determination. Parameters A and B of the Weltman model gave the information regarding the initial shear stress and extent of structural destruction respectively. The mean of Weltman model parameters A and B of the emulsions ranged from 235 to 250 Pa and 19.8 to 22.0 Pa, respectively. The high values of Weltman model parameters indicated high emulsion viscosity which was a product of high oil droplets interaction and matrix strength of the BGNF varieties used to achieve emulsion stabilization. BGNF varieties had closely related effects on the rate of structural destruction (parameter B) of all oil-in-water emulsions (Table 4.38).

Table 4.38 Effect of bambara groundnut flour varieties on Weltman model parameters

BGNF varieties	A (Pa)	-B (Pa)	R^2
Black-eye	238 ± 3.68^{a}	20.1 ± 0.14^{a}	0.96
Red	250 ± 7.19^{b}	20.9 ± 0.18^{ab}	0.99
Brown-eye	235 ± 14.01^{a}	19.8 ± 1.27^{a}	0.98
Brown	263 ± 27.1^{d}	22.0 ± 2.66^{b}	0.99

[1] Values are mean ± standard deviation; Means with different letters within the same column are significantly different from each other ($p < 0.05$).
[2] A equals the initial shear rate of Weltman model; B is the extent of structural break down of Weltman model; R^2 is the coefficient of determination between the experimental data and Weltman model prediction volume-mean diameter of the emulsions.

The identical behaviour of all the emulsions suggested that all the BGNF varieties investigated possessed closely related structure and this was due to their comparable BGNF matrix strength.

4.6.6 Effect of BGNF varieties on rheological properties with regard to viscoelastic properties

Figures 4.63 and 4.64 show the results of the frequency sweep experiments obtained for emulsions containing 40% (w/w) SFO stabilized with 7% (w/w) BGNF from four varieties of bambara groundnut (BGN). All the emulsions exhibited both the elastic ($G^{'}$) and viscous ($G^{''}$) moduli. Both G' and G" showed significant independence on the frequency and tended to form a plateau at high frequency for all the emulsions. The spectrum of all emulsions showed solid-like behaviour at all the frequencies where G' dominated and was higher than the G'' curve and tended to show a constant limiting value. The predominance of the elastic characteristics (G') over viscous characteristics (G") at the selected frequency range for all the emulsions suggested that all the emulsions were weak gels. The η^* of all the emulsions was also observed to rise increasingly towards an infinitely high value which is a characteristic of gel structures. All the emulsions possessed high values of G' at low frequencies which implied high structural strength and long term storage stability. These emulsions therefore have the tendencies to be rigid and also possessed high flow resistance. Figure 4.65 shows the effect of the four BGNF varieties on the material functions (G' and G'') of the oil-in-water emulsion formulated with 40% (w/w) SFO. The effect of the four varieties on material functions was comparable at all studied frequencies. The G' and G" curves of all emulsions did not show a clear distinction and overlapped at most of the frequencies considered. The similarity in the properties of the emulsions was as a result of very close matrix strength of the BGNFs. BGNFs from the four varieties investigated therefore produced similar rheological characteristics in the emulsions regardless of their slightly dissimilar proximate composition as reported by Ojimelukwe and Ayenor. (1992).

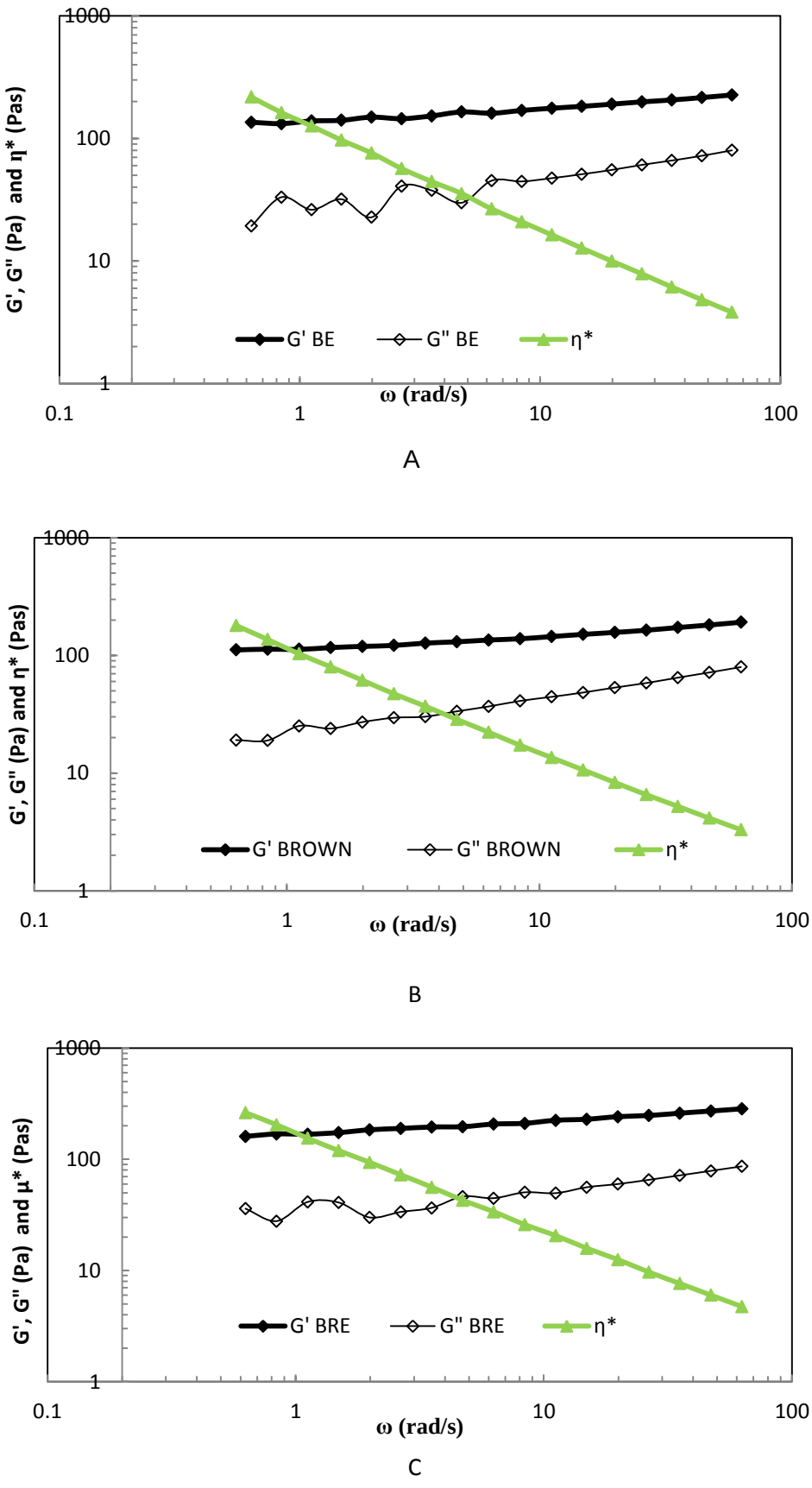

Figure 4.63 **Frequency sweep of o/w emulsion containing 40% (w/w) SFO stabilized with (A) Black-eye (B) Brown-eye (C) Brown bambara groundnut flour**

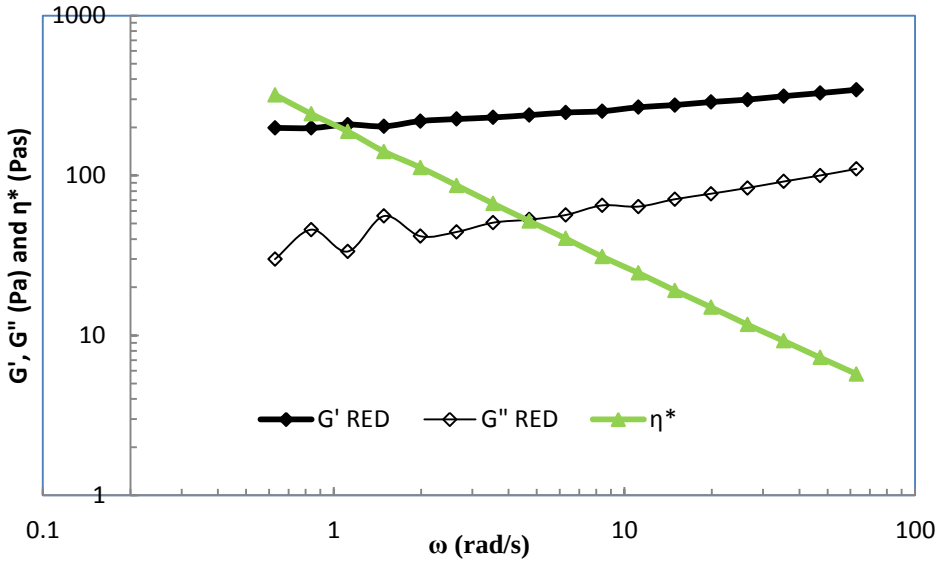

Figure 4.64 **Frequency sweep of o/w emulsion containing 40% (w/w) SFO stabilized with 7% Red bambara groundnut flour**

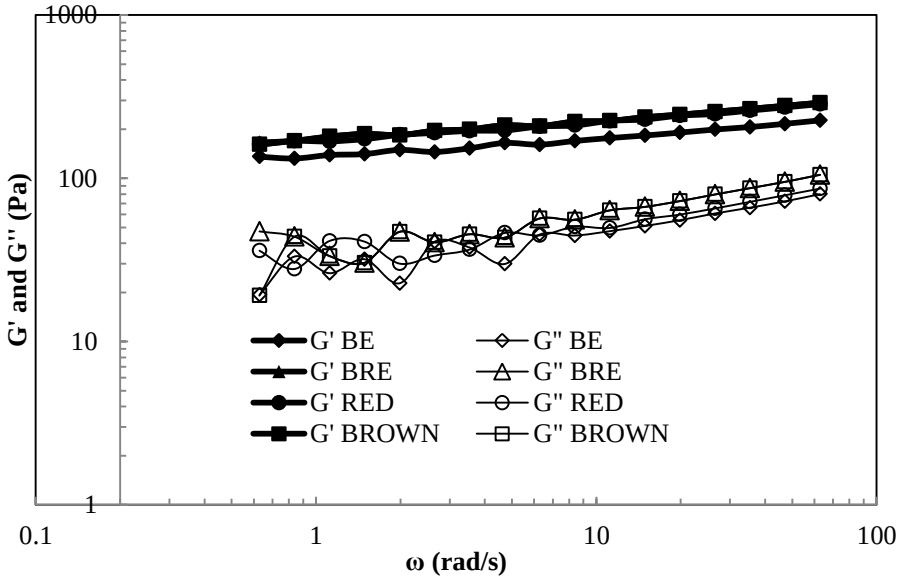

Figure 4.65 **Storage (G') and loss moduli (G") as a function of angular frequency during dynamic oscillatory tests of o/w emulsion with 40% (w/w) SFO stabilized with 7% (w/w) Bambara groundnut flour from four varieties.**

4.6.7 Effect of BGNF varieties on rheological properties with regard to compliance and recoverable strain

Figure 4.66 shows the compliance (J) against time (s) for emulsions containing 40% (w/w) SFO, stabilized with 7% BGNF from four different varieties of BGN. Like other similar previous experiments, a load of 0.5 Pa was imposed on the structure of all the emulsions in the first part of the experiment for 500 s while the second part involved sudden removal of the load and compliance was monitored for the next 500 s. All the emulsions showed similar viscoelastic characteristics during creep and recovery phases. Compliance steadily increased when a stress of 0.5 Pa was imposed on all the emulsions during the creep stage and the elastic component of the deformation recovered instantaneously when the load was removed (Figure 4.66). The creep and recovery graphs of all the emulsions were similar and overlapped indicating a closely related structure and viscoelastic properties. The similarities in properties of all the emulsions stabilized by four varieties of BGNF indicated that the BGNFs possessed comparable characteristics and were able to impact similar viscoelastic properties on the emulsions.

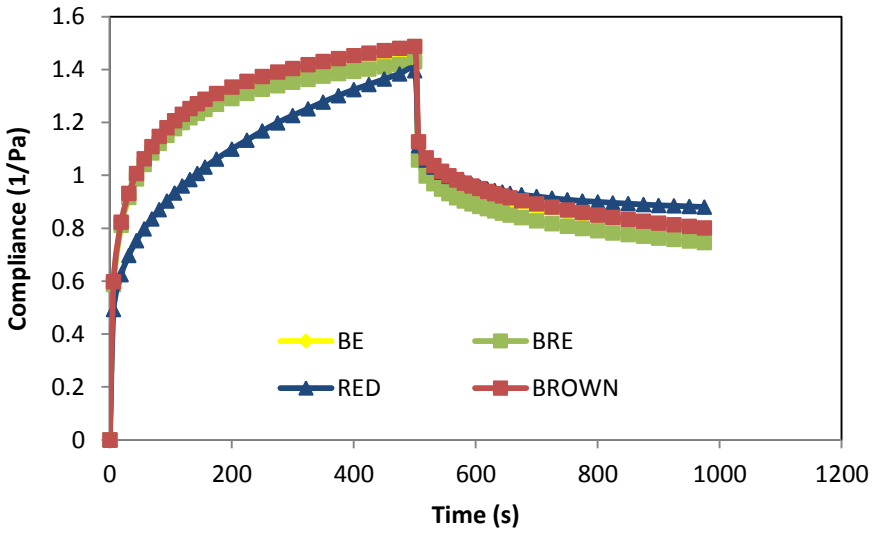

Figure 4.66 **Creep and recovery curves of emulsion containing 40% (w/w) SFO stabilized with 7% (w/w) Bambara groundnut flour from four varieties**

4.6.8 Summary on the effect of different varieties of bambara groundnut flour (BGNF) on O/W emulsion stability and rheology

Various emulsion stability and rheological parameters were quantified and compared in order to determine the relative strength of four varieties of BGNF to stabilize oil-in-water emulsion. All the emulsions stabilized with the four varieties showed the same stability and rheological behaviour. This could be attributed to the comparable matrix strength of all the varieties. All the emulsions showed similar structure, comparable particle size and initial backscattering flux. This close characteristics could be responsible for similar emulsion stability obtained when BGNF of the four varieties were used to achieve emulsion stabilization. The result of the rheological studies buttressed what was observed in emulsion stability. All the emulsion showed the same rheological behaviour when assessed using shear stress sweep, oscillatory tests and creep and recovery experiment. They were all thixotropic - time dependent fluids and possessed both elastic and viscous properties. The parameters of the power law also indicated that the emulsions were pseudoplastic non-Newtonian fluids. However, both of the parameters of power law model, magnitude of hysteresis loop area and parameter B of Wetman model were not significantly different among the emulsions. The G' and G'' curves were similar at all investigated frequencies and creep and recovery graphs also showed an overlap indicating closely related viscoelastic properties. This implied that the emulsions had comparable structural strength (both oil droplet - oil droplet interactions and oil droplet - BGN matrix interactions). The comparable structural strength of all the emulsions was as a result of equal matrix strength of the BGNF varieties.

4.7 Effect of Food Additives on Emulsion Stability and Rheological Properties of Optimum Formulation

This section reported the effect of sodium chloride (NaCl), vinegar and citric acid on the optimal emulsion stability and rheological properties. Brown bambara groundnut was used for this investigation because of its comparable ability with other varieties to stabilize oil-in-water emulsions as reported in section 4.6. It also conferred good rheological properties on the emulsions. The influence of these additives on the stability parameters such as oil-droplet distribution, emulsion microstructure, oil droplet size ($d_{3,2}$ and $d_{4,3)}$ and initial backscattering (BS_{AVO}) and on rheological properties such as time-dependent, time-independent and viscoelastic properties were evaluated. Attempts were made to identify the most stable additive containing emulsions based on their stability and rheological properties.

4.7.1 Effect of NaCl on the stability and rheological properties of optimum emulsion

4.7.1.1 Effect of NaCl on the stability of optimum emulsion with regard to droplet size distribution

Figure 4.67 shows the droplet size distributions of the optimum emulsion (7% (w/w) BGNF and 40% (w/w) SFO) containing a range of concentration of NaCl (0 - 300 mM). All the droplet size distributions presented a nearly Gaussian shape with few secondary populations. This indicated that the droplets were poly-dispersed in nature. The presence of NaCl at various concentrations in the BGNF emulsions affected the width and population of the oil droplets in a dissimilar manner. When compared with the emulsion without NaCl the width of the distribution shifted to the right implying an increase in oil droplet size.

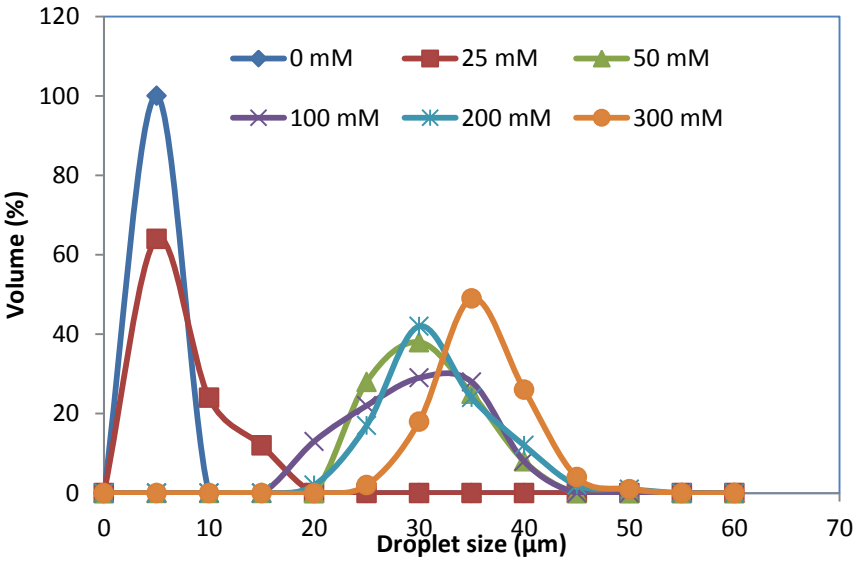

Figure 4.67 **Droplet size distribution of dispersed phase particles in emulsion formulated with 7% (w/w) BGNF and 40% (w/w) SFO containing various concentrations of NaCl**

Table 4.39 shows the effect of NaCl concentrations on the oil-droplet size of the emulsion. The volume surface mean diameter $d_{3,2}$ which provided information where most particle fell (Gu *et al.,* 2005), ranged between 3.45 - 34.5 µm while $d_{4,3,}$ the equivalent volume-mean diameter which is related to changes in droplet size involving destabilization process (Camino and Pilosof, 2011) ranged between 3.66 - 35.1 µm. The range of $d_{4,3}$ obtained from this work was relatively higher than those reported by Charoen *et al.* (2011) on the effect of NaCl concentrations (0 – 500 mM) on the particle size of biopolymer stabilized emulsions.

Increased in the NaCl concentrations had an observable negative effect on microstructure of the emulsions by increasing the oil droplet size. Both $d_{3,2}$ and $d_{4,3}$ increased significantly ($p < 0.05$) with increased NaCl concentration.

Table 4.39 Effect of NaCl on oil-droplet size[1,2]

Concentration of NaCl (mM)	$d_{3,2}$ (µm)	$d_{4,3}$ (µm)
0	3.45 ± 0.10[a]	3.66 ± 0.11[a]
25	8.72 ± 0.42[b]	10.1 ± 0.04[b]
50	29.3 ±0.49[c]	30.0 ± 0.41[c]
100	29.7 ± 0.82[c]	30.6 ± 0.51[c]
200	31.3 ± 1.11[d]	32.4 ± 0.87[d]
300	34.5 ± 0.69[e]	35.1 ± 0.13[e]

[1] Values ± standard deviations; Means with different letters within the same column are significantly different from each other ($p < 0.05$).
[2] $d_{3,2}$ refers to the volume surface mean diameter of the emulsions; $d_{4,3}$ is the equivalent volume-mean diameter of the emulsions.

Various articles have reported the influence of NaCl on droplet size and emulsion stability which largely depended on the nature of the emulsion system in question. As an example, similar observation of an increase in oil droplet size with increase in NaCl concentration was reported by Onsaard *et al.* (2005) for emulsion stabilized with coconut skim milk protein isolate (CSPI), coconut skim milk protein concentrate (CSPC) and whey protein isolate (WPI) and their observation was explained in terms of electrostatic interactions between the emulsion droplets. On the contrary, the microstructure of low in fat oil-in-water emulsion stabilized with polysaccharides (potato starch and xanthan gum) containing salt at 0 and 0.5 M showed no difference in oil-droplet distribution and size (Quintana, 2002). This was also supported by the report of Yilmazar and Kokini (1992), that addition of NaCl at 1% or 2% to 0.4% xanthan gum stabilized emulsions did not cause any change in mean droplet size upon aging. The report of Charoen *et al.* (2011) also showed that the $d_{4,3}$ of emulsions stabilized with whey protein isolate showed an appreciable increase at NaCl concentration of 200 mM and greater. They also reported that NaCl concentrations had little effect on the emulsion stabilized by gum Arabic and modified starch. However, increased NaCl concentration from 0 to 25 mM in the BGNF stabilized emulsion showed a nearly doubled increase in oil-droplet size in addition to, noticeable significant increase as NaCl increased from 50 to 300 mM.

Emulsion containing 25 mM NaCl had the minimum d_{32} and $d_{4,3}$ with corresponding values of 8.72 and 10.1 µm, respectively. Smaller oil-droplets have been said to contribute to greater emulsion stability while the larger the mean droplet size the higher the creaming

rate (Tantayotai and Pongsawatmanit, 2005), coalescence rate and the probability of flocculation (Walstra 1987, Stewart and Mazza, 2000). When compared with other systems that were stabilized mainly by polysaccharides such as the gum Arabic, modified starch, potato starch and xanthan gum, the influence of NaCl was very noticeable and deleterious on the oil droplet size of BGNF stabilized emulsions. This could be due to the method of incorporation of NaCl into the BGNF stabilized emulsions. BGNF has been reported to be sensitive to different kinds of electrolytes and its gelation property has been found to respond differently to the effect of NaCl (Aremu *et al.,* 2008). During the course of continuous phase preparation in this research, aqueous phase containing NaCl at various concentrations were used to gelatinize the BGNF prior to emulsification. NaCl which was present in the aqueous phase might probably have interfered with the polysaccharides network negatively during formation thereby reducing the matrix strength necessary for emulsion formation and stabilization. Giami and Bekebrain (1992) reported that the presence of salt at some concentration during gelatinization may cause denaturation of seed protein and probable neutralization of charges stabilizing gel formation. However, NaCl at a level of less than 25 mM seemed to have caused less harm to the polymer network while NaCl concentration of more than 50 mM greatly hindered the emulsion formation and promoted large oil droplet.

4.7.1.2 Effect of NaCl on the stability of optimum emulsion with regard to microstructure

Figure 4.68 shows the effect of NaCl on the microscopic images of the optimized formulation (7% (w/w) BGNF and 40% (w/w) SFO). The images are the microstructure of the recently prepared emulsions containing various concentrations of NaCl (0 - 300 mM). The images showed that the droplets are poly-dispersed systems. In comparison with the emulsion without NaCl (Figure 4.68A), the effect of NaCl concentration on the microstructure was noticeable and deleterious. Increased NaCl concentration from 0 to 25 mM resulted in relatively fewer large oil-droplet. The microstructure of the emulsion containing 25 mM NaCl was the least affected among emulsion systems containing NaCl. Increasing the concentration of NaCl in the gelatinized BGNF matrix resulted into increased size of the oil-droplets in the resulting emulsions. This was indicative of relative impediment caused by the presence of NaCl to BGNF polymer network formation and droplet - droplet interactions. The aggregated droplets that stood side by side could have coalesced to form bigger oil droplets as a result of the weakened matrix and film strength of the BGNF responsible for emulsion stabilization which was induced by the presence of NaCl. Onsaard *et al.* (2005) also reported that the extent of aggregation and creaming increased with an increase in

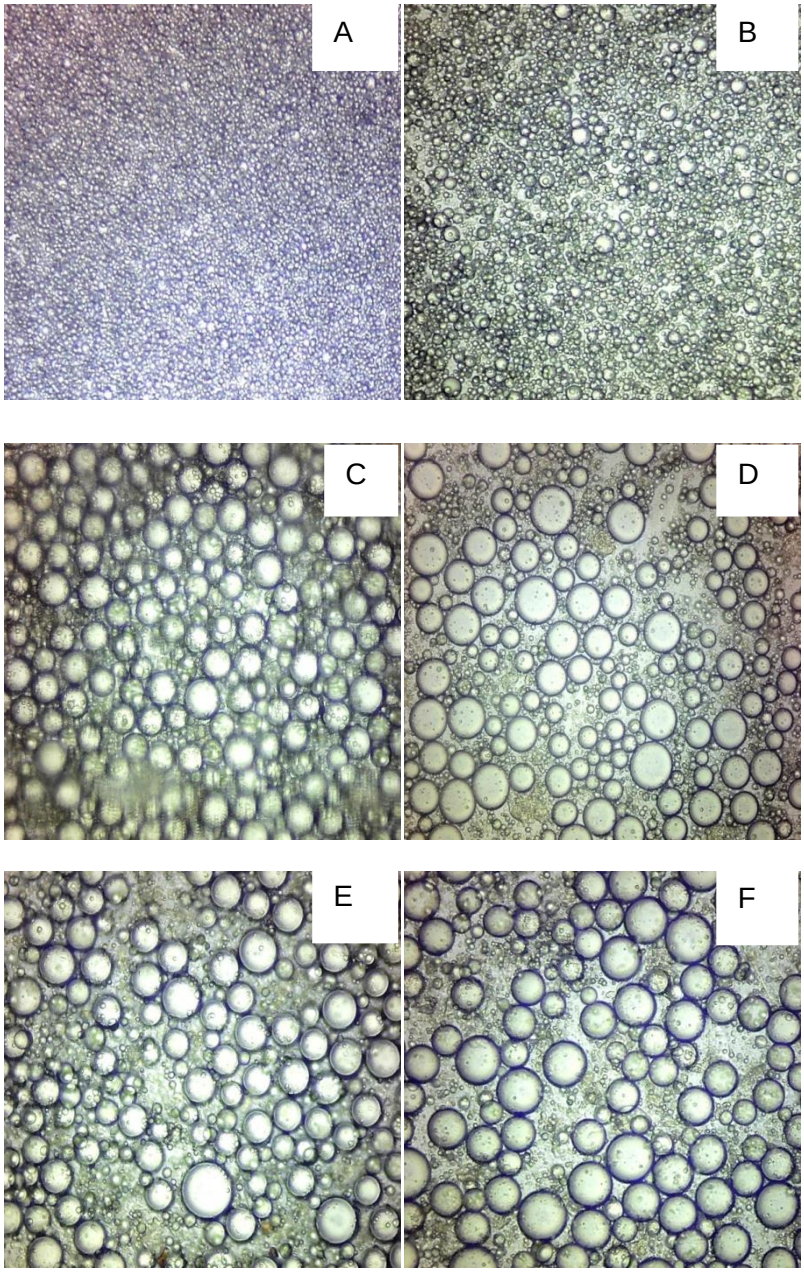

Figure 4.68 **Micrographs (X40 magnification) of 40% SFO and 7% BGNF emulsions containing (A) 0 mM NaCl (B) 20 mM NaCl (C) 50 mM NaCl (D) 100 mM NaCl (E) 200 mM NaCl (F) 300 mM NaCl**

NaCl concentration for an oil-in-water emulsion stabilized by coconut skim milk protein. The micrographs of emulsions with 50 mM and above presented a higher number of bigger oil droplets relative to smaller ones and showed areas of unoccupied aqueous phase. Presence of big oil-droplets is an indication of high tendencies of the emulsions to destabilize faster relative to the emulsion without NaCl. However not a very clear difference

was observed among the microstructures of the emulsions containing 50 mM, 100 mM, 200 mM and 300 mM NaCl.

4.7.1.3 Effect of NaCl on the storage stability of optimum emulsion

Figures 4.69 and 4.70 show the Turbiscan profile of emulsions containing 0 (A), 25 mM (B), 50 mM (C), 100 mM (D) 200 mM (E), and 300 mM (F) of NaCl scanned at 30 mins interval for 360 mins stored at 20^{o}C. The profiles were presented in both the normal Turbiscan mode (left) and the reference mode (right). In the reference mode, the first profile of all the six emulsions were used as a reference profile and its backscattering flux was represented as 0% relative to other profiles. The normal mode showed the backscattering flux (%) of all the profiles against the tube length. The first scan was the initial backscattering flux BS_{AVo} (%), and it gave the information about the microstructure of the freshly prepared emulsion. The BS_{AVo} (%) was directly related to the number of the oil-droplets in an emulsion system. The BS_{Avo} (%) of the emulsion containing between 0 and 300 mM NaCl is detailed in Table 4.40

Table 4.40 Effect of NaCl concentration on Initial backscattering[1]

NaCl (mM)	Initial backscattering [BS_{AVo}] (%)
0	95.3 ± 0.01^{a}
25	88.5 ± 0.01^{b}
50	78.7 ± 0.01^{c}
100	69.2 ± 0.02^{d}
200	69.3 ± 0.03^{d}
300	69.0 ± 0.02^{d}

[1]Mean values with different letters within the same column are significantly different from each other ($p < 0.05$)

The mean of BS_{Avo} (%) ranged from 95.3 to 69.0% for emulsions containing 0 to 300 mM NaCl. The NaCl concentration had significant influence on the BS_{Avo} (%). NaCl concentration decreased the BS_{AVO} (%) value until NaCl concentration of 100 mM was attained. When compared with other formulations containing NaCl, emulsion with 25 mM had the highest BS_{Avo} (%). As mentioned earlier, the presence of NaCl in the continuous phase during gelatinization of BGNF dispersions might have impeded the polymer network formation and weakened the matrix strength. This process might have hindered emulsion formation which consequently was observed as lowered backscattering flux relative to emulsion without NaCl.

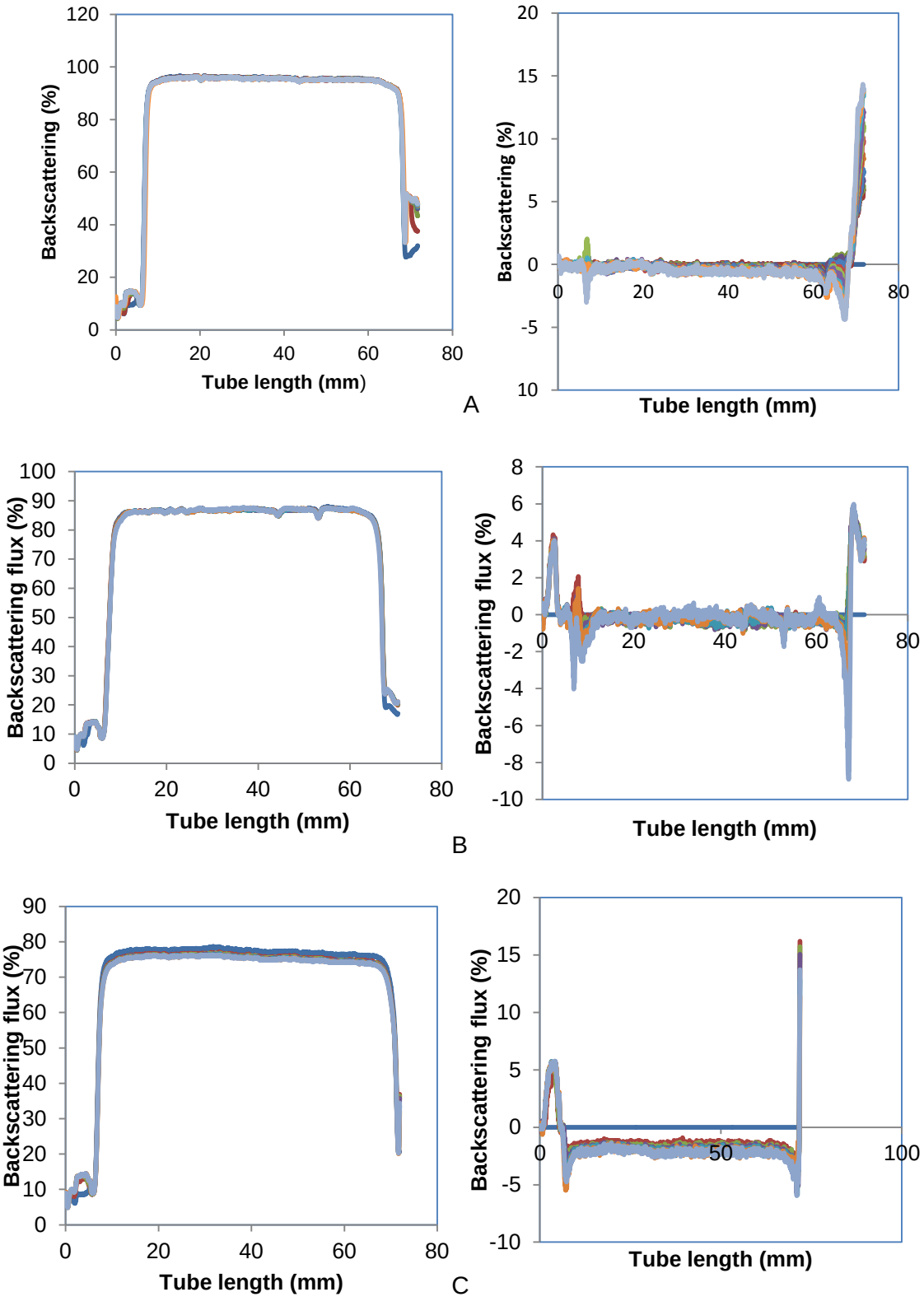

Figure 4.69 **Changes in the backscattering profile (BS%) as a function of sample height during storage of optimum emulsion containing (A) 0 mM NaCl (B) 25 mM NaCl (C) 50 mM NaCl**

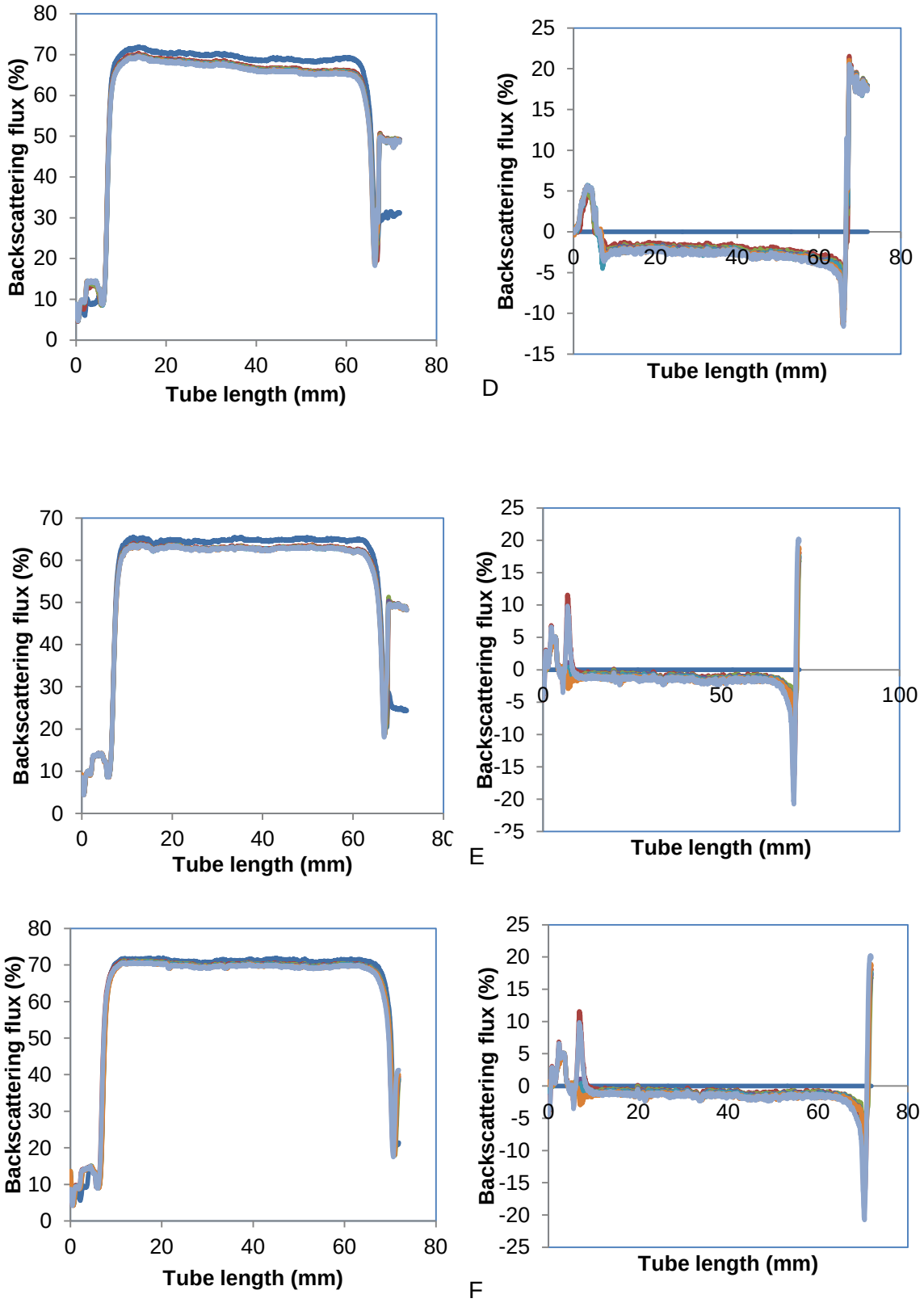

Figure 4.70 **Changes in the backscattering profile (BS%) as a function of sample height during storage of optimum emulsion containing (D) 100 mM NaCl (E) 200 mM NaCl (F) 300 mM NaCl**

The relative increase or decrease of the initial backscattering flux (%) was therefore an indication of the emulsion forming ability of the BGNF dispersions containing different concentration of NaCl and also presented a measure of the microstructure of the resulting emulsions. Therefore emulsion system with 25 mM NaCl seemed to form BGNF matrix with a firmer film thickness which was responsible for a better emulsion formation relative to other NaCl containing emulsions. Emulsions with 100 mM NaCl and greater seemed to possess similar weakened BGNF polymer matrix.

The result of the reference mode showed relative changes in the Turbiscan profile of the emulsions over time. The backscattering flux decreased along the whole length of the tube with time and there was presence of a peak at the bottom region of the tube (0 - 10 mm) indicative of oil-droplet aggregation (flocculation or coalescence) and creaming phenomena, respectively. Decrease in the backscattering flux was as a result of an increase in the oil-droplet size which correspondingly caused the mean path of photon (l*) to increase because of an increase in the average distance between the oil-droplets.

Figure 4.71 showed that NaCl concentrations had dissimilar effects on emulsion stability over time. The presence of NaCl in the emulsions at all concentrations had a negative effect on emulsion stability. NaCl in the BGNF stabilized emulsion systems tended to decrease the average backscattering flux relative to emulsion without NaCl and this invariably implied a decrease in emulsion stability. NaCl has been reported to have various noticeable effects on the emulsion stability and this largely depended on the compositions of emulsion systems. As an example, Martinez *et al.* (2007) investigated the effect of NaCl contents on the properties of salad dressing-type emulsion which were stabilized by emulsifier blends of protein origin. They reported that an increase in salt concentration led to a significant increase in emulsion stability. Similarly Stewart and Mazza (1999) observed that a salad dressing emulsion type with low NaCl content of 1% was found to be less stable relative to a system with higher NaCl content (4%). They explained their observation based on the inability of egg protein to act as a good emulsifier at low NaCl concentration. Charoen *et al.* (2011) investigated the effect of NaCl concentrations on the emulsions stability of emulsion systems stabilized by whey protein isolate (WPI), gum Arabic (GA), and modified starch (MS). The authors reported emulsion instability of WPI stabilized emulsion at higher salt concentration of (≤ 200 mM NaCl) and stability of GA and MS emulsions at all NaCl concentrations. BGNF stabilized emulsion containing 25 mM NaCl however showed highest stability followed by 50 mM NaCl. The stability of emulsions containing 100, 200 and 300 mM NaCl could not be clearly resolved beyond 100 minutes of study. The emulsion systems became relatively unstable as NaCl concentration increased. This could be directly related to the extent of impediment caused by different NaCl concentrations to polymer network formation during preparation of the continuous phase.

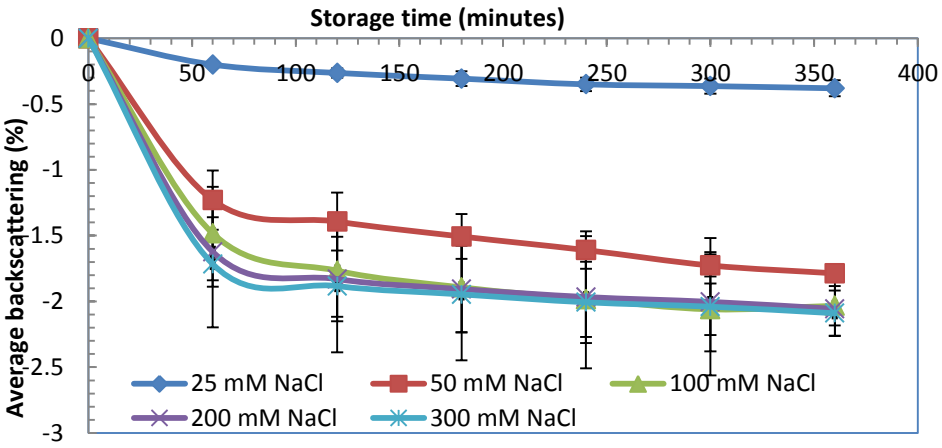

Figure 4.71 **Variation in backscattering in the 20 – 40 mm zone monitored over 360 minutes for sample stored in quiescent condition at 20°C (emulsion containing different concentrations of NaCl)**

The backscattering flux (%) at equilibrium was plotted against NaCl concentration in order to analyze emulsion stability at equilibrium time. The equilibrium backscattering flux (%) is the final backscattering flux attained at the equilibrium time. All of the studied emulsions reached equilibrium at about 360 mins (Figure 4.71). Therefore, the backscattering flux (%) values at 360 mins were plotted against the respective NaCl concentrations. The graph of the equilibrium backscattering flux (%) against concentration (Figure 4.72) showed clearly that NaCl concentrations affected the average equilibrium backscattering flux (%).

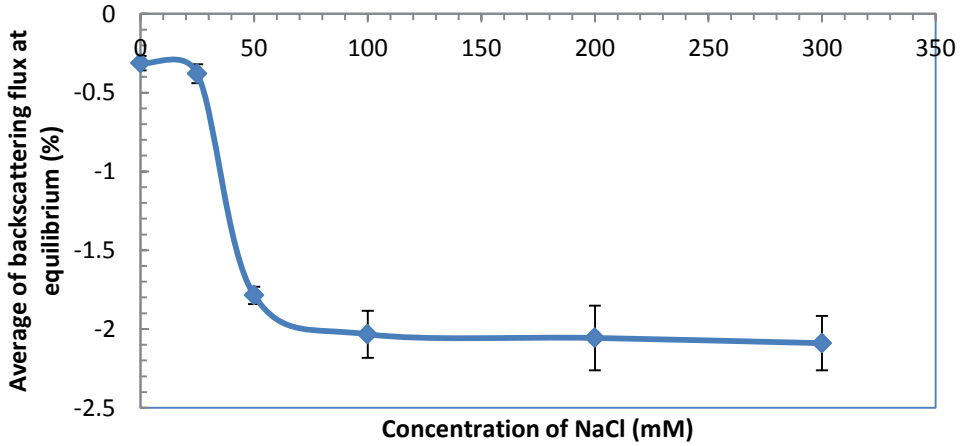

Figure 4.72 **Effect of NaCl on emulsion stability (Average backscattering flux at equilibrium state)**

Emulsion without NaCl remained the most stable within the studied time interval. However emulsion formulated with 25 mM NaCl induced the least structural breakdown. Emulsion containing 100, 200, and 300 mM NaCl showed similar destabilization profile and therefore their equilibrium backscattering values (%) were not judged to be different from one another.

4.7.1.4 Effect of NaCl on the rheological properties of optimum emulsion with regard to flow curves and hysteresis loop area

The rheological properties of the emulsions with and without NaCl can be assessed from their respective rheograms in Figure 4.73. The upper curves were developed first and therefore were at the top relative to the other and this showed that the emulsion samples were time dependent. The relative position of the curves with time showed that the structure of the emulsions was destroyed during the forward curve resulted in a decrease in shear stress during the backward curve. The structural destruction resulted into hysteresis loop areas created between the forward and the backward curves.

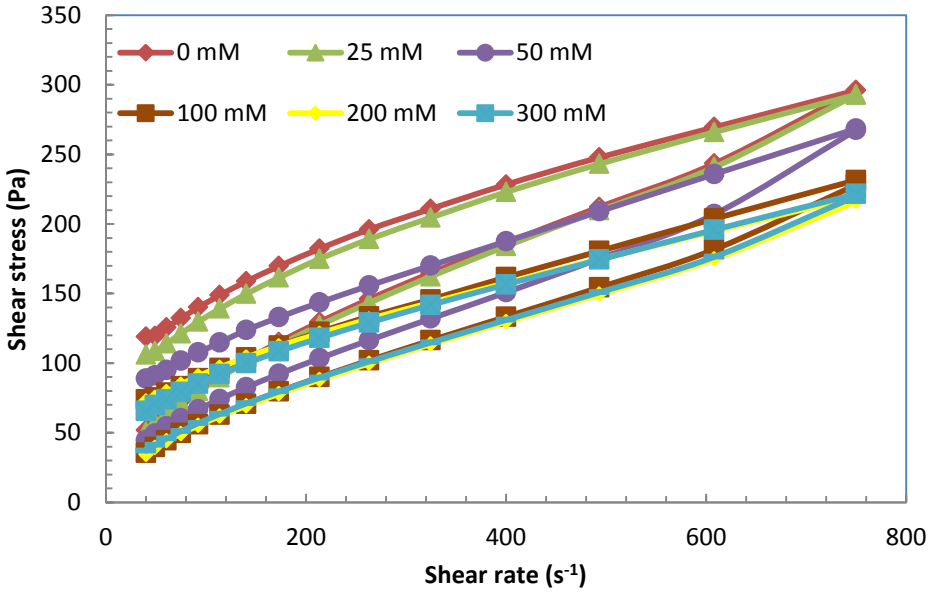

Figure 4.73 Effect of NaCl concentrations on the rheological behavior of optimized emulsion

All the emulsions exhibited hysteresis loop area irrespective of the concentration of the NaCl and the rheological behaviour of the emulsions with NaCl was similar to that of emulsion without NaCl. The existence of the hysteresis loop in the flow curves is an indication that the emulsions are thixotropic in nature. The viscosity of thixotropic fluids tends to decrease with

shearing time, showing a marked structural destruction with time. Similar time-dependent properties were observed in oil-in-water emulsions containing vitamin C and its derivatives at different concentrations (Goncalves and Maia Campos, 2009). Close examination of the ascending and descending curves revealed similarities and differences among the emulsions. The rheograms of all the emulsions started above the origin implying a positive yield stress which is desirable for the stability of semi-solid fluids (Goncalves and Maia Campos, 2009).

Figure 4.74 showed the effect of NaCl on the steady state apparent viscosity of the optimum BGNF emulsion. The apparent viscosities of all the emulsions decreased with increased shear rate which is characteristic performance of shear thinning fluids. Tantayotai and Pongsawatmanit (2005) also reported shear thinning behaviour in coconut oil-in-water emulsion containing NaCl, stabilized by whey protein isolate. The apparent viscosities of BGNF stabilized emulsion was sensitive to the influence of NaCl and tended to decrease with an increase in NaCl concentration. Similar observation was reported for emulsions stabilized with flaxseed gum and this was as a result of the deteriorative effect of electrolytes on the viscosity of flaxseed gum (Stewart and Mazza, 1999). On the contrary, Tantayotai and Pongsawatmanit (2005) reported an increase in apparent viscosity of coconut oil-in-water emulsion stabilized by whey protein isolate with an increase in NaCl concentration measured after two hours of the addition of NaCl. The internal structure of the BGNF stabilized emulsion without NaCl remained totally flocculated and hence its apparent viscosities were the highest due to the oil-droplets interactions and high matrix and film strength.

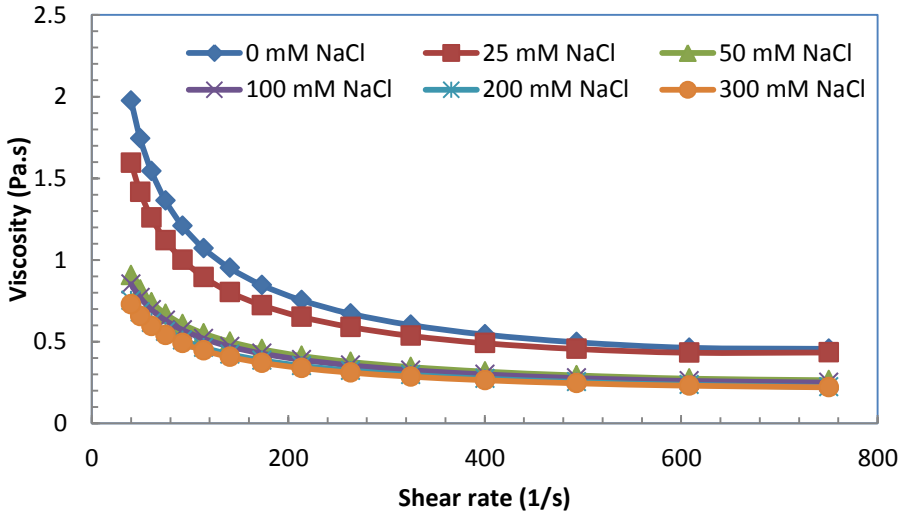

Figure 4.74 **Effect of NaCl on the apparent viscosity of the optimum emulsion (40% SFO + 7% BGNF)**

Emulsion containing 25 mM NaCl showed relatively higher apparent viscosities compare to the other emulsion systems containing NaCl. The apparent viscosity flow curve of emulsions with 50, 100, 200 and 300 mM NaCl showed an overlap and could not be completely resolved. The presence of NaCl in the emulsions systems must have affected the polysaccharide network during formation, thereby weakening the strength and reducing the emulsion forming ability of the NaCl containing BGNF dispersions. This must have led to reductions in apparent viscosities as the NaCl concentration increased in the emulsion system. However it seemed that NaCl concentration of 100 mM was enough to provide optimum inhibition of structuration in the polymer network during formation as there was no significant difference between the flow properties of emulsions containing 100, 200 and 300 mM NaCl.

For comparative purposes, the minimum apparent viscosities of all the emulsions were measured at the maximum point of shear gradient (750 s^{-1}). Table 4.41 shows the effect of NaCl on the minimum apparent viscosity of the optimum emulsion obtained at the loop apex (Figure 4.73) analyzed immediately after preparation. The values were the apparent viscosities of all the emulsions at a point where the forward and backward curve share the same properties. The minimum apparent viscosities of the emulsions containing NaCl were significantly different ($p < 0.05$) from the emulsion without NaCl.

Table 4.41 Effect of NaCl on the minimum apparent viscosity of the optimized emulsions at ambient temperature of 22°C[1,2].

NaCl concentration (mM)	Viscosity at 750 s^{-1} (Pas)
0	0.39 ± 0.00^{a}
25	0.37 ± 0.00^{b}
50	0.35 ± 0.01^{c}
100	0.31 ± 0.00^{d}
200	0.29 ± 0.01^{e}
300	0.29 ± 0.00^{e}

[1] Values are means ± standard deviations; Means with different letters in the same column are significantly different ($P < 0.05$)
[2]Values calculated at the maximum point of the shear gradient

The mean minimum apparent viscosity of all the emulsions ranged from 0.39 to 0.29 Pas with the highest value belonging to emulsion without NaCl. The emulsion containing 25 mM NaCl however possessed the highest value among other NaCl containing emulsions. This implied that emulsion with 25 mM NaCl was relatively viscous compared to other NaCl

containing emulsions. This may be explained in terms of the presence of a relative stronger BGNF matrix which favored emulsion formation and promoted oil-droplet interactions. The apparent viscosity of emulsions containing 200 and 300 mM NaCl were however not significantly different ($p < 0.05$).

Power law rheological model was used to analyze the developed flow curves and calculate the hysteresis loop areas because of its suitability in describing the time-independent properties of BGNF emulsions (Section 4.4). Dematrides *et al.* (1997), Tantayotai and Pongsawatmanit (2005), and Gonclves and Maia Campos (2009) have used power law model to evaluate the effect of additives on the rheological properties of emulsions. Table 4.42 shows the effects of NaCl concentrations on the power law rheological parameters and hysteresis loop area. The high coefficient of determination, $R^2 > 0.98$ indicated that power law model can adequately predict the rheological data. The NaCl had peculiar effects on the parameters of power law and hysteresis loop area. The mean consistency coefficient, a measure of the viscosity of the emulsion system (Tantayotai and Pongsawatmanit, 2005; Dematrides *et al.,* 1997) ranged from 30.1 to 13.6 Pas^n and 5.90 to 4.17 Pas^n for the forward and backward curves, respectively. While the flow behaviour index (n and n^i), a measure of fluid resistance to flow were in the range 0.34 to 0.41 and 0.58 to 0.61 for forward and backward curves respectively. The flow behaviour index for the forward and backward curve were less than unity indicating that all the emulsions were pseudoplastic in nature. Similar behavior was reported by Dematrides *et. al.* (1997) on the effect of NaCl and pH on the whey protein stabilized emulsion. The K and n were however relatively higher and lower respectively than those reported by Dematrides *et al.* (1997) and Tantayotai and Pongsawatmanit (2005) for protein stabilized emulsions.

The values of consistency coefficients of the forward curve were higher than the corresponding values for the backward curve while the values of the flow behavior index of the forward curve were lower than the corresponding values of backward curves indicative of structural destruction of the emulsion systems. In both cases (forward and backward curves), the consistency coefficient was observed to increase with a corresponding decrease in flow behavior. The consistency coefficients however showed significant decrease with the presence of NaCl for both forward and backward curves suggesting a decrease in emulsion viscosity. The decrease of consistency behaviour with an increase in NaCl concentration was contrary to the report of Tantayotai and Pongsawatmanit (2005) on the effect of NaCl on rheological properties of coconut oil-in-water emulsion stabilized with whey protein isolate. For the forward curve, the decrease was obvious up to NaCl concentration of 100 mM. Emulsions containing 100, 200 and 300 mM NaCl had the mean consistency coefficient values of 14.0, 13.8 and 13.6 Pas^n and were not significantly ($p > 0.05$) different from one to

Table 4.42 Effect of NaCl concentration on Power law parameters and hysteresis loop area[1,2]

Conc. NaCl (% w/w)	K (Pas^n)	n	R^2	K' (Pas^n)	n'	R^2	Hysteresis loop area (Pas^{-1})
0	44.9 ± 5.01^{a}	0.28 ± 0.01^{a}	0.99	7.60 ± 0.53^{a}	0.55 ± 0.34^{a}	0.99	772 ± 44^{a}
25	26.5 ± 1.78^{b}	0.36 ± 0.02^{b}	0.99	5.78 ± 0.14^{b}	0.58 ± 0.01^{a}	0.99	649 ± 22^{ab}
50	20.3 ± 2.99^{bc}	0.37 ± 0.03^{b}	0.99	5.11 ± 0.18^{bc}	0.57 ± 0.01^{a}	0.99	563 ± 19^{abc}
100	14.0 ± 2.51^{c}	0.41 ± 0.03^{b}	0.98	3.57 ± 0.06^{bcd}	0.61 ± 0.00^{a}	0.99	421 ± 58^{c}
200	13.8 ± 4.09^{c}	0.41 ± 0.04^{b}	0.99	3.70 ± 0.04^{d}	0.59 ± 0.00^{a}	0.99	395 ± 107^{c}
300	13.6 ± 3.28^{c}	0.41 ± 0.04^{b}	0.99	4.17 ± 0.05c^{d}	0.58 ± 0.00^{a}	0.99	389 ± 50^{bc}

[1] Values are means ± standard deviations; Means with different letters within the same column are significantly different from each other ($p < 0.05$).

[2]K refers to the consistency coefficient of the forward sweep; K' is the consistency coefficient of the backward sweep; n is the flow behaviour index of the forward sweep; n' is the flow behaviour index of the backward sweep; R^2 is the coefficient of determination between the experimental data and power law model prediction

the another. The relative difference and similarities in the emulsion with NaCl was a product of the degree of impediment caused by the various concentrations of NaCl on BGNF polymer network formation and droplet interactions in the emulsion systems. The quantification of hysteresis loop (magnitude) is detailed in Table 4.42. The magnitude of hysteresis loop quantified the extent of structural break down in an emulsion. The mean of the observed hysteresis loop area ranged from 771.50 to 389.9 Pas^{-1}. The magnitude of hysteresis loop area of emulsion without NaCl is significantly different ($p < 0.05$) from emulsion with NaCl. However the emulsions with NaCl showed significant and non-significant difference among themselves. The differences and similarities observed in the emulsions is a measure of relative disparities in both the BGNF matrix strength and the structural interactions in the emulsion systems. BGNF stabilized emulsion without and with 300 mM NaCl recorded the highest and lowest values, respectively. High value of BGNF emulsion without NaCl is an indication of high structural interactions and matrix strength which subsequently led to high emulsion viscosity.

4.7.1.5 Effect of NaCl on the rheological properties of optimum emulsion with regard to steady shear decay

In order to describe the time dependent behavior observed earlier in section 4.7.1.4, steady shear decay method was employed. Emulsions with and without NaCl were sheared and their behaviors were compared at constant shear rate of 50 s^{-1}. Figure 4.75 shows the effect of shearing time on the viscosity of the emulsions containing different concentration of NaCl measure at a constant shear rate of 50 s^{-1}. All the emulsions showed a time dependent thixotropic characteristics as there was a noticeable decrease in the viscosity with increased shearing time. In addition, different NaCl contents in the emulsions had altered thixotropic properties of the emulsion in a dissimilar manner (Figure 4.75). The viscosity of the emulsions with and without NaCl at initial and final time of shearing can be visualized from the ordinate of the viscosity-shearing time graph (Figure 4.75). The figure suggested that the presence of NaCl had reduced the viscosity of the emulsions relative to emulsion without NaCl. The curve of the emulsion with no NaCl was at the top while emulsions containing 25, 50, 100, 200 and 300 mM NaCl were below. Although the highest changes in viscosity between the initial and final time of shearing was found in the emulsion without NaCl, emulsion containing 25 mM NaCl showed the highest change in viscosity among the emulsions containing various concentrations of NaCl. However, after 1200 seconds of shearing, emulsion with 25 mM NaCl had the highest apparent viscosity among other BGNF emulsions containing NaCl. The observed influence of NaCl on

time dependent characteristics in the emulsions was modeled using Wetman model. Table 4.43 shows the Weltman model parameters at a constant shear rate of 50 s^{-1} as a function of NaCl concentrations.

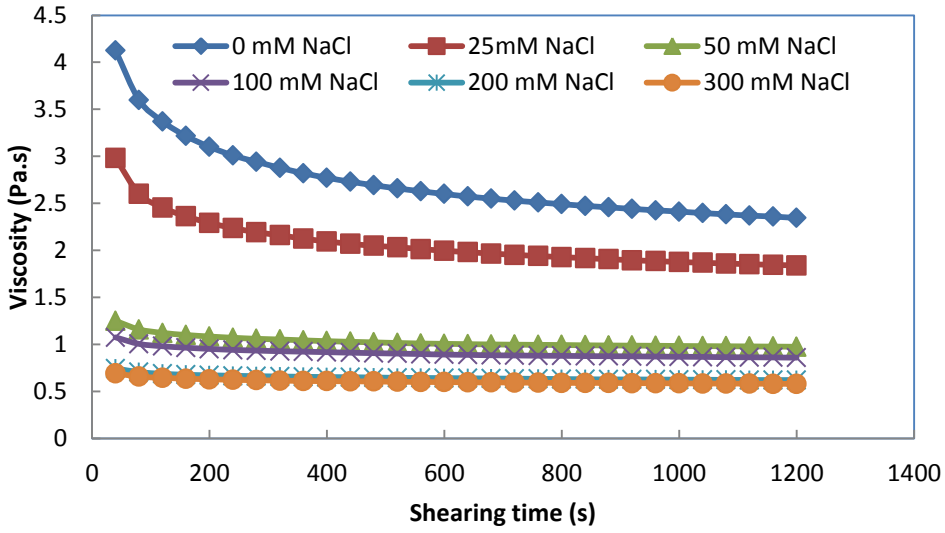

Figure 4.75 Effect of NaCl on time dependent characteristics of optimized emulsion at 50 s^{-1}

The high coefficient of determination (>0.97) suggested that Weltman model was able to represent the time-dependent rheological data. Table 4.43 showed that both parameters (A and B) of Weltman model were influenced by different NaCl concentrations. The mean of Weltman model parameter A ranged from 24.2 to 1.49 Pa and parameter B was from 286 to 39.5 Pa for emulsion without NaCl to 300 mM NaCl. Emulsion without NaCl was significantly different ($p < 0.05$) from emulsions with NaCl. The highest and lowest values of parameter A and B belonged to emulsion without NaCl and emulsion containing 300 mM NaCl respectively. However a comparison among emulsions prepared with different concentrations of NaCl suggested that emulsion containing 25 mM NaCl had the highest values of Weltman model parameters A and B which can be interpreted as high emulsion stability due to its relatively higher viscosity.

Table 4.43 Effect of NaCl concentrations on Weltman model parameters[1,2]

Concentration of NaCl (mM)	- B (Pa)	A (Pa)	R^2
0	24.2 ± 1.64[a]	285 ± 13.11[a]	0.98
25	15.0 ± 0.22[b]	196 ± 1.44[b]	0.97
50	3.63 ± 0.21[c]	73.8 ± 6.88[c]	0.97
100	2.92 ± 0.08[c]	59.0 ± 7.09[d]	0.98
200	1.63 ± 0.07[d]	42.4 ± 1.82[e]	0.98
300	1.49 ± 0.12[d]	39.5 ± 2.05[e]	0.99

[1]values are means ± standard deviations; Means with different letters within the same column are significantly different from each other ($p < 0.05$).
[2] A equals to the initial shear rate of Weltman model; B is the extent of structural break down of Weltman model; R^2 is the coefficient of determination between the experimental data and Weltman model prediction

4.7.1.6 Effect of NaCl on the rheological properties of optimum emulsion with regard to viscoelastic properties (storage and loss moduli)

Figures 4.76 and 4.77 show the frequency sweep obtained for optimum emulsion formulated with 0, 25, 100, 200 and 300 mM NaCl respectively. The logarithms of G', G'' and complex viscosity (η^*) were plotted as a function of logarithm of the frequency. Both the emulsions without and with NaCl exhibited both the G' and G". Both G' and G" showed significant dependence on the frequency and were increased with increase in frequency for the emulsions with NaCl. Emulsion without NaCl showed less dependence on frequency and tended to form a plateau at high frequency. Emulsions containing 0 mM, 25 mM, 50 mM, 100 mM and 200 mM NaCl showed a solid-like behaviour at all the studied frequencies where G' dominated and was higher than the G'' curve and tended to show a constant limiting value. This implied predominance in elastic characteristic over viscous behaviour at the frequency range investigated suggesting that the emulsions were weak gels. The spectrum of emulsion with 300 mM NaCl showed that the G" was higher than G' at the lower frequencies which was an indication of liquid character at a very low frequency. There was a cross over at higher frequency of about 20.0 rad/s and G' was observed to be higher than G" there by showing a solid-like behaviour at higher frequency. This behaviour is typical of viscoelastic material.

The η^* of all the emulsions also increased towards an infinitely high value. These observations are typical of gel structures. The high G' at low frequency indicated high structural strength of the emulsions without NaCl and with 25 mM, 50 mM, 100 mM and 200 mM NaCl.

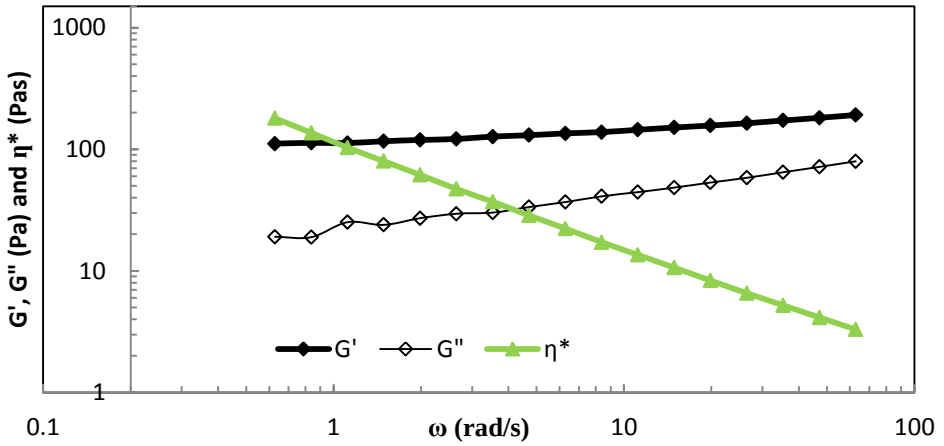

A

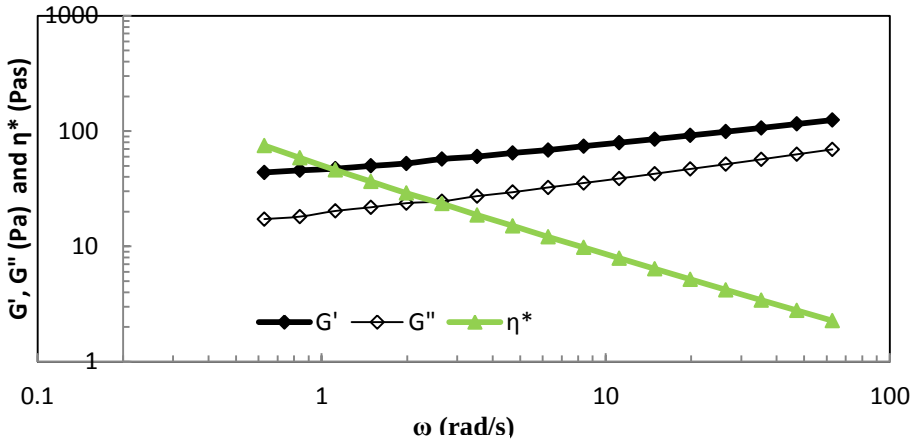

B

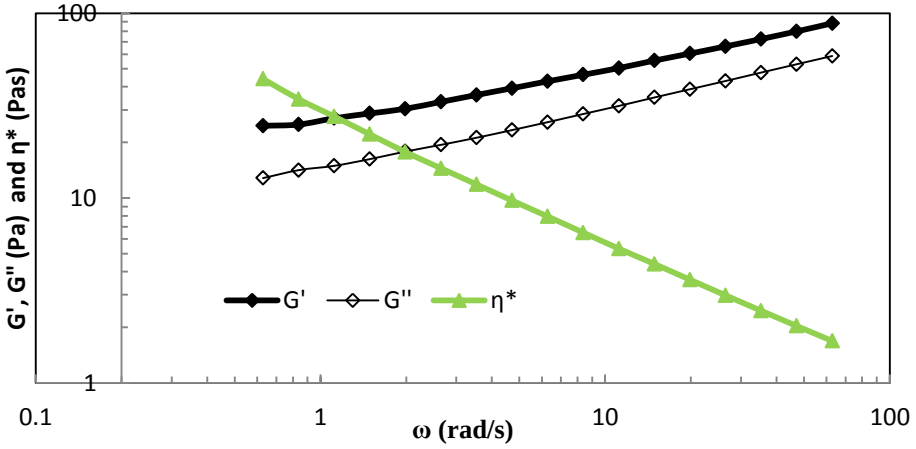

C

Figure 4.76 **Frequency sweep of optimum emulsion containing (A) 0 mM (B) 25 mM (C) 50 mM NaCl**

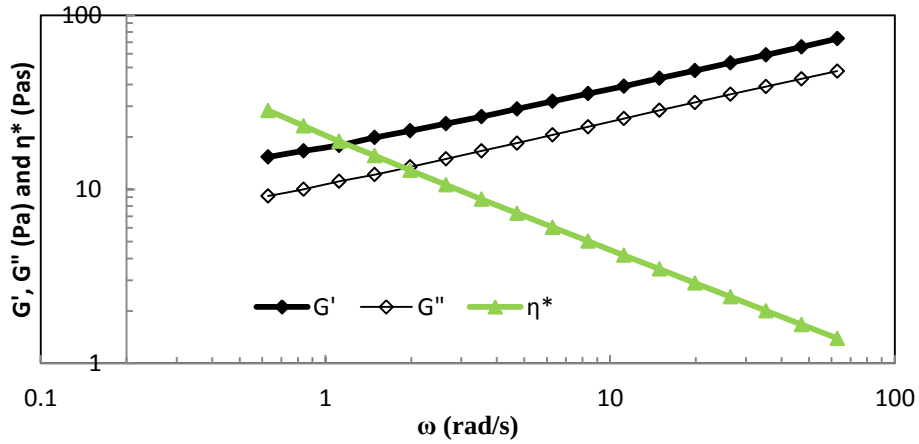

D

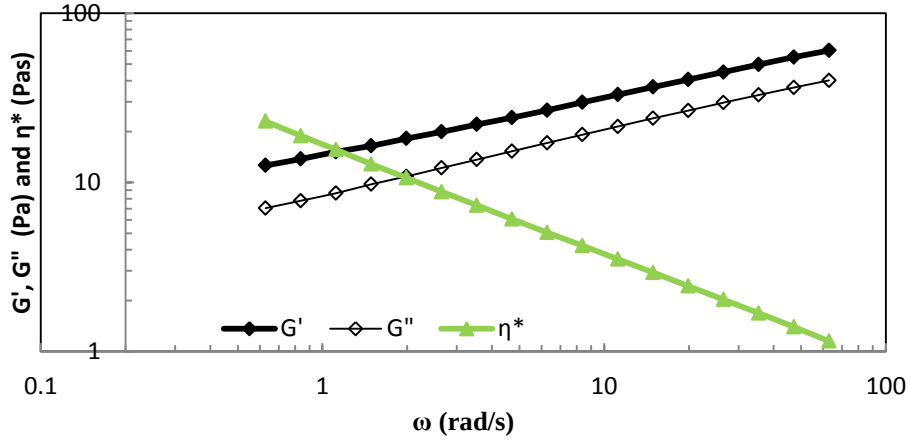

E

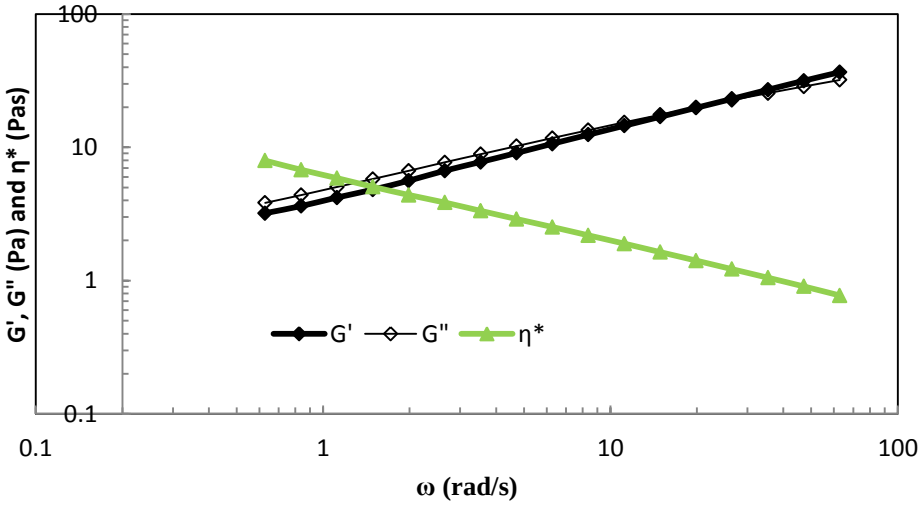

F

Figure 4.77 **Frequency sweep of optimum emulsion containing (D) 100 mM (E) 200 mM (F) 300 mM NaCl**

These emulsions therefore exhibit the tendencies to be rigid, possess high flow resistance and therefore have high stability at rest (during storage). Emulsion with 300 mM NaCl had low structural strength and this was as a result of change in molecular conformation of BGNF matrix by NaCl which inhibited emulsion formation during homogenization.

Figure 4.78 shows the effect of NaCl concentrations on the G' and G'' of the optimum emulsion. The effect of NaCl concentrations was noticeable on the material functions. Both G' and G'' decreased with increase in NaCl concentrations. Decreased G' and G" were as a result of decreased flocculation in the emulsions as the concentrations of the NaCl increased resulting into less interactions and consequent emulsion instability. The decrease in material function as the concentration of NaCl increased was a result of impediment posed by the NaCl to BGNF polymer network formation. The NaCl reduced the BGNF matrix strength necessary for emulsion formation. Table 4.44 shows the G' and G'' obtained for the emulsions with and without NaCl at low frequency of 0.628 rad/s.

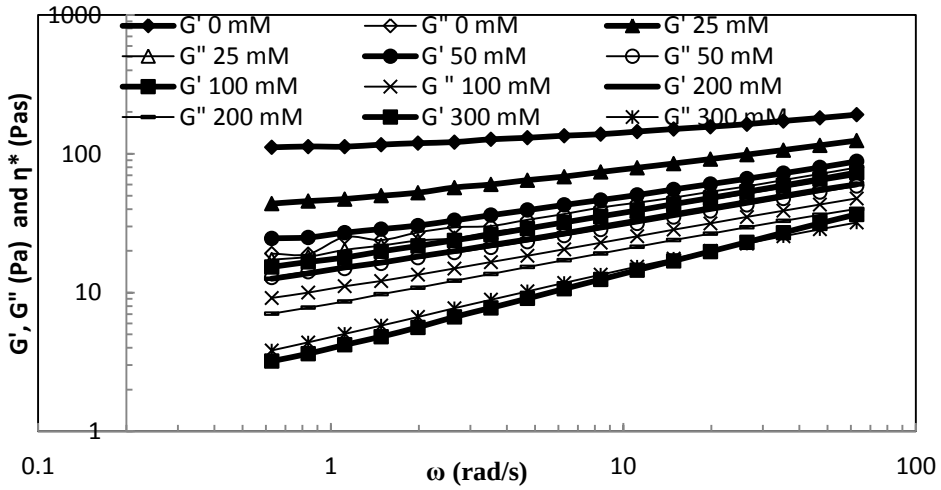

Figure 4.78 Storage (G') and loss (G") moduli as a function of angular frequency during dynamic oscillatory tests of sunflower oil-in-water emulsion containing various concentration of NaCl.

The means of G' and G'' ranged from 3.21 to 111 Pa and 3.83 to 19.1 Pa, respectively. Emulsions without and 300 mM NaCl recorded the highest and lowest values of G' and G'' ($p < 0.05$), respectively. However, emulsion with 25 mM NaCl had the highest G' and G" among the emulsions with NaCl.

Table 4.44 Effect of NaCl concentration on the storage and loss modulus at 0.628 rad/s[1,2]

NaCl (mM)	Storage modulus (G') Pa	Loss modulus (G") Pa
0	111 ± 2.70[e]	19.1 ± 1.38[d]
25	43.8 ± 1.23[d]	17.3 ± 0.20[d]
50	24.6 ± 1.21[c]	12.8 ± 1.18[c]
100	15.3 ± 0.17[b]	9.15 ± 0.69[b]
200	12.6 ± 1.37[b]	7.04 ± 0.87[b]
300	3.21 ± 0.04[a]	3.83 ± 0.37[a]

[1] Values are means ± standard deviations; Means with different letters within the same column are significantly different from each other ($p < 0.05$).
[2] G' equals the storage modulus; G" is the loss modulus

4.7.1.7 Effect of NaCl on the rheological properties of optimum emulsion with regard to compliance and recoverable strain

Figure 4.79 shows the compliance (J) against time (s). A load of 0.5 Pa was imposed on the structure of the emulsions in the first part of the experiment for 500 s while the second part involved sudden removal of the load and compliance was monitored for the next 500 s.

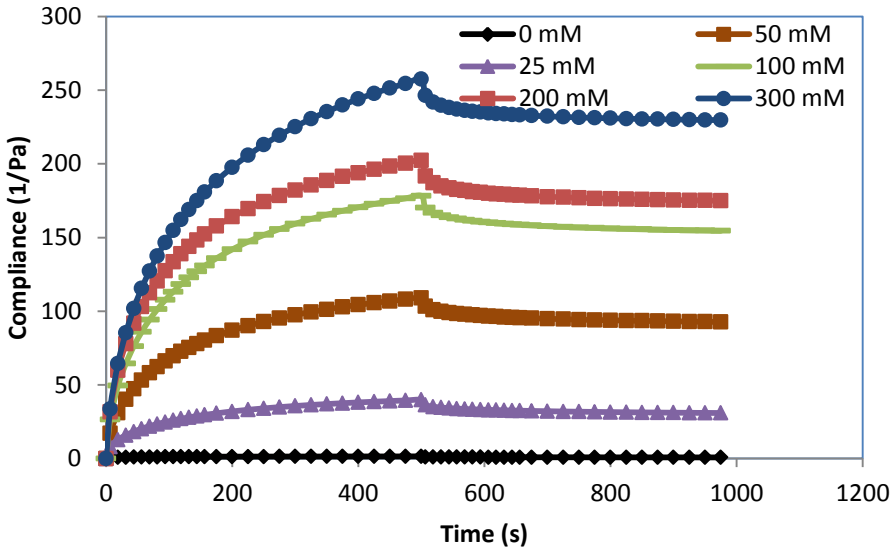

Figure 4.79 Creep and recovery curves of emulsions containing various concentrations of NaCl

All the emulsions with and without NaCl showed similar viscoelastic characteristics during creep and recovery phases. For instance, J increased steadily when a stress of 0.5 Pa was imposed on all the emulsions during the creep stage and the elastic component of the deformation recovered instantaneously when the load was removed. The emulsion without NaCl recorded the lowest while emulsion containing 300 mM NaCl recorded the highest J. The high J for 300 mM NaCl emulsion indicated a negligible instantaneous elastic compliance and implied that the network of the emulsion structure is weak and less rigid. Emulsions with lower J possess stronger structural interactions (high rigidity) hence gave small deformation when the stress was imposed on them. NaCl had profound influence on the compliance. Increase in NaCl concentrations (Figure 4.79) increased J. This was as a result of decreased structural formation (droplet – droplet interaction) as NaCl concentration increased and this subsequently decreased emulsion rigidity. However, among the emulsions containing NaCl, emulsion with 25 mM NaCl had the lowest J.

Table 4.45 shows the effect of NaCl concentrations on the recoverable strain, Q (t)% of the studied emulsion.

Table 4.45 Effect of NaCl concentration on the recoverable strain[1,2]

NaCl concentration (mM)	Recoverable strain Q(t)%
0	46.2 ± 1.49^{d}
25	22.4 ± 1.53^{c}
50	15.0 ± 0.59^{b}
100	13.3 ± 0.35^{b}
200	13.5 ± 0.55^{b}
300	10.8 ± 0.58^{a}

[1] Values are mean ± standard deviations; Mean values with different letters within the same column are significantly different from each other ($p < 0.05$).
[2] Q (t)% equals the recoverable strain

Q (t)% indicated how much percentage of the structure was able to recover when the load was withdrawn from the emulsions and hence it was a measure of the elasticity of the emulsion. Increased Q (t)% can therefore be linked to increased elasticity of the emulsions. The mean of Q (t)% ranged between 10.8 to 46.3% for all the emulsions. Increased concentration of NaCl in the BGNF matrix had a profound significant decrease ($p < 0.05$) on the elasticity. The emulsion

containing 300 mM NaCl, had the lowest Q (t)% indicating that this emulsion had the lowest elasticity and stability among the emulsions. Emulsion with 25 mM NaCl, recorded the highest elasticity among emulsions with NaCl.

4.7.1.8 Summary on the effect of NaCl on the stability and rheological properties of optimum emulsion

The relative impediments caused by the presence of NaCl to the BGNF network formation during the continuous phase preparations brought about significant difference to the characteristics of emulsions. The stability of the emulsion seemed to be dependent on the microstructural properties of the emulsion. Emulsion that contained the least concentration (25 mM) had the least oil droplet size, high BS_{Avo} (%) and flocculated microstructure relative to other emulsions with NaCl. The difference in properties could be a measure of extent of relative imposition of NaCl on BGNF structuration and emulsification. Rheological results showed a similar observation. The presence of NaCl in the BGNF matrix showed a significant reduction in emulsion properties relative to emulsion without NaCl. However the presence of NaCl at 25 mM is thought not to cause much severity to both BGNF polymer strength and structural interactions. Although both the emulsions with and without NaCl had similar rheological properties, the influence of NaCl on the BGNF matrix appeared to reduce some characteristics such as thixotropy, pseudoplasticity and viscoelasticity. The stability of BGNF emulsion may therefore not be unconnected with its rheological properties. The changes in the microstructure of the emulsions due to the presence of NaCl in the BGNF polymer network had manifested as differences in the rheological properties such as significant reduction in apparent viscosities and viscoelasticity with consequent disparities in their stabilities.

4.7.2 Effect of vinegar on the stability and rheological properties of optimum emulsion

4.7.2.1 Effect of vinegar on emulsion stability of optimum emulsion with regard to droplet size distribution

Figure 4.80 shows the oil-droplet size distribution of the optimum emulsion (7% (w/w) BGNF and 40% (w/w) SFO) containing various concentrations of vinegar (0 - 8% w/w). All the oil-droplet distributions presented a similar Gaussian shape. The presence of vinegar at various concentrations affected the oil droplet distribution curves relative to emulsion without vinegar. Similar observation was reported by Romero *et al.* (2009) on the effect of pH on oil droplet distribution of highly concentrated O/W crayfish flour-based emulsions. The influence of vinegar

on the droplet size distribution of emulsions whose BGNF matrix contained vinegar in the range of 0.5 - 8% (w/w) were similar as there was no much difference in the oil-droplet distribution curves. When compared with the distribution of emulsion without vinegar, the oil droplet size distribution curves of all other emulsions with vinegar, irrespective of concentration, have shifted to the right and broader indicating an increase in oil-droplet size (Romero *et al.,* 2009).

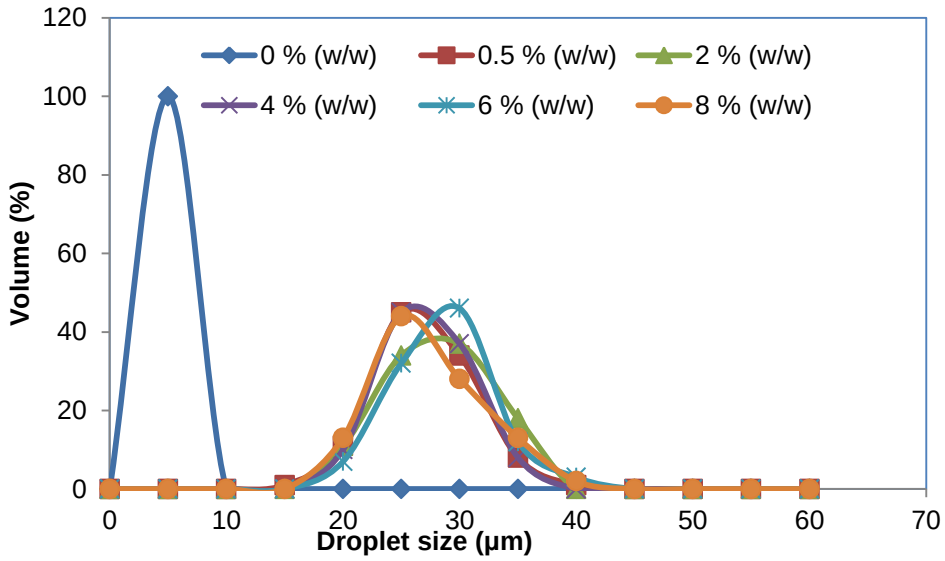

Figure 4.80 Droplet size distribution of dispersed phase particles in emulsion formulated with 7% (w/w) BGNF and 40% (w/w) SFO containing vinegar at various concentrations

Table 4.46 is the particle size volume surface mean diameter ($d_{3,2}$) and the equivalent volume mean diameter ($d_{4,3}$) of the emulsions with and without vinegar measured immediately after emulsion preparation. The $d_{3,2}$ gave information regarding size of the emulsion where most oil-droplet fell while $d_{4,3}$ was a measure of changes in oil-droplet size involving emulsion destabilization process. The mean of oil-droplet size ranged from 3.45 to 27.6 µm and 3.66 to 28.4 µm for $d_{3\ 2}$ and $d_{4,3}$, respectively as affected by vinegar concentrations (0 to 8% (w/w)). The influence of vinegar in the BGNF matrix was deleterious to emulsion as its presence at all concentrations increased the droplet sizes of the resulting oil-in-water emulsions relative to BGNF matrix without vinegar. Vinegar is a sour tasting liquid which contained acetic acid as its main component. Like other studied additives in this work, vinegar at various concentration

Table 4.46 Effect of Vinegar on droplet size[1,2]

Conc of Vinegar (% w/w)	$d_{3,2}$ (μm)	$d_{4,3}$ (μm)
0	3.45 ± 0.10^{a}	3.66 ± 0.11^{a}
0.5	26.2 ± 0.86^{bc}	26.9 ± 0.42^{bc}
2.0	27.1 ± 0.49^{bc}	27.7 ± 0.54^{cd}
4.0	25.9 ± 0.23^{b}	26.4 ± 0.29^{b}
6.0	27.6 ± 0.91^{c}	28.4 ± 0.64^{d}
8.0	26.4 ± 0.46^{bc}	27.2 ± 0.52^{bc}

[1]Values are means ± standard deviations; Means with different letters within the same column are significantly different from each other ($p < 0.05$).
[2]$d_{3,2}$ refers to the volume surface mean diameter of the emulsions; $d_{4,3}$ is the equivalent volume-mean diameter of the emulsions.

had been incorporated into the BGNF during continuous phase preparation by gelatinizing BGNF dispersions with vinegar prior to emulsification process. The presence of vinegar during the gelatinization of BGNF dispersion must have weakened the strength of the BGNF matrix responsible for emulsion formation. Ohishi *et al.* (2007) reported a decrease in viscosity of rice starch and flour pastes when gelatinized with acetic acid. The authors attributed decreased viscosity to loosening or destruction of the structures during gelatinization with acetic acid. Generally there appeared to be no trend on the oil droplet sizes ($d_{3,2}$ and $d_{4,3}$) with increase in vinegar concentration (Table 4.46). However, the presence of vinegar as low as 0.5% (w/w) increased the oil droplet sizes more than seven time relative to the emulsion without vinegar. There was a significant difference ($p < 0.05$) between the particle sizes of emulsions without and with vinegar. Some of the emulsions containing vinegar however showed significant difference in droplet size while others were not significantly different. The differences and similarities in droplet sizes could be as a result of different levels at which vinegar at various concentrations in the emulsions caused BGNF structural loosening.

4.7.2.2 Effect of vinegar on emulsion stability of optimum emulsion with regard to microstructure

Figure 4.81 shows the microstructures of emulsions whose BGNF matrix contained vinegar at various concentrations. The images were obtained immediately after emulsion preparation and thus showed the influence of vinegar on the emulsion forming ability of BGNF matrix. The micrographs showed that vinegar had a negative effect on the ability of the BGNF matrix to form

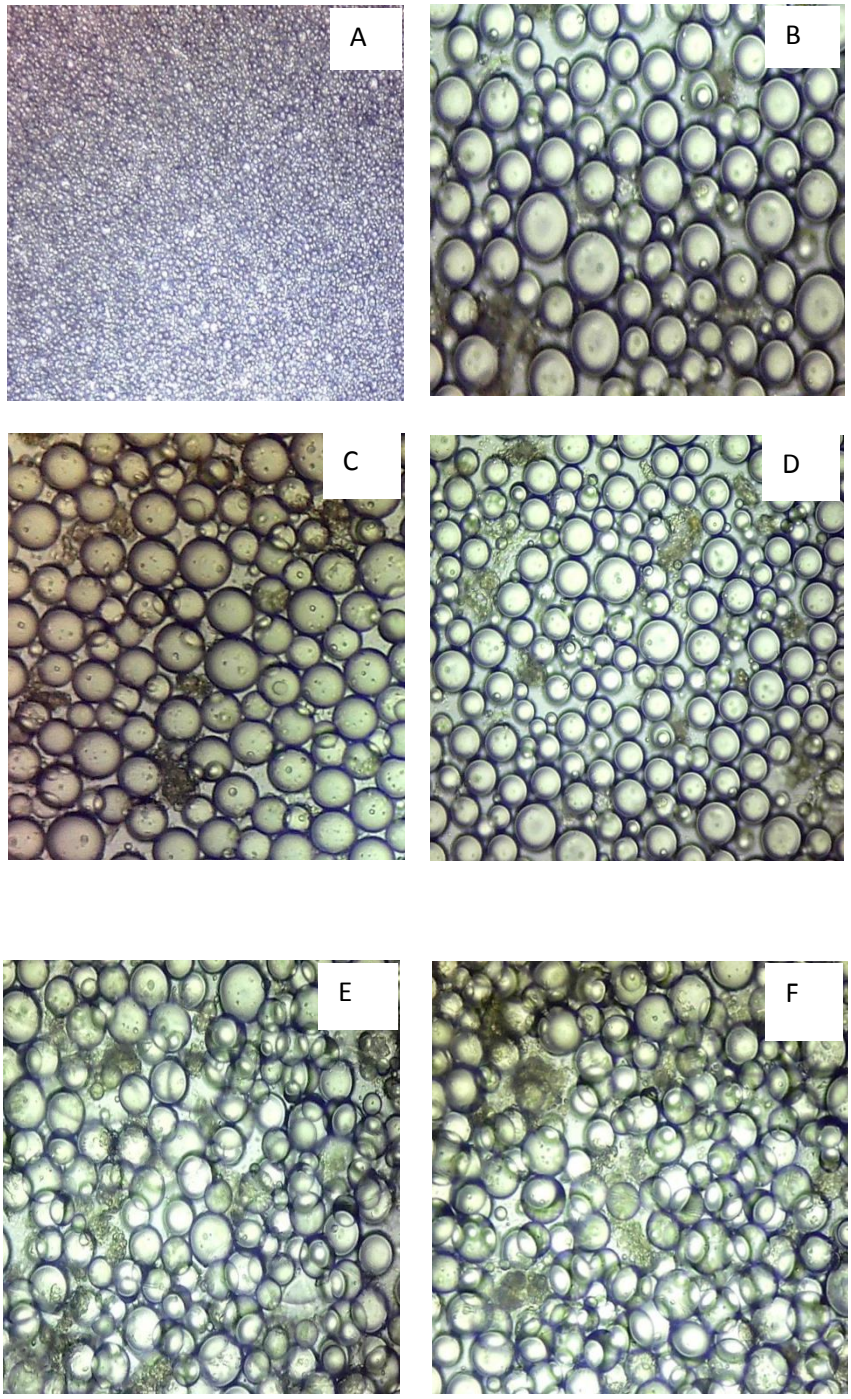

Figure 4.81 Micrographs (X 40 magnifications) of emulsions containing vinegar at (A) 0 % (w/w) (B) 0.5% (w/w) (C) 2% (w/w) (D) 4% (w/w) (E) 6% (w/w) (F) 8% (w/w)

emulsions. The micrographs of emulsions presented relatively larger particles with some fewer smaller oil droplets which indicated a polydispersed system. Creaming and oil droplet aggregation phenomena in an emulsion system had been explained to depend on the oil-droplet

size and distribution of such systems. Emulsions of high polydispersity are more prone to creaming due to differential creaming speeds of individual large and small droplets (Nor Hayati, 2009). The presence of vinegar in the BGNF matrix at all studied concentrations had produced emulsions with bigger droplet sizes relative to the matrix without vinegar as can be visualized in the micrographic images. This probably was because of the weakened strength of the BGNF matrix containing vinegar relative to the BGNF matrix without the vinegar. The weakening of the strength during gelatinization might probably have been a result of the hindrance posed by vinegar to form polymer network of required strength necessary for emulsion formation and stabilization. The microstructures of the emulsions with vinegar were however difficult to differentiate micro graphically. This is an indication of comparable influences of vinegar at all studied concentrations on the emulsion forming ability of BGNF polymer.

4.7.2.3 Effect of vinegar on storage stability of optimum emulsion

Figure 4.82 and 4.83 are the Turbiscan profile (physical stability graph) of the BGNF emulsions with vinegar concentration of (A) 0% (w/w); (B) 0.5% (w/w); (C) 2% (w/w); (D) 4% (w/w); (E) 6% (w/w) and (F) 8% (w/w) measured at 30 mins interval for a period of 360 mins at 20^{o}C. The emulsion stability curves were presented in both the normal and reference Turbiscan mode with backscattering flux (%) at ordinate and tube length at abscissa respectively. The reference modes (positioned right to the normal mode in Figures 4.82 and 4.83) were the alternative representation of the stability curves where the firstly scanned profile was used as the reference profile relative to the other scans and was assigned a value of 0%. The first scans in all of the emulsion stability curves gave the intrinsic information regarding the emulsions and its backscattering flux (%) gave the representation of the microstructure of the recently prepared emulsions.

The initial backscattering, BS_{AVo} (%) is a parameter that is highly dependent on the number of oil droplets in an emulsion system. The higher the number of the oil droplets in the emulsion system, the higher the BS_{AVo} (%). Table 4.47 shows the effect of vinegar concentrations on BS_{AVo} (%). Vinegar had observable influence on BS_{AVo} (%). The mean of BS_{AVo} (%) ranged between 95.2 and 70.5% for vinegar concentration between 0 and 8% (w/w). There was no general trend of increase or decrease of BS_{AVo} (%) in relation to increase in the concentration of vinegar.

However, there was a general significant decrease ($p < 0.05$) in BS_{AVo} (%) of the emulsions containing vinegar relative to emulsion without vinegar. The reduction in the initial backscattering (BS_{AVo} (%)) of emulsions with vinegar relative to emulsion without vinegar was a

Table 4.47 Effect of vinegar concentration on Initial backscattering value[1,]

Concentration of vinegar (% w/w)	Initial backscattering [BS_{AVo}] value (%)
0	95.2 ± 0.01^{a}
0.5	71.2 ± 0.87^{b}
2.0	72.0 ± 1.75^{b}
4.0	70.5 ± 0.29^{b}
6.0	71.3 ± 1.63^{b}
8.0	70.8 ± 0.23^{b}

[1]Values are means ± standard deviations; Means with different letters within the same column are significantly different from each other ($p < 0.05$).

result of less numerous oil-droplets in the BGNF matrix containing vinegar. Although there was no significant difference in the BS_{AVo} (%) of all the emulsions containing vinegar ($p < 0.05$), emulsion without vinegar showed a significant difference ($p < 0.05$) from other emulsions with vinegar and recorded the highest BS_{AVo} (%).

The result of the reference mode of Turbiscan profile in Figures 4.82 and 4.83 (right hand side) showed relative changes with respect to time in all emulsions. Backscattering flux (%) decreased along the entire tube length in all the emulsion with and without vinegar. Decreased backscattering flux (%) was as a result of oil droplet aggregation which could be as a result of oil-droplet flocculation or coalescence. The observed decrease in the backscattering flux overtime was because of increased oil-droplet size which caused the mean path of photon (l*) to increase because of an increase in the average distance between the oil-droplets. The presence of vinegar at all concentrations induced similar destabilization mechanism to emulsion without vinegar. In order to understand the effect of different concentrations of vinegar on emulsion stability, the mean value kinetics for oil-droplet aggregation in the middle of the tube (20 - 40 mm) from backscattering flux (%) was analysed. Figure 4.84 showed the effect of vinegar concentrations on the backscattering flux (%) mean value kinetics. Vinegar concentrations had dissimilar effects on emulsion stability over time. The farther the graph from the origin the less stable the emulsion becomes. Although the effect of vinegar on the emulsion has induced destabilization at all studied concentrations, the destabilization kinetics did not however follow any particular trend. The graph showed that there were no clear differences between the effects of various concentrations of vinegar on emulsion stability within the period of study. However the destabilization kinetic graph of emulsion containing 8% (w/w) vinegar

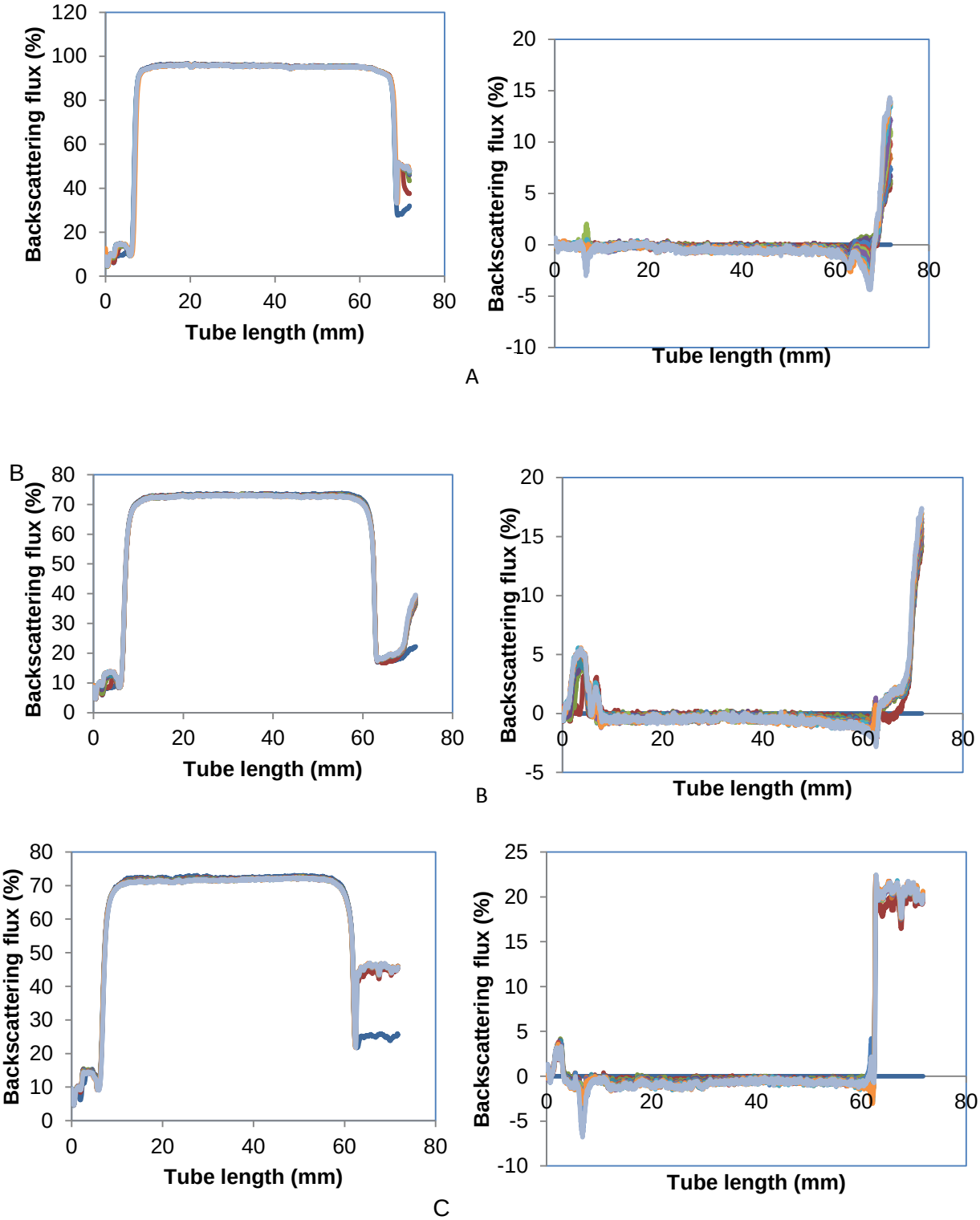

Figure 4.82 **Changes in the backscattering profile (BS%) as a function of sample height with storage time of BGNF (7% (w/w) stabilized emulsion containing vinegar at (A) 0% (w/w) (B) 0.5% (w/w) (C) 2% (w/w)**

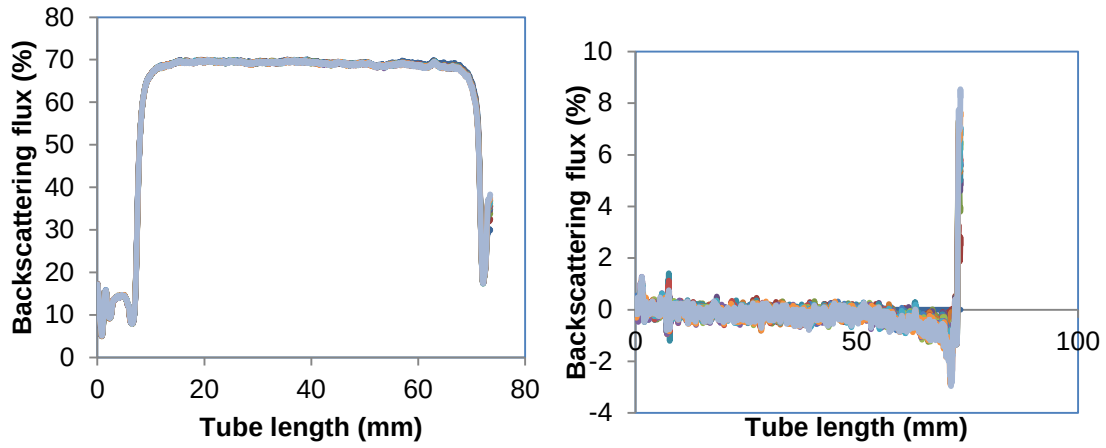

D

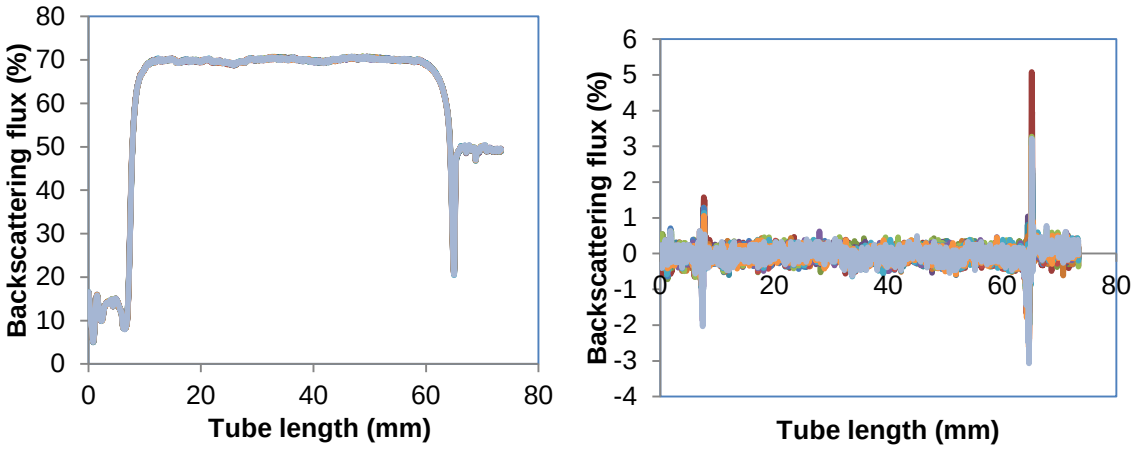

E

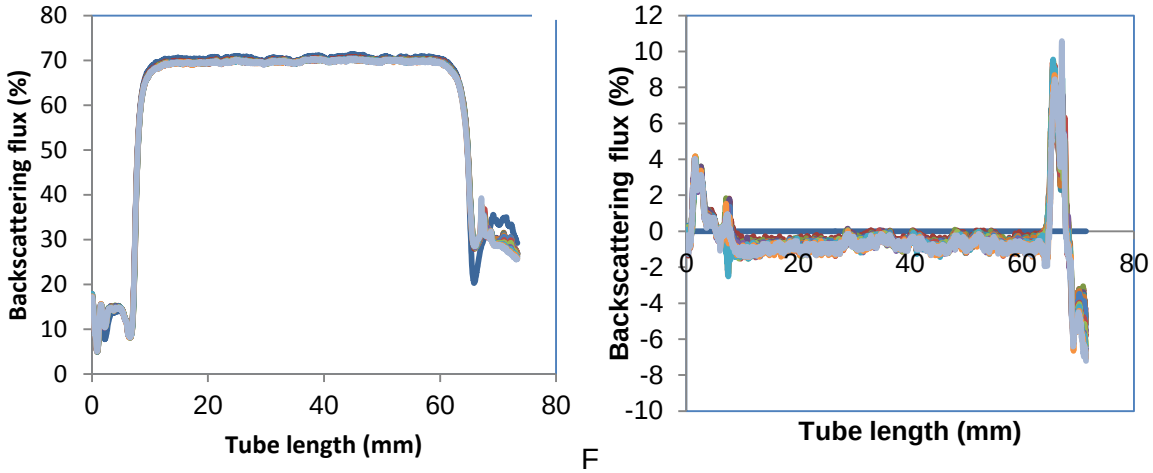

F

Figure 4.83 **Changes in the backscattering profile (BS%) as a function of sample height with storage time of BGNF (7% (w/w) stabilized emulsion containing vinegar at (D) 4% (w/w) (E) 6% (w/w) (F) 8% (w/w)**

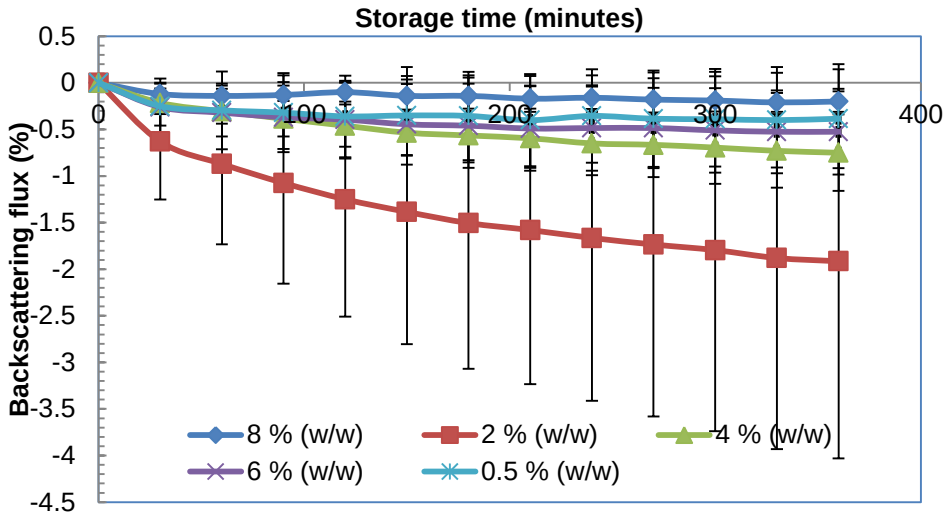

Figure 4.84 **Variation in backscattering in the 20-40mm zone monitored over 360 minutes for samples stored in quiescent condition at 20^{o}C for emulsion containing different concentrations of vinegar**

was the closest to the origin among emulsions containing vinegar. In order to analyze emulsion stability at equilibrium time, the backscattering flux (%) at equilibrium was plotted against vinegar concentration. The equilibrium backscattering flux (%) is the final backscattering flux attained at the equilibrium time. Figure 4.84 showed that all of the studied emulsions have reached equilibrium at about 360 mins. Therefore the backscattering flux (%) at the 360th minutes was plotted against the respective vinegar concentrations. Figure 4.85 is the graph of the equilibrium backscattering flux (%) against concentration of vinegar and it showed clearly that vinegar concentrations affected the average equilibrium backscattering flux (%). Although there was no definite trend on the effect of vinegar on the equilibrium backscattering flux (%), emulsion containing, 8% (w/w) of vinegar had the least average backscattering flux (%) at the end of 360 minutes.

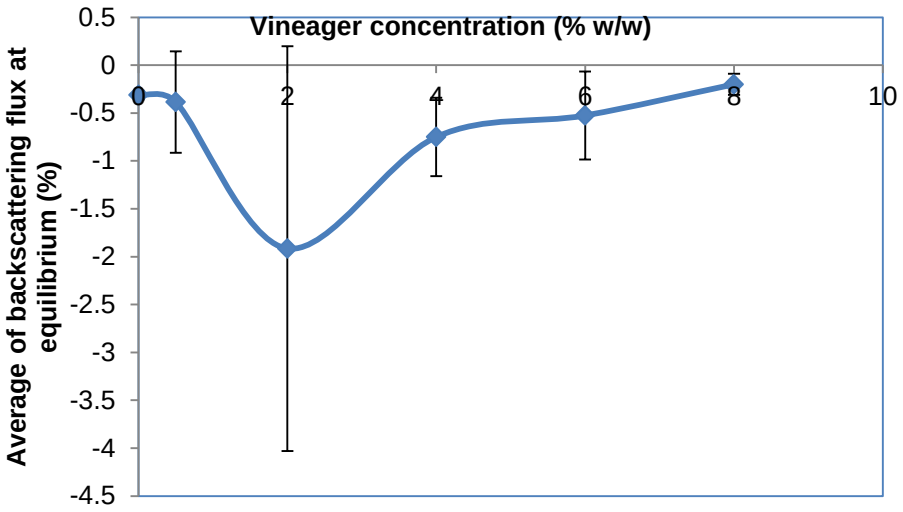

Figure 4.85 **Effect of addition of vinegar on emulsion stability (Average backscattering flux at equilibrium state)**

4.7.2.4 Effect of vinegar on rheology of optimum emulsion with regard to flow curves and hysteresis loop area

In order to describe and compare the rheology of the emulsions with and without vinegar, forward and backward shear stress sweep experiments were conducted. Figure 4.86 shows the ascending and descending flow curves developed for the emulsions with and without vinegar. The relative position of the forward and backward curves showed that the emulsions were time dependent, and the structure of the samples had been destroyed during the forward sweep and this has resulted in a decrease in shear stress during the backward sweep. The structural destruction caused by forward sweep has therefore resulted into hysteresis loop areas between the forward and backward curves. All the emulsions exhibited hysteresis loop area irrespective of the concentration of the vinegar. The presence of the hysteresis loop areas between the forward and backward flow curves and relative positions of the forward and backward curves indicated that all of the emulsions were thixotropic in nature. The viscosity of a thixotropic fluid decreases progressively with shearing time which could be as a result of structural breakdown (Barbosa-Cánovas *et al.,* 1996). Comparison of the loop areas revealed similarities and differences among emulsions with and without vinegar. Although some of the rheological behaviors of the emulsions with and without vinegar were similar, the closed loop area showed that emulsion without vinegar had a relatively larger loop area compared to emulsions with vinegar. However, all the emulsions with vinegar have closely identical

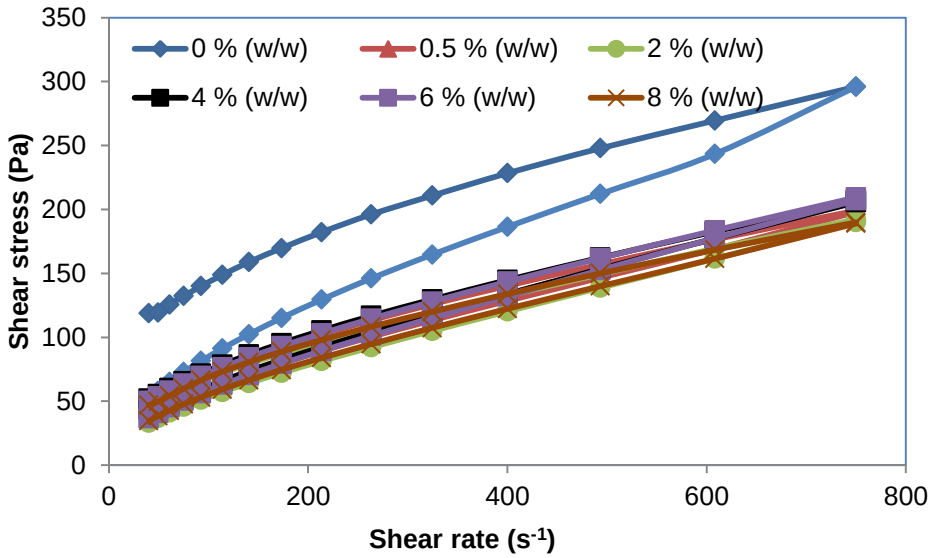

Figure 4.86 Effect of vinegar on the rheological behavior of optimized emulsion

hysteresis loop areas. This may be attributed to the structural similarities (droplet-droplet and BGNF – droplets interactions) among the emulsions with vinegar.

Figure 4.87 shows the effect of vinegar on the steady state apparent viscosity curves of the optimum BGNF emulsion. All the emulsions were shear thinning in nature since the apparent viscosities decreased with increased shear rate (Dolores and Canet, 2013). The apparent viscosities of BGNF stabilized emulsion were sensitive to the influence of vinegar and tended to decrease in the presence of vinegar (Figure 4.87). BGNF matrix with vinegar at all concentrations were unable to form a comparable oil droplet structures to BGNF matrix without vinegar and this has resulted into a decrease in apparent viscosities of the emulsions. All the emulsions formed by BGNF matrix with vinegar recorded lower and overlapped apparent viscosities at all shear rates investigated. The decrease in apparent viscosity for emulsion containing vinegar could probably be as a result of both weakened BGNF strength and big droplet sizes which subsequently reduced droplet interactions. The internal structure of the emulsion without vinegar remained totally flocculated and hence its apparent viscosities at all tested shear rates were the highest due to the droplet-droplet and BGNF-oil droplet interactions and high matrix strength which enhanced good oil-droplet structural formation. Regarding apparent viscosities, the behaviour of all the emulsions containing vinegar cannot be resolved. However, it seemed that vinegar concentration of 0.5% (w/w) was enough to provide optimum

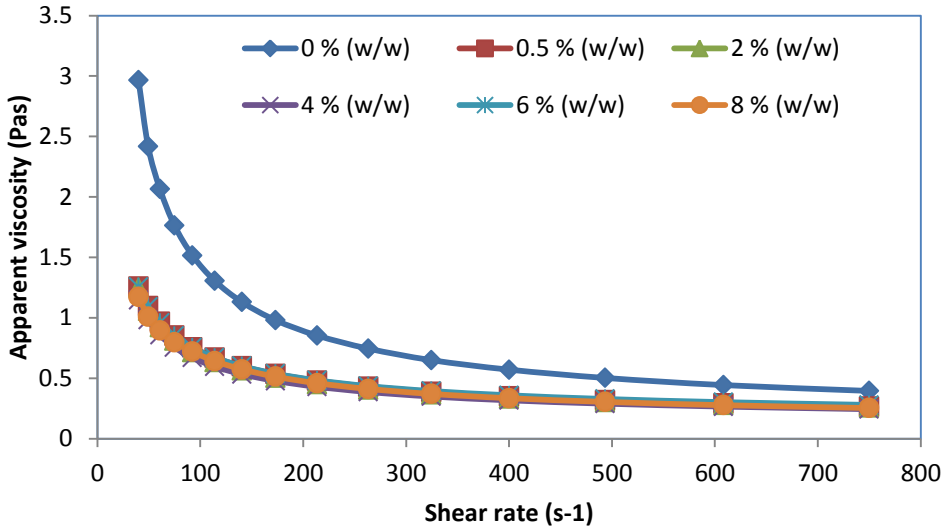

Figure 4.87 Effect of vinegar concentrations on the apparent viscosity of the optimum emulsion

inhibition of structuration in the polymer network during formation as there was no difference between the flow properties of emulsions containing 0.5, 2, 4, 6 and 8% (w/w).

Single point comparison of the minimum apparent viscosities among the emulsions at the maximum point of shear gradient (750 s^{-1}) was made for comparative purposes. Table 4.48 shows the effect of vinegar on the minimum apparent viscosity of the recently prepared optimum emulsion obtained at the loop apex (Figure 4.86).

Table 4.48 Effect of vinegar on the minimum apparent viscosity of the optimum emulsion at ambient temperature of 22°C [1,2].

Vinegar (% (w/w))	Viscosity at 750 s^{-1} (Pas)
0	0.39 ± 0.00[a]
0.5	0.27 ± 0.00[b]
2.0	0.26 ± 0.01[bc]
4.0	0.24 ± 0.00[c]
6.0	0.27 ± 0.01[b]
8.0	0.25 ± 0.00[c]

[1]Values are means ± standard deviations; Different letters within the same column are significantly different from each other ($p < 0.05$)
[2]Values calculated at the maximum point of the shear gradient.

The table showed that the minimum apparent viscosities of the emulsions containing vinegar were significantly different ($p < 0.05$) from the emulsion without vinegar.

The mean of the minimum apparent viscosity of all the emulsions ranged from 0.39 to 0.24 Pas with the highest value belonging to emulsion without vinegar. Hence, the minimum apparent viscosity of emulsion without vinegar is significantly different from emulsions with vinegar. This may be explained in terms of a relatively stronger matrix possessed by emulsion without vinegar which favored emulsion formation and promoted stronger oil droplet - oil droplet and BGNF-oil droplets interactions. The minimum apparent viscosities of emulsions with vinegar however showed significant similarities and differences probably based on the level of structural inhibition and droplet-interactions imposed by various concentrations of vinegar.

Table 4.49 shows the data obtained when the flow curves of Figure 4.86 were further analysed using power law rheological model. The hysteresis loop area was also included in the Table 4.49. High coefficient of determination indicated the ability of power law rheological model to describe the intrinsic rheological properties of the emulsions. Ohishi *et al.* (1997) also used power law model to evaluate the effect of acetic acid on the flow curves of gelatinized rice starch and pastes. Vinegar concentrations had observable effects on the power law parameters and hysteresis loop area. The mean of consistency coefficient ranged from 7.09 to 30.1 and 4.19 to 5.90 Pas for forward and backward curves, respectively while the flow behaviour index (n and n^i), a measure of fluid resistance to flow was in the range 0.34 to 0.49 and 0.58 to 0.62 for forward and backward curves respectively. The flow behaviour index for the forward and backward curve were less than unity indicating that all the emulsions were pseudoplastic in nature. For all the formulation studied, the consistency coefficients of the forward curve were higher than those of corresponding values for the backward curve while the flow behavior index of the forward curve were lower than those of corresponding values of backward curves indicative of structural destruction in the emulsion systems during forward shear stress sweep. There was a significant decrease and increase in the consistency coefficient and flow behaviour index, respectively for the forward and backward curves of emulsions with vinegar relative to emulsion without vinegar. This indicated that the presence of vinegar had decreased the emulsion viscosity and this probably could be due to inability of BGNF matrix containing vinegar to form structured emulsion of comparable strength to BGNF matrix without vinegar. The viscosity of BGNF matrix could probably have decreased and strength weakened by vinegar and hence it reduced ability to form emulsion. Ohishi *et al.* (2007) reported a significant decrease in viscosity of rice starch and flour gelatinized in the presence of acetic acid relative to

distilled water. The effect of vinegar concentrations of 0.5, 2, 4, 6 and 8% (w/w) did not show a significant ($p < 0.05$) difference on consistency coefficient and flow behavior index.

The effect of vinegar concentration on the magnitude of hysteresis loop area is shown in Table 4.49. The magnitude of hysteresis loop area gave information regarding the thixotropy of a material and has been explained to be an index of energy required to eliminate the structure responsible for flow time dependence. The area enclosed by the curves indicated the degree of structural breakdown (Barbosa-Cánovas *et al.,* 1996). The presence of vinegar at all concentrations in the emulsions decreased the magnitude of hysteresis loop area significantly. The mean hysteresis loop area ranged from 694 to 162 Pas^{-1} with the highest value belonging to emulsion without vinegar. All the emulsions containing vinegar showed closely related small magnitude of hysteresis loop area relative to emulsion without vinegar. Ohishi *et al.* (2007) found time dependency in rice starch and flour and reported remarkably small degree of thixotropy for rice starch and flour gelatinized with acetic acid. Their observation was attributed to loosened structure of starch during heating with acetic acid. There was no specific trend when vinegar was increased from 0 to 8% (w/w) on the magnitude of hysteresis loop area. However it showed a significant ($p < 0.05$) decrease when vinegar was increased from 0 to 0.5% (w/w). The magnitudes of hysteresis loop area of emulsions with vinegar were not significantly different. Although the emulsion without vinegar showed the highest thixotropic effect, the high value of magnitude of hysteresis loop area was an indication of high structural interactions and stronger strength which resulted into a correspondingly high viscosity. However, as it was reported by Tarrega *et al.* (2004) and Koocheki and Razavi (2009), a high viscous thixotropic fluid may show a larger hysteresis area than a lower viscosity one even if the latter undergoes a stronger structural destruction.

4.7.2.5 Effect of vinegar on emulsion rheology of optimum emulsion with regard to steady shear decay

In order to elucidate the time dependent behavior observed by hysteresis loop area method, steady shear decay method was employed. Emulsions with and without vinegar were sheared and their behaviors were compared at constant shear rate of 50 s^{-1}. Figure 4.88 shows the effect of shearing time on the viscosity of the emulsions containing different concentration of vinegar measured at a constant shear rate of 50 s^{-1}. All the emulsions showed a time dependent thixotropic characteristics evident from an observable decrease in the viscosity with increased shearing time (Dolores and Canet, 2013).

Table 4.49 Effect of Vinegar on Power law parameters and hysteresis loop area[1,2]

Conc. vinegar (% w/w)	K (Pas^n)	n	R^2	K' (Pas^n)	n'	R^2	Hysteresis loop area (Pas^{-1})
0	44.9 ± 0.87[a]	0.28 ± 0.02[a]	0.99	7.60 ± 0.53[a]	0.55 ± 0.34[a]	0.99	771 ± 44[a]
0.5	7.62 ± 1.18[b]	0.49 ± 0.03[b]	0.99	4.36 ± 0.25[b]	0.57 ± 0.01[a]	0.99	162 ± 55[b]
2.0	7.24 ± 1.43[b]	0.49 ± 0.03[b]	0.99	3.61 ± 0.06[b]	0.59 ± 0.02[a]	0.99	180 ± 27[b]
4.0	7.09 ± 0.31[b]	0.48 ± 0.01[b]	0.99	4.23 ± 0.62[b]	0.62 ± 0.08[a]	0.99	160 ± 1.1[b]
6.0	7.60 ± 0.31[b]	0.49 ± 0.00[b]	0.99	4.19 ± 0.16[b]	0.58 ± 0.01[a]	0.99	167 ± 12[b]
8.0	7.47 ± 0.16[b]	0.48 ± 0.00[b]	0.99	4.08 ± 0.04[b]	0.57 ± 0.00[a]	0.99	167 ± 10[b]

[1] Values are means ± standard deviations; Mean values with different letters within the same column are significantly different from each other ($p < 0.05$).

[2]K refers to the consistency coefficient of the forward sweep; K' is the consistency coefficient of the backward sweep; n is the flow behaviour index of the forward sweep; n' is the flow behaviour index of the backward sweep; R^2 is the coefficient of determination between the experimental data and power law model prediction

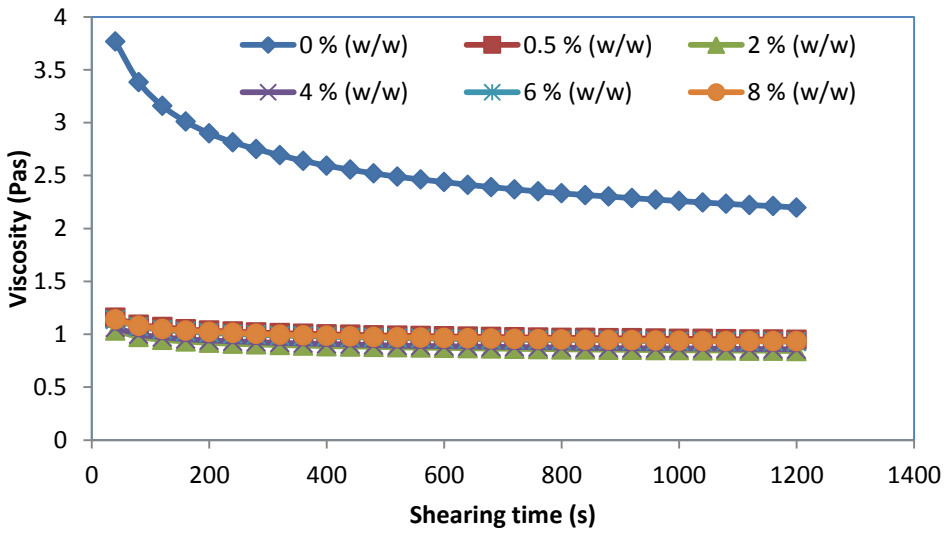

Figure 4.88 **Effect of vinegar on time dependent characteristics of optimum emulsion at 50 s^{-1}**

In addition, different vinegar contents in the emulsions had changed thixotropic properties of the emulsion in a different manner. The viscosity of the emulsions with and without vinegar at initial and final time of shearing can be visualized from the ordinate of the viscosity-shearing time graph (Figure 4.88). The presence of vinegar in the emulsion had reduced the viscosity of the emulsions relative to emulsion without vinegar. The curve of the emulsion with no vinegar was at the uppermost while emulsions containing 0.5, 2, 4, 6 and 8% (w/w) vinegar were below and unresolved. The highest changes in viscosity between the initial and final time of shearing was found in the emulsion without vinegar while emulsions containing 0.5, 2, 4, 6 and 8% (w/w) showed similar changes.

The observed influence of vinegar on time dependent characteristics in the emulsion was modeled using Weltman model. Table 4.50 shows the Weltman model parameters at a constant shear rate of 50 s^{-1} as a function of vinegar concentration. The high coefficient of determination (> 0.97) suggested that Weltman model was able to represent the time-dependent rheological data. The presence of vinegar in the BGNF emulsion had produced different significant ($p < 0.05$) effects on Weltman model parameters. The mean of Weltman model parameter A ranged from 24.2 to 2.55 Pa and parameter B was from 286 to 59.9 Pa for emulsion without vinegar to 8% (w/w) vinegar. Both parameters of Weltman model showed a sharp decline up till vinegar concentration of 0.5% (w/w) and remained nearly constant afterwards. The highest of parameters A and B belonged to emulsion without vinegar. However, a comparison among emulsions prepared with different concentrations of

Table 4.50 Effect of vinegar concentrations on Weltman model parameters[1,2]

Concentration of vinegar (% w/w)	- B (Pa)	A (Pa)	R^2
0	24.2 ± 1.64[a]	286.0 ± 13.1[a]	0.98
0.5	2.76 ± 0.18[b]	66.7 ± 39.2[b]	0.98
2.0	2.55 ± 0.17[b]	59.9 ± 6.05[b]	0.98
4.0	2.72 ± 1.19[b]	61.9 ± 9.31[b]	0.98
6.0	2.75 ± 1.37[b]	65.6 ± 8.60[b]	0.98
8.0	2.84 ± 0.75[b]	66.5 ± 5.68[b]	0.99

[1]Mean values with different letters within the same column are significantly different from each other ($p < 0.05$).
[2]A equals to the initial shear rate of Weltman model; B is the extent of structural break down of Weltman model; R^2 is the coefficient of determination between the experimental data and Weltman model prediction

vinegar showed that the effect of all vinegar concentration produced similar ($p < 0.05$) effect on Weltman model. This implies that the extent of structural destruction in the BGNF stabilized emulsions was a function of both BGNF matrix and oil droplets interactions. The high value of parameter B indicated in emulsion without vinegar showed the strong contribution of BGNF matrix to structural formation in terms of droplet-droplet interactions which consequently increased emulsion viscosity relative to the weakened BGNF-matrix. High viscosity possessed by emulsion without vinegar made it to suffer greater structural destruction relative to emulsions with vinegar. All emulsions with vinegar were not able to form emulsion of high viscosity which could be due to weakened matrix and poor droplet-droplet interaction. Emulsion containing 8% (w/w) however possessed marginally higher parameters A and B.

4.7.2.6 Effect of vinegar on emulsion rheology of optimum emulsion with regard to viscoelastic characteristics

Figures 4.89 and 4.90 show the results of the frequency sweep obtained for optimum emulsion without vinegar and with 0, 0.5, 2, 4, 6 and 8% (w/w) vinegar. The logarithms of storage modulus, G', loss modulus, G'' and complex viscosity (η*) were plotted as a function of logarithm of the frequency. All the emulsions exhibited both the $G^{'}$ and $G^{''}$. Both of the material functions (G' and G") showed significant dependence on the frequency and increased with increase in frequency for the emulsions with and without vinegar. The spectra of emulsions with and without vinegar showed solid-like behaviour at all the frequencies where G' dominated and was higher than the G'' curve and tended to show a constant limiting value. The predominance of the elastic characteristics (G') over viscous

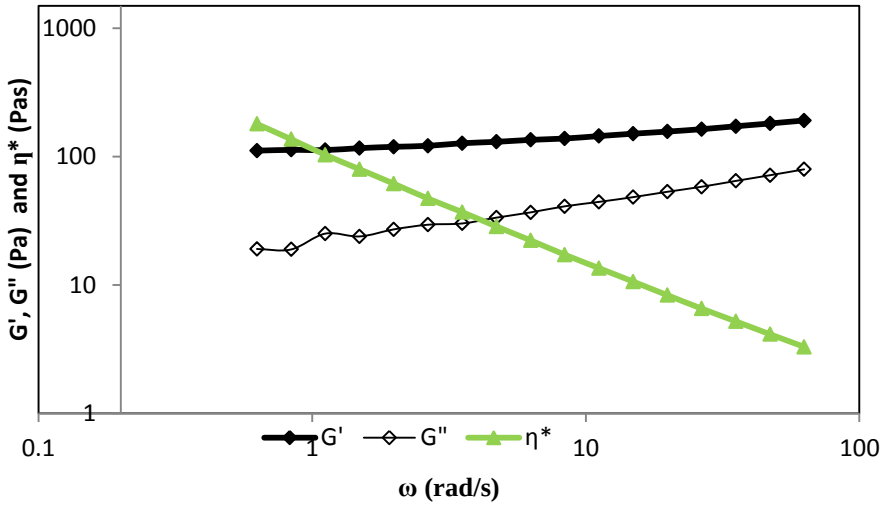

A

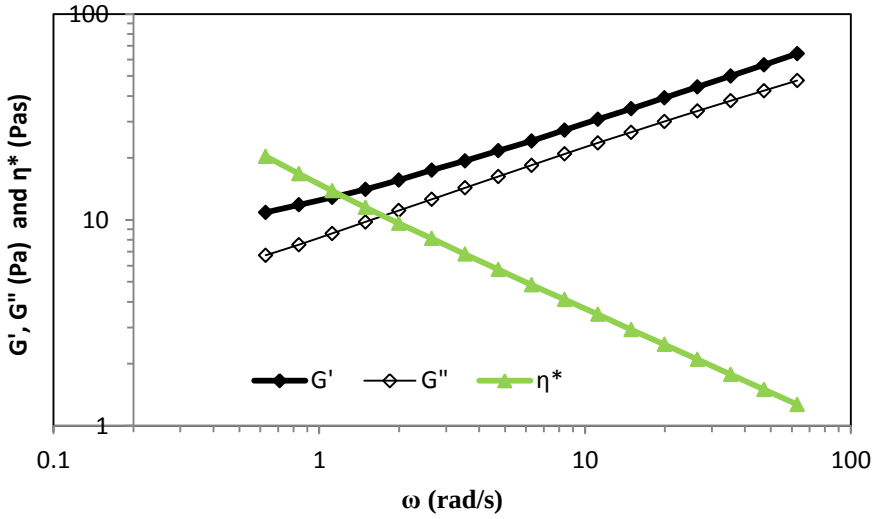

B

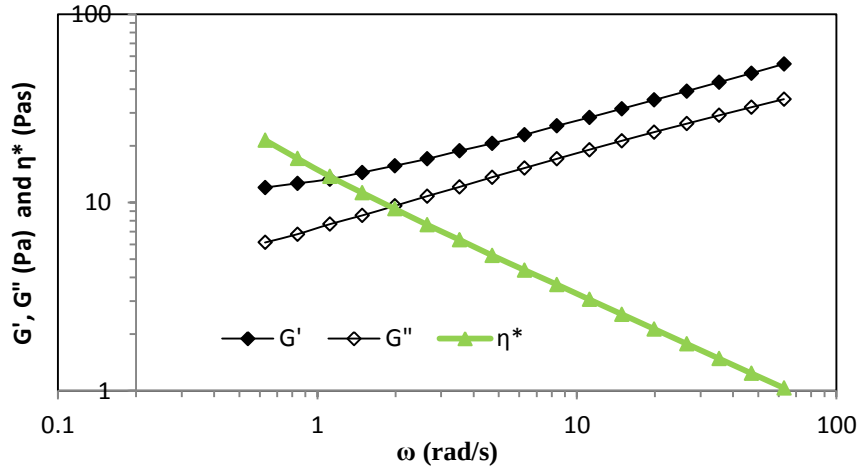

C

Figure 4.89 **Frequency sweep of optimum emulsion formulated with (A) 0 (B) 0.5 (C) 2% (w/w) vinegar**

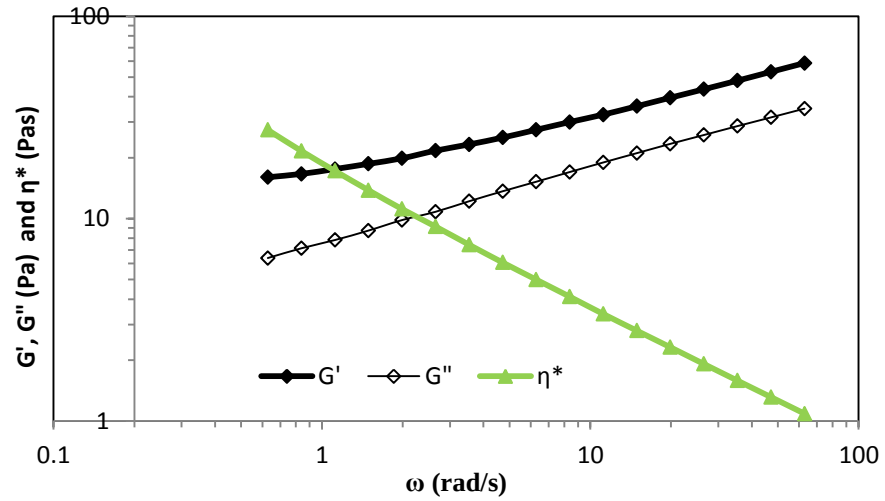

D

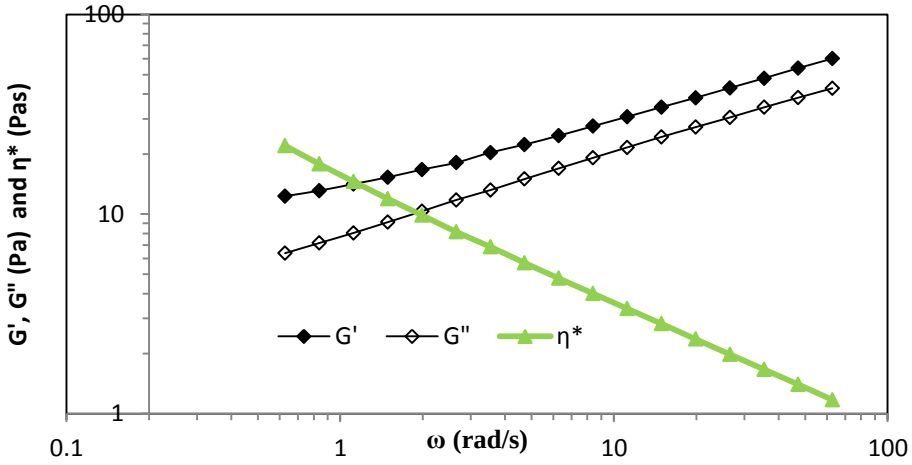

E

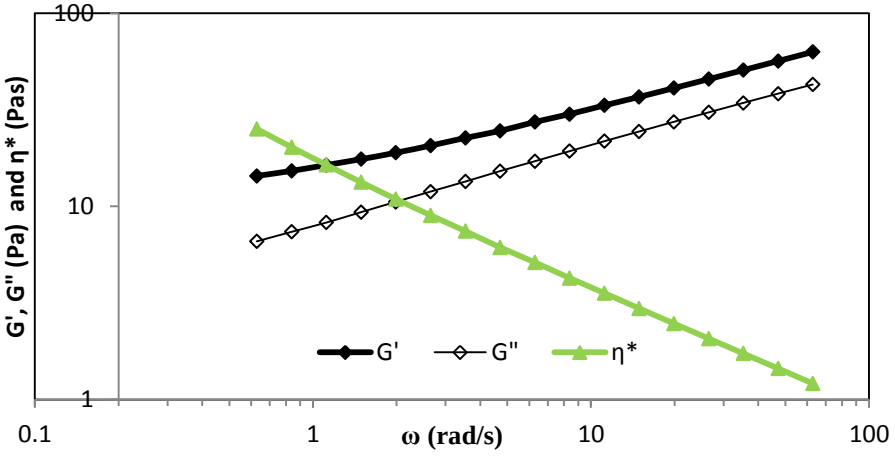

F

Figure 4.90 **Frequency sweep of optimum emulsion formulated with (D) 4 (E) 6 (F) 8% (w/w) vinegar**

characteristics (G") at the considered frequency range for all the emulsions suggested that all the studied emulsions were weak gels. The η* of all the emulsions was observed to rise increasingly towards an infinitely high value. These observations are also typical of gel structures. The emulsions possessed high G' values at the low frequencies. This indicated high structural strength of the emulsions without and with vinegar. These emulsions therefore exhibited the tendencies to be rigid, possessed high flow resistance and therefore had good stability during storage.

Figure 4.91 shows the effect of vinegar on the G' and G'' of the optimum emulsion. The effect of vinegar was noticeable on the material functions when compared with emulsion without vinegar. Both G' and G'' were observed to decrease in the presence of vinegar. Decreased G' and G" was due to decreased structural interactions in the emulsions. The observed decrease in material function in the presence of vinegar was a result of weakening of BGNF matrix by vinegar. The vinegar reduced the BGNF matrix strength necessary for emulsion formation relative to emulsion without vinegar. However, the G' and G" curves of emulsions whose BGNF matrix contained 0.5, 2, 4, 6 and 8% (w/w) vinegar did not show a clear distinction. There were overlaps among emulsions with vinegar at the frequency range considered. Table 4.51 shows the G' and G'' obtained for the emulsions with and without vinegar at low frequency of 0.628 rad/s. The means of G' and G'' ranged from 12.30 to 111 Pa and 6.37 to 19.1 Pa, respectively.

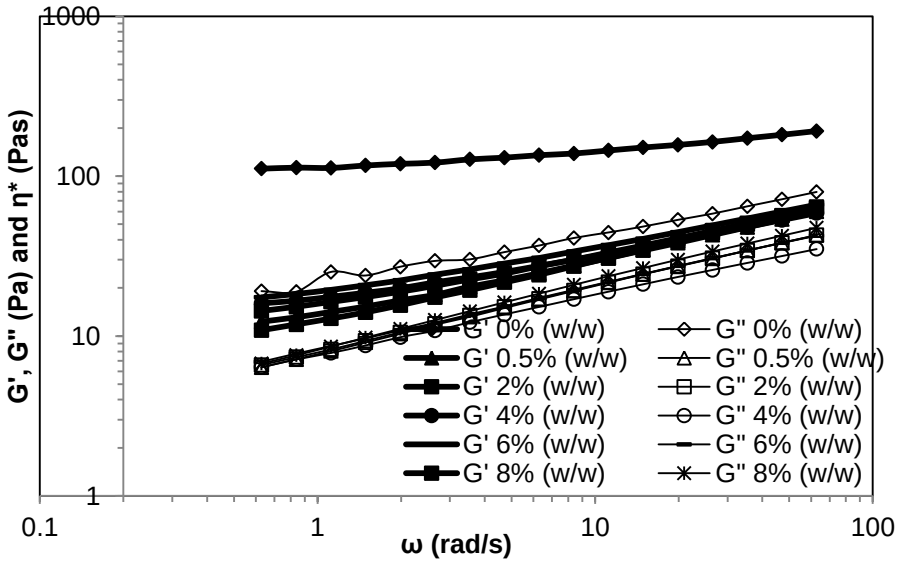

Figure 4.91 Storage (G') and loss moduli as a function of angular frequency during dynamic oscillatory tests of sunflower oil-in-water emulsion containing various concentrations of vinegar

The G' and G" of emulsions with and without vinegar were significantly ($p < 0.05$) different while the G' of emulsions formulated with 2, 4, and 6% (w/w) were not significantly different from each other ($p > 0.05$). The G' of emulsions containing 0.5% (w/w) and 8% (w/w) vinegar were not significantly different ($p > 0.05$). The viscous properties of all the emulsions with vinegar were not significantly different ($p > 0.05$).

Table 4.51 Effect of vinegar concentration on the storage and loss moduli at 0.628 rad/s

Vinegar Concentration (% w/w)	Storage modulus (G') Pa	Loss modulus (G") Pa
0	111 ± 2.70^{c}	19.1 ± 1.38^{b}
0.5	12.3 ± 0.47^{a}	6.37 ± 0.20^{a}
2.0	14.4 ± 0.28^{b}	6.59 ± 0.18^{a}
4.0	16.0 ± 0.80^{b}	6.39 ± 0.72^{a}
6.0	17.5 ± 0.82^{b}	6.90 ± 0.98^{a}
8.0	10.9 ± 1.80^{a}	6.73 ± 0.23^{a}

[1]Values are means ± standard deviations; Mean values with different letters within the same column are significantly different from each other ($p < 0.05$).
[2] G' equals the storage modulus; G" is the loss modulus

4.7.2.7 Effect of vinegar on emulsion rheology of optimum emulsion with regard to compliance and recoverable strain

Figure 4.92 shows the plot of compliance (J) against time (s) for emulsions with and without vinegar. A load of 0.5 Pa was imposed on the structure of all the emulsions in the first part of the experiment for 500 s while the second part involved sudden removal of the load and compliance was monitored for the next 500 s. Both of the emulsions with and without vinegar showed similar viscoelastic characteristics during creep and recovery phases. As an example, J steadily increased when a stress of 0.5 Pa was imposed on all the emulsions during the creep stage and the elastic component of the deformation recovered instantaneously when the load was removed (Figure 4.92). The emulsion without vinegar recorded the lowest J while emulsion with vinegar showed very similar and overlapping creep and recovery graphs. The presence of vinegar in the emulsion drastically increased J. The higher J showed by emulsions with vinegar relative to emulsion without vinegar indicated a negligible instantaneous elastic compliance. This implied that the network of the emulsion structures with vinegar were weaker and less rigid when compared with emulsion without vinegar. Emulsions with lower J possessed stronger structural interactions (high rigidity) hence gave small deformation when the stress was imposed on them. All concentrations of vinegar tested had very similar influence on the J.

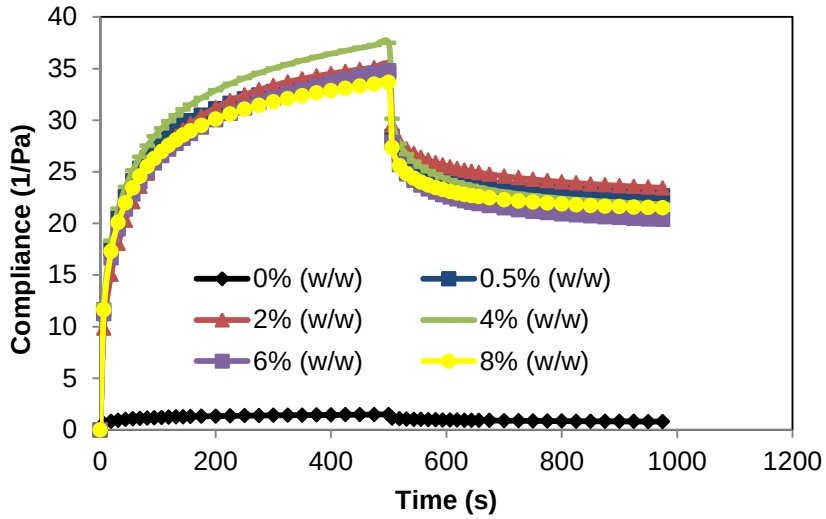

Figure 4.92 Creep and recovery curves of emulsions containing various concentrations of vinegar

Table 4.52 shows the effect of vinegar on the recoverable strain, Q (t)% of the emulsion. Q (t)% indicated how much percentage of the structure was able to recover when the load was withdrawn from the emulsions and hence it was a measure of the elasticity of the emulsion. Increased Q (t)% can therefore be linked to increased elasticity of emulsions.

Table 4.52 Effect of vinegar concentration on the recoverable strain[1,2]

Vinegar concentration (% (w/w))	Recoverable strain Q (t)%
0	46.2 ± 1.49[c]
0.5	34.5 ± 0.83[a]
2.0	33.5 ± 1.34[a]
4.0	41.7 ± 1.64[b]
6.0	41.4 ± 0.77[b]
8.0	39.3 ± 1.30[b]

[1] Values are means ± standard deviations; Mean values with different letters within the same column are significantly different from each other ($p < 0.05$).
[2] Q (t)% equals the recoverable strain

The mean of Q (t)% ranged between 33.5 to 46.2% for all the emulsions. Emulsion without vinegar was significantly ($p < 0.05$) different from emulsions formulated with vinegar. Although there was a significant ($p < 0.05$) difference between the emulsions with 0.5 and

2% (w/w) and emulsions with 4, 6 and 8% (w/w) there was no clearly observable difference in their creep and recovery graphs.

4.7.2.8 Summary on the effect of vinegar on emulsion stability and rheology of optimum emulsion

From the results of oil droplet size distribution, emulsion microstructure and initial backscattering flux, the effect of the vinegar on the BGNF matrix strength can be evaluated. The results showed that comparable strength was possessed by BGNF matrix at all studied vinegar concentrations and this had affected their emulsion forming ability similarly. Related structures of emulsions containing vinegar had influenced the particle aggregation and hence destabilization in a comparable similar and complicated manner. All emulsions containing vinegar possessed very large oil-droplets compared to emulsion whose BGNF matrix did not contain vinegar. Vinegar had therefore caused changes in the properties of the BGNF polymer network during continuous phase preparations. The observation of relative weakening of BGNF by vinegar concentration was confirmed by rheological results. There were observed significant decrease in the emulsion apparent viscosity and viscoelasticity with the presence of vinegar in the BGNF matrix. This is an indication of both weakness in BGNF polymer network and oil droplet interactions. The behaviour of all emulsions containing vinegar as determined by many rheological methods could not be resolved, indicating very comparable structures.

4.7.3 Effect of citric acid on emulsion stability and rheological properties

4.7.3.1 Effect of citric acid on emulsion stability with regard to particle size distribution

Figure 4.93 present the oil-droplet size distribution of optimum BGNF emulsion (7% (w/w) BGNF and 40% (w/w) SFO) as affected by various concentrations of citric acid. Citric acid had a notable effect on the oil droplet size distibutions of the emulsions. Franco *et al.* (2000) also reported observable effect of pH and previous protein thermal treatments on the droplet size distribution of pea protein stabilized oil-in-water emulsion. Although they all have closely comparable height, the oil droplet distribution curve widths of BGNF emulsions with citric acid shifted a bit to the right when compared with the BGNF emulsion without citric acid. All the curves of emulsions containing citric acid, irrespective of concentration were closely related. The presence of citric acid in the BGNF emulsions increased the oil-droplet size relative to the emulsion without citric acid. Table 4.53 compares the droplet size of the emulsions in terms of volume surface mean diameter ($d_{3,2}$) and equivalent volume-mean

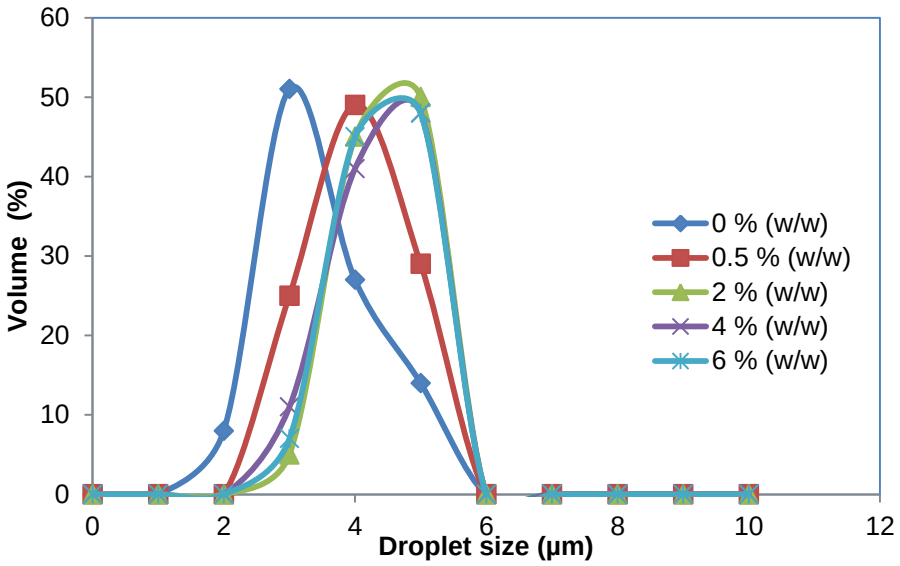

Figure 4.93 Particle size distribution of emulsions whose BGNF matrix contained various concentrations of citric acid

diameter ($d_{4,3}$). Both the $d_{3,2}$ and $d_{4,3}$ of the emulsions depended on the concentrations of citric acid. The $d_{3,2}$ and $d_{4,3}$ ranged between 3.55 – 4.19 µm and 3.66 – 4.23 µm, respectively. The oil droplet sizes of emulsion without citric acid was significantly different from emulsions with citric acid

Table 4.53 Effect of citric acid concentration on the particle size [1, 2]

Citric acid concentration (% (w/w))	$d_{3,2}$ (µm)	$d_{4,3}$ (µm)
0	3.45 ± 0.10^{a}	3.66 ± 0.11^{a}
0.5	3.85 ± 0.98^{b}	3.94 ± 0.59^{b}
2.0	4.03 ± 0.84^{bc}	4.06 ± 0.56^{bc}
4.0	4.02 ± 0.42^{bc}	4.06 ± 0.42^{bc}
6.0	4.19 ± 0.28^{c}	4.23 ± 0.14^{c}

[1]Values are means ± standard deviations; Mean values with different letters within the same column are significantly different from each other ($p < 0.05$).
[2]$d_{3,2}$ refers to the volume surface mean diameter of the emulsions; $d_{4,3}$ is the equivalent volume-mean diameter of the emulsions.

The smallest and largest $d_{3,2}$ and $d_{4,3}$ were found in emulsions without citric acid and 6% (w/w) respectively. Citric acid is an acidulant and has been reported as an agent for adjusting the pH of various systems including emulsions (Solowiej, 2007; Miquelim *et al.,*

2010; Taherian *et al.,* 2007). Contrary to the observations above, Franco *et al.* (2000) reported significant decrease in oil-droplet size with increase in pH up to emulsion pH close to protein isoelectric point for pea protein stabilized emulsion. Chanamai and McClements (2002) also reported that the droplet sizes of gum Arabic and modified starch stabilized emulsions were insensitive to acid within pH range of 3 - 9. The difference in our results with other researchers on the influence of pH on particle size may probably be connected to the method used for the incorporation of citric acid into the emulsion system and some physicochemical properties of BGNF. Like other organic acids, citric acid might have hydrolysed and changed the molecular conformation of the BGNF (Majzoobi and Beparva, 2014) during continuous phase preparation and this could have decreased the matrix strength necessary for emulsion formation.

4.7.3.2 Effect of citric acid on emulsion stability with regard to microstructure

Figure 4.94 presents the photomicrographs of freshly prepared emulsions formed with BGNF matrix containing various concentrations of citric acid.

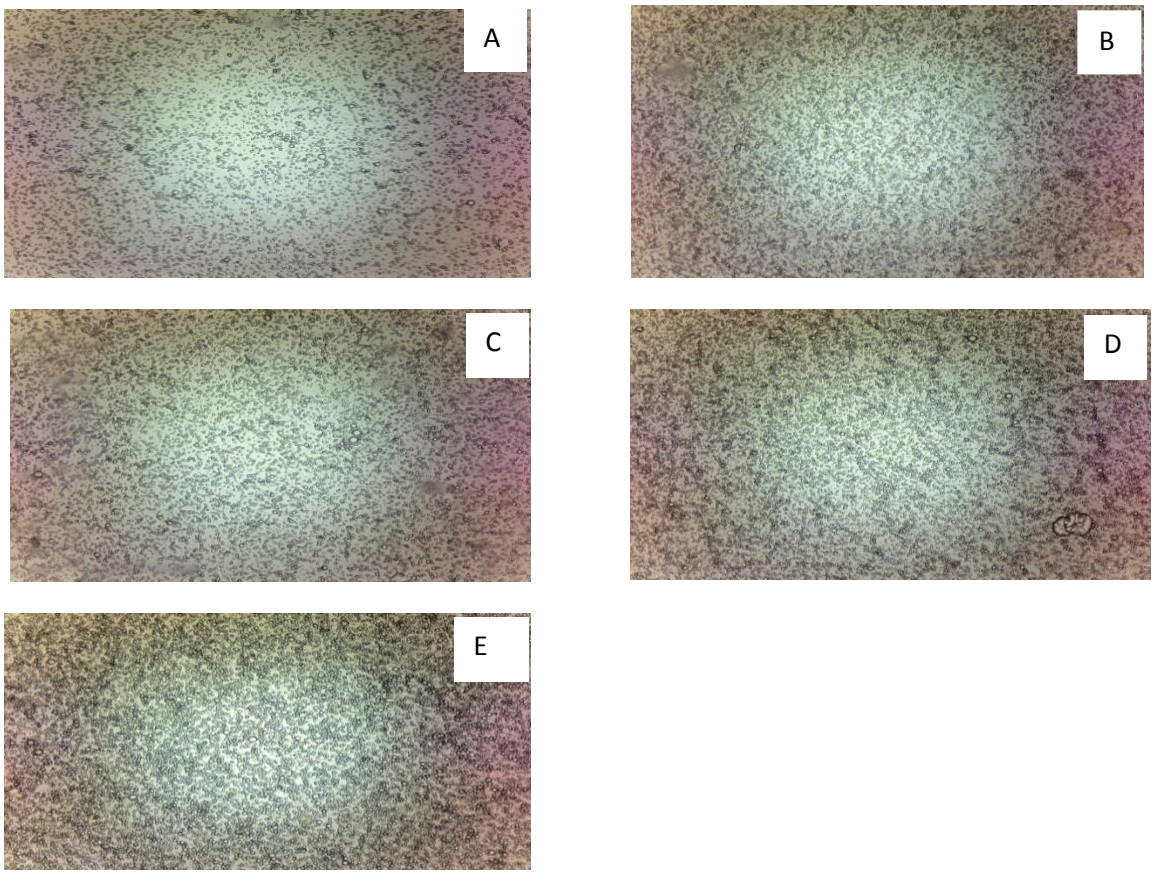

Figure 4.94 **Photo micrographs of emulsions formulated with 7% (w/w) BGNF and 40% (w/w) SFO containing citric acid at concentrations of (A) 0%(w/w) (B) 0.5% (w/w) (C) 2% (w/w) (D) 4% (w/w) (E) 6% (w/w)**

The figure compares the emulsion forming characterstics of BGNF matrix containing various concentrations of citric acid as well as also the influnce of citric acid on the matrix-droplet and droplet-droplet interactions. The oil-droplet sizes of the emulsion with citric acid however showed some similarities and differences which could therefore be indicative of levels of the changes caused by citric acid concentrations in the molecular structure of BGNF. Figure 4.94 shows that all the emulsions were made up of evenly dispersed small spherical oil droplets surrounded by continuous phase BGNF matrix, irrespective of the concentrations of citric acid. The presence of citric acid at all concentrations in the BGNF dispersion during continuous phase gelatinization did not seem to greatly affect the emulsion forming properties of the resulting BGNF matrix. When compared with the BGNF matrix without citric acid, matrix with citric acid had comparable emulsion forming ability. As can be seen in the figure, there was no serious flocculation of the oil-droplets and this phenomenon of oil-droplet aggreagtions were not different in both the emulsion with and without citric acid.

4.7.3.3 Effect of citric acid on emulsion storage stability

Figures 4.95 and 4.96 present the stability of BGNF emulsions with citric acid at various concentrations (0 – 6% (w/w)). The graphs are the normal and reference modes of Turbisacn profiles of emulsions scanned at a regular interval of 30 minutes for 360 minutes at 20^{o}C. The reference modes of the Turbiscan graphs were placed right of the normal modes in Figure 4.95 and 4.96 and were constructed relative to the initial or the first scan. The initial scans of all the emulsions were assigned a value of 0% when constructing the reference mode and can be visualized at the ordinate of the normal turbiscan mode. The initial bacscattering flux (BS_{AVo} (%)) provided the information regarding the structure of the freshly prapared emulsions and it is dependent on the oil droplet numbers. The more numerous the oil droplets in an emulsion the greater the backscattered light and hence the higher the backscattering flux. Since all the emulsions contained fixed amounts of SFO and BGNF, the information regarding the effect of various concentrations of citric acid in the BGNF matrix on their respective emulsion forming ability can be obtained from BS_{AVo} (%).

Table 4.54 presents BS_{AVo} (%) of the emulsions formed by BGNF matrix containing citric acid in the range of 0 – 6% (w/w). The mean of BS_{AVo} (%) was between 95.2 and 90.1 with the highest and lowest values belonging to emulsion without citric acid and emulsion whose BGNF matrix contained 6% (w/w) citric acid respectively. All the emulsions with citric acid showed closely related BS_{AVo} (%) which is an indication that the presence of citric acid at all studied concentrations in the BGNF matrix affected the emulsion forming abilities in a similar way. Although the result indicated a significant difference between the emulsion without citric acid and emulsions containing citric acid, there seemed not to be much observable difference in their photomicrographs. The presence of citric acid in the

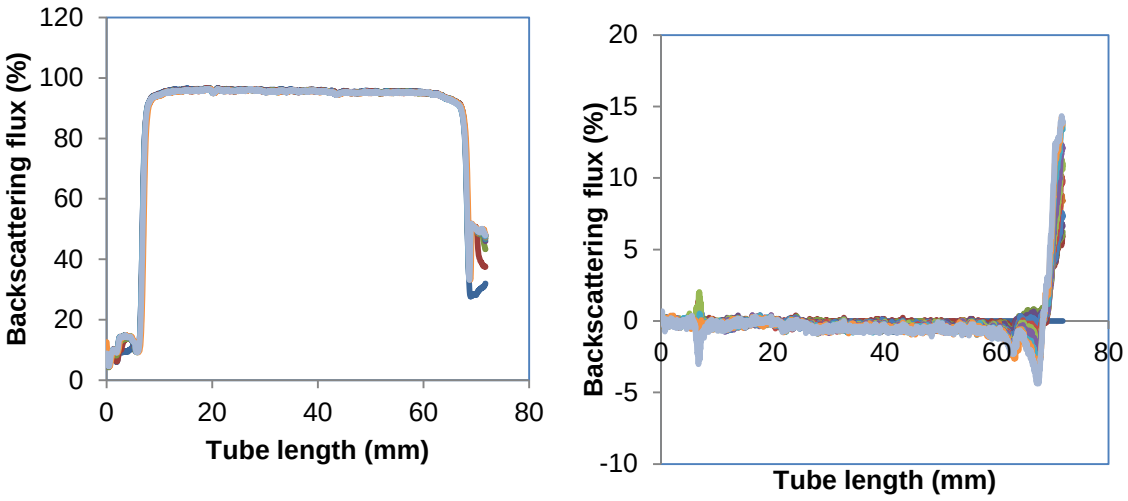

A

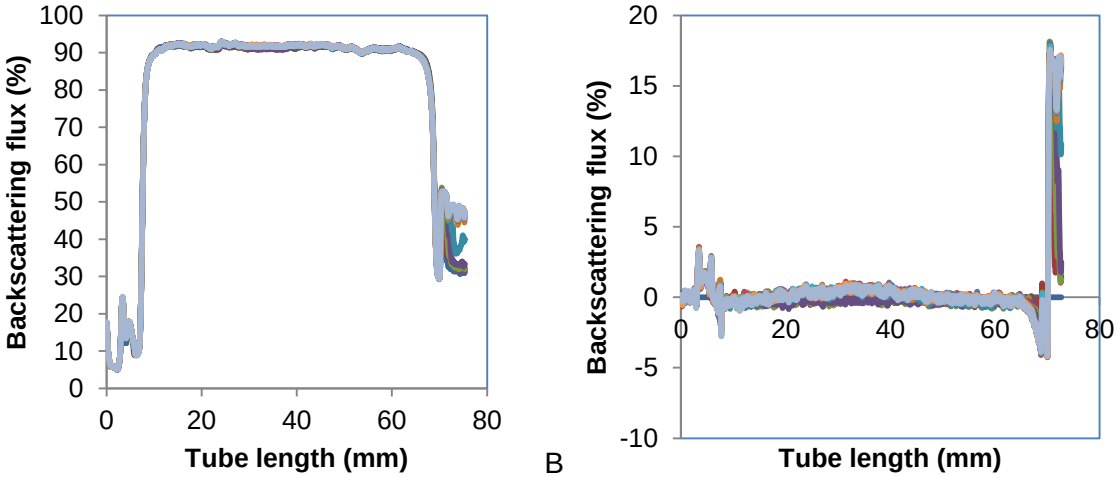

B

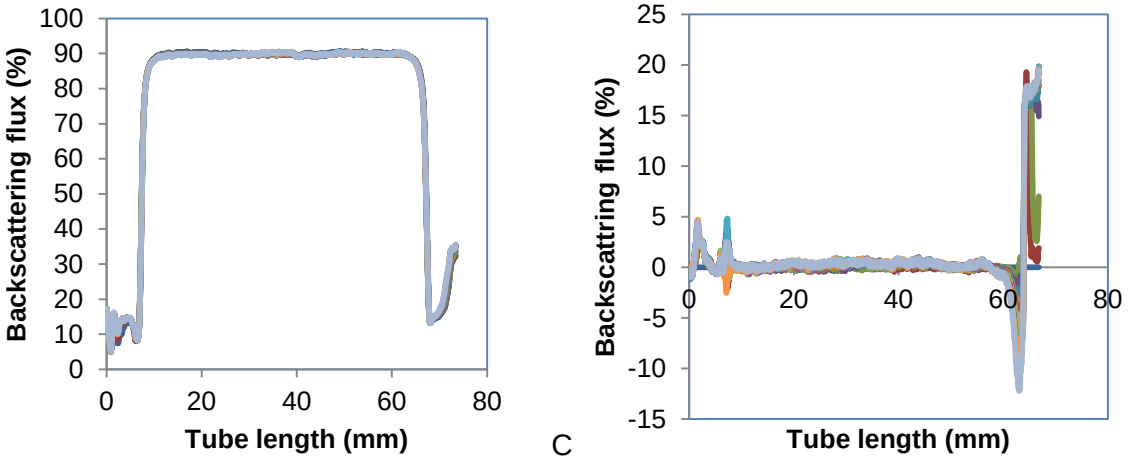

C

Figure 4.95 **Changes in the backscattering profile (BS%) as a function of sample height with storage time of BGNF (7% (w/w) stabilized emulsions containing citric acid at (A) 0% (w/w) (B 0.5% (w/w) (C) 2% (w/w)**

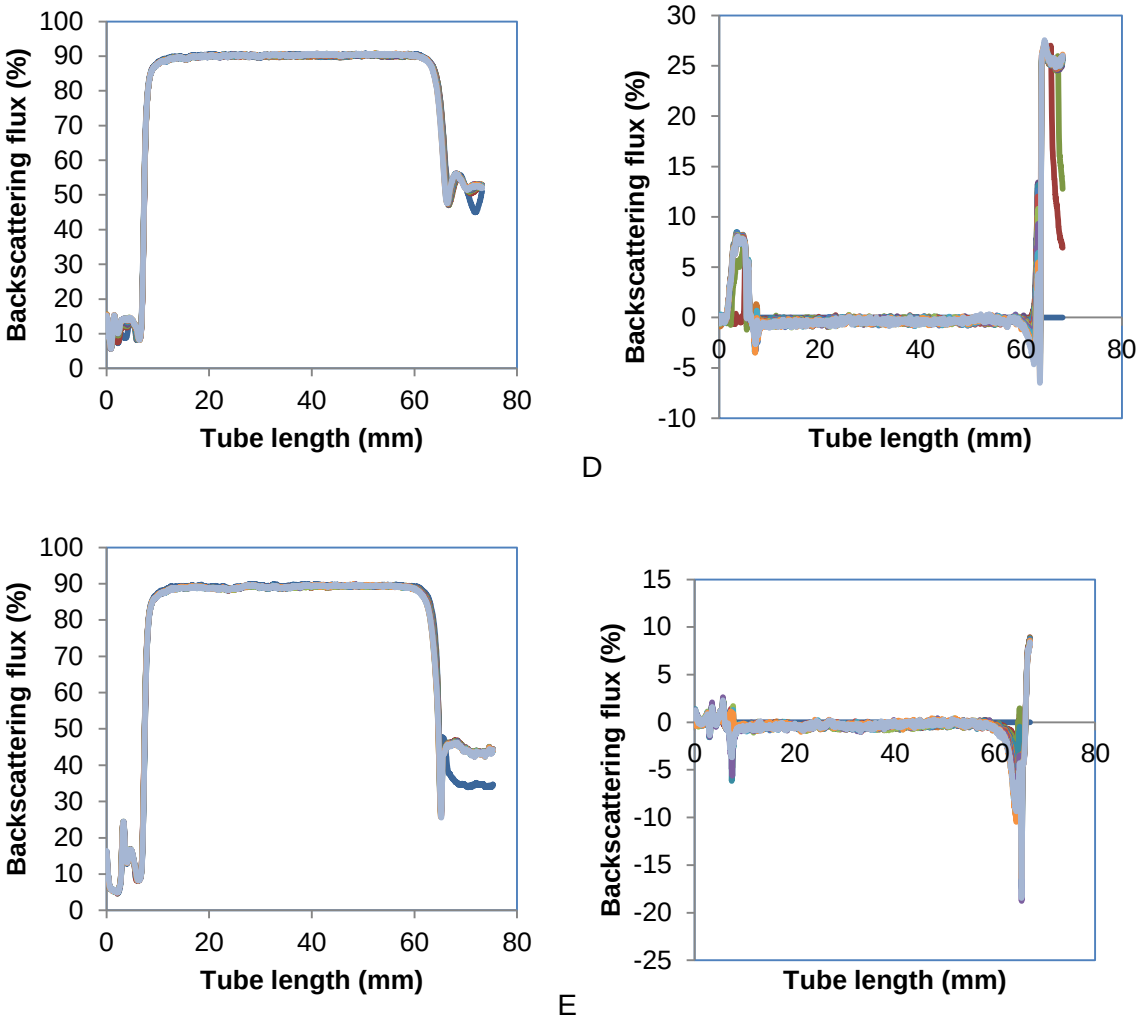

Figure 4.96 **Changes in the backscattering profile (BS%) as a function of sample height with storage time of BGNF (7% (w/w) stabilized emulsions containing citric acid at (D) 4% (w/w) (E) 6% (w/w)**

Table 4.54 **Effect of citric acid concentration on Initial backscattering value[1]**

Citric acid concentration (% (w/w))	Initial backscattering flux (%)
0	95.2 ± 0.01^{a}
0.5	90.9 ± 1.19^{b}
2.0	90.8 ± 0.69^{bc}
4.0	90.2 ± 0.11^{bc}
6.0	90.1 ± 0.07^{c}

[1]Values are means ± standard deviations; Mean values with different letters within the same column are significantly different from each other ($p < 0.05$)

BGNF dispersions during gelatinization caused little impediment to polymer network formation even at high concentration of 6% (w/w) and has consequently affected the matrix strength mildly.

The result of the Turbiscan reference mode showed the various destabilization mechanisms which characterized emulsions with and without citric acid. There were no observable differences between the graphs of emulsion with and without citric acid. There were peaks between 0 - 10 mm region and notable increases and decreases in the backscattering flux (%) along the entire tube length of all the turbiscan profiles which was indicative of possible creaming and particle aggregation phenomenon, respectively. Particle aggregation phenomenon showed as decrease and increase in backscattering flux depending on the oil droplet sizes in an emulsion system. Decrease in the backscattering flux was as a result of an increase in the oil-droplet size which correspondingly caused the mean path of photon (l*) to increase because of an increase in the average distance between the oil-droplets (Celia *et al.,* 2009). This relationship between the backscattering flux and the oil-droplet size variation is presented in equation 3.5 and 3.6 according to Mie theory.

However, if the oil-droplet size is smaller than the wavelength of the light source and is increasing by flocculation or coalescence, then the backscattering flux can identify an increase and this is called Raleigh diffusion (Park *et al.,* 2010). Therefore, the more the oil-droplets sizes increased the higher the backscattering flux in the Raleigh diffusion zone (Park *et al.,* 2010). No substantial information was obtained for creaming phenomenon as the migration rates obtained for all the emulsions were zeros. This is an indication that the droplet movement was very minimal within the time frame of study. In addition, no physical separation was observed with the naked eye. Figure 4.97 showed the oil-droplet aggregation kinetics obtained in the middle of the Turbiscan tube (zone 20 - 40 mm) and was reported in the Turbiscan MA 2000 reference mode. It was expected that the graphs in Figure 4.97 should fall below the zero line if the subsequently scanned profiles decreased with time of scanning relative to the first scan (Mie diffusion zone). However, some of the graphs were higher than the zero line which is an indication that successive scans increased relative to the first scan (Raleigh diffusion zone). The graphs compared the influence of citric acid at various concentrations on the oil droplet aggregation phenomenon. The farther the graphs from the origin, the less stable the emulsion. Figure 4.97 showed that citric acid concentrations had different effects on the droplet aggregation kinetics. No meaningful conclusion can however be drawn on the trend of increase or decrease with citric acid concentrations. The oil-droplet aggregation kinetics was marked with high standard deviations which did not allow any valid conclusions within the time frame of study.

The destabilization velocity of oil-in-water emulsion was strongly dependent on the droplet size and concentration (Perrechil and Cunha, 2010). The unresolved stability

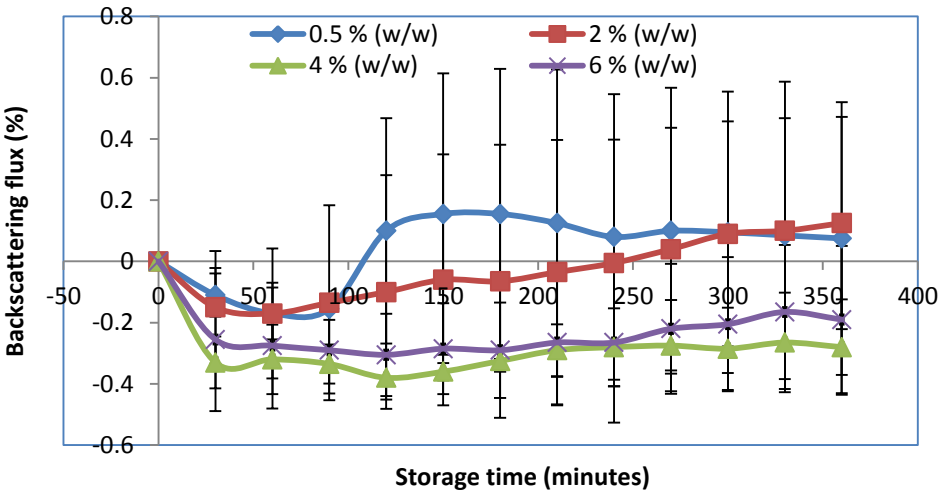

Figure 4.97 Effect of citric acid on backscattering in the 20-40 mm zone at 20°C

behaviour of all the emulsions containing citric acid may be as a result of the similar manner it has affected the microstructure of the emulsion. The results of the oil-droplet distribution, image analysis and initial backscattering flux showed that citric acid had produced similar characteristics at all concentrations.

The equilibrium backscattering flux is detailed in Figure 4.98 and it provides information regarding the influence of citric acid on the emulsion stability at the equilibrium time.

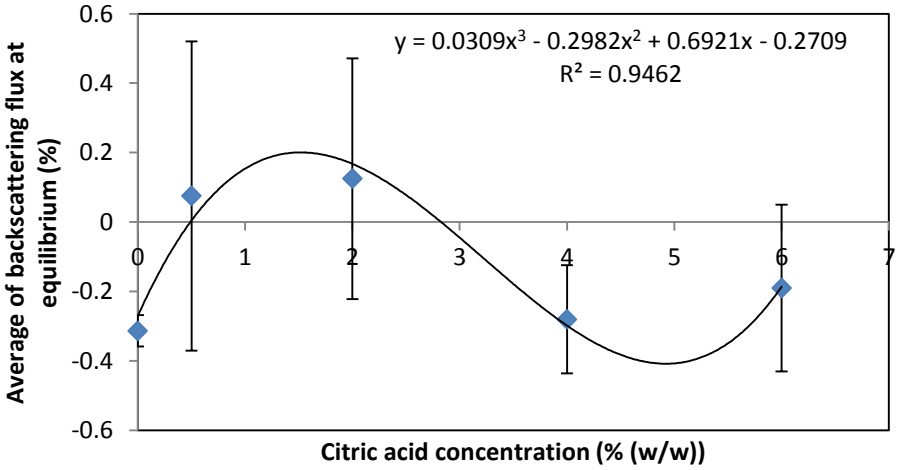

Figure 4.98 Effect of citric acid on emulsion stability (Average backscattering flux at equilibrium state)

The graph was generated by plotting the backscattering flux attained at the equilibrium studied time (360th minute) against the citric acid concentrations. It was expected that a stable formulation will be very close to the origin at the 360th minute. A third order polynomial was found to describe the effect of citric acid concentrations on emulsion stability with high coefficient of determination.

Although the graph was marked with high standard deviations, the mean of the backscattering flux at the 360th minute showed that emulsion containing 0.5% (w/w) citric acid was marginally better.

4.7.3.4 Effect of citric acid on emulsion rheology with regard to flow curves and hysteresis loop area

The flow curves of the emulsions were superimposed in order to identify similarities and differences in their behaviours. The forward and backward shear rate sweeps are presented in Figure 4.99. All the emulsions showed some similarities in behaviour. For example, the shear stress increased with increased shear rates and that all of the emulsions possessed hysteresis loop area. The presence of hysteresis loop area was an indication of shearing effect on the molecular structure of the emulsions such that the apparent viscosity has decreased (Habibi-Najafi and Alaei, 2006). Although there was little difference in the flow properties of the emulsions with and without citric acid, the flow curves of emulsions with citric acid overlapped.

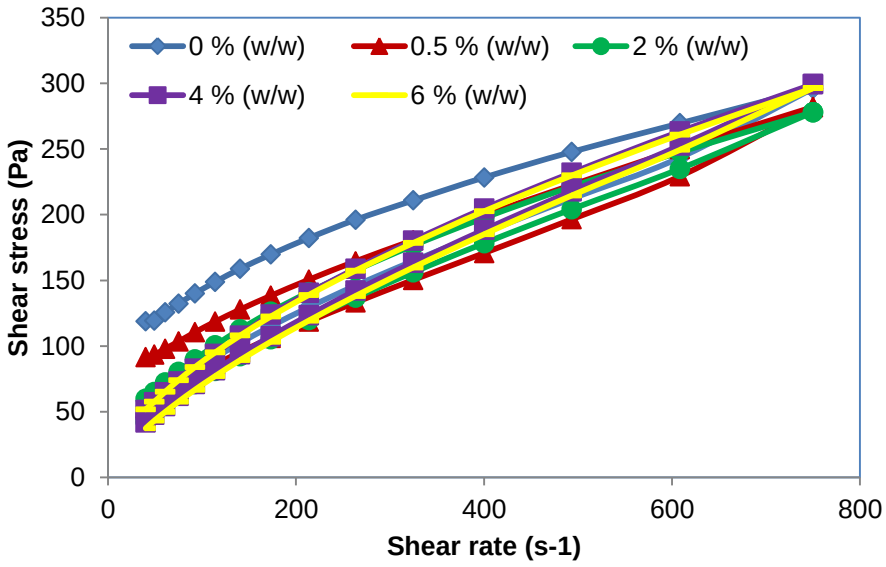

Figure 4.99 Effect of citric acid on the rheological behavior of optimum emulsion

The overlap in flow curves showed closely related rheological behaviours among emulsions with citric acid. The relative difference in the flow properties between the emulsions with and without citric acid was as a result of the influence of citric acid on the properties of the BGNF matrix. The present observation has influenced both the BGNF matrix-oil droplet and oil droplet-oil droplet interactions. The closed loop sweep area of the emulsion without citric acid was the highest among the studied formulations.

Figure 4.100 is the comparison of the apparent viscosities of the forward sweep when the structures have not been destroyed.

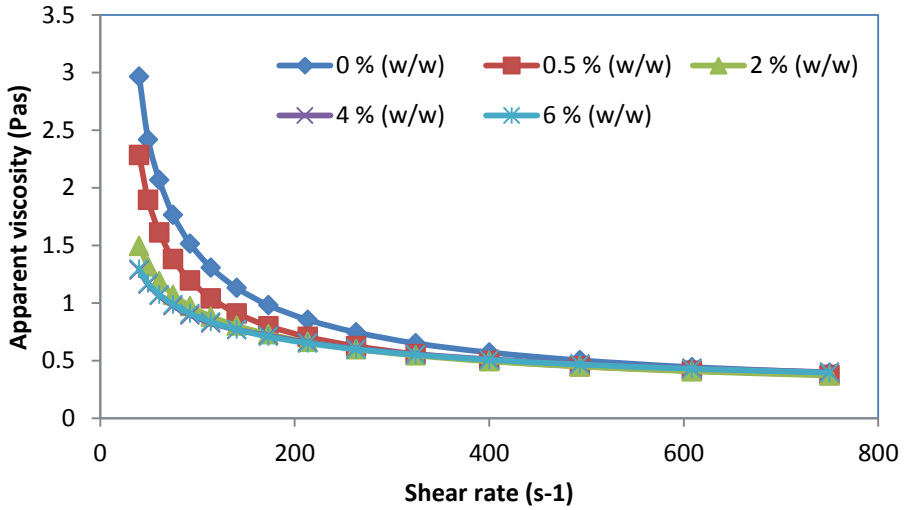

Figure 4.100 Effect of citric acid on the apparent viscosity of the optimum emulsion.

The figure showed that citric acid had observable different effects on the apparent viscosities of the emulsions compared to emulsion without citric acid. There were some identical characteristics among all of the emulsions. The apparent viscosities decreased with shear rate and this was a characteristic behavior of shear thinning fluids. Overlaps were observed in the flow curves of the emulsions at higher shear rates while differences were seen at lower shear rates. Therefore, there was a high tendency that all the emulsions behaved in similar manners at high shear rate operations such as during pumping. High similarity in the apparent viscosities was an indication of closely related structures which were formed by the BGNF matrix with and without citric acid. It appeared that the presence of in the BGNF dispersions during gelatinization did not alter significantly the polymer strength necessary for emulsion formation. Hence, the emulsions formed by BGNF matrix with and without citric

acid have comparable matrix-oil droplet and oil droplet-oil droplet interactions and therefore remained flocculated.

In order to gain more insights into the structural similarities and differences, single point viscosity comparison was made at the maximum point of shear gradient (750 s^{-1}). The maximum point of shear gradient is the point at which the upward and downward curves have common properties and share the same viscosity in Figure 4.99. Table 4.55 presents the effect of citric acid on the apparent viscosity at the maximum point of shear gradient. Citric acid concentrations had observable effects on minimum apparent viscosities.

Table 4.55 Effect of citric acid on the minimum apparent viscosity of the optimum emulsion at 22°C[1, 2].

Citric acid concentration (% w/w)	Viscosity at 750 s^{-1} (Pas)[2]
0	0.39 ± 0.00[a]
0.5	0.37 ± 0.02[b]
2.0	0.37 ± 0.01[b]
4.0	0.39 ± 0.00[a]
6.0	0.39 ± 0.00[a]

[1] Values are means ± standard deviations; Different letters within the same column are significantly different from each other ($p < 0.05$)
[2]Values calculated at the maximum point of the shear gradient

Table 4.55 showed that there was significant ($p < 0.05$) difference in the minimum apparent viscosity of the emulsions. The result of minimum apparent viscosity had grouped the emulsions into two parts. Emulsions with 0.5 and 2% (w/w) citric acid did not differ significantly ($p > 0.05$) while emulsions whose BGNF matrix contained 0, 4 and 5% (w/w) behaved similarly.

Power law rheological model were used to characterize the forward and backward flow curves developed in Figure 4.99 (Kuş *et al.,* 2005). Table 4.56 presents the parameters of power law rheological model alongside the magnitude of hysteresis loop area. The high coefficient of determination was an indication that power law model was suitable to describe and predict changes in rheological properties. Citric acid of different concentrations has different effects on the power law parameters. The mean of consistent coefficient was in the range 5.55 - 30.05 and 2.85 - 5.90 Pas^n for the forward and backward curves respectively. The mean of flow behaviour index for the forward and backward curves was between 0.34 - 0.60 and 0.58 - 0.69 respectively. The range of the flow behaviour index for both the forward and backward curves (n and n^i< 1) suggested that the fluids were pseudoplastic in nature (Habibi-Najafi and Alaei, 2006). There were observed increase in consistency coefficient

Table 4.56 Effect of citric acid concentration on Power law parameters and magnitude of hysteresis loop area[1, 2]

Conc. citric (% w/w)	K (Pas^n)	n	R^2	K' (Pas^n)	n'	R^2	Hysteresis loop area (Pas^{-1})
0	44.87 ± 5.01[a]	0.28 ± 0.02[a]	0.99	7.60 ± 0.15[a]	0.55 ± 0.34[a]	0.99	771.50 ± 44.23[a]
0.5	19.93 ± 0.48[b]	0.38 ± 0.01[b]	0.99	5.61 ± 1.38[b]	0.59 ± 0.03[a]	0.99	508.1 ± 69.07[b]
2.0	8.76 ± 1.43[c]	0.54 ± 0.01[c]	0.99	5.54 ± 0.19[b]	0.60 ± 0.01[a]	0.99	227.77 ± 0.23[c]
4.0	5.62 ± 0.38[d]	0.59 ± 0.01[d]	0.99	3.60 ± 0.12[c]	0.66 ± 0.01[b]	0.99	200.22 ± 12.67[c]
6.0	5.55 ± 0.07[d]	0.60 ± 0.03[d]	0.99	2.85 ± 0.05[c]	0.69 ± 0.02[b]	0.99	241.42 ± 0.93[c]

[1] Value are means ± standard deviations; Mean values with different letters within the same column are significantly different from each other ($p < 0.05$).

[2] K refers to the consistency coefficient of the forward sweep; K' is the consistency coefficient of the backward sweep; n is the flow behaviour index of the forward sweep; n' is the flow behaviour index of the backward sweep; R^2 is the coefficient of determination between the experimental data and power law model prediction

with corresponding decrease in the flow behaviour index for all cases studied. Both the consistency coefficient and flow behaviour index for the forward and backward curves decreased and increased ($p < 0.5$) with increased citric acid concentration, respectively. Decrease in the consistency coefficient was connected to an overall decrease in both the BGNF matrix-oil droplet and oil droplet-oil droplet interactions as the concentration of citric acid increases. Emulsion with no citric acid was significantly ($p < 0.05$) different from emulsion without citric acid.

The consistency coefficients and the flow behaviour index of the forward curve were higher and lower than the backward curves, respectively at all the citric acid concentration. This observation implies that thixotropic structural destruction had occurred in the emulsions during the shear rate sweep. Furthermore, the difference in consistency coefficient of the forward and backward measurement showed that the emulsions were time dependent (Habibi-Najafi and Alaei, 2006). The magnitude of hysteresis loop area is detailed in Table 4.56. Magnitude of hysteresis loop area quantifies the thixotropy of a material (Razavi *et al.,* 2008; Steffe, 1996). The magnitude of hysteresis loop area ranged from 694 ± 64 to 200 ± 13 Pas^{-1} with the highest and lowest values belonging to emulsions without citric acid and 6% (w/w) citric acid, respectively. The magnitude of hysteresis loop area decreased significantly ($p < 0.05$) up till citric acid concentration of 2% (w/w) and remained significantly constant after. Decrease in the magnitude of the hysteresis loop area implies a decrease in index of energy necessary to remove the phenomenon of time in the flow behaviour of emulsions as citric acid concentrations increased. This property is directly related to the viscosity of the emulsion system which invariably depended on the structural interactions and BGNF matrix strength responsible for the emulsion formation. No significant difference existed in the emulsions containing 2, 4 and 6% (w/w) indicating a close similarity in both the oil droplets interactions and BGNF matrix strength responsible for structural formation.

4.7.3.5 Effect of citric acid on emulsion rheology with regard to steady shear decay

Constant shear rate of 50 s^{-1} was applied on the emulsions with and without citric acid in order to study the time dependent properties more closely since hysteresis loop method considers shear rate change and time at the same time. Figure 4.101 showed the effect of citric acid concentrations on the thixograms of the emulsions. The figure showed a decrease in emulsion viscosity with increase in shearing time. There were clear differences in the thixograms of emulsion with and without citric acid. Emulsion without citric acid showed greater dependence on time and recorded the highest changes in viscosity. Emulsions that were formulated with BGNF matrix containing citric acid had their thixograms below the emulsion without citric acid.

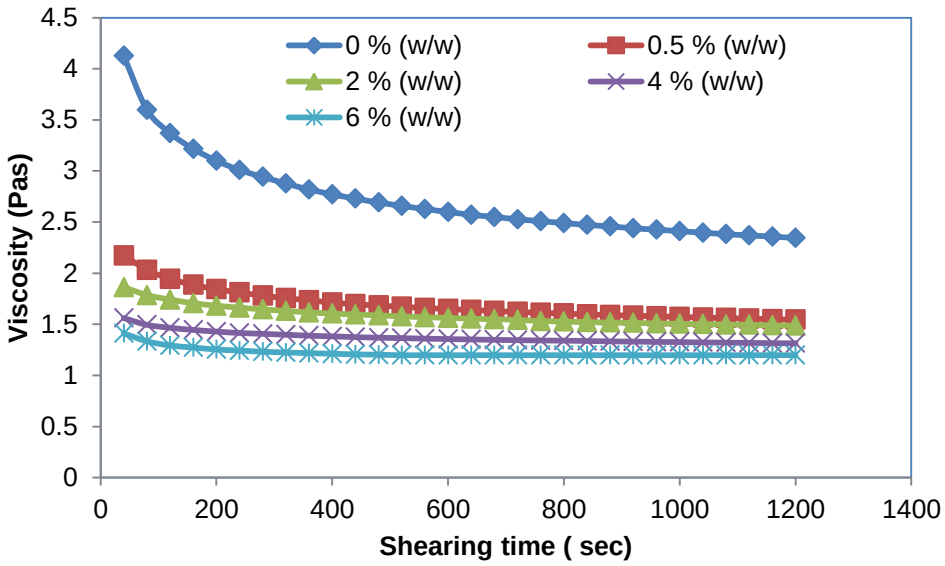

Figure 4.101 Effect of citric acid on time dependent characteristics of optimum emulsion at 50 s^{-1}

The initial viscosity on the viscosity–shearing time graph showed that citric acid had reduced the viscosity of the emulsions. This could probably be as a result of changes in BGNF molecular structure/conformation brought about by citric acid during gelatinization and or that citric acid had caused reduction in oil droplet interactions.

The time dependent characteristics observed in Figure 4.101 were quantified and described by Weltman model (Abu-Jdayil *et al.,* 2002). Table 4.57 presented the result of the parameters of Weltman model.

Table 4.57 Effect of citric acid on Weltman model parameters[1, 2]

Citric acid (% (w/w)	- B (Pa)	A (Pa)	R^2
0	24.2 ± 1.64^{a}	286 ± 13^{a}	0.96
0.5	8.54 ± 0.64^{b}	132 ± 11^{b}	0.99
2.0	4.89 ± 0.94^{c}	103 ± 14^{c}	0.99
4.0	2.86 ± 0.81^{d}	85.0 ± 7^{cd}	0.98
6.0	2.44 ± 0.25^{d}	76.0 ± 2^{d}	0.92

[1]Values are means ± standard deviations; Mean values with different letters within the same column are significantly different from each other ($p < 0.05$).
[2] A equals to the initial shear rate of Weltman model; B is the extent of structural break down of Weltman model; R^2 is the coefficient of determination between the experimental data and Weltman model prediction

The high coefficients of determination (0.92 - 0.99) showed that Weltman model was able to predict the thixotropic properties. Parameter B of Weltman model measured the extent of

thixotropy (Razavi and Karazhiyan, 2009) and ranged from 2.44 ± 0.25 to 24.2 ± 1.64 Pa, while A is the initial shear stress (Kuş *et al.,* 2005) and it ranged from 76.0 ± 2 to 286 ± 13 Pa. Both parameters A and B of Weltman model decreased significantly ($p < 0.05$) up to citric acid concentration of 0.5% (w/w) and there were no significant decrease afterwards. Emulsions containing 2, 4 and 6% (w/w) did not show any significant difference. The highest Weltman parameters A and B belonged to emulsion without citric acid. However, when emulsions with citric acid were compared, the emulsion system whose BGNF matrix contained 0.5% (w/w) recorded the highest of both Weltman parameter A and B. The high value recorded by emulsion without citric acid relative to emulsion with citric acid showed the high contributions of BGNF matrix to the thixotropic properties of BGNF stabilized emulsions. All the emulsions whose BGNF matrix contained citric acid had relatively weakened and probable hydrolyzed BGNF as a result of the presence of citric acid in the continuous phase. This had reduced overall viscosity of the emulsions and led to decreased Weltman parameter A and B.

4.7.3.6 Effect of citric acid on emulsion rheology with regard to viscoelastic properties (storage and loss moduli)

Figures 4.102 and 4.103 show the results of the frequency sweep obtained for optimum emulsion whose BGNF matrix was formulated with 0, 0.5, 2, 4, and 6% (w/w) citric acid respectively. The figure showed a log-log graphs of storage modulus, (G'), loss modulus, (G"), complex viscosity, (η^*) and frequency. Both G' and G" showed significant dependence on the frequency and were increased with increase in frequency for the emulsions with and without citric acid. However, the frequency dependence of the G' and G" of optimum emulsion was less when compared with emulsions with citric acid. In general, the spectrum of emulsions with and without citric acid showed solid-like behaviour at all the studied frequencies where G' dominated and was higher than the G'' curve and tended to show a constant limiting value. The G' curve was observed to be higher than the G" for all the emulsions at all the investigated frequency range. The predominance of the elastic characteristics (G') over viscous characteristics (G") at the considered frequency range for all the emulsions suggested that all the emulsions were weak gels. The η^* of all the emulsions was observed to rise increasingly towards an infinitely high value which is typical of gel structures. Emulsions possessed high G' values at the low frequency suggested high structural strengths of the emulsions without and with citric acid. Emulsions with and without citric acid therefore exhibited the tendencies to be rigid, possess high flow resistance and

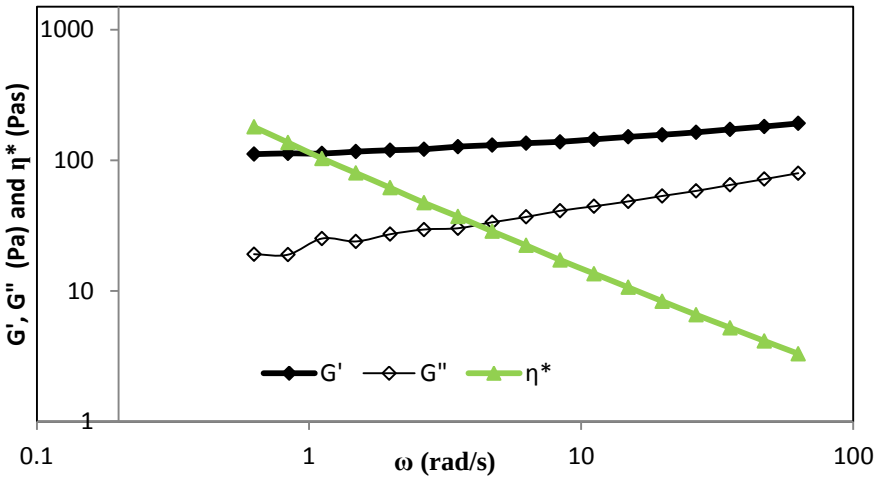

A

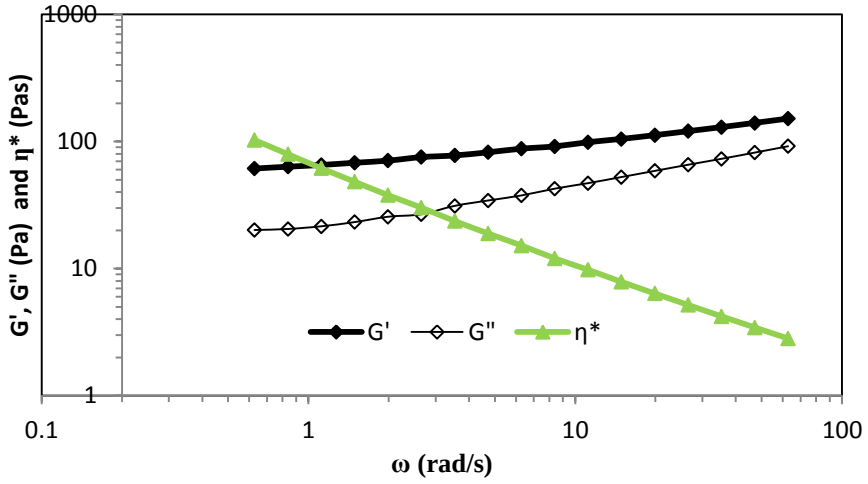

B

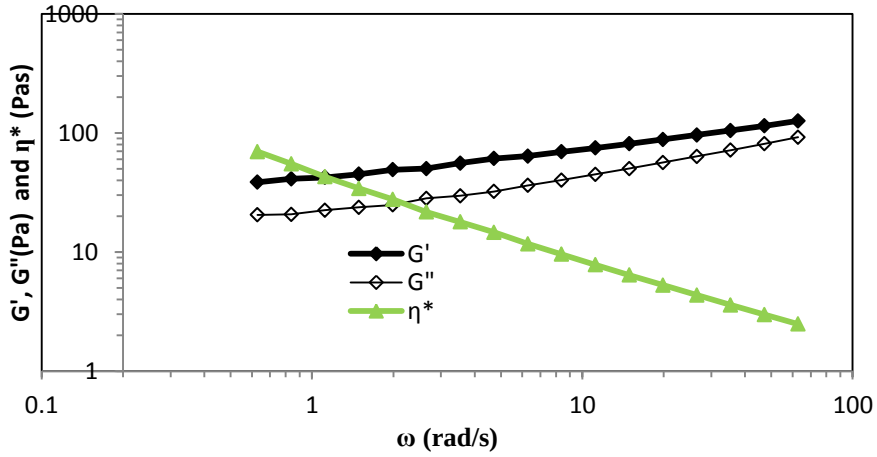

C

Figure 4.102 Frequency sweep of optimized emulsion formulated with (A) 0 (B) 0.5 (C) 2% (w/w) citric acid

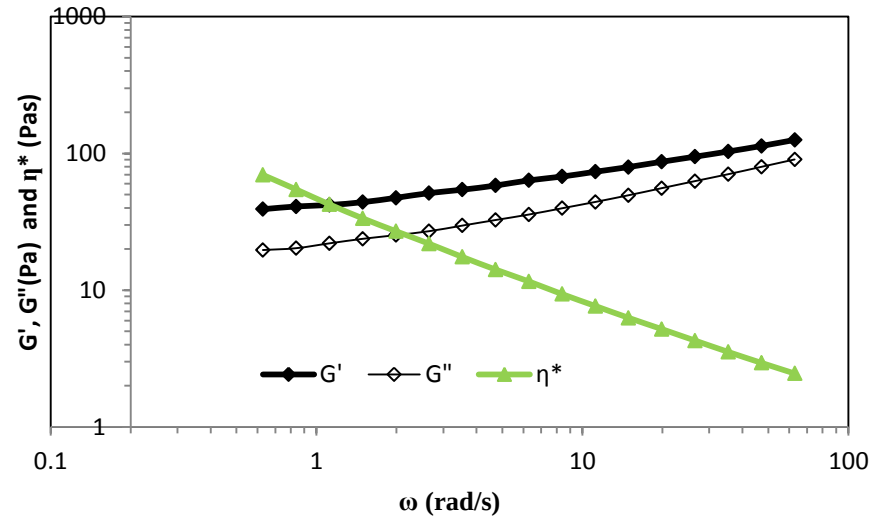

D

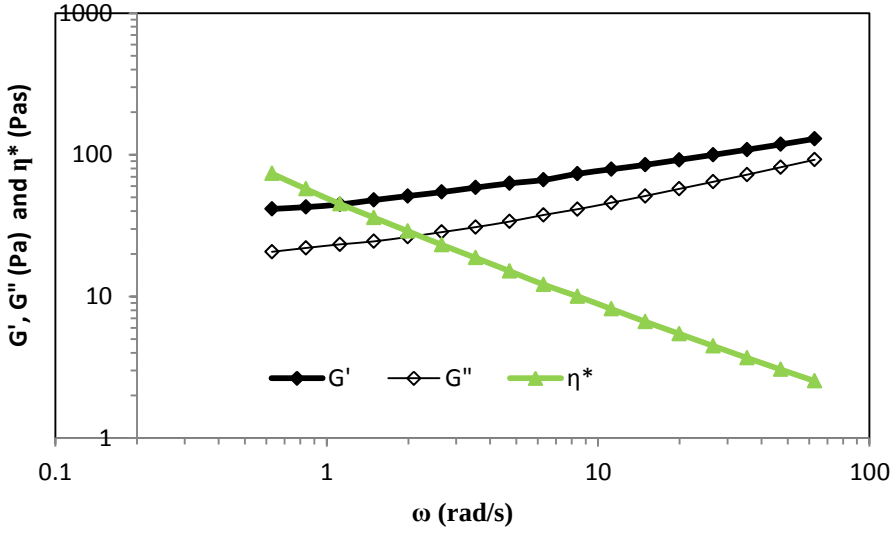

E

Figure 4.103 Frequency sweep of optimum emulsion formulated with (A) 0 (B) 0.5 (C) 2 (D) 4 (E) 6% (w/w) citric acid

therefore had good stability during storage.

Figure 4.104 shows the comparison between the G' and G" of emulsions with different concentrations of citric acid. The effect of citric acid was noticeable on the material function (G') when compared with emulsion without citric acid. G' curves of emulsions with citric acid were observed to be located below the G' curve of emulsion without citric acid. The relative lower position of the G' curves of the emulsion with citric acid suggested that there were decreases in the G' values at all frequency range considered for the emulsion with citric acid. Decreased G' at all frequency range were as a result of decreased elasticity due to the influence of citric acid on the molecular conformation of BGNF gels. This could

have caused decreased structural interactions among oil-droplets. The observed decrease in G' of the emulsions in the presence of citric acid was a result of impediment posed by the citric acid to BGNF polymer network formation. The citric acid reduced the BGNF matrix strength necessary for emulsion formation relative to emulsion without citric acid. It was surprising however that the G" of emulsions with and without citric acid overlap at all tested frequency range. This implied that the presence of citric acid in the emulsion did not alter significantly the viscous properties of the BGNF matrix responsible for emulsion formation. This observation explained the very close similarities observed in the micrographs and apparent viscosities at minimum shear rate of emulsions without and with citric acid in sections 4.7.3.2 and 4.7.3.4, respectively. Table 4.58 shows the G' and G'' obtained for the emulsions with and without citric acid at low frequency of 0.628 rad/s. The mean values of G' and G'' ranged from 38.6 to 111 Pa and 19.1 to 20.7 Pa respectively. The G' values of emulsions with and without citric acid was significantly ($p < 0.05$) different while emulsion formulated with 2, 4, and 6% (w/w) were not significantly ($p < 0.05$) different from each other. On the other hand the G" values of both the emulsions with and without citric acid were not significantly ($p > 0.05$) different from each other.

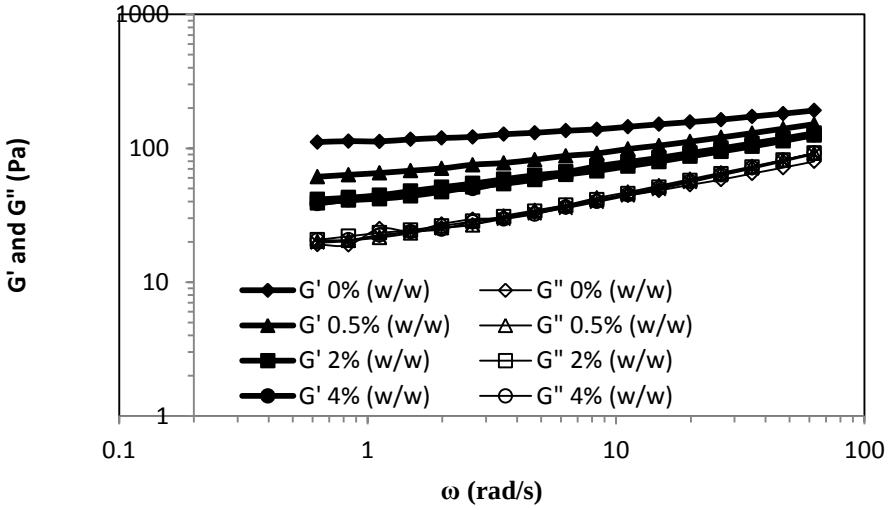

Figure 4.104 Storage (G') and loss (G") moduli as a function of angular frequency during dynamic oscillatory tests of sunflower oil-in-water emulsion containing various concentration of citric acid

Table 4.58 Effect of citric acid concentration on the storage and loss moduli at 0.628 rad/s

Citric acid concentration (% w/w)	Storage modulus (G') Pa	Loss modulus (G") Pa
0	111 ± 2.70[c]	19.1 ± 1.38[a]
0.5	61.3 ± 2.19[b]	20.1 ± 1.40[a]
2.0	41.5 ± 1.23[a]	20.7 ± 1.28[a]
4.0	38.6 ± 1.96[a]	20.5 ± 1.83[a]
6.0	39.1 ± 0.58[a]	19.7 ± 0.80[a]

[1]Values are means ± standard deviations; Mean values with different letters within the same column are significantly different from each other ($p < 0.05$).
[2] G' equals the storage modulus; G" is the loss modulus

4.7.3.7 Effect of citric acid on emulsion rheology with regard to compliance and recoverable strain

Figure 4.105 shows the plot of compliance (J) against time (s) for emulsions with and without citric acid. In the first part of the experiment, a load of 0.5 Pa was imposed on the structure of all the emulsions for 500 s while the second part involved sudden removal of the load and compliance was monitored for the next 500 s. The results of the creep and recovery test were similar for both the emulsions with and without citric acid. Similar viscoelastic characteristic were observed where, J steadily increased when a stress of 0.5 Pa was imposed on all the emulsions during the creep stage and the elastic component of the deformation recovered instantaneously when the load was removed as shown in Figure 4.105.

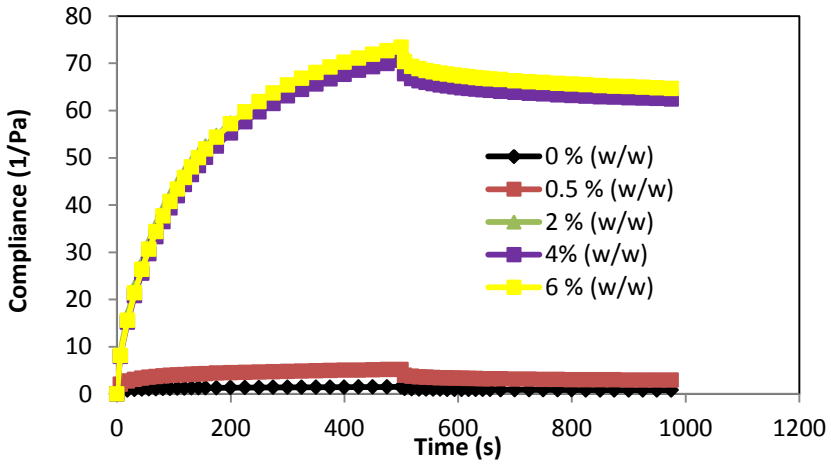

Figure 4.105 Creep and recovery curves of emulsions containing various concentrations of citric acid

The emulsion without citric acid recorded the lowest J, followed by emulsion with 0.5% (w/w) citric acid. Emulsion with 2, 4 and 6% (w/w) citric acid showed very similar and overlapping creep and recovery graphs. The presence of citric acid in the emulsion increased J relative to emulsion whose BGNF matrix did not contain citric acid. The higher J indicated a negligible instantaneous elastic compliance. This suggested that the network of the emulsion structures with citric acid were weaker and less rigid when compared with emulsion without citric acid. Emulsion without citric acid with the least value of J possessed stronger structural interactions and hence gave least deformation when the stress of 0.5 Pa was imposed on it. Citric acid concentrations of 2, 4 and 6% (w/w) had very similar influence ($p < 0.05$) on the J values. Table 4.59 shows the effect of citric acid concentrations on the recoverable strain, Q (t)% of the emulsion. Q (t)% indicated the elasticity of the structure when the load was withdrawn. Higher value of Q (t)% therefore implied higher elasticity of the sample.

Table 4.59 Effect of citric acid concentration on the recoverable strain of BGNF optimum emulsion[1,2]

Citric acid concentration (% w/w)	Recoverable strain Q (t)%
0	46.2 ± 1.49^{b}
0.5	44.1 ± 2.66^{b}
2.0	13.7 ± 0.94^{a}
4.0	11.5 ± 0.91^{a}
6.0	11.9 ± 1.03^{a}

[1]Values are means ± standard deviations; Mean values with different letters within the same column are significantly different from each other ($p < 0.05$).

[2] Q (t) % equals the recoverable strain

The mean of Q (t)% ranged between 11.5 to 46.2% for all the emulsions. Emulsion without citric acid and that with 0.5% citric acid were similar but were significant ($p < 0.05$) difference from others with citric acid. Emulsions with 2, 4 and 6% (w/w) citric acid did not show any significant ($p < 0.05$) difference.

4.7.3.8 Summary on the effect of citric acid on emulsion stability and rheology of optimum emulsion

Citric acid although had affected the BGNF molecular conformation and strength responsible for emulsions stability relative to virgin gelatinized BGNF dispersion, its effect at all concentrations had produced very similar effects on the emulsion forming ability of

gelatinized BGNF dispersion. The initial backscattering showed that comparable concentrations of the droplets were formed by all the gelatinized BGNF dispersions containing citric acid. And this was strongly supported by the result of oil droplet size and microscopic analysis of the emulsions formed by citric acid containing gelatinized BGNF dispersions. The similarities in the behaviour of emulsions formed by citric acid containing BGNF matrix showed that the emulsion stability characteristic is pH dependent. Citric acid had altered the pH of the emulsions to a more acidic region and affected the matrix strength and droplet-droplet interaction of emulsions comparably. Citric acid weakened the BGNF matrix and reduced the strength.

The result of the rheological studies, confirmed the changes in molecular conformation brought about by the presence of citric acid. The presence of citric acid at all concentrations had reduced the consistencies of the emulsion as a result of either decreased viscosity of the BGNF matrix or droplet-droplet interactions relative to emulsion without citric acid. However, it should be pointed out that some rheological studies identified changes in conformation, structuration and droplet-droplet interactions as the citric acid concentration increased in the BGNF polymer network. Citric acid had produced progressive decrease in viscosity as concentration increased. The viscoelastic properties were altered significantly ($p < 0.05$). Emulsion containing 0.05% (w/w) recorded the relatively higher rheological properties among emulsions with citric acid. Decreases in rheological properties when compared with emulsion without citric acid however did not seem to have significant effect on the emulsion stability properties such as droplet size, and oil-droplet aggregation. Addition of citric acid into the BGNF dispersion could therefore be used as a way of controlling the rheology of the BGNF stabilized emulsions without significant change in the microstructure and stability of the emulsion. This is an advantage in food deliveries where small oil droplets (for high sensory properties) are required with yet controlled rheology.

4.8 Effect of Storage Temperature and Time on Emulsion Stability and Rheological Properties of Optimum and Most Stable Additive Containing Emulsions

The ageing of the optimum emulsion and most stable additive contaning emulsions as a function of temperature was reported in this section. The stability and rheological behaviour of the emulsions were reported over a period of 20 days. The equilibrium backscattering value (BS_{eq}) was evaluated in order to understand the long term storage properties of the BGNF-stabilized emulsion. The time independent rheological properties of these emulsions were also investigated at different temperatures during storage. Attempts were made to relate rheological properties to the long term stability data.

4.8.1 Effect of storage temperature and time on stability of optimum and most stable additive containing emulsions

Optimum emulsion in section 4.2.4 and relatively most stable additive containing emulsions in section 4.7 (Figure 106) were studied for their behavior during storage.

Figure 4.106 Optimum emulsion (A) and most stable emulsions containing NaCl (B), Vinegar (C) and Citric acid (D)

The storage stability was conducted at low temperatures of 5^{o}C, room temperature of 20^{o}C and elevated temperature of 45^{o}C and emulsion stability were measured on 1st, 3rd, 9th, 15th and 20th day of storage. The stability of the optimum emulsion (A) and emulsions containing 25 mM NaCl (B), 8% vinegar (C), and 0.5% citric acid (D) (Figure 106) analyzed for 20 days at temperatures of 5^{o}C, 25^{o}C and 45^{o}C is presented in Figures 4.107, 4.108, 4.109 and 4.110. The stability graphs were presented both in the Turbiscan normal mode (left) and reference mode (right). The Turbiscan normal mode showed that all the emulsions had destabilized over time and the destabilization was dependent on both the storage temperature and composition of emulsion system. The mechanism of destabilization and quantification can be easily analyzed in the reference modes of the stability graphs. The reference mode of the emulsion stability graph was constructed by using the first scan as the reference and its backscattering flux was assigned a value of zero. The subsequent scans were afterwards overlaid to show the relative changes in the backscattering overtime. The reference mode of the stability curves showed that multiple mechanism of destabilization characterized all the emulsion systems. Creaming phenomenon manifested as a decrease in the backscattering at the bottom of the tube (0 - 20 mm zone) and subsequently increased

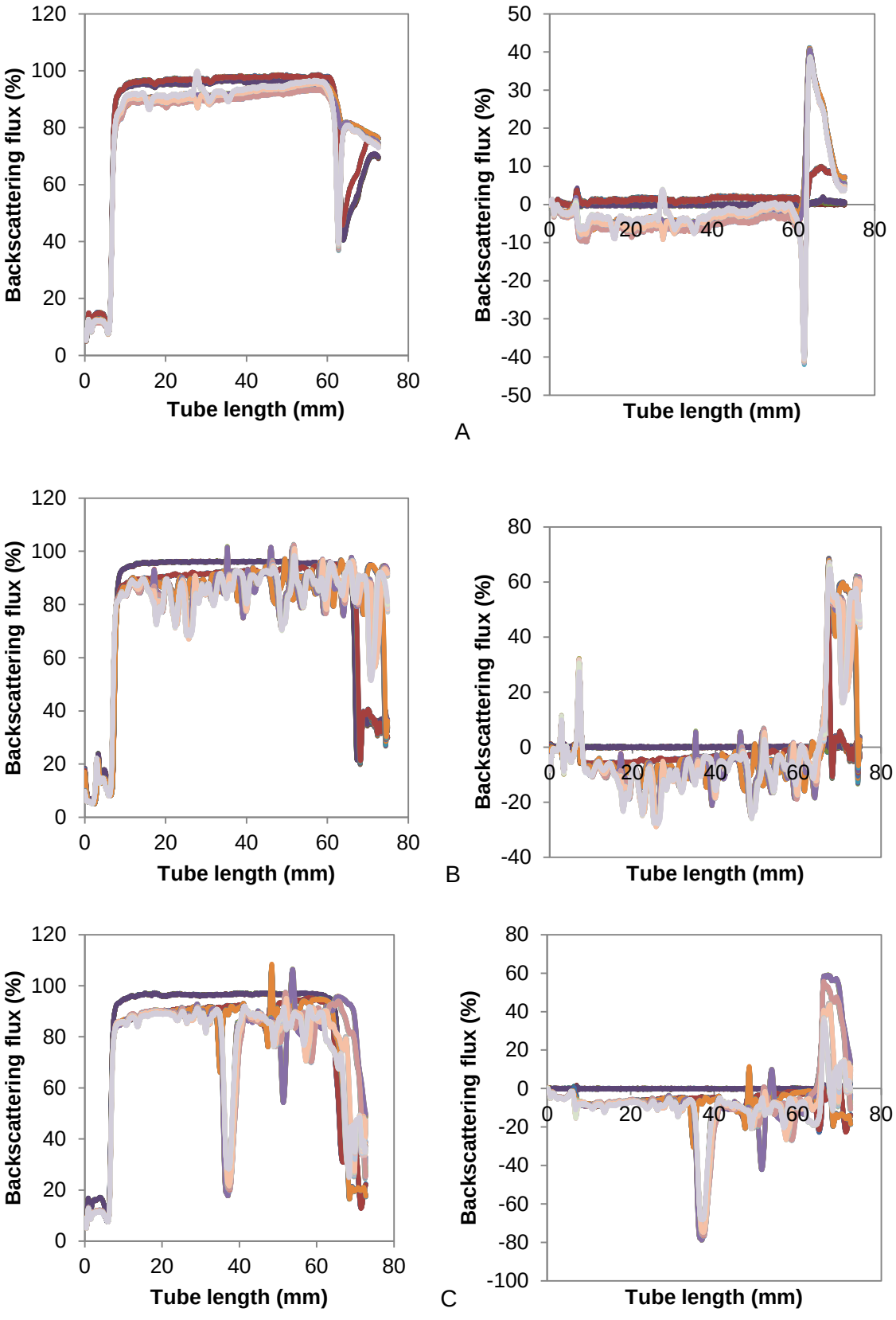

Figure 4.107 **Changes in the backscattering profile (BS%) as a function of sample height with storage time of optimized emulsion at different temperatures (A) 5°C (B) 20°C (C) 45°C**

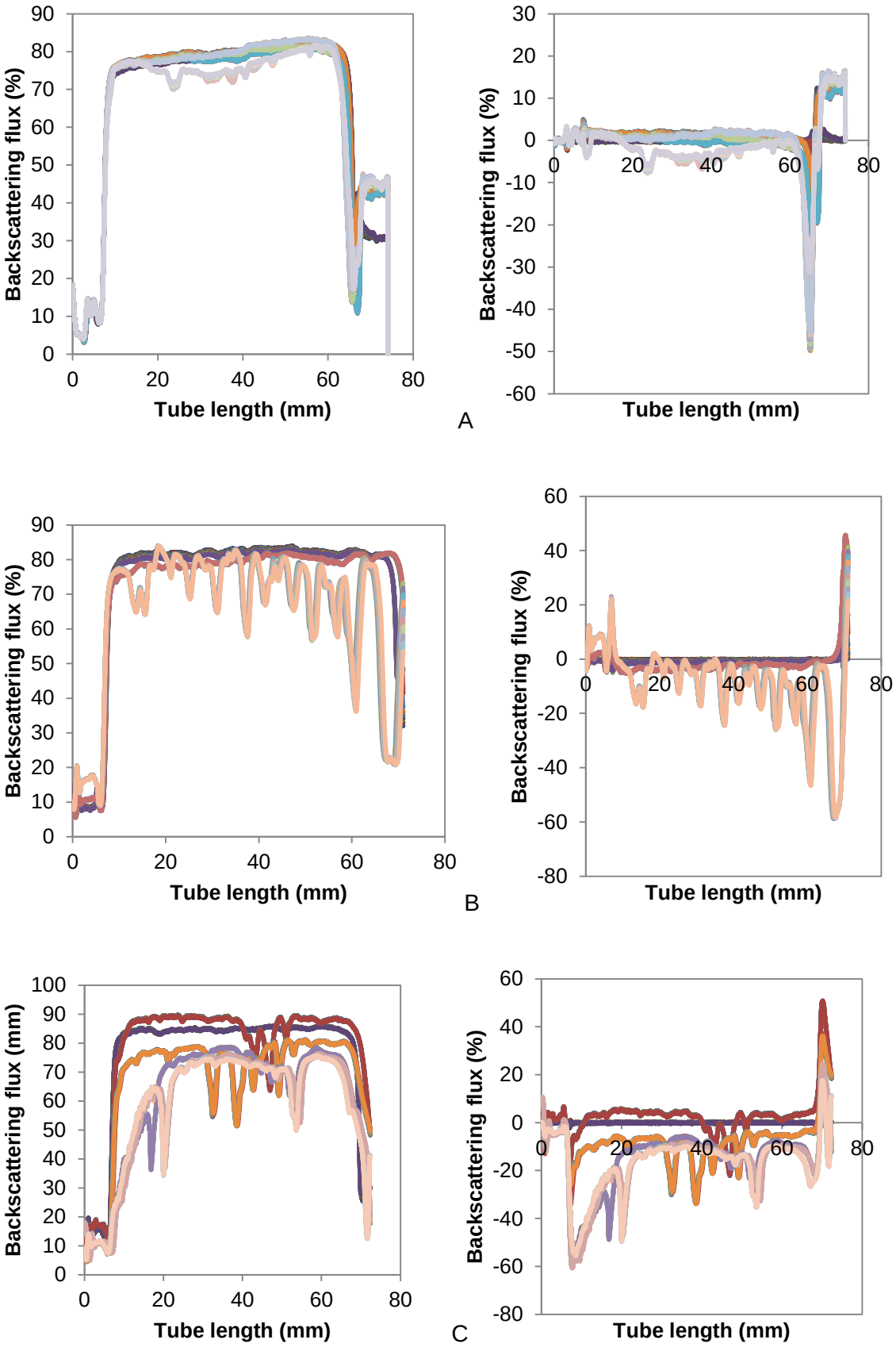

Figure 4.108 **Changes in the backscattering profile (BS%) as a function of sample height with storage time of emulsion containing 25 mM NaCl at different temperatures (A) 5°C (B) 20°C (C) 45°C**

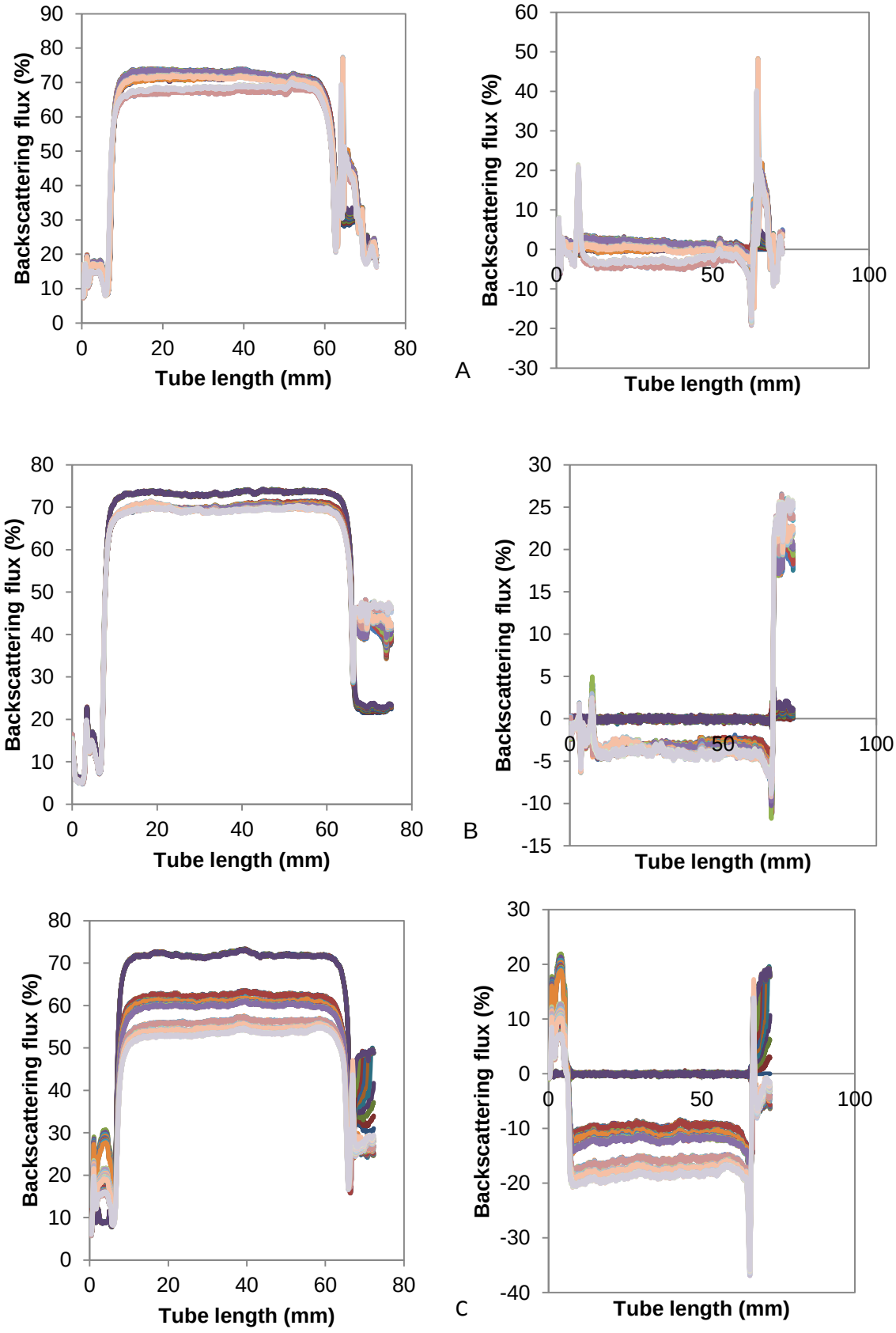

Figure 4.109 **Changes in the backscattering profile (BS%) as a function of sample height with storage time of emulsion containing 8% vinegar at different temperatures (A) 5°C (B) 20°C (C) 45°C**

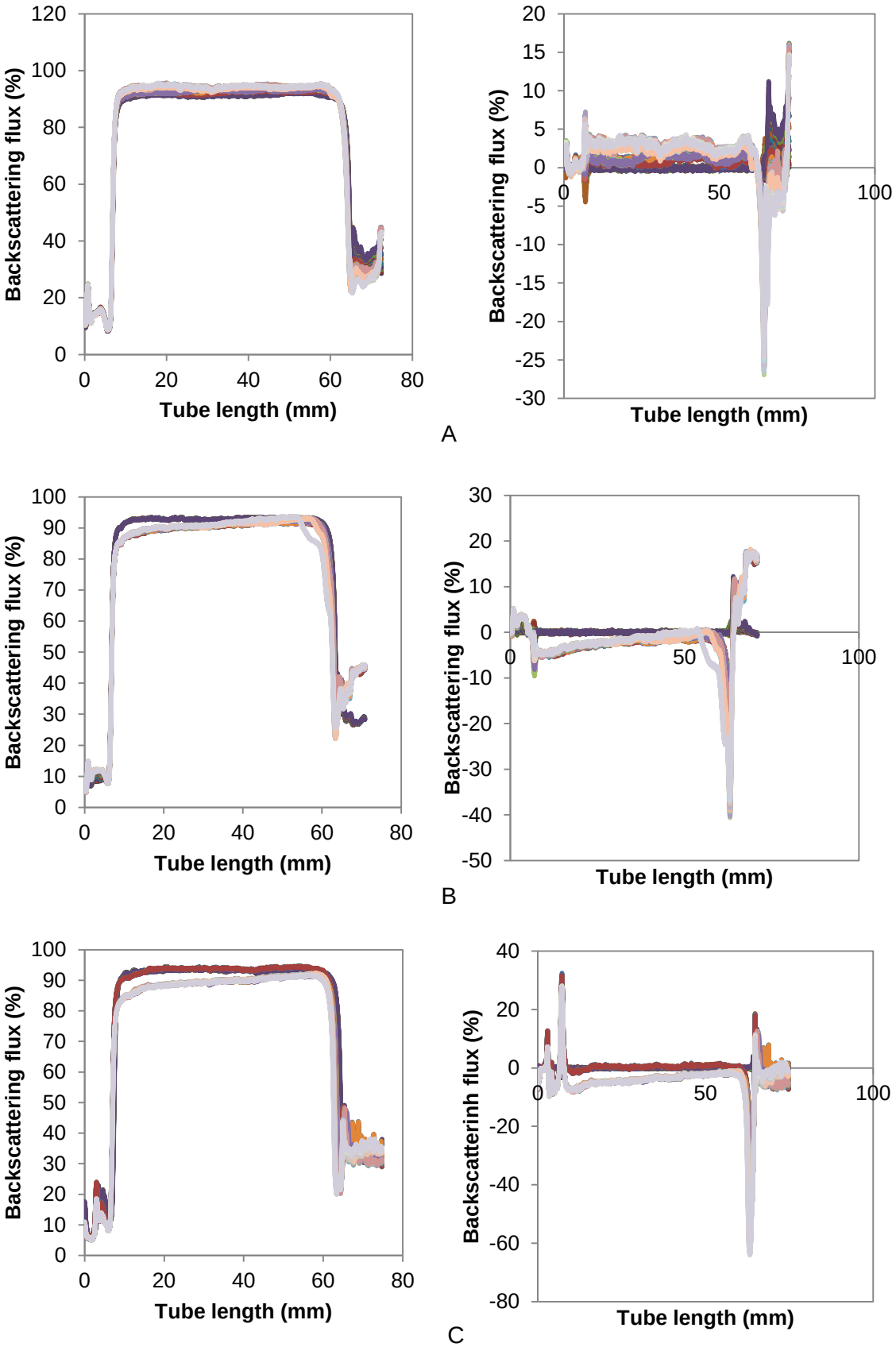

Figure 4.110 **Changes in the backscattering profile (BS%) as a function of sample height with storage time of emulsion containing 0.5% citric acid at different temperatures (A) 5°C (B) 20°C (C) 45°C**

at the top of the tube (50 – 60 mm). Destabilization phenomenon that related to oil-droplet aggregations showed as a continuous increase or decrease in backscattering usually in the middle of the tube (20 – 40 mm zone) depended on the size of the oil droplets. If the oil droplet is smaller than the wavelength of the light source and the particles are destabilizing by particle aggregation, the backscattering manifests as an increase (Raleigh diffusion zone). Whereas if the wavelength of the light source is bigger than the oil droplet and the destabilization by flocculation or coalescence is taking place then the backscattering manifests as a decrease (Mie zone). This is because of the increase in the mean path of photon due to increase in the distance between the oil droplets. For comparative purposes and to gain insight into the destabilization phenomenon relating to particle migration (creaming) and particle aggregation (flocculation and coalescence), the emulsions were analyzed at the bottom (0 – 20 mm) and middle (20 – 40 mm) of the Turbiscan tube. Figures 4.111 and 4.112 show the oil droplet aggregation kinetics evaluated at the middle of the tube. All the emulsion systems did not substantially cream overtime. The kinetics of oil droplet aggregation in the middle of the tube however showed that both temperature and the nature of emulsion system had influence on the extent of destabilization. Generally, most emulsion destabilization reached equilibrium on the third day of storage. The low temperature of 5^{o}C inhibited the aggregation of oil droplets while high destabilization was observed at high temperature (45^{o}C).

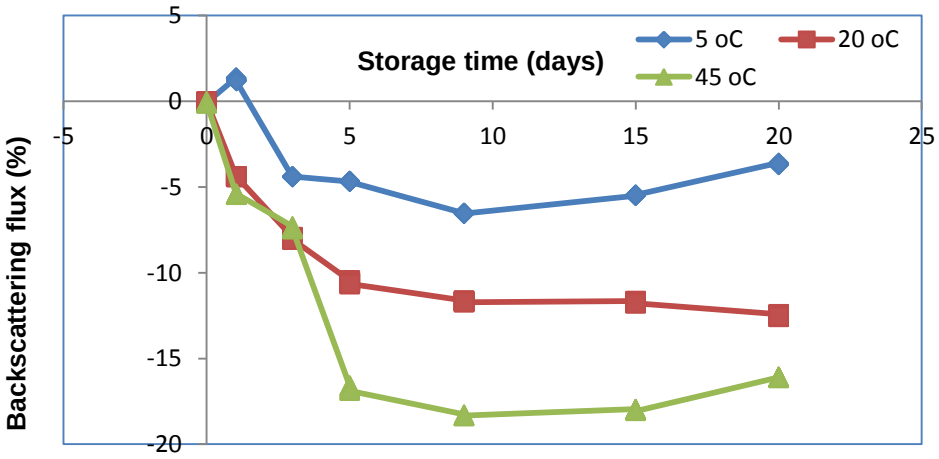

Figure 4.111 **Variation in backscattering in the 20 - 40 mm zone monitored over 20 days for optimum emulsion stored at 5^{o}C, 20^{o}C and 45^{o}C**

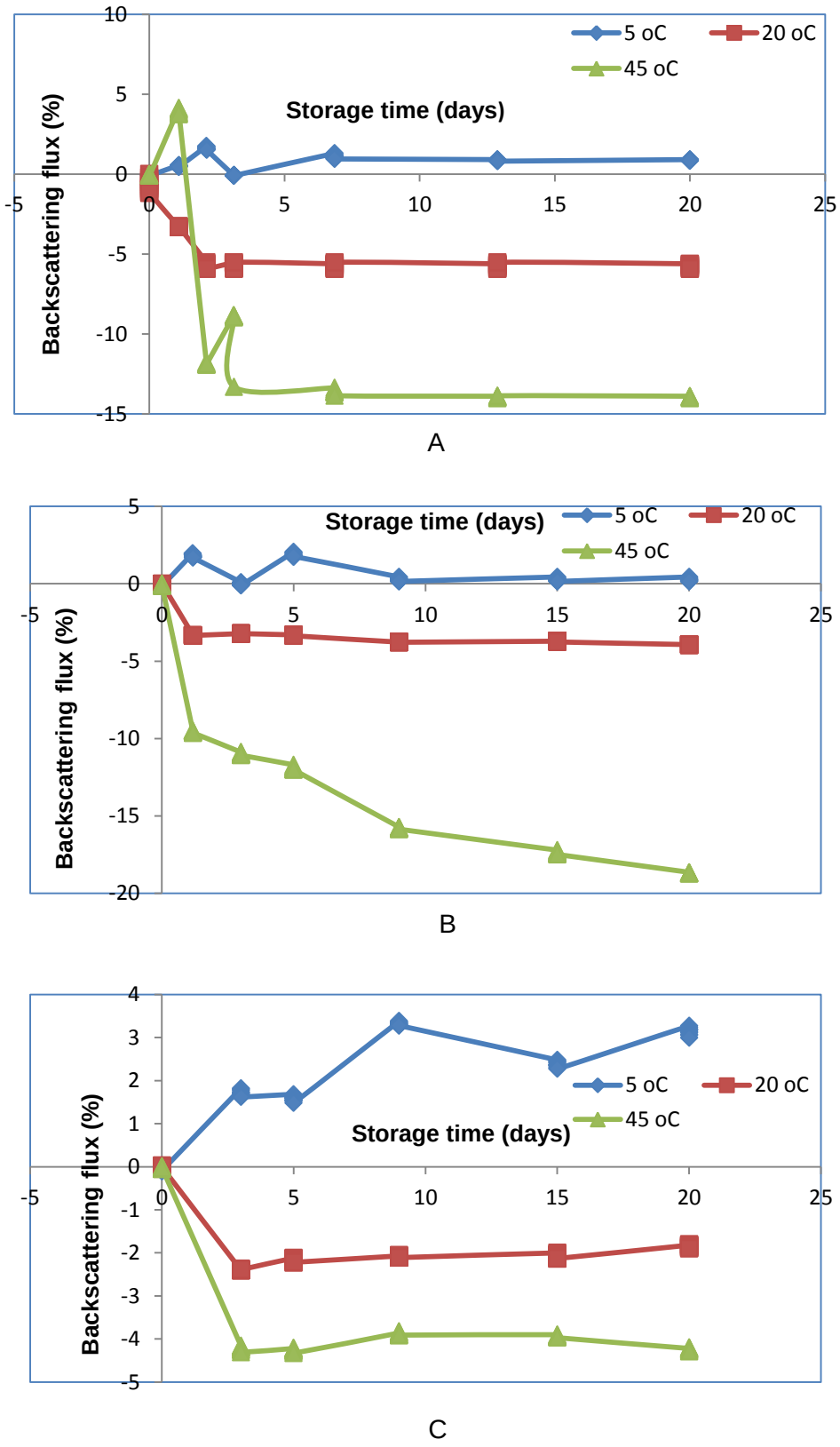

Figure 4.112 **Variation in backscattering in the 20 - 40 mm zone monitored over 20 days for emulsions stored at 5°C, 20°C and 45°C (A) emulsion containing 25 mM NaCl (B) emulsion containing 8% vinegar (C) emulsion containing 0.5% citric acid**

Kiokias *et al.* (2004) and Boode *et al.* (1991) also reported high stability for whey protein stabilized emulsions and triglyceride oil-in-water emulsions respectively at 5^{o}C. The increased destabilization observed at high temperature may be connected with reduced viscosity of the BGNF matrix at high temperature thereby encouraging oil-droplets movements and aggregations (Gonçalves and Maia Campos, 2009).

4.8.2 Effect of storage temperature and time on the rheological properties of optimum and most stable additive containing emulsions with regard to flow curves and hysteresis loop area

The storage stability experiment was conducted at low temperatures of 5^{o}C, room temperature of 20^{o}C and elevated temperature of 45^{o}C and the rheological properties were measured on days 1, 3, 9, 15 and 20. Figures 4.113, 4.114, 4.115 and 4.116 are the shear sweep conducted on optimum emulsion and emulsions containing 25 mM NaCl, 8% (w/w) vinegar and 0.5% (w/w) citric acid respectively at different temperature and time. The behaviour of emulsions containing additives were similar to optimized emulsion at all storage times and temperatures. There were observed structural destruction in all the emulsions at all storage temperatures and times. This was revealed in the relative positions of the ascending and descending flow curves and this had resulted into thixotropic loop between the two curves. Moreover, both the storage time and temperature had dissimilar influence on the flow curves. The rheograms of all the emulsions at all studied conditions showed a positive yield stress which was desirable for the stability of semi-solid fluids (Goncalves and Maia Campos, 2009). The apparent viscosity at the loop apex is shown in Tables 4.60 and 4.61. Both the storage temperature and time influenced the apparent viscosity of all the emulsions and this was peculiar to each formulation. Generally, the viscosity of the optimum emulsion was the highest on the first day relative to emulsions containing additives. Although the changes (increase or decrease) in the viscosity with storage time were a peculiarity of each formulation, the viscosities at temperatures of 5^{o}C and 45^{o}C were the highest and lowest respectively at all storage times (except for the optimum emulsion on day 3).

Regarding the optimum emulsion, there were observed structuration in the emulsion over time and this manifested as increased viscosity ($p < 0.05$). The structuration over time was a characteristics of the gelatinized BGNF used to achieve emulsion stability. The viscosity of the emulsions at all the three temperatures showed initial increase with storage time before a final decline. It appeared that the low temperature of 5^{o}C preserved the initial characteristics of the emulsion as there were no significant difference between the viscosity on day 1 and day 20. The viscosity at 20 and 45^{o}C showed a relative decrease at the final

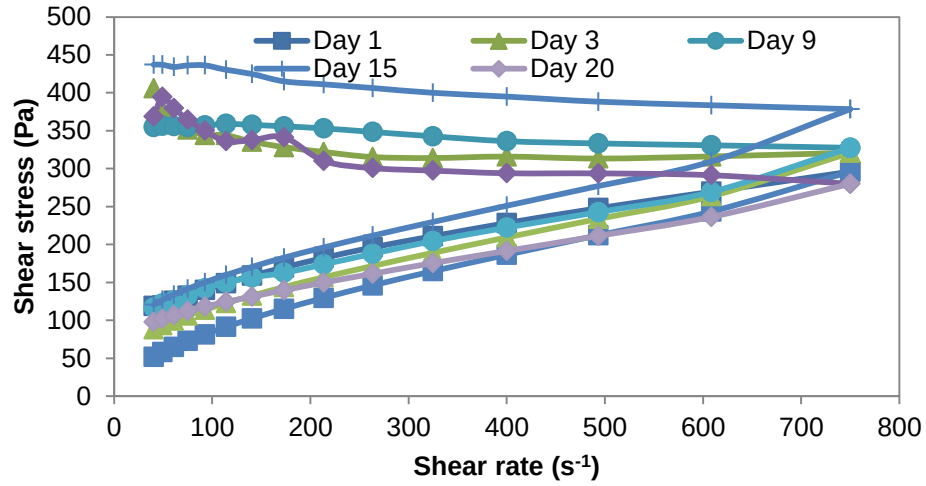

A

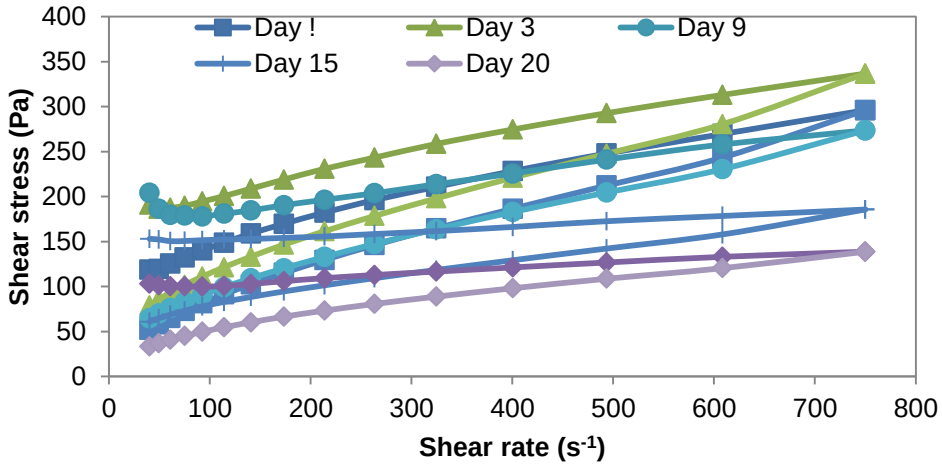

B

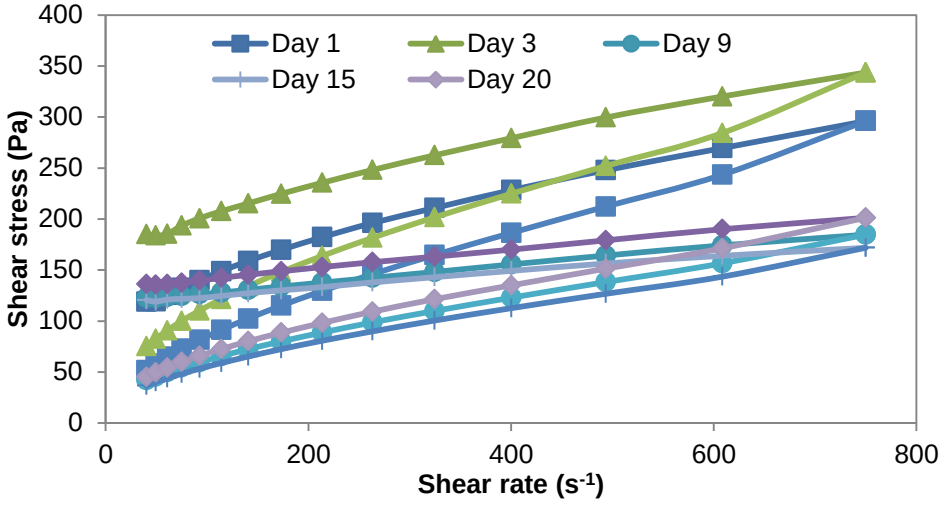

C

Figure 4.113 Effect of storage time and temperatures on the properties of optimum emulsion (A) 5°C (B) 20°C (C) 45°C

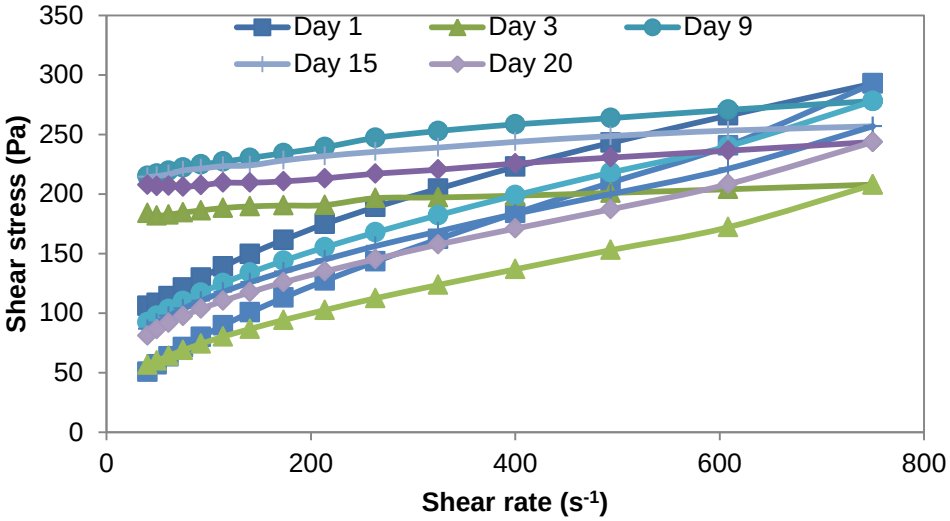

A

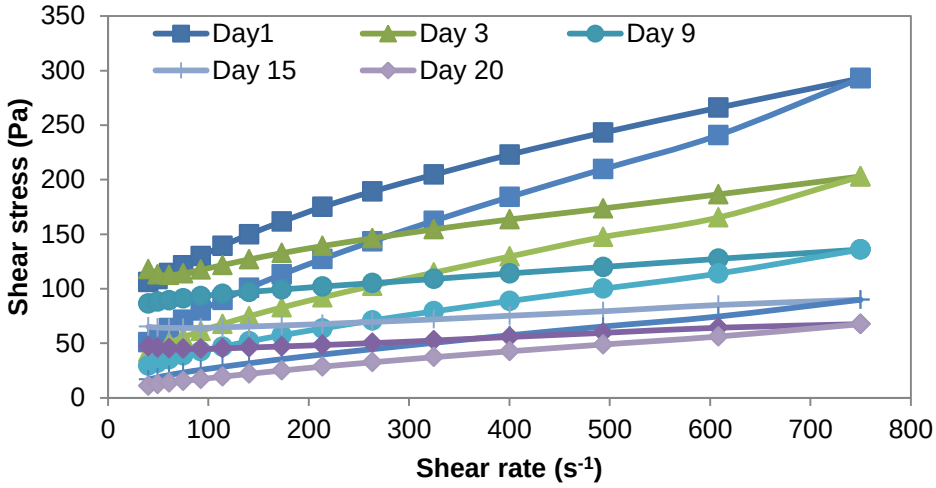

B

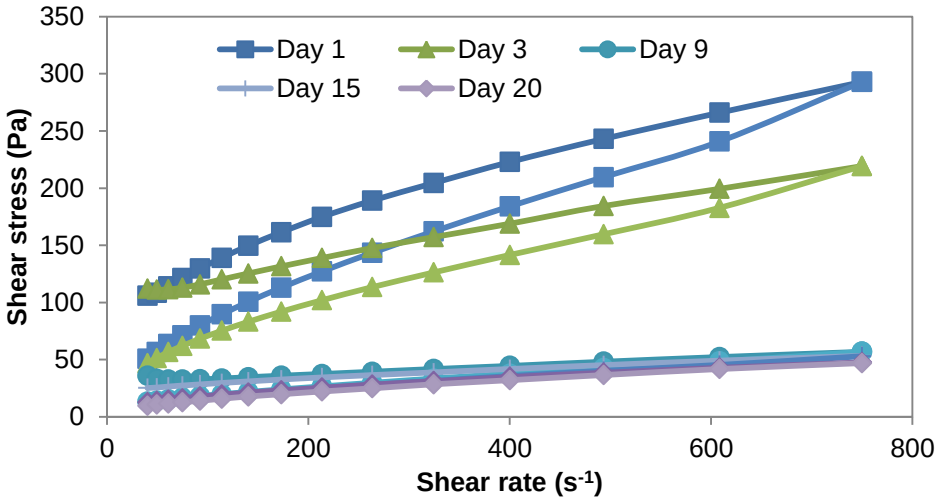

C

Figure 4.114 Effect of storage time and temperatures on the property of emulsion containing 25 mM NaCl. (A) 5°C (B) 20°C (C) 45°C

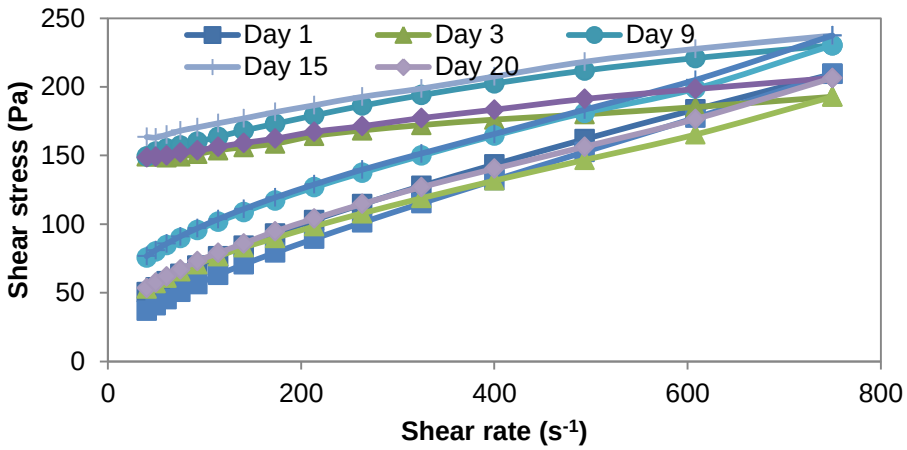

A

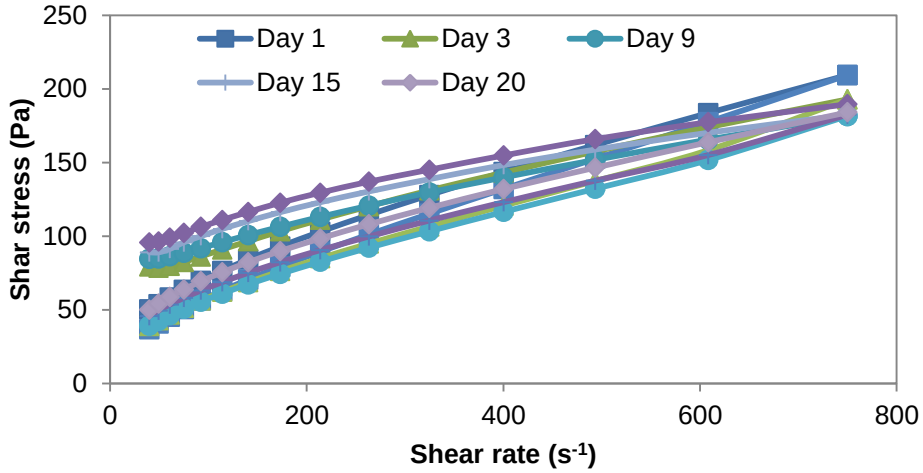

B

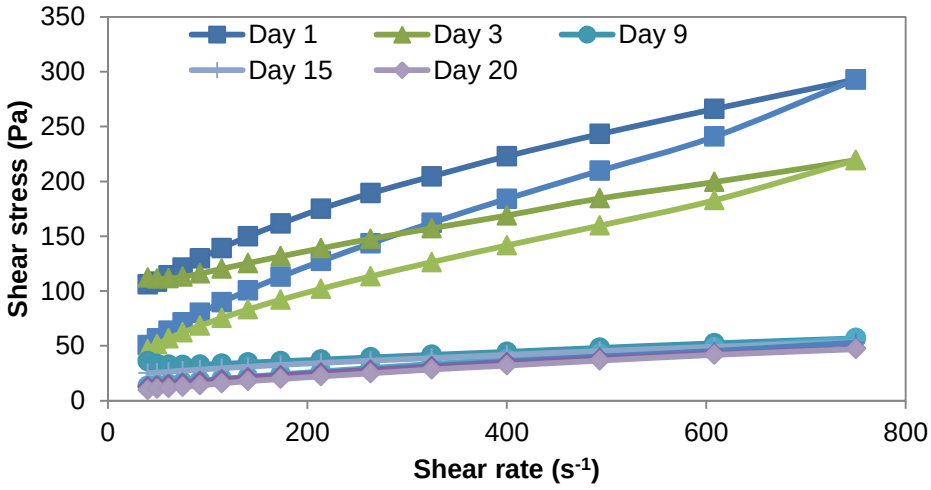

C

Figure 4.115 Effects of storage time and temperatures on the property of emulsion formulated with 8% (w/w) vinegar (A) 5°C (B) 20°C (C) 45°C

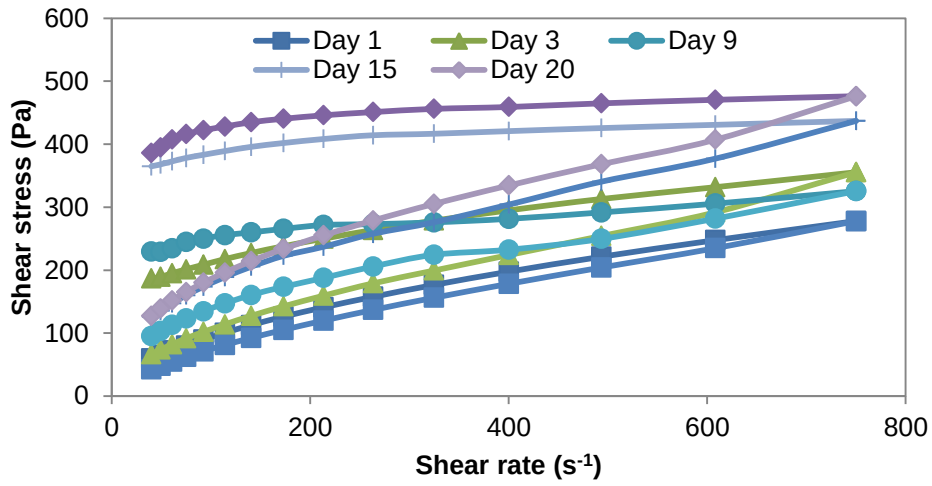

A

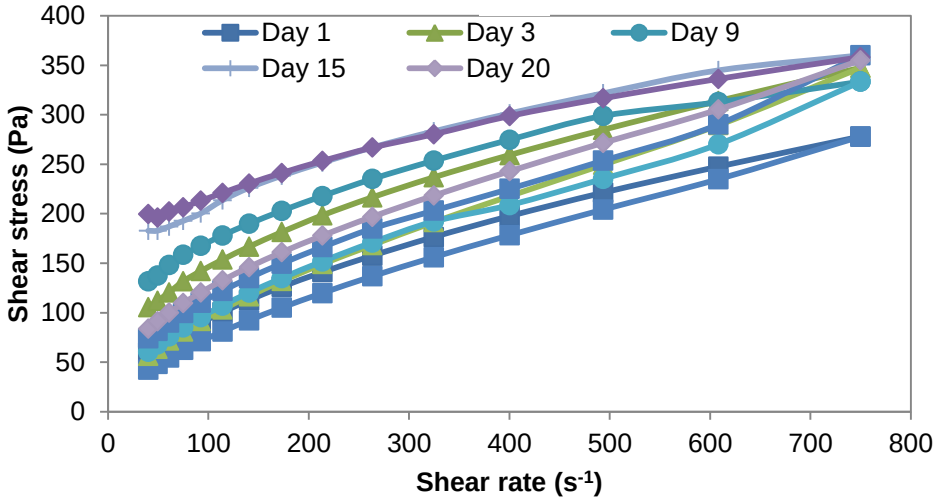

B

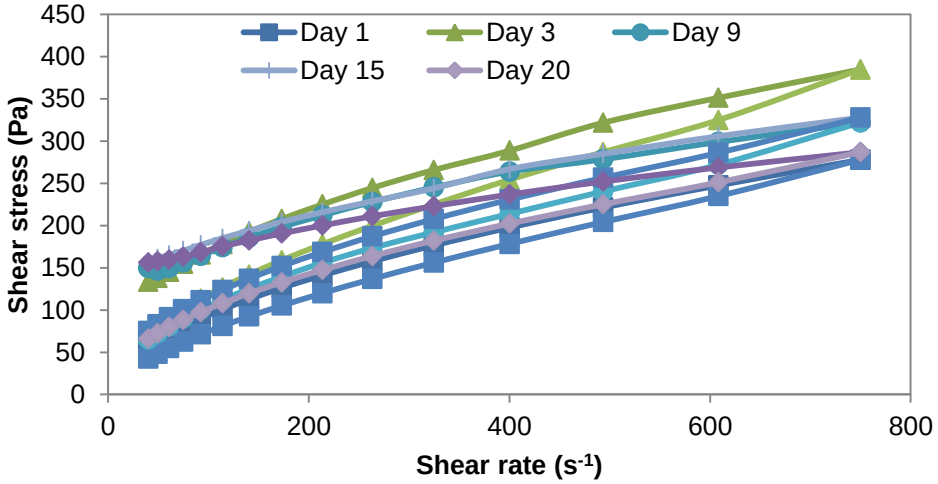

C

Figure 4.116 Effects of storage time and temperatures on the property of emulsion formulated with 0.5% citric acid (A) 5°C (B) 20°C (C) 45°C

storage time (day 20) when compared with the initial viscosity at the first day of manufacture ($p < 0.05$). The storage temperature can alter the viscosity of a product and higher temperatures promote droplet mobility and phase interactions in emulsions by decreasing the viscosity of the continuous phase (Gonçalves and Maia Campos, 2009). Significant decrease ($p < 0.05$) in viscosity observed at 20^{o}C for the optimum emulsion on the 20th day of storage was probably as a result of the decreased BGNF matrix strength and subsequent increased droplet coalescence which could be a result of microbial spoilage in the emulsion. The behaviour of emulsion with 25 mM NaCl was in some ways similar to the optimum emulsion during storage. For example the initial characteristic of the emulsion was preserved at low temperature (5^{o}C) and the viscosities of the emulsions were observed to decrease significantly ($p < 0.05$) at the room temperature (20^{o}C) and at the elevated temperature (45^{o}C) on the 20th day of storage relative to the first day of preparation. Contrary to what was observed in the optimize emulsion there was no initial surge in the viscosity before decline. This could be as a result of the weakened polysaccharide stabilizing strength induced by the presence of NaCl during continuous phase preparation. The weakened matrix must have reduced the effect of BGNF structuration in the emulsion. Decrease in viscosity was however very pronounced at elevated temperatures. It was interesting to note that the presence of NaCl did not seem to preserve the initial properties of the emulsion at elevated temperatures. The presence of NaCl seemed to have a deteriorating effect on the polymer gel structure over time. The viscosities at room temperature (20^{o}C) and elevated temperature of 45^{o}C were significantly reduced on the 20th day of storage. This was an evidence of weakened polymer gels structure due probably to spoilage by age and high temperature. It appeared that the presence of NaCl at a concentration of 25 mM NaCl made the emulsion more susceptible to structural breakdown (destabilization) at room temperature (20^{o}C) and elevated temperature of 45^{o}C.

Emulsion containing 8% (w/w) of vinegar behaved very similar at all storage temperatures. The viscosity at low temperature 5^{o}C was relatively higher than the corresponding temperatures of 20^{o}C and 45^{o}C and the initial properties (viscosity on the first day of manufacture) of the emulsion seemed to be fairly preserved at the 20th day of storage. The initial viscosity of the emulsions at the 20^{o}C and 45^{o}C decreased significantly ($p < 0.05$) with age. Vinegar is an acidulant and it has been reported to possess preservative properties. The polymer gel structure of the emulsion containing 8% (w/w) vinegar at 5^{o}C was properly kept and this had maintained and preserved the polymer gel strength needed for long term stability. Although the presence of vinegar in the emulsion at 8% (w/w) greatly reduced the viscosity of the optimum emulsion (from 0.39 to 0.28 Pas) on the first day of preparation, the structuration of the emulsion with vinegar did not seem significant ($p < 0.05$) over time especially at 5^{o}C

Table 4.60 Effect of storage time and temperature on the minimum apparent viscosity of the optimum and emulsions with NaCl

Days	Viscosity (Pas) Optimized Emulsion			Viscosity (Pas) Emulsion with 25 mM NaCl		
	5°C	20°C	45°C	5°C	20°C	45°C
1	0.39 ± 0.00[a]	0.39 ± 0.00[a]	0.39 ± 0.00[a]	0.37 ± 0.00[a]	0.37 ± 0.00[a]	0.37 ± 0.00[a]
3	0.43 ± 0.00[b]	0.45 ± 0.00[b]	0.46 ± 0.01[b]	0.37 ± 0.00[a]	0.27 ± 0.00[b]	0.29 ± 0.01[b]
9	0.44 ± 0.01[b]	0.36 ± 0.00[c]	0.25 ± 0.01[c]	0.37 ± 0.00[a]	0.18 ± 0.00[c]	0.08 ± 0.00[c]
15	0.50 ± 0.01[c]	0.25 ± 0.01[d]	0.24 ± 0.07[d]	0.34 ± 0.01[c]	0.12 ± 0.02[d]	0.07 ± 0.00[c]
20	0.37 ± 0.00[a]	0.18 ± 0.07[e]	0.23 ± 0.00[c]	0.33 ± 0.00[d]	0.09 ± 0.01[e]	0.06 ± 0.00[d]

[1]Values are means ± standard deviations; Different letters within the same column are significantly different from each other ($p < 0.05$)
[2]Values calculated at the maximum point of the shear gradient

.

Table 4.61 Effect of storage time and temperature on the minimum apparent viscosity of emulsions with vinegar and citric acid

Days	Viscosity (Pas) Emulsion with 8% (w/w) Vinegar			Viscosity (Pas) Emulsion with 0.5% (w/w) Citric acid		
	5°C	20°C	45°C	5°C	20°C	45°C
1	0.28 ± 0.00[a]	0.28 ± 0.00[a]	0.28 ± 0.00[a]	0.37 ± 0.00[a]	0.37 ± 0.00[a]	0.37 ± 0.00[a]
3	0.28 ± 0.00[a]	0.26 ± 0.00[b]	0.24 ± 0.00[b]	0.47 ± 0.01[b]	0.46 ± 0.00[b]	0.46 ± 0.00[b]
9	0.31 ± 0.02[b]	0.25 ± 0.00[c]	0.23 ± 0.00[c]	0.44 ± 0.00[c]	0.44 ± 0.00[c]	0.43 ± 0.00[c]
15	0.32 ± 0.00[b]	0.24 ± 0.00[d]	0.22 ± 0.07[d]	0.58 ± 0.00[d]	0.48 ± 0.00[d]	0.44 ± 0.00[c]
20	0.28 ± 0.07[a]	0.24 ± 0.02[d]	0.21 ± 0.00[e]	0.64 ± 0.01[e]	0.48 ± 0.00[d]	0.38 ± 0.02[a]

[1] Values are means ± standard deviations; Different letters within the same column are significantly different from each other ($p < 0.05$)
[2] Values calculated at the maximum point of the shear gradient

The presence of citric acid at a concentration of 0.5% (w/w) showed significant increase in viscosity at all temperatures. The presence of citric acid in the emulsion had promoted structuration which could be as a result of magnified intrinsic structural characteristics of the BGNF matrix and improved oil droplet interaction in the emulsion over time. Surprisingly, the viscosity of the emulsion on the 20th day of storage at the high temperature did not different significantly ($p < 0.05$) from the first day of manufacture. The viscosities at 5 and 20^{o}C were relatively higher than those at 45^{o}C at all storage times.

Beside the one point analysis at the loop apex, the whole length of the flow curves was further analyzed for information regarding the fluid consistency, resistance to flow and extent of structural destruction during storage. For this purpose, power law rheological model was used. Tables 4.62, 4.63, 4.64 and 4.65 were the parameters of power law model and magnitude of hysteresis loop area of optimum emulsion, emulsions with 25 mM NaCl, 8% (w/w) vinegar and 0.5% (w/w) citric acid, respectively as a function of storage time and temperature. The high coefficients of determination showed that power law rheological model described the changes in the rheological behaviour at all conditions. Both the storage temperatures and time had significant effect on the power law parameters of the forward and backward curves and the effect was a peculiarity of individual emulsion systems. The observed characteristics of the emulsions under storage at different temperatures were similar to what was observed previously in all the BGNF stabilized emulsions. For instance, the consistency coefficient was observed to increase with corresponding decrease in flow behaviour index. Also, there were observed decreases and increases in the consistency coefficients and flow behaviour index, respectively for the backward curves relative to the corresponding forward curve. There were differences in consistency coefficients and flow behaviour index of the forward and backward flow curves suggesting that the emulsions were thixotropic time dependent fluids. The flow behaviour indexes were all less than unity which implied a pseudoplastic non-Newtonian behaviour. Pseudoplastic non-Newtonian property is desirable in emulsions, since the viscosity was observed to decrease with applied stress thereby making it possible to spread (Gonçalves and Campos, 2009). Similar to the observation of the apparent viscosity at the loop apex, in most cases, the consistency coefficients of the forward and backward curves were highest and lowest at temperatures of 5^{o}C and 45^{o}C, respectively at all times. The power law flow behaviour index parameter n, was found to be negative for the optimum emulsion stored at 5^{o}C on days 3, 9, 15 and 20. The negative n-parameters showed severe shear thinning behaviour of the optimum emulsion. Fraiha *et al.* (2011) also reported negative n-parameters in their study to investigate the rheological behavior of corn and soy mix as feed ingredients. Padmanabhan and Bhattacharya (1991) explained the negative n-parameter to be due to molecular degradation of the sample, viscous dissipation, fluid slip along the capillary wall and

Table 4.62 Effect of storage time and temperature on power law parameters and Hysteresis loop area of optimum emulsion

Days	K (Pas^n)	n	R^2	K′ (Pas^n)	n′	R^2	HL (Pas^{-1})
5°C							
1	44.9 ± 0.87[a]	0.28 ± 0.06[a]	0.99	7.60 ± 0.53[a]	0.56 ± 0.03[a]	0.99	772 ± 44[a]
3	406 ± 13.4[b]	-0.06 ± 0.02[b]	0.90	16.3 ± 1.46[a]	0.41 ± 0.01[b]	0.98	2236 ± 572[b]
9	413 ± 9.80[b]	-0.02 ± 0.02[c]	0.88	28.9 ± 5.75[b]	0.35 ± 0.04[bc]	0.97	2642 ± 187[bc]
15	546 ± 23.2[bc]	-0.05 ± 0.02[c]	0.95	29.4 ± 3.59[b]	0.36 ± 0.02[bc]	0.97	3202 ± 268[c]
20	579 ± 14.6[c]	-0.11 ± 0.01[d]	0.92	26.5 ± 4.87[b]	0.33 ± 0.02[d]	0.97	2623 ± 144[bc]
20°C							
1	44.9 ± 0.87[a]	0.28 ± 0.06[a]	0.99	7.60 ± 0.53[ab]	0.56 ± 0.00[a]	0.99	772 ± 44[a]
3	87.4 ± 11.3[b]	0.19 ± 0.02[b]	0.96	13.9 ± 1.33[c]	0.47 ± 0.01[b]	0.99	1077 ± 46[b]
9	103 ± 6.34[bc]	0.13 ± 0.00[c]	0.88	8.93 ± 2.14[b]	0.50 ± 0.03[ab]	0.99	1055 ± 3[b]
15	117 ± 2.89[c]	0.06 ± 0.00[d]	0.81	16.8 ± 1.32[c]	0.35 ± 0.01[c]	0.99	851 ± 3[a]
20	56.9 ± 8.60[a]	0.12 ± 0.01[c]	0.86	5.17 ± 1.02[a]	0.49 ± 0.02[b]	0.99	553 ± 40[d]
45°C							
1	44.0 ± 0.87[a]	0.28 ± 0.06[a]	0.99	7.60 ± 0.53[a]	0.56 ± 0.00[a]	0.99	772 ± 44[a]
3	68.7 ± 12.9[ab]	0.23 ± 0.01[a]	0.95	11.2 ± 1.44[b]	0.47 ± 0.07[a]	0.99	986 ± 46[b]
9	69.1 ± 17.1[ab]	0.14 ± 0.03[b]	0.90	6.44 ± 0.14[a]	0.50 ± 0.00[a]	0.99	756 ± 57[a]
15	71.7 ± 11.6[ab]	0.12 ± 0.00[b]	0.91	5.23 ± 1.42[a]	0.51 ± 0.01[a]	0.99	806 ± 18[a]
20	78.3 ± 5.96[b]	0.13 ± 0.01[b]	0.92	7.10 ± 2.27[a]	0.49 ± 0.00[a]	0.99	838 ± 91[a]

[1]Values are means ± standard deviations; Mean values with different letters within the same column are significantly different from each other ($p < 0.05$). [2]K refers to the consistency coefficient of the forward sweep; K′ is the consistency coefficient of the backward sweep; n is the flow behaviour index of the forward sweep; n′ is the flow behaviour index of the backward sweep; HL equals the hysteresis loop area; R^2 is the coefficient of determination between the experimental data and power law model prediction

Table 4.63 Effect of storage time and temperature on power law parameters and Hysteresis loop area of emulsion containing 25 mM NaCl

Days	K (Pas^n)	n	R^2	K' (Pas^n)	n'	R^2	HL (Pas^{-1})
5°C							
1	26.5 ± 1.78[a]	0.36 ± 0.02[a]	0.99	5.78 ± 0.14[a]	0.58 ± 0.01[a]	0.99	648 ± 22[a]
3	153 ± 5.81[b]	0.04 ± 0.00[b]	0.95	11.0 ± 1.56[b]	0.43 ± 0.01[b]	0.99	1302 ± 99[b]
9	162 ± 20.8[b]	0.07 ± 0.00[c]	0.95	23.7 ± 1.45[c]	0.33 ± 0.04[c]	0.99	1309 ± 124[b]
15	166 ± 11.6[b]	0.06 ± 0.00[c]	0.87	23.0 ± 0.26[c]	0.35 ± 0.00[c]	0.99	1004 ± 110[c]
20	164 ± 114[b]	0.05 ± 0.00[c]	0.87	21.5 ± 3.62[c]	0.35 ± 0.07[c]	0.99	1137 ± 28[bc]
20°C							
1	26.5 ± 1.78[a]	0.36 ± 0.02[a]	0.99	5.78 ± 0.14[a]	0.58 ± 0.01[ac]	0.99	648 ± 22[a]
3	48.7 ± 1.17[b]	0.21 ± 0.01[b]	0.93	6.02 ± 0.02[a]	0.52 ± 0.00[b]	0.99	707 ± 2[b]
9	48.3 ± 0.54[b]	0.16 ± 0.00[c]	0.95	4.46 ± 0.09[b]	0.50 ± 0.00[b]	0.99	574 ± 3[c]
15	41.8 ± 1.62[c]	0.10 ± 0.00[d]	0.80	2.18 ± 0.07[c]	0.55 ± 0.00[ab]	0.99	447 ± 13[d]
20	25.8 ± 0.01[a]	0.12 ± 0.01[d]	0.88	1.05 ± 0.08[c]	0.61 ± 0.00[c]	0.99	309 ± 13[e]
45°C							
1	26.5 ± 1.78[a]	0.36 ± 0.02[a]	0.99	5.78 ± 0.14[a]	0.58 ± 0.01[a]	0.99	649 ± 22[a]
3	41.1 ± 1.03[b]	0.24 ± 0.00[b]	0.93	6.83 ± 0.12[a]	0.51 ± 0.00[b]	0.99	575 ± 11[b]
9	13.5 ± 3.20[c]	0.20 ± 0.03[b]	0.84	1.76 ± 0.42[b]	0.51 ± 0.03[b]	0.99	162 ± 18[c]
15	9.12 ± 1.81[c]	0.26 ± 0.01[b]	0.97	1.72 ± 0.15[b]	0.50 ± 0.00[b]	0.99	137 ± 40[c]
20	1.81 ± 0.75[d]	0.48 ± 0.05[c]	0.99	1.05 ± 0.28[b]	0.56 ± 0.03[ab]	0.99	33 ± 13[d]

[1]Values are means ± standard deviations; Mean values with different letters within the same column are significantly different from each other ($p < 0.05$). [2]K refers to the consistency coefficient of the forward sweep; K' is the consistency coefficient of the backward sweep; n is the flow behaviour index of the forward sweep; n' is the flow behaviour index of the backward sweep; HL equals the hysteresis loop area; R^2 is the coefficient of determination between the experimental data and power law model prediction

Table 4.64 Effect of storage time and temperature on power law parameters and Hysteresis loop area of emulsion containing 8% (w/w) vinegar

Days	K (Pas^n)	n	R^2	K′ (Pas^n)	n′	R^2	HL (Pas^{-1})
5°C							
1	7.60 ± 0.31[a]	0.49 ± 0.00[a]	0.99	4.19 ± 0.16[a]	0.58 ± 0.01[a]	0.99	167 ± 12[a]
3	92.8 ± 6.11[b]	0.11 ± 0.02[b]	0.97	16.7 ± 1.75[b]	0.36 ± 0.02[b]	0.99	941 ± 5[b]
9	92.9 ± 9.23[b]	0.12 ± 0.06[c]	0.97	16.3 ± 2.40[b]	0.37 ± 0.01b	0.99	941 ± 26[b]
15	93.5 ± 3.92[b]	0.13 ± 0.00[bc]	0.96	16.3 ± 2.93[b]	0.38 ± 0.02[b]	0.99	899 ± 52[b]
20	93.0 ± 0.51[b]	0.12 ± 0.07[bc]	0.95	13.0 ± 4.56[b]	0.41 ± 0.05[b]	0.99	901 ± 51[b]
20°C							
1	7.60 ± 0.31[a]	0.49 ± 0.00[a]	0.99	4.19 ± 0.16[a]	0.58 ± 0.01[a]	0.99	167 ± 12[a]
3	20.3 ± 1.92[b]	0.33 ± 0.01[b]	0.96	5.29 ± 0.01[b]	0.53 ± 0.00[b]	0.99	433 ± 53[b]
9	30.6 ± 2.89[c]	0.26 ± 0.01[c]	0.95	5.72 ± 0.14[b]	0.51 ± 0.00[c]	0.99	472 ± 30[b]
15	34.1 ± 2.72[cd]	0.25 ± 0.01[c]	0.98	8.16 ± 0.20[c]	0.46 ± 0.00[d]	0.97	470 ± 17[b]
20	36.9 ± 0.59[d]	0.24 ± 0.00[c]	0.98	9.37 ± 0.33[d]	0.44 ± 0.00[e]	0.99	466 ± 18[b]
45°C							
1	7.60 ± 0.31[a]	0.49 ± 0.00[a]	0.99	4.19 ± 0.16[a]	0.58 ± 0.01[a]	0.99	167 ± 12[a]
3	11.9 ± 0.19[b]	0.39 ± 0.00[b]	0.99	5.58 ± 0.04[b]	0.51 ± 0.00[b]	0.99	134 ± 2[a]
9	13.0 ± 0.63[b]	0.38 ± 0.00[c]	0.99	5.76 ± 0.04[b]	0.50 ± 0.01[cb]	0.99	148 ± 26[a]
15	13.2 ± 0.57[b]	0.37 ± 0.00[c]	0.98	5.78 ± 0.00[b]	0.50 ± 0.00[c]	0.99	153 ± 13[a]
20	12.7 ± 1.38[b]	0.36 ± 0.01[c]	0.98	5.08 ± 0.31[c]	0.51 ± 0.01[bc]	0.99	165 ± 17[a]

[1]Mean values with different letters within the same column are significantly different from each other ($p < 0.05$).

[2]K refers to the consistency coefficient of the forward sweep; K′ is the consistency coefficient of the backward sweep; n is the flow behaviour index of the forward sweep; n' is the flow behaviour index of the backward sweep; HL equals the hysteresis loop area; R^2 is the coefficient of determination between the experimental data and power law model prediction

Table 4.65 Effect of storage time and temperature on power law parameters and Hysteresis loop area of emulsion containing 0.5% (w/w) citric acid

Days	K (Pas^n)	n	R^2	K′ (Pas^n)	n′	R^2	HL (Pas^{-1})
5°C							
1	19.9 ± 0.48[a]	0.38 ± 0.01[a]	0.99	5.61 ± 1.37[a]	0.57 ± 0.03[a]	0.99	508 ± 69[a]
3	76.3 ± 1.28[b]	0.22 ± 0.01[b]	0.98	7.85 ± 0.77[b]	0.57 ± 0.02[a]	0.99	1265 ± 54[b]
9	155 ± 3.51[c]	0.13 ± 0.04[c]	0.98	22.6 ± 0.63[c]	0.42 ± 0.03[b]	0.99	1686 ± 94[c]
15	287 ± 7.23[d]	0.06 ± 0.00[d]	0.99	28.1 ± 0.21[d]	0.40 ± 0.01[b]	0.99	2437 ± 127[d]
20	308 ± 3.31[e]	0.06 ± 0.00[d]	0.97	26.0 ± 0.06[e]	0.43 ± 0.01[b]	0.99	2808 ± 97[e]
20°C							
1	19.9 ± 0.48[a]	0.38 ± 0.01[a]	0.99	5.61 ± 1.37[a]	0.57 ± 0.03[a]	0.99	508 ± 69[a]
3	22.1 ± 0.76[a]	0.41 ± 0.00[a]	0.99	5.89 ± 0.08[a]	0.60 ± 0.01[a]	0.99	618 ± 47[a]
9	36.2 ± 3.44[b]	0.34 ± 0.02[b]	0.99	7.40 ± 0.36[a]	0.57 ± 0.02[a]	0.99	874 ± 104[b]
15	68.8 ± 2.22[c]	0.24 ± 0.01[c]	0.98	10.9 ± 0.06[b]	0.51 ± 0.00[b]	0.99	1158 ± 98[c]
20	98.4 ± 1.96[d]	0.19 ± 0.00[d]	0.95	14.7 ± 0.56[c]	0.47 ± 0.00[c]	0.99	1234 ± 2[c]
45°C							
1	19.9 ± 0.48[a]	0.38 ± 0.01[a]	0.99	5.61 ± 1.37[a]	0.57 ± 0.03[a]	0.99	508 ± 69[a]
3	30.4 ± 1.86[b]	0.37 ± 0.00[a]	0.99	8.69 ± 0.55[b]	0.56 ± 0.00[ab]	0.99	647 ± 29[ab]
9	42.5 ± 6.37[c]	0.30 ± 0.02[b]	0.98	9.19 ± 0.55[bc]	0.53 ± 0.00[b]	0.99	728 ± 142[b]
15	56.4 ± 2.09[d]	0.26 ± 0.00[c]	0.98	11.7 ± 0.39[d]	0.50 ± 0.00[c]	0.99	749 ± 11[b]
20	62.5 ± 4.57[d]	0.23 ± 0.02[c]	0.97	10.7 ± 0.37[cd]	0.49 ± 0.00[c]	0.99	789 ± 34[c]

[1]Mean values with different letters within the same column are significantly different from each other ($p < 0.05$).

[2]K refers to the consistency coefficient of the forward sweep; K′ is the consistency coefficient of the backward sweep; n is the flow behaviour index of the forward sweep; n' is the flow behaviour index of the backward sweep; ; HL equals the hysteresis loop area; R^2 is the coefficient of determination between the experimental data and power law model prediction

influence of the yield stress. In this study, the optimum emulsion was semi solid viscous fluid, therefore viscous dissipation and influence of the yield stress may account for the observed negative values.

The structuration of the optimum emulsion, which is a typical behaviour of BGNF used to achieve stabilization, was observable in terms of increased consistency coefficient and or decrease in flow behaviour index with storage time. Both the K and K' increased significantly ($p < 0.05$) at 5°C during storage. The K' however reached equilibrium on the 3rd day of storage and there was no significant change afterwards. The properties (K and K') of the optimum emulsion on the 20th day of storage were significantly improved compared to the first day of manufacture. At room temperature however, K and K' of the optimum emulsion showed significant ($p < 0.05$) decline on the 20th day of storage. The sudden decline was as a result of structurally weakened strength of BGNF emulsion as a function of time and this may probably be due to accelerated microbial activities in the emulsion at room temperature. Study at 45°C showed that the K of the optimized emulsion significantly increased on the 20th day of storage while K' was not significantly different from the first day of manufacture. Although there was increase ($p < 0.05$) within the 3rd day of storage, a significant decrease was observed after the 3rd day of study. The behaviour of the optimum emulsion at room temperature and elevated temperature of 45°C were closely related. There were relative differences between the parameters of power law for the forward and backward curves at all storage temperature, no general trend for the K' as a function of time were observed at 20 and 45°C.

Table 4.63 shows the effect of 25 mM NaCl on the power law parameters as a function of storage time and temperature. The observed structuration and structural weakness in the emulsion, which manifested as significant increase and decrease in consistency coefficient (K and K') respectively of the 25 mM NaCl emulsion over time was dependent on the storage temperature. Both K and K' at 5°C increased significantly in the first three days and reached equilibrium on the 9th day of study. The consistency coefficients of the 9th, 15th, and 20th day were not different. The consistency coefficient at 20 and 45°C increased significantly till 9th and 3rd day of storage respectively. Significant decline in K and K' were recorded at both temperatures of 20 and 45°C on the 20th day of storage relative to the 15th day. Although there was no significant difference in K of the first day (26.51 Pas^n) and that of the 20th day (25.75 Pas^n) at 20°C their corresponding K' showed significant difference (5.78 and 1.05 Pas^n) respectively. This was an indication that both the BGNF matrix structure and droplet-droplet interactions had been weakened with age. Significant ($p < 0.05$) decrease in properties (K and K') were observed at 45°C relative to first day of storage. A comparison between storage at

room temperature and elevated temperature of 45^{o}C however, showed that decrease in K and K' were more pronounced at 45^{o}C on the 20th day of study relative to the 15th day of storage. However, there was no significant difference ($p < 0.05$) between the K on the 20th day of storage and that on the first day of manufacture, at 20^{o}C. K at 45^{o}C showed a significant difference on the 20th day of storage compared to the first day of manufacture. Decreases in K and K' of emulsion with NaCl were more intense when compared with optimum emulsion at 20 and 45^{o}C. Pronounced decline in K and K' in the emulsion with NaCl relative to optimum emulsion was probably a result of combined effect of temperature, age and the long term deteriorative effect of NaCl in the emulsion. The flow behaviour index for the forward and backward curve at 5^{o}C also showed significant decrease with storage time indicating a loss of fluidity and high resistance to flow over time and more pronounced pseudoplasic behaviour (Ma and Boye, 2013). This is linked to product of low storage temperature and the intrinsic characteristics of the BGNF matrix used to achieve stabilization of the emulsion. The increase in n was more observable at 45^{o}C and this was because of loss of consistency at this temperature. The n' was observed to increase relative to n with storage time for NaCl containing emulsion and this was more pronounced at 45^{o}C and 20^{o}C.

Table 4.64 shows the effect of vinegar on the power law parameters as a function of storage time and temperature. Both the K and K' at 5^{o}C increased significantly within the first three days of storage and reached equilibrium around the 3rd day. The changes afterwards were not significantly different from the consistency coefficients of day 3. In a similar manner, the flow behaviour of the forward curve showed a correspondingly significant decrease till day 3 and no significant decrease were observed afterwards. Similar behaviour was observed at 20 and 45^{o}C. It should be noted that both the K and K' and n and n' of the emulsion containing vinegar at the 20th day of storage at 5, 20 and 45^{o}C were significantly higher and lower respectively, than on the first day of manufacture. This shows that the properties of the emulsions were well kept after the initial equilibrium of BGNF emulsion structuration was attained. This was an indication that the presence of vinegar in the emulsion, though hindered polymer structuration by altering the molecular structure of BGNF during formation, was able to preserve the polymer networks from spoilage at all storage temperature and time. The constancy of these parameters after equilibrium time has been reached was as a result of the intactness of both the polymer gel/network and the oil-droplet structures and their interactions. When the influence of time was considered on shearing, however, there were structural breakdown indicated by the marked decrease in K' relative to K at all storage time and temperature. The behaviour of the emulsions stored at 20^{o}C and 45^{o}C was however similar (all

the parameters of power law are very close in value). However the storage at 5^{o}C was relatively better since the parameters of power law model after structural destruction (K' and n') were relatively improved than at the temperatures of 20 and 45^{o}C.

The significant increase (K and K') and decrease (n and n') in the parameters of power law model throughout the storage time and at all temperatures in the emulsions with 0.5% (w/w) citric acid was an indication that citric acid at the studied concentration possessed a preservative properties. When compared with the optimum emulsion, emulsion with 0.5% (w/w) citric acid had similar characteristics of structuration with age. Like other studied BGNF emulsions, emulsions with citric acid were thixotropic and the parameters of the forward curves were quantitatively improved than the backward curves. The behaviour of the 0.5% (w/w) citric acid containing emulsion stored at 20^{o}C was comparable to 45^{o}C. After shearing however the emulsion remained non-Newtonian pseudoplastic fluid suggesting a decreasing viscosity with increasing shear rate. Although storage time and temperature affected the behaviour of this emulsion, the properties of the emulsion were greatly improved (significantly increased) at all the storage conditions.

Tables 4.62, 4.63, 4.64 and 4.65 presented the hysteresis loop of all the emulsions at all storage conditions. Although hysteresis loop is a measure of extent of thixotropy/structural breakdown, as established earlier for BGNF emulsions, its magnitude is a function of the relative viscosity of the system which is related to both the BGNF-matrix strength and oil droplet - oil droplet and the BGNF matrix - oil droplets interactions. The structures of all the categories of emulsions were the same on the first day of preparation at all temperatures and therefore changes in this value (magnitude of thixotropy) were ascribed to decrease or increase of the BGNF polymer strength used to achieve stabilization and associated structural interactions (droplet-droplet and BGNF matrix-oil droplet) with age. The higher the magnitude of hysteresis the more viscous the system was and hence the more intact the structure and droplet interaction in the emulsion. The result of the magnitude of hysteresis loop areas showed peculiarity to each studied system, however the magnitude of hysteresis at 5^{o}C was higher than those at 20 and 45^{o}C for all the emulsions. Regarding, the optimum emulsion, the magnitude of hysteresis loop area showed a wide difference between the storage at low temperature and higher temperatures. Structural destruction was pronounced at low temperature, while the magnitude of hysteresis loop at higher temperatures were relatively lower. This may be connected with the high and low viscosities of the emulsions at low and high temperatures, respectively. Although the structures at both 20 and 45^{o}C condition of storage were both closely related, the magnitude of hysteresis loop on the 20th day of storage showed a reduction ($p <$

0.05) and lower than at 45^{o}C. The drastic reduction was as a result of weakened emulsion structure which could be as a result of age.

The effect of NaCl at higher temperature on the emulsion structure is presented in Table 4.63. The magnitude of hysteresis significantly ($p < 0.05$) decreased at 20 and 45^{o}C with storage time. Emulsion containing NaCl showed a great reduction ($p < 0.05$) in the magnitude of hysteresis loop on the 15th and 20th day of study at 45^{o}C relative to 20^{o}C. The implication was that the structure of NaCl containing emulsion has become less viscous due to loss of BGNF matrix strength and oil-droplet interactions at high temperature. Storage at 5^{o}C was however greatly improved. This could be as a result of decreased emulsion fluidity at low temperature.

The structuration of emulsion with vinegar was minimal (particularly at 20 and 45^{o}C) and the structures were comparable ($p < 0.05$) after an initial equilibrium was reached. The magnitudes of hysteresis loop area were constant and not different after the 3rd day of storage at all temperatures. This shows the preservative characteristics of vinegar on the emulsion, by maintaining both polymeric strength and structural interaction in the emulsion. The behaviour of emulsions with vinegar was however different at all the studied temperatures.

The magnitude of hysteresis obtained for 0.5% citric acid was relatively higher at all temperatures and time than other emulsion systems. Although there were observed increase in time dependency and structural breakdown when sheared, increase in the magnitude of hysteresis loop area gave information on the extent of structuration and hence viscosity with time. It seemed that citric acid did not only preserve the structures, it also magnified the structuration of BGNF emulsions which made it more viscous over time and at all storage temperatures.

4.8.3 Summary on the effect of storage temperature and time on emulsion stability and rheological properties of optimum and most stable additive containing emulsions

Emulsion stability studies over 20 days of storage at three temperatures showed oil droplets movements and aggregations and this was conspicuously noticed in the first three days of storage before equilibrium condition set in using Turbiscan MA 2000. The changes in oil droplets sizes due to aggregation was manifested in terms of increasing and decreasing in backscattering flux and this was dependent on the size of the oil droplets relative to the wavelength of the light source of the Turbiscan vertical scanner. Generally, all emulsions were more stable at low temperature (5^{o}C) than at room temperature (20^{o}C) and high temperature (45^{o}C). Good stability at low temperature could be explained in terms of high viscosity and good

structural formation of BGNF gels which restrained the oil droplet movement. All the emulsion characteristics at 5^{o}C were properly kept and preserved. The rheological studies on the other hand showed differently interesting results. The apparent viscosity at the maximum point of shear gradient, quantification by power law model and magnitude of hysteresis loop showed that the apparent viscosity, consistency coefficient and magnitude of hysteresis loop were relatively higher at 5^{o}C for all of the emulsions at all storage conditions. It was however interesting to note that the apparent viscosity at maximum point of shear gradient, consistency coefficients of power law rheological model and magnitude of hysteresis loop area for some emulsions either increased significantly throughout storage time and temperature or experience an initial significant increase before decline. Interestingly, the initial increase in rheological properties was observed during the first three days of storage where most oil aggregation had reached optimum. The droplet-droplet interaction should at this point be minimum and hence a significant reduction in rheological properties. Most studies on storage stabilities reported decrease or insignificant difference in all of these properties with time. For example Ma and Boye (2013) investigated the storage stability of salad dressing emulsions supplemented with various pulse flours using power law parameters as indicator. They reported significant decrease in the consistency coefficients between the first day of manufacture and 12th day of storage. Mandala *et al.* (2004) also reported a decrease in consistency index for white model sauce emulsion during a 10-day storage investigation. Decrease in consistency coefficient over time was explained to be connected with decreased droplet interaction with age. A non-significant increase in apparent viscosity and negative magnitude of hysteresis loop area was reported by Gonçalves and Maia Campos (2009) in their study on shelf life and rheology of emulsions containing vitamin C and its derivatives. This behaviour of structuration over time observed in BGNF stabilized emulsions was therefore linked to the intrinsic properties of BGNF gel and less to the oil droplet aggregations. It therefore seemed that the rheological behaviours of BGNF stabilized emulsions (including the additive containing emulsions) were completely masked by the intrinsic behaviour of the BGNF matrix. Although the influence of the additive resulted into changes in the molecular configuration of the BGNF polymer structure during continuous phase preparation, intrinsic properties (thickening or structuration with time) of the BGNF matrix did not fail to manifest. An attempt to link stability to the measured rheological properties was therefore very complicated as the rheological properties of BGNF stabilized emulsion was a product of both the behaviour of oil interactions and dominating structuration properties of BGNF matrix.

CHAPTER FIVE

SUMMARY, CONCLUSION AND RECOMMENDATION

The overall purpose of this research work was the assessment of the suitability of the BGNF as a natural emulsifier/stabilizer in food emulsion systems. Two properties of interest were the emulsion stability and rheological properties of BGNF-stabilized emulsion. Emulsion stability parameters were determined microscopically and in terms of oil droplet sizes and by using Turbiscan MA 2000 while the rheological measurements were carried out using a rotational and dynamic rheometer. The rheological measurements included flow curves, magnitude of hysteresis loop area and time dependency, frequency dependency and creep and recovery measurement.

The preliminary part of this work involved the determination of the optimum conditions necessary for the processing of BGNF-stabilized emulsions. The effect of processing parameters like homogenization time and speed was investigated on emulsion properties such as oil droplet size and emulsion apparent viscosities. In order to achieve objective 1 in this study, optimal workable processing conditions were used for the optimization of the emulsion components that resulted into highest stability (optimum emulsion) and to investigate the effects of emulsion components on the physical stability parameters. Stability parameters such as the microstructure, oil droplet size, initial backscattering, BS_{avo} and equilibrium backscattering, BS_{eq} were investigated on emulsion components. The experiments for this investigation were designed by using response surface methodology (RSM). All important emulsion stability characteristics were modeled as a function of emulsion components (SFO and BGNF) in accordance with objective 1.

Rheological properties of the BGNF-stabilized emulsions were also investigated and efforts were made to relate the rheological properties to stability data (objective 7). The time dependent, steady shear and viscoelastic rheological properties of the BGNF-stabilized emulsion were investigated and modeled as a function of emulsion components (BGNF and SFO) according to objectives 2, 3 and 4. Both the hysteresis loop method and steady shear decay were used for the investigations of time-dependent properties and decay data were described using Weltman model, Figoni-Shoemaker model, Hahn model and first order stress decay with zero equilibrium stress value. The steady shear rheological data were fitted to different popular rheological models that are useful in the design of processing operations and related equipment such as Power law, Herschel-Bulkley, Bingham and Casson equations. Effect of the emulsion components at different levels on the rheological parameters of the fitted

models was also determined. Comparative studies of the suitability of the model equations were made to ascertain the appropriateness of the rheological equations to describe BGNF stabilized emulsion systems.

In order to achieve objective 4, the effect of BGN varieties and food additives was investigated on the stability and rheological properties of the optimum emulsion. Four varieties of bambara groundnut flour (BGNF) used to stabilized oil-in-water emulsion at optimal ingredient (BGNF and SFO) level were the black eye, brown eye, red, and brown varieties. The respective ability of BGNF to stabilize oil-in-water emulsion was evaluated and compared. The additives examined were sodium chloride (NaCl), citric acid and vinegar. Among the parameters considered for judging the relative effect of the additives on emulsion properties are the droplet size, BS_{Avo}, BS_{eq}, power law parameters (K and n), magnitude of hysteresis loop area, Weltman parameters (A and B), G' and G" and Q (t). The most stable additive containing emulsions were identified and used for storage analysis.

The behaviour of optimum emulsion and most stable additive containing emulsions were investigated during storage at three different temperatures in accordance with objective 6. Additive emulsions studied were emulsions containing 25 mM NaCl, 0.5% (w/w) citric acid and 8% vinegar. Both the emulsion stability and rheological properties were assessed on the 1st, 3rd, 9th, 15th, and 20th day of storage.

The following conclusions can be made based on each section

1.0 Effect of processing parameters

1.1 Gelatinized BGNF was able to form a semi solid emulsion.

1.2 Processing conditions affected the emulsion stability and rheological properties

1.3 The droplet sizes and emulsion viscosity decreased and increased, respectively as the homogenization time and speed increased.

2.0 Emulsion stability and components optimization of O/W emulsion stabilized by BGNF

2.1 All the BGNF stabilized emulsions were macro (μm) emulsions, the higher the BGNF concentration the lower the particle size and the higher the stability. This is in line with hypothesis 1. Macro (μm) emulsions are desirable in some food delivery systems.

2.2 The emulsions were stable to creaming and predominantly affected by destabilization mechanism involving oil droplet aggregation.

2.3 The empirical models developed for *BS* showed that the mutual increase of both BGNF and SFO played significant roles in structural formation.

2.4 Emulsion system that contained highest 7% (w/w) BGNF and 40% (w/w) SFO was selected as the most stable emulsion in line with hypothesis 3.

3.0 Effect of emulsion components on time-dependent, time-independent and viscoelastic properties

3.1 All the BGNF-stabilized oil-in-water emulsions studied were time-dependent thixotropic fluids. This is desirable in mastication and chewing.

3.2 The thixotropy of the emulsions was SFO and BGNF concentrations and shear rate dependent.

3.3 Both hysteresis loop and constant decay methods showed that emulsion containing 7% (w/w) BGNF and 40% (w/w) SFO possessed the highest percentage of thixotropy.

3.4 Weltman, Hahn and Figoni and Shoemaker models were suitable to describe the time dependent rheological behaviour of BGNF stabilized emulsions because of high R^2 values and low RMSE and SE values. This is in line with hypothesis 2. First order stress decay with zero equilibrium model was found not suitable to describe the time dependent behaviour.

3.5 Empirical model developed for magnitude of hysteresis loop area showed that the presence of both BGNF and SFO in an emulsion system increases thixotropic characteristics of BGNF-stabilized emulsion.

3.6 All the emulsions were non-Newtonian pseudoplastic fluids. Pseudo-plasticity is desirable in product spreadability and processability.

3.7 The pseudoplastic nature was as a result of both droplet defloculation and non-Newtonian characteristics of BGNF matrix.

3.8 Both BGNF and SFO had pronounced effect on the pseudo plasticity of the emulsion.

3.9 Power law, Herschel-Bulkley, Bingham and Casson rheological models were able to predict the steady shear properties of BGNF-stabilized emulsions in line with hypothesis 2. However, Casson model was a better predictor because of its high R^2 and low RMSE and SE values.

3.10 All emulsions possessed yield stress according to the Herschel-Bulkley, Bingham and Casson models. Yield stress is desirable in product stability and rigidity.

3.11 All the BGNF-stabilized emulsions were visco-elastic fluids. A high viscoelastic property is desirable during product transportation and in long term storage stability.

3.12 Emulsion containing 7% (w/w) BGNF and 40% (w/w) SFO is the most structured, viscous and elastic emulsion among the emulsion investigated.

3.13 Increased BGNF and SFO in the emulsions increased the viscous (G') and elastic (G") properties in line with hypothesis 2.

3.14 Emulsion formulated with 7% (w/w) SFO and 40% (w/w) possessed the least and highest compliance and recoverable strain respectively.

4.0 Effect of BGN varieties on optimal emulsion stability and rheological properties

4.1 All the bambara groundnut flour (BGNF) varieties formed stable oil-in-water emulsions at concentrations of BGNF and SFO investigated.

4.2 The effects of BGNF of the four varieties were not significantly different on the stability and rheological properties of oil-in-water emulsions.

4.3 Probable difference in proximate compositions did not seem to have pronounced effect on the matrix strength of the BGNF properties of the emulsions.

4.4 All emulsions were thixotropic, pseudoplastic and viscoelastic in nature.

5.0 Effect of food additives on optimal emulsion stability and rheological properties

5.1 BGNF emulsion was sensitive to the presence of food additives in the BGNF matrix and this had caused changes in emulsion structural properties in line with hypothesis 1.

5.2 The presence of NaCl, vinegar and citric acid in the BGNF matrix reduced the emulsion stability, apparent viscosities and decreased the time dependent thixotropic properties of the optimal emulsion.

5.3 NaCl, citric acid and vinegar all decreased viscoelastic properties (G' and G") and consistency coefficient (K) and recoverable strain (Q (t)%) at all tested concentrations.

5.4 Vinegar induced large particle size which may have impact on sensory values and long term stability of BGNF stabilized emulsion while the presence of citric acid had little effect of the microstructure and emulsion stability.

6.0 Effect of storage time and temperature on optimal and most stable additive containing emulsion stability and rheological properties

6.1 Emulsion destabilization mainly by oil droplet aggregation occurred at all storage conditions and the extent is largely dependent on the nature of the emulsions.

6.2 Generally, stability was improved at low temperature relative to high temperatures in line with hypothesis 4.

6.3 All emulsions remained thixotropic at all storage temperatures and time.

6.4 There was observed structuration of some of the emulsions with storage time and temperatures and this observation was relatively higher at low temperature of $5^{o}C$.

6.5 The intrinsic properties of BGNF matrix seemed to dominate the rheological properties of BGNF stabilized emulsion relative to the droplet-droplet interactions.

6.6 Long term stability of emulsion implied that NaCl might have a deteriorative effect on the BGNF matrix structure thereby affecting both the long term viscosity and stability negatively contrary to hypothesis 4.

6.7 Influence of vinegar and citric acid showed a preservative potential in the BGNF stabilized emulsions. Although the acidulants promoted the BGNF intrinsic properties they however, preserved the BGNF matrix.

The following may however be of interest for future investigation

- Interaction of BGNF with other naturally available bio-polymers such as proteins and hydrocolloids in emulsion systems.
- Use of thermally processed BGNF seeds as supplements in food emulsion system
- Use of isolated and modified BGNF protein in food emulsion systems
- Use of native and modified starch of BGNF and their interaction with proteins in food emulsion system
- Interaction of protein isolates and hydrolase with modified starches and surfactants may also be considered for investigation in emulsion system.

REFERENCES

Abdel-Raouf ME (2011). Factors Affecting the Stability of Crude Oil Emulsions, www.intechopen.com. Assessed 3rdNovember 2-12. pp. 188

Abu-Jdayil, B., Al-Malah, K. & Asoud, H.(2002). Rheological characterization of milled sesame (tehineh). *Food Hydrocolloid*. 16, 55–61.

Adebowale, K.O. & Lawal, O.S. (2002). Effect of annealing and heat moisture conditioning on the physicochemical characteristics of bambara groundnut (*Voandzeia subterranean*) starch. *Nahrung/Food*. 46: 311-316.

Agboola, S. O., & Dalgleish, D. G. (1996). Effects of pH and Ethanol on the Kinetics of Destabilisation of Oil-in-Water Emulsions Containing Milk Proteins. *Journal of the Science of Food and Agriculture*, *72*(4), 448-454.

Agboola, S. O., Singh, H., Munro, P. A., Dalgleish, D. G., & Singh, A. M. (1998). Destabilization of oil-in-water emulsions formed using highly hydrolyzed whey proteins. *Journal of Agricultural and Food Chemistry*, *46*(1), 84-90.

Akoh, C. C. (Ed.). (1994). *Carbohydrate polyesters as fat substitutes* (Vol. 62). CRC Press.

Aktaş, N., & Genccelep, H. (2006). Effect of starch type and its modifications on physicochemical properties of bologna-type sausage produced with sheep tail fat. *Meat Science*, *74*(2), 404-408.

Alparslan, M. & Hayta, M. (2002). Rheological and sensory properties of pekmez (grape molasses) / tahin (sesame paste) blends. *Journal of Food Engineering* 54: 89-93.

Altan, A. Kus, S. and Kaya, A.(2005). Rheological Behaviour and Time Dependent Characterization of Gilaboru Juice (Viburnum opulus L.). *Food Science and Technology International*. 11:129.

Álvarez Cerimedo, M. S., Iriart, C. H., Candal, R. J., & Herrera, M. L. (2010). Stability of emulsions formulated with high concentrations of sodium caseinate and trehalose. *Food Research International*, *43*(5), 1482-1493.

Aremu, M. O., Olaofe, O., Akintayo, E. T., & Adeyeye, E. I. (2008).Foaming, Water Absorption, Emulsification and Gelation Properties of Kersting's Groundnut {Kerstingiellageocarpa) and Bambara Groundnut {Vigna subterranean) Flours as Influenced by Neutral Salts and Their Concentrations.*Pakistan Journal of Nutrition*, *7*(1), 194-201.

Arora, A., Chism, G. W. & Shellhammer, T.H. (2003).Rheology and Stability of Acidified Food Emulsions treated with High Pressure. *Journal of Agricultural and Food Chemistry.* 51 : 2591-2596.

Augosto, P.E.D., Falguera, V., Cristianini, M., & Ibarz, A. (2012). Rheological Behavior of Tomato Juice: Steady- State Shear and Time-Dependent Modeling. Food Bioprocess Technology. 5: 1715-1723.

Ayamdoo, A. J., Badii, K. B., & Sowley, E. N. K. (2013). Storage Systems For Bambara Groundnut (Vigna Subterranean) And Their Implications For Bruchid Pest Management In Talensi-Nabdam District, Upper East Region, Ghana. *International Journal of Scientific & Technology Research*, *2*(2).

Bagley, E.B. & Christianson, D.D. (1982). Swelling capacity of starch and its relationship to suspension viscosity-effect of cooking time, temperature and concentration. *Journal of Texture Studies.* 13: 115-126.

Bamshaiye, O.M., Adeghola, J.A. & Bamishaiye, E.I. (2011). Bambara groundnut: an under-utilized nut in Africa. *Advances in Agricultural Biotechnology.* 1: 60-70.

Barbosa-Cánovas, G. V., Kokini, J. L., Ma, L., & Ibarz, A. (1996). The rheology of semiliquid foods. *Advances in Food and Nutrition Research*, *39*, 1-69.

Barnes, H. A. (1997). Thixotropy—a review. *Journal of Non-Newtonian Fluid Mechanics*, *70*(1), 1-33.

Bellalta, P., Troncoso, E., Zuniga, R.N. & Aguilera, J.M. (2012). Rheological and microstructural characterization of WPI-stabilized emulsions exhibiting time-dependent flow behaviour. *LWT-Food Science and Technology*. 46 : 375-381.

Blijdenstein, T. B., Hendriks, W. P., van der Linden, E., van Vliet, T., & van Aken, G. A. (2003). Control of strength and stability of emulsion gels by a combination of long-and short-range interactions. *Langmuir*, *19*(17), 6657-6663.

Blijdenstein, T. B. J., Zoet, F. D., van Vliet, T., van der Linden, E., & van Aken, G. A. (2004). Dextran-induced depletion flocculation in oil-in-water emulsions in the presence of sucrose. *Food Hydrocolloids*, *18*(5), 857-863.

Boode, K., Bisperink, C., & Walstra, P. (1991). Destabilization of O/W emulsions containing fat crystals by temperature cycling. *Colloids and Surfaces*, *61*, 55-74.

Bortnowska, G., Balejko, J., Tokarczyk, G., Romanowska-Osuch, A., & Krzemińska, N. (2014). Effects of pregelatinized waxy maize starch on the physicochemical properties and stability of model low-fat oil-in-water food emulsions. *Food Hydrocolloids*, *36*, 229-237.

Brough, S. H., Azam-Ali, S. N., & Taylor, A. J. (1993). The potential of bambara groundnut (*Vigna subterranea*) in vegetable milk production and basic protein functionality systems. *Food Chemistry*, *47*(3), 277-283.

Can Karaca, A., Nickerson, M. T., & Low, N. H. (2011). Lentil and chickpea protein-stabilized

emulsions: Optimization of emulsion formulation. *Journal of Agricultural and Food Chemistry*, *59*(24), 13203-13211.

Camino, N & Pilosof, A.M.R. (2011) Hydroxypropymethylcellulose at the oil-waterinterface. Part II. Submicron-emulsions as affected by pH. *Food Hydrocolloids* 25(5) :1051-1062.

Campanalla, O.H, Dorward N.M & Singh, H (1995). A study of the rheological properties of concentrated food emulsions. *Journal of Food Engineering 25*: 427-440.

Caubet, S.,Guer, Y.L.,Grassil, B., Omari, K.E. and Normandin, E. (2011). A low-enegy emulsification batch mixer for concentrated oil-in-water emulsion. *AlChe Journal* 57, 27-39.

Celia, C., Trapasso, E., Cosco, D., Paolino, D., & Fresta, M. (2009). Turbiscan Lab Expert analysis of the stability of ethosomes and ultradeformable liposomes containing a bilayer fluidizing agent. *Colloids and Surfaces B: Biointerfaces*, *72*(1), 155-160.

Cerimedo, M.S.A., Iriart, C.H.,Canda,R.J. & Herrera, M.L. (2010). Stability of emulsions formulated with high concentrations of sodium caseinate and trehalose. *Food Research International*, 43, 1482-1493..

Chanamai, R. & McClements, D. J. (2000). Dependence of creaming and rheology of monodisperse oil-in-water emulsions on droplet size and concentration. *Colloids and Surfaces A: Physicochemical and Engineering Aspects*, *172*(1), 79-86.

Chanamai, R. A. D. J. M., & McClements, D. J. (2002). Comparison of gum arabic, modified starch, and whey protein isolate as emulsifiers: influence of pH, CaCl2 and temperature. *Journal of Food Science*, *67*(1), 120-125.

Charoen, R., Jangchud, A., Jangchud, K., Harnsilawat, T., Naivikul, O., & McClements, D. J. (2011). Influence of Biopolymer Emulsifier Type on Formation and Stability of Rice Bran Oil-in-Water Emulsions: Whey Protein, Gum Arabic, and Modified Starch. *Journal of Food Science*, *76*(1), E165-E172

Cheng, D. C., & Evans, F. (1965). Phenomenological characterization of the rheological behaviour of inelastic reversible thixotropic and antithixotropic fluids. *British Journal of Applied Physics*, *16*(11), 1599.

Chin, N.L, Chan, S.M., Yusof, Y.A., Chuah, T.G. & Talib, R.A. (2009). Modelling of rheological behavior of pummelo juice concentrates using master curve. *Journal of Food Engineering* 93: 134-140.

Chuah, T.G., Hairulnisah, H., Thomaschoong, S.Y., Chin, N.L., & Nazimah Sheikh, AL. (2007). Effects of temperature on viscosity of dodo l (concoction). *Journal of Food Engineering*. 80: 423–430.

Daoud-Mahammed, S., Couvreur, P., & Gref, R. (2007). Novel self-assembling nanogels: stability and lyophilisation studies. *International Journal of Pharmaceutics*, *332*(1), 185-191.

Dapčević Hadnađev, T., Dokić, P., Krstonošić, V., & Hadnađev, M. (2013). Influence of oil phase concentration on droplet size distribution and stability of oil-in-water emulsions. *European Journal of Lipid Science and Technology*, *115*(3), 313-321.

de Castro Santana, R., Kawazoe Sato, A. C., & Lopes da Cunha, R. (2012). Emulsions stabilized by heat-treated collagen fibers. *Food Hydrocolloids*, *26*(1), 73-81.

Demetriades, K., Coupland, J. N., & McClements, D. J. (1997). Physical properties of whey protein stabilized emulsions as related to pH and NaCl. *Journal of Food Science*, *62*(2), 342-347.

Dluzewska, E., Stobiecka, A., & Maszewska, M. (2006). Effect of oil phase concentration on rheological properties and stability of beverage emulsions. *Acta Scientiarum Polonorum. Technologia Alimentaria*, *5*(2), 147-156.

Dolores Alvarez, M., & Canet, W. (2013). Time-independent and time-dependent rheological characterization of vegetable-based infant purees. *Journal of Food Engineering*.

Emadzadey, B. & Razavi, S.M.A. (2012). Effect of Fat Replacers and Sweeteners on the Time-Dependent Rheological Characteristics and Emulsion Stability of Low-Calorie Pistachio Butter: A Response Surface Methodology. *Food Bioprocess Technology* 5: 1581-1591.

Erçelebi, E. A., & Ibanoğlu, E. (2009a). Rheological properties of whey protein isolate stabilized emulsions with pectin and guar gum. *European Food Research and Technology*, *229*(2), 281-286.

Erçelebi, E. A., & Ibanoğlu, E. (2009b). Characterization of phase separation behavior, emulsion stability, rheology, and microstructure of egg white–polysaccharide mixtures. *Journal of food science*, *74*(6), C506-C512.

Figoni, P.I., & Shoemaker, C. F. (1983). Characterization of time dependent flow properties of mayonnaise under steady shear. *Journal of Texture Studies* 14(4), 431-442.

Fischer, P., & Windhab, E. J. (2011). Rheology of food materials. *Current Opinion in Colloid & Interface Science*, *16*(1), 36-40.

Floury, J. Desrumaux, A. & Lardieres, J. (2000). Effect of high-pressure homogenization on the droplet size distributions and rheological properties of model oil-in-water emulsions. *Innovative Food Science and Emerging Technologies* 1: 127-134.

Fraiha, M., Biagi, J. D., &Ferraz, A. C. D. O. (2011). Rheological behavior of corn and soy mix as feed ingredients. *Food Science and Technology (Campinas)*, *31*(1), 129-134.

Franco, J. M., Raymunds, A., Sousa, I., & Gallegos, C (1998). Influence of processing variables on the rheological and textural properties of lupin protein stabilized emulsions. *Journal of Agricultural and Food Chemistry, 46 (80, 3109-3115.*

Franco, J. M., Partal, P., Conde, B., & Gallegos, C. (2000). Influence of pH and protein thermal treatment on the rheology of pea protein-stabilized oil-in-water emulsions. *Journal of the American Oil Chemists' Society*, *77*(9), 975-984.

Freire, M. G., Dias, A., Coelho, M. A., Coutinho, J. A., & Marrucho, I. M. (2005). Aging mechanisms of perfluorocarbon emulsions using image analysis. *Journal of Colloid and Interface Science*, *286*(1), 224-232.

Friberg S, Larsson, K. (1997). Food Emulsions: Revised and Expanded.3rd ed. Marcel Dekker, Inc., New York.

Gallegos, C., Franco, J.M. & Partal, P. (2004) Rheology of food dispersions. The British Society of rheology, pp19 – 65.

Gao, T., Hu, H. H., & Castañeda, P. P. (2011). Rheology of a suspension of elastic particles in a viscous shear flow. *Journal of Fluid Mechanics*, *687*, 209.

Gharsallaoui, A., Saurel, R., Chambin, O., & Voilley, A. (2012). Pea (Pisum sativum, L.) protein isolate stabilized emulsions: a novel system for microencapsulation of lipophilic ingredients by spray drying. *Food and Bioprocess Technology*, *5*(6), 2211-2221.

Gharibzahedi, S. M. T., Mousavi, S. M., Hamedi, M., & Ghasemlou, M. (2012). Response surface modeling for optimization of formulation variables and physical stability assessment of walnut oil-in-water beverage emulsions. *Food Hydrocolloids*, *26*(1), 293-301.

Giami, S.Y. & Bekebain O.A., (1992). Proximate composition and functional properties of raw and processed full fat fluted pumpkin seed flour. J. Sci. Food Agric., 59: 321-325.

Gonçalves, G. M. S., & Maia Campos, P. M. B. G. (2009).Shelf life and rheology of emulsions containing vitamin C and its derivatives.*Rev. Ciênc. Farm.Básica.Apl*, *30*(2), 217-224.

Gu, Y., Decker, E., & McClements, D. J. (2005). Production and characterization of oil-in-water emulsions containing droplets stabilized by multilayer membranes consisting of b-lactoglobulin, i-carrageenan and gelatin. *Langmuir*, 21, 5752-5760.

Guo, Q., & Mu, T. H. (2011). Emulsifying properties of sweet potato protein: effect of protein concentration and oil volume fraction. *Food Hydrocolloids*, *25*(1), 98-106.

Habibi-Najafi, M. B., & Alaei, Z. (2006). Rheological properties of date syrup/sesame paste blend. *World Journal of Dairy and Food Sciences*, *1*(1), 01-05.

Heyman, B., Depypere, F., Delbaere, C., & Dewettinck, K. (2010). Effects of non-starch hydrocolloids on the physicochemical properties and stability of a commercial béchamel sauce. *Journal of Food Engineering*, *99*(2), 115-120.

Higuchi, W. I., Okada, R., & Lemberger, A. P. (1962). Aggregation in oil-in-water emulsions. Effects of dioctyl sodium sulfosuccinate concentration. *Journal of Pharmaceutical Sciences*, *51*(7), 683-687

Holdsworth, S.D. (1993). Rheological Models used for the prediction of the flow properties of food products: a literature Review. Trans I chem E Part C 71: 139-179.

Huck-Iriart, C., Candal, R. J., & Herrera, M. L. (2011). Effect of processing conditions and composition on sodium caseinate emulsions stability. *Procedia Food Science*, *1*, 116-122.

Ibrahim, N.H. & Achudan, S. N., (2011). Physical properties and stability of Emulsions as affected by Native and Modified Yam Starches. *World Academy of Science , Engineering and Technology* 81: 470-474.

Ibrahim, N. H., & Najwa Md Yusof, N. (2012). Properties and Stability of Catfish Oil-in-water Emulsions as Affected by Oil and Emulsifier Concentrations. *International Proceedings of Chemical, Biological & Environmental Engineering*, *33*.

Ikhu-Omoregbe, D. and Bushi, G.M.(2008). Rheological characteristics of South African commercial sauces. *International Journal of Food Science and Technology* .43:2230-2236.

Ishii, F., Sasaki, I., & Ogata, H. (1990). Effect of phospholipid emulsifiers on physicochemical properties of intravenous fat emulsions and/or drug carrier emulsions. *Journal of Pharmacy and Pharmacology*, *42*(7), 513-515.

Izidoro, D.R, Scheer, A, Sierakowski, M. (2008). Rheological properties of emulsions stabilized by green Banana (Musa cavendishii) pulp fitted by power law model. *Brazilian Archives of Biolology and Technology* 52: 1516-8913.

Jafari, S. M., Beheshti, P., & Assadpoor, E. (2012). Rheological behavior and stability of d-limonene emulsions made by a novel hydrocolloid (Angum gum) compared with Arabic gum. *Journal of Food Engineering*, *109*(1), 1-8.

Kaur, M. & Singh N. (2005): Studies on functional, thermal and pasting properties of flours from different chickpea (Cicerarietinum L.) cultivars. *Food Chemistry*. 91: 403-411

Keshani, S., Luqman, C., Russly, A.R. (2012). Effect of temperature and concentration on rheological properties of pomelo juice concentrates. *International Food Research Journal* 19: 553-562.

Keowmaneechai, E., & McClements, D. J. (2002). Influence of EDTA and citrate on physicochemical properties of whey protein-stabilized oil-in-water emulsions containing CaCl2. *Journal of Agricultural and Food Chemistry*, *50*(24), 7145-7153.

Kiokias, S., Reiffers-Magnani, C. K., & Bot, A. (2004). Stability of whey-protein-stabilized oil-in-water emulsions during chilled storage and temperature cycling.*Journal of Agricultural and Food Chemistry*, *52*(12), 3823-3830.

Klinkesorn, U., Sophanadora, P., Chinachoti, P. & McClements, D.J. (2004). Stability and rheology of cornoil-in-water emulsions containing maltodextrin. *Food Resources International. 37***:** 851–859.

Kobayashi, I., & Nakajima, M. (2002). Effect of emulsifiers on the preparation of food-grade oil-in-water emulsions using a straight-through extrusion filter. *European Journal of L ipid Science and Technology*, *104*(11), 720-727.

Koksoy,A & Kilic, M. (2003). Effects of water and salt level on rheological properties of ayran, a Turkish yoghurt drink. *International Dairy Journal* 13:835-839.

Koocheki, A., & Razavi, S.M.A (2009). Effect of Concentration and Temperature on Flow properties of Alyssum homolocarpum Seed Gum Solution: Assessment of Time Dependency and Thixotropy. *Food Biophysics.* 4:353-364.

Koocheki, A., & Kadkhodaee, R. (2011). Effect of *Alyssum homolocarpum* seed gum, Tween 80 and NaCl on droplets characteristics, flow properties and physical stability of ultrasonically prepared corn oil-in-water emulsions. *Food Hydrocolloids*, *25*(5), 1149-1157.

Kuş, S., Altan, A., & Kaya, A. (2005). Rheological Behavior and Time-Dependent Characterization of Ice Cream Mix with Different Salep Content. *Journal of Texture Studies*, *36*(3), 273-288.

Lemarchand, C., Couvreur, P., Vauthier, C., Costantini, D., & Gref, R. (2003). Study of emulsion stabilization by graft copolymers using the optical analyzer Turbiscan. *International Journal of Pharmaceutics*, *254*(1), 77-82.

Lorenzo, G., Zaritzky, N, & Califano A (2008). Modeling rheological properties of low-in fat O/W emulsions stabilized with xanthan/guar mixtures. *Food Resources International* 41: 452-494.

Lorenzo, G., Checmarev, G., Zaritzky, N., & Califano, A. (2011). Linear viscoelastic

assessment of cold gel-like emulsions stabilized with bovine gelatin. *LWT-Food Science and Technology*, *44*(2), 457-464.

Lupi, F. R., Gabriele, D., De Cindio, B., Sánchez, M. C., & Gallegos, C. (2011). A rheological analysis of structured water-in-olive oil emulsions. *Journal of Food Engineering*, *107*(3), 296-303.

Ma, Z., & Boye, J. I. (2013). Microstructure, Physical Stability, and Rheological Properties of Salad Dressing Emulsions Supplemented with Various Pulse Flours. *Journal of Food Research*, *2*(2).

Ma, Z., Boye, J. I., Fortin, J., Simpson, B. K., & Prasher, S. O. (2013). Rheological, physical stability, microstructural and sensory properties of salad dressings supplemented with raw and thermally treated lentil flours. *Journal of Food Engineering*, *116*(4), 862-872.

Majzoobi, M., & Beparva, P. (2014). Effects of acetic acid and lactic acid on physicochemical characteristics of native and cross-linked wheat starches. *Food Chemistry*, *147*, 312-317.

Mandala, I. G., Savvas, T. P., & Kostaropoulos, A. E. (2004). Xanthan and locust bean gum influence on the rheology and structure of a white model-sauce. *Journal of Food engineering*, *64*(3), 335-342.

Martinez, I., Riscardo, M. A., & Franco, J. M. (2007). Effect of salt content on the rheological properties of salad dressing-type emulsions stabilized by emulsifier blend. *Journal of Food Engineering* 1272-1281.

Marquez, A.L., Palazolo, G.G. & Wagner, J.R. (2005). Emulsiones tipo crema preparadas a base de leche de soja l: Estudios de estabilidad y determinacion de las formulaciones. Grasas y Aceited*. International Journal of Fat and Oils.* 56:59-66.

Mathias, T.R.S., Carvalho Junior, I.C., Carvalho, C.W.P & Servulo, E.F.C (2011). Rheological characterization of coffee flavored yogurt with different types of thickener. Alim. Nutr., Araraquara 22(4):521-529

McClements, D. J. (1999). Food emulsions, principles, practise and techniques. LLC:CRC Press.

McClements D.J. (2005). Food Emulsions: Principles, Practice, and Techniques. Boca Raton: CRC Press

McClements D.J, & Jochen Weiss (2005) Lipid Emulsions 6th edition Freidon Shahidi (Ed) New York.

Mengual, O, Meunier, G., cayre, L., Puech, K., & Snabre, P. (1999). Turbiscan M.A 2000: multiple light scattering measurement for concentrated emulsion and suspension instability analysis. *Talanta*, 50: 445-456.

Mezger, T.G. (2006). The rheology handbook: for users of rotational and oscillatory rheometers.2nd ed. Vincentz Network, Hannover, Germany.

Mine, Y. (1998). Emulsifying characterization of hens egg yolk proteins in oil-in-water emulsions.*Food Hydrocolloids*, *12*(4), 409-415.

Miquelim, J. N., Lannes, S., & Mezzenga, R. (2010). pH Influence on the stability of foams with protein–polysaccharide complexes at their interfaces. *Food Hydrocolloids*, *24*(4), 398-405.

Mirhosseini, H., Tan, C. P., Hamid, N. S., & Yusof, S. (2008). Effect of Arabic gum, xanthan gum and orange oil contents on zeta potential, conductivity, stability, size index and pH of orange beverage emulsion. *Colloids and Surfaces A: Physicochemical and Engineering Aspects*, *315*(1), 47-56.

Moghaddam, M. Y., Mizani, M., Salehifar, M., & Gerami, A. (2013). Effect of waxy maize starch (modified, native) on physical and rheological properties of French dressing during storage. *World Applied Sciences Journal*, *21*(6), 819-824.

Moreira de Morais, J., David Henrique dos Santos, O., Delicato, T., Azzini Gonçalves, R., & Alves da Rocha-Filho, P. (2006). Physicochemical Characterization of Canola Oil/Water Nano-emulsions Obtained by Determination of Required HLB Number and Emulsion Phase Inversion Methods. *Journal of Dispersion Science and Technology*, *27*(1), 109-115.

Moros, J.E, Franco, J.M. & Gallegos, C. (2002). Rheology of spray-dried egg yolk stabilized emulsions. International Journal of Food Science and Technology. 37: 297-310.

Mothé, C.G., Azevedo, A.D. & Antoniassi, R. (2001). Rheological characterization of emulsions from soymilk, 3rd internationalSymposium on Food Rheology and Structure: 531 – 532.

Murevanhema, Y. Y., & Jideani, V. A. (2013). Potential of Bambara Groundnut (Vignasubterranea (L.) Verdc) Milk as a Probiotic Beverage—A Review. *Critical Reviews in Food Science and Nutrition*, *53*(9), 954-967.

Nayebzedey, K., Chen, J., & Mousavi, M.S.M. (2007). Interaction of WPI and Xanthan in microstructure and Rheological Properties of Protein Gels and O/W Emulsion. *International Journal of food Engineering*. Vol. 3., issue 4,Art 9

Nguyen, Q.D., Jensen, C.T.B., Kristensen, P.G. (1998). Experimental and modelling studies of the flow properties of maize and waxy starch pastes. *Chemical. Engineering Journal*. 70, 165–171.

Nikovska, K. (2010). Oxidative stability and rheological properties of oil-in-water emulsions with walnut oil. *Advance Journal of Food Science and Technology*, *2*(3), 172-177.

Nindo, C.I., Tang, J., Powers, J.R. & Takhar, P.S. (2007). Rheological properties of blueberry puree for processing applications. *LWT-Food Science and Technology* 40: 292-299.

Nor Hayati, I., Che Man, Y. B., Tan, C. P., & Nor Aini, I. (2009). Droplet characterization and stability of soybean oil/palm kernel olein O/W emulsions with the presence of selected polysaccharides. *Food Hydrocolloids*, *23*(2), 233-243.

Ohishi, K., Kasai, M., Shimada, A., & Hatae, K. (2007). Effects of acetic acid on the rice gelatinization and pasting properties of rice starch during cooking. *Food Research International*, *40*(2), 224-231.

Ojimelukwe, P. C., Ayernor, G. S. (1992). Oligosaccharide composite and functional properties of flour and starch isolates from four cultivars of Bambara groundnutseeds. *Journal of Food Science and Technology*, 29, 319-321.

Okpuzor, J., Oghunugafor, H.A, Okafor, U. & Sofidiya, M.O. (2010). Identification of protein types in bambara nut seeds: Perspectives for dietary protein supply in developing countries. *EXCLI Journal* 9: 17-28.

Onsaard, E., Vittayanont, M., Srigam, S. & McClements, D. J. (2005). Properties and stability of oil-in-water emulsions stabilized by coconut skim milk proteins. *Journal of Agricultural and Food Chemistry*, *53*(14), 5747-5753.

Padmanabhan, M., & Bhattacharya, M. (1991). Flow behavior and exit pressures of corn mealunder high-shear–high-temperature extrusion conditions using a slit diea). *Journal of Rheology (1978-present)*, *35*(3), 315-343.

Pal, R. (1996) Viscoelastic properties of polymer thickened oil-in-water emulsion. *Chemical Engineering Science*. 5: 3299-3305.

Palazolo, G.G., Sorgentini, D.A. & Wagner, J.R. (2005). Coalescence and flocculation in o/w emulsions of native denatured whey soy proteins In comparison with soy protein isolates. *Food Hydrocolloids*, 19: 595-604.

Partal, P., Guerrero, A., Berjano, M., Muñoz, J., & Gallegos, C. (1994). Flow behaviour and stability of oil-in-water emulsions stabilized by a sucrose palmitate. *Journal of Texture Studies*, *25*(3), 331-348.

Papalamprou, E., Doxastakis, G., & Kiosseoglou, V. (2006). Model salad dressing emulsion stability as affected by the type of the lupin seed protein isolate. *Journal of the Science of Food and Agriculture*, *86*(12), 1932-1937.

Paredes, M. D. C., Rao, M. A., & Bourne, M. C. (1988). Rheological characterization of salad dressings. 1. Steady shear, thixotropy and effect of temperature. *Journal of Texture Studies*, *19*(3), 247-258.

Park, K. M., Lim, S. Y., Chung, M. S., Kang, D., Choi, Y. J., Lee, J., & Chang, P. S. (2010). Effect of 1-monocaprin addition on the emulsion stability and the storage stability of mayonnaise. *Food Science and Biotechnology*, *19*(5), 1227-1232.

Payet, L., & Terentjev, E. M. (2008). Emulsification and stabilization mechanisms of O/W emulsions in the presence of chitosan. *Langmuir*, *24*(21), 12247-12252.

Pearce, K. N., & Kinsella, J. E. (1978). Emulsifying properties of proteins: evaluation of a turbidimetric technique. *Journal of Agricultural and Food Chemistry*, *26*(3), 716-723.

Perrechil, F. A., & Cunha, R. L. (2010). Oil-in-water emulsions stabilized by sodium caseinate: Influence of pH, high-pressure homogenization and locust bean gum addition. *Journal of Food Engineering*, *97*(4), 441-448.

Perrechil, F. D. A., Santana, R. D. C., Fasolin, L. H., Silva, C. A. S. D., & Cunha, R. L. D. (2010). Rheological and structural evaluations of commercial italian salad dressings. *Ciência e Tecnologia de Alimentos*, *30*(2), 477-482.

Prinyawwiwatkul, W., Beuchat, L.R., Mcwatters, K.H. & Phillips, R.D. (1997). Functional properties of Cowpea (Vignaunguiculata) Flour As Affected by Soaking, Boiling, and Fungal Fermentation. *Journal of Agriculture and Food Chemistry*. 45, 480–486.

Quintana, J. M., Califano, A. N., Zaritzky, N. E., & Partal, P. (2002). Effect of salt on the rheological properties of low-in-fat O/W emulsions stabilised with polysaccharides. *Food Science and Technology International*, *8*(4), 213-221.

Rao, M. A. (2014). Flow and functional models for rheological properties of fluid foods. In *Rheology of Fluid, Semisolid, and Solid Foods* (pp. 27-61). Springer US.

Rao, M.A., Okechukwu, P.E. & Da Silva, J.C. (1997). Rheological behavior of heated starch dispersions in excess water: role of starch granule. *Carbohydrare Polymers* 33: 273-283.

Razavi, S. M. A., & Habibi-Najafi, M. B. (2006). The effect of fat substitutes on the time dependent rheological properties of low fat sesame paste/date syrup blends (Halwa-Ardeh). *Journal of Mathematics*

Razavi, S.M.A, Najafi M.H. & Alaee Z (2008), Rheological characterization of low fat sesame paste blended with date syrup. *International Journal of Food Properties* 11, 92–101

Razavi, S., & Karazhiyan, H. (2009). Flow properties and thixotropy of selected hydrocolloids: experimental and modeling studies. *Food Hydrocolloids*, *23*(3), 908-912.

Razavi, S.M.A.,Taghizadeh & Ardekani, A.S. (2010). Modeling the Time-Dependent rheological Properties of Pistachio Butter. *International Journal of Nuts and Related Science*. 1(1):38-45.

Roberts, G.P., Banes, H.A., & Carew, P. (2001). Modeling the flow behaviour of very shear-thinning liquids. *Chemical Engineering Science.* 56: 5617-5623.

Roland, I., Piel, G., Delattre, L. & Evrard, B. (2003). Systematic characterization of oil-in-water emulsions for formulation design. *International Journal of Pharmaceutics* 263: 85-94.

Romero, A., Cordobés, F., & Guerrero, A. (2009). Influence of pH on linear viscoelasticity and droplet size distribution of highly concentrated O/W crayfish flour-based emulsions. *Food Hydrocolloids*, *23*(2), 244-252.

Saley, N., Sarbu, T., Sirk, K., Lowry, G. V., Matyjaszewski, K. & Tilton, R. D. (2005). Oil-in-water Emulsions Stabilized by Highly Charged polyelectrolyte-Grafted silica Nano particles. *Langmuir* 21: 9873-9878.

Samavati, V., Emama-Djomeh, Z., Mohammadifar, M.A., Omid, M., & Mehdinia A.L.I. (2011). Stability and rheology of dispersions containing polysaccharide, oleic acid and whey protein Isolate. *Journal of Texture Studies* 1: 14.

Santana, R. C., Perrechil, F. A., Sato, A. C. K., & Cunha, R. L. (2011). Emulsifying properties of collagen fibers: Effect of pH, protein concentration and homogenization pressure. *Food Hydrocolloids*, *25*(4), 604-612.

Sarker, D. K. (2013). What is an emulsion?. *Pharmaceutical Emulsions: A Drug Developer's Toolbag*, 15-48.

Schmidt, R.H. (1981) Gelation and coagulation. In J. P. Cherry (Ed.), Protein functionality in foods, ACS symposium series, 147: 131–147. Washington, DC: American chemical Society.

Sherman, P. (1983). Rheological properties of emulsions. In P. Becher (Ed.). Encyclopedia of emulsion Technology, 1: 405-437.

Silset, A. (2008). Emulsions (w/o and o/w) of Heavy Crude Oils. Characterization, Stabilization, Destabilization and Produced Water Quality.

Sikorski, Z.E. (2002). Proteins. In Z.E. Sikorski (Ed). Chemical and functional properties of Food components Florida:CRS Press Inc. 133-178.

Singla, N., Verma, P., Ghoshal, G. and Basu, S. (2013). Steady state and time dependent rheological behavior of mayonnaise (egg and eggless). *International Food Research Journa*l 20(4) 2009-2016

Singh, U. (2001). Functional properties of grain legume flours. *Journal of Food Science and Technology* 38 (3): 191–199

Sirivongpaisal, P. (2008). Structure and functional properties of starch and flour from Bambara groundnut. *Songlanakarin Journal of Science and Technolology.* 30 (1):51-56.

Sołowiej, B. (2007). Effect of pH on rheological properties and meltability of processed cheese analogs with whey products. *Polish Journal of Food and Nutrition Sciences*. 57, 3(A), 125-128.

Steffe, J.F. (1996). Rheological methods in food process engineering, Freeman Press, East Lansing, MI.USA. pp. 86-91.

Stewart, S., & Mazza, G. (2000).Effect of flaxseed gum on quality and stability of a model salad dressing1.*Journal of Food Quality*, *23*(4), 373-390.

Swanevelder, C. J. (1998). Bambara:Food for Africa. Printed and published by the National Department of Agriculture of the ARC-Grain Crops Institute, South Africa.

Sun, C., & Gunasekaran, S. (2009). Effects of protein conentration and oil-phase volume fraction on the stability and rheology of menhaden oil-in-water emulsions stabilized by whey protein isolate with xanthan gum. *Food Hydrocolloid* 23: 165-174.

Surh, J., Decker, E. A., & McClements, D. J. (2006). Influence of pH and pectin type on properties and stability of sodium-caseinate stabilized oil-in-water emulsions. *Food Hydrocolloids*, *20*(5), 607-618.

Tadros, T. (2004). Application of rheology for assessment and prediction of the long-term physical stability of emulsions. *Advances in Colloid and Interface Science*, *108*, 227-258.

Tadros, T. F. (2009). Emulsion science and technology: a general introduction. *Emulsion Science and Technology. Wiley-VCH, Weinheim*, 1-56.

Taherian, A.R, Frustier P. & Ramaswamy, H.S (2006): Effect of added oil and modified starch on rheological properties, droplet size distribution, opacity and stability of beverage cloud emulsions. *Journal of Food Engineering*. 77:687-696.

Taherian, A. R., Fustier, P., & Ramaswamy, H. S. (2007). Effects of added weighting agent and xanthan gum on stability and rheological properties of beverage cloud emulsions formulated using modified starch. *Journal of Food Process Engineering*, *30*(2), 204-224.

Tantayotai, T., & Pongsawatmanit, R. (2005).Effect of Homogenizer Types and Sodium Chloride Concentrations on the Physical Properties of Coconut Oil-in-Water Emulsions.*KASETSART JOURNAL*, 1.

Tan, C. P., & Nakajima, M. (2005). Effect of polyglycerol esters of fatty acids on physicochemical properties and stability of β-carotene nanodispersions prepared by emulsification/evaporation method. *Journal of the Science of Food and Agriculture*, *85*(1), 121-126

Tarrega, A.,Duran, L. & Costell, E. (2004). Flow behaviour of semi-solid dairy desserts. Effects of temperature. *International Dairy Journal* 14:345-353.

Tcholakova, S., Denkov, N. & Danner, T. (2004). Role of Surfactant Type and Concentration for the Mean Drop Size during Emulsification in Turbulent Flow. *Langmuir*, 20 : 7444-7458.

Thiebaud, M., Dumay, E., Picart, L., Guiraud, J. P., & Cheftel, J. C. (2003). High-pressure homogenisation of raw bovine milk. Effects on fat globule size distribution and microbial inactivation. *International Dairy Journal*, *13*(6), 427-439.

Tse, K. Y., & Reineccius, G. A. (1995, January). Methods to predict the physical stability of flavor-cloud emulsion. In *ACS Symposium Series* (Vol. 610, pp. 172-182). American Chemical Society.

Trindade, J. R., Freire, M. G., Amaral, P. F., Coelho, M. A. Z., Coutinho, J. A., & Marrucho, I. M. (2008). Aging mechanisms of oil-in-water emulsions based on a bioemulsifier produced by *Yarrowia lipolytica*. *Colloids and Surfaces A: Physicochemical and Engineering Aspects*, *324*(1), 149-154.

Tunan, F., & Tiu, C. (1991). Steady-shear viscosity and transient stress response for elasto-thixotropic fluids. *Acta Mechanica Sinica*, *7*(1), 46-50.

Vega, C., Dalgleish, D. G., & Goff, H. D. (2005). Effect of κ-carrageenan addition to dairy emulsions containing sodium caseinate and locust bean gum. *Food Hydrocolloids*, *19*(2), 187-195.

Verwey, E. J. W., Overbeek, J. T. G., & Overbeek, J. T. G. (1999). *Theory of the stability of lyophobic colloids*. Courier Dover Publications.

Vurayai, R., Emongor, V., & Moseki, B. (2011). Physiological responses of bambara groundnut (Vigna subterranea L. Verdc) to short periods of water stress during different developmental stages. *Asian Journal of Agricultural Sciences*, *3*.

Walpole, R.E, Myers RH, Myers, S.L. & Ye, K. (2002). Probability and statistics for Engineers and Scientists, seventh Ed. Prentice Hall. Nj USA. P 367.

Walstra, P. 1987. Physical principles of emulsion science.In *Food Structure and Behaviour,* (J.M.V. Blanshard and P. Lillford, eds.) pp. 87-106, AcademicPress, New York.

Wang, B., Li, D., Wang, L., Adhikari, B. & Shi, J. (2010a). Ability of flaxseed and soybean protein concentrates to stabilize oil-in-water emulsions. *Journal of Food Engineering* 100: 417-426.

Wang, Bo, Li, D. Wang,L. & Ozkan, N. (2010b). Effect of concentrated faxseed protein on the stability and rheological properties of soybean oil-in-water emulsion. *Journal of Food Engineering.* 555-561.

Wang, B., Wang, L. J., Li, D., Adhikari, B., & Shi, J. (2011). Effect of gum Arabic on stability of oil-in-water emulsion stabilized by flaxseed and soybean protein. *Carbohydrate Polymers*, *86*(1), 343-351.

Yang, Y., Leser, M. E., Sher, A. A., & McClements, D. J. (2013). Formation and stability of emulsions using a natural small molecule surfactant: Quillaja saponin (Q-Naturale®). *Food Hydrocolloids*, *30*(2), 589-596.

Yilmazer, G., & Kokini, J. L. (1992). effect of salt on the stability of propylene glycol alginate/xanthan gum/polysorbate-60 stabilized oil-in-water emulsions. *journal of Texture Studies*, *23*(2), 195-213.

Young, L. L. (1976). Composition and properties of an animal protein isolate prepared from bone residue. *Journal of Food Science*, *41*(3), 606-608.

Yusuf, A.A., Ayedun, H. & Sanni, L.O. (2007). Chemical composition and functional properties of raw and roasted Nigerian benniseed (*sesamumindicum)* and bambara groundnut (*Vigna Subterranean*). *Food Chemistry. III* :277-282.

Zhang, T., Jiang, B., Mu, W., & Wang, Z. (2009). Emulsifying properties of chickpea protein isolates: Influence of pH and NaCl. *Food Hydrocolloids*, *23*(1), 146-152.

Zúñiga, R. N., Skurtys, O., Osorio, F., Aguilera, J. M., & Pedreschi, F. (2012). Physical properties of emulsion-based hydroxypropyl methylcellulose films: Effect of their microstructure. *Carbohydrate Polymers*, *90*(2), 1147-1158.

APPENDICES

APPENDIX A: DATA ON EFFECT OF PROCESSING VARIABLES ON APPARENT VISCOSITY

Table A1 Effect of homogenization time on apparent viscosity at various processing time

Shear rate	4mins	6mins	8 mins	10 mins	12 mins
40.00	0.2678	0.3108	0.3414	0.3719	0.3887
49.32	0.2478	0.2831	0.3136	0.3346	0.3586
60.8	0.2295	0.258	0.2886	0.3031	0.3311
74.97	0.2125	0.235	0.2682	0.2742	0.3033
92.43	0.2005	0.2206	0.2464	0.2509	0.2787
114	0.1884	0.2034	0.2247	0.227	0.2556
140.5	0.1729	0.1866	0.2051	0.2058	0.2325
173.2	0.1596	0.1731	0.1879	0.1866	0.212
213.5	0.146	0.1591	0.1715	0.1698	0.194
263.3	0.1358	0.1488	0.156	0.1538	0.1776
324.6	0.1264	0.1383	0.142	0.1403	0.1625
400.2	0.1184	0.1271	0.1297	0.1272	0.1489
493.4	0.1114	0.116	0.1197	0.1154	0.136
608.3	0.1042	0.1071	0.1109	0.1039	0.1241
750	0.09666	0.09834	0.1018	0.09493	0.1131

Table A2 Effect of homogenization speed on apparent viscosity at various processing speed

Shear rate	4000 rpm	6000 rpm	8000 rpm	10000 rpm	12000 rpm
40.00	0.2456	0.267	0.2903	0.3887	0.4685
49.32	0.2344	0.2482	0.261	0.3586	0.4179
60.8	0.2245	0.2359	0.2441	0.3311	0.3823
74.97	0.2106	0.2236	0.229	0.3033	0.3407
92.43	0.1974	0.2065	0.2123	0.2787	0.3057
114	0.1844	0.1921	0.1969	0.2556	0.2734
140.5	0.1728	0.1782	0.1816	0.2325	0.2445
173.2	0.1574	0.1659	0.1686	0.212	0.2171
213.5	0.1453	0.1514	0.1556	0.194	0.1924
263.3	0.1356	0.1402	0.1443	0.1776	0.1681
324.6	0.1264	0.1322	0.1344	0.1625	0.1504
400.2	0.1171	0.1222	0.1236	0.1489	0.1361
493.4	0.109	0.1126	0.1142	0.136	0.1283
608.3	0.1014	0.1057	0.1057	0.1241	0.116
750	0.09453	0.09739	0.09951	0.1131	0.1153

APPENDIX B: MEAN DATA ON TIME DEPENDENT PROPERTIES OF BGNF-STABILIZED EMULSION

Table B1 Emulsion stabilized with 5% (w/w) BGNF containing 30, 35 and 40% (w/w) SFO

Shear rate	Shear stress of forward and backward sweep					
	30% SFO		35% SFO		40% SFO	
40.00	7.961	6.208	13	8.502	27.32	16.58
49.32	9.037	6.938	14.33	9.674	29.3	18.61
60.8	10.14	7.832	15.91	10.91	31.86	21.1
74.97	11.35	8.987	17.65	12.4	34.85	23.91
92.43	12.79	10.3	19.7	14.31	38.39	27.16
114	14.53	11.78	22.02	16.46	42.17	30.84
140.5	16.44	13.51	24.7	18.96	46.48	35.11
173.2	18.61	15.52	27.75	21.71	51.38	40.02
213.5	21.08	17.96	31.13	25.08	56.73	45.54
263.3	23.86	20.76	35.13	29.1	62.9	52.37
324.6	27.23	24.02	39.26	33.62	69.95	59.72
400.2	31.04	27.9	44.4	38.57	77.8	68.38
493.4	35.4	32.48	50.37	44.93	86.91	78.79
608.3	40.28	37.84	57.01	52.62	97.1	90.98
750	45.77	45.77	64.13	64.13	108.1	108.1

Table B2 Emulsion stabilized with 6% (w/w) BGNF containing 30, 35 and 40% (w/w) SFO

Shear rate	Shear stress for forward and backward sweep					
	30% SFO		35% SFO		40% SFO	
40.00	12.79	9.236	18.49	12.2	52.14	28.3
49.33	13.96	10.41	20.37	13.79	55.32	32.13
60.8	15.63	11.94	22.81	15.85	59.48	36.31
74.97	17.58	13.64	25.36	18.12	64.49	41.05
92.43	19.82	15.58	28.42	20.81	70.33	46.45
114	22.36	17.84	31.88	23.91	76.84	52.8
140.5	25.28	20.48	35.85	27.48	84.01	60.01
173.2	28.72	23.62	40.33	31.66	92.1	68.31
213.5	32.66	27.48	45.4	36.56	101	77.85
263.3	37.14	32.04	51.09	42.07	110.9	88.76
324.6	42.14	36.92	57.67	48.53	122.2	101.4
400.2	47.77	42.8	63.68	56.13	135.1	116
493.4	53.93	49.68	71.84	65.1	149.3	132.6
608.3	60.85	57.72	80.63	75.53	165.7	152.4
750	69.68	69.68	90.35	90.35	182.4	182.4

Table B3 Emulsion stabilized with 7% (w/w) BGNF containing 30, 35 and 40% (w/w) SFO

Shear rate	Shear stress for forward and backward sweep					
	30% SFO		35% SFO		40% SFO	
40.00	18.89	12.76	45.2	25.92	118.9	51.73
49.32	20.7	14.51	47.85	29.37	119.3	57.99
60.8	23	16.49	51.76	33.37	125.6	64.95
74.97	25.68	18.85	56.25	37.76	132.2	72.74
92.43	28.81	21.7	61.66	42.88	140	81.39
114	32.45	24.98	67.48	48.71	148.8	91.26
140.5	36.46	28.79	74.28	55.38	158.8	102.3
173.2	41.02	33.18	81.98	63.15	169.7	115.1
213.5	46.17	38.15	90.54	72.03	182.2	129.5
263.3	51.9	43.94	100.3	82.24	196.1	146
324.6	58.69	50.78	111.5	93.97	210.8	164.7
400.2	66.25	58.78	123.9	107.6	228.3	186.4
493.4	74.76	68.03	138.1	123.6	247.8	212.2
608.3	84.17	79.05	153.8	142.6	269.5	243.4
750	95.12	95.12	171.4	171.4	296	296

APPENDIX C: MEAN DATA OF STEADY SHEAR DECAY OF BGNF –STABILIZED EMULSIONS

Table C1 Emulsion stabilized with 5% (w/w) BGNF at 50 s^{-1}

Time (s)	Apparent viscosity (Pas)		
	30% SFO	35% SFO	40% SFO
0	0	0	0
40	0.193927	0.344667	0.665667
80	0.187767	0.319333	0.596133
120	0.184627	0.308067	0.576467
160	0.182207	0.2996	0.5632
200	0.17908	0.293	0.555733
240	0.177193	0.287733	0.548667
280	0.175173	0.283667	0.544333
320	0.173727	0.28	0.5382
360	0.172347	0.276733	0.531067
400	0.172087	0.274	0.5234
440	0.170907	0.271733	0.517067
480	0.16996	0.269867	0.510867
520	0.168173	0.2682	0.504467
560	0.1667	0.2666	0.4998
600	0.166153	0.265733	0.4956
640	0.165273	0.264067	0.491267
680	0.164727	0.262733	0.4876
720	0.164393	0.260867	0.484733
760	0.164087	0.259733	0.482133
800	0.16396	0.258867	0.480133
840	0.16346	0.257667	0.479067
880	0.162673	0.256733	0.4772
920	0.162293	0.253867	0.475333
960	0.161747	0.2532	0.473533
1000	0.16198	0.253333	0.471133
1040	0.161793	0.254133	0.4706
1080	0.161087	0.2526	0.4698
1120	0.16132	0.253267	0.469067
1160	0.161013	0.252533	0.468
1200	0.160407	0.2526	0.4672

Table C2 Emulsion stabilized with 5% (w/w) BGNF at 100 s^{-1}

Time (s)	Apparent viscosity (Pas)		
	30% SFO	35% SFO	40% SFO
0	0	0	0
40	0.1651	0.2435	0.492233
80	0.153867	0.223067	0.442733
120	0.1497	0.214433	0.426933
160	0.146567	0.208567	0.4161
200	0.1445	0.203467	0.4082
240	0.1428	0.200333	0.4019
280	0.141367	0.197233	0.3963
320	0.1401	0.194933	0.391533
360	0.1386	0.1929	0.387767
400	0.137467	0.1913	0.384467
440	0.136733	0.189933	0.381467
480	0.135933	0.188533	0.378733
520	0.135133	0.187467	0.3763
560	0.134467	0.1863	0.374267
600	0.1337	0.185367	0.371967
640	0.133033	0.1845	0.370333
680	0.1324	0.183633	0.3683
720	0.132	0.182567	0.366467
760	0.131633	0.182033	0.364967
800	0.131333	0.181567	0.364233
840	0.131033	0.180867	0.363267
880	0.130767	0.1801	0.362533
920	0.1305	0.1795	0.361767
960	0.130333	0.179	0.361033
1000	0.129933	0.178667	0.3605
1040	0.1296	0.1782	0.3599
1080	0.129367	0.1779	0.359333
1120	0.129267	0.177867	0.358933
1160	0.129167	0.177533	0.3586
1200	0.1289	0.177267	0.358233

Table C3 **Emulsion stabilized with 5% (w/w) BGNF at 150 s^{-1}**

Time (s)	Apparent shear rate (Pas)		
	30% SFO	35% SFO	40% SFO
0	0	0	0
40	0.139822	0.205711	0.392156
80	0.128689	0.187178	0.349556
120	0.124467	0.179911	0.336644
160	0.121667	0.174511	0.329222
200	0.119378	0.1704	0.321978
240	0.117778	0.167511	0.316556
280	0.116222	0.165156	0.312067
320	0.114933	0.163	0.308489
360	0.113978	0.1612	0.3056
400	0.112933	0.159733	0.302778
440	0.112156	0.158467	0.3006
480	0.111356	0.157444	0.298511
520	0.110733	0.156556	0.296311
560	0.110156	0.155467	0.294289
600	0.109911	0.154756	0.292578
640	0.110111	0.154111	0.291222
680	0.110022	0.153533	0.289911
720	0.109867	0.153089	0.288444
760	0.109756	0.152533	0.287044
800	0.109622	0.152089	0.285978
840	0.109578	0.151556	0.285
880	0.109489	0.151356	0.283956
920	0.1094	0.151	0.282867
960	0.109311	0.150756	0.282044
1000	0.109267	0.150578	0.281378
1040	0.109222	0.150333	0.280844
1080	0.109156	0.150111	0.280556
1120	0.109111	0.149867	0.280311
1160	0.109067	0.149733	0.279844
1200	0.109022	0.149578	0.279644

Table C4 **Emulsion stabilized with 6% (w/w) BGNF at 50 s^{-1}**

Time (s)	Apparent viscosity (Pas)		
	30% SFO	35% SFO	40% SFO
0	0	0	0
40	0.5684	0.6312	1.4408
80	0.497133	0.578	1.312467
120	0.476733	0.56	1.266
160	0.4656	0.5482	1.239133
200	0.4584	0.5394	1.22
240	0.452867	0.5326	1.202
280	0.4478	0.5274	1.187133
320	0.442733	0.5224	1.1738
360	0.439667	0.5186	1.1634
400	0.4358	0.5152	1.153733
440	0.4324	0.5136	1.144867
480	0.429333	0.5112	1.136
520	0.426733	0.5074	1.128
560	0.4244	0.5022	1.123067
600	0.422	0.4992	1.1166
640	0.419733	0.4976	1.1118
680	0.4176	0.4932	1.1068
720	0.416267	0.4896	1.102
760	0.414133	0.4884	1.0988
800	0.4126	0.4868	1.094267
840	0.410467	0.4836	1.089933
880	0.4096	0.4816	1.084933
920	0.4082	0.4782	1.081067
960	0.407	0.4762	1.077533
1000	0.405667	0.4746	1.0744
1040	0.404733	0.4732	1.071333
1080	0.4038	0.4704	1.068267
1120	0.402267	0.4684	1.065533
1160	0.401067	0.4678	1.062067
1200	0.400333	0.4658	1.0598

Table C5 **Emulsion stabilized with 6% (w/w) BGNF at 100 s^{-1}**

Time (s)	Apparent viscosity (Pas)		
	30% SFO	35% SFO	40% SFO
0	0	0	0
40	0.3746	0.5672	1.0298
80	0.332267	0.496933	0.910267
120	0.321233	0.476767	0.866767
160	0.3143	0.4632	0.841633
200	0.310333	0.453733	0.8213
240	0.306933	0.445833	0.803933
280	0.303933	0.439433	0.790333
320	0.301167	0.433833	0.779533
360	0.299	0.428567	0.770167
400	0.2972	0.4244	0.7622
440	0.295567	0.4208	0.7547
480	0.294233	0.417667	0.7488
520	0.293133	0.414867	0.743333
560	0.292067	0.412533	0.737967
600	0.2908	0.4106	0.7331
640	0.289967	0.408667	0.728733
680	0.289233	0.406867	0.7244
720	0.288533	0.404933	0.721867
760	0.287867	0.403067	0.718967
800	0.287667	0.4013	0.715333
840	0.2872	0.399467	0.711867
880	0.286833	0.3982	0.709
920	0.2861	0.396633	0.705967
960	0.2855	0.395167	0.703333
1000	0.284967	0.393833	0.700833
1040	0.284867	0.392633	0.699233
1080	0.284633	0.391567	0.697167
1120	0.2844	0.390633	0.6944
1160	0.284333	0.389733	0.6926
1200	0.284267	0.388867	0.690833

Table C6 Emulsion stabilized with 6% (w/w) BGNF at 150 s^{-1}

Time (s)	Apparent viscosity (Pas)		
	30% SFO	35% SFO	40% SFO
0	0	0	0
40	0.271022	0.497867	0.886
80	0.242311	0.435089	0.769778
120	0.232889	0.4152	0.727333
160	0.227778	0.4024	0.701778
200	0.223778	0.393422	0.687778
240	0.220644	0.386622	0.672422
280	0.218422	0.380933	0.660533
320	0.216178	0.375978	0.650533
360	0.214467	0.371667	0.642178
400	0.212644	0.367956	0.635067
440	0.211422	0.364244	0.628867
480	0.2102	0.360933	0.623489
520	0.208889	0.358178	0.6186
560	0.207911	0.355378	0.613933
600	0.206956	0.353422	0.609911
640	0.206422	0.351644	0.605778
680	0.205644	0.349844	0.602044
720	0.204867	0.348	0.598822
760	0.204111	0.347067	0.595822
800	0.203511	0.345933	0.592778
840	0.2028	0.344844	0.589733
880	0.202356	0.343644	0.586444
920	0.201489	0.342778	0.583222
960	0.200822	0.341844	0.580689
1000	0.200356	0.341378	0.584467
1040	0.199756	0.340778	0.583022
1080	0.199533	0.340422	0.580733
1120	0.198778	0.339556	0.579067
1160	0.198556	0.338711	0.576978
1200	0.198222	0.338111	0.574933

Table C7 Emulsion stabilized with 7% (w/w) BGNF at 50 s^{-1}

Time (s)	Apparent viscosity (Pas)		
	30% SFO	35% SFO	40% SFO
0	0	0	0
40	0.781267	1.302533	3.768
80	0.684733	1.164733	3.384
120	0.656733	1.114467	3.159334
160	0.643067	1.0828	3.009334
200	0.631	1.062667	2.898666
240	0.6218	1.045733	2.815334
280	0.614133	1.037	2.750666
320	0.6088	1.0252	2.692666
360	0.6028	1.015067	2.639334
400	0.598467	1.0058	2.594
440	0.594067	0.997333	2.555334
480	0.592133	0.991267	2.520666
520	0.5906	0.985	2.489334
560	0.587267	0.979467	2.462666
600	0.585467	0.9744	2.438666
640	0.5826	0.969867	2.412666
680	0.580267	0.965267	2.391334
720	0.577533	0.961933	2.369334
760	0.5756	0.958933	2.35
800	0.574133	0.954133	2.332
840	0.5726	0.9502	2.316
880	0.5706	0.945867	2.302
920	0.567	0.941733	2.286666
960	0.567	0.939	2.272666
1000	0.5658	0.936467	2.259334
1040	0.564867	0.933933	2.245334
1080	0.563267	0.9324	2.232666
1120	0.563067	0.930067	2.220666
1160	0.561067	0.928867	2.211
1200	0.558267	0.927733	2.197534

Table C8 Emulsion stabilized with 7% (w/w) BGNF at 100 s^{-1}

Time (s)	Apparent viscosity (Pas)		
	30% SFO	35% SFO	40% SFO
0	0	0	0
40	0.632933	0.863333	2.192
80	0.5421	0.7667	1.926333
120	0.516733	0.733933	1.806333
160	0.4994	0.715567	1.718667
200	0.487633	0.700467	1.653667
240	0.4783	0.6878	1.606333
280	0.470767	0.677767	1.569
320	0.4643	0.670067	1.537333
360	0.458533	0.6632	1.510667
400	0.4531	0.6577	1.487667
440	0.4481	0.652267	1.467333
480	0.444033	0.648233	1.449333
520	0.440533	0.644033	1.432
560	0.4382	0.640633	1.417
600	0.436233	0.636533	1.404
640	0.433533	0.633433	1.391333
680	0.430933	0.630767	1.380333
720	0.4286	0.627233	1.372333
760	0.426367	0.623833	1.362333
800	0.424433	0.6209	1.353
840	0.4228	0.6184	1.344
880	0.4211	0.615767	1.336333
920	0.418167	0.613167	1.329333
960	0.417567	0.611667	1.325
1000	0.416833	0.610767	1.320667
1040	0.416067	0.6103	1.317
1080	0.415033	0.611667	1.314
1120	0.4141	0.6112	1.310333
1160	0.4135	0.610667	1.307
1200	0.412433	0.6106	1.303667

Table C9 Emulsion stabilized with 7% (w/w) BGNF at 150 s^{-1}

Time (s)	Apparent viscosity (Pas)		
	30% SFO	35% SFO	40% SFO
0	0	0	0
40	0.369867	0.708845	1.604667
80	0.325978	0.620356	1.366222
120	0.311178	0.592667	1.269555
160	0.3026	0.5742	1.207333
200	0.296889	0.560622	1.162667
240	0.292489	0.550333	1.132
280	0.289089	0.541933	1.108889
320	0.285667	0.535311	1.089333
360	0.2828	0.530089	1.07
400	0.280378	0.524889	1.053778
440	0.278378	0.520644	1.039778
480	0.276844	0.517044	1.026889
520	0.275689	0.513644	1.015111
560	0.273911	0.510533	1.006667
600	0.272733	0.507711	0.997778
640	0.271467	0.505333	0.990889
680	0.270133	0.503133	0.982445
720	0.268933	0.501333	0.976667
760	0.268133	0.499622	0.979555
800	0.267	0.498133	0.973111
840	0.265911	0.496756	0.967778
880	0.265644	0.495689	0.962445
920	0.264978	0.494889	0.958
960	0.264533	0.493933	0.953778
1000	0.263511	0.492511	0.949111
1040	0.262644	0.491667	0.945111
1080	0.261956	0.490622	0.941333
1120	0.261889	0.489622	0.937555
1160	0.262422	0.489333	0.933333
1200	0.262489	0.489311	0.929555

APPENDIX D: MEAN DATA ON TIME INDEPENDENT PROPERTIES OF GELATINIZED BGNF DISPERSIONS AND BGNF-STABILIZED EMULSION

Table D1 Gelatinized BGNF dispersions at various concentrations

Shear Rate [1/s]	Apparent viscosity (Pas)		
	5% (w/w)	6% (w/w)	7% (w/w)
750	0.0249	0.04881	0.08099
608.3	0.02558	0.05026	0.08523
493.4	0.02732	0.05399	0.09118
400.2	0.02943	0.05808	0.09894
324.6	0.032	0.06378	0.1082
263.3	0.03559	0.07013	0.1186
213.5	0.03983	0.07779	0.1304
173.2	0.04436	0.08568	0.143
140.5	0.04983	0.09463	0.1584
113.9	0.0552	0.105	0.1745
92.43	0.06236	0.1164	0.1947
74.97	0.06893	0.129	0.2177
60.8	0.07626	0.1441	0.2439
49.32	0.08687	0.1622	0.2736
40	0.09989	0.1839	0.3068

Table D2 5% (w/w) BGNF dispersion and emulsion stabilized with 5% (w/w) BGNF containing 30, 35 and 40% (w/w) SFO

Shear Rate [1/s]	Apparent viscosity (Pas)			
	5% BGNF	30% SFO	35% SFO	40% SFO
750	0.02352	0.049817	0.07409	0.1408
608.3	0.024757	0.051137	0.07762	0.146733
493.4	0.026637	0.053413	0.081803	0.156667
400.2	0.028867	0.056237	0.086577	0.167467
324.6	0.031563	0.05927	0.091773	0.1804
263.3	0.035073	0.062327	0.09712	0.193167
213.5	0.039187	0.06548	0.102967	0.207533
173.2	0.043747	0.069187	0.109	0.222833
140.5	0.049297	0.073697	0.1154	0.2393
113.9	0.05513	0.077833	0.123167	0.257733
92.42	0.062433	0.0832	0.131433	0.2765
74.96	0.070227	0.089347	0.140367	0.297433
60.79	0.0784	0.096867	0.149733	0.3201
49.32	0.089497	0.104043	0.159867	0.3434
40	0.100247	0.10847	0.171867	0.373167

Table D3 **6% (w/w) BGNF dispersion and emulsion stabilized with 6% (w/w) BGNF containing 30, 35 and 40% (w/w) SFO**

Shear Rate [1/s]	Apparent viscosity (Pas)			
	6% BGNF	30% SFO	35% SFO	40% SFO
750	0.04829	0.066367	0.1399	0.292167
608.3	0.05008	0.067147	0.143	0.300667
493.4	0.05409	0.069963	0.151133	0.322767
400.2	0.05876	0.073673	0.161167	0.351467
324.6	0.064553	0.077853	0.1724	0.3851
263.3	0.071183	0.08236	0.184667	0.424867
213.5	0.078903	0.086987	0.198367	0.4682
173.2	0.08712	0.09211	0.212933	0.517033
140.5	0.096503	0.09799	0.229067	0.572133
113.9	0.106967	0.104327	0.2473	0.633933
92.42	0.118833	0.1116	0.2672	0.7026
74.96	0.1323	0.119067	0.2885	0.7778
60.79	0.149133	0.126533	0.3122	0.8627
49.32	0.168833	0.133233	0.335267	0.955233
40	0.1915	0.1421	0.361767	1.0586

Table D4 **7% (w/w) BGNF dispersion and emulsion stabilized with 7% (w/w) BGNF containing 30, 35 and 40% (w/w) SFO**

Shear Rate [1/s]	Apparent viscosity (Pas)			
	7% BGNF	30% SFO	35% SFO	40% SFO
750	0.081317	0.140133	0.260533	0.4567
608.3	0.08688	0.142033	0.2648	0.463033
493.4	0.093183	0.1493	0.2796	0.4968
400.2	0.101403	0.158333	0.299333	0.543833
324.6	0.1107	0.1687	0.322867	0.6023
263.3	0.1216	0.180133	0.350133	0.6718
213.5	0.133967	0.1929	0.3811	0.754
173.2	0.147167	0.206733	0.4154	0.846567
140.5	0.1626	0.222033	0.4535	0.951367
113.9	0.1799	0.239033	0.4963	1.0714
92.42	0.201033	0.2576	0.543767	1.208
74.96	0.224267	0.278067	0.5954	1.364333
60.79	0.252333	0.300233	0.653567	1.543
49.32	0.283	0.323467	0.717	1.743667
40	0.320067	0.3494	0.7887	1.975333

APPENDIX E: MEAN DATA ON VISCOELASTIC PROPERTIES OF BGNF-STABILIZED EMULSION

(A) Data on amplitude sweep at 1 Hz

Table E1 Emulsion stabilized with 5% (w/w) BGNF containing 30, 35 and 40% (w/w) SFO

	30% (w/w) SFO		35% (w/w) SFO		40% (w/w) SFO	
Oscillation stress	Storage modulus	Loss modulus	Storage modulus	Loss modulus	Storage modulus	Loss modulus
Pa	Pa	Pa	Pa	Pa	Pa	Pa
0.012192	5.08967	3.65842	9.20971	5.76419	230.414	37.7639
0.019376	5.08019	3.602	9.13492	5.6845	235.132	37.8062
0.030792	5.02307	3.55203	9.06957	5.60719	234.937	34.1336
0.04893	4.95954	3.50643	8.95809	5.54711	231.14	41.1678
0.077712	4.86446	3.47962	8.81159	5.49617	222.623	50.8266
0.123601	4.68518	3.43644	8.60991	5.44952	227.049	44.6318
0.196655	4.43866	3.3894	8.25806	5.3883	228.811	43.6029
0.313401	4.09495	3.3103	7.74333	5.2966	228.623	43.7319
0.500173	3.66345	3.18639	7.03569	5.13934	230.198	40.783
0.798611	3.16359	3.00791	6.17963	4.90057	228.55	41.6828
1.26905	2.63176	2.79575	5.25583	4.60156	225.901	42.2979
1.98365	2.13203	2.61164	4.32748	4.30364	221.786	42.3066
3.02634	1.75248	2.5557	3.49183	4.09742	214.155	42.6034
4.58113	1.55426	2.71805	2.96728	4.17654	201.132	43.2559
6.97725	1.40813	2.96789	2.92789	4.73883	179.784	43.3722
10.5866	1.12537	3.03539	3.09819	5.59121	145.154	41.8036
15.7208	0.699671	2.72193	2.98719	6.31463	93.8925	35.0635
22.4114	0.341002	2.12658	2.22358	6.3105	48.6696	25.8611
30.4153	0.151916	1.55717	1.08973	5.11703	31.8868	26.9554
39.7508	0.068864	1.14241	0.355558	3.33896	22.3207	31.1529
51.072	0.032129	0.859786	0.104619	2.014	7.53311	24.637

Table E2 Emulsion stabilized with 6% (w/w) BGNF containing 30, 35 and 40% (w/w) SFO

	30% (w/w) SFO		35% (w/w) SFO		40% (w/w) SFO	
Oscillation stress	Storage modulus	Loss modulus	Storage modulus	Loss modulus	Storage modulus	Loss modulus
Pa	Pa	Pa	Pa	Pa	Pa	Pa
0.011146	9.18588	6.6	27.4	14.0756	335.678	48.807
0.01769	9.49551	6.40647	28.2015	13.5666	326.074	65.3415
0.028039	9.72217	6.31808	28.2337	13.3331	333.997	50.38
0.044451	9.81701	6.25453	27.9141	13.1966	322.762	69.0557
0.070474	9.86387	6.20921	28.0504	12.9919	333.048	57.6053
0.111768	9.81874	6.1715	27.8221	12.8749	322.114	70.6782
0.1774	9.58446	6.1335	27.4942	12.7989	325.345	65.7197
0.281849	9.18075	6.07854	26.7521	12.7498	325.428	64.9995
0.448596	8.54579	5.96202	25.5434	12.6757	328.392	62.5979
0.715781	7.68258	5.74288	23.6458	12.4481	328.146	62.68
1.14522	6.66337	5.41163	20.8719	11.9441	327.183	61.9641
1.83465	5.59124	5.02275	17.4936	11.0407	324.906	61.2749
2.92798	4.53526	4.6791	13.8847	9.83892	318.186	61.9312
4.60827	3.55278	4.48521	10.5349	8.68032	306.019	62.2038
7.10946	2.82301	4.57945	8.05411	8.13575	284.723	62.8791
10.9097	2.29914	4.84379	7.01455	8.7569	249.897	62.0705
16.7223	1.58205	4.67002	7.06626	10.3601	193.69	57.7224
25.2195	0.785213	3.78707	6.83286	12.0341	116.362	45.721
36.6943	0.307839	2.68031	5.09938	12.3701	59.4297	36.6894
50.8061	0.117038	1.84345	2.23081	9.87894	38.1793	40.9037
67.3894	0.048471	1.30541	0.526732	6.00922	20.4411	40.3232

Table E3 Emulsion stabilized with 7% (w/w) BGNF containing 30, 35 and 40% (w/w) SFO

	30% (w/w) SFO		35% (w/w) SFO		40% (w/w) SFO	
Oscillation stress	Storage modulus	Loss modulus	Storage modulus	Loss modulus	Storage modulus	Loss modulus
Pa	Pa	Pa	Pa	Pa	Pa	Pa
0.010422	28.4736	14.8912	25.7541	14.1608	759.7	132.771
0.016547	27.4434	14.2539	29.9287	9.69564	919.16	-188.027
0.026259	26.4786	13.9105	28.7142	11.5065	712.808	270.419
0.041661	26.0827	13.4244	29.7147	10.767	932.357	-108.54
0.066087	25.5839	13.1891	30.4688	10.1016	861.675	150.745
0.104818	25.2672	12.9582	30.7942	9.81091	843.56	150.249
0.166258	24.7334	12.8113	30.7893	9.55986	862.784	122.721
0.263743	24.083	12.7049	30.2209	9.3758	849.364	150.758
0.418621	22.9831	12.593	28.824	9.2924	850.689	149.155
0.665021	21.3219	12.4123	26.5244	9.07408	876.035	113.89
1.0578	19.1151	12.0383	23.2251	8.59528	860.004	139.926
1.68596	16.3816	11.3477	19.1001	7.84279	861.568	138.725
2.69401	13.3406	10.336	14.7632	6.83343	864.232	132.562
4.31396	10.2659	9.17595	10.9167	5.85901	859.351	135.628
6.89018	7.55454	8.21991	8.00606	5.56432	850.927	135.506
10.8642	5.91337	8.06097	6.02697	6.19827	834.582	137
16.9744	5.40527	8.83781	4.36628	6.77802	806.747	139.239
26.5341	4.9165	9.71436	2.37229	6.10682	761.167	142.109
41.4785	3.49478	9.5201	0.741726	3.95428	686.222	144.189
64.4191	1.53651	7.40006	0.112012	1.66587	565.895	142.874
97.9185	0.436761	4.5972	6.67E-03	0.507485	375.302	129.424

(B) Frequency sweep data for emulsion stabilized with BGNF

Table E4 Emulsion stabilized with 5% (w/w) BGNF containing 30, 35 and 40% (w/w) SFO

	30% SFO		35% SFO		40% SFO	
Angular frequency	Storage modulus	Loss modulus	Storage modulus	Loss modulus	Storage modulus	Loss modulus
rad/s	Pa	Pa	Pa	Pa	Pa	Pa
62.8319	6.34418	8.34589	7.69227	9.96964	30.8299	22.9477
47.117	6.3179	7.21114	7.36496	8.44215	28.0657	20.1676
35.3326	5.86856	6.13312	6.57829	7.12411	25.1789	17.7274
26.4957	5.35999	5.25541	5.83739	6.04016	22.3744	15.532
19.8689	4.78453	4.48696	5.03462	5.09218	20.4341	13.6791
14.8998	4.17276	3.81574	4.2221	4.27268	18.984	12.083
11.1733	3.59613	3.23183	3.52684	3.57023	17.674	10.6946
8.37882	3.17637	2.76043	3.03498	3.00273	16.4935	9.48497
6.28319	2.87833	2.37987	2.68756	2.55054	15.3915	8.40613
4.71167	2.62373	2.06168	2.4009	2.17583	14.4265	7.46783
3.53331	2.40649	1.79314	2.165	1.86356	13.5263	6.66862
2.64958	2.20956	1.5635	1.95992	1.59945	12.7159	5.9884
1.9869	2.03535	1.36725	1.78013	1.37527	12.0482	5.35509
1.48998	1.88727	1.20015	1.63206	1.18645	11.5547	4.77638
1.11733	1.76699	1.05886	1.51427	1.02954	11.0662	4.38057
0.837875	1.66951	0.9393	1.42341	0.900257	10.7796	3.98647
0.628319	1.59991	0.838825	1.36149	0.792773	10.6294	3.64052

Table E5 Emulsion stabilized with 6% (w/w) BGNF containing 30, 35 and 40% (w/w) SFO

	30% SFO		35% SFO		40% SFO	
Angular frequency	Storage modulus	Loss modulus	Storage modulus	Loss modulus	Storage modulus	Loss modulus
rad/s	Pa	Pa	Pa	Pa	Pa	Pa
62.8319	18.8295	14.8595	50.554	33.0734	73.4621	45.0063
47.117	17.0248	12.804	46.9073	28.7253	67.9549	40.0071
35.3326	15.5062	11.1471	43.3012	25.1343	63.3211	35.516
26.4957	14.0458	9.69108	40.4963	22.0857	59.4549	31.6421
19.8689	12.574	8.44712	38.1027	19.4298	55.8765	28.1569
14.8998	11.4986	7.39425	35.9637	17.1928	52.6951	25.1363
11.1733	10.6735	6.49064	33.9759	15.2104	49.9701	22.4508
8.37882	9.93394	5.71813	32.3452	13.5251	47.0337	20.1983
6.28319	9.2548	5.05307	30.7736	12.0753	44.8212	18.0777
4.71167	8.65415	4.47403	29.4421	10.77	42.774	16.2856
3.53331	8.11882	3.97299	28.3296	9.61835	40.7575	14.7258
2.64958	7.64332	3.54354	27.3546	8.57214	39.5603	12.8725
1.9869	7.22231	3.16629	26.5004	7.74355	38.0144	11.7728
1.48998	6.84649	2.85543	25.7448	7.16238	36.9774	10.4993
1.11733	6.56084	2.57962	25.0621	7.03466	35.8824	10.0011
0.837875	6.3588	2.32037	25.0636	6.31861	35.4322	9.12895
0.628319	6.19099	2.13123	25.3929	5.54126	35.2515	8.6649

Table E6 Emulsion stabilized with 7% (w/w) BGNF containing 30, 35 and 40% (w/w) SFO

	30% SFO		35% SFO		40% SFO	
Angular frequency	Storage modulus	Loss modulus	Storage modulus	Loss modulus	Storage modulus	Loss modulus
rad/s	Pa	Pa	Pa	Pa	Pa	Pa
62.8319	58.5328	35.3431	106.911	49.2867	191.452	79.6746
47.117	53.0737	31.1131	99.8619	43.7535	181.387	71.6765
35.3326	48.3083	27.4796	93.9821	39.038	172.529	64.7288
26.4957	44.5142	24.2332	88.3702	34.6351	163.703	58.28
19.8689	41.3079	21.4324	83.7803	31.0771	156.826	53.2889
14.8998	38.4356	18.9755	79.5872	27.8207	150.984	48.3923
11.1733	35.9692	16.8004	75.7275	25.2272	144.656	44.4465
8.37882	33.7245	14.9822	73.1685	22.2936	138.464	41.0446
6.28319	31.8971	13.3124	69.4404	20.5953	135.202	36.8103
4.71167	30.3883	11.7584	67.4512	18.1115	130.476	33.4942
3.53331	28.6225	10.729	65.4265	15.8519	127.281	30.1734
2.64958	27.3811	9.6122	63.487	14.1158	121.507	29.5095
1.9869	26.2651	8.72039	60.6615	14.0267	119.363	27.133
1.48998	25.2871	7.9055	58.7133	13.6248	116.525	23.9127
1.11733	24.8031	6.9438	58.1627	11.3825	112.565	25.1639
0.837875	23.9416	6.80272	56.2075	12.694	112.954	18.9387
0.628319	23.8495	6.07863	56.1423	10.3925	111.36	19.0945

APPENDIX F: EFFECT OF BAMBARA GROUNDNUT VARIETIES ON EMULSION RHEOLOGY.

TableF1 Mean data of frequency sweep on different varieties

	Black eye		Brown eye		Red		Brown	
Angular frequency	Storage modulus	Loss modulus	Storage modulus	Loss modulus	Storage modulus	Loss modulus	Storage modulus	Loss modulus
rad/s	Pa	Pa	Pa	Pa	Pa	Pa	Pa	Pa
62.8319	226.38	79.95	290.392	105.048	284.564	86.4323	290.392	105.048
47.117	215.636	72.2062	278.107	95.0901	271.846	78.7022	278.107	95.0901
35.3326	206.1	66.0494	266.405	86.9738	259.984	71.6707	266.405	86.9738
26.4957	198.918	60.8561	255.898	79.5549	247.835	65.3502	255.898	79.5549
19.8689	190.474	55.3485	245.327	72.4831	241.83	59.9223	245.327	72.4831
14.8998	182.821	51.0451	236.735	66.7776	229.39	56.0398	236.735	66.7776
11.1733	176.429	47.4053	224.876	63.5899	224.438	49.6207	224.876	63.5899
8.37882	169.242	44.5832	222.176	55.6954	210.881	50.452	222.176	55.6954
6.28319	160.695	45.231	208.94	56.7343	207.426	44.6964	208.94	56.7343
4.71167	164.601	29.8577	211.198	43.2704	196.587	46.2477	211.198	43.2704
3.53331	152.681	37.6478	199.67	45.4009	195.243	36.5892	199.67	45.4009
2.64958	144.941	40.8623	195.384	40.4882	189.569	33.6096	195.384	40.4882
1.9869	149.303	22.74	184.02	47.0016	184.275	30.0028	184.02	47.0016
1.48998	140.731	31.9152	186.983	30.3346	173.807	40.8987	186.983	30.3346
1.11733	138.827	26.2082	180.224	33.3852	168.226	41.2854	180.224	33.3852
0.837875	132.202	33.1536	169.643	43.8682	169.078	27.8092	169.643	43.8682
0.628319	135.497	19.2765	166.032	47.2632	160.898	35.9905	160.898	19.0945

Table F2 Data of creep and compliance on different varieties

Time (s)	Black eye Strain (%)	Brown eye Strain (%)	Red Strain (%)	Brown Strain (%)
0	0	0	0	0
6.25008	0.581354	0.587179	0.492163	0.59826
18.7502	0.804649	0.810476	0.624134	0.822943
31.2503	0.911699	0.916186	0.697704	0.931805
43.7504	0.984899	0.986516	0.753081	1.006652
56.2505	1.04127	1.04136	0.797913	1.062908
68.7506	1.08675	1.0848	0.835704	1.109198
81.2507	1.12471	1.12082	0.869984	1.147038
93.7508	1.15602	1.15123	0.902891	1.179615
106.251	1.18259	1.17683	0.933094	1.206837
118.751	1.20563	1.19885	0.960048	1.231428
131.251	1.22554	1.21777	0.984209	1.25232
143.751	1.2438	1.2342	1.00753	1.270685
156.251	1.26063	1.24869	1.03116	1.28723
175.001	1.28262	1.26835	1.0619	1.309475
200.002	1.3068	1.29043	1.09951	1.33395
225.002	1.32738	1.3092	1.1333	1.35529
250.002	1.34563	1.32522	1.16739	1.373555
275.002	1.36095	1.3392	1.19879	1.39036
300.002	1.37519	1.35162	1.22622	1.404535
325.003	1.38758	1.36314	1.25186	1.418085
350.003	1.39867	1.37447	1.27727	1.430235
375.003	1.40906	1.38463	1.30146	1.441805
400.003	1.41824	1.39362	1.32373	1.45202
425.003	1.42686	1.40204	1.34364	1.462295
450.003	1.43517	1.41029	1.3635	1.47133
475.004	1.44198	1.41832	1.38299	1.47991
500	1.44845	1.42881	1.39535	1.487035
506.25	1.08552	1.05751	1.11172	1.127142
518.75	1.02669	0.997235	1.05788	1.066474
531.25	0.998955	0.968222	1.03119	1.037077
543.75	0.979561	0.94773	1.01216	1.015975
556.25	0.963211	0.931302	0.996525	0.998787
568.751	0.948782	0.915512	0.983989	0.983924
581.251	0.936864	0.902468	0.973686	0.971219
593.751	0.926143	0.892118	0.964634	0.959791
606.251	0.917206	0.882478	0.955877	0.9496
618.751	0.908865	0.873529	0.948655	0.939505
631.251	0.900512	0.865	0.942389	0.930623
643.751	0.893008	0.857139	0.936494	0.922233
656.251	0.886825	0.850137	0.93226	0.914464
675.001	0.878199	0.83987	0.926574	0.904251
700.002	0.867646	0.82842	0.920071	0.891459
725.002	0.858873	0.817105	0.913487	0.879893
750.002	0.851374	0.807089	0.907864	0.869015
775.002	0.843609	0.798741	0.903027	0.859128
800.002	0.836895	0.790481	0.89966	0.850173
825.003	0.830999	0.782264	0.895969	0.841481
850.003	0.824293	0.775416	0.892727	0.833606
875.003	0.819679	0.769386	0.889615	0.82637
900.003	0.814708	0.763097	0.886518	0.819494
925.003	0.810082	0.757136	0.884826	0.813289
950.003	0.804727	0.751266	0.882271	0.807004
975.004	0.801186	0.745513	0.880377	0.800705

APPENDIX G: EFFECT OF FOOD ADDITIVES ON EMULSION STABILITY AND RHEOLOGY

(1) Data on the effect of NaCl on storage stability and rheology of BGNF-stabilized emulsion

Table G1 Effect of NaCl on mean backscattering values

Time (s)	Mean backscattering value (%)				
	25 mM	50 mM	100 mM	200 mM	300 mM
0	0	0	0	0	0
60	-0.2	-1.23	-1.48333	-1.62333	-1.71667
120	-0.26333	-1.39333	-1.76667	-1.83	-1.88333
180	-0.30667	-1.50667	-1.89333	-1.90667	-1.94667
240	-0.35	-1.61	-1.98333	-1.96667	-2.00667
300	-0.36333	-1.72667	-2.06	-2.00333	-2.04
360	-0.38	-1.7866	-2.03333	-2.05667	-2.09

Table G2 Shear stress sweep of optimum emulsion (7% (w/w) BGNF and 40% SFO) containing 0, 25, 50, 100, 200 and 300 mM NaCl

Shear Rate [1/s]	Shear stress (Pa) for forward and backward sweep											
	0 mM NaCl		25 mM NaCl		50 mM NaCl		100 mM NaCl		200 mM NaCl		300 mM NaCl	
40	118.9	51.73	106	50.68	88.84	44.655	73.97	35.35	72.81	34.34	65.485	36.975
49.34	119.3	57.99	108.5	56.77	91.225	49.26	75.31	39.6	75.31	39.43	69.71	41.125
60.81	125.6	64.95	114.1	63.63	95.13	54.485	78.66	44.38	79.27	44.14	73.97	45.81
74.98	132.2	72.74	121.3	71.31	101.7	60.27	83.34	49.74	84.69	49.27	79.215	51.01
92.44	140	81.39	129.7	79.91	107.65	66.78	89.14	55.83	90.76	55.2	85.205	56.83
114	148.8	91.26	139.1	89.64	114.8	74.155	96.29	62.79	96.97	61.9	92.02	63.42
140.5	158.8	102.3	149.7	100.6	123.75	82.62	103.9	70.61	104.2	69.37	99.77	71.025
173.2	169.7	115.1	161.5	113	133	92.255	112.5	79.59	112.3	77.99	108.45	79.605
213.6	182.2	129.5	174.9	127.2	143.55	103.45	122.4	89.92	121.3	88.13	118.05	89.575
263.3	196.1	146	189.1	143.4	155.7	116.45	133.5	102	131.7	99.81	129.1	101.15
324.6	210.8	164.7	204.5	162.2	170.05	131.95	145.7	116.3	143.4	113.6	141.75	114.75
400.2	228.3	186.4	222.9	184.1	187.55	150.85	161.7	133.3	157.6	129.7	156.55	131.05
493.4	247.8	212.2	243.1	209.7	209.05	175.1	180.5	154.4	174.5	149.5	174.3	150.9
608.4	269.5	243.4	266	240.8	235.85	207	203.8	181.7	194.9	174.9	195.85	176.4
750	296	296	292.9	292.9	268.45	267.5	231.5	228.1	219.7	216.2	221.5	220

Table G3 Effect of NaCl on the viscosity of optimum emulsion (7% (w/w) BGNF and 40% SFO)

Shear Rate [1/s]	Viscosity (Pas)					
	0 mM	25 mM	50 mM	100 mM	200 mM	300 mM
750	0.4567	0.434233	0.264667	0.2503	0.223267	0.221067
608.3	0.463033	0.432733	0.274133	0.260067	0.236167	0.231033
493.4	0.4968	0.455733	0.293833	0.2775	0.253667	0.245833
400.2	0.543833	0.490967	0.317367	0.300067	0.274033	0.2647
324.6	0.6023	0.5359	0.344967	0.325833	0.297167	0.286433
263.3	0.6718	0.5902	0.3765	0.3557	0.323667	0.311233
213.5	0.754	0.652067	0.4129	0.389833	0.353267	0.339433
173.2	0.846567	0.7232	0.454033	0.427933	0.386367	0.370933
140.5	0.951367	0.803133	0.4999	0.4706	0.423667	0.406733
113.9	1.0714	0.895633	0.550533	0.5184	0.4647	0.446133
92.42	1.208	1.001367	0.6067	0.5724	0.5101	0.4908
74.96	1.364333	1.121	0.670233	0.631267	0.561133	0.540867
60.79	1.543	1.258667	0.740967	0.696067	0.6178	0.596067
49.32	1.743667	1.415333	0.8183	0.770367	0.6808	0.656267
40	1.975333	1.595333	0.9063	0.852267	0.752467	0.729433

Table G4 Effect of NaCl on the steady shear decay of optimum emulsion

Time (s)	Viscosity (Pas)					
	0 mM	25 mM	50 mM	100 mM	200 mM	300 mM
40	4.126	2.980333	1.249	1.074	0.7436	0.692467
80	3.599333	2.602333	1.158667	1.0044	0.7043	0.656667
120	3.370667	2.454	1.121333	0.9793	0.686567	0.6439
160	3.215667	2.361333	1.099333	0.9641	0.675933	0.634367
200	3.100333	2.291333	1.082967	0.95105	0.6702	0.627967
240	3.009333	2.237	1.069833	0.94085	0.665467	0.622567
280	2.942	2.192333	1.058733	0.9331	0.661167	0.617933
320	2.877333	2.16	1.051333	0.9265	0.657633	0.6141
360	2.819667	2.123667	1.042033	0.9218	0.654867	0.610167
400	2.771333	2.094667	1.033433	0.91625	0.6518	0.608333
440	2.729333	2.068667	1.0269	0.91105	0.649833	0.606
480	2.692	2.048	1.020633	0.90585	0.646933	0.604367
520	2.658333	2.033	1.0143	0.9014	0.6436	0.601833
560	2.628	2.013	1.008833	0.8965	0.642133	0.599567
600	2.599	1.995667	1.005233	0.89065	0.6406	0.5983
640	2.572	1.98	1.001667	0.88755	0.6388	0.5956
680	2.549667	1.965333	0.998567	0.8835	0.6361	0.595
720	2.527667	1.951667	0.996233	0.88125	0.634533	0.5935
760	2.509333	1.939	0.994433	0.8786	0.632667	0.591033
800	2.490667	1.927667	0.992533	0.8773	0.630667	0.59
840	2.472667	1.916333	0.989633	0.8747	0.6284	0.589233
880	2.457	1.905333	0.987567	0.87325	0.626567	0.5893
920	2.440333	1.894333	0.986033	0.87195	0.626467	0.587233
960	2.425333	1.884667	0.984633	0.8694	0.625	0.586033
1000	2.411667	1.875667	0.9822	0.86755	0.624033	0.584933
1040	2.396	1.867667	0.980767	0.866	0.623233	0.5832
1080	2.382333	1.859333	0.979333	0.86295	0.621533	0.5827
1120	2.369333	1.852	0.977733	0.8619	0.6211	0.581533
1160	2.358667	1.845	0.9758	0.86015	0.619567	0.580367
1200	2.344	1.838667	0.974267	0.85795	0.620333	0.5794

Table G5 **Frequency sweep of optimum emulsion containing various concentration of NaCl**

	0 mM		25 mM		50 mM		100 mM		200 mM		300 mM	
Angular frequency	Storage modulus	Loss modulus	Storage modulus	Loss modulus	Storage modulus	Loss modulus	Storage modulus	Loss modulus	Storage modulus	Loss modulus	Storage modulus	Loss modulus
rad/s	Pa	Pa	Pa	Pa	Pa	Pa	Pa	Pa	Pa	Pa	Pa	Pa
62.8319	191.452	79.6746	124.602	69.3649	88.2092	58.6965	73.3193	47.7511	60.1801	40.0991	36.6174	32.0001
47.117	181.387	71.6765	115.155	62.882	79.7592	52.9483	65.7518	43.1352	54.9829	36.3655	31.5861	28.594
35.3326	172.529	64.7288	106.505	56.8742	72.4943	47.7333	59.1418	38.9121	49.712	32.8476	27.04	25.4742
26.4957	163.703	58.28	98.7643	51.5988	66.1396	42.9711	53.3124	35.1193	44.911	29.5976	23.0892	22.5827
19.8689	156.826	53.2889	91.6763	46.9373	60.4783	38.7884	48.0424	31.5477	40.4955	26.5638	19.7869	19.9402
14.8998	150.984	48.3923	85.1696	42.6621	55.4317	34.9974	43.4465	28.4158	36.6119	23.9203	16.9426	17.5312
11.1733	144.656	44.4465	79.3483	38.8035	50.4665	31.5013	39.059	25.4616	32.9693	21.4012	14.5227	15.4053
8.37882	138.464	41.0446	73.9848	35.4636	46.4545	28.4919	35.4373	22.8635	29.7557	19.1398	12.4295	13.4473
6.28319	135.202	36.8103	68.5348	32.4649	42.8067	25.7339	32.0238	20.5304	26.7099	17.1167	10.6436	11.746
4.71167	130.476	33.4942	64.6644	29.5215	39.2753	23.3181	28.9661	18.4287	24.1514	15.2835	9.0718	10.2056
3.53331	127.281	30.1734	60.1113	27.3076	36.1154	21.1938	26.1259	16.6081	21.997	13.6238	7.76532	8.88001
2.64958	121.507	29.5095	57.1954	24.6327	33.1378	19.3997	23.829	14.9297	19.891	12.1758	6.67901	7.72186
1.9869	119.363	27.133	52.4448	23.7081	30.4101	17.8464	21.6772	13.4385	18.1699	10.8444	5.6219	6.66879
1.48998	116.525	23.9127	49.9021	21.8276	28.6864	16.2375	19.8195	12.133	16.4419	9.74325	4.81584	5.78993
1.11733	112.565	25.1639	47.2081	20.2971	27.0127	14.9399	17.8827	11.1092	15.1653	8.63301	4.20201	5.04259
0.837875	112.954	18.9387	45.644	18.1228	24.9833	14.1561	16.6257	9.99652	13.7496	7.79142	3.62581	4.38008
0.628319	111.36	19.0945	43.7724	17.2562	24.6017	12.8222	15.3118	9.1499	12.5916	7.04106	3.20576	3.82991

(2) Data on the effect of vinegar on storage stability and rheology of optimum BGNF-stabilized emulsion

Table G6 Effect of vinegar concentration on backscattering mean value of optimum emulsion

Time	Mean Backscattering				
	0.50%	2%	4%	6%	8%
0	0	0	0	0	0
30	-0.12	-0.63	-0.215	-0.26	-0.25
60	-0.14	-0.87	-0.305	-0.32	-0.295
90	-0.13	-1.075	-0.385	-0.37	-0.32
120	-0.1	-1.25	-0.46	-0.395	-0.36
150	-0.14	-1.385	-0.535	-0.445	-0.35
180	-0.14	-1.505	-0.565	-0.46	-0.355
210	-0.17	-1.58	-0.595	-0.49	-0.4
240	-0.16	-1.665	-0.65	-0.485	-0.355
270	-0.18	-1.735	-0.665	-0.485	-0.385
300	-0.19	-1.795	-0.695	-0.51	-0.39
330	-0.21	-1.88	-0.73	-0.525	-0.4
360	-0.2	-1.915	-0.75	-0.525	-0.385

Table G7 Effect of vinegar on equilibrium backscattering value of optimum emulsion

Vinegar (%)	BS_{eq}
0	-0.31333
0.5	-0.385
2	-1.915
4	-0.75
6	-0.525
8	-0.2

Table G8 Effect of vinegar concentrations (%w/w) on apparent viscosity

	0%	0.5%	2%	4%	6%	8%
Shear Rate [1/s]	Viscosity [Pa·s]	Viscosity [Pa·s]	Viscosity [Pa·s]	Viscosity [Pa·s]	Viscosity [Pa·s]	Viscosity [Pa·s]
40	2.965	1.257	1.248	1.147	1.256	1.172
49.33	2.418	1.096	1.057	0.9826	1.091	1.008
60.8	2.066	0.966	0.921	0.8566	0.9584	0.8937
74.97	1.763	0.8515	0.8094	0.7556	0.8489	0.7968
92.43	1.515	0.7547	0.7149	0.6695	0.7536	0.7189
114	1.306	0.6704	0.634	0.5959	0.6706	0.6419
140.5	1.13	0.5984	0.5644	0.533	0.6	0.5732
173.2	0.9797	0.5344	0.5039	0.4774	0.5368	0.5124
213.6	0.8532	0.4788	0.4511	0.4287	0.4823	0.4585
263.3	0.7447	0.4301	0.4055	0.3859	0.4347	0.4113
324.6	0.6494	0.3878	0.3653	0.3486	0.3939	0.3698
400.2	0.5705	0.3504	0.3312	0.3169	0.3586	0.3345
493.4	0.5022	0.3183	0.3026	0.2894	0.3281	0.304
608.3	0.4431	0.2902	0.2784	0.2651	0.3018	0.2768
750	0.3947	0.2654	0.2563	0.2436	0.2792	0.2532

Table G9 Frequency sweep data of optimum emulsion containing vinegar at various concentrations

	0%		0.50%		2%		4%		6%		8%	
Angular frequency	Storage modulus	Loss modulus	Storage modulus	Loss modulus	Storage modulus	Loss modulus	Storage modulus	Loss modulus	Storage modulus	Loss modulus	Storage modulus	Loss modulus
rad/s	Pa	Pa	Pa	Pa	Pa	Pa	Pa	Pa	Pa	Pa	Pa	Pa
62.8319	191.452	79.6746	60.1293	42.7034	62.936	42.7226	58.7225	34.9787	66.2886	42.4115	64.1699	47.4965
47.117	181.387	71.6765	53.8442	38.3052	56.4848	38.3105	53.1565	31.6371	60.0434	38.1907	56.5929	42.4156
35.3326	172.529	64.7288	47.9278	34.2573	50.6677	34.2963	48.0733	28.6618	54.3349	34.2305	50.0056	37.8854
26.4957	163.703	58.28	42.8522	30.4836	45.5109	30.6248	43.5961	25.8986	49.225	30.664	44.2495	33.7873
19.8689	156.826	53.2889	38.2637	27.267	40.9002	27.3656	39.5985	23.4182	44.6358	27.4415	39.1626	30.0397
14.8998	150.984	48.3923	34.3455	24.3501	36.8141	24.3858	35.9359	21.0675	40.5403	24.483	34.6349	26.6411
11.1733	144.656	44.4465	30.7345	21.585	33.2872	21.7253	32.6687	18.9469	36.9786	21.8325	30.8122	23.6626
8.37882	138.464	41.0446	27.5737	19.1304	29.9956	19.292	30.0172	16.9939	33.8009	19.4364	27.3231	20.8951
6.28319	135.202	36.8103	24.7118	16.9393	27.3193	17.1147	27.4717	15.2166	30.7684	17.2997	24.1815	18.4254
4.71167	130.476	33.4942	22.3018	14.9795	24.5747	15.216	25.1535	13.6512	28.4174	15.299	21.6604	16.2382
3.53331	127.281	30.1734	20.3396	13.1865	22.6038	13.4298	23.265	12.1861	26.1016	13.6611	19.3685	14.3032
2.64958	121.507	29.5095	18.1099	11.7663	20.6146	11.924	21.6763	10.8112	24.2096	12.0867	17.4547	12.5848
1.9869	119.363	27.133	16.714	10.3276	18.9378	10.5463	19.8744	9.83654	22.2759	10.8601	15.6025	11.0951
1.48998	116.525	23.9127	15.2934	9.11295	17.54	9.32928	18.6582	8.73049	20.7872	9.67471	14.0763	9.77734
1.11733	112.565	25.1639	14.1515	8.04475	16.3564	8.24068	17.5877	7.83872	19.4413	8.66615	12.8656	8.59562
0.837875	112.954	18.9387	13.1072	7.1637	15.2542	7.37721	16.6365	7.13652	18.3268	7.76576	11.8257	7.57872
0.628319	111.36	19.0945	12.302	6.37088	14.3619	6.58849	16.022	6.38792	17.4762	6.90422	10.8758	6.73241

Table G9 **Creep and compliance data of optimum emulsion containing various concentrations of vinegar (%w/w)**

Time (s)	Strain (%)					
	0	0.50	2	4	6	8
0	0	0	0	0	0	0
6.25008	0.59826	11.63036	9.84434	12.12718	11.23558	11.61316
18.7502	0.822943	17.54849	15.07124	18.31982	16.6832	17.28799
31.2503	0.931805	20.52505	18.06046	21.4084	19.45884	20.07526
43.7504	1.006652	22.57481	20.2968	23.5398	21.39	21.98056
56.2505	1.062908	24.11766	22.094	25.1538	22.8584	23.41785
68.7506	1.109198	25.33902	23.5894	26.4508	24.0348	24.56045
81.2507	1.147038	26.3391	24.8604	27.5226	25.011	25.50097
93.7508	1.179615	27.1766	25.9562	28.4258	25.8382	26.29419
106.251	1.206837	27.8884	26.9052	29.2062	26.5542	26.9727
118.751	1.231428	28.502	27.728	29.8862	27.186	27.561
131.251	1.25232	29.0398	28.4478	30.4862	27.745	28.0771
143.751	1.270685	29.5105	29.0872	31.0208	28.2504	28.5348
156.251	1.28723	29.9315	29.6564	31.5032	28.707	28.9437
175.001	1.309475	30.4783	30.395	32.1388	29.3146	29.4805
200.002	1.33395	31.0947	31.223	32.8786	30.0248	30.0912
225.002	1.35529	31.6086	31.9012	33.5186	30.6508	30.6078
250.002	1.373555	32.0491	32.467	34.0754	31.201	31.0523
275.002	1.39036	32.434	32.944	34.5692	31.6998	31.4429
300.002	1.404535	32.7734	33.351	35.0148	32.152	31.7888
325.003	1.418085	33.0756	33.7004	35.4188	32.5664	32.0983
350.003	1.430235	33.3504	34.0058	35.7848	32.9494	32.3793
375.003	1.441805	33.5976	34.2736	36.1212	33.3016	32.6339
400.003	1.45202	33.8256	34.513	36.4338	33.6368	32.8698
425.003	1.462295	34.036	34.7256	36.7276	33.9462	33.0892
450.003	1.47133	34.2313	34.9182	37.0008	34.2406	33.2928
475.004	1.47991	34.413	35.0958	37.2544	34.5202	33.4834
500	1.487035	34.5845	35.2638	37.4906	34.7956	33.6562
506.25	1.127142	28.4173	29.5512	30.1212	27.8282	27.3422
518.75	1.066474	26.7032	27.9356	27.7236	25.7098	25.57961
531.25	1.037077	25.9849	27.2398	26.6824	24.7912	24.84395
543.75	1.015975	25.50664	26.7684	25.9886	24.1736	24.35504
556.25	0.998787	25.14822	26.409	25.472	23.7112	23.98998
568.751	0.983924	24.86457	26.1184	25.061	23.3438	23.70185
581.251	0.971219	24.63032	25.876	24.7242	23.0412	23.46428
593.751	0.959791	24.43146	25.667	24.4376	22.7848	23.26378
606.251	0.9496	24.26233	25.4842	24.1776	22.5656	23.09335
618.751	0.939505	24.11434	25.3234	23.9648	22.3716	22.94474

631.251	0.930623	23.9838	25.177	23.7774	22.1972	22.81316
643.751	0.922233	23.86833	25.0456	23.6088	22.0452	22.6979
656.251	0.914464	23.76486	24.9248	23.4568	21.907	22.59419
675.001	0.904251	23.62788	24.7642	23.2588	21.724	22.45779
700.002	0.891459	23.47008	24.5752	23.0346	21.5134	22.30038
725.002	0.879893	23.33691	24.4112	22.8394	21.3346	22.16919
750.002	0.869015	23.22329	24.2654	22.676	21.1822	22.0576
775.002	0.859128	23.12654	24.1368	22.533	21.0488	21.96148
800.002	0.850173	23.0425	24.0218	22.4094	20.9284	21.87696
825.003	0.841481	22.96877	23.9164	22.302	20.823	21.80257
850.003	0.833606	22.90393	23.8206	22.2036	20.7292	21.73882
875.003	0.82637	22.84393	23.7326	22.1178	20.6434	21.68022
900.003	0.819494	22.79059	23.6532	22.0388	20.5674	21.62731
925.003	0.813289	22.7434	23.5794	21.9674	20.5	21.58083
950.003	0.807004	22.70044	23.5126	21.9048	20.44	21.53857
975.004	0.800705	22.65998	23.4474	21.8476	20.3846	21.4986

(3) Data on the effect of citric acid on storage stability and rheology of optimum BGNF-stabilized emulsion

Table G10 Effect of citric acid concentration on backscattering mean value of optimum emulsion

Time	Mean Backscattering			
	0.50%	2%	4%	6%
0	0	0	0	0
30	-0.11	-0.15	-0.33	-0.255
60	-0.17	-0.17	-0.32	-0.275
90	-0.155	-0.135	-0.335	-0.29
120	0.1	-0.1	-0.38	-0.305
150	0.155	-0.06	-0.36	-0.285
180	0.155	-0.065	-0.325	-0.29
210	0.125	-0.035	-0.29	-0.265
240	0.08	-0.005	-0.28	-0.265
270	0.1	0.04	-0.275	-0.22
300	0.095	0.09	-0.285	-0.205
330	0.085	0.1	-0.265	-0.165
360	0.075	0.125	-0.28	-0.19

Table G11Effect of citric acid concentrations (%w/w) on apparent viscosity

	0%	0.50%	2%	4%	6%
Shear Rate [1/s]	Viscosity [Pa·s]	Viscosity [Pa·s]	Viscosity [Pa·s]	Viscosity [Pa·s]	Viscosity [Pa·s]
40.08	2.965	2.283	1.494	1.284	1.295
49.34	2.418	1.894	1.317	1.161	1.169
60.81	2.066	1.612	1.189	1.063	1.073
74.98	1.763	1.38	1.071	0.9749	0.9873
92.44	1.515	1.195	0.9712	0.896	0.9089
114	1.306	1.04	0.8819	0.8249	0.8351
140.5	1.13	0.9093	0.8018	0.768	0.7689
173.2	0.9797	0.7984	0.7284	0.7159	0.7073
213.6	0.8532	0.7047	0.6601	0.6574	0.6503
263.3	0.7447	0.6249	0.5987	0.6036	0.5979
324.6	0.6494	0.5561	0.5437	0.5555	0.5495
400.2	0.5705	0.4987	0.4936	0.5113	0.5063
493.4	0.5022	0.4511	0.4485	0.47	0.4657
608.4	0.4431	0.4109	0.4069	0.4329	0.4289
750	0.3947	0.3759	0.3707	0.3991	0.395

Table G12 **Shear stress sweep of optimum emulsion (7% (w/w) BGNF and 40% SFO) containing 0, 0.5, 2, 4, and 6 % (w/w) citric acid**

Shear Rate [1/s]	Shear stress (Pa) for forward and backward sweep									
	0% (w/w)		0,5% (w/w)		2% (w/w)		4% (w/w)		6% (w/w)	
40.11	118.9	51.73	91.51	52.61	59.83	42.37	51.44	41.84	51.86	37.44
49.34	119.3	57.99	93.45	57.79	64.96	48.28	57.26	47.7	57.66	43.29
60.81	125.6	64.95	97.99	63.52	72.3	54.83	64.67	54.39	65.23	49.85
74.98	132.2	72.74	103.4	70.1	80.29	62.43	73.1	62.18	74.03	57.67
92.44	140	81.39	110.5	77.48	89.78	71.15	82.82	71.17	84.01	66.73
114	148.8	91.26	118.6	85.87	100.5	81.03	94.01	81.63	95.17	77.15
140.5	158.8	102.3	127.8	95.34	112.7	92.35	107.9	93.64	108	89.27
173.2	169.7	115.1	138.3	106.2	126.2	105.2	124	107.5	122.5	103.3
213.6	182.2	129.5	150.5	118.7	141	119.9	140.4	123.5	138.9	119.4
263.3	196.1	146	164.5	133.2	157.6	136.8	158.9	142.2	157.4	138.1
324.6	210.8	164.7	180.5	150.3	176.5	156.1	180.3	163.5	178.4	159.8
400.2	228.3	186.4	199.6	170.8	197.6	178.3	204.7	188.5	202.6	185.1
493.4	247.8	212.2	222.6	196.5	221.3	204.2	231.9	217.8	229.8	214.6
608.4	269.5	243.4	250	229.2	247.6	234.9	263.3	252.6	260.9	249.3
750	296	296	281.9	281.9	278	278	299.3	299.3	296.3	296.3

Table G13 **Effect of citric acid on the steady shear decay of optimum emulsion**

Time (s)	Viscosity (Pas)				
	0% (w/w)	0.5% (w/w)	2% (w/w)	4% (w/w)	6% (w/w)
40	4.126	2.174	1.864	1.561	1.411
80	3.599333	2.032	1.786	1.495	1.334
120	3.370667	1.944	1.742	1.466	1.293
160	3.215667	1.887	1.707	1.445	1.273
200	3.100333	1.843	1.682	1.429	1.254
240	3.009333	1.812	1.663	1.415	1.243
280	2.942	1.78	1.646	1.407	1.232
320	2.877333	1.756	1.631	1.398	1.225
360	2.819667	1.734	1.617	1.389	1.218
400	2.771333	1.713	1.605	1.382	1.212
440	2.729333	1.696	1.596	1.375	1.206
480	2.692	1.684	1.587	1.369	1.203
520	2.658333	1.671	1.578	1.365	1.198
560	2.628	1.66	1.57	1.36	1.198
600	2.599	1.649	1.563	1.356	1.198
640	2.572	1.64	1.555	1.352	1.198
680	2.549667	1.63	1.549	1.348	1.198
720	2.527667	1.621	1.543	1.345	1.198
760	2.509333	1.613	1.532	1.342	1.198
800	2.490667	1.605	1.527	1.34	1.198
840	2.472667	1.597	1.521	1.337	1.198
880	2.457	1.591	1.517	1.333	1.198
920	2.440333	1.584	1.514	1.331	1.198
960	2.425333	1.578	1.509	1.328	1.198
1000	2.411667	1.572	1.505	1.326	1.198
1040	2.396	1.566	1.502	1.323	1.198
1080	2.382333	1.561	1.498	1.321	1.198
1120	2.369333	1.555	1.495	1.318	1.198
1160	2.358667	1.55	1.49	1.316	1.198
1200	2.344	1.546	1.486	1.314	1.198

Table G10 Frequency sweep data of optimum emulsion containing citric acid at various concentrations

	0 % (w/w)		0.5% (w/w)		2% (w/w)		4% (w/w)		6% (w/w)	
Angular frequency	Storage modulus	Loss modulus	Storage modulus	Loss modulus	Storage modulus	Loss modulus	Storage modulus	Loss modulus	Storage modulus	Loss modulus
rad/s	Pa	Pa	Pa	Pa	Pa	Pa	Pa	Pa	Pa	Pa
62.8319	191.452	79.6746	151.467	91.7183	129.553	92.198	126.084	91.966	125.477	90.3634
47.117	181.387	71.6765	140.043	81.7488	118.323	81.6492	114.855	81.0475	113.406	79.8031
35.3326	172.529	64.7288	129.745	73.0512	108.585	72.3087	104.812	71.6414	103.292	70.486
26.4957	163.703	58.28	120.501	65.5977	99.8147	64.3727	96.0254	63.4372	94.6725	62.7473
19.8689	156.826	53.2889	112.117	58.6896	92.0559	57.401	88.1585	56.3975	86.9282	55.7109
14.8998	150.984	48.3923	104.741	52.4765	84.8302	51.148	81.1547	50.1535	79.5302	49.4369
11.1733	144.656	44.4465	98.7061	46.9874	78.9797	45.8421	74.711	44.9417	73.4454	44.1839
8.37882	138.464	41.0446	91.4605	42.5316	73.3095	41.2322	69.4345	40.1713	67.7319	39.7216
6.28319	135.202	36.8103	87.7348	37.607	66.4213	37.5753	63.9673	36.2865	63.5184	35.7311
4.71167	130.476	33.4942	82.1934	34.3278	62.8042	33.7515	61.0443	32.215	58.2384	32.596
3.53331	127.281	30.1734	77.6348	31.1418	58.6547	30.8397	55.7442	29.6596	54.2777	29.6771
2.64958	121.507	29.5095	75.3195	26.744	54.4783	28.4259	50.1046	28.1858	51.2877	26.9981
1.9869	119.363	27.133	70.6597	25.5657	51.1432	26.2876	49.0958	24.8517	47.3597	25.2601
1.48998	116.525	23.9127	68.0032	23.2112	47.8684	24.4651	45.0532	23.7206	44.0096	23.7441
1.11733	112.565	25.1639	65.3347	21.5079	44.6065	23.313	42.3356	22.452	41.9882	22.0043
0.837875	112.954	18.9387	63.3163	20.497	42.7392	21.985	41.1843	20.6754	40.9566	20.2845
0.628319	111.36	19.0945	61.2605	20.1089	41.4512	20.6613	38.5856	20.5404	39.1078	19.6696

Table G11 **Creep and compliance data of optimum emulsion containing various concentrations of citric acid (%w/w)**

Time (s)	Strain %				
	0%(w/w)	0.5% (w/w)	2% (w/w)	4% (w/w)	6% (w/w)
0	0	0	0	0	0
6.25008	0.59826	2.060473	8.6378	7.94232	8.10766
18.7502	0.822943	2.727	16.58474	15.18802	15.6119
31.2503	0.931805	3.06979	22.55726	20.773	21.4114
43.7504	1.006652	3.31343	27.5686	25.5484	26.356
56.2505	1.062908	3.50322	31.8525	29.6638	30.62
68.7506	1.109198	3.65736	35.5896	33.2538	34.3634
81.2507	1.147038	3.7858	38.8975	36.4562	37.7024
93.7508	1.179615	3.8973	41.832	39.3436	40.693
106.251	1.206837	3.99351	44.4341	41.9422	43.3862
118.751	1.231428	4.07913	46.7503	44.2798	45.8122
131.251	1.25232	4.15529	48.8275	46.3966	48.007
143.751	1.270685	4.22368	50.7069	48.3226	50.008
156.251	1.28723	4.28701	52.4147	50.0876	51.8406
175.001	1.309475	4.3698	54.685	52.4506	54.3136
200.002	1.33395	4.47035	57.3032	55.2266	57.2152
225.002	1.35529	4.55667	59.5417	57.6218	59.7084
250.002	1.373555	4.63483	61.479	59.6928	61.8606
275.002	1.39036	4.70375	63.1716	61.4894	63.726
300.002	1.404535	4.76741	64.6672	63.0546	65.354
325.003	1.418085	4.82812	66.0013	64.4112	66.7818
350.003	1.430235	4.88365	67.2112	65.6116	68.0478
375.003	1.441805	4.9379	68.3107	66.6786	69.1702
400.003	1.45202	4.99012	69.3277	67.6282	70.18
425.003	1.462295	5.04167	70.2575	68.4742	71.0932
450.003	1.47133	5.0886	71.1034	69.2336	71.9184
475.004	1.47991	5.13453	71.874	69.9272	72.6696
500	1.487035	5.17204	72.5903	70.5724	73.3764
506.25	1.127142	3.95031	69.2861	67.7364	70.347
518.75	1.066474	3.7106	68.1165	66.7724	69.3366
531.25	1.037077	3.60062	67.515	66.281	68.828
543.75	1.015975	3.5244	67.076	65.9172	68.4502
556.25	0.998787	3.46378	66.7257	65.6248	68.1472
568.751	0.983924	3.41321	66.4224	65.378	67.8902
581.251	0.971219	3.37063	66.1565	65.1582	67.6656
593.751	0.959791	3.33134	65.9161	64.962	67.4672
606.251	0.9496	3.29779	65.707	64.7862	67.2856
618.751	0.939505	3.26565	65.5122	64.626	67.124
631.251	0.930623	3.23851	65.3307	64.4772	66.971
643.751	0.922233	3.21194	65.1613	64.3416	66.8288
656.251	0.914464	3.18968	65.0074	64.2108	66.695

675.001	0.904251	3.16098	64.7934	64.0382	66.513
700.002	0.891459	3.12272	64.5374	63.8258	66.2936
725.002	0.879893	3.08856	64.3026	63.633	66.0914
750.002	0.869015	3.06146	64.0875	63.4564	65.9082
775.002	0.859128	3.03546	63.8852	63.296	65.7392
800.002	0.850173	3.01152	63.7013	63.15	65.5804
825.003	0.841481	2.99075	63.5319	63.018	65.43
850.003	0.833606	2.96927	63.3703	62.8946	65.2846
875.003	0.82637	2.95184	63.2166	62.788	65.1468
900.003	0.819494	2.93358	63.0746	62.6878	65.0176
925.003	0.813289	2.91977	62.9399	62.5956	64.8932
950.003	0.807004	2.90497	62.8053	62.5082	64.77
975.004	0.800705	2.89158	62.6838	62.4278	64.6552

APPENDIX H: EFFECT OF STORAGE TIME AND TEMPERATURE ON EMULSION RHEOLOGY

[1] Optimum emulsion (mean values)

Table H1 Data of optimum emulsion at 5°C

Shear rate[1/s]	Shear stress of forward and backward sweep (Pa)									
	Day 1		day 3		Day 9		Day 15		Day 20	
40	118.9	51.73	405.9	88.08	354.7	116.9	437.1	120.5	368.6	97.79
49.37	119.3	57.99	378.1	93.47	356.5	122.1	437	126.8	394.3	101.9
60.81	125.6	64.95	360.6	99.39	355.9	126.1	434.1	133.8	379.9	106.7
74.98	132.2	72.74	351.6	106.2	354.8	132.6	436.1	141.5	364.6	112
92.44	140	81.39	344.3	113.9	356.9	142	436.2	150	350	118
114	148.8	91.26	344.1	122.6	358.9	149.8	430.4	159.7	336.3	124.2
140.5	158.8	102.3	335.5	132.5	357.7	156.6	424.8	170.4	337.4	131.2
173.2	169.7	115.1	328.4	143.9	355.8	162.6	415.1	182.7	341.5	139.7
213.6	182.2	129.5	322	156.8	353.1	173.8	411.2	196.1	310.2	149.8
263.3	196.1	146	315.3	171.6	348.4	187.7	406.3	211.6	300.7	161.4
324.6	210.8	164.7	314	188.9	342.6	204.5	400	229.6	297.4	175.4
400.2	228.3	186.4	315.9	209.3	336.2	222.3	395	251.1	293.9	191.5
493.4	247.8	212.2	313.3	233.8	333.2	242.7	388.3	277.1	293.7	211.4
608.3	269.5	243.4	316.1	263.5	330.8	269.2	383.6	309.4	291.3	236.3
750	296	296	320.9	320.9	327.5	327.5	378.5	378.5	280	280

Table H2 Data of optimum emulsion at 20°C

Shear rate [1/s]	Shear stress of forward and backward sweep									
	Day 1		Day 3		Day 9		Day 15		Day 20	
40	118.9	51.73	191.1	78.86	204.3	64.67	153	60.85	103.1	33.35
49.34	119.3	57.99	186.4	85.73	186.5	69.98	152.3	64.7	101.4	36.96
60.81	125.6	64.95	187.5	93.26	179.7	76.08	150.4	68.73	100.4	40.92
74.98	132.2	72.74	189.6	101.7	178.8	82.92	150.6	73.09	100.1	45.01
92.44	140	81.39	194.5	111	177.9	90.54	151.5	77.83	99.74	49.59
114	148.8	91.26	200.5	121.4	181	99.28	152.2	82.9	100.7	54.6
140.5	158.8	102.3	208.7	133.1	184.5	109	152.8	88.32	102.8	60.19
173.2	169.7	115.1	218.8	146.5	190.4	120.2	154.1	94.47	105.9	66.47
213.6	182.2	129.5	230.8	161.4	196.4	132.8	155.6	101.3	109.3	73.18
263.3	196.1	146	243.3	178.4	203.7	147.3	158.4	109.3	112.8	80.64
324.6	210.8	164.7	258.5	198	213.7	163.7	161.6	118.4	116.6	88.72
400.2	228.3	186.4	274.5	220.9	225.6	182.8	166.2	129.2	121.2	98.06
493.4	247.8	212.2	292.7	247.6	241.1	204.5	172.6	142.2	126.7	108.6
608.4	269.5	243.4	313	280.4	257.9	230.5	178.4	157.9	133	120.4
750	296	296	336.7	336.7	273.6	273.6	185.6	185.6	138.7	138.7

Table H3 Data of optimum emulsion at 45°C

Shear rate[1/s]	Shear stress (Pa) of forward and backward sweep									
	Day 1		Day 3		Day 9		Day 15		Day 20	
40	118.9	51.73	185	75.1	122.5	42.01	120.5	36.49	136	45.04
49.35	119.3	57.99	183.9	82.51	122.6	45.56	119.1	40.04	135.4	49.51
60.81	125.6	64.95	185.3	90.74	123.6	49.69	121	43.82	136	54.29
74.98	132.2	72.74	193.5	100	124.6	54.38	121.8	48.28	137.4	59.74
92.44	140	81.39	200.6	110.1	126.3	59.69	122.5	53.23	139.5	65.83
114	148.8	91.26	207.6	121.4	128	65.61	124.6	58.83	142.3	72.47
140.5	158.8	102.3	215.2	134	130.6	72.42	127.3	65.17	145.3	80.12
173.2	169.7	115.1	224.7	148.1	133.9	80.03	130.1	72.45	148.8	88.59
213.6	182.2	129.5	235.5	163.8	137.7	88.76	133.3	80.69	152.9	98.12
263.3	196.1	146	248.1	181.6	142.4	98.66	137.9	89.85	157.7	109.2
324.6	210.8	164.7	262.5	201.7	148.1	109.9	143	100.5	163.1	121.4
400.2	228.3	186.4	279.2	224.8	155.5	122.9	149.2	112.6	170	135
493.4	247.8	212.2	299.5	252	164.2	138.2	156.4	126.7	179.1	151.3
608.4	269.5	243.4	320.1	284.3	174.2	156.6	164	143.5	190	171.3
750	296	296	343.6	343.6	184.7	184.7	171.8	171.8	201.2	201.2

[2] 25 mM NaCl Emulsion (mean values)

Table H4 Data of emulsion containing 25 mM NaCl at 5°C

Shear rate [1/s]	Shear stress (Pa) of forward and backward sweep									
	Day 1		Day 3		Day 9		Day 15		Day 20	
40	106	50.68	184	56.5	215.3	92.34	214.4	86.72	207.7	81.13
49.34	108.5	56.77	181.8	60.07	217	97.63	215.2	91.95	206.5	86.32
60.81	114.1	63.63	182.8	64.2	219.5	103.5	216.7	97.65	206.8	91.72
74.98	121.3	71.31	184.5	68.9	222.1	110.1	219.9	103.8	206.1	97.51
92.44	129.7	79.91	186.3	74.25	224.9	117.2	221.4	110.4	207.4	103.7
114	139.1	89.64	188.3	80.28	227.2	125.2	223.5	117.8	209.5	110.3
140.5	149.7	100.6	189.7	86.76	230.4	134	224.2	125.9	209.6	117.6
173.2	161.5	113	190.4	94.27	234.4	144	228.3	134.8	210.7	125.9
213.6	174.9	127.2	190.8	102.6	239.4	155.3	232	145	213.2	135.1
263.3	189.1	143.4	196.6	112.6	247.2	167.9	235.6	156.4	217.2	145.4
324.6	204.5	162.2	197.2	123.7	253	182.3	239.1	168.7	220.5	157.7
400.2	222.9	184.1	198.7	136.9	258.6	199	243.9	183.5	225.7	171.1
493.4	243.1	209.7	201	153	263.8	218.1	248.8	200.1	230.7	187.3
608.4	266	240.8	204.1	172.2	270.8	240.3	253.4	221.3	236.5	208.4
750	292.9	292.9	208	208	278.2	278.2	257	257	243.8	243.8

Table H5 Data of emulsion containing 25 mM NaCl at 20°C

Shear rate(s-1)	Shear stress (Pa) of forward and backward sweep									
	Day 1		Day 3		Day 9		Day 15		Day 20	
40	106	50.68	117.8	41.77	86.44	29.27	65.12	16.72	47	10.94
49.34	108.5	56.77	112.9	45.82	88.04	32.06	64.35	18.57	45.78	12.32
60.81	114.1	63.63	112.4	50.39	89.36	35.27	64.07	20.82	45.12	13.66
74.97	121.3	71.31	114	55.47	91.05	38.78	63.95	23.12	44.83	15.32
92.44	129.7	79.91	117.3	61.11	93.19	42.57	64.08	25.57	44.81	17.06
114	139.1	89.64	121.6	67.48	95.05	46.8	64.61	28.33	45.24	19.3
140.5	149.7	100.6	126.8	74.7	97	51.69	65.28	31.58	46.04	21.88
173.2	161.5	113	132.6	82.82	99.26	57.27	66.32	35.38	47.02	24.96
213.6	174.9	127.2	139.1	92.01	102	63.54	67.61	39.64	48.34	28.51
263.3	189.1	143.4	146.2	102.6	105.1	70.82	69.55	44.53	50.11	32.49
324.6	204.5	162.2	154.4	114.7	108.9	79.17	71.84	50.36	52.46	37.16
400.2	222.9	184.1	163.5	129.5	114	88.7	75.2	57.31	55.71	42.56
493.4	243.1	209.7	173.6	147.4	119.9	99.99	79.28	65.32	59.49	48.82
608.3	266	240.8	186.5	165.3	127.4	113.9	85.06	74.53	64.21	56.14
750	292.9	292.9	202.9	202.9	135.9	135.9	89.89	89.89	67.5	67.5

Table H6 Data of emulsion containing 25 mM NaCl at 45°C

Shear rate [s^{-1}]	Shear stress of forward and backward sweep									
	Day 1		Day 3		Day 9		Day 15		Day 20	
40	106	50.68	112.1	46.88	36.07	13.35	25.24	11.98	12.79	9.743
49.34	108.5	56.77	111.2	51.44	33.24	14.26	25.63	12.9	13.81	10.76
60.81	114.1	63.63	111.5	56.59	32.63	15.35	26.46	14	15.02	11.59
74.98	121.3	71.31	112.9	62.11	32.59	16.63	27.41	15.29	16.21	12.73
92.44	129.7	79.91	115.9	68.34	32.85	18.17	28.39	16.65	17.78	14.07
114	139.1	89.64	120.2	75.31	33.51	19.86	29.65	18.31	19.32	15.82
140.5	149.7	100.6	125.4	83.17	34.67	21.76	31.01	20.24	21.21	17.83
173.2	161.5	113	131.6	92.02	36	24	32.65	22.47	23.2	19.77
213.6	174.9	127.2	138.9	102	37.5	26.65	34.48	25	25.49	22.19
263.3	189.1	143.4	147.6	113.4	39.44	29.75	36.52	28.09	28.17	24.93
324.6	204.5	162.2	157.2	126.3	41.82	33.5	38.88	31.47	31.17	28.47
400.2	222.9	184.1	168.9	141.6	44.56	37.74	41.88	35.67	34.73	32.08
493.4	243.1	209.7	184.4	159.7	48.19	42.69	45.25	40.24	38.55	36.58
608.4	266	240.8	199.4	182.8	52.31	48.53	49.18	45.4	42.89	41.8
750	292.9	292.9	219.3	219.3	56.86	56.86	53.32	53	47.62	47

[3] 8% (w/w) Vinegar (mean values)

Table H7 Data of emulsion containing 8% (w/w) vinegar at 5°C

Shear rate [1/s]	Shear stress (Pa) of forward and backward sweep									
	Day 1		Day 3		Day 9		Day 15		Day 20	
40	50.3	36.79	149.3	52.99	149.2	75.71	163.5	76.66	148.7	53.4
49.33	53.8	40.74	149.3	56.94	152.9	79.95	163.1	80.96	149	57.32
60.8	58.28	45.32	148.5	60.89	155.2	84.7	165.2	85.77	149.9	61.75
74.97	63.64	50.58	149.3	65.48	157.3	89.8	168.1	91.1	152	66.86
92.43	69.66	56.33	151.1	70.7	160	95.59	170.5	96.98	153.7	73.02
114	76.43	63	153.8	76.48	163.6	101.8	173.5	103.6	156.2	78.99
140.5	84.3	70.59	156.1	83.02	168.2	108.7	177	111	159.2	85.92
173.2	92.99	79.28	158.7	89.88	173.1	117.2	181.6	119.4	162.3	94.73
213.6	103	89.37	164.3	98.36	179.2	126.8	186.6	128.9	167.3	104
263.3	114.5	101.2	168.3	107.9	186.3	137.5	192.8	139.7	171.4	114.7
324.6	127.9	115.2	172.2	118.9	194	149.9	198.8	151.5	177.3	127
400.2	143.5	132.1	176.2	131.7	202.5	164.5	207.6	165.7	183.4	140.4
493.4	161.9	152.6	180	146.8	211.9	181.1	218.3	183.4	191.2	156.4
608.3	183.6	177.5	185.3	165.3	221	198.7	227.7	205.1	198.4	176.6
750	209.4	209.4	192.8	192.8	230.3	230.3	237.4	237.4	206.5	206.5

Table H8 Data of emulsion containing 8% (w/w) vinegar at 20°C

Shear rate[1/s]	Shear stress (Pa) of forward and backward sweep									
	Day 1		Day 3		Day 9		Day 15		Day 20	
40	50.3	36.79	149.3	52.99	149.2	75.71	163.5	76.66	148.7	53.4
49.33	53.8	40.74	149.3	56.94	152.9	79.95	163.1	80.96	149	57.32
60.8	58.28	45.32	148.5	60.89	155.2	84.7	165.2	85.77	149.9	61.75
74.97	63.64	50.58	149.3	65.48	157.3	89.8	168.1	91.1	152	66.86
92.43	69.66	56.33	151.1	70.7	160	95.59	170.5	96.98	153.7	73.02
114	76.43	63	153.8	76.48	163.6	101.8	173.5	103.6	156.2	78.99
140.5	84.3	70.59	156.1	83.02	168.2	108.7	177	111	159.2	85.92
173.2	92.99	79.28	158.7	89.88	173.1	117.2	181.6	119.4	162.3	94.73
213.6	103	89.37	164.3	98.36	179.2	126.8	186.6	128.9	167.3	104
263.3	114.5	101.2	168.3	107.9	186.3	137.5	192.8	139.7	171.4	114.7
324.6	127.9	115.2	172.2	118.9	194	149.9	198.8	151.5	177.3	127
400.2	143.5	132.1	176.2	131.7	202.5	164.5	207.6	165.7	183.4	140.4
493.4	161.9	152.6	180	146.8	211.9	181.1	218.3	183.4	191.2	156.4
608.3	183.6	177.5	185.3	165.3	221	198.7	227.7	205.1	198.4	176.6
750	209.4	209.4	192.8	192.8	230.3	230.3	237.4	237.4	206.5	206.5

Table H9 Data of emulsion containing 8% (w/w) vinegar at 45°C

Shear rate [1/s]	Shear stress (Pa) of forward and backward sweep									
	Day 1		Day 3		Day 9		Day 15		Day 20	
40	50.3	36.79	55.61	38.87	57.25	38.55	56.1	37.84	54.45	34.8
49.33	53.8	40.74	58.23	42.68	59.79	42.29	58.91	41.26	57.1	38.29
60.8	58.28	45.32	61.6	47.08	62.78	46.5	62.01	45.25	60.03	42.12
74.97	63.64	50.58	65.43	51.9	67.02	51.2	65.38	49.55	63.41	46.31
92.43	69.66	56.33	70.05	57.31	72.16	56.36	69.35	54.44	66.93	51.04
114	76.43	63	75.33	63.48	76.86	62.2	73.76	60.02	70.89	56.45
140.5	84.3	70.59	81.37	70.44	82.33	68.81	78.89	66.26	75.59	62.34
173.2	92.99	79.28	88.14	78.22	88.52	76.27	84.88	73.34	81.16	69.01
213.6	103	89.37	95.73	87.19	95.69	84.74	91.52	81.55	87.36	76.38
263.3	114.5	101.2	104.4	97.3	103.9	94.41	99.32	90.71	94.78	84.9
324.6	127.9	115.2	114.3	108.9	113.2	105.7	108.6	101.2	103.5	95.05
400.2	143.5	132.1	125.9	122.4	124.2	118.6	119.5	113.4	113.6	106.5
493.4	161.9	152.6	140.1	138	137.7	133.6	132.3	127.6	125.7	119.8
608.3	183.6	177.5	156.8	156.5	154.1	151.6	147.3	144.6	139.6	135.6
750	209.4	209.4	177.7	177.5	173.5	173.5	165.3	165.3	155.6	155.6

[4] 0.5% (w/w) citric acid (mean values)

Table H10 Data of emulsion containing 0.5 % (w/w) citric acid at 5°C

Shear rate [s^{-1}]	Shear stress (Pa) of forward and backward sweep									
	Day 1		Day 3		Day 9		Day 15		Day 20	
40	59.83	42.37	186.8	66.37	229.4	95.23	364.9	125.8	386	127.3
49.33	64.96	48.28	189.3	73.8	229.2	103.7	368	135.6	394.9	138.9
60.81	72.3	54.83	195	82.17	234.6	113.2	372.7	147.2	407.4	151.6
74.97	80.29	62.43	201.3	91.54	244.7	123.4	378.2	159.9	416.2	165.2
92.44	89.78	71.15	208.6	102	250.1	134.7	383.2	173.7	422.2	180.1
114	100.5	81.03	217.5	113.8	255.6	147.1	389.1	188.9	428	196.2
140.5	112.7	92.35	227.2	127.4	259.9	160.6	395.8	205.4	434.9	214.2
173.2	126.2	105.2	238	142.5	265.6	173.5	401.9	222.7	440.4	233.9
213.6	141	119.9	250	159.5	271.6	187.7	408.3	237.2	445.9	255.2
263.3	157.6	136.8	263.7	179	273.1	205.8	414.2	257.7	451	278.8
324.6	176.5	156.1	278.6	199.3	275.9	224.4	416.6	276	456.1	305.1
400.2	197.6	178.3	295	224	281.5	232.5	420.8	304.1	459.1	334.5
493.4	221.3	204.2	313	254.2	291.7	249.6	425.6	340.5	464.9	368.2
608.3	247.6	234.9	331.8	291.9	305.6	281.8	430.8	377.1	470.5	407.2
750	278	278	355.5	355.5	325.5	325.5	437	437	476.3	476.3

Table H11 Data of emulsion containing 0.5 % (w/w) citric acid at 20°C

Shear rate [s^{-1}]	Shear stress (Pa) of forward and backward sweep									
	Day 1		day 3		Day 9		Day 15		Day 20	
40	59.83	42.37	105.7	56.54	131.7	60.63	182.8	74.17	199.7	83.78
49.33	64.96	48.28	112.1	63.68	137.7	67.97	182.9	81.74	196.1	91.4
60.81	72.3	54.83	120.5	71.91	148.2	76.12	187.1	90.2	202.1	100
74.97	80.29	62.43	131.8	81.07	158.5	85.31	192.8	99.73	206.6	109.7
92.44	89.78	71.15	142.1	91.57	167.6	95.55	200.3	110.2	213.1	120.5
114	100.5	81.03	153.6	103.2	178.1	107.2	213.6	122	221	132.6
140.5	112.7	92.35	166.7	116.7	189.8	120.3	226.2	135.1	230.5	146.1
173.2	126.2	105.2	181.5	132	203	135	238.4	149.7	241.2	161.1
213.6	141	119.9	198.4	149.2	217.9	151.9	251.7	166.3	253.3	177.9
263.3	157.6	136.8	216.6	168.4	235.1	171	266.9	185	266.8	196.9
324.6	176.5	156.1	236.8	191.5	253.6	192.2	283.2	203.1	280.3	218.3
400.2	197.6	178.3	259.3	217.8	274.7	208.7	301.3	225.1	298.7	242.9
493.4	221.3	204.2	284.8	249.5	298.8	235.3	321.6	253.6	316.6	271.6
608.3	247.6	234.9	313.9	289.4	312.7	270.2	344.8	290.2	336.2	305.3
750	278	278	347.4	347.4	333.4	333.4	360	360	358.2	355

Table H12 Data of emulsion containing 0.5 % (w/w) citric acid at 45°C

Shear rate [s^{-1}]	Shear stress of forward and backward sweep									
	Day 1		Day 3		Day 9		Day 15		Day 20	
40	59.83	42.37	133.5	72.46	149.9	65.12	156.7	75.18	156	65.99
49.34	64.96	48.28	137.9	80.92	146.8	72.48	161.2	82.83	157.8	72.56
60.81	72.3	54.83	145	90.55	149.8	80.79	165.2	91.23	159.7	79.95
74.98	80.29	62.43	154.6	101.2	156	90.15	170.4	100.8	163.1	88.23
92.44	89.78	71.15	165.8	113.2	164.3	100.5	177.2	111.6	168.1	97.57
114	100.5	81.03	178.2	126.7	174.2	112.1	185.1	123.5	175.3	108.1
140.5	112.7	92.35	192.4	141.9	185.6	125	194	137	182.3	119.8
173.2	126.2	105.2	207.8	158.9	198.3	139.6	204.4	152	190.7	132.8
213.6	141	119.9	225	178	212.1	155.9	215.8	168.6	200.1	147.4
263.3	157.6	136.8	244.5	199.7	227.9	173.5	228.8	187.2	211	163.9
324.6	176.5	156.1	265.8	225	245.1	192	244.1	207.7	222.9	182.1
400.2	197.6	178.3	288.7	254.3	263.9	213.9	266.9	230.7	236.8	202.3
493.4	221.3	204.2	321.7	287	278.4	240.4	284.9	256.6	252.1	225.1
608.4	247.6	234.9	351.3	325	299	272.1	305.8	286.2	268.8	251.2
750	278	278	384.9	384.9	322.1	322.1	327.9	327.9	286.9	286.9